900-231

ORBITING ASTRONOMICAL OBSERVATORY A-2 SPACE VEHICLE RESPONSE TO TRANSIENT LOADING AT ATLAS BOOSTER ENGINE CUTOFF

December 21, 1968

J. A. Garba
R. D. Simpson

JET PROPULSION LABORATORY
CALIFORNIA INSTITUTE OF TECHNOLOGY
PASADENA, CALIFORNIA

CONTENTS

TABLES

FIGURES

FIGURES (contd)

FIGURES (contd)

FIGURES (contd)

FIGURES (contd)

FIGURES (contd)

FIGURES (contd)

FIGURES (contd)

FIGURES (contd)

FIGURES (contd)

FIGURES (contd)

FIGURES (contd)

FIGURES (contd)

FIGURES (contd)

FIGURES (contd)

FIGURES (contd)

ORBITING ASTRONOMICAL OBSERVATORY A-2 SPACE VEHICLE RESPONSE TO TRANSIENT LOADING AT ATLAS BOOSTER ENGINE CUTOFF

I. INTRODUCTION

The analyses described herein were undertaken in response to a request[1] made by the NASA Goddard Space Flight Center (GSFC). They have utilized analysis concepts and computer programs developed by the Applied Mechanics Section of JPL for treating various classes of problems in the field of structural dynamics. The specific problem dealt with in this document is the prediction of the Orbiting Astronomical Observatory (OAO A-2) spacecraft structural response to be expected during Atlas booster engine cutoff (BECO).

The analyses documented in this report closely parallel the torsion analyses performed by JPL for GSFC on the Orbiting Geophysical Observatory (OGO-E) space vehicle, described in Ref. 1.

II. NORMAL MODE ANALYSIS

A. Input Data

Input data for the normal mode analysis were obtained from two sources: (1) The OAO A-2 spacecraft model was supplied to JPL by GSFC. (2) The model for the launch vehicle system consisting of the General Dynamics Convair Division (GD/C) Atlas/Centaur SLV-3C data, including the nose fairing, was supplied to JPL by GD/C, San Diego, California.

1. The OAO A-2 Spacecraft. A reduced structural model for the OAO A-2 spacecraft was used in this analysis. The torsional model consisted of nine mass points and eight spring elements connecting these points. The data for

[1] GSFC letter, File No. 6234, dated October 4, 1968, to Dr. W. H. Pickering, Director, JPL, from John F. Clark, Director, GSFC; subject: OAO A-2 Torsion Analysis.

this lumped parameter model, revised as of July 30, 1968, consisted of nine inertia values, eight torsional compliances, and the associated Grumman Aircraft Engineering Company (GAEC) vehicle station numbers. The spacecraft is modeled by one major torsion branch beam made up of eight inertia elements and a branch beam consisting of one element. The branch attaches to the main beam through an infinitely stiff spring. The spacecraft model terminates in a mass point at GAEC spacecraft station number 174.0, GD/C vehicle station number 31.0. The spacecraft model data were transmitted to JPL as an enclosure to the GSFC request letter.

Within the overall launch vehicle system the spacecraft is represented by joints 10 through 17 and joint 39; see JPL Documentation Codes, Fig. A-1. All pertinent spacecraft data are given in Appendix A.

2. The Atlas/Centaur Launch Vehicle. The data describing the Atlas/Centaur SLV-3C launch vehicle, including the nose fairing and an OAO spacecraft model, were transmitted to JPL via Ref. 2.

The launch vehicle model description consists of a lumped parameter representation of the Atlas/Centaur vehicle including the nose fairing and the OAO spacecraft. The OAO spacecraft representation was compatible in format with the OAO A-2 model received from GSFC. The numerical values for this spacecraft model were obtained by GD/C from a GSFC correspondence dated August 22, 1967.

The launch vehicle data are similar to the data used by JPL in the torsion analysis of the Surveyor space vehicle, described in Ref. 3. GD/C has modified these data by:

(1) Replacing the Surveyor payload, nose fairing, and adapters with the OAO payload configuration, nose fairing, and adapters.

(2) Adding new sustainer tank data to reflect the 51 in. extension of the SLV-3C vehicle.

B. Data Processing

1. Data Modification. The composite vehicle data of Ref. 2 were updated using the revised GSFC OAO A-2 spacecraft inertia values of July 30, 1968.

The OAO spacecraft model contains a stiffness element of zero compliance, connecting joints 14 and 63, Appendix A, JPL Documentation Codes, Fig. A-1. An infinitely stiff spring is not acceptable for computational purposes. A spring constant of 1×10^{12} in.-lb/in. was used in the mathematical model for the element connecting joint 14 to joint 63. This element is stiffer than any other element in (1) the spacecraft model by more than two orders of magnitude and (2) the composite vehicle model by more than one order of magnitude. The adequacy of this modeling is justified by the modal deflections of joint 14 and joint 63 as shown in Table B-1, Appendix B.

2. The Composite Vehicle. All pertinent data of the composite vehicle are given in Appendix A. In the processing of the composite vehicle data to obtain normal modes, the vehicle was first divided into two parts at GD/C station 685.0. The cantilevered normal modes of each part of the vehicle were obtained using the stiffness matrix structural analysis program, Ref. 4.

The two parts of the composite vehicle were then combined to obtain the overall vehicle normal modes using the modal combination program, Ref. 5. Thirty normal modes of the upper half and 20 normal modes of the lower half were retained in this analysis.

C. Free-Free Torsional Modes

Appendix B contains plots of the first 19 free-free normal modes of the composite vehicle as well as other pertinent modal data in tabular form.

For the plotting of mode shapes, the Atlas booster engine modal participation is represented by the angle

$$\phi_B^{(n)} = \phi_{59}^{(n)} + 0.5725\left(\phi_{60}^{(n)} - \phi_{59}^{(n)} + 0.4273\left(\phi_{61}^{(n)} - \phi_{59}^{(n)}\right)\right) \qquad (1)$$

where

$\phi_B^{(n)}$ is the booster engine modal participation in the n^{th} mode.

$\phi_{59}^{(n)}, \phi_{60}^{(n)}, \phi_{61}^{(n)}$ are the modal participations of joints 59, 60, and 61, respectively.

The Centaur engine modal participation is represented by the angle

$$\phi_6^{(n)} = \phi_{30}^{(n)} + 0.7067 \left(\phi_{31}^{(n)} - \phi_{30}^{(n)}\right) \tag{2}$$

where

$\phi_6^{(n)}$ is the Centaur engine modal participation in the n^{th} mode.

$\phi_{30}^{(n)}$, $\phi_{31}^{(n)}$ are the modal participations of joints 30 and 31, respectively.

The mathematical representation of the Atlas and Centaur engines and the derivations of equations (1) and (2) are described in Ref. 3.

Examination of the mode shape plots of Appendix B shows a slight discontinuity of the curvature at GD/C station 685.0. This discontinuity is the result of the method of analysis, where the cantilever normal modes of two parts of the vehicle are used to obtain free-free normal modes.

The modal deflections for joints within the OAO A-2 spacecraft listed in Table B-1 (Appendix B) are those required for the response analysis requested by GSFC. In order to represent the torque time history clearly, assume the following indicial notation:

Joint 10 = JT(1), Joint 11 = JT(2), Joint 12 = JT(3),
Joint 13 = JT(4), Joint 63 = JT(5), Joint 14 = JT(6),
Joint 15 = JT(7), Joint 16 = JT(8), Joint 17 = JT(9).

The computation of the torque time history just below each joint within the OAO A-2 spacecraft requires the evaluation of the following quantity

$$\tau_n^{JT(K)} = \sum_{\ell=1}^{K} I_{JT(\ell)} U_{JT(\ell)n} \tag{3}$$

where

$\tau_n^{JT(K)}$ - Modal quantity used to compute torque response where the superscript K refers to the point number at which the torque is to be computed and the subscript n refers to the n^{th} normal mode.

$I_{JT(\ell)}$ - Moment of inertia, lb-in.-sec^2, of the $JT(\ell)^{th}$ joint.

$U_{JT(\ell)n}$ - The n^{th} mode shape at joint $JT(\ell)$ in the overall launch vehicle free-free mode.

The summation in equation (3) is to be interpreted such that all joints $JT(\ell)$ are included affecting the torque at joint JT(K).

For example, if

$$\tau_n^{14} \left[= \tau_n^{JT(6)}\right]$$

is required for the computation of the torque time history just below joint 14, Fig. A-1, JPL Documentation Codes, equation (3) is interpreted as the following expression.

$$\tau_n^{14} = \tau_n^{JT(6)} = I_{10}U_{10n} + I_{11}U_{11n} + I_{12}U_{12n} + I_{13}U_{13n} + I_{63}U_{63n} + I_{14}U_{14n} \quad (4)$$

Values of $\tau_n^{JT(K)}$ for the joints at which torque time histories within the OAO A-2 spacecraft were requested by GSFC are listed in Table B-2, Appendix B.

III. RESPONSE ANALYSES

A. Method

The method used to compute the response of the spacecraft at booster engine cutoff (BECO) is indicated in the JPL Technical Memorandum 33-350, (Ref. 6), modified to accommodate certain types of responses. Two types of responses were required:

(1) Responses of angular acceleration versus time at each gridpoint.

(2) Responses of torque versus time at each gridpoint.

Item 1 is readily computed by the digital program of Ref. 6, for which Φ_{1n} is identical to $U_{JT(\ell)n}$.

Item 2 requires a slight modification in the interpretation of equation (8) of Ref. 6 in order to use the same program as indicated below.

Using the same notation in torque computation as used in Section II-C, the computation of the torque $T_{JT(K)} = T_{JT(K)}(t)$ at a joint JT(K) is the sum of the inertia torques due to the elements of inertia $I_{JT(\ell)}$, $\ell = 1, 2, \ldots K$, of each mass point ℓ of the spacecraft model (cantilever normal mode of spacecraft) about the longitudinal axis above the joint JT(K).

The inertia torque due to each inertia I_ℓ is:

$$T_{JT(\ell)} = I_{JT(\ell)}\ddot{\theta}_{JT(\ell)} = I_{JT(\ell)}\sum_{n=0}^{N} U_{JT(\ell)n}\,\ddot{q}_n \qquad (N = 20) \qquad (5)$$

where

$\ddot{\theta}_{JT(\ell)}$ = The angular rotation at mass point

$U_{JT(\ell)n}$ = The n^{th} mode shape at mass point JT(ℓ) in the overall vehicle free-free modes.

$\ddot{q}_n$ = The n^{th} generalized coordinate.

The total torque at joint JT(K) is

$$T_{JT(K)} = \sum_{\ell=1}^{K} I_{JT(\ell)}\sum_{n=0}^{N} U_{JT(\ell)n}\,\ddot{q}_n \qquad (6)$$

or,

$$T_{JT(K)} = \sum_{n=0}^{N}\left(\sum_{\ell=1}^{K} I_{JT(\ell)}\,U_{JT(\ell)n}\right)\ddot{q}_n \qquad (7)$$

where

$$K = 1, 2, \ldots M \qquad (M = 9)$$

Let

$$\tau_n^{JT(K)} = \sum_{\ell=1}^{K} I_{JT(\ell)} U_{JT(\ell)n} \tag{8}$$

then the torque at joint JT(K) is

$$T_{JT(K)} = \sum_{n=0}^{N} \ddot{q}_n \, \tau_n^{JT(K)} \tag{9}$$

Taking the Fourier transform of $T_{JT(K)}$ and using equation (5) of Ref. 6 we finally obtain

$$F_{JT(K)}(\omega) = F(\omega) \sum_{n=0}^{N} \frac{\Phi_{2n} \tau_n^{JT(K)}}{m_n} \frac{1}{\left[1 - \left(\frac{\omega_n}{\omega}\right)^2 - 2i\xi_n \frac{\omega_n}{\omega}\right]} \tag{10}$$

This is the same as equation (8) of Ref. 6 if we replace

$$\Phi_{1n} \text{ by } \tau_n^{JT(K)}$$

and

$$V_1(\omega) \text{ by } F_{JT(K)}(\omega)$$

The column of

$$\tau_n^{JT(K)}$$

used in the computation of the torque is indicated in Appendix B.

B. Input Data

The time history of the angular acceleration at the Ranger adapter was obtained during the Ranger flight, Ranger VI through IX, at booster engine cut-off (Ref. 7). It was assumed that this acceleration was due to the transient torque applied at the gimbal blocks of the Atlas engine at BECO. The Fourier transforms of the gimbal torque for the Ranger flights were obtained as indicated in Ref. 7, and used as input data for the OAO. Figures C-1 through C-12 (in Appendix C) display the four gimbal torque Fourier transforms and gimbal torque time histories.

C. Normal Modes

In addition to the rigid body mode, the first 19 elastic free-free normal modes covering a frequency range from 11.59 to 132.08 cps were retained to represent the Atlas/Centaur/OAO A-2 vehicle (see Appendix B).

D. Damping

A modal damping of 3 percent critical ($\xi = C/C_c$) was used for all modes of the Atlas/Centaur/OAO A-2 vehicle in accordance with previous calculations of Ref. 7.

E. Responses

The time histories of the responses were computed together with their Fourier transforms. In addition, the vehicle transfer function at each joint was also computed. Peak responses were noted and are indicated in Tables 1 and 2. Time histories and Fourier transforms are shown in Figs. C-13 through C-263 in Appendix C.

Examination of the peak acceleration responses in Tables 1 and 2 for joint 14 and joint 63 show some differences between the two. Since these two joints were to be connected by an infinitely stiff spring element, their acceleration responses should be identical. The differences are attributed to the type of mathematical model used as discussed in Section II, B-1. The differential modal deflection across the spring connecting the two points in question is

Table 1. Acceleration responses for 3% modal damping (RA-6, 7, 8, 9 data input)

Location	Excitation	Peak acceleration rad/sec^2
Joint 10	Pulse 1	11.18
	Pulse 2	10.03
	Pulse 3	17.81
	Pulse 4	9.66
Joint 11	Pulse 1	7.78
	Pulse 2	7.78
	Pulse 3	9.65
	Pulse 4	7.33
Joint 12	Pulse 1	4.34
	Pulse 2	3.95
	Pulse 3	12.59
	Pulse 4	4.41
Joint 13	Pulse 1	6.13
	Pulse 2	4.09
	Pulse 3	10.85
	Pulse 4	4.55
Joint 63	Pulse 1	8.15
	Pulse 2	7.32
	Pulse 3	12.84
	Pulse 4	6.71
Joint 14	Pulse 1	8.61
	Pulse 2	7.24
	Pulse 3	11.92
	Pulse 4	6.49
Joint 15	Pulse 1	10.22
	Pulse 2	7.47
	Pulse 3	12.72
	Pulse 4	6.73
Joint 16	Pulse 1	13.53
	Pulse 2	6.97
	Pulse 3	17.12
	Pulse 4	7.10
Joint 17	Pulse 1	4.24
	Pulse 2	4.09
	Pulse 3	10.20
	Pulse 4	3.85

Table 2. Torque responses for 3% modal damping (RA-6, 7, 8, 9 data input)

Location	Excitation	Peak torque lb-in.
Joint 10	Pulse 1 Pulse 2 Pulse 3 Pulse 4	8179 7337 13032 7069
Joint 11	Pulse 1 Pulse 2 Pulse 3 Pulse 4	18971 17914 26274 16656
Joint 12	Pulse 1 Pulse 2 Pulse 3 Pulse 4	24461 23790 28334 24495
Joint 13	Pulse 1 Pulse 2 Pulse 3 Pulse 4	13447 19532 25843 21760
Joint 63	Pulse 1 Pulse 2 Pulse 3 Pulse 4	4755 3145 8350 3551
Joint 14	Pulse 1 Pulse 2 Pulse 3 Pulse 4	19976 13891 45400 18234
Joint 15	Pulse 1 Pulse 2 Pulse 3 Pulse 4	34032 20840 55993 24681
Joint 16	Pulse 1 Pulse 2 Pulse 3 Pulse 4	44551 23576 44243 33837
Joint 17	Pulse 1 Pulse 2 Pulse 3 Pulse 4	44591 23218 43019 33860

negligible for most modes, as shown in Table B-1, Appendix B. Small differences in modal deflection are, however, apparently magnified in the response solution.

For design purposes the larger of the two numbers should be used.

REFERENCES

1. Gayman, W. H., Trubert, M. R., and Garba, J. A., OGO-E--Space Vehicle Response to Transient Loading at Atlas Booster Engine Cutoff; JPL Report No. 900-128; April 1968.

2. OAO AC-16 Torsional Model; General Dynamics Convair Division Inter-office Memorandum No. SD-68-183-CEN to R. S. Shorey, 966-4 from Structural Dynamics, 966-9; 19 November 1968.

3. Garba, J. A., Gayman, W. H., and Wada, B. K.; Computation of Torsional Vibration Modes of Ranger and Surveyor Space Vehicles; JPL Technical Memorandum 33-277; 1 April 1968.

4. Wada, B. K.; Stiffness Matrix Structural Analysis; JPL Technical Memorandum 32-774; 31 October 1965.

5. Bamford, R. M.; A Modal Combination Program for Dynamic Analysis of Structures; JPL Technical Memorandum 33-290; 1 July 1967.

6. Trubert, M. R.; A Fourier Transform Technique for the Prediction of Torsional Transients for a Spacecraft from Flight Data of Another Spacecraft Using the Same Booster; JPL Technical Memorandum 33-350; 15 October 1967.

7. Trubert, M. R.; Use of Ranger Flight Data in the Synthesis of a Torsional Acceleration Transient for Surveyor Vibration Qualification Testing; JPL Technical Memorandum 33-237; 19 April 1966.

APPENDIX A

ATLAS/CENTAUR OAO A-2 TORSION MODEL NUMERICAL VALUES

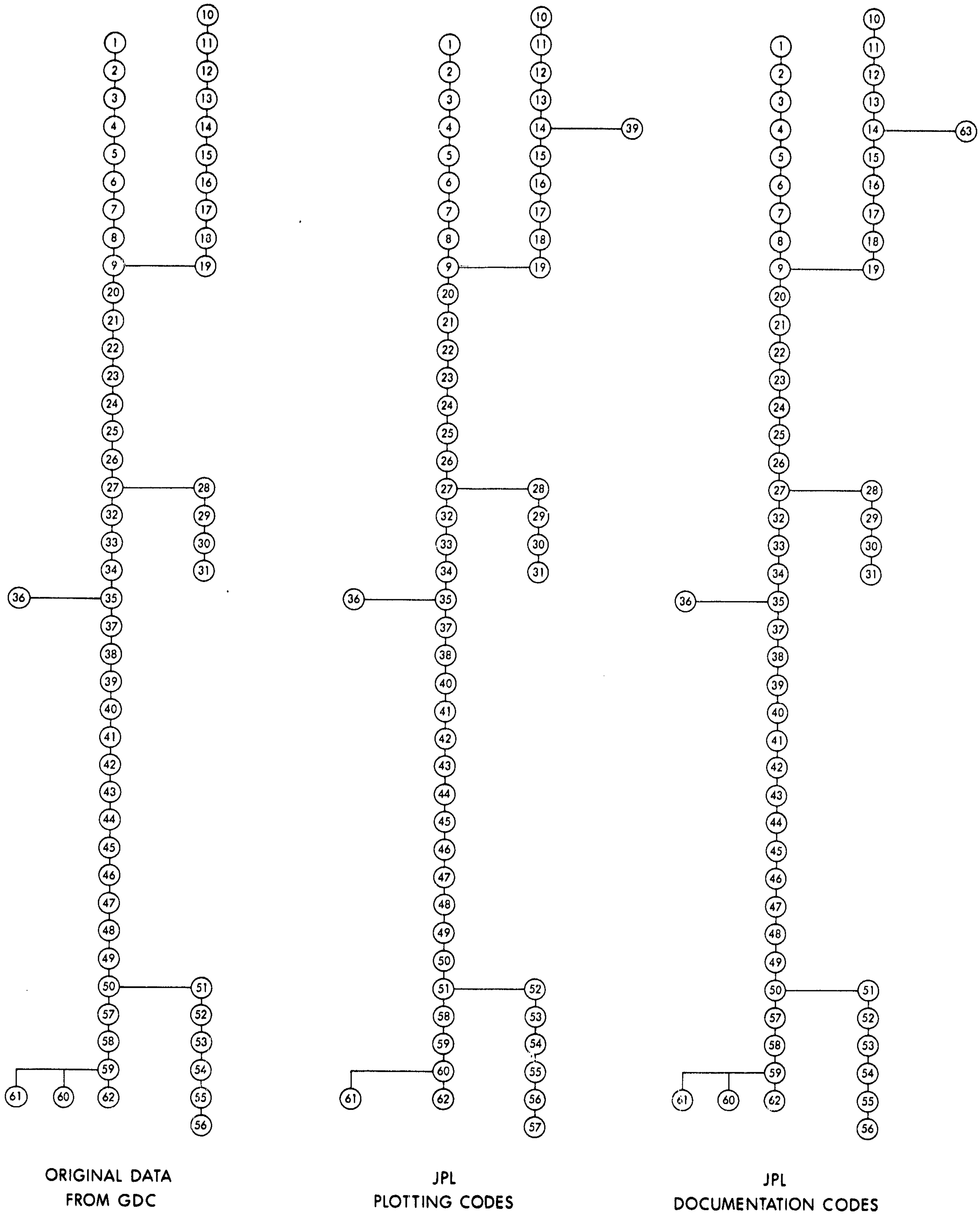

Fig. A-1. Mathematical model of the Atlas/Centaur/OAO A-2 space vehicle

JOINT	GD/C STATION, INCHES
1	-300.0
2	-250.0
3	-200.0
4	-150.0
5	-100.0
6	-50.0
7	0.0
8	50.0
9	75.0
10	-99.0
11	-82.0
12	-62.0
13	-43.0
14	-25.0
15	-4.0
16	12.0
17	31.0
18	45.0
19	60.0
20	120.0
21	150.0
22	190.0
23	226.0
24	260.0
25	296.0
26	335.0
27	360.0
28	368.0
29	390.0
30	410.0
31	430.0
32	405.0
33	440.0
34	475.0
35	510.0
36	499.0
37	550.0
38	630.0
39	685.0
40	745.0
41	805.0
42	835.0
43	860.0
44	890.0
45	920.0
46	980.0
47	1040.0
48	1090.0
49	1120.0
50	1133.0
51	1140.0
52	1160.0
53	1180.0
54	1200.0
55	1220.0
56	1240.0
57	1155.0
58	1190.0
59	1212.0
60	1242.0
61	1242.0
62	1250.0
63	-45.0

Fig. A-2. Atlas/Centaur/OAO A-2 torsion model - joint coordinates

JOINT A	JOINT B	K, IN-LB/RADIAN
1	2	1.0 E 08
2	3	3.0 E 08
3	4	7.0 E 08
4	5	1.3 E 09
5	6	1.5 E 09
6	7	1.5 E 09
7	8	1.5 E 09
8	9	1.65 E 10
10	11	5.076 E 08
11	12	4.237 E 08
12	13	4.505 E 08
13	14	6.135 E 08
14	15	1.042 E 09
15	16	3.125 E 08
16	17	1.919 E 08
17	18	4.0 E 09
18	19	6.0 E 09
9	19	1.0 E 10
9	20	4.5 E 09
20	21	1.8 E 09
21	22	4.5 E 09
22	23	6.66 E 09
23	24	6.66 E 09
24	25	6.66 E 09
25	26	6.66 E 09
26	27	8.64 E 09
27	28	3.17 E 10
28	29	8.50 E 09
29	30	1.30 E 09
30	31	4.59 E 06
27	32	7.68 E 09
32	33	9.43 E 09
33	34	9.43 E 09
34	35	9.43 E 09
35	36	1.8 E 10
35	37	9.43 E 09
37	38	3.17 E 09
38	39	4.63 E 09
39	40	4.87 E 09
40	41	5.05 E 09
41	42	1.13 E 10
42	43	1.24 E 10
43	44	2.04 E 10
44	45	1.10 E 10
45	46	7.80 E 09
46	47	7.30 E 09
47	48	9.75 E 09
48	49	1.24 E 10
49	50	3.02 E 10
50	51	6.0 E 10
51	52	1.4 E 10
52	53	7.01 E 09
53	54	1.4 E 09
54	55	1.4 E 09
55	56	1.4 E 09
50	57	3.13 E 10
57	58	2.4 E 10
58	59	4.14 E 10
59	60	5.976 E 07
59	61	8.998 E 08
59	62	2.25 E 10
14	63	1.0 E 12

Fig. A-3. Atlas/Centaur/OAO A-2 torsion model - spring constants

JOINT	INERTIA, POUND INCHES SQUARED	
1	6.0	E 04
2	4.0	E 05
3	5.0	E 05
4	1.3	E 06
5	1.5	E 06
6	1.5	E 06
7	1.5	E 06
8	4.55	E 05
9	4.55	E 05
10	2.827	E 05
11	5.361	E 05
12	9.332	E 05
13	8.389	E 05
14	9.727	E 05
15	5.871	E 05
16	5.684	E 05
17	7.40	E 04
18	8.9	E 04
19	4.88	E 05
20	1.8	E 06
21	1.8	E 06
22	7.92	E 05
23	1.14	E 06
24	1.78	E 06
25	8.87	E 06
26	1.46	E 06
27	3.03	E 06
28	2.543	E 05
29	7.519	E 05
30	7.55	E 05
31	3.12	E 05
32	4.72	E 05
33	2.35	E 06
34	4.34	E 05
35	5.22	E 05
36	3.54	E 05
37	6.84	E 05
38	6.84	E 05
39	1.15	E 05
40	6.53	E 05
41	3.08	E 05
42	5.46	E 05
43	3.22	E 05
44	6.36	E 05
45	6.5	E 05
46	3.46	E 06
47	4.85	E 06
48	4.26	E 06
49	2.36	E 06
50	5.79	E 05
51	5.62	E 05
52	4.521	E 05
53	5.55	E 05
54	2.34	E 05
55	2.59	E 05
56	4.18	E 05
57	2.83	E 06
58	4.51	E 06
59	7.92	E 06
60	4.09	E 06
61	3.05	E 06
62	5.22	E 06
63	1.72	E 05

Fig. A-4. Atlas/Centaur/OAO A-2 torsion model - joint inertias

APPENDIX B

FREE-FREE TORSIONAL MODES FOR THE OAO A-2 SPACE VEHICLE

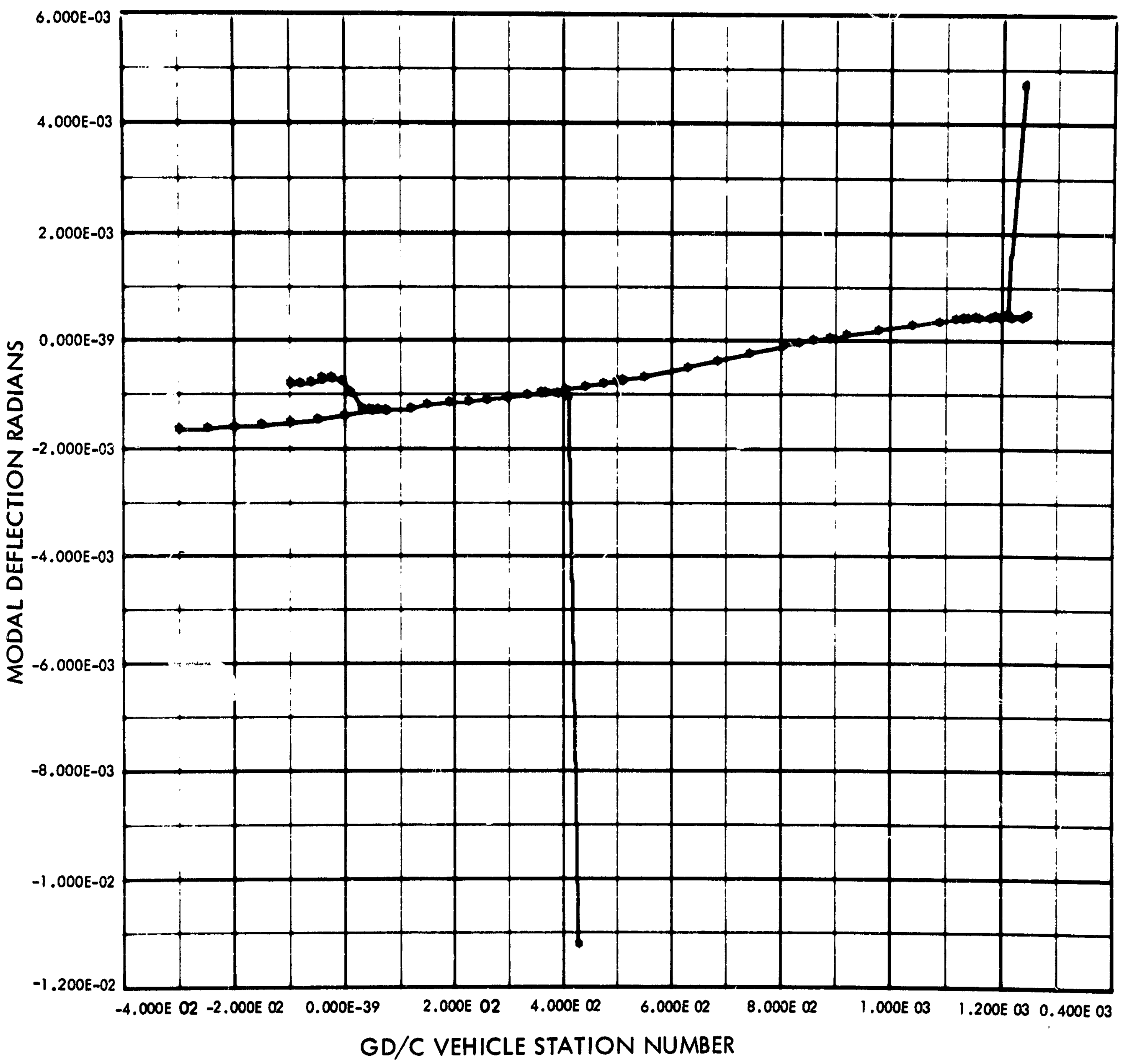

Fig. B-1. Atlas/Centaur/OAO torsion mode shape
Mode No. 1 Freq. = 0.1159E 02 cps

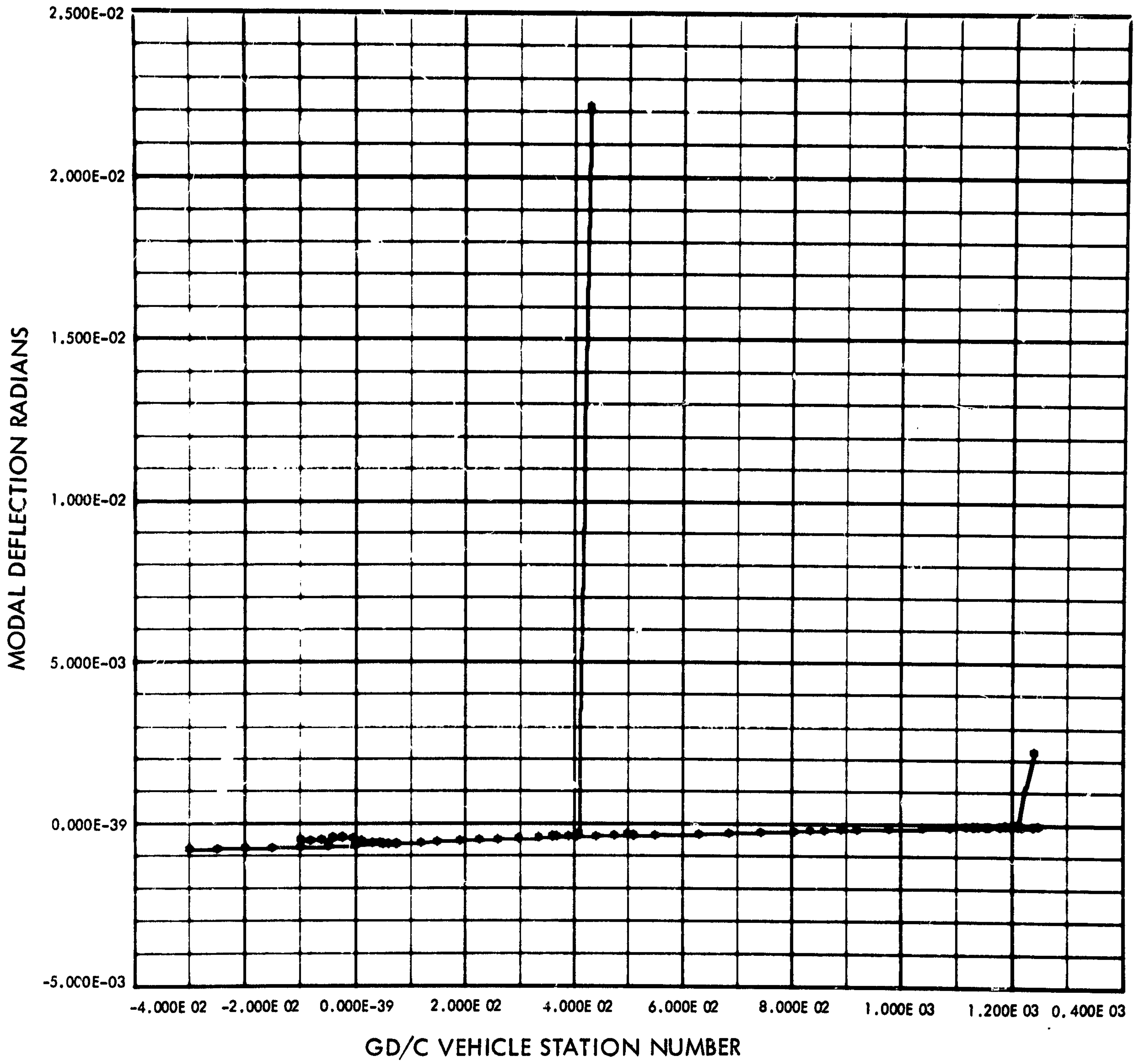

Fig. B-2. Atlas/Centaur/OAO torsion mode shape
Mode No. 2 Freq. = 0.1206E 02 cps

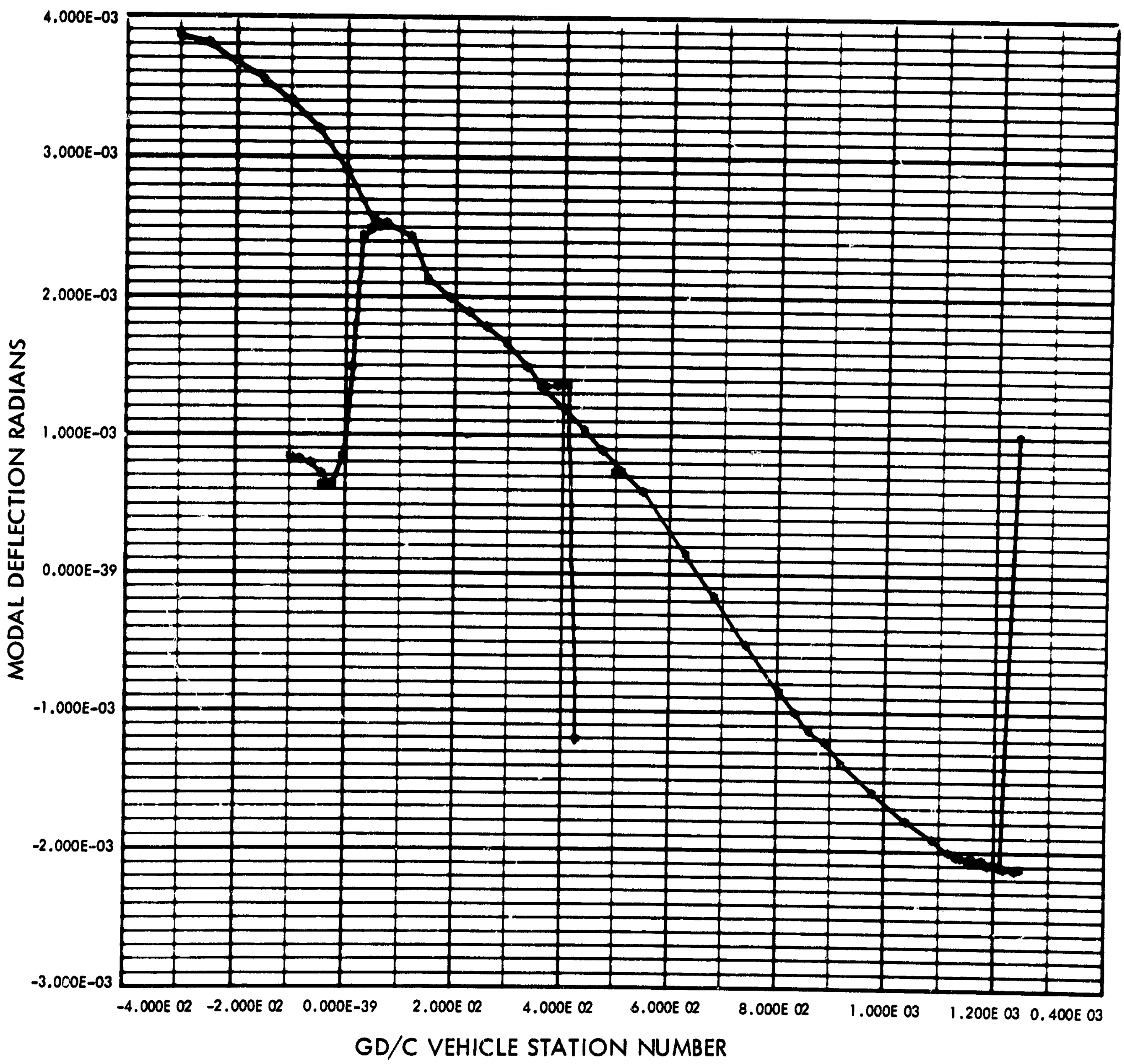

Fig. B-3. Atlas/Centaur/OAO torsion mode shape
Mode No. 3 Freq. = 0.1517E 02 cps

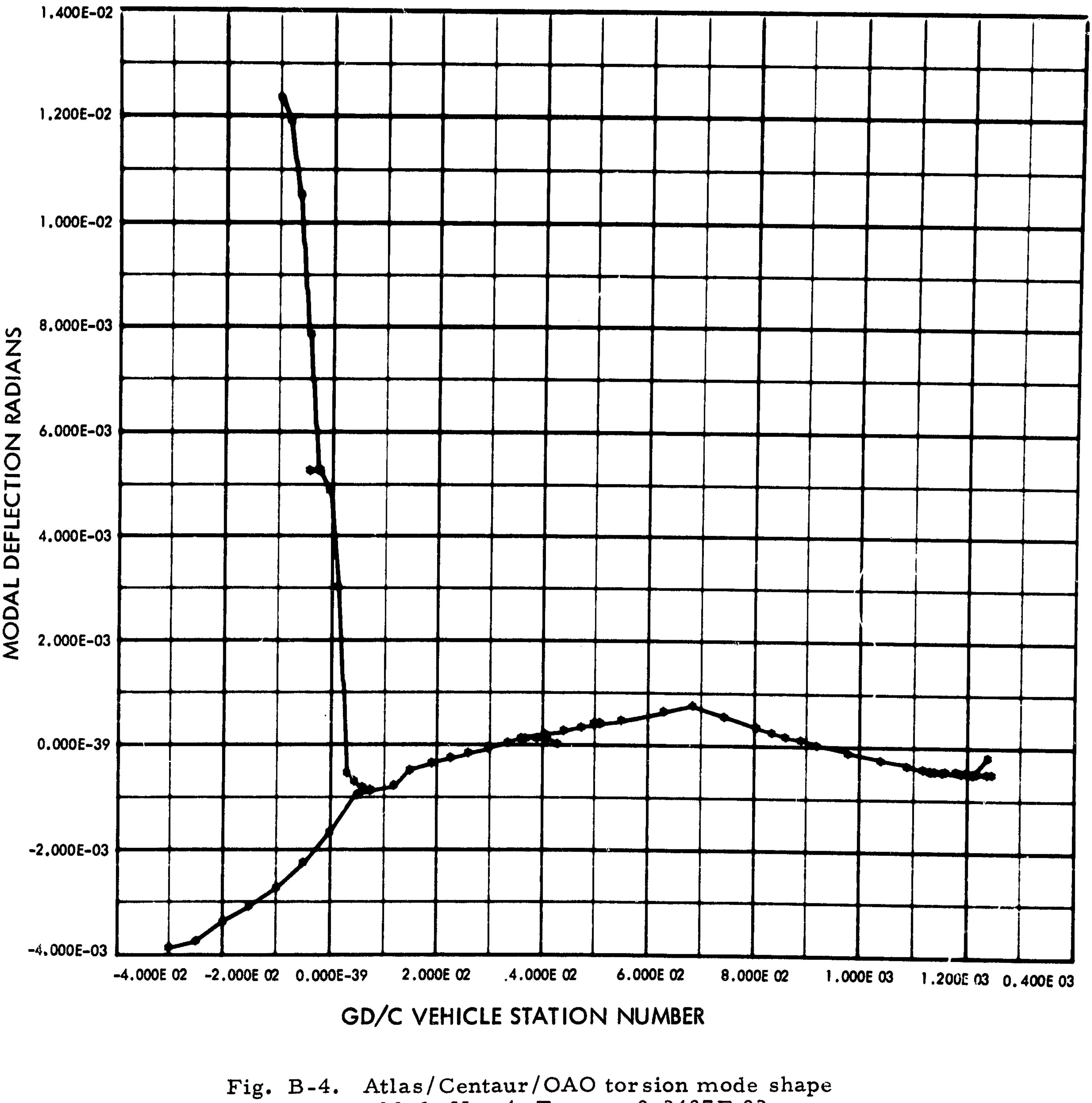

Fig. B-4. Atlas/Centaur/OAO torsion mode shape
Mode No. 4 Freq. = 0.2437E 02 cps

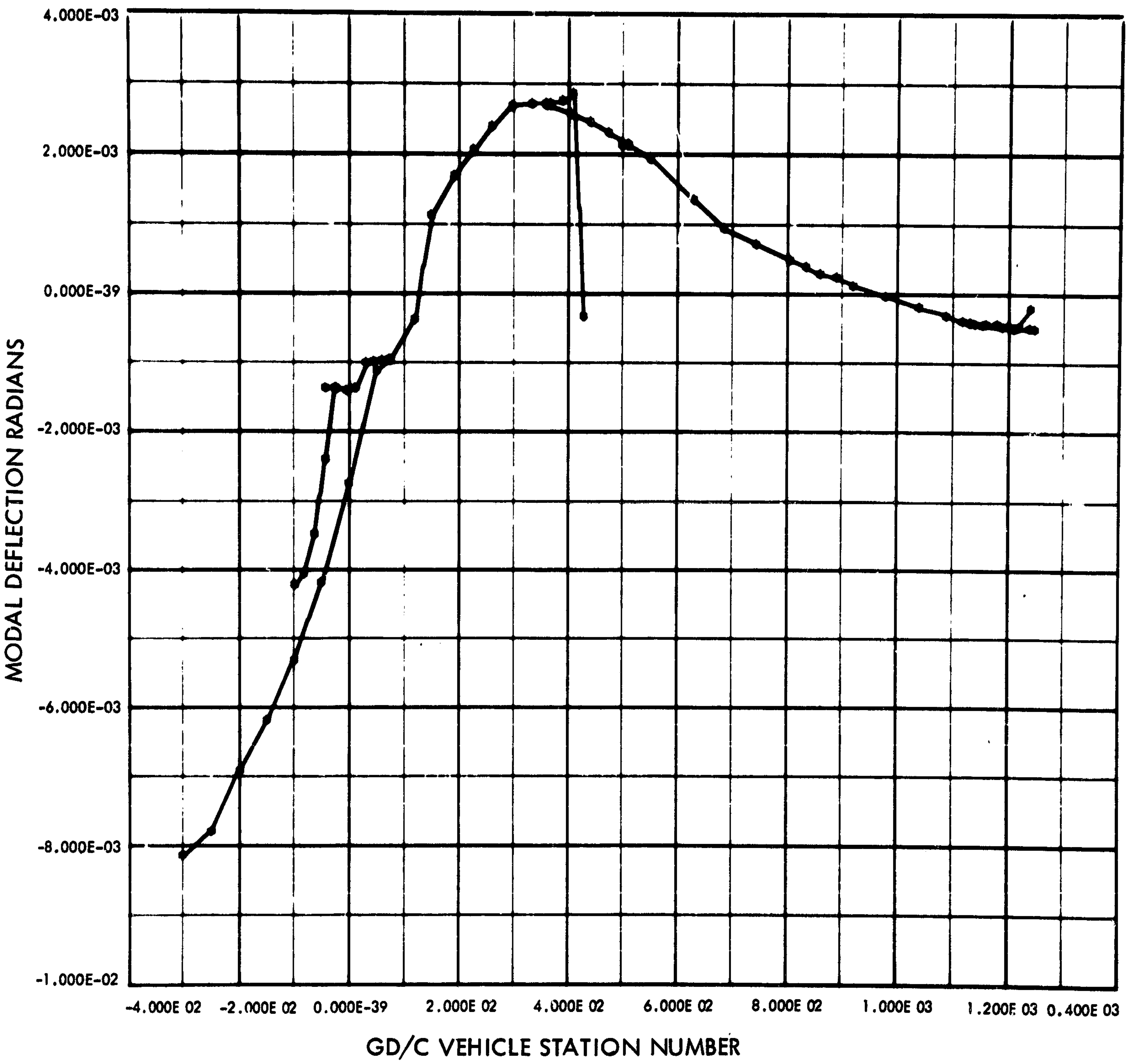

Fig. B-5. Atlas/Centaur/OAO torsion mode shape
Mode No. 5 Freq. = 0.2680E 02 cps

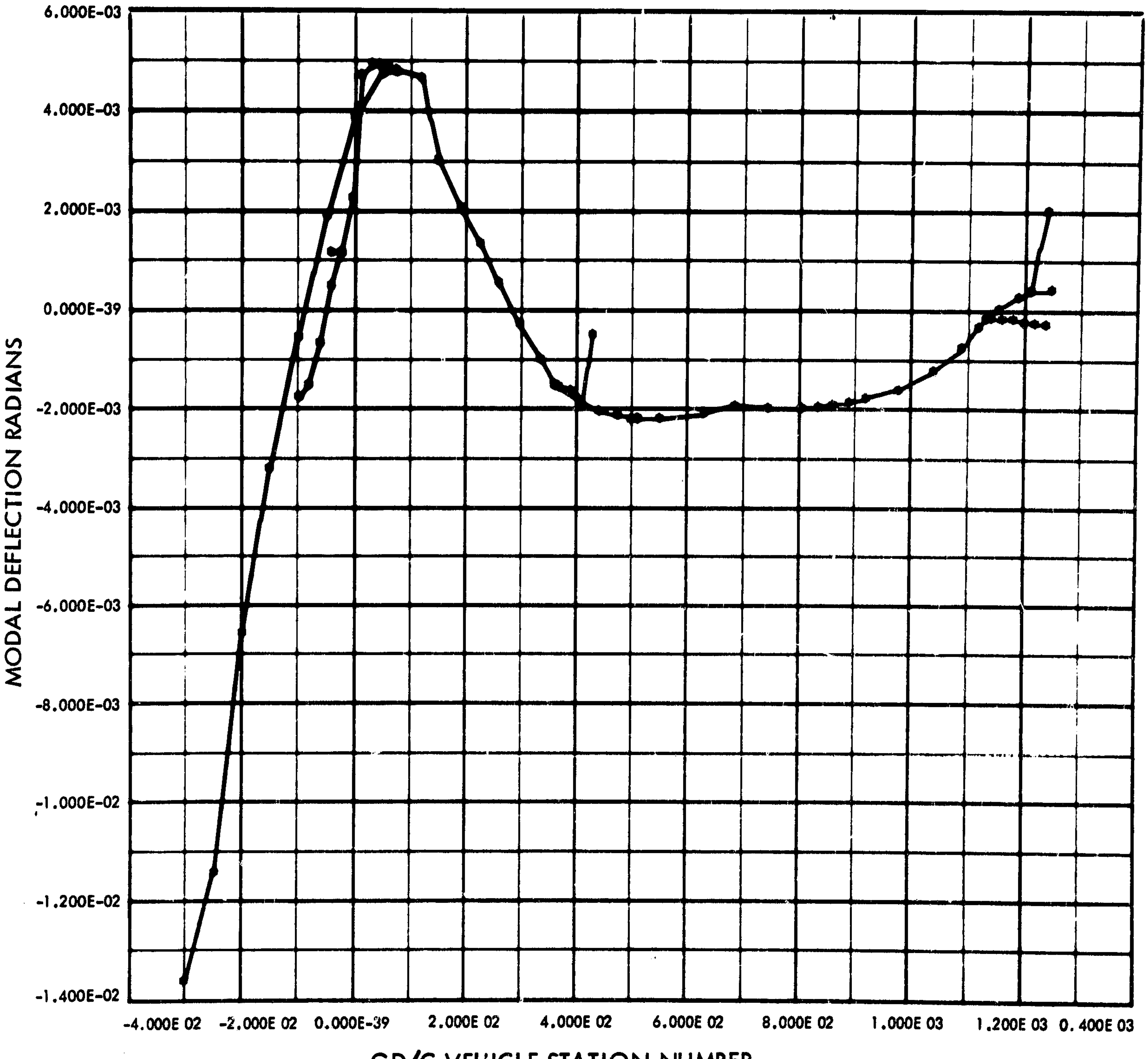

Fig. B-6. Atlas/Centaur/OAO torsion mode shape
Mode No. 6 Freq. = 0.5147E 02 cps

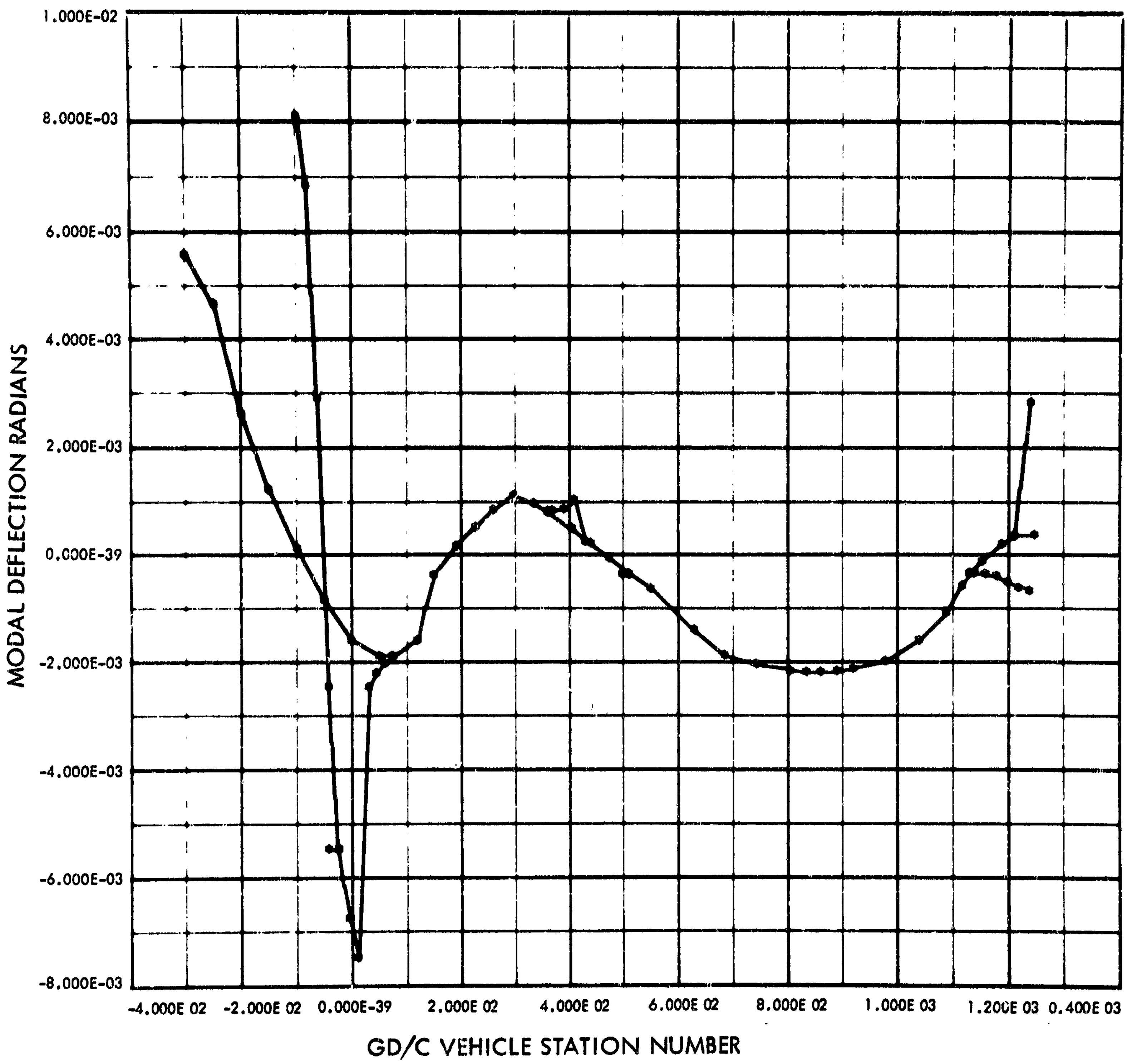

Fig. B-7. Atlas/Centaur/OAO torsion mode shape
Mode No. 7 Freq. = 0.5233E 02 cps

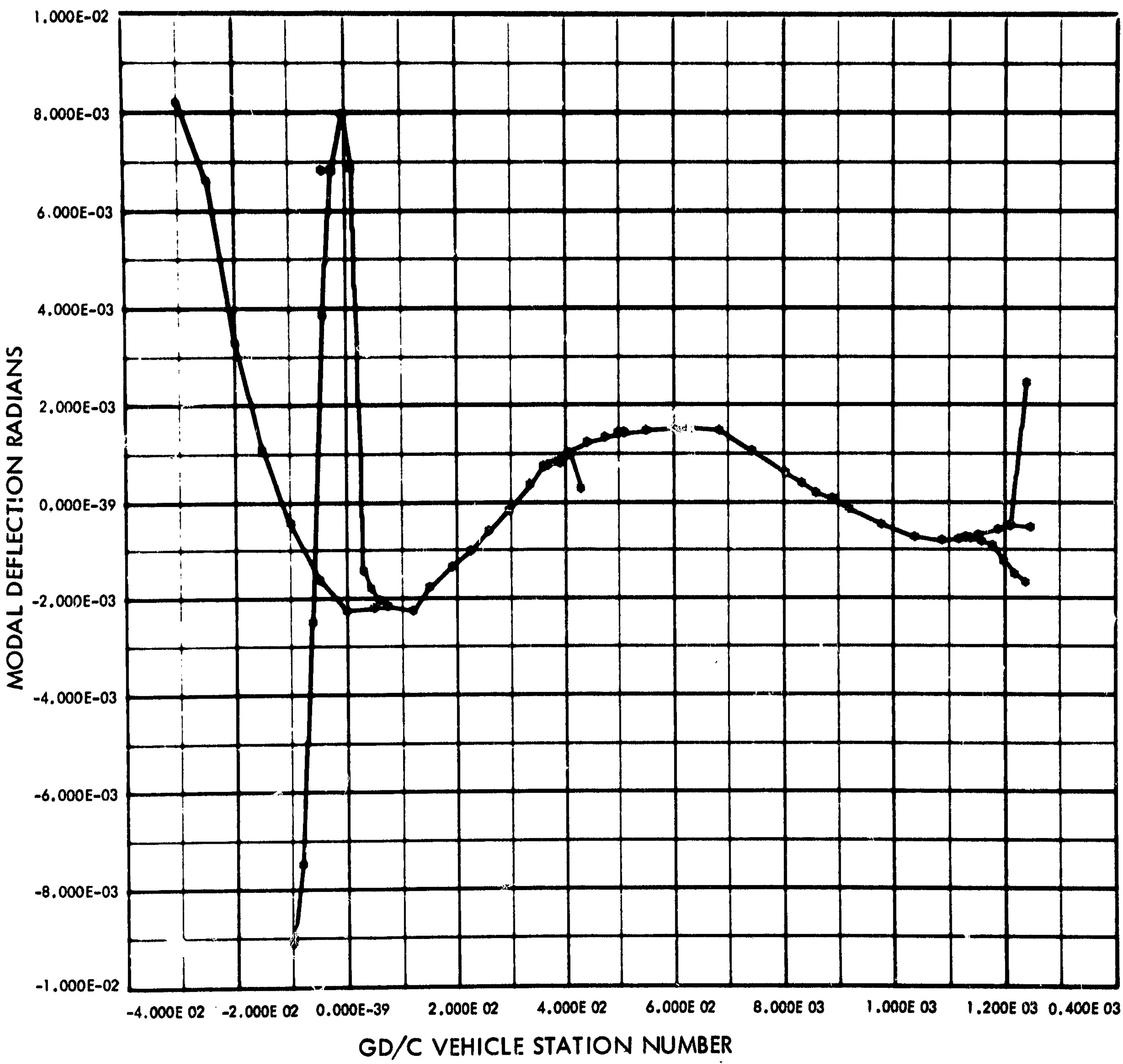

Fig. B-8. Atlas/Centaur/OAO torsion mode shape
Mode No. 8 Freq. = 0.5607E 02 cps

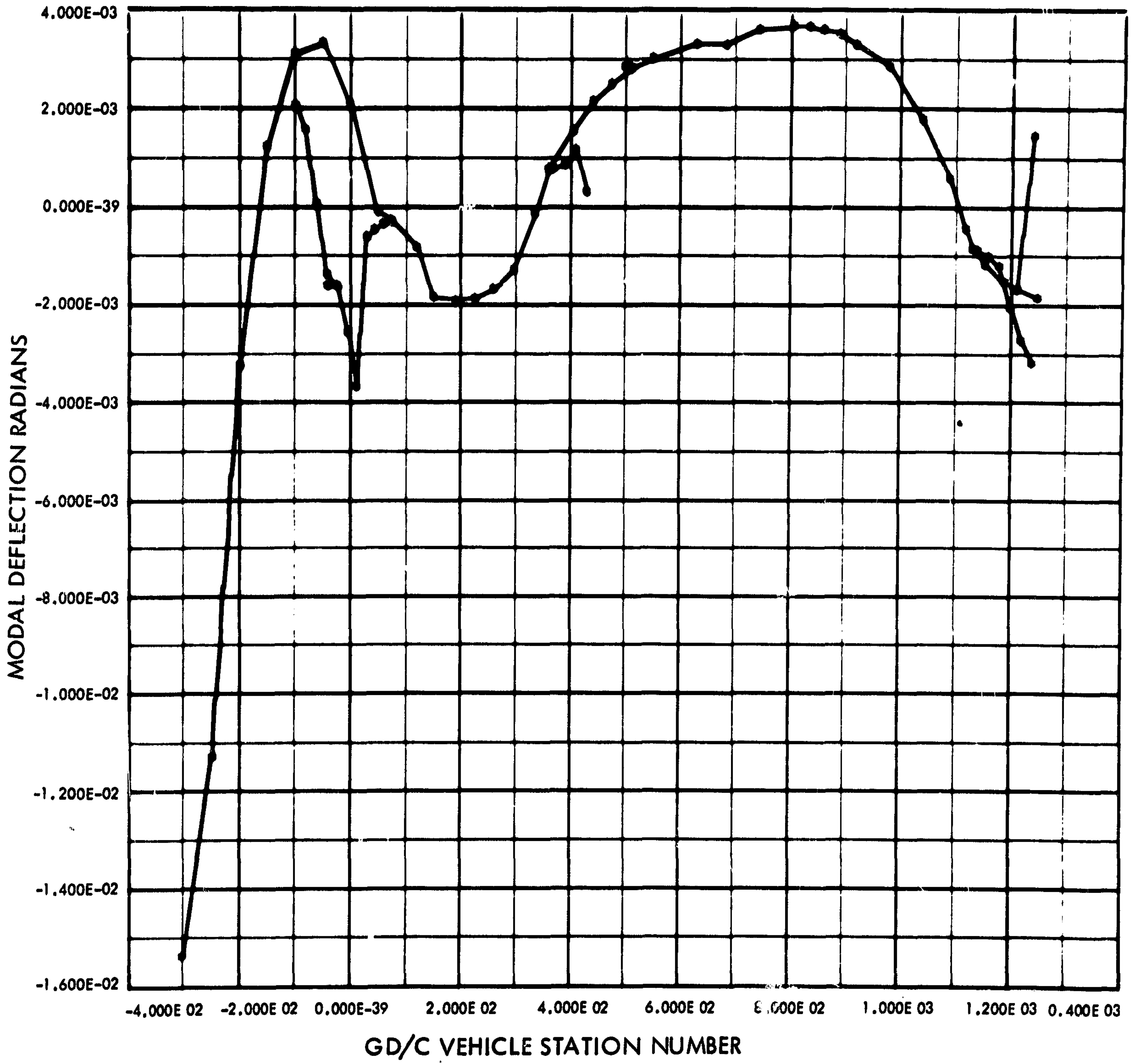

Fig. B-9. Atlas/Centaur/OAO torsion mode shape
Mode No. 9 Freq. = 0.6594E 02 cps

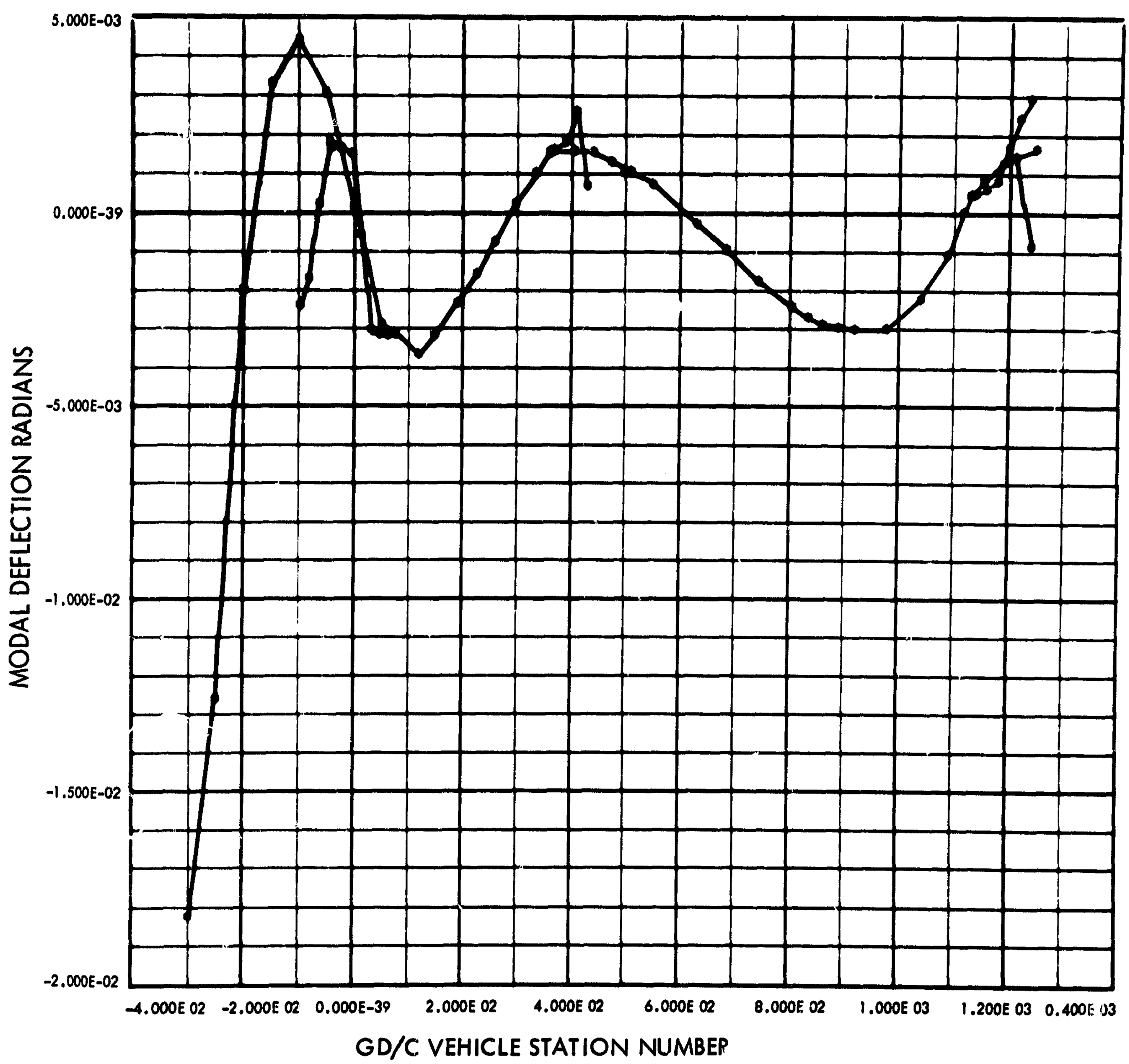

Fig. B-10. Atlas/Centaur/OAO torsion mode shape
Mode No. 10 Freq. = 0.7137E 02 cps

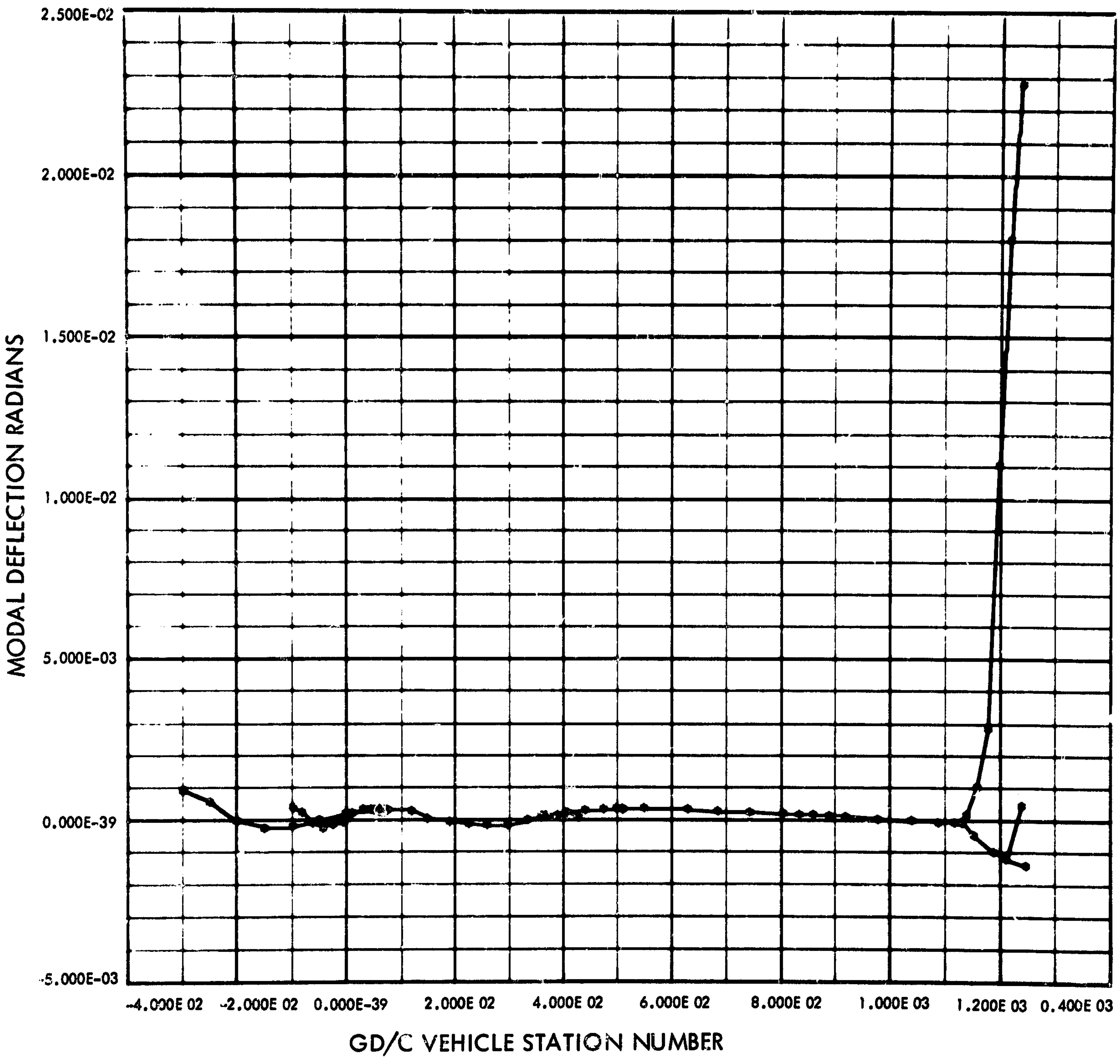

Fig. B-11. Atlas/Centaur/OAO torsion mode shape
Mode No. 11 Freq. = 0.7987E 02 cps

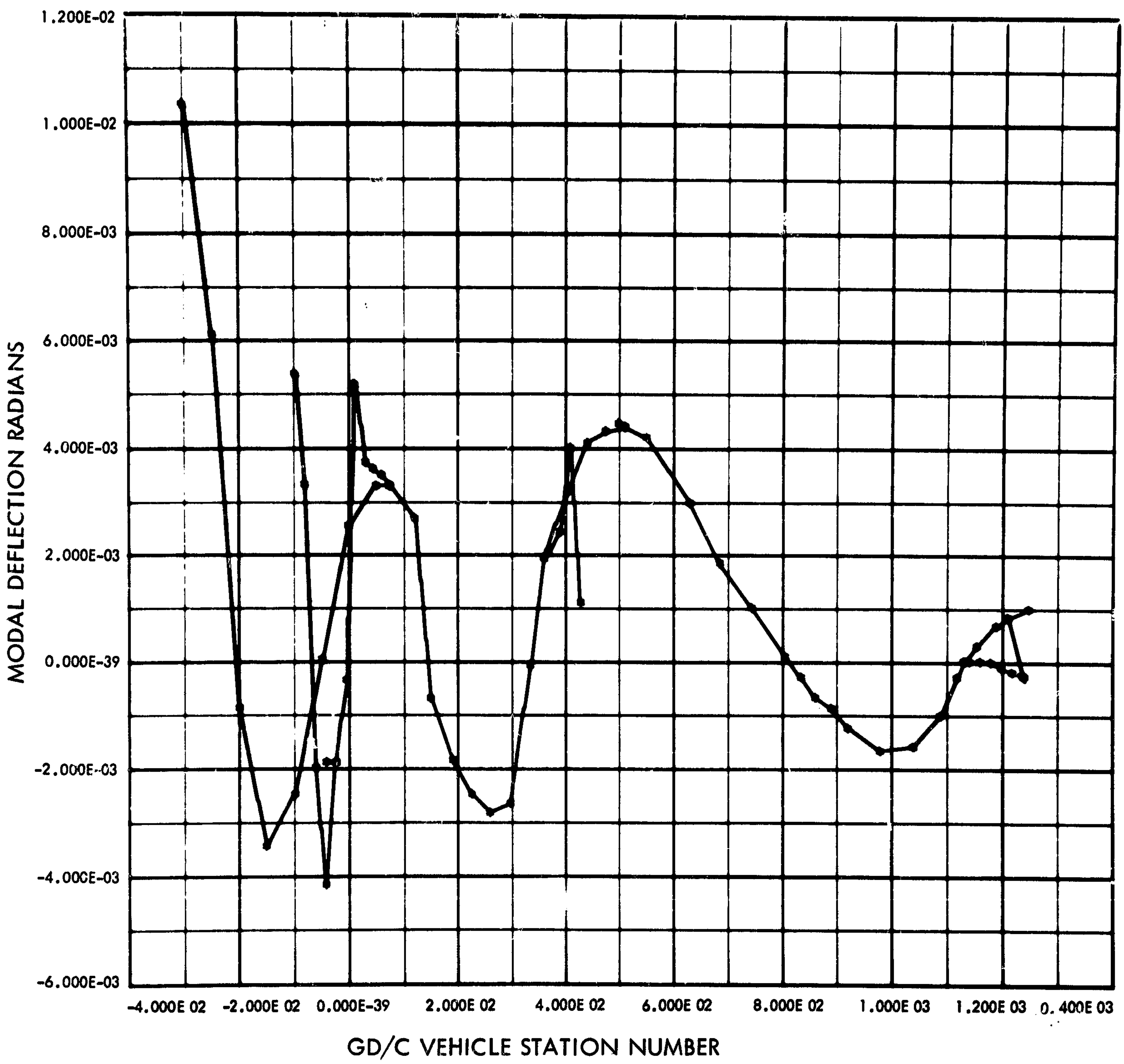

Fig. B-12. Atlas/Centaur/OAO torsion mode shape
Mode No. 12 Freq. = 0.8178E 02 cps

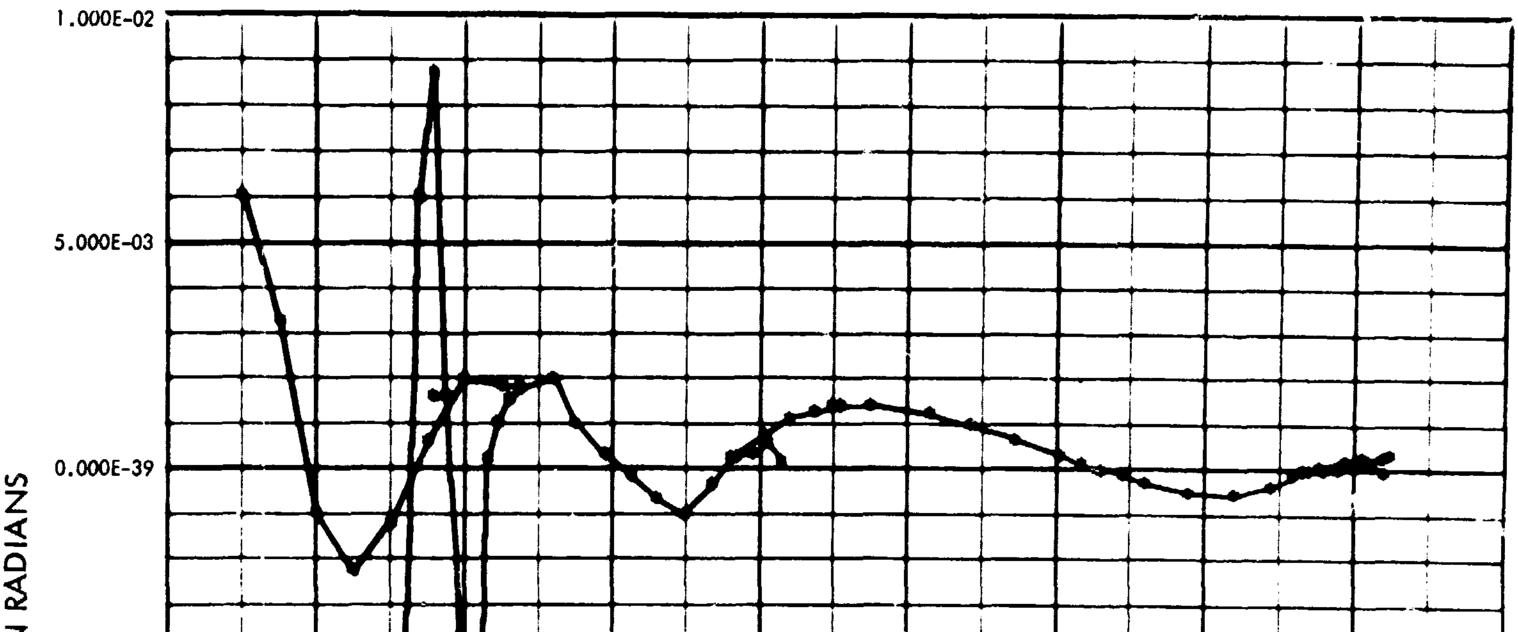

Fig. B-13. Atlas/Centaur/OAO torsion mode shape
Mode No. 13 Freq. = 0.8657E 02 cps

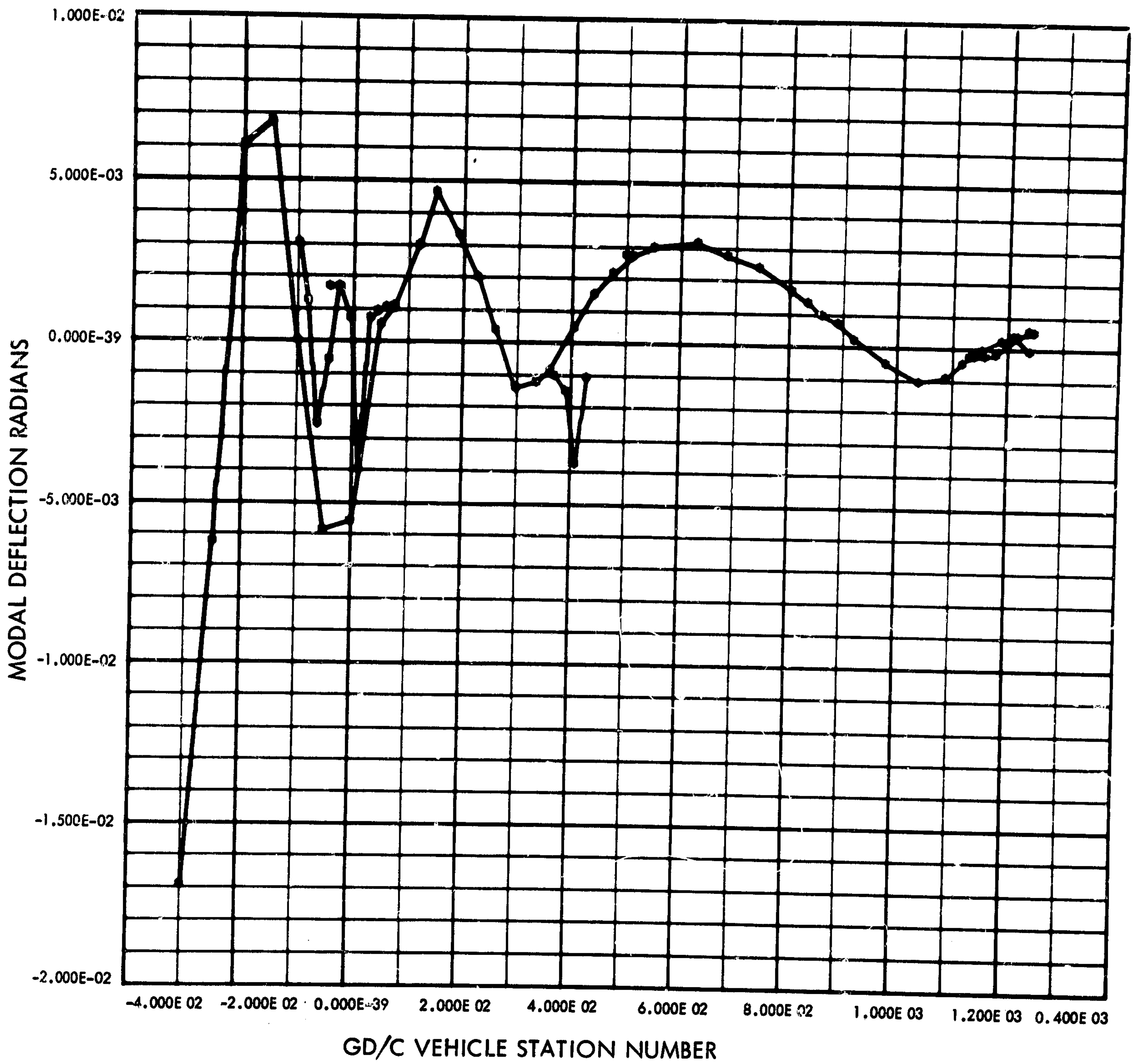

Fig. B-14. Atlas/Centaur/OAO torsion mode shape
Mode No. 14 Freq. = 0.1015E 03 cps

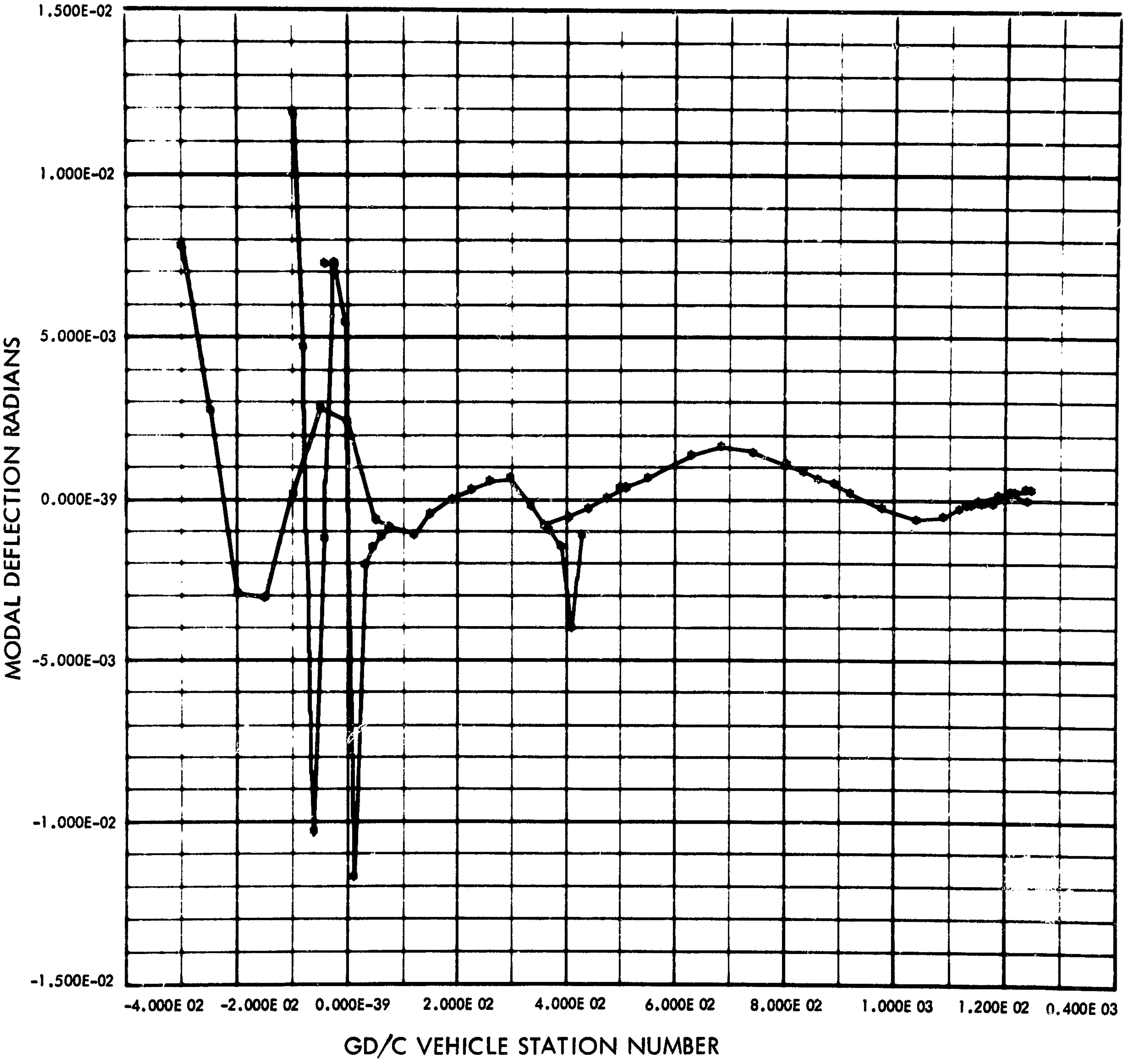

Fig. B-15. Atlas/Centaur/OAO torsion mode shape
Mode No. 15 Freq. = 0.1031E 03 cps

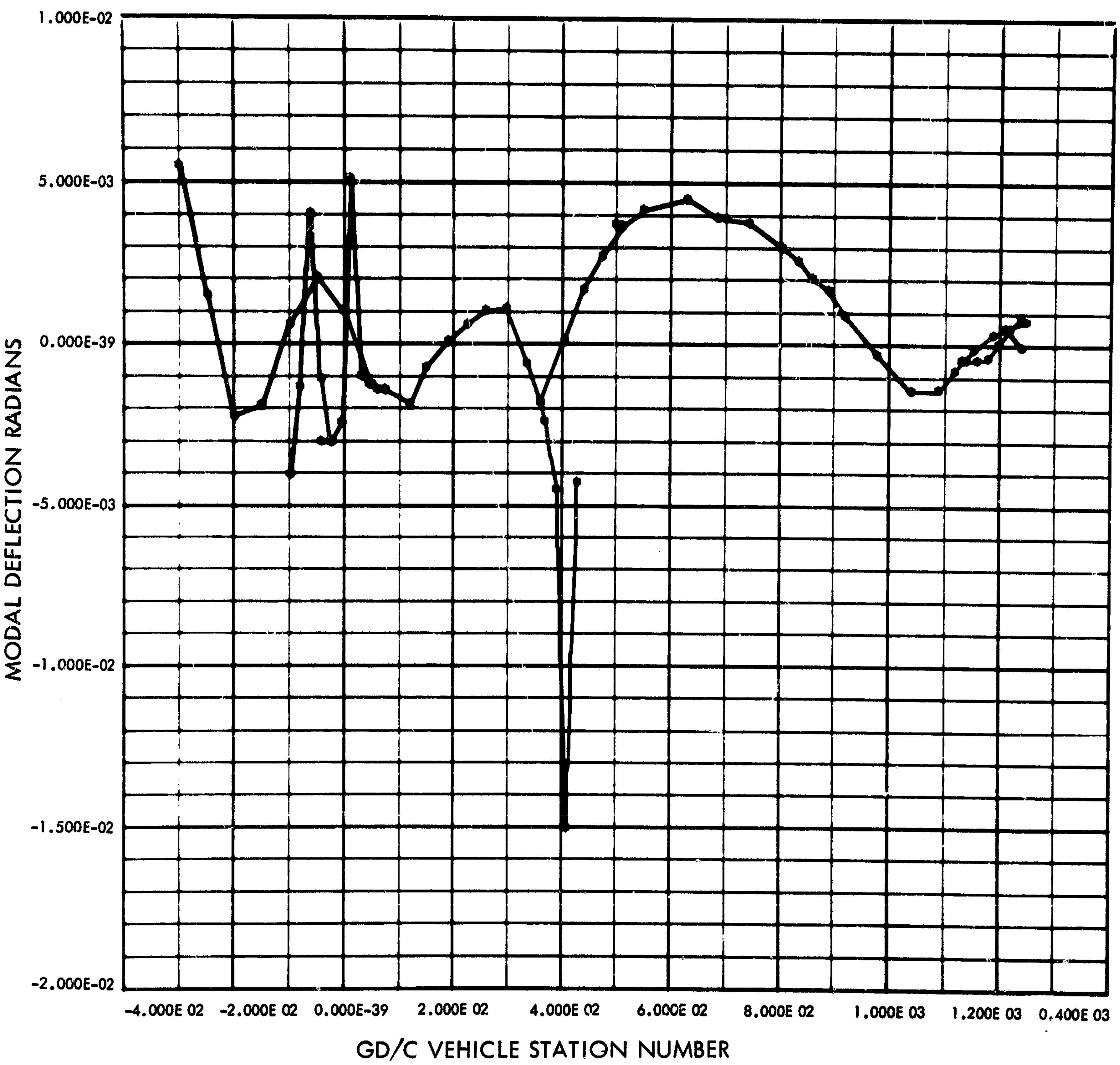

Fig. B-16. Atlas/Centaur/OAO torsion mode shape
Mode No. 16 Freq. = 0.1091E 03 cps

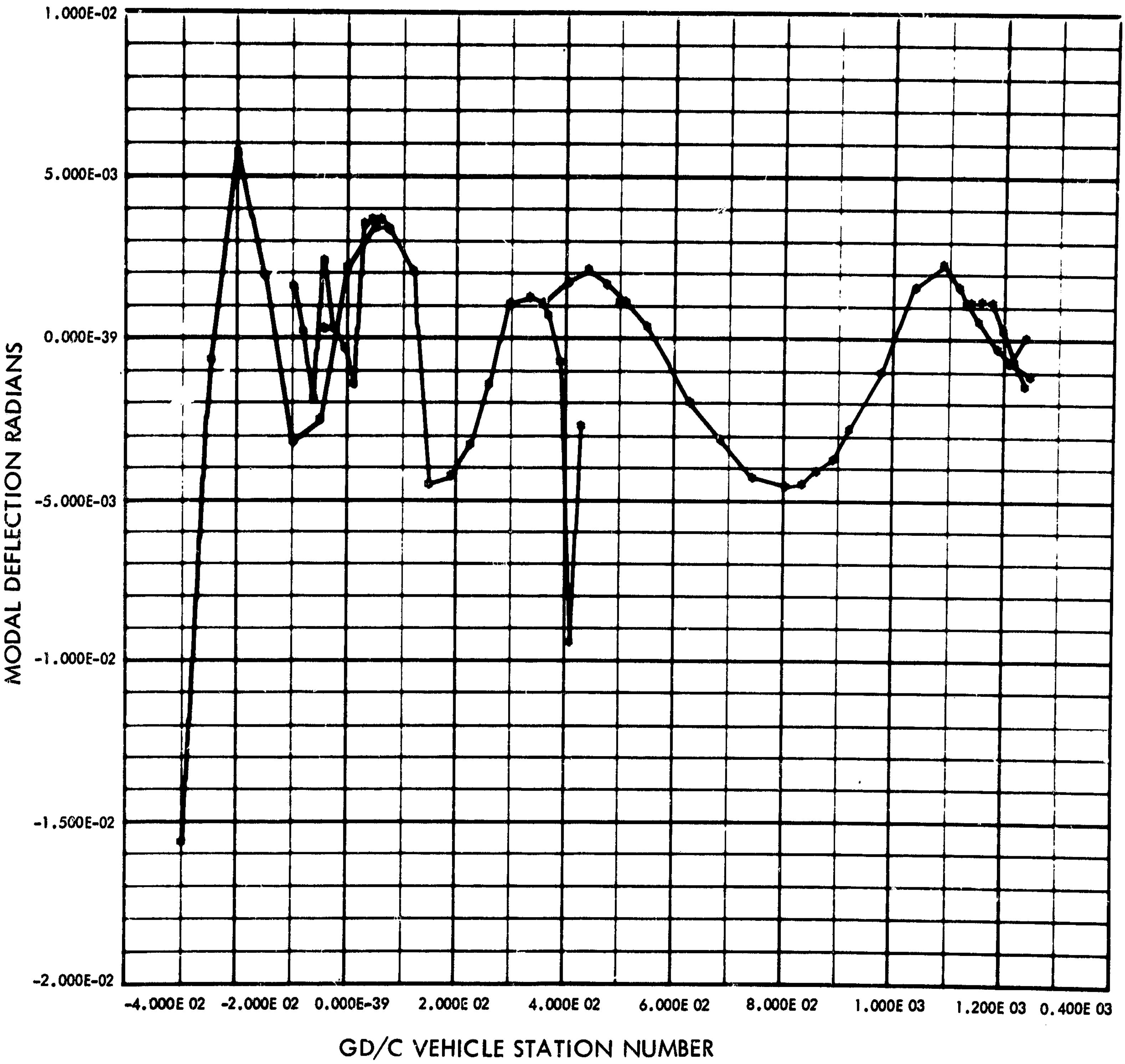

Fig. B-17. Atlas/Centaur/OAO torsion mode shape
Mode No. 17 Freq. = 0.1251E 03 cps

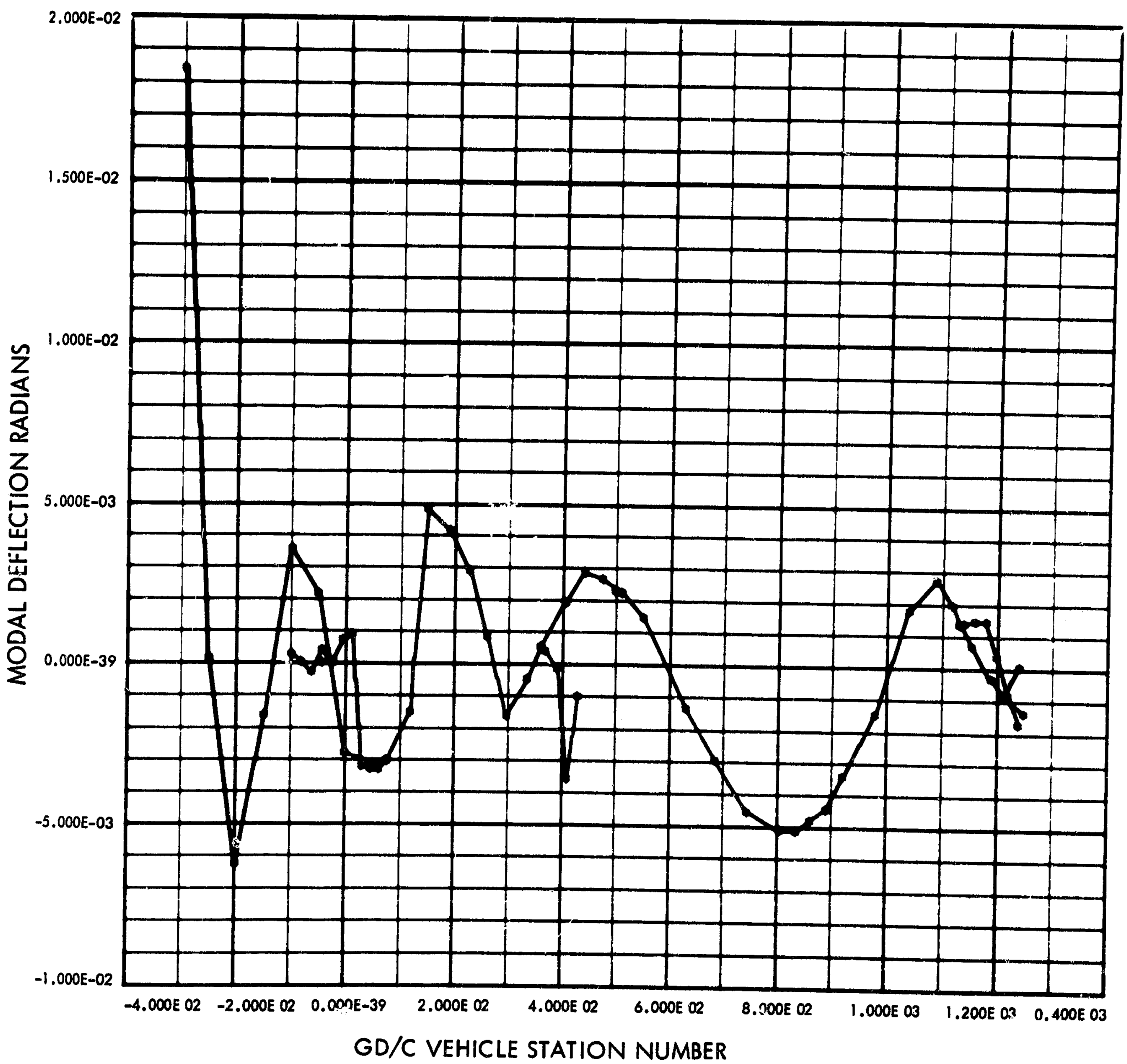

Fig. B-18. Atlas/Centaur/OAO torsion mode shape
Mode No. 18 Freq. = 0.1272E 03 cps

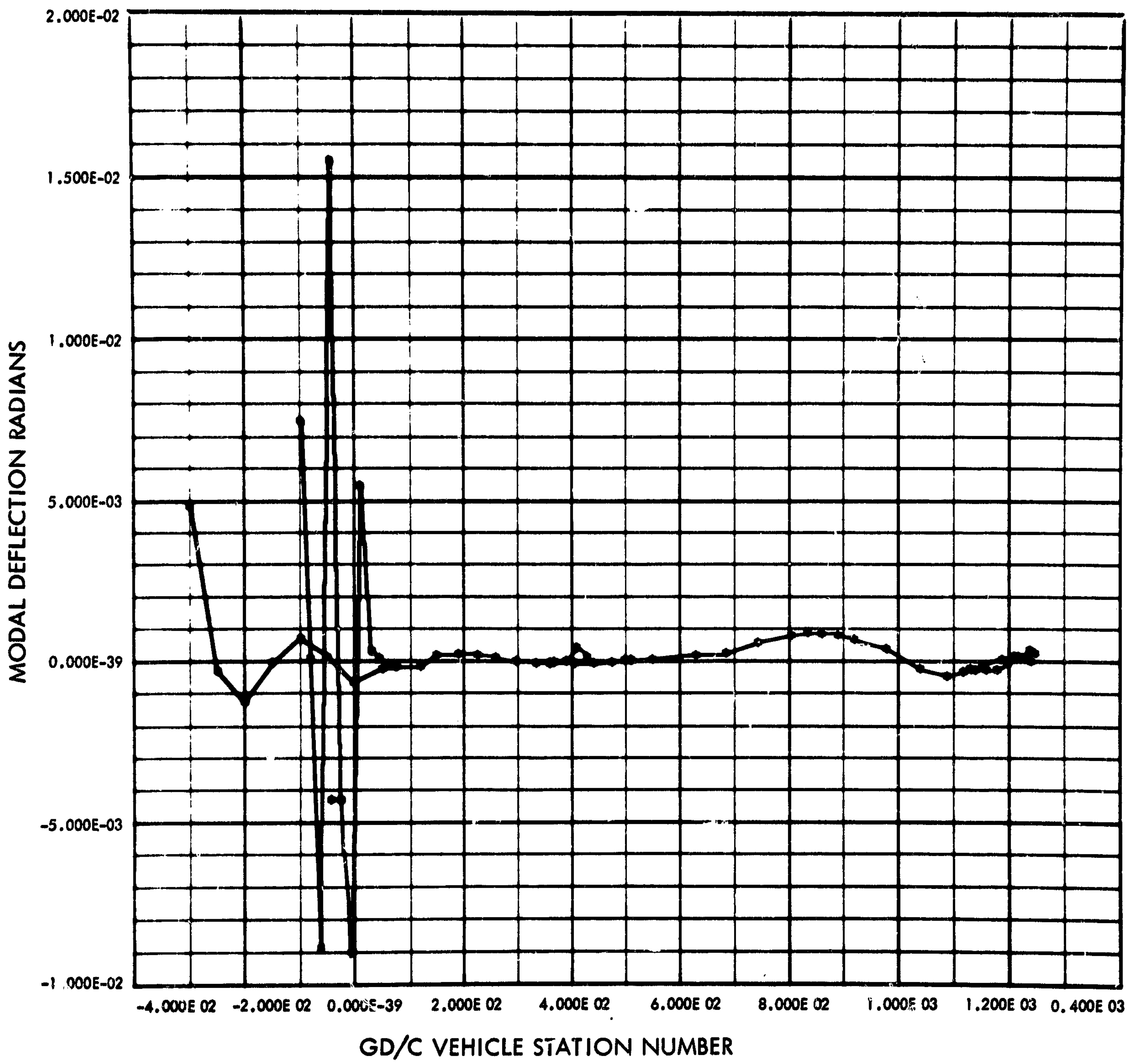

Fig. B-19. Atlas/Centaur/OAO torsion mode shape
Mode No. 19 Freq. = 0.1321E 03 cps

FOLDOUT FRAME

PRECEDING PAGE BLANK NOT FILMED.

Mode No. n	Generated mass (Inertia) m_n lb-in-sec^2	Freq. cps	Gimbal block deflection JT. 59 $\phi_{59}^{(n)}$ (ϕ_{2n})	JT. 10 (rad) U_{10n} (ϕ_{1n})	JT. 11 (rad) U_{11n} (ϕ_{1n})	JT. 12 (rad) U_{12n} (ϕ_{1n})	JT. 13 (rad) U_{13n} $(\phi_{1}$
0	233,800	0	1	1	1	1	1
1	1	11.59	$.48135\times10^{-3}$	$-.80559\times10^{-3}$	$-.79943\times10^{-3}$	$-.77814\times10^{-3}$	$-.73605\times10$
2	1	12.06	$-.65142\times10^{-4}$	$-.54353\times10^{-3}$	$-.53905\times10^{-3}$	$-.52351\times10^{-3}$	$-.49279\times10$
3	1	15.17	$-.21160\times10^{-2}$	$.83633\times10^{-3}$	$.82539\times10^{-3}$	$.78761\times10^{-3}$	$.71392\times10$
4	1	24.37	$-.51749\times10^{-3}$	$.12344\times10^{-1}$	$.11928\times10^{-1}$	$.10513\times10^{-1}$	$.78607\times10$
5	1	26.80	$-.50441\times10^{-3}$	$-.42454\times10^{-2}$	$-.40719\times10^{-2}$	$-.34860\times10^{-2}$	$-.24052\times10$
6	1	51.47	$.39762\times10^{-3}$	$-.17939\times10^{-2}$	$-.15234\times10^{-2}$	$-.67847\times10^{-3}$	$.49753\times10$
7	1	52.33	$.35415\times10^{-3}$	$.8117\times10^{-2}$	$.68538\times10^{-2}$	$.29180\times10^{-2}$	$-.24735\times10$
8	1	56.07	$-.50037\times10^{-3}$	$-.91318\times10^{-2}$	$-.74998\times10^{-2}$	$-.24997\times10^{-2}$	$.38649\times10$
9	1	65.94	$-.16743\times10^{-2}$	$.20626\times10^{-2}$	$.15529\times10^{-2}$	$.70775\times10^{-4}$	$-.13887\times10$
10	1	71.37	$.14578\times10^{-2}$	$-.23957\times10^{-2}$	$-.17019\times10^{-2}$	$.24864\times10^{-3}$	$.18153\times10$
11	1	79.87	$-.12107\times10^{-2}$	$.34302\times10^{-3}$	$.21863\times10^{-3}$	$-.11042\times10^{-3}$	$-.27105\times10$
12	1	81.78	$.83101\times10^{-3}$	$.53649\times10^{-2}$	$.33247\times10^{-2}$	$-.19908\times10^{-2}$	$-.41754\times10$
13	1	86.57	$.25431\times10^{-3}$	$-.12237\times10^{-1}$	$-.70227\times10^{-2}$	$.60233\times10^{-2}$	$.87465\times10$
14	1	101.51	$.38955\times10^{-3}$	$.30553\times10^{-2}$	$.12661\times10^{-2}$	$-.25640\times10^{-2}$	$-.58048\times10$
15	1	103.13	$.22480\times10^{-3}$	$.11848\times10^{-1}$	$.46843\times10^{-2}$	$-.10330\times10^{-1}$	$-.12229\times10$
16	1	109.11	$.52758\times10^{-3}$	$-.40879\times10^{-2}$	$-.13220\times10^{-2}$	$.40243\times10^{-2}$	$-.10755\times10$
17	1	125.07	$-.72611\times10^{-3}$	$.15841\times10^{-2}$	$.17621\times10^{-3}$	$-.18659\times10^{-2}$	$.23833\times10$
18	1	127.25	$-.84313\times10^{-3}$	$.24497\times10^{-3}$	$.19064\times10^{-4}$	$-.29252\times10^{-3}$	$.41584\times10$
19	1	132.08	$.14734\times10^{-3}$	$.74325\times10^{-2}$	$.62893\times10^{-4}$	$-.89062\times10^{-2}$	$.15506\times10$

FOLDOUT FRAME 2

Table B-1. Pertinent modal information - modal deflections

12) ϕ_{1n})	JT. 13 (rad) U_{13n} (ϕ_{1n})	JT. 63 (rad) U_{63n} (ϕ_{1n})	JT. 14 (rad) U_{14n} (ϕ_{1n})	JT. 15 (rad) U_{15n} (ϕ_{1n})	JT. 16 (rad) U_{16n} (ϕ_{1n})	JT. 17 (rad) U_{17n} (ϕ_{1n})
	1	1	1	1	1	1
$x10^{-3}$	$-.73605x10^{-3}$	$-.69131x10^{-3}$	$-.69131x10^{-3}$	$-.75973x10^{-3}$	$-.96822x10^{-3}$	$-.12684x10^{-2}$
$x10^{-3}$	$-.49279x10^{-3}$	$-.46024x10^{-3}$	$-.46024x10^{-3}$	$-.48321x10^{-3}$	$-.54631x10^{-3}$	$-.62507x10^{-3}$
$x10^{-3}$	$.71392x10^{-3}$	$.63677x10^{-3}$	$.63677x10^{-3}$	$.84192x10^{-3}$	$.14887x10^{-2}$	$.24382x10^{-2}$
$x10^{-1}$	$.78607x10^{-2}$	$.52624x10^{-2}$	$.52624x10^{-2}$	$.48718x10^{-2}$	$.30137x10^{-2}$	$-.55247x10^{-3}$
$x10^{-2}$	$-.24052x10^{-2}$	$-.13705x10^{-2}$	$-.13705x10^{-2}$	$-.14171x10^{-2}$	$-.13768x10^{-2}$	$-.10121x10^{-2}$
$x10^{-3}$	$.49753x10^{-3}$	$.11761x10^{-2}$	$.11761x10^{-2}$	$.22565x10^{-2}$	$.47106x10^{-2}$	$.49337x10^{-2}$
$x10^{-2}$	$-.24735x10^{-2}$	$-.54870x10^{-2}$	$-.54869x10^{-2}$	$-.67693x10^{-2}$	$-.74925x10^{-2}$	$-.24700x10^{-2}$
$x10^{-2}$	$.38649x10^{-2}$	$.68429x10^{-2}$	$.68429x10^{-2}$	$.79571x10^{-2}$	$.68776x10^{-2}$	$-.14175x10^{-2}$
$x10^{-4}$	$-.13887x10^{-2}$	$-.16179x10^{-2}$	$-.16179x10^{-2}$	$-.25886x10^{-2}$	$-.36672x10^{-2}$	$-.60141x10^{-3}$
$x10^{-3}$	$.18153x10^{-2}$	$.16752x10^{-2}$	$.16752x10^{-2}$	$.14991x10^{-2}$	$-.55202x10^{-3}$	$-.30418x10^{-2}$
$x10^{-3}$	$-.27105x10^{-3}$	$-.14766x10^{-3}$	$-.14766x10^{-3}$	$-.97555x10^{-4}$	$.18881x10^{-3}$	$.29100x10^{-3}$
$x10^{-2}$	$-.41754x10^{-2}$	$-.18808x10^{-2}$	$-.18809x10^{-2}$	$-.35289x10^{-3}$	$.51942x10^{-2}$	$.37223x10^{-2}$
$x10^{-2}$	$.87465x10^{-2}$	$.15960x10^{-2}$	$.15958x10^{-2}$	$-.37477x10^{-2}$	$-.16179x10^{-1}$	$.24070x10^{-3}$
$x10^{-2}$	$-.58048x10^{-3}$	$.17118x10^{-2}$	$.17111x10^{-2}$	$.73084x10^{-3}$	$-.39785x10^{-2}$	$.74450x10^{-3}$
$x10^{-1}$	$-.12229x10^{-2}$	$.72814x10^{-2}$	$.72805x10^{-2}$	$.54694x10^{-2}$	$-.11726x10^{-1}$	$-.20268x10^{-2}$
$x10^{-2}$	$-.10755x10^{-2}$	$-.30342x10^{-2}$	$-.30336x10^{-2}$	$-.24391x10^{-2}$	$.51104x10^{-2}$	$-.98700x10^{-3}$
$x10^{-2}$	$.23833x10^{-2}$	$.30046x10^{-3}$	$.30044x10^{-3}$	$-.32510x10^{-3}$	$-.14345x10^{-2}$	$.35407x10^{-2}$
$x10^{-3}$	$.41584x10^{-3}$	$-.27346x10^{-5}$	$-.26682x10^{-5}$	$.72677x10^{-3}$	$.90285x10^{-3}$	$-.32275x10^{-2}$
$x10^{-2}$	$.15506x10^{-1}$	$-.43188x10^{-2}$	$-.43172x10^{-2}$	$-.90461x10^{-2}$	$.54485x10^{-2}$	$.31615x10^{-3}$

F[illegible] FRAME

PRECEDING PAGE BLANK NOT FILMED.

Mode No.	Frequency cps	Joint 10	Joint 11	Joint 12	Joint 13
n		τ_n^{10}	τ_n^{11}	τ_n^{12}	τ_n^{13}
0	0	731.63	2119.05	4534.16	6705.23
1	11.59	-0.58939	-1.69854	-3.57783	-5.17584
2	12.06	-0.39766	-1.14555	-2.40989	-3.47977
3	15.17	0.61188	1.75704	3.65921	5.20918
4	24.37	9.03118	25.58036	50.97045	68.03655
5	26.80	-3.10604	-8.75549	-17.17458	-22.39642
6	51.47	-1.31246	-3.42606	-5.06465	-3.98447
7	52.33	5.93860	15.44772	22.49502	17.12489
8	56.07	-6.68106	-17.08645	-23.12351	-14.73255
9	65.94	1.50905	3.66358	3.83451	0.81955
10	71.37	-1.75275	-4.11401	-3.51351	0.42762
11	79.87	0.25096	0.55430	0.28762	-0.30085
12	81.78	3.92510	8.53786	3.72985	-5.33522
13	86.57	-8.95290	-18.69635	-4.14939	14.83984
14	101.51	2.23533	3.99195	-2.20040	-3.46067
15	103.13	8.66830	15.1[illegible]	-9.78073	-12.43572
16	109.11	-2.99081	-4.82498	4.89416	2.55918
17	125.07	1.15897	1.40344	-3.10292	2.07138
18	127.25	0.17923	0.2[illegible]8	-0.50079	0.40202
19	132.08	5.43781	5.52506	-15.98444	17.68013

FOLDOUT FRAME 2

Table B-2. Pertinent modal information - torque parameters

nt	Joint 63	Joint 14	Joint 15	Joint 16	Joint 17
3	τ_n^{63}	τ_n^{14}	τ_n^{15}	τ_n^{16}	τ_n^{17}
23	445.13	9667.70	11187.11	12658.13	12849.64
17584	-0.30773	-7.22383	-8.37817	-9.80244	-10.04535
47977	-0.20487	-4.84322	-5.57741	-6.38104	-6.50075
20918	0.28345	7.09559	8.37481	10.56471	11.03166
03655	2.34248	83.62627	91.02854	95.46173	95.35593
39642	-0.61006	-26.45649	-28.60965	-30.63494	-30.82877
98447	0.52352	-0.50031	2.92824	9.85760	10.80246
2489	-2.44245	0.87004	-9.41530	-20.43687	-20.90991
73255	3.04601	5.53936	17.62946	27.74651	27.47504
31955	-0.72018	-3.97344	-7.90658	-13.30108	-13.41626
2762	0.74569	5.39036	7.66811	6.85608	6.27354
0085	-0.06573	-0.73829	-0.88652	-0.60877	-0.55304
3522	-0.83721	-10.90729	-11.44348	-3.80274	-3.08987
3984	0.71043	19.56745	13.87315	-9.92639	-9.88030
6067	0.76198	1.60874	2.71918	-3.13325	-2.99067
3572	3.24120	9.13297	17.44323	0.19411	-0.19404
5918	-1.35063	-6.42805	-10.13404	-2.61657	-2.80559
7138	0.133745	2.96143	2.47072	0.36054	1.03862
0202	-0.00122	0.39409	1.49835	2.82645	2.20835
8013	-1.92245	4.88982	8.85491	-0.84009	-0.77954

APPENDIX C

RESPONSE PLOTS

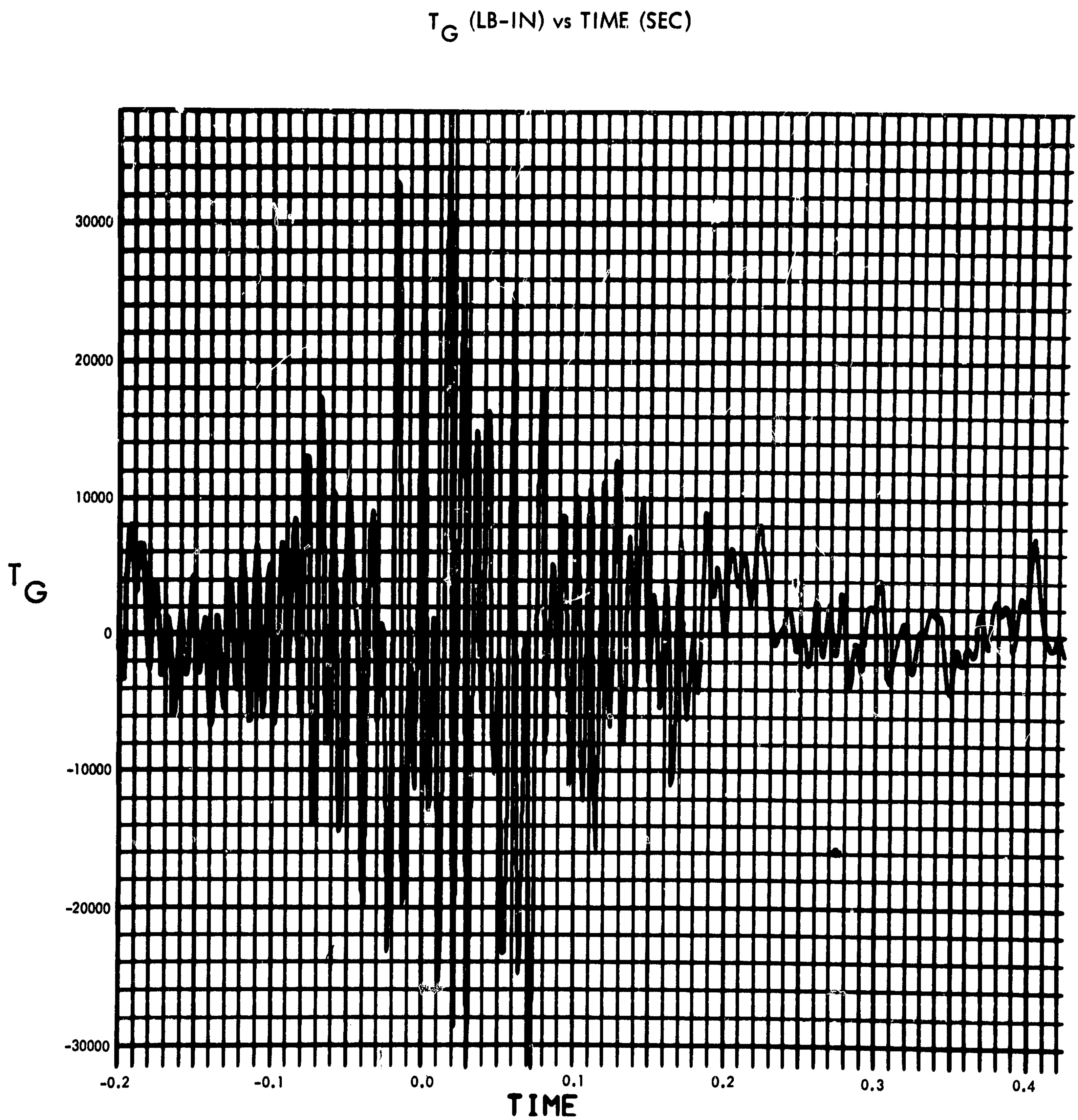

Fig. C-1. RA-6 gimbal torque, time history (pulse 1)

MODULUS OF F(F) (LB-IN-SEC) vs FREQUENCY (CYCLES/SEC)

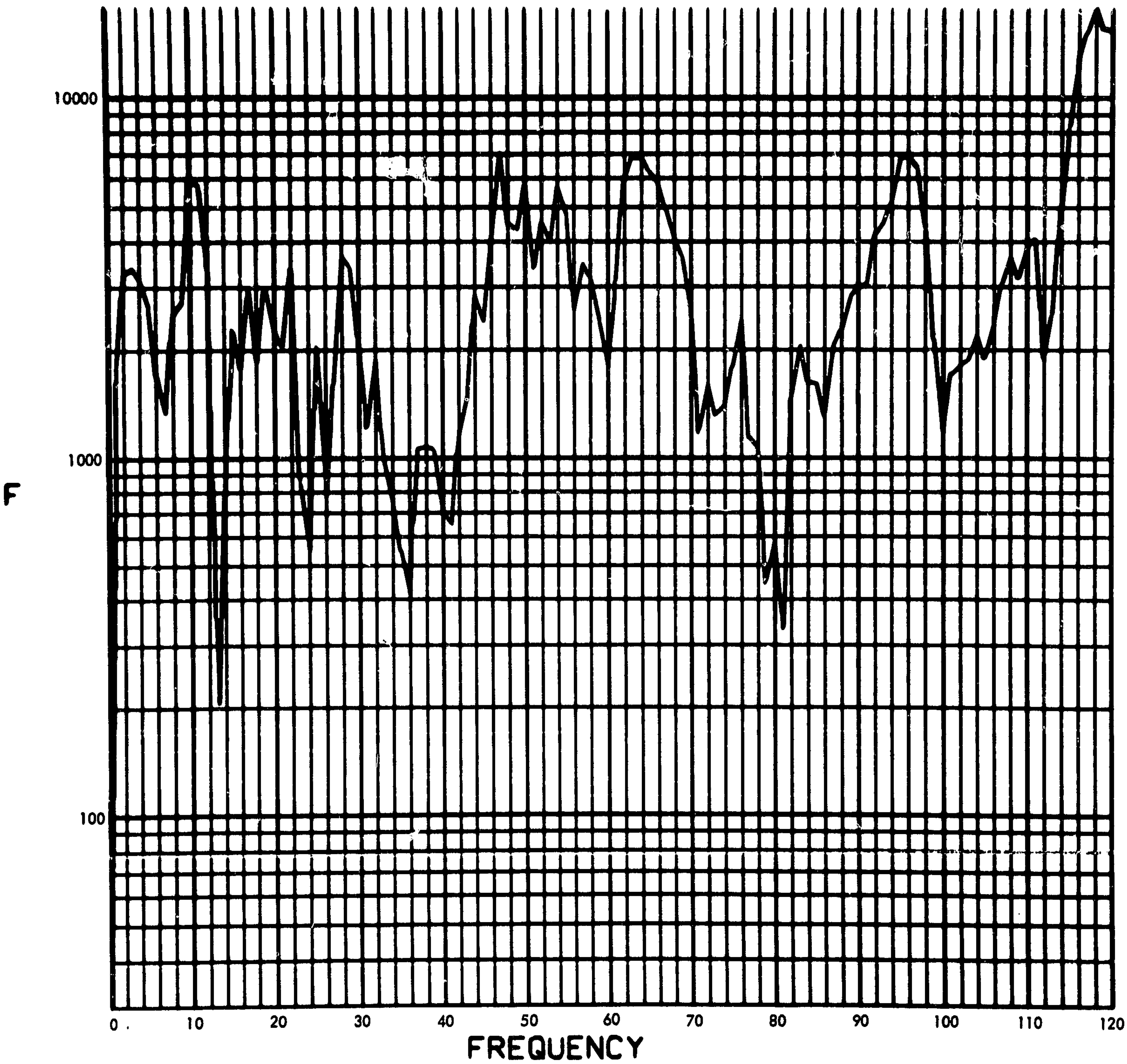

Fig. C-2. RA-6 gimbal torque, Fourier transform, modulus (pulse 1)

PHASE ANGLE OF F(F) (RAD) vs FREQUENCY (CYCLES/SEC)

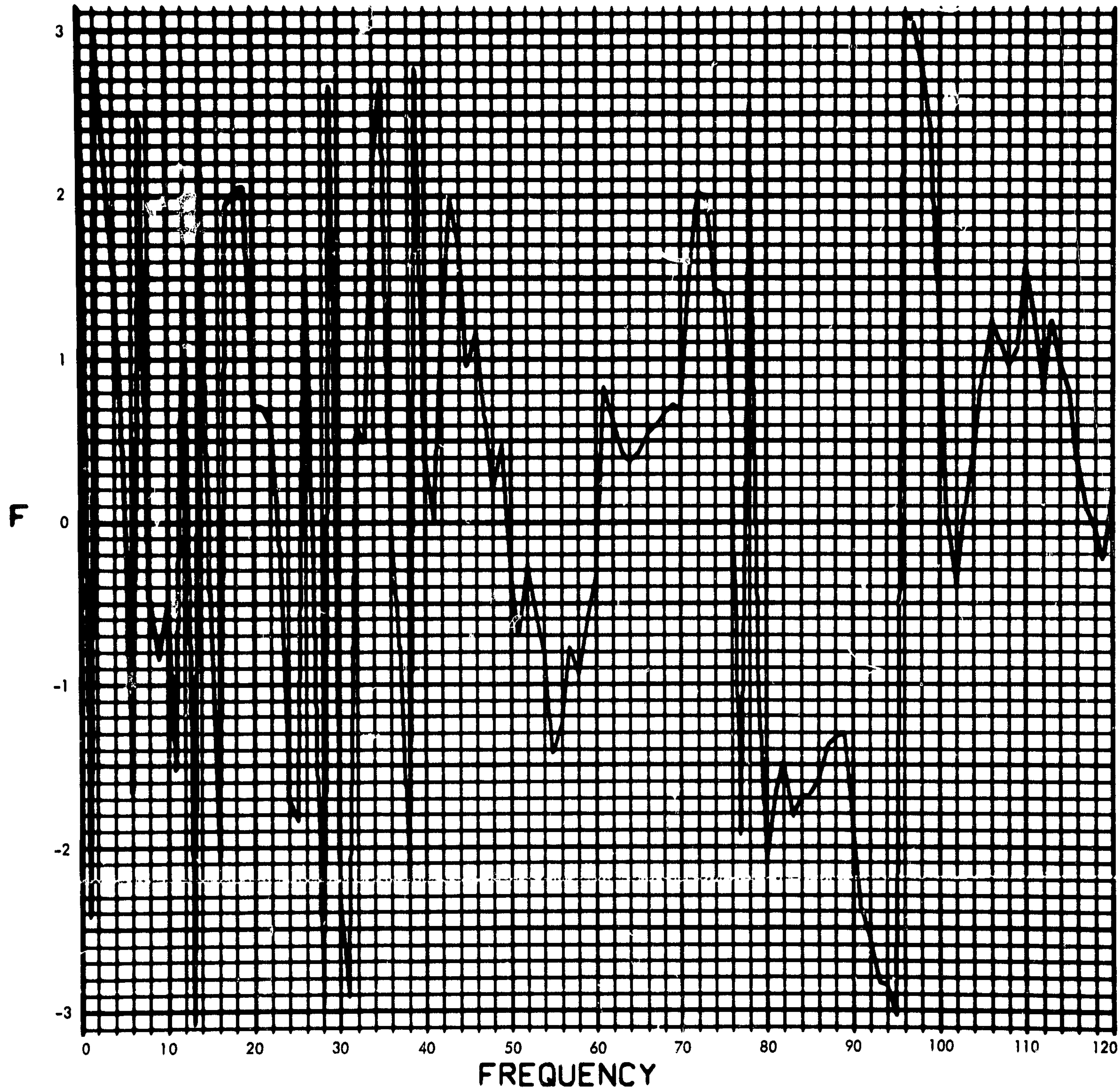

Fig. C-3. RA-6 gimbal torque, Fourier transform, phase angle (pulse 1)

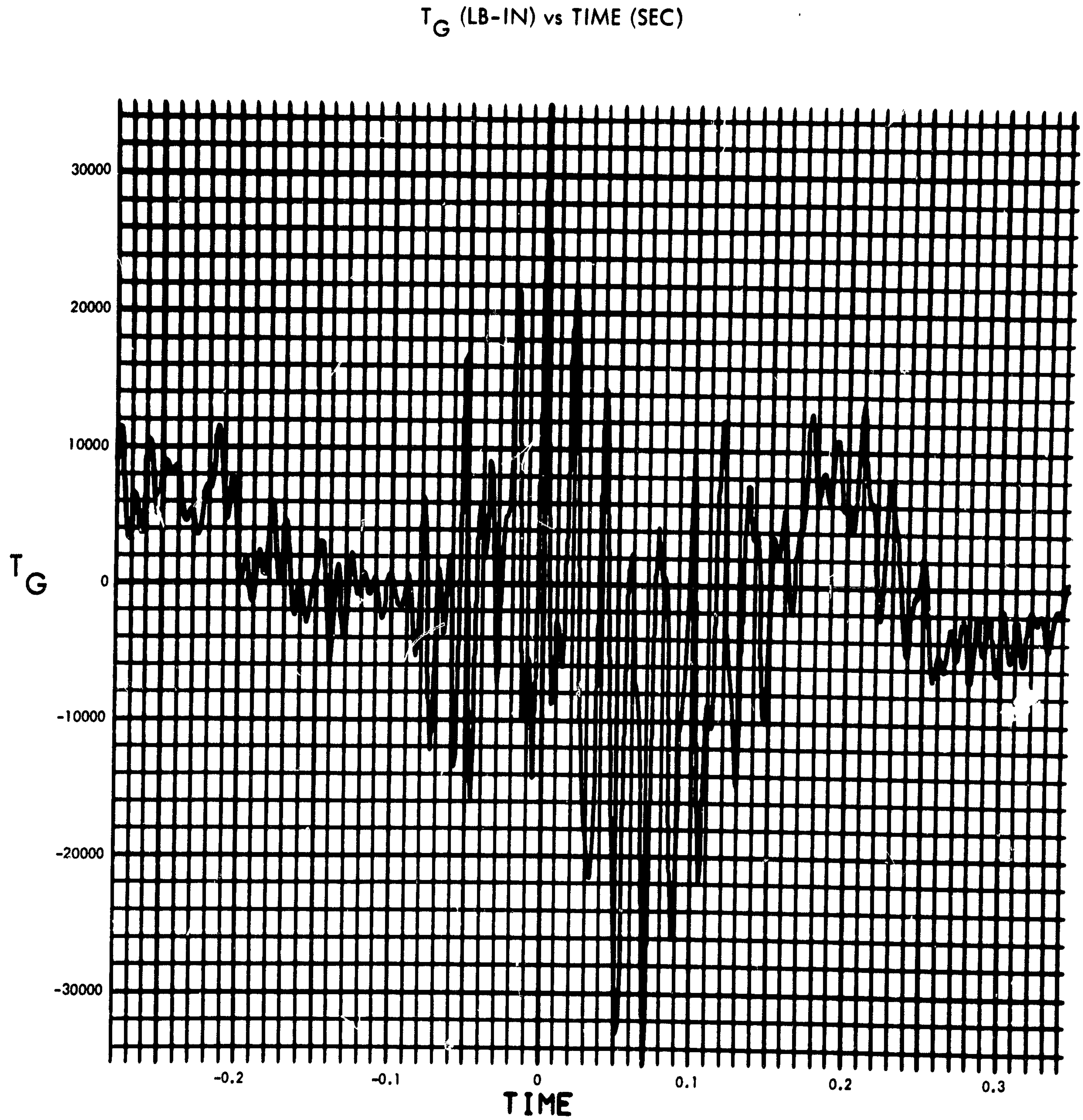

Fig. C-4. RA-7 gimbal torque, time history (pulse 2)

MODULUS OF F(F) (LB-IN-SEC) vs FREQUENCY (CYCLES/SEC)

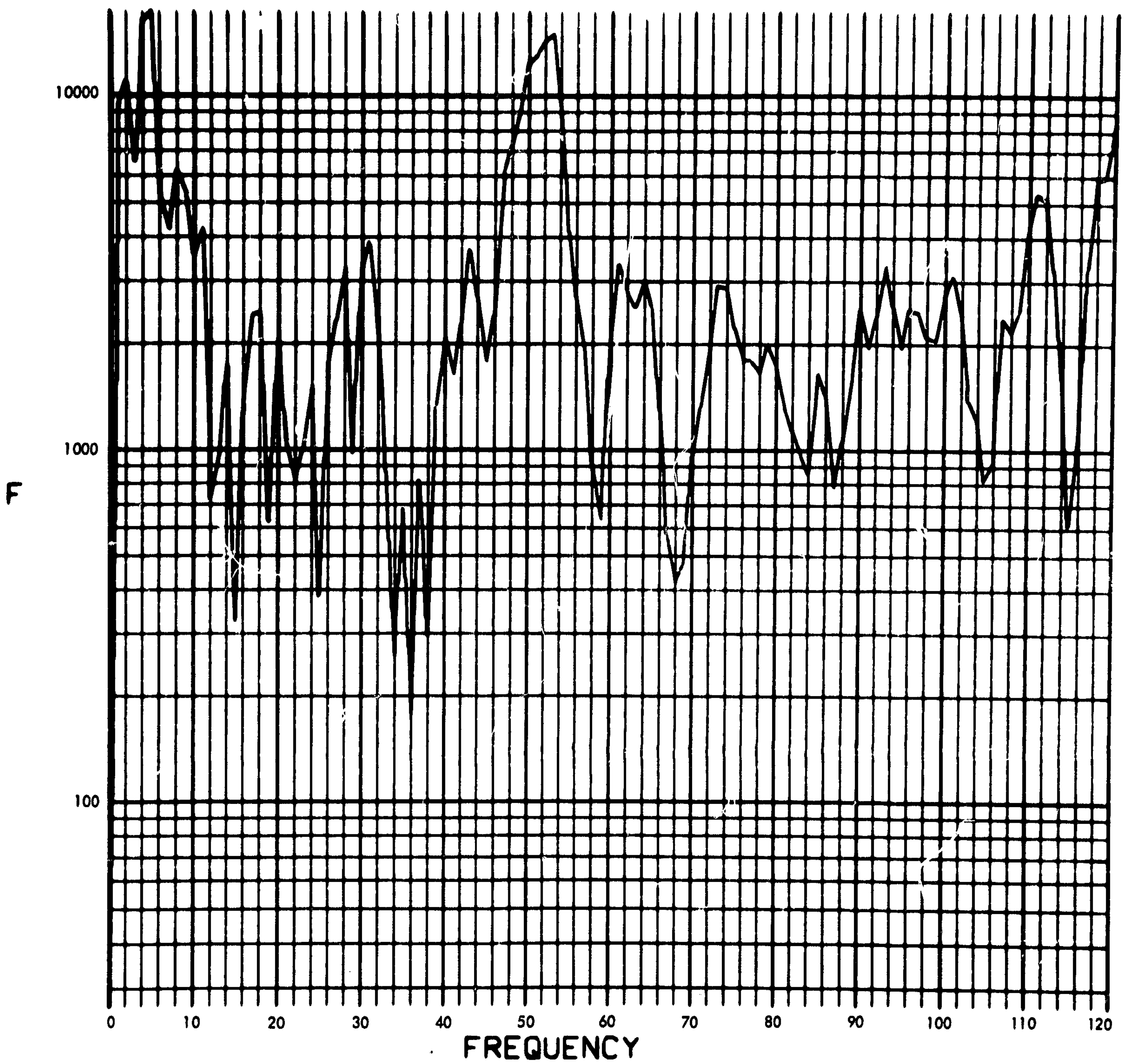

Fig. C-5. RA-7 gimbal torque, Fourier transform, modulus (pulse 2)

PHASE ANGLE OF F(F) (RAD) vs FREQUENCY (CYCLES/SEC)

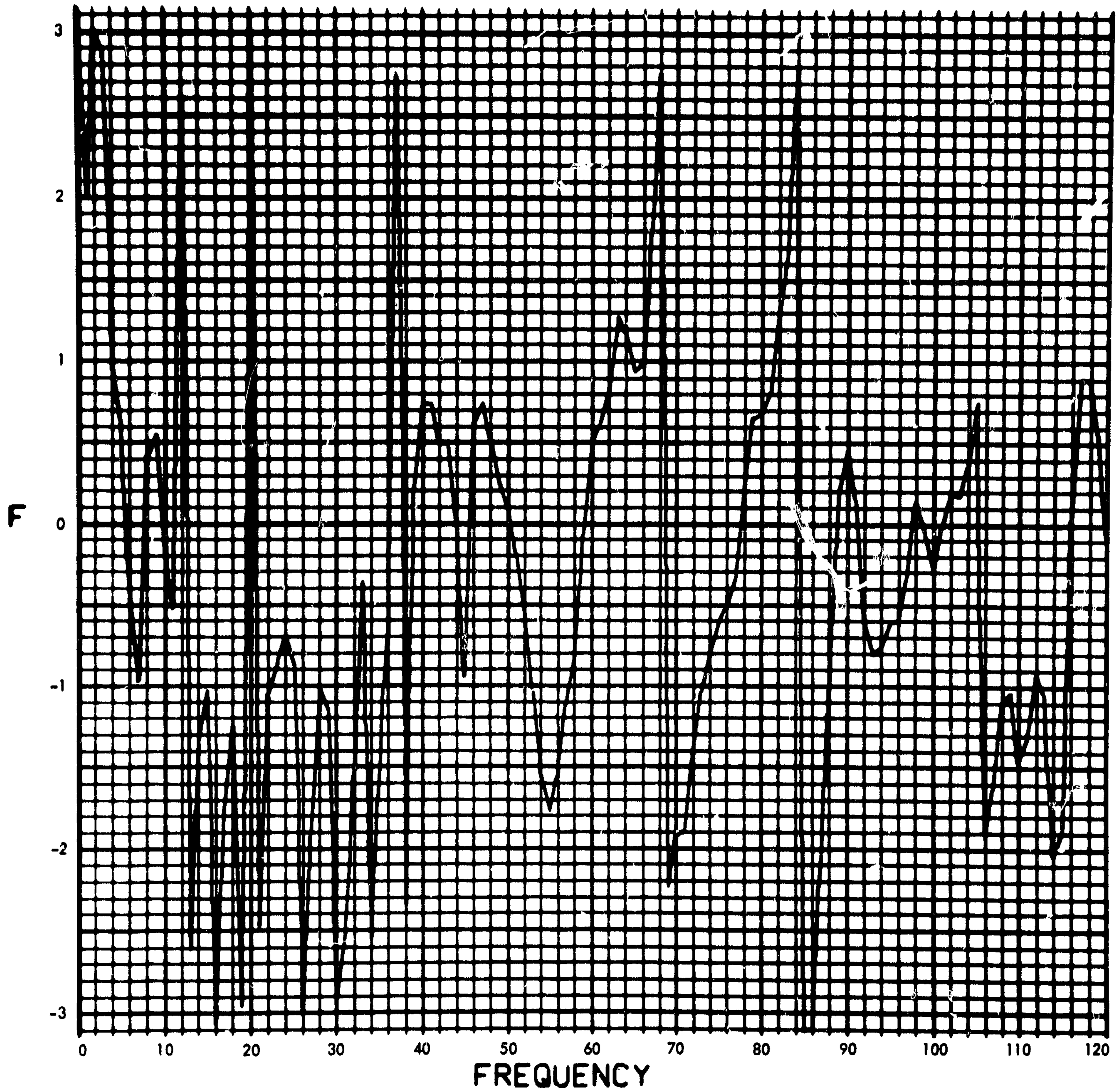

Fig. C-6. RA-7 gimbal torque, Fourier transform, phase angle (pulse 2)

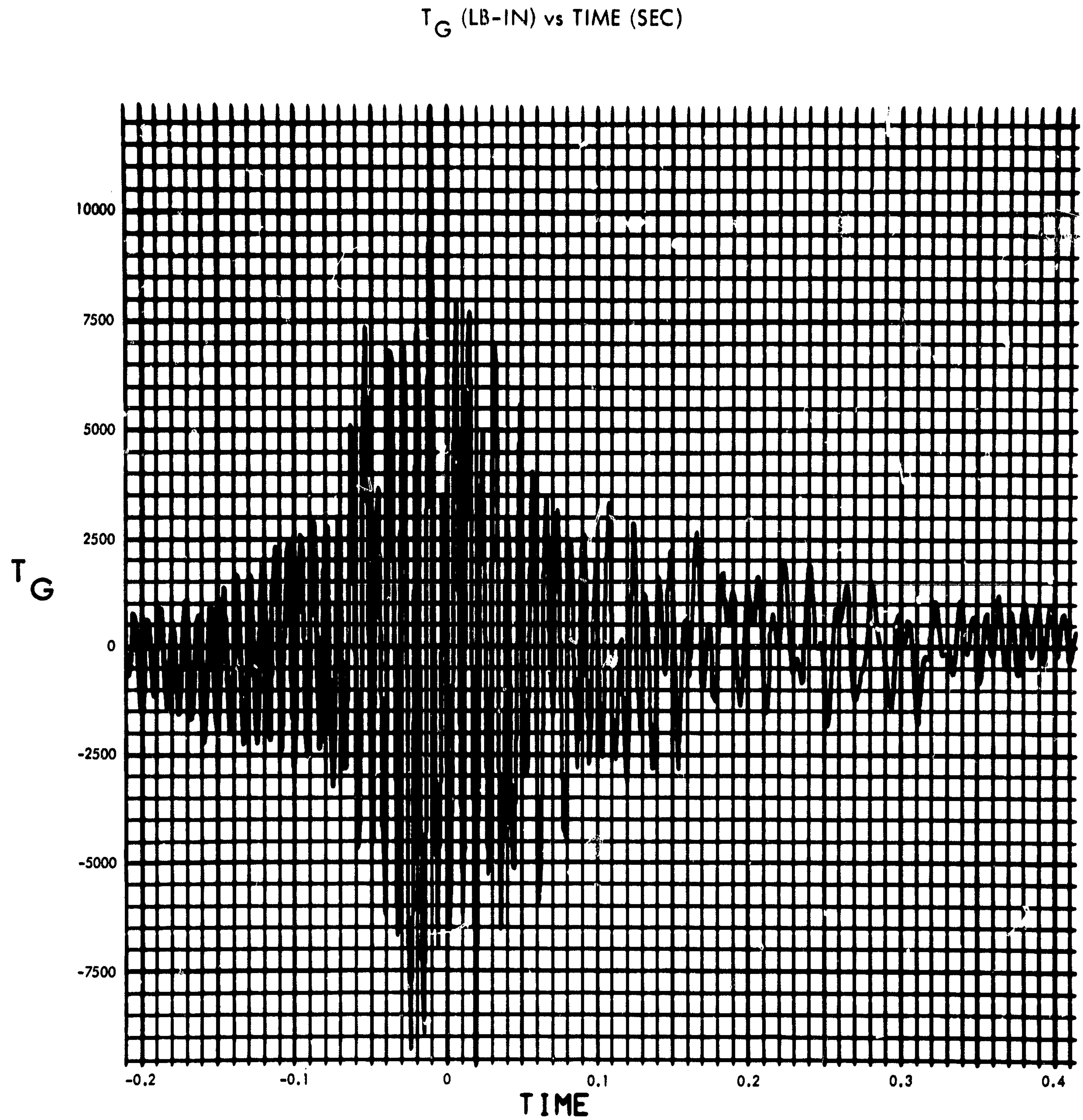

Fig. C-7. RA-8 gimbal torque, time history (pulse 3)

MODULUS OF F(F) (LB-IN-SEC) vs FREQUENCY (CYCLES/SEC)

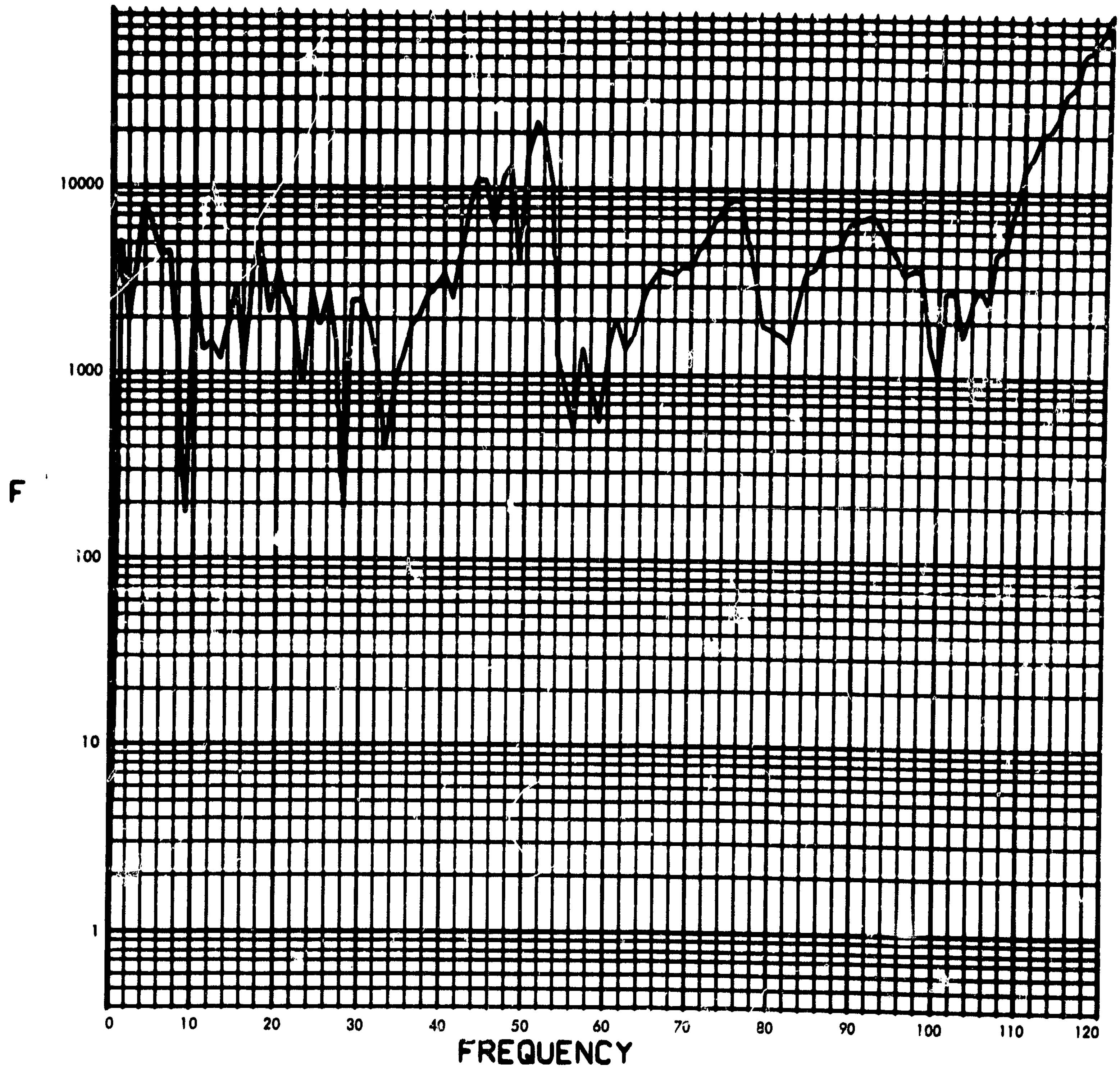

Fig. C-8. RA-8 gimbal torque, Fourier transform, modulus (pulse 3)

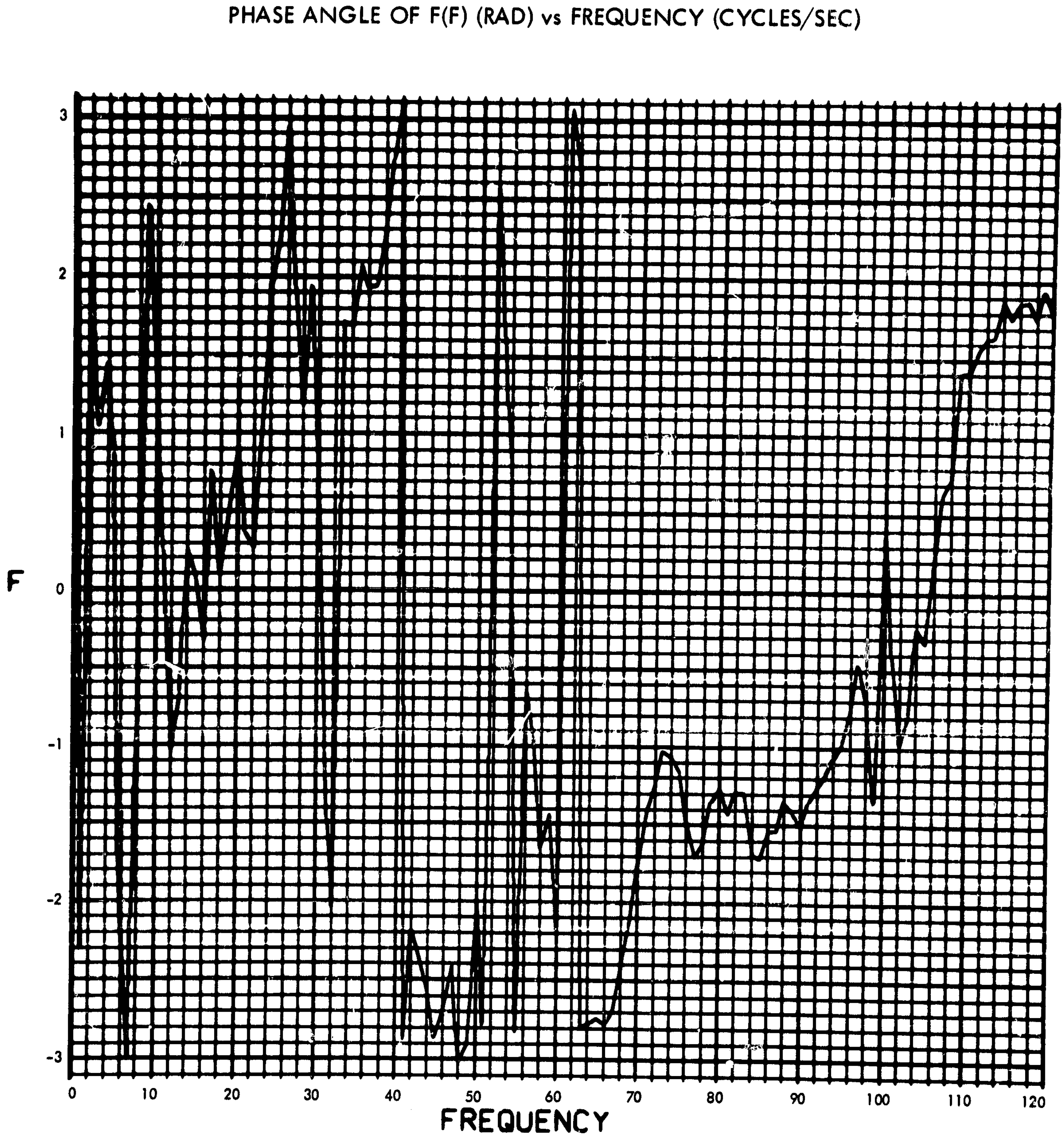

Fig. C-9. RA-8 gimbal torque, Fourier transform, phase angle (pulse 3)

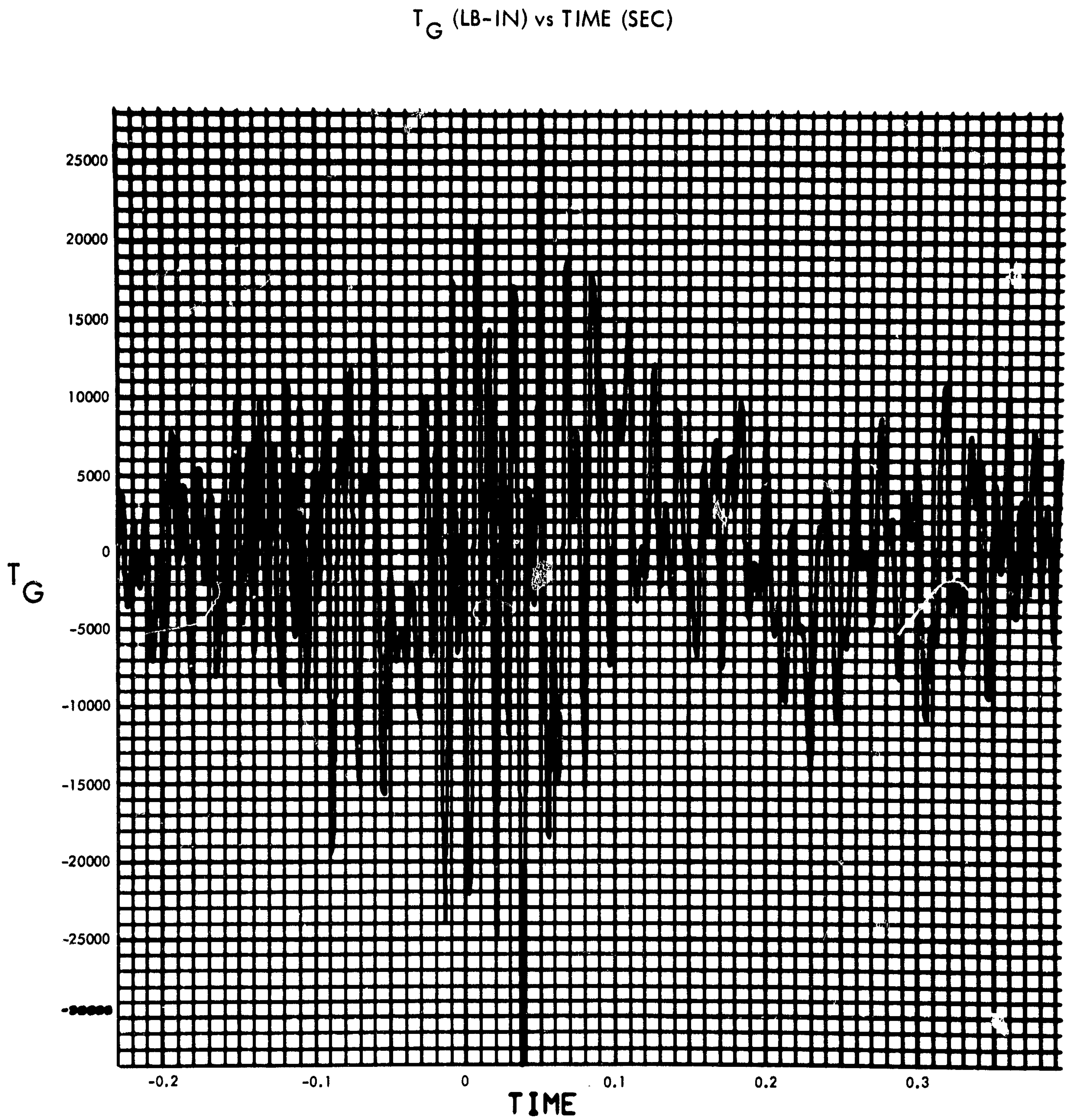

Fig. C-10. RA-9 gimbal torque, time history (pulse 4)

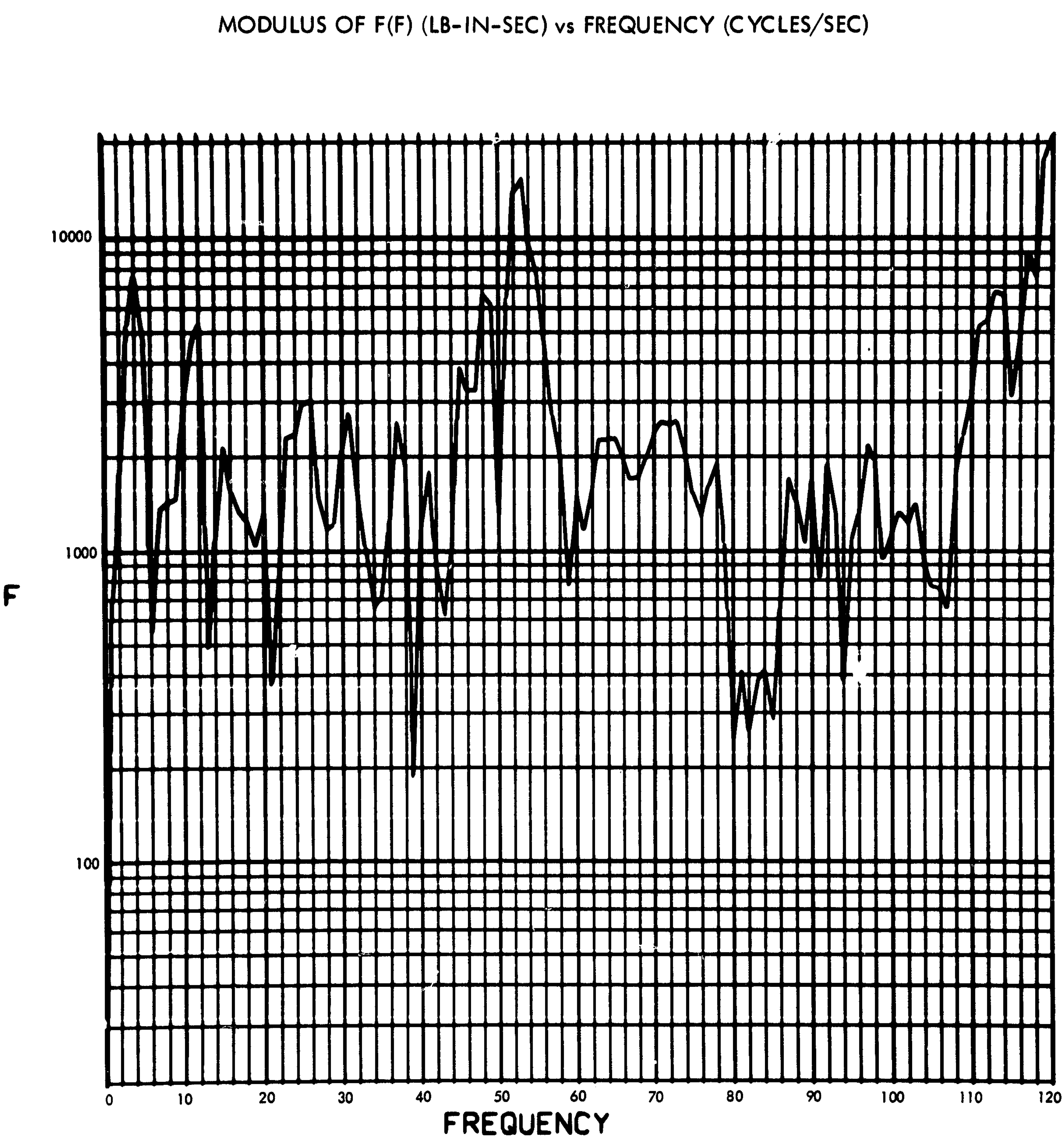

Fig. C-11. RA-9 gimbal torque, Fourier transform, modulus (pulse 4)

PHASE ANGLE OF F(F) (RAD) vs FREQUENCY (CYCLES/SEC)

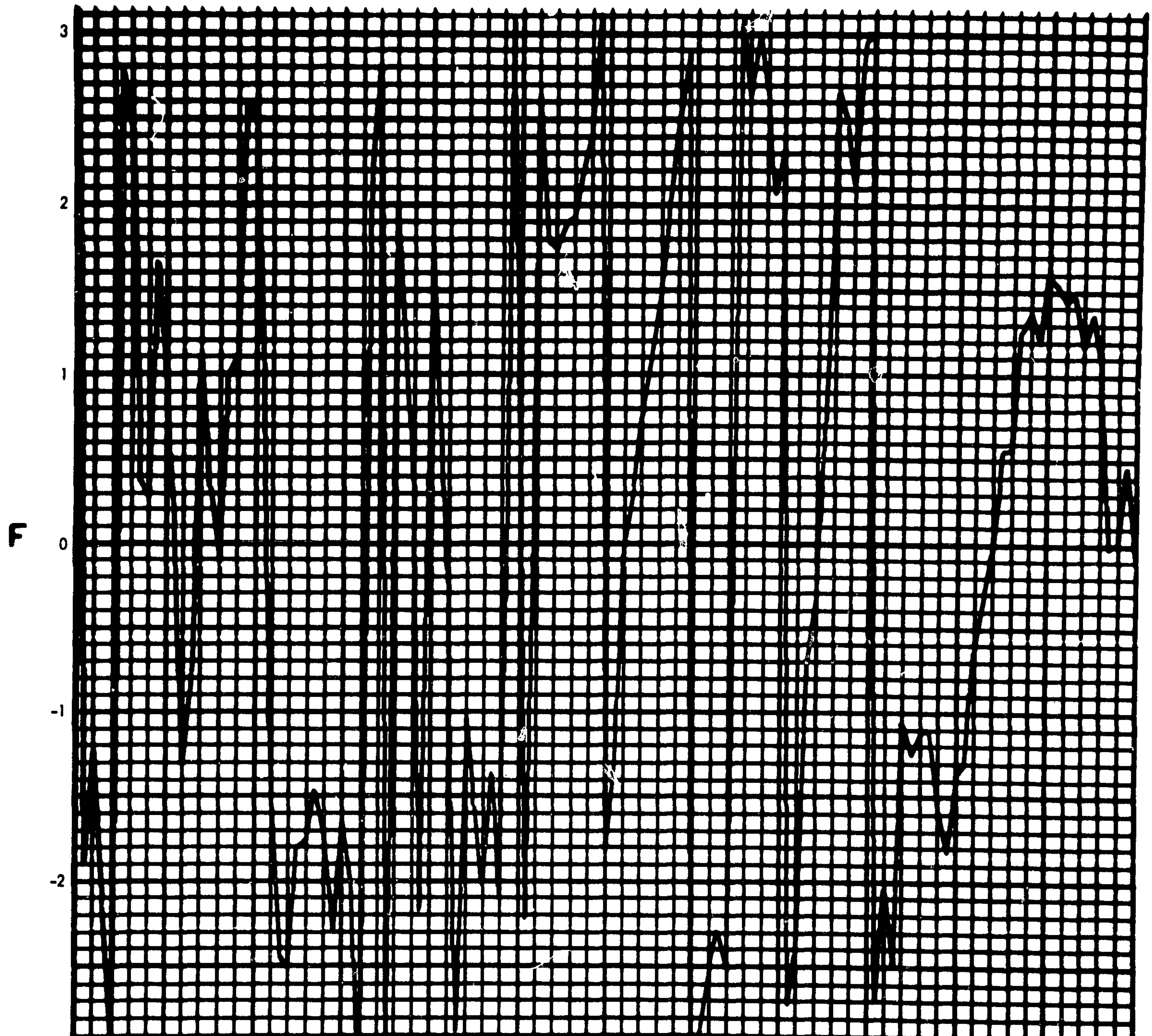

Fig. C-12. RA-9 gimbal torque, Fourier transform, phase angle (pulse 4)

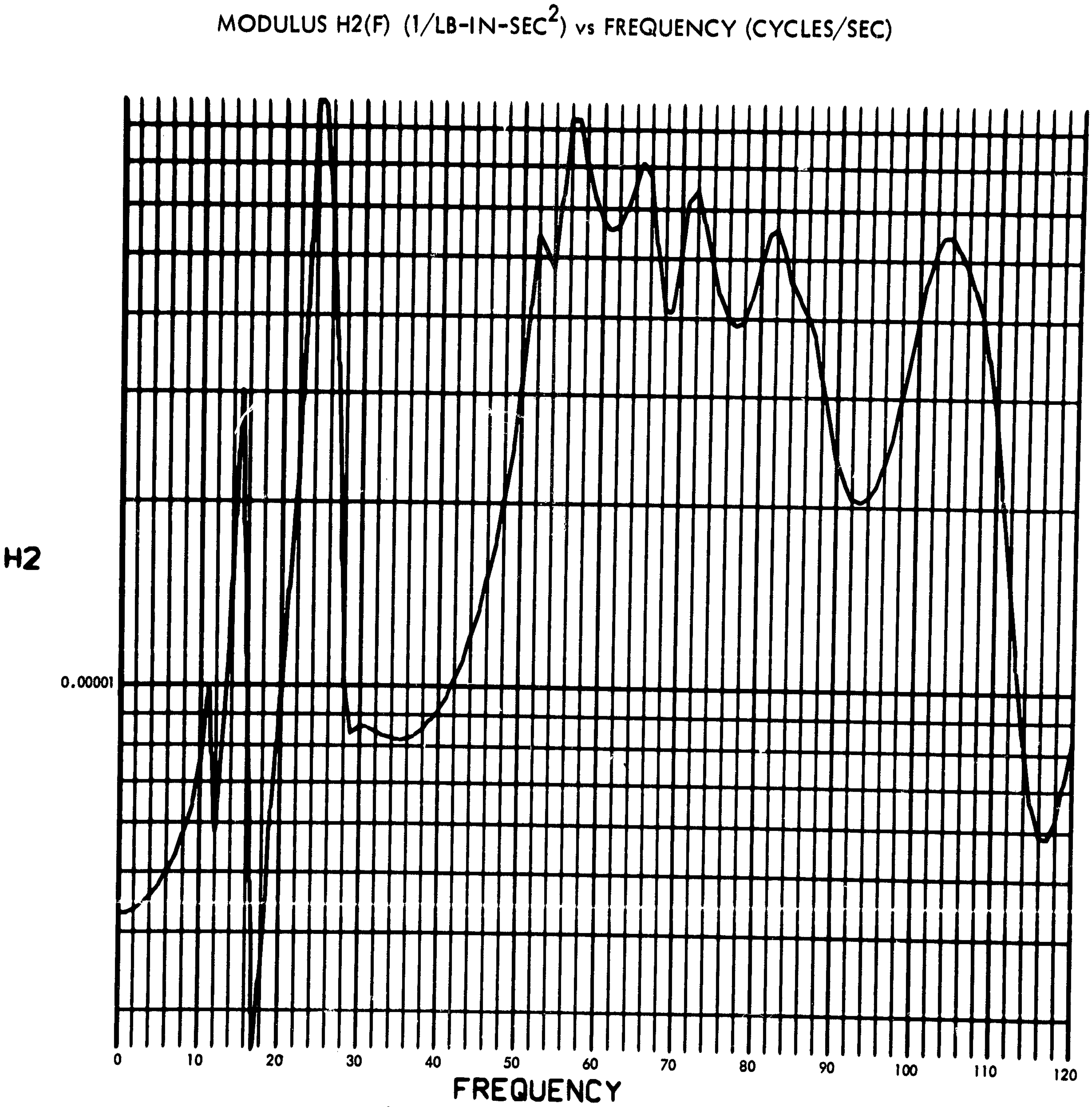

Fig. C-13. Joint 10, acceleration transfer function, Fourier transform, modulus

PHASE ANGLE OF H2(F) (RAD) vs FREQUENCY (CYCLES/SEC)

Fig. C-14. Joint 10, acceleration transfer function, Fourier transform, phase angle

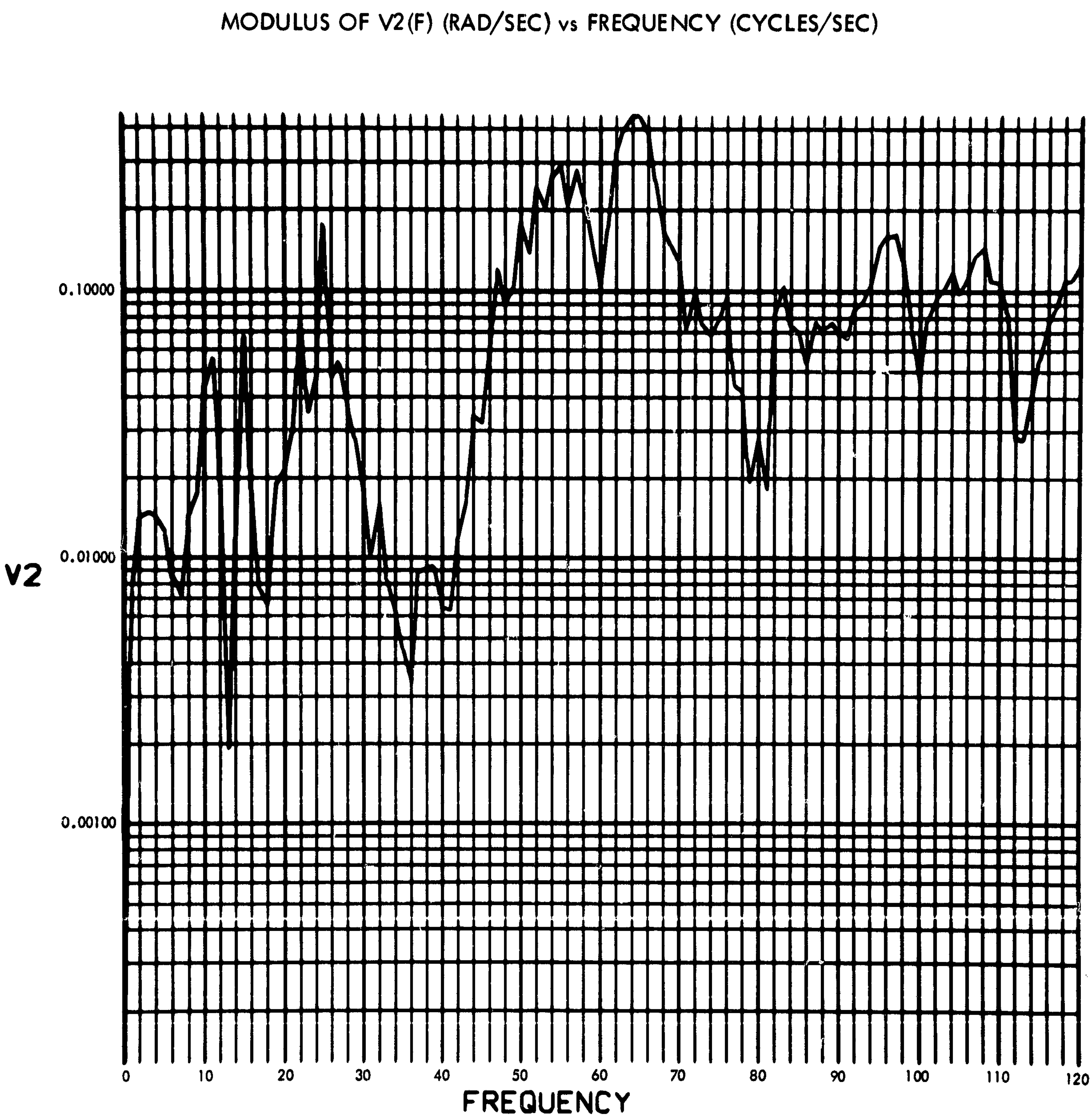

Fig. C-15. Joint 10, acceleration response, Fourier transform, modulus (pulse 1)

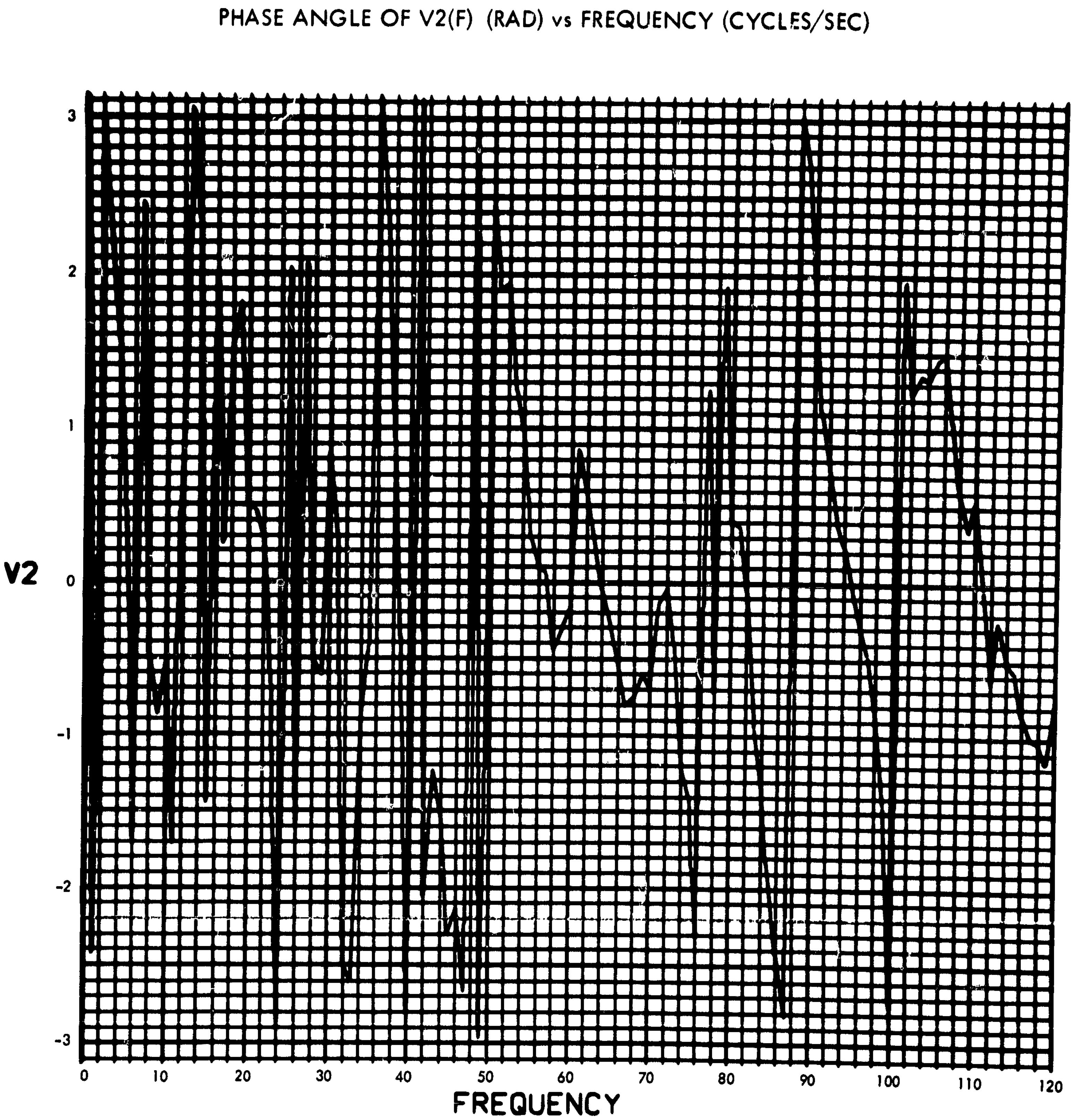

Fig. C-16. Joint 10, acceleration response, Fourier transform, phase angle (pulse 1)

U2(T) (RAD/SEC^2) vs TIME (SEC)

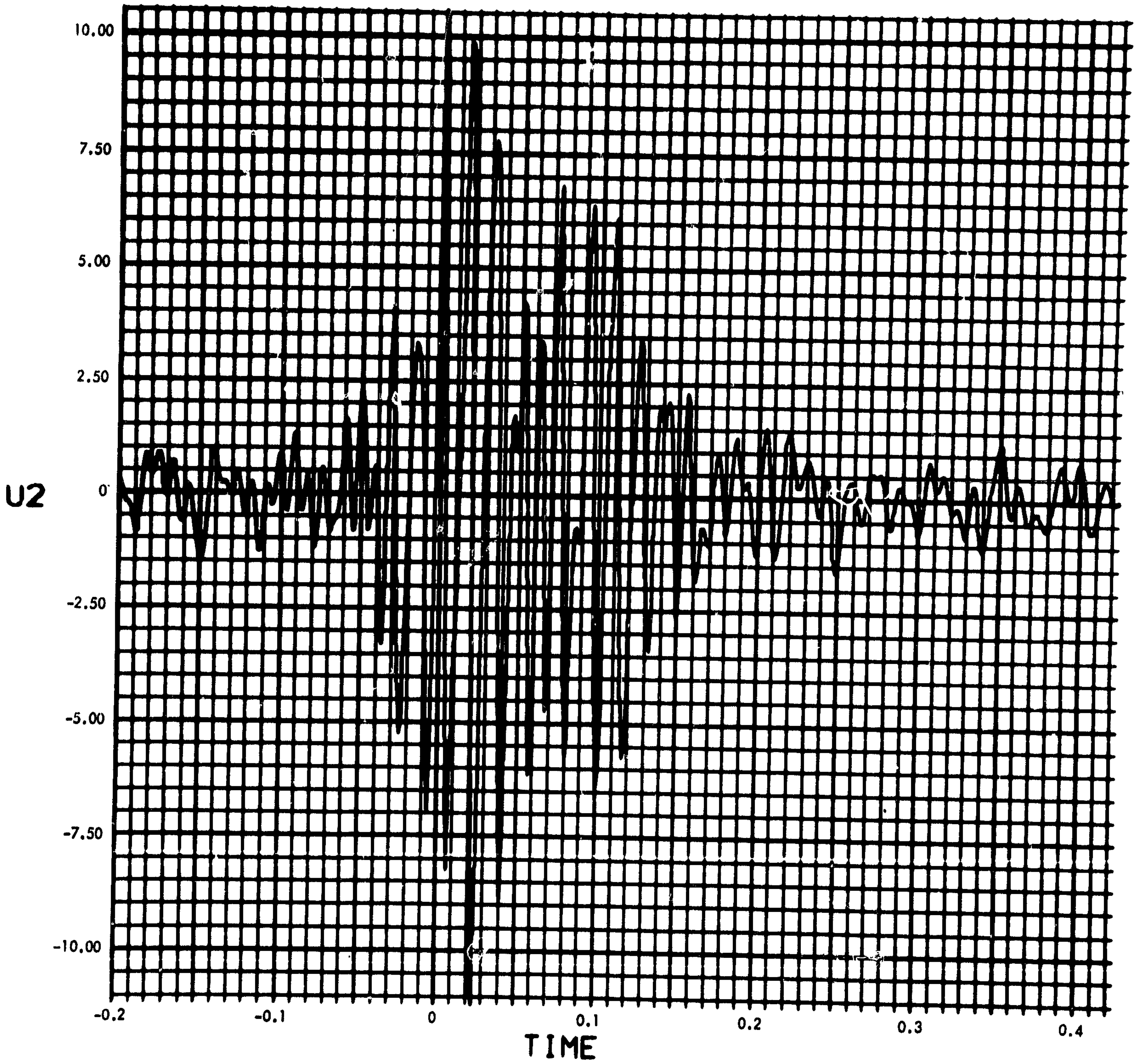

Fig. C-17. Joint 10, acceleration response, time history (pulse 1)

MODULUS OF V2(F) (RAD/SEC) vs FREQUENCY (CYCLES/SEC)

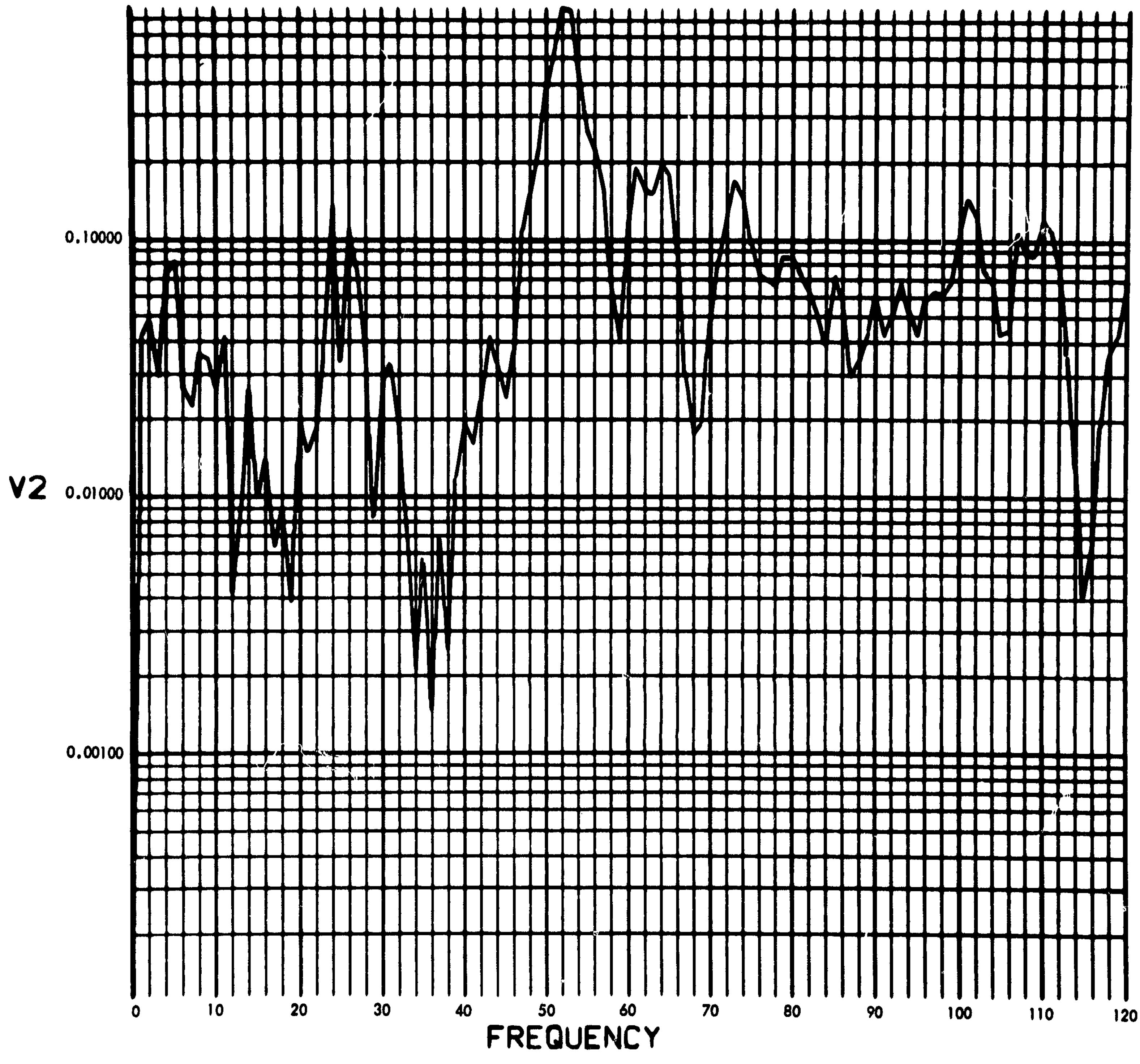

Fig. C-18. Joint 10, acceleration response, Fourier transform, modulus (pulse 2)

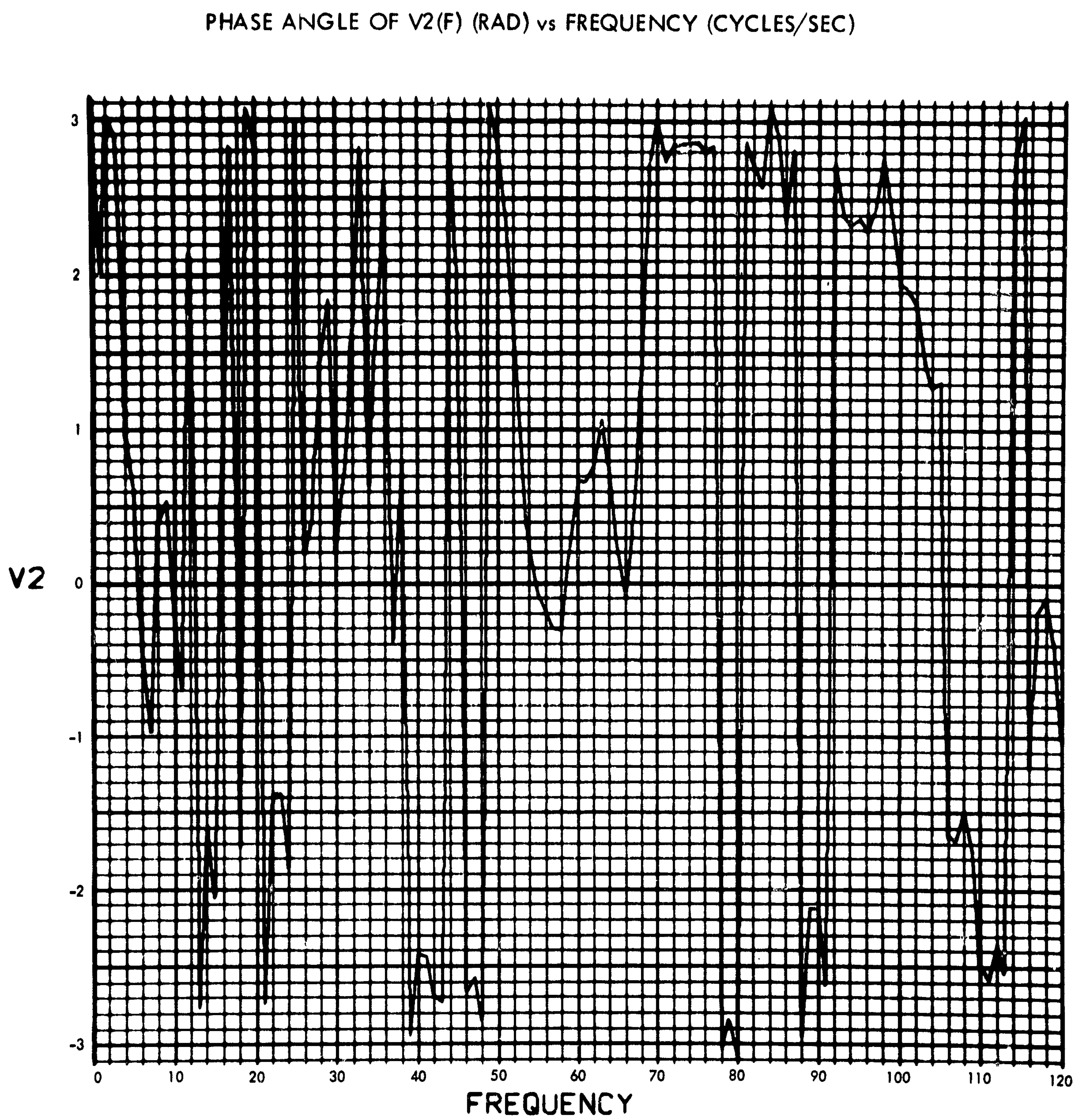

Fig. C-19. Joint 10, acceleration response, Fourier transform, phase angle (pulse 2)

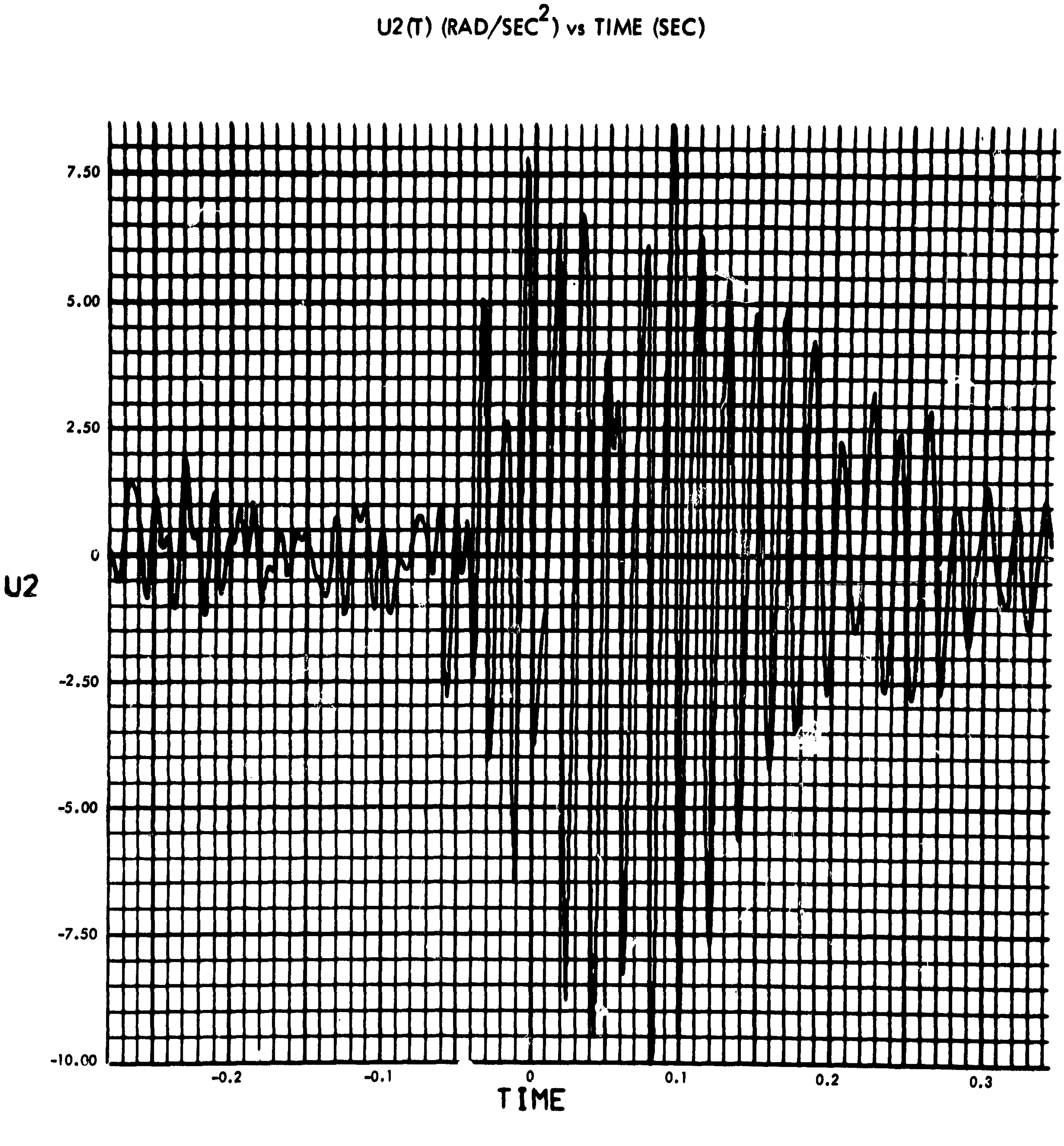

Fig. C-20. Joint 10, acceleration response, time history (pulse 2)

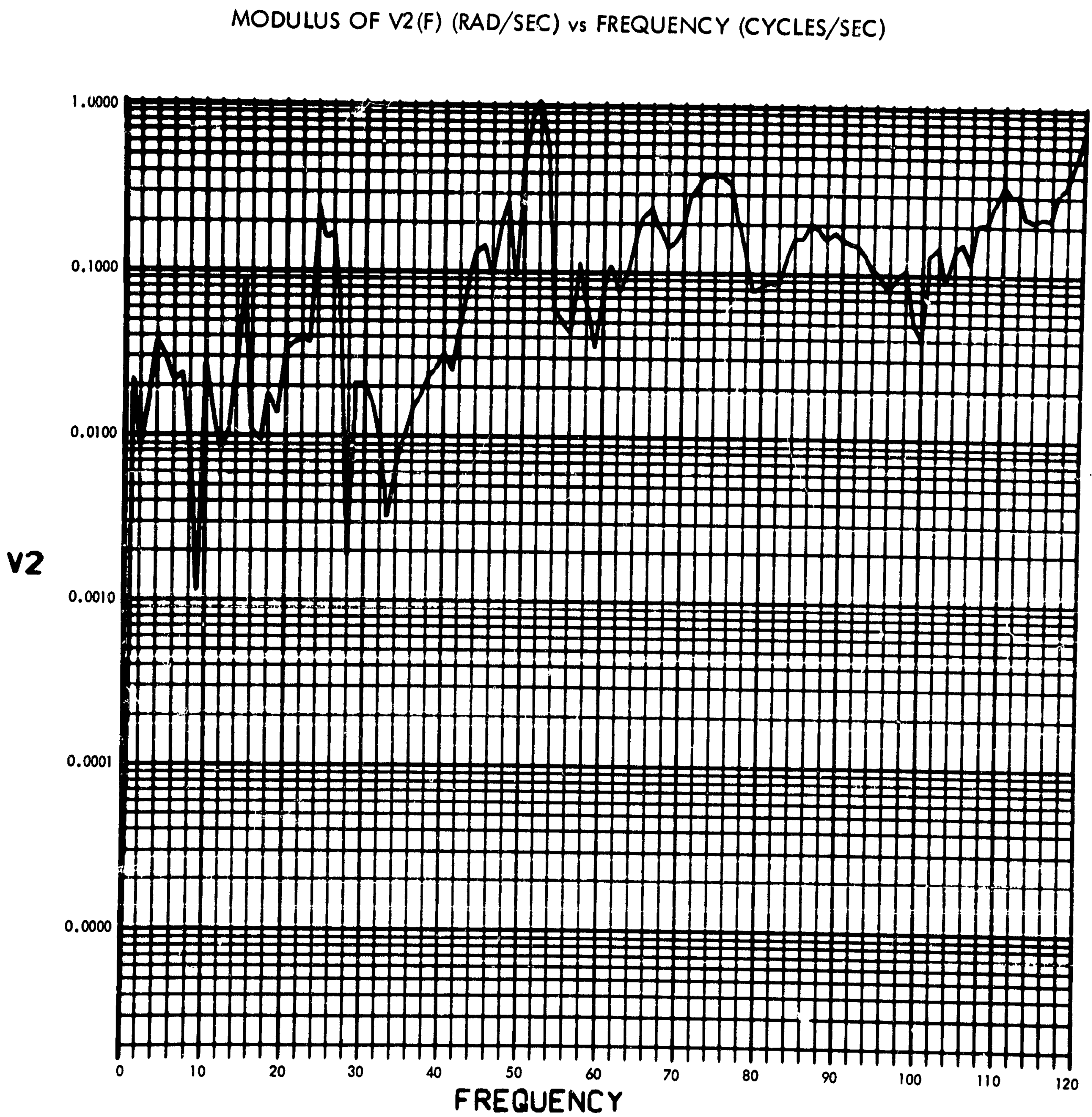

Fig. C-21. Joint 10, acceleration response, Fourier transform, modulus (pulse 3)

PHASE ANGLE OF V2(F) (RAD) vs FREQUENCY (CYCLES/SEC)

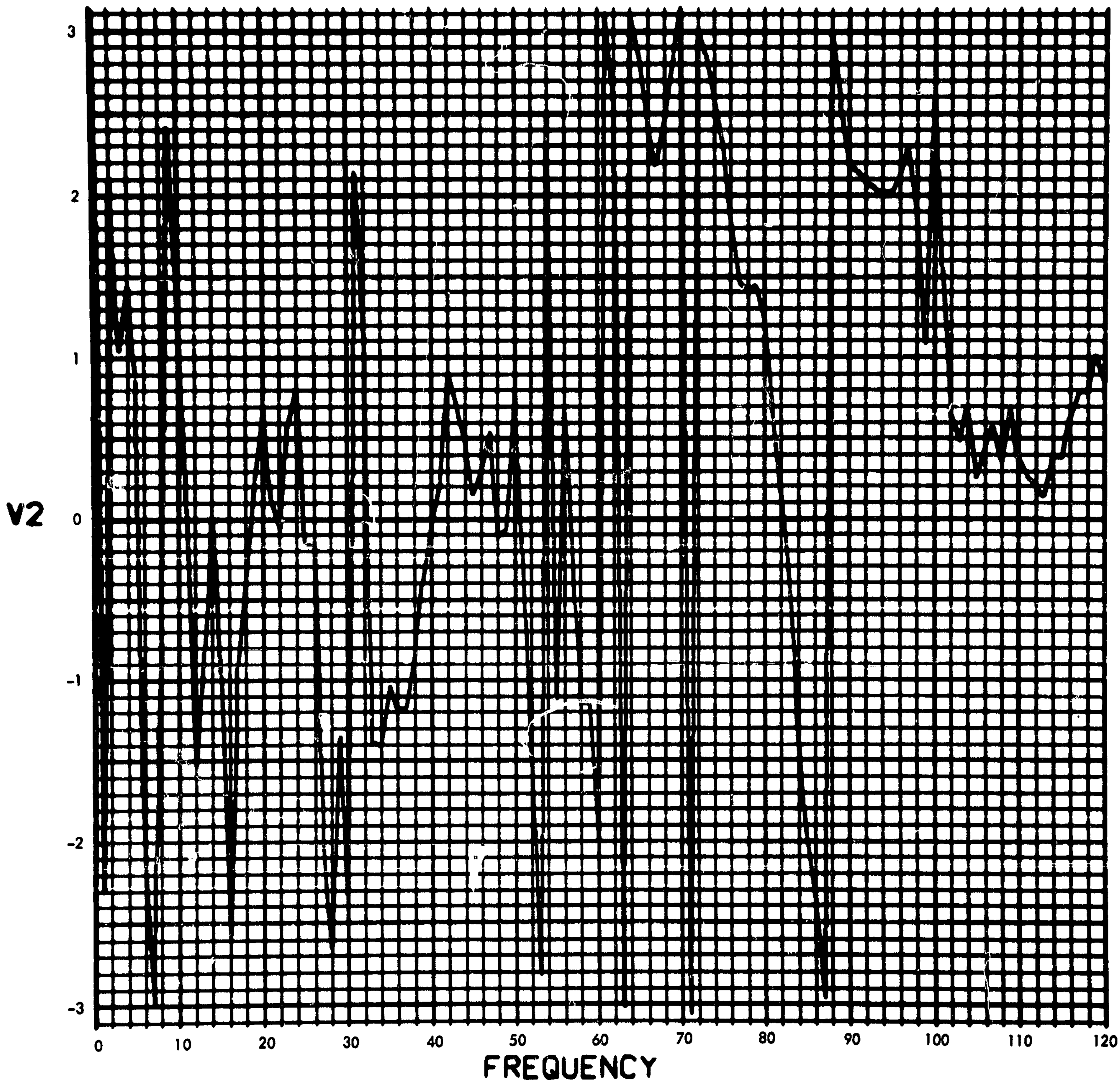

Fig. C-22. Joint 10, acceleration response, Fourier transform, phase angle (pulse 3)

U2(T) (RAD/SEC^2) vs TIME (SEC)

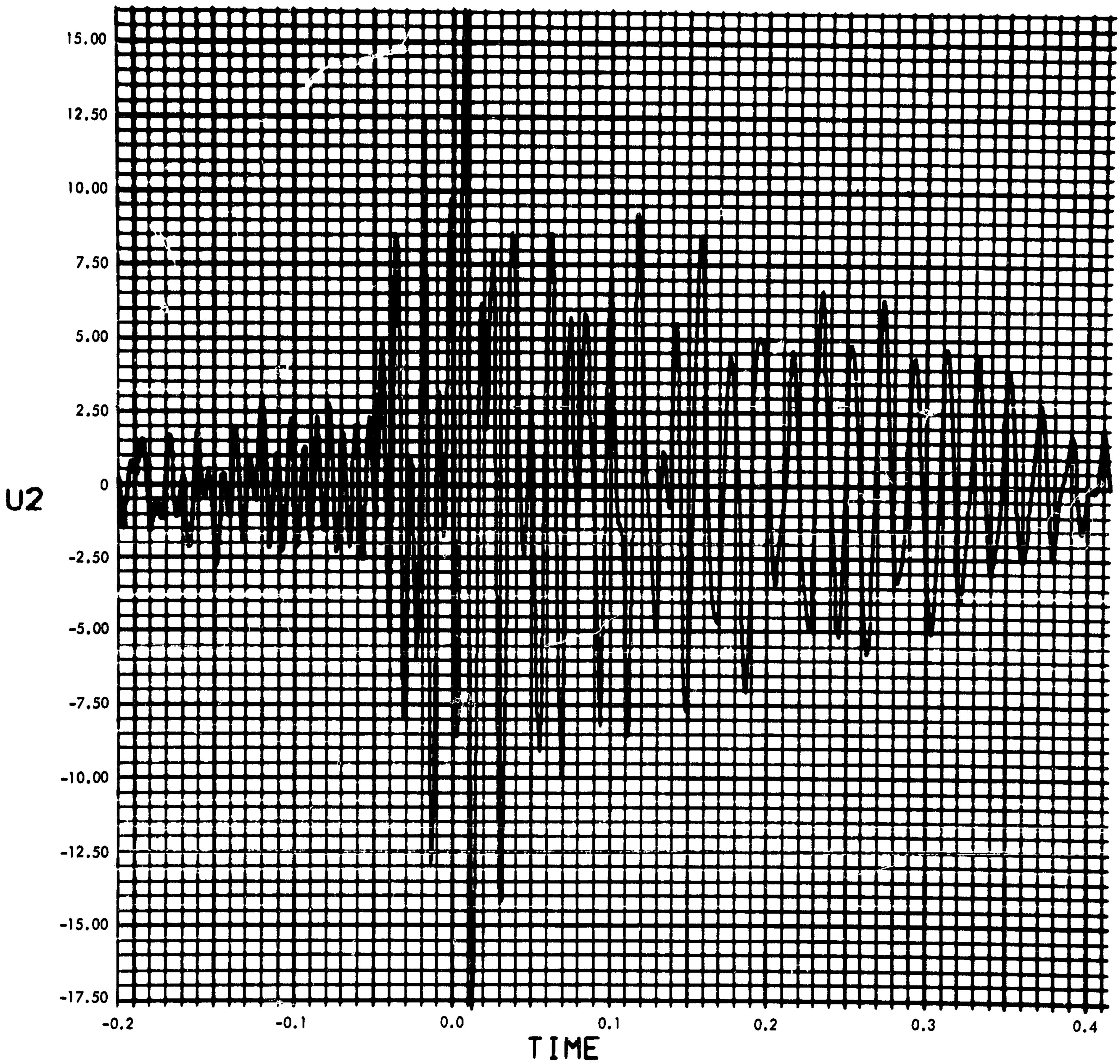

Fig. C-23. Joint 10, accele[illegible]on response, time history (pulse 3)

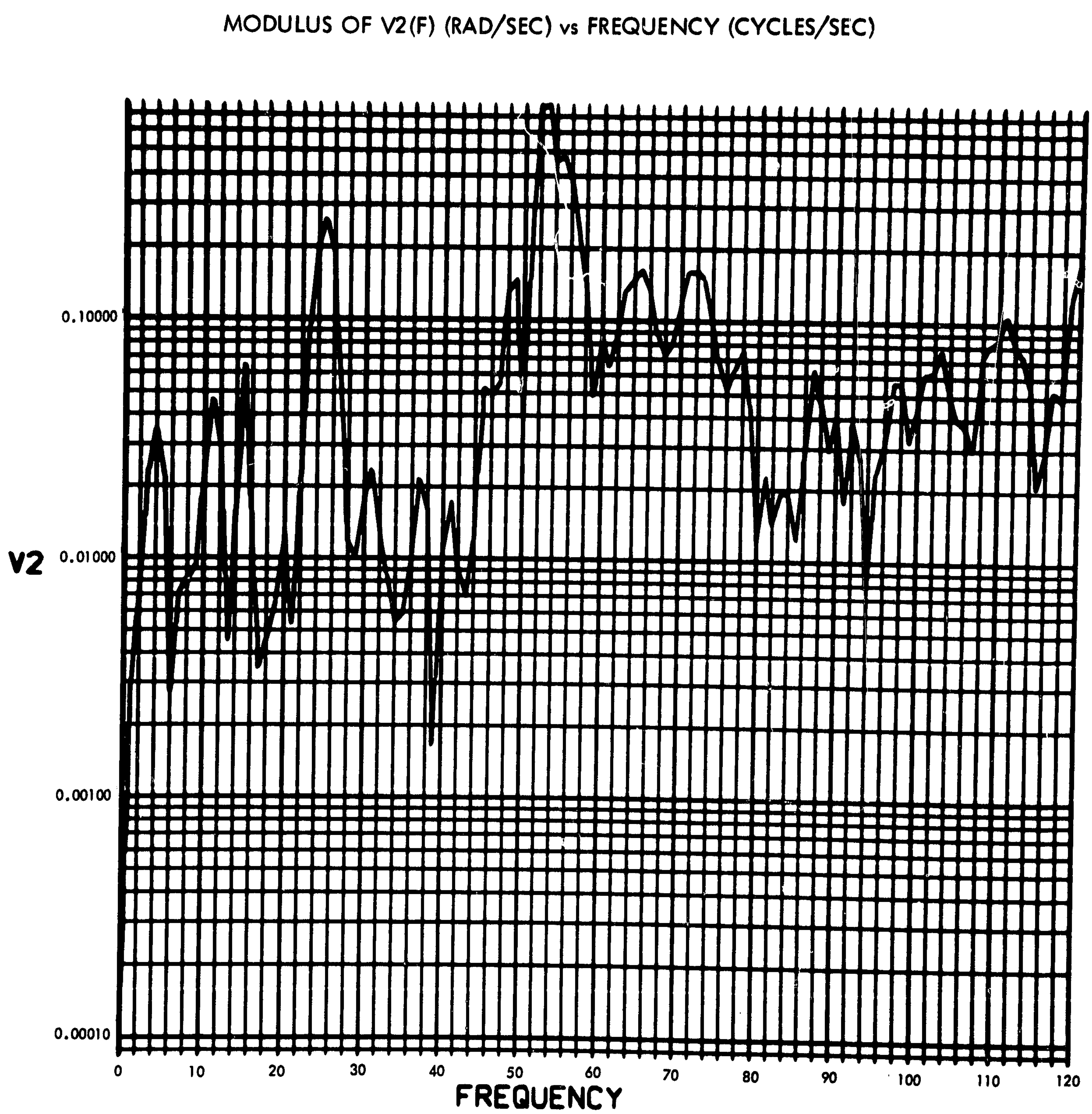

Fig. C-24. Joint 10, acceleration response, Fourier transform, modulus (pulse 4)

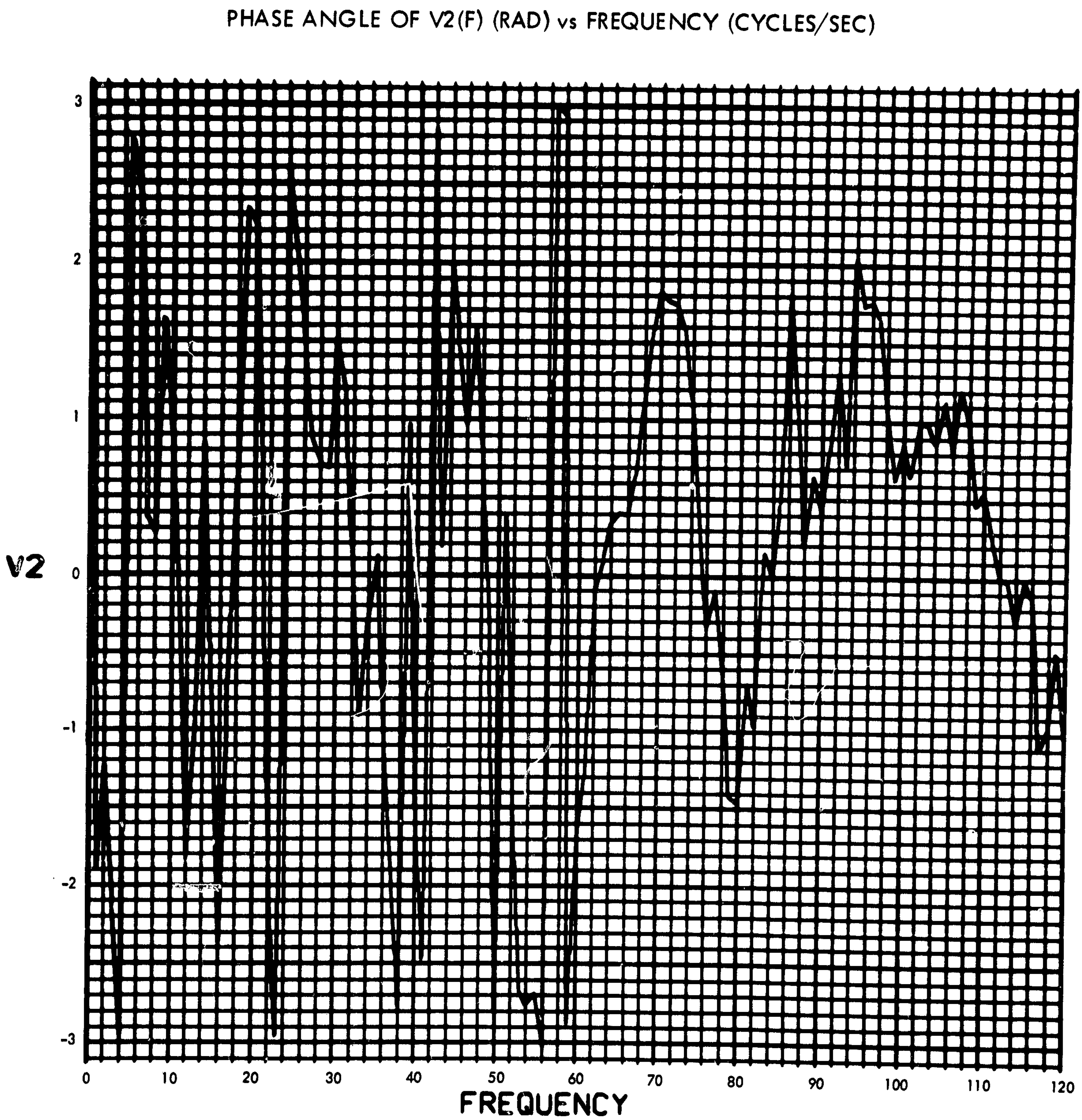

Fig. C-25. Joint 10, acceleration response, Fourier transform, phase angle (pulse 4)

U2(T) (RAD/SEC^2) vs TIME (SEC)

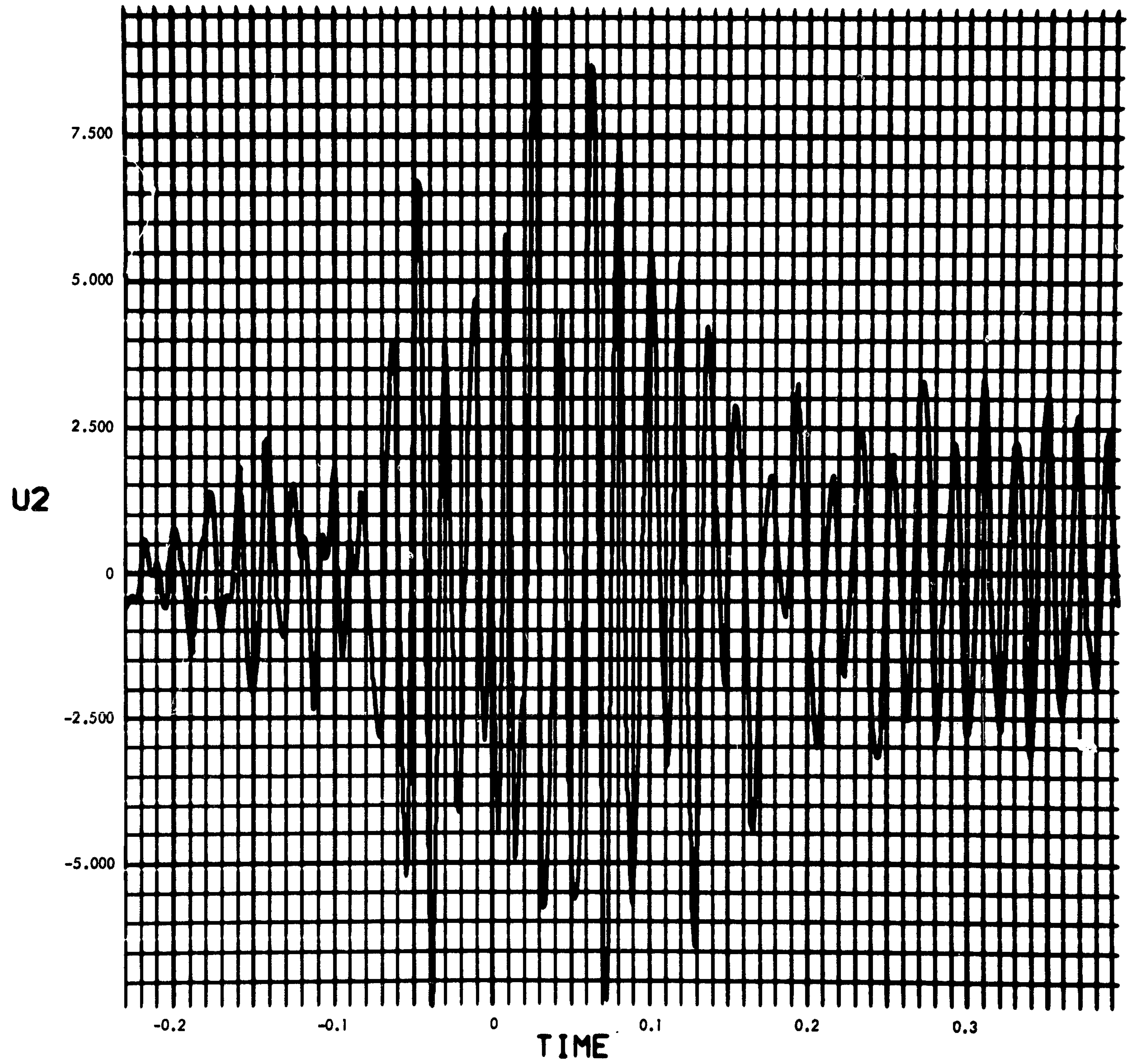

Fig. C-26. Joint 10, acceleration response, time history (pulse 4)

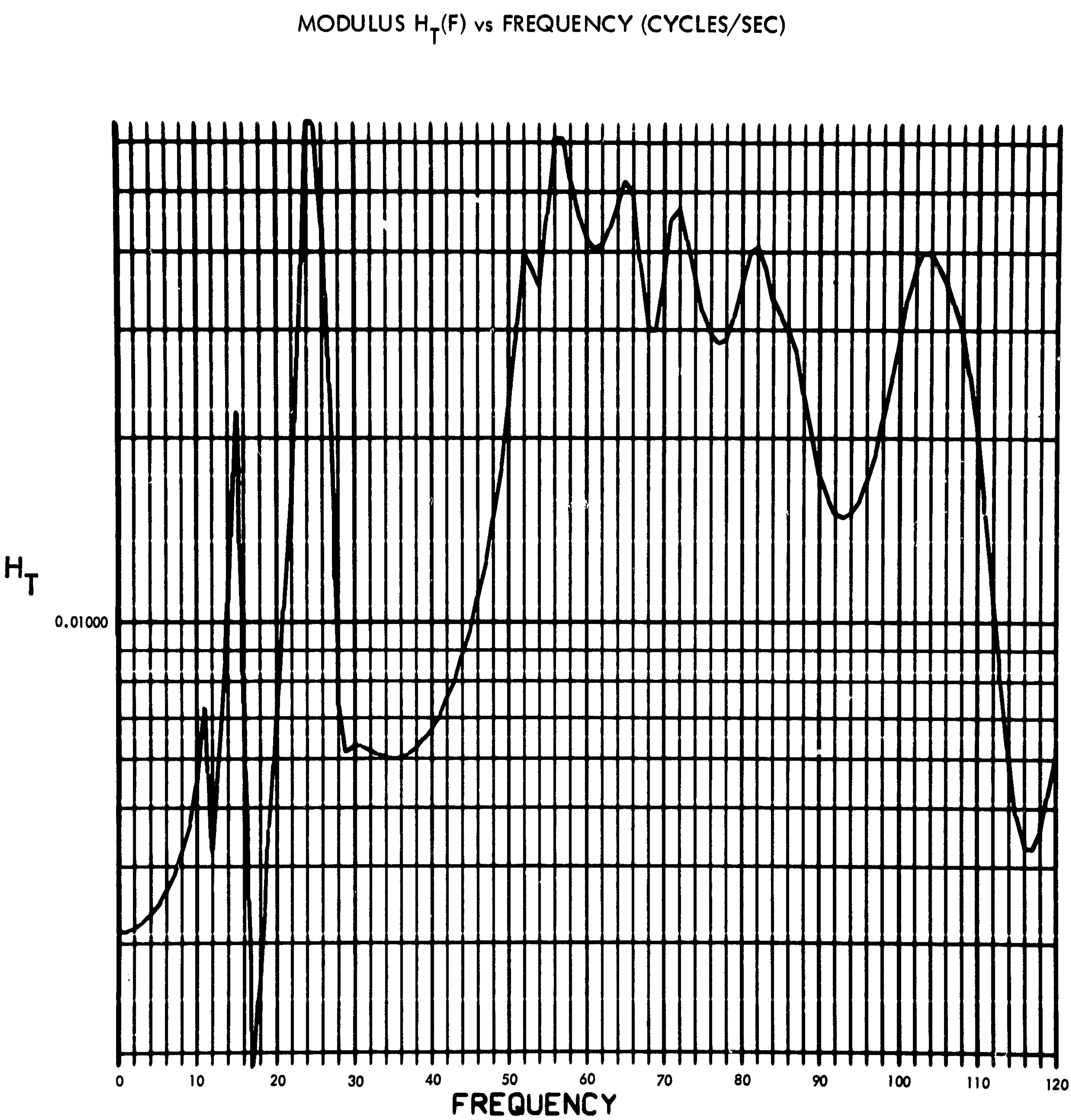

Fig. C-27. Joint 10, torque transfer function, Fourier transform, modulus

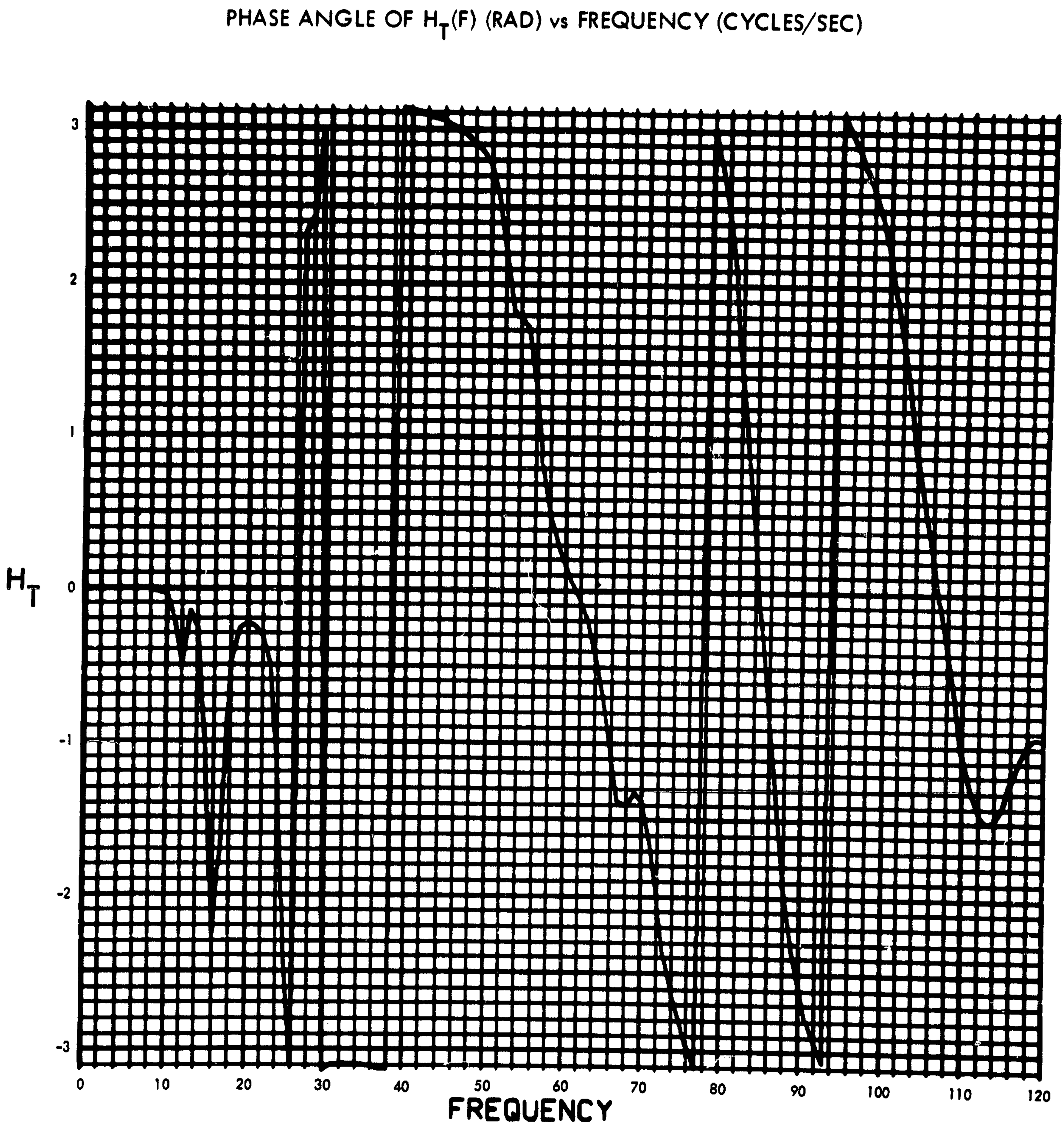

Fig. C-28. Joint 10, torque transfer function, Fourier transform, phase angle

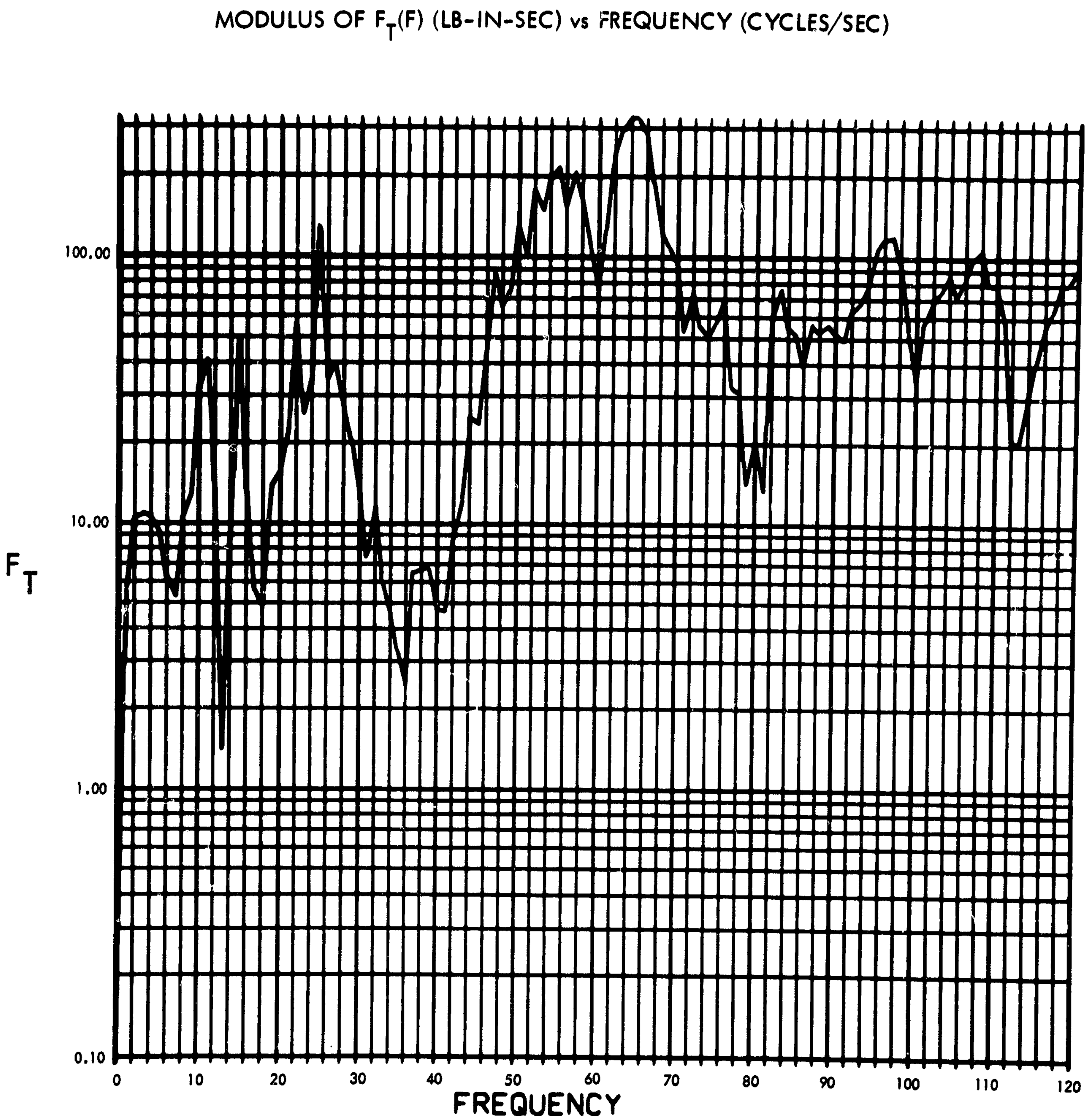

Fig. C-29. Joint 10, torque response, Fourier transform, modulus (pulse 1)

PHASE ANGLE OF $F_T(F)$ (RAD) vs FREQUENCY (CYCLES/SEC)

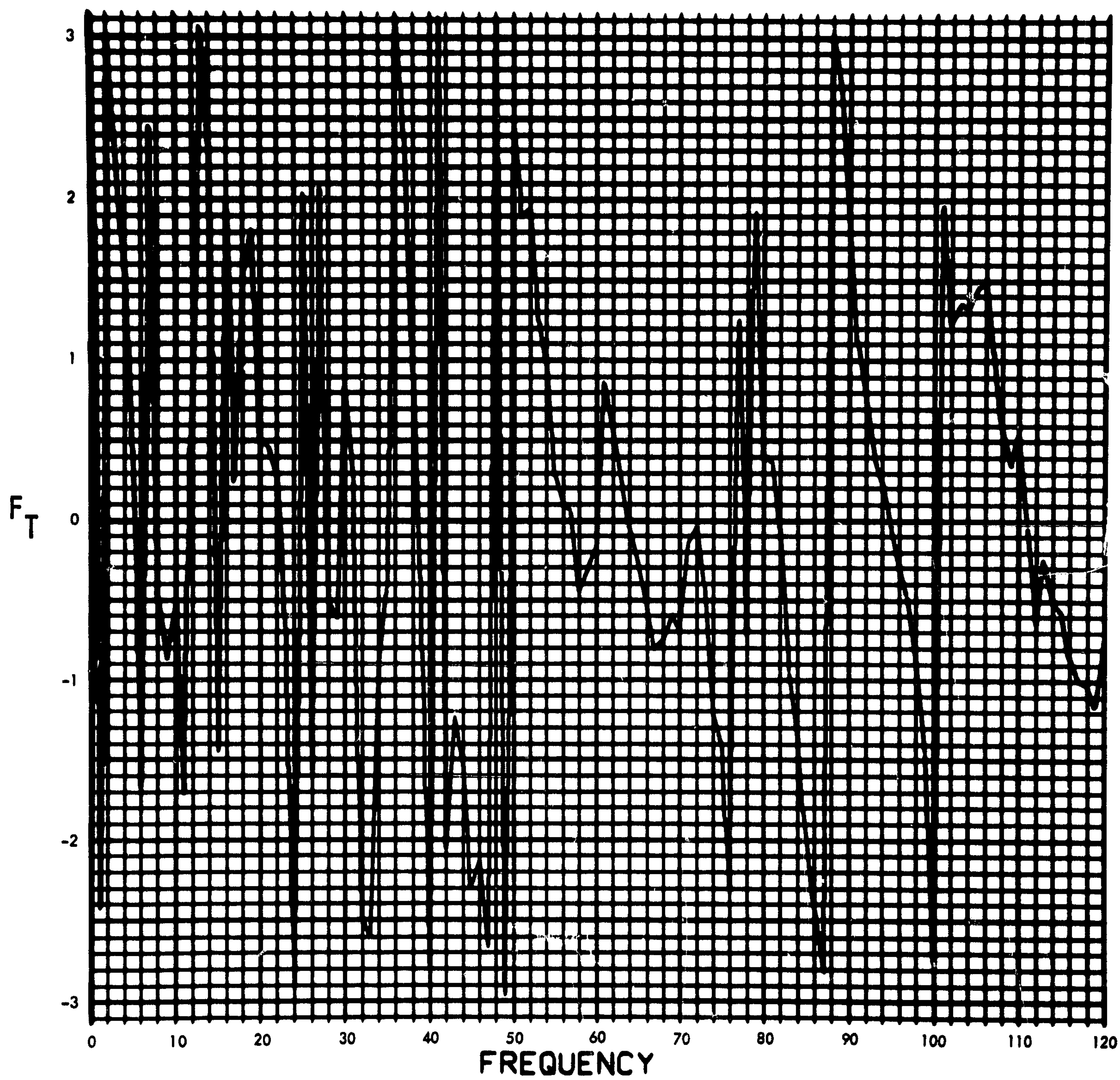

Fig. C-30. Joint 10, torque response, Fourier transform, phase angle (pulse 1)

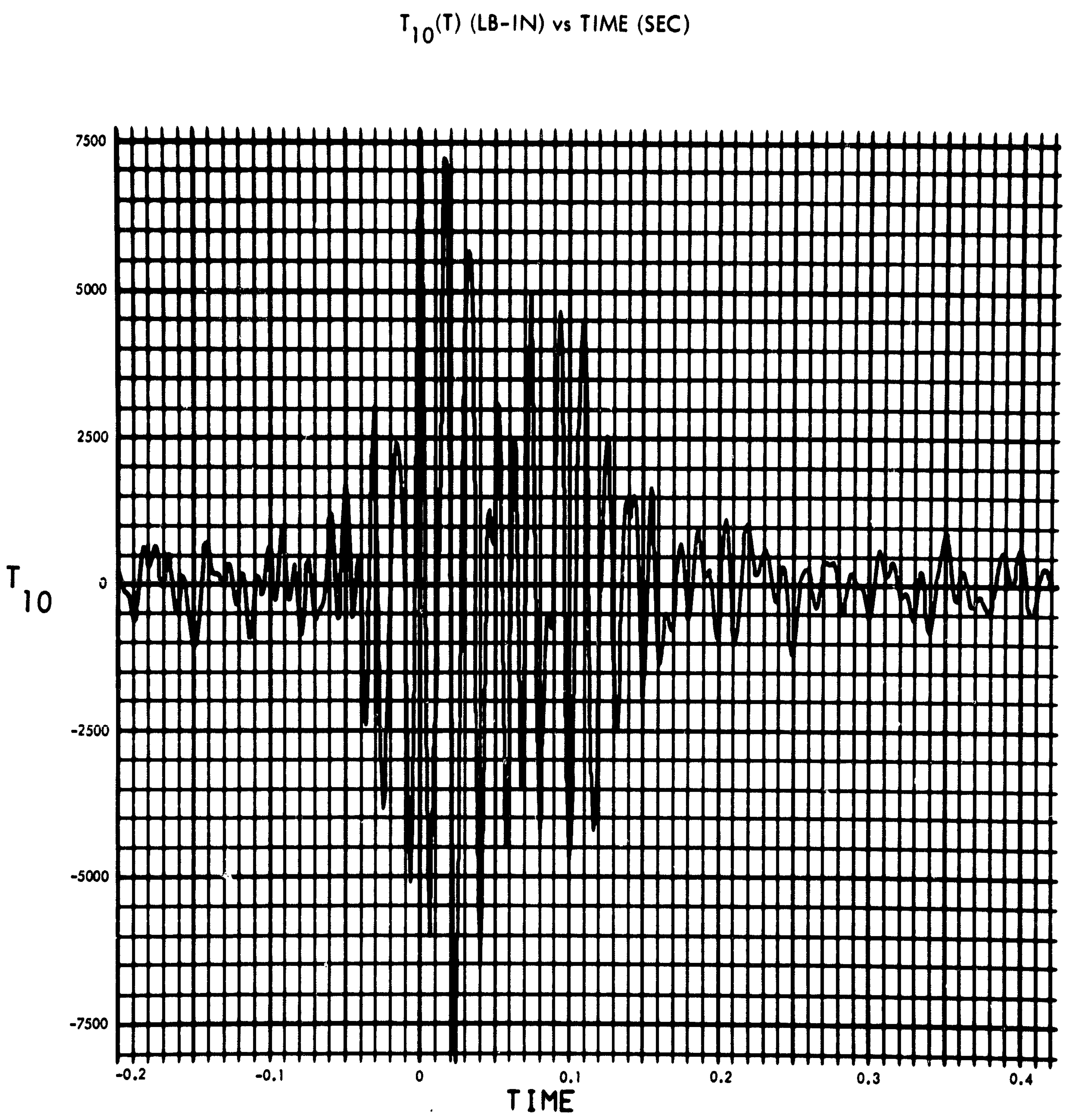

Fig. C-31. Joint 10, torque response, time history (pulse 1)

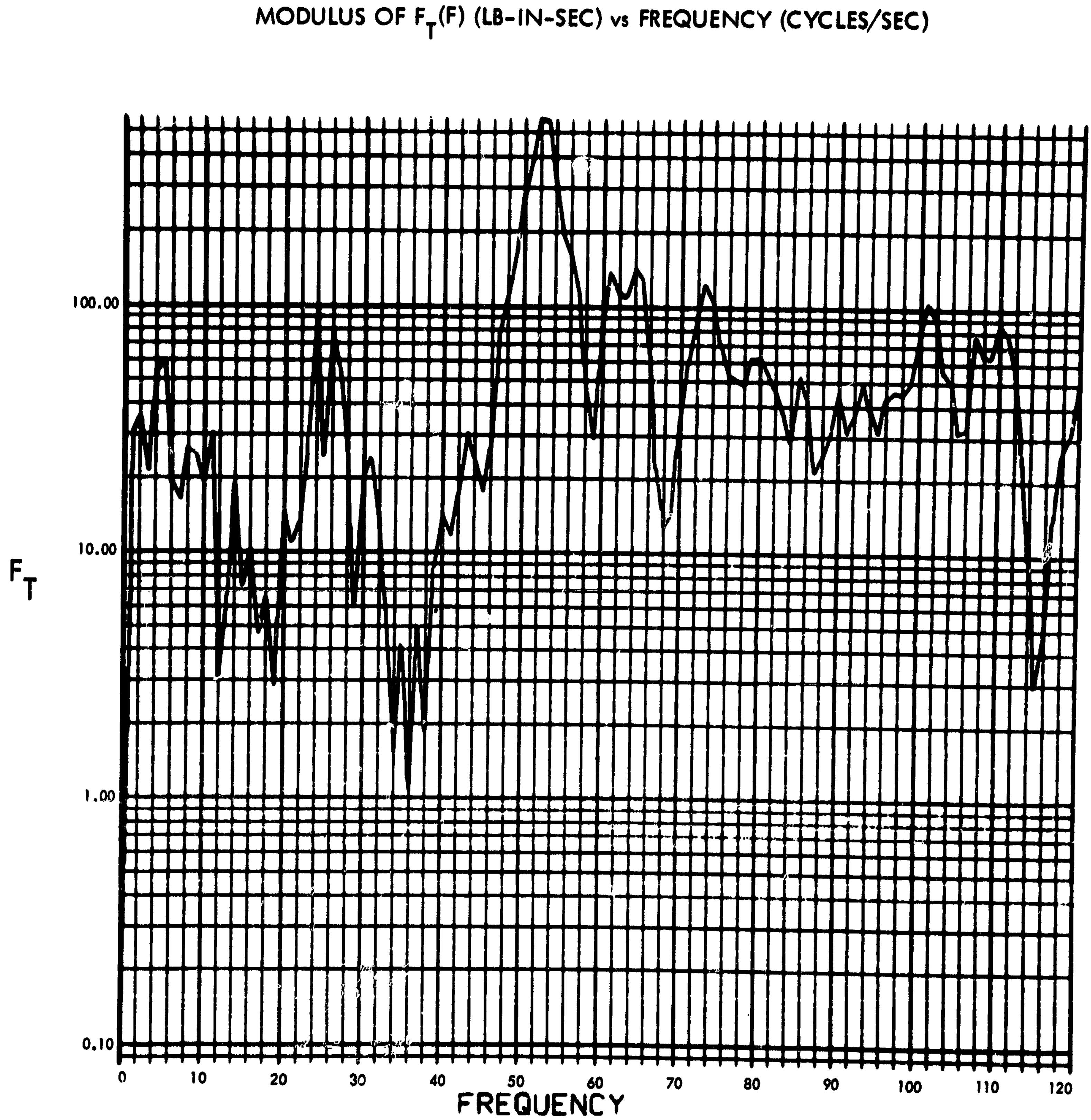

Fig. C-32. Joint 10, torque response, Fourier transform, modulus (pulse 2)

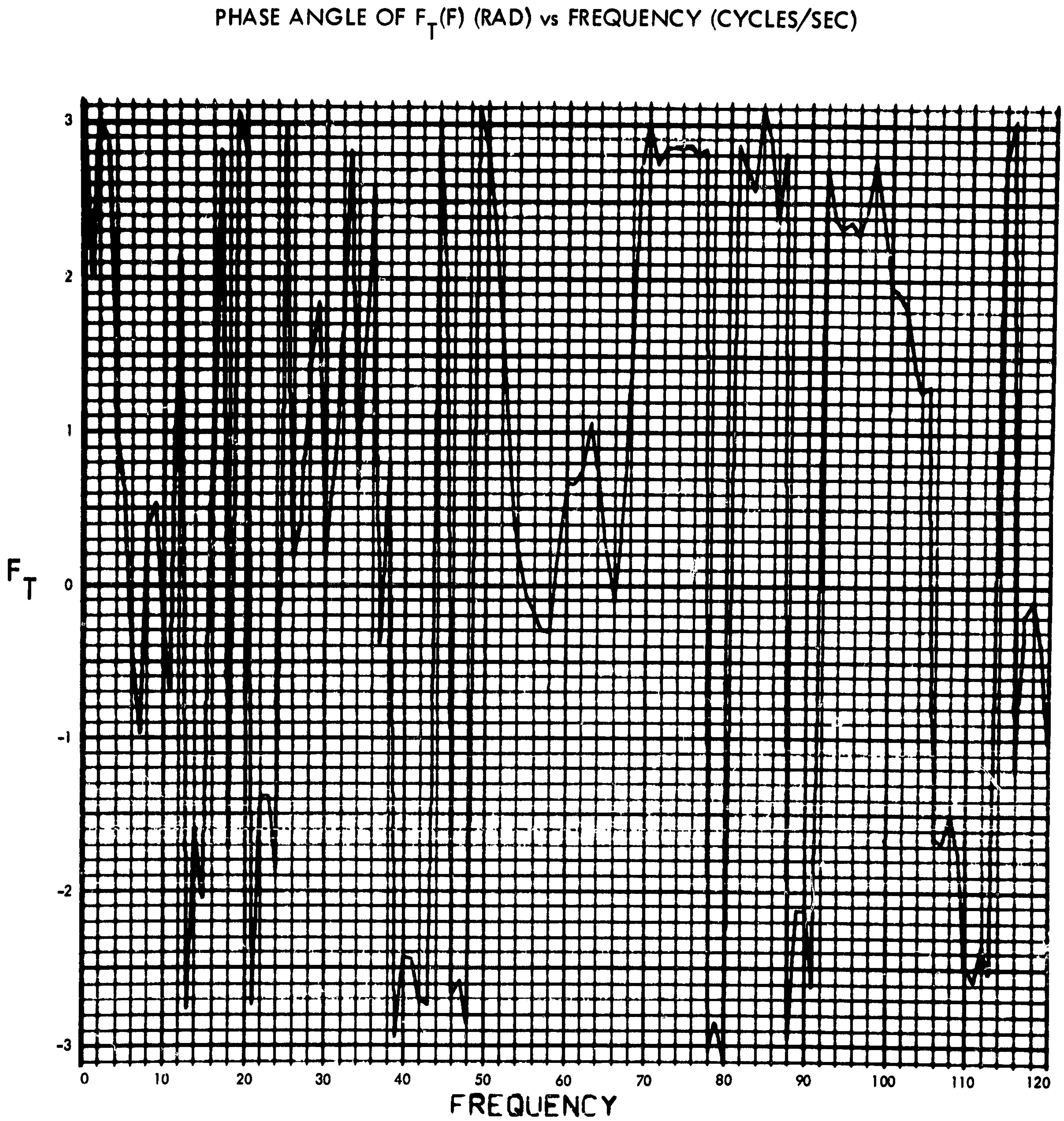

Fig. C-33. Joint 10, torque response, Fourier transform, phase angle (pulse 2)

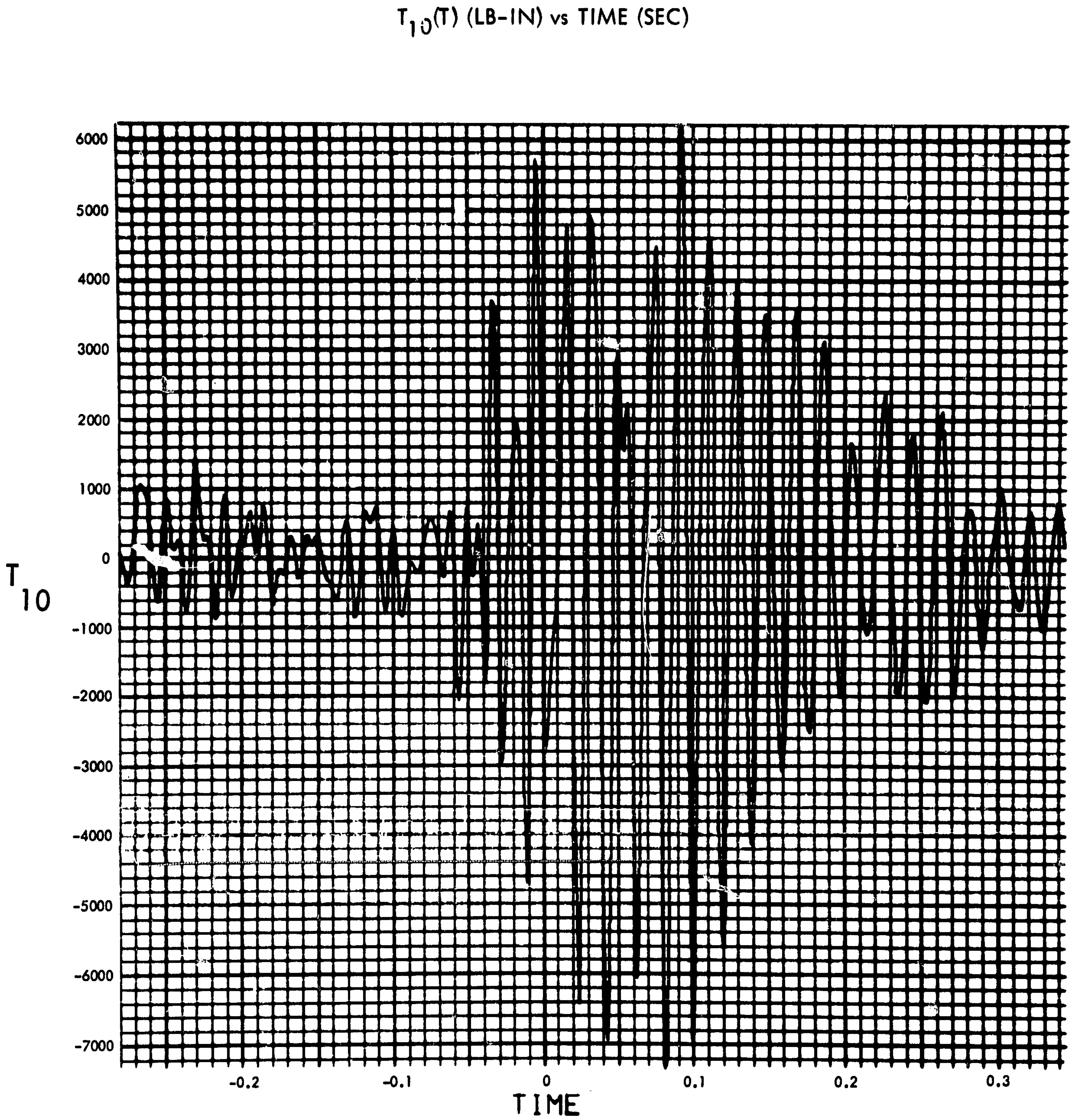

Fig. C-34. Joint 10, torque response, time history (pulse 2)

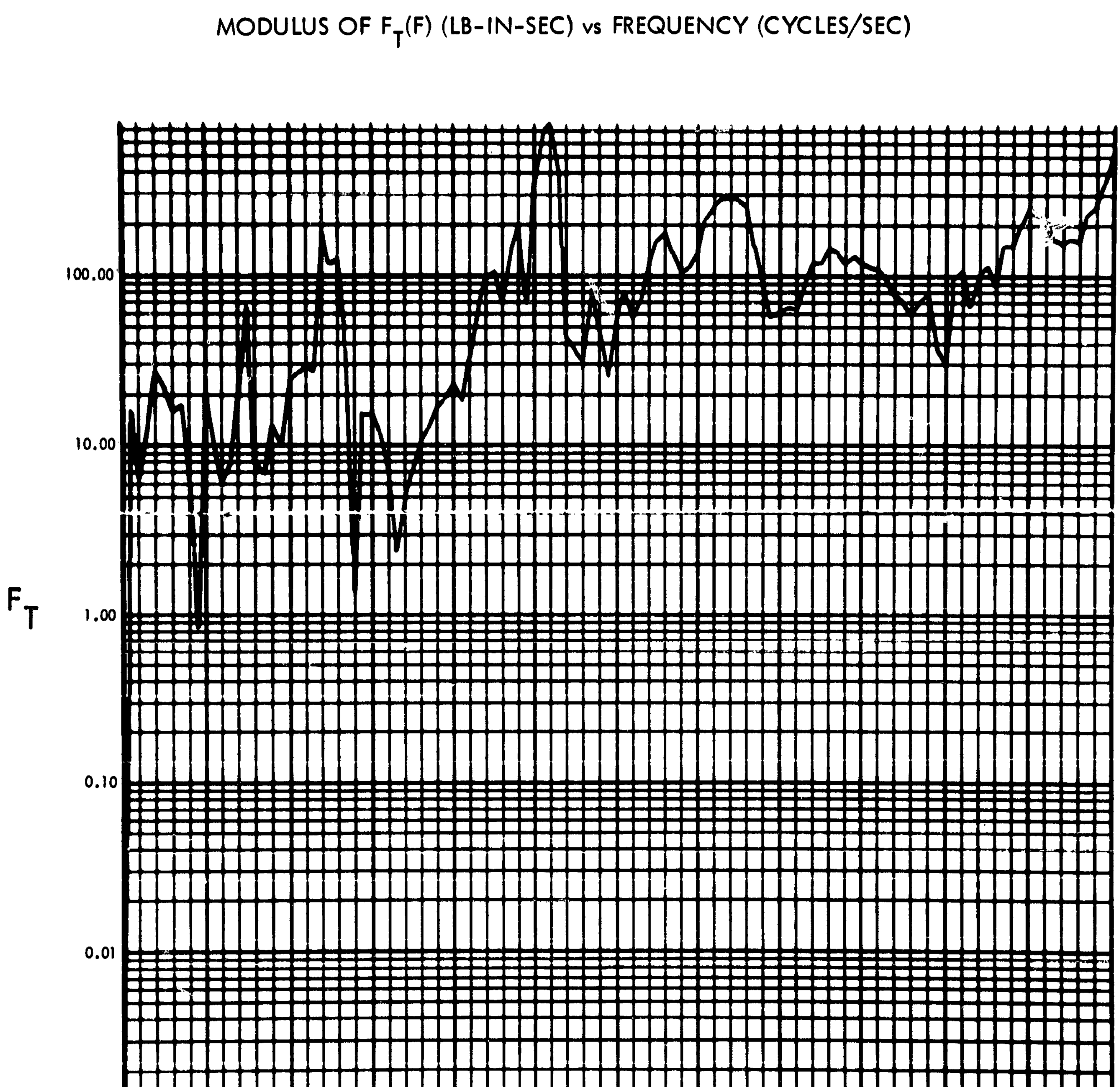

Fig. C-35. Joint 10, torque response, Fourier transform, modulus (pulse 3)

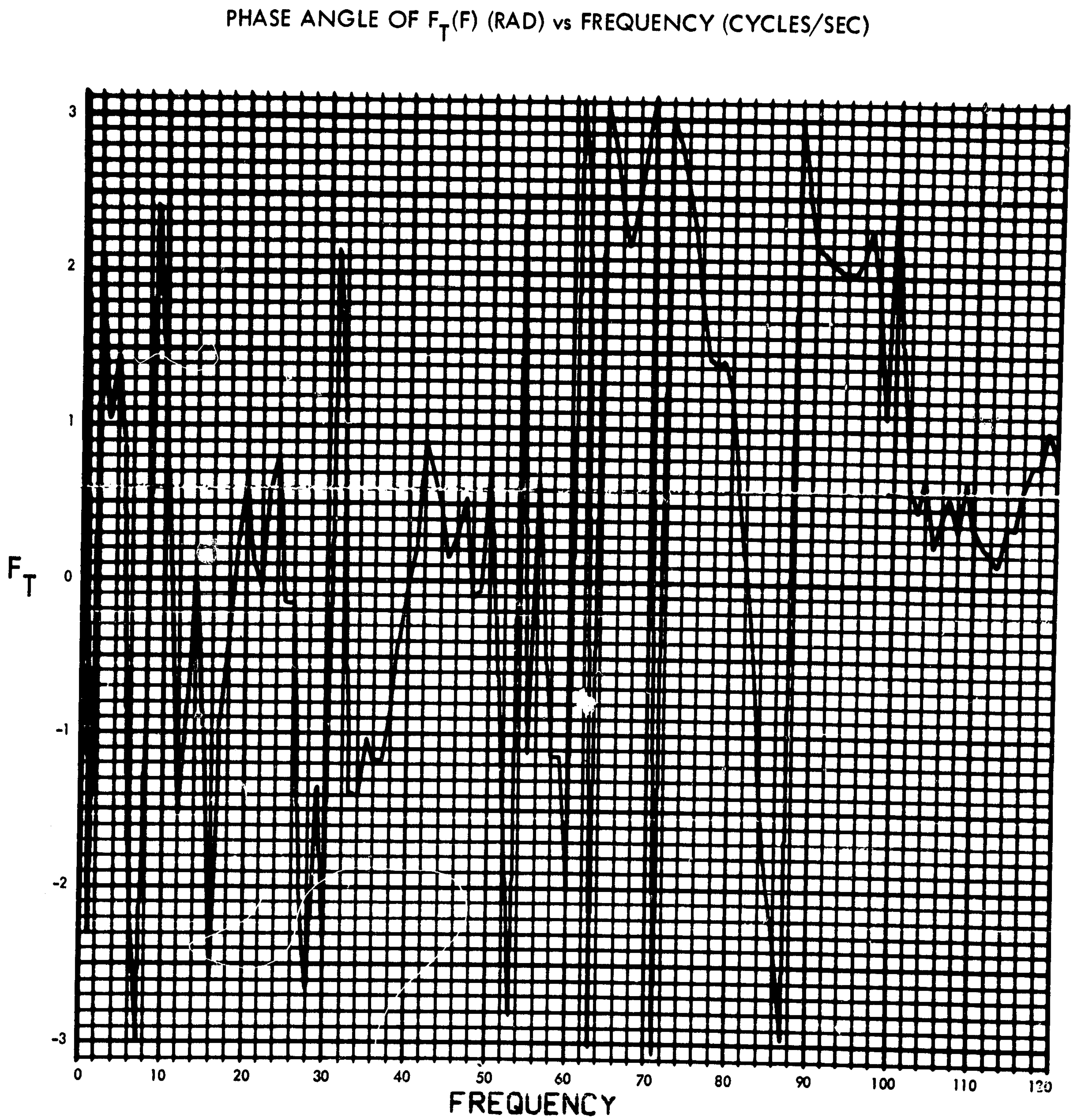

Fig. C-36. Joint 10, torque response, Fourier transform, phase angle (pulse 3)

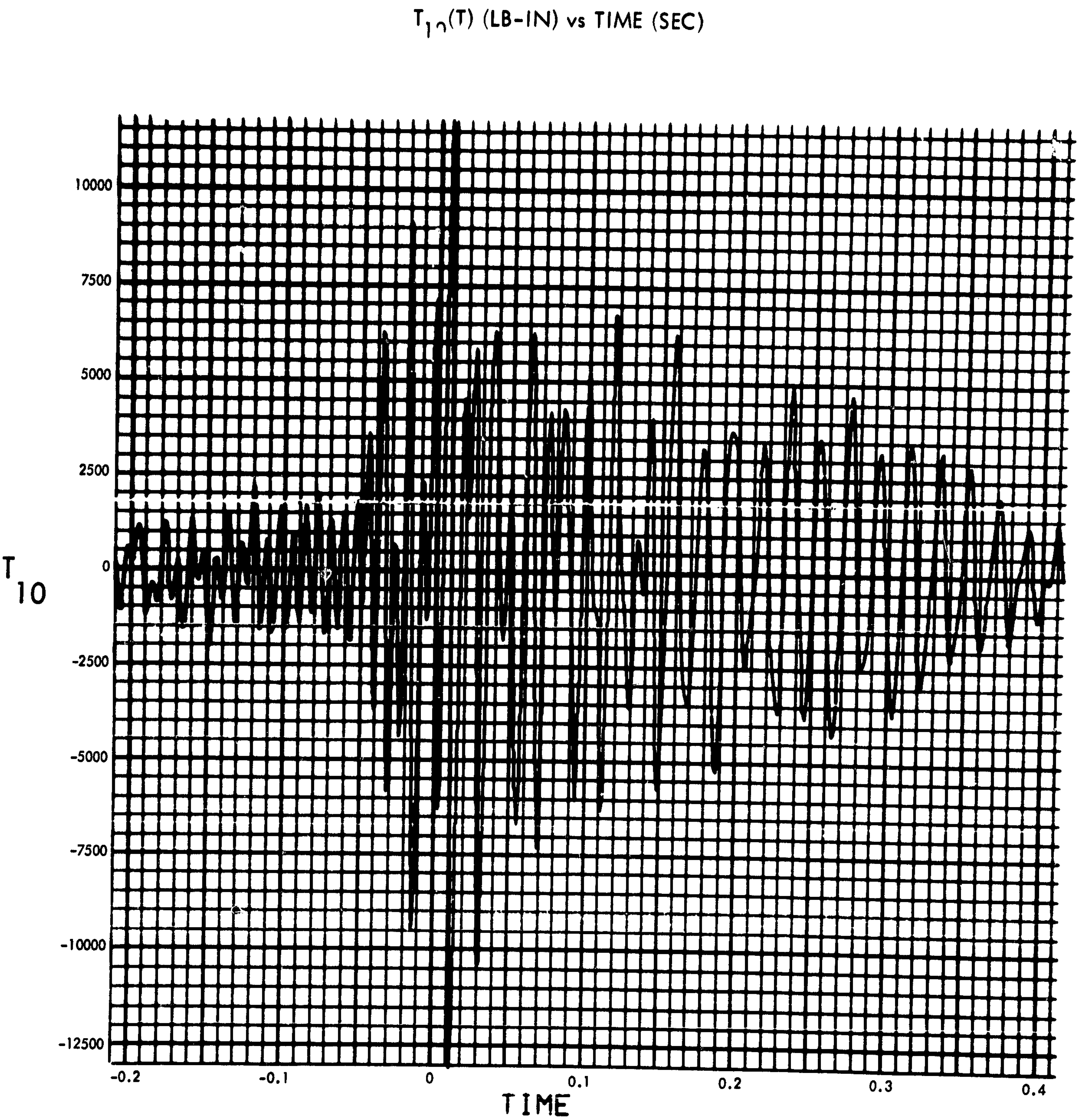

Fig. C-37. Joint 10, torque response, time history (pulse 3)

MODULUS OF $F_T(F)$ (LB-IN-SEC) vs FREQUENCY (CYCLES/SEC)

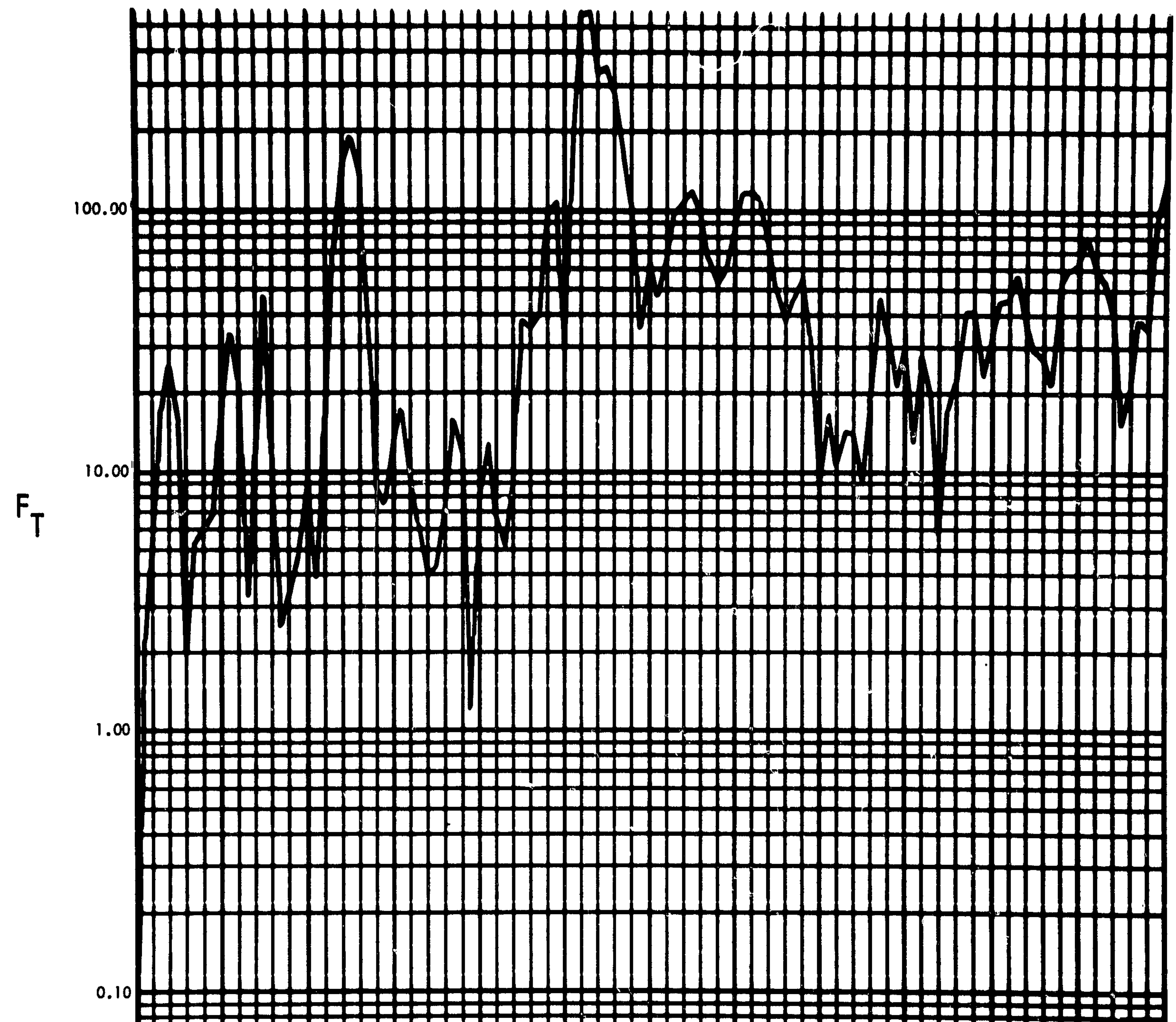

Fig. C-38. Joint 10, torque response, Fourier transform, modulus (pulse 4)

PHASE ANGLE OF $F_T(F)$ (RAD) vs FREQUENCY (CYCLES/SEC)

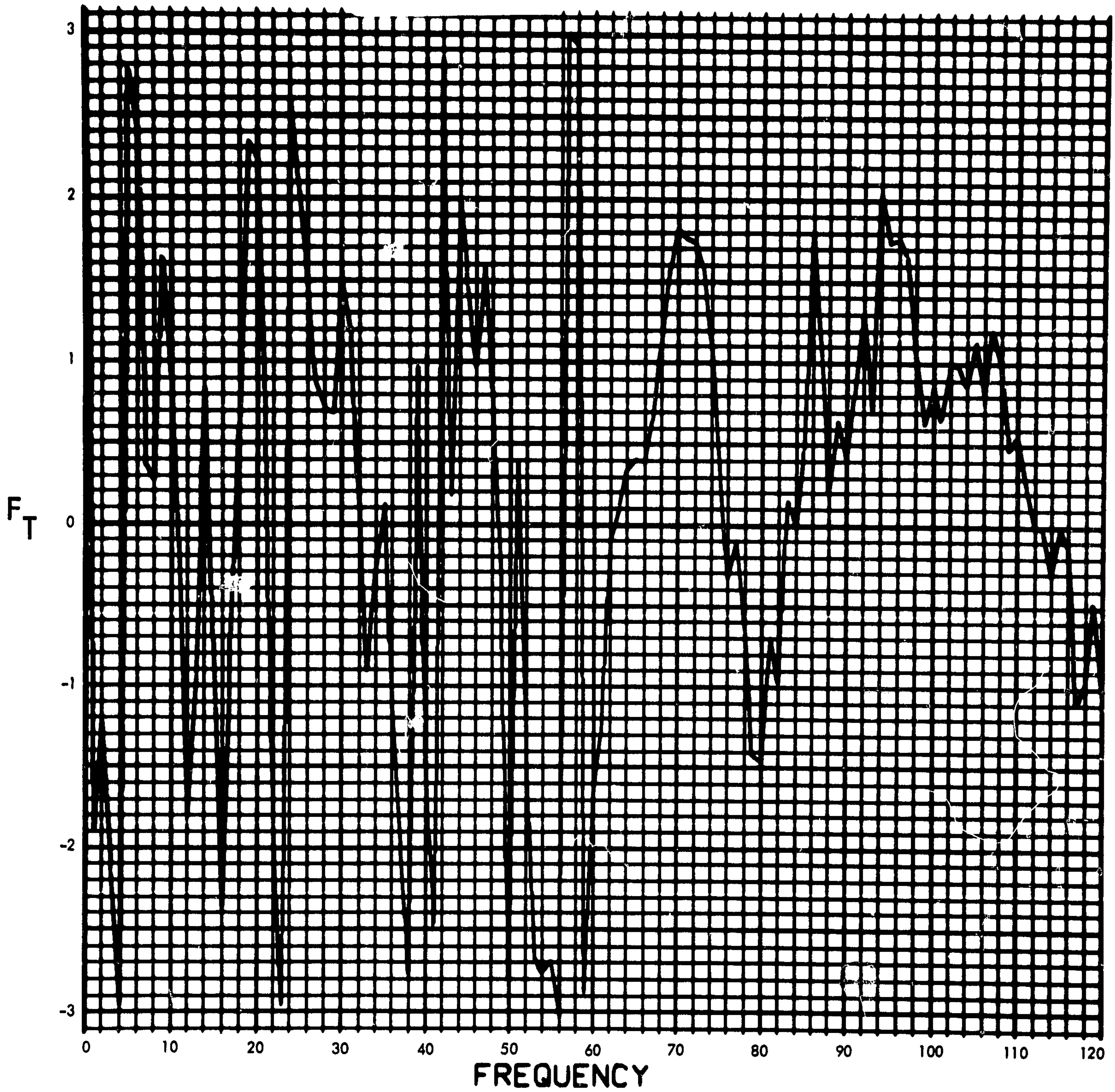

Fig. C-39. Joint 10, torque response, Fourier transform, phase angle (pulse 4)

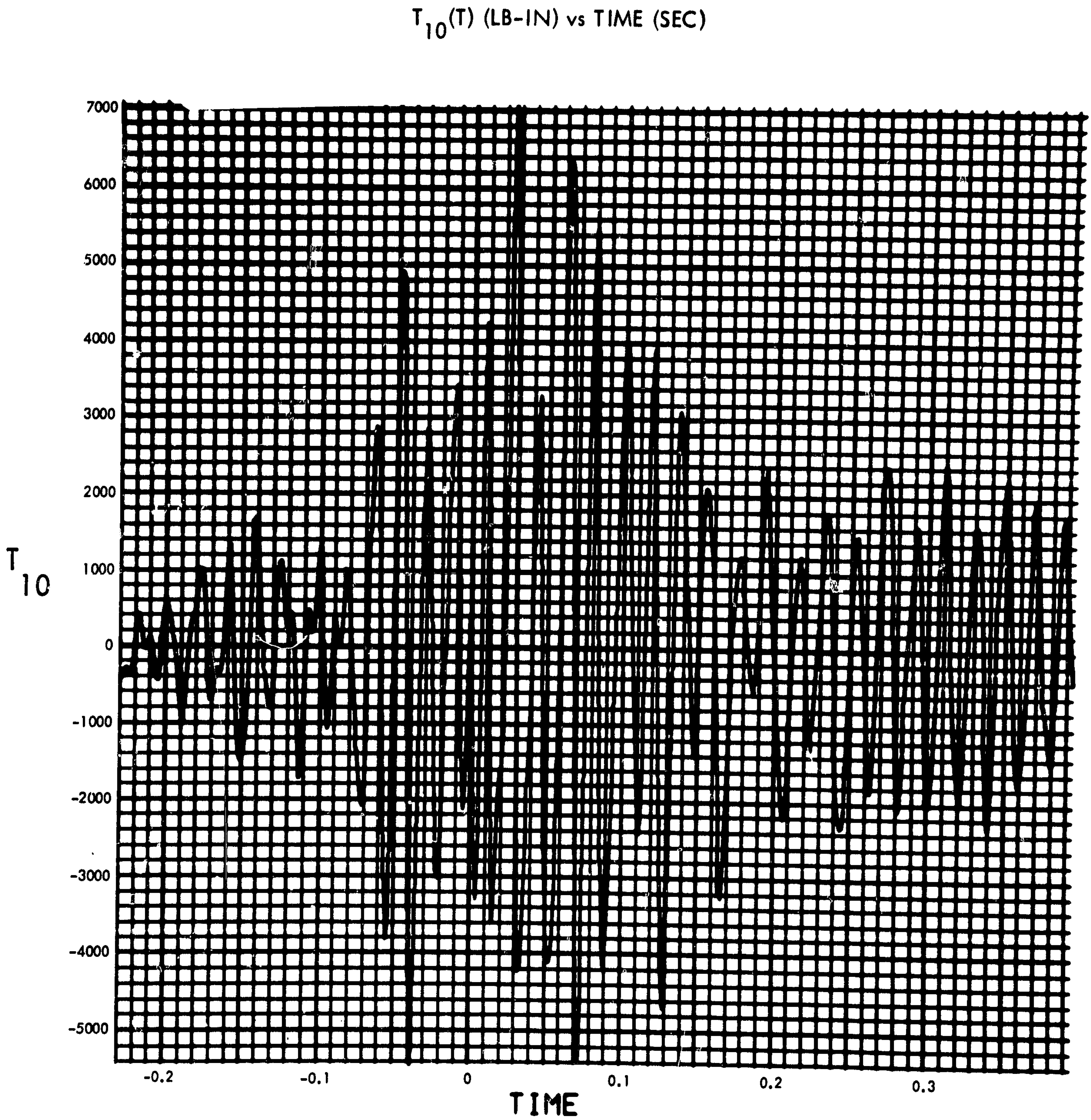

Fig. C-40. Joint 10, torque response, time history (pulse 4)

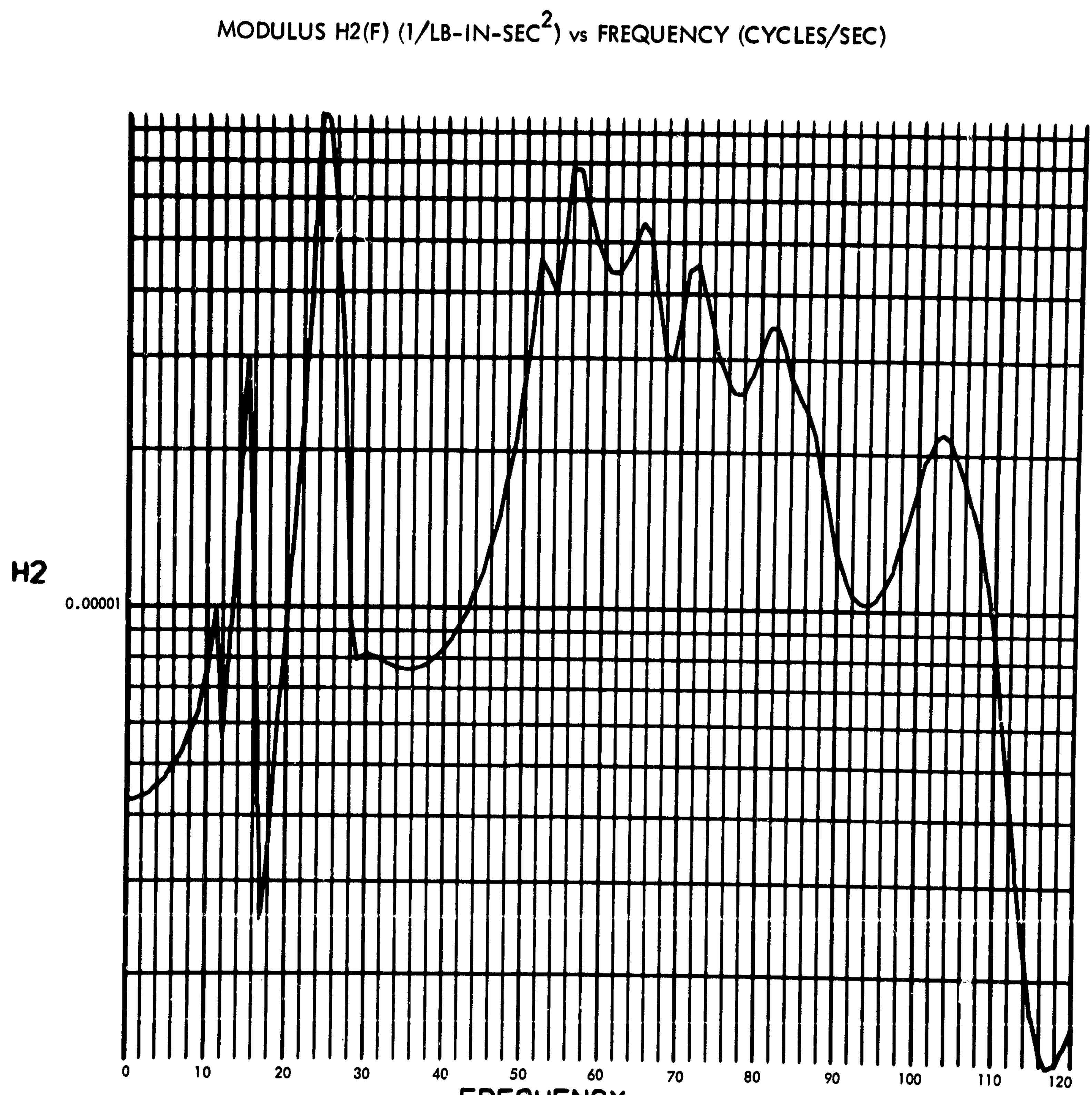

Fig. C-41. Joint 11, acceleration transfer function, Fourier transform, modulus

PHASE ANGLE OF H2(F) (RAD) vs FREQUENCY (CYCLES/SEC)

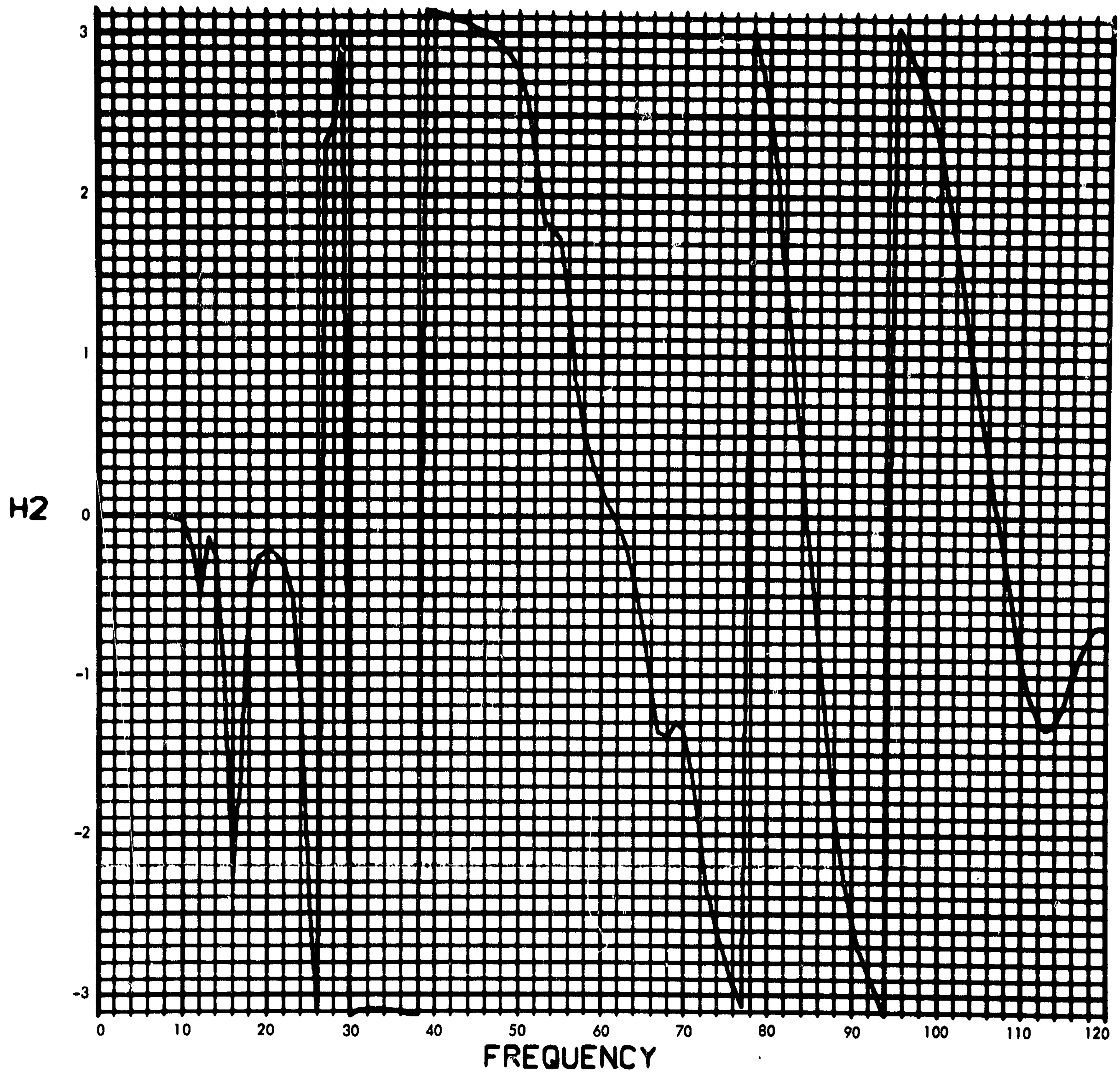

Fig. C-42. Joint 11, acceleration transfer function, Fourier transform, phase angle

MODULUS OF V2(F) (RAD/SEC) vs FREQUENCY (CYCLES/SEC)

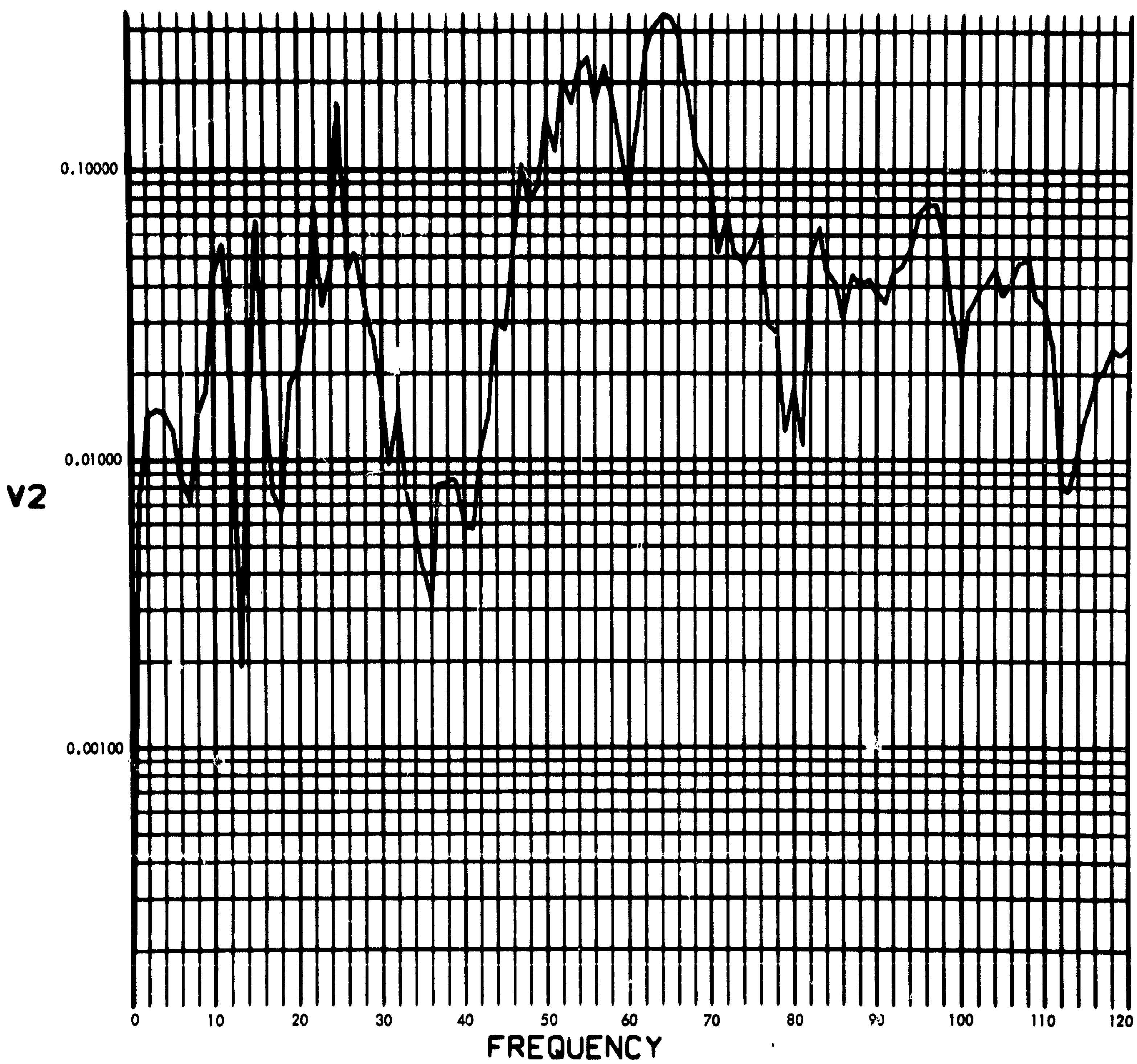

Fig. C-43. Joint 11, acceleration response, Fourier transform, modulus (pulse 1)

PHASE ANGLE OF V2(F) (RAD) vs FREQUENCY (CYCLES/SEC)

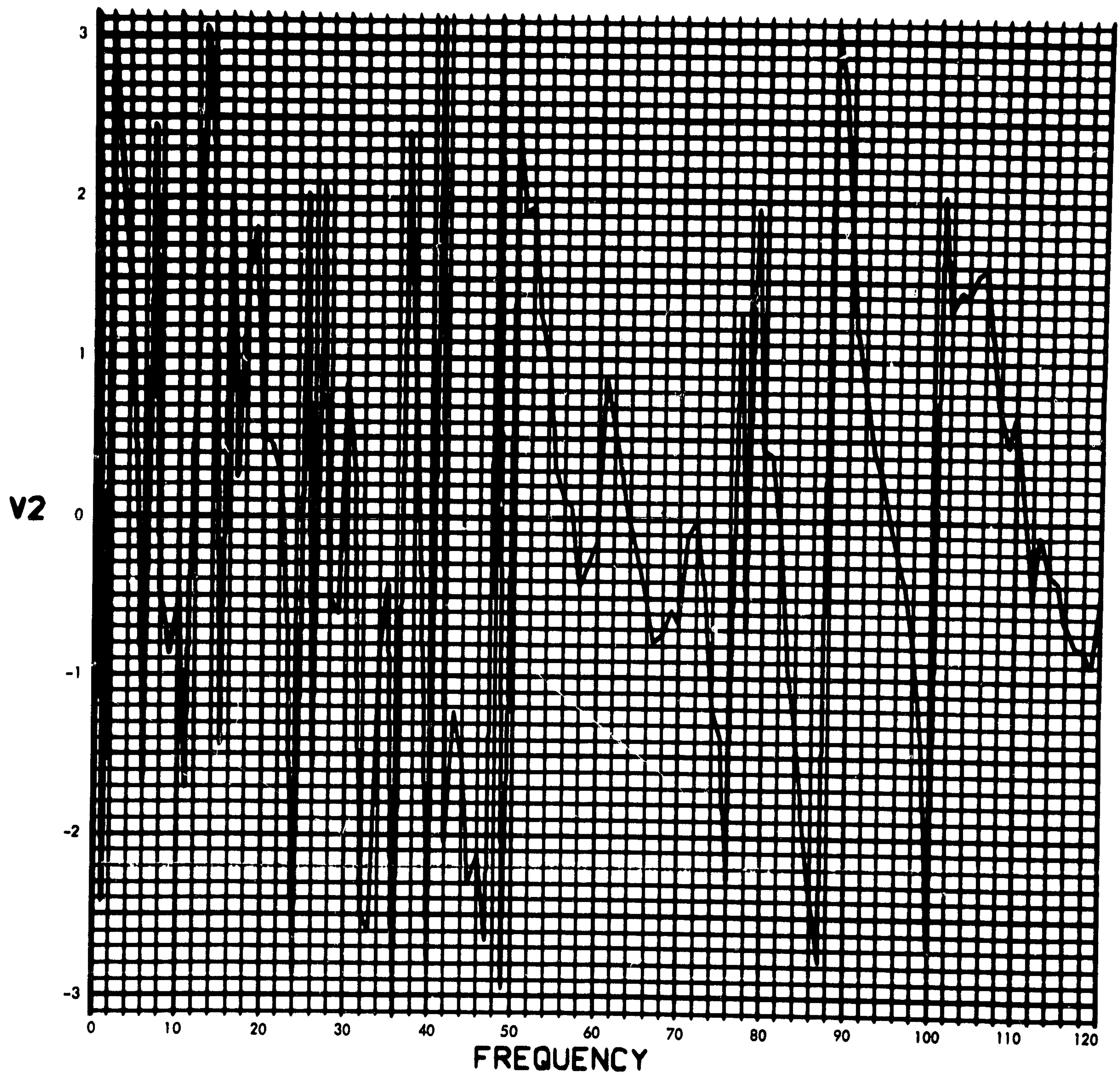

Fig. C-44. Joint 11, acceleration response, Fourier transform, phase angle (pulse 1)

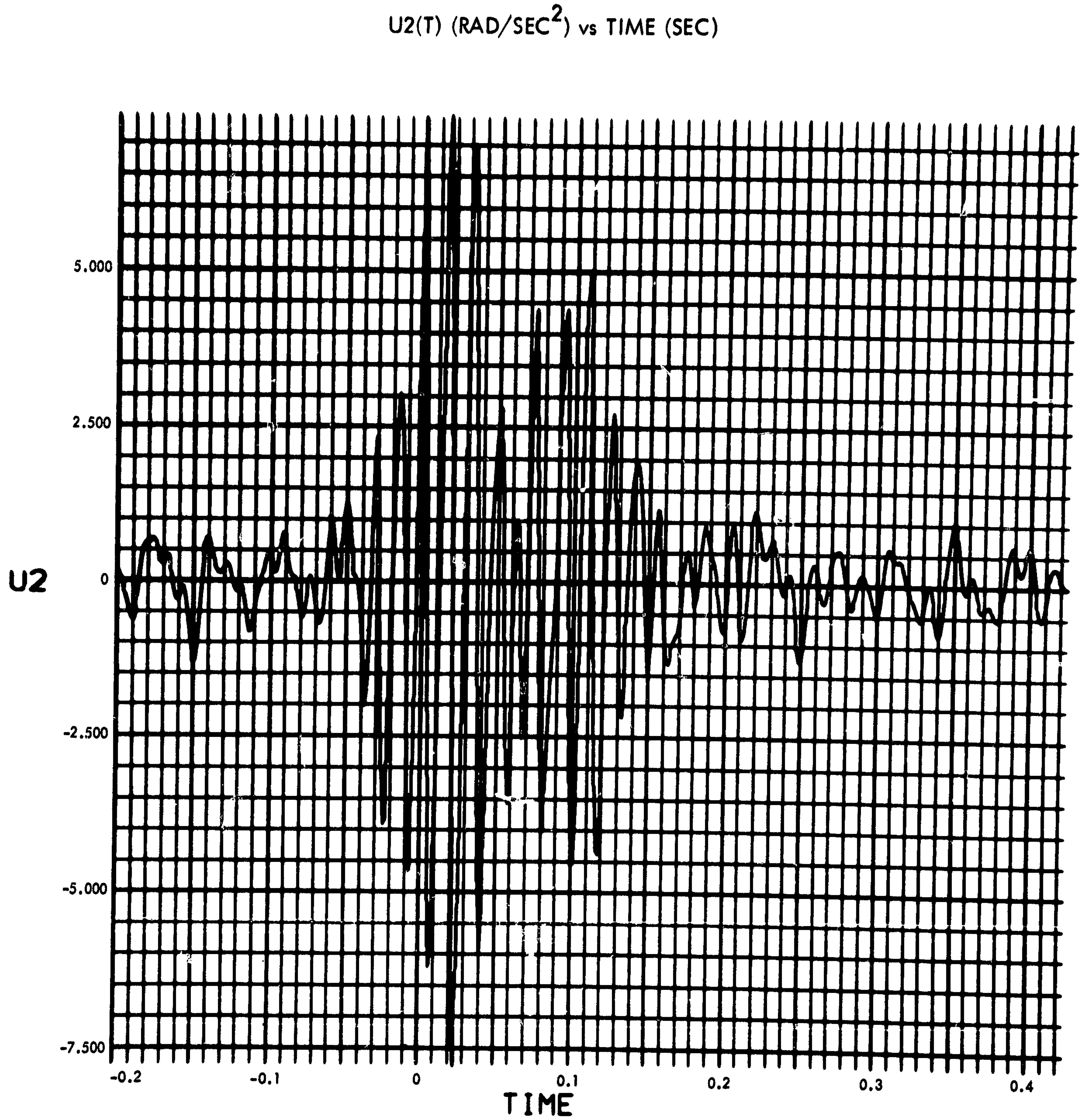

Fig. C-45. Joint 11, acceleration response, time history (pulse 1)

MODULUS OF V2(F) (RAD/SEC) vs FREQUENCY (CYCLES/SEC)

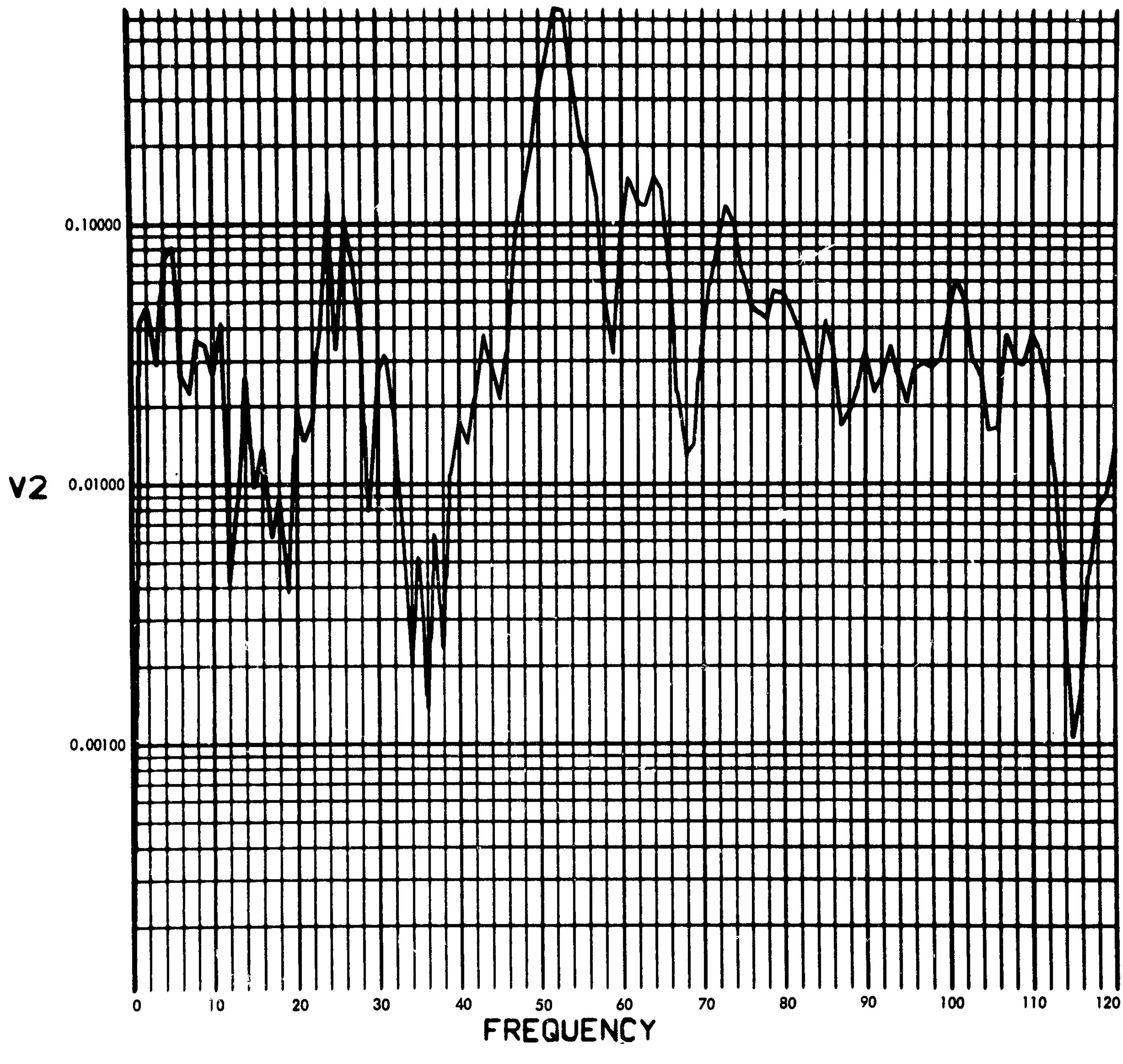

Fig. C-46. Joint 11, acceleration response, Fourier transform, modulus (pulse 2)

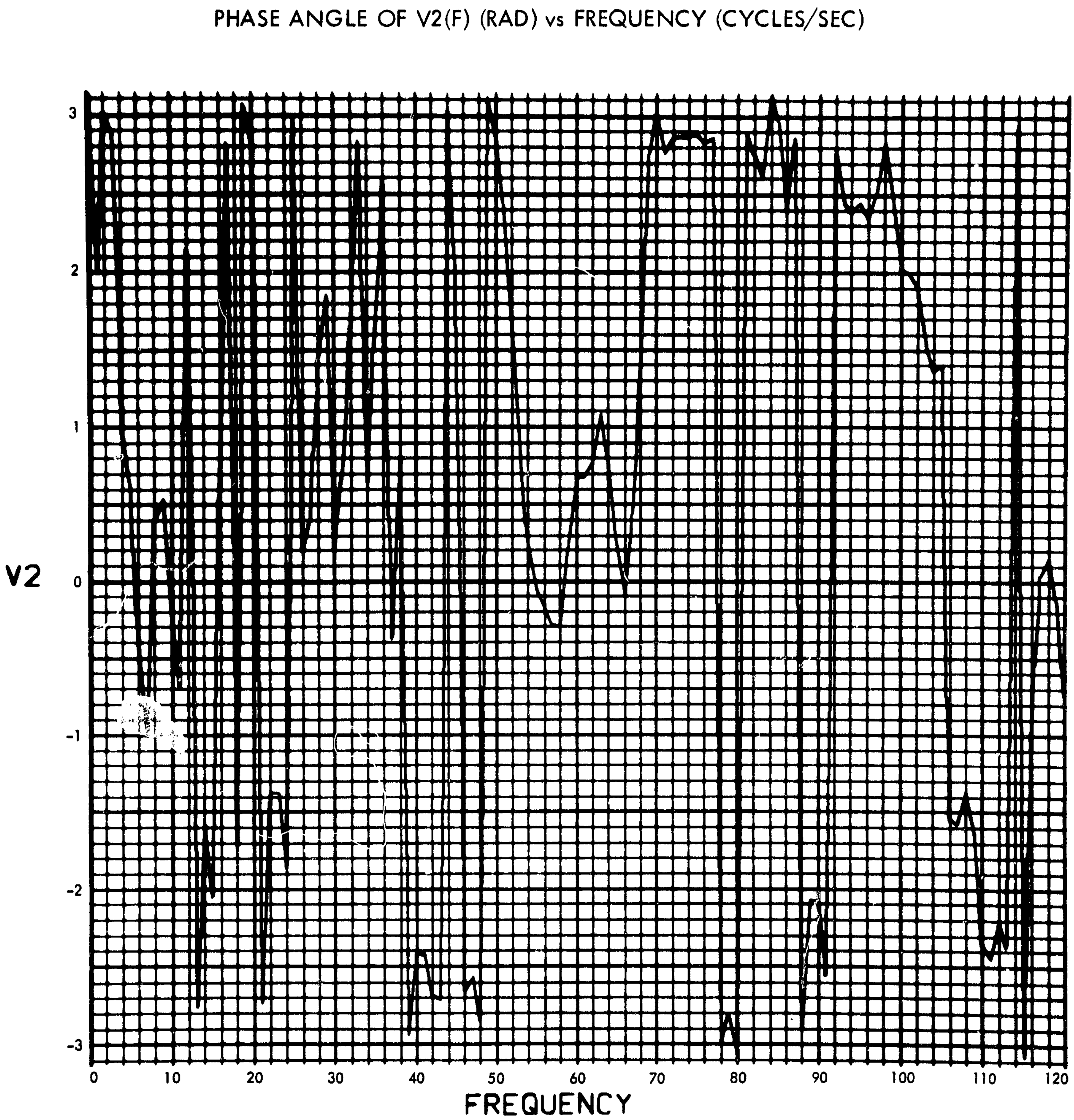

Fig. C-47. Joint 11, acceleration response, Fourier transform, phase angle (pulse 2)

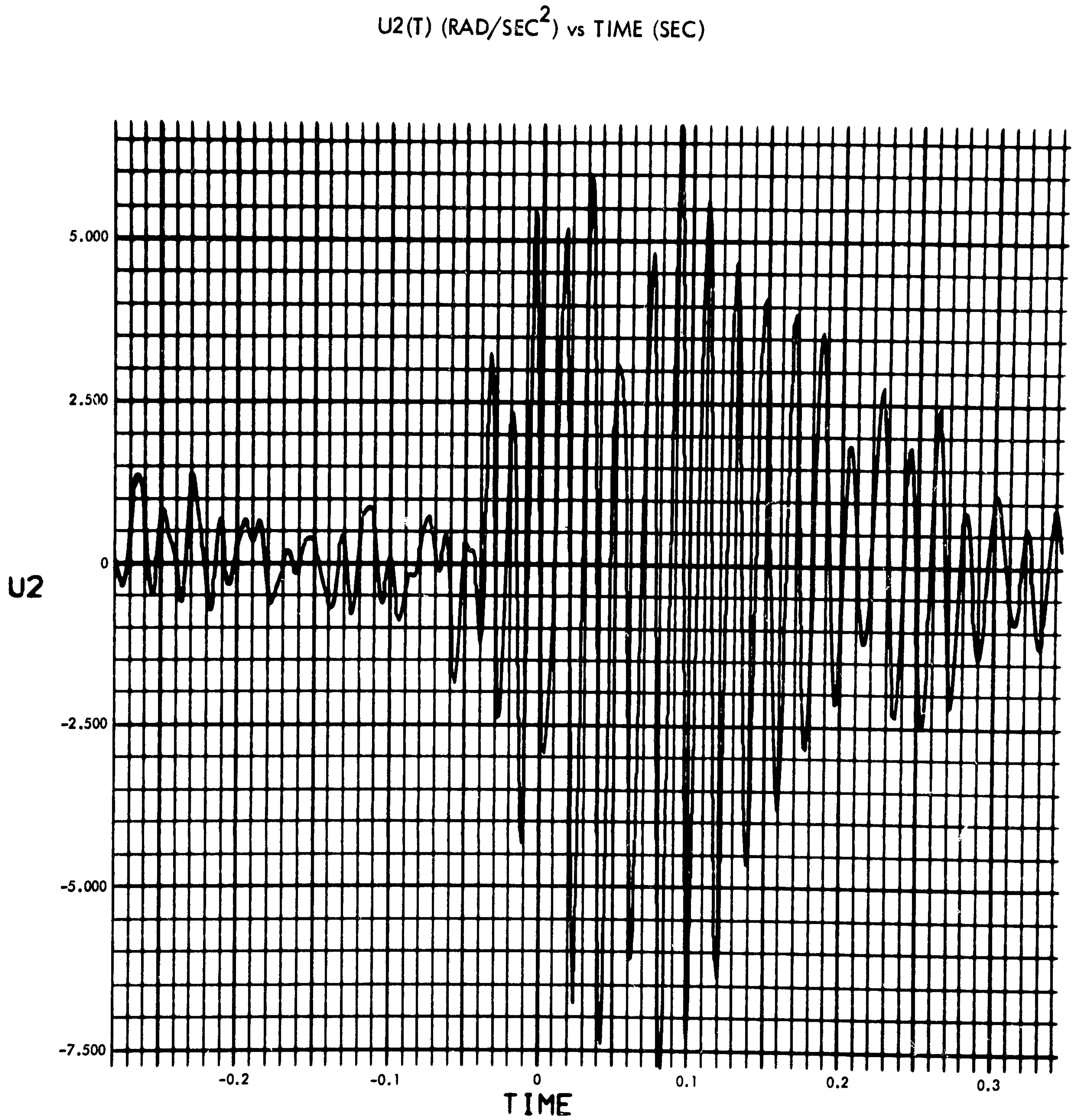

Fig. C-48. Joint 11, acceleration response, time history (pulse 2)

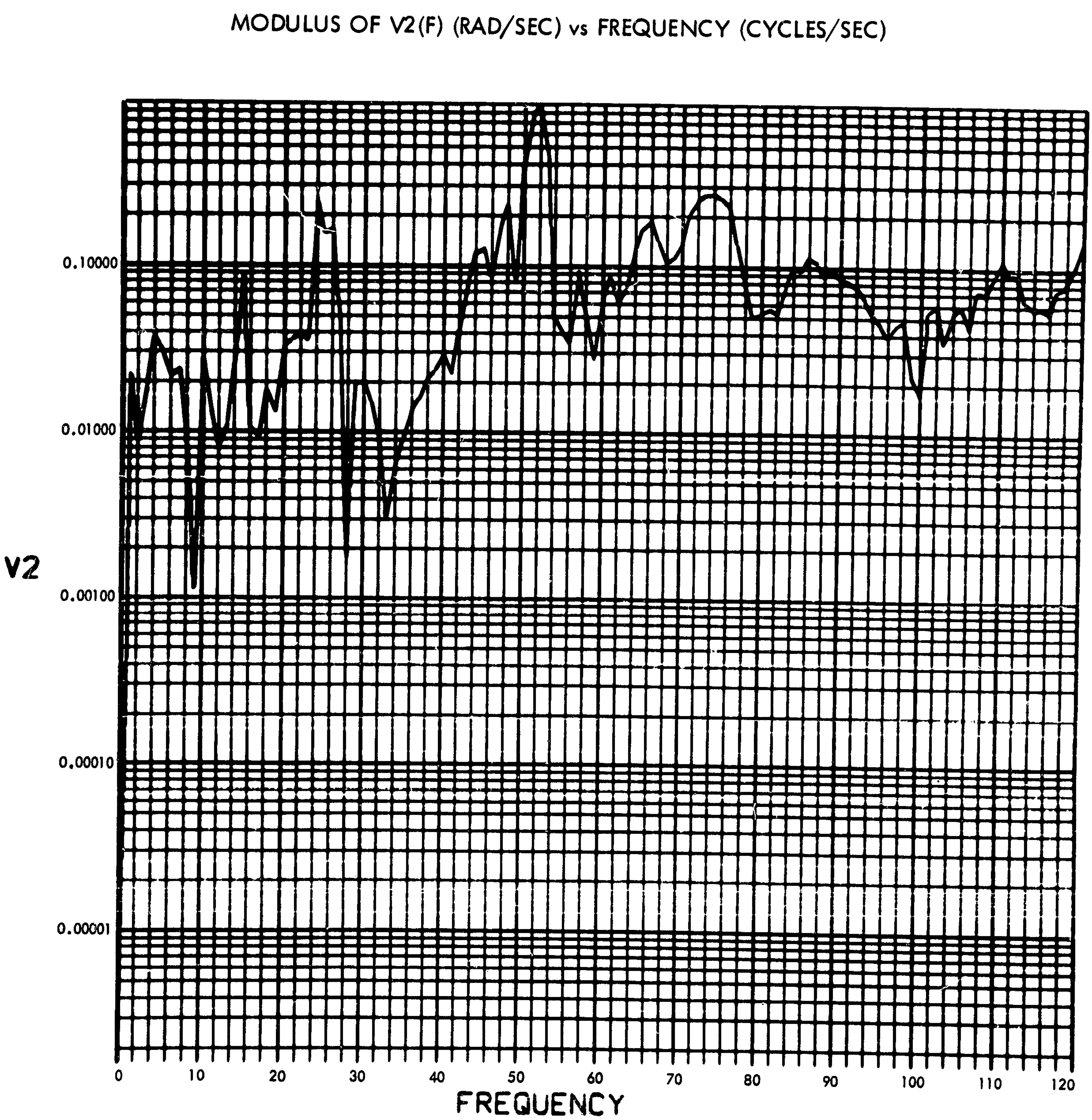

Fig. C-49. Joint 11, acceleration response, Fourier transform, modulus (pulse 3)

PHASE ANGLE OF V2(F) (RAD) vs FREQUENCY (CYCLES/SEC)

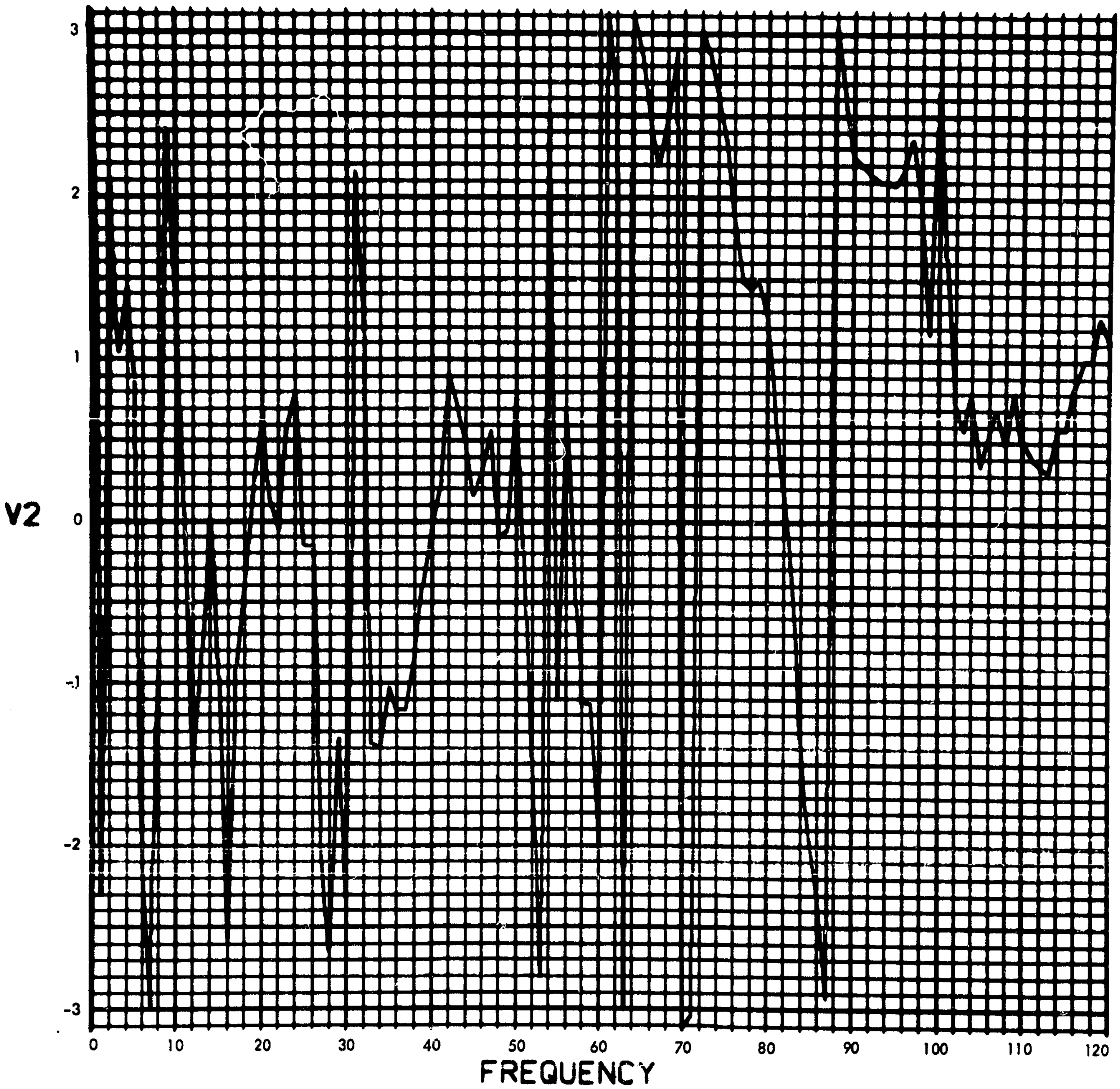

Fig. C-50. Joint 11, acceleration response, Fourier transform, phase angle (pulse 3)

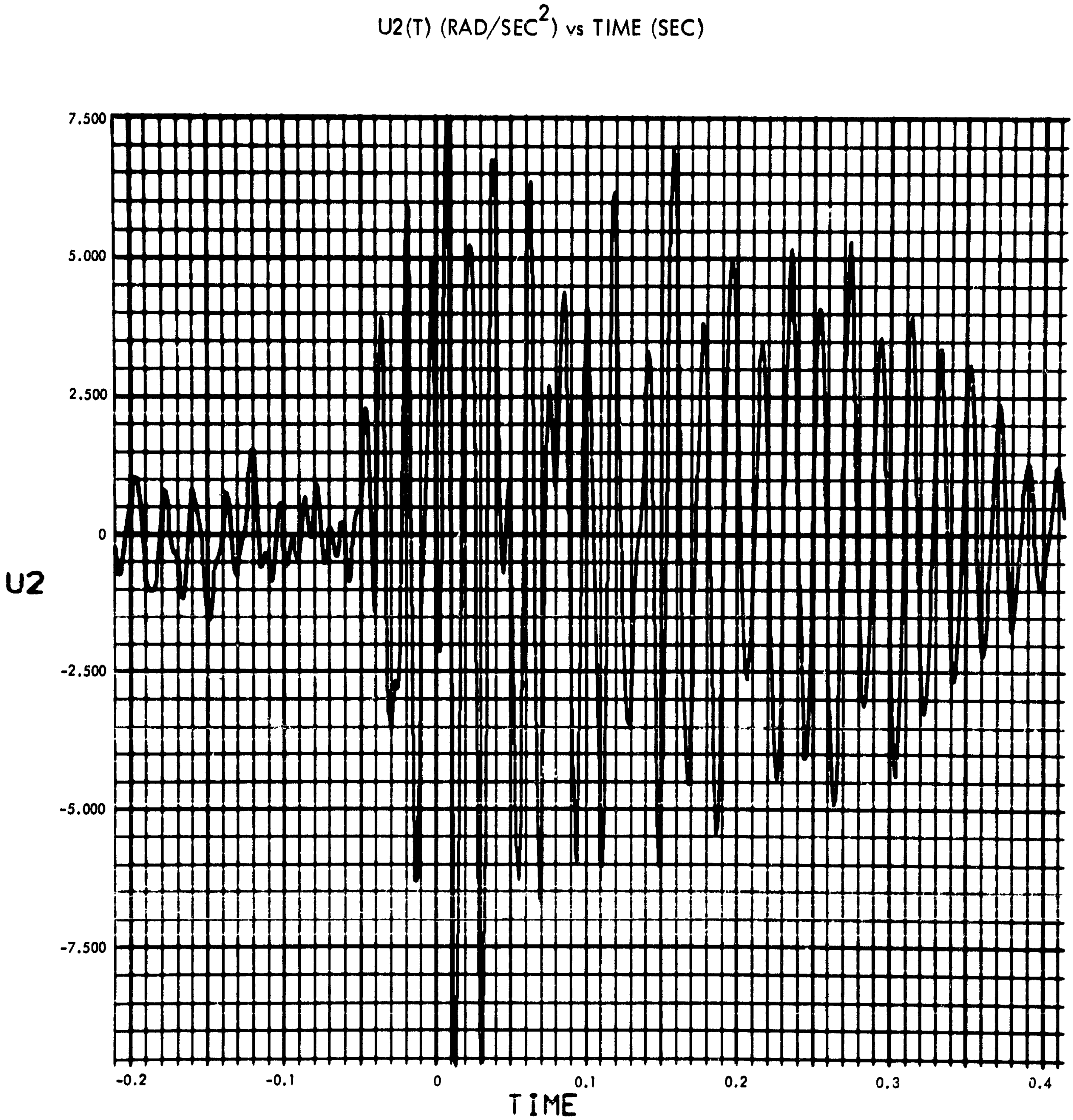

Fig. C-51. Joint 11, acceleration response, time history (pulse 3)

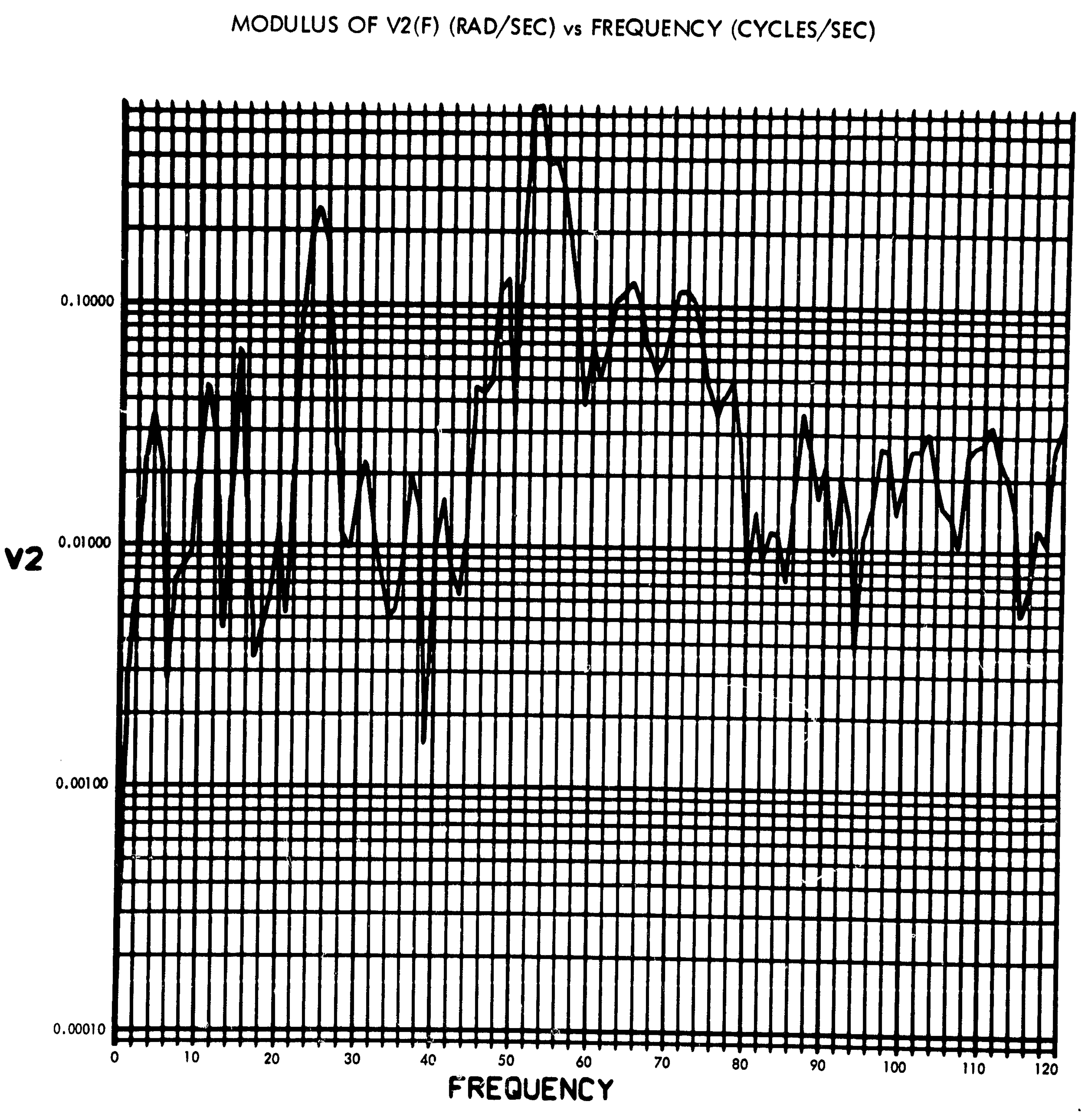

Fig. C-52. Joint 11, acceleration response, Fourier transform, modulus (pulse 4)

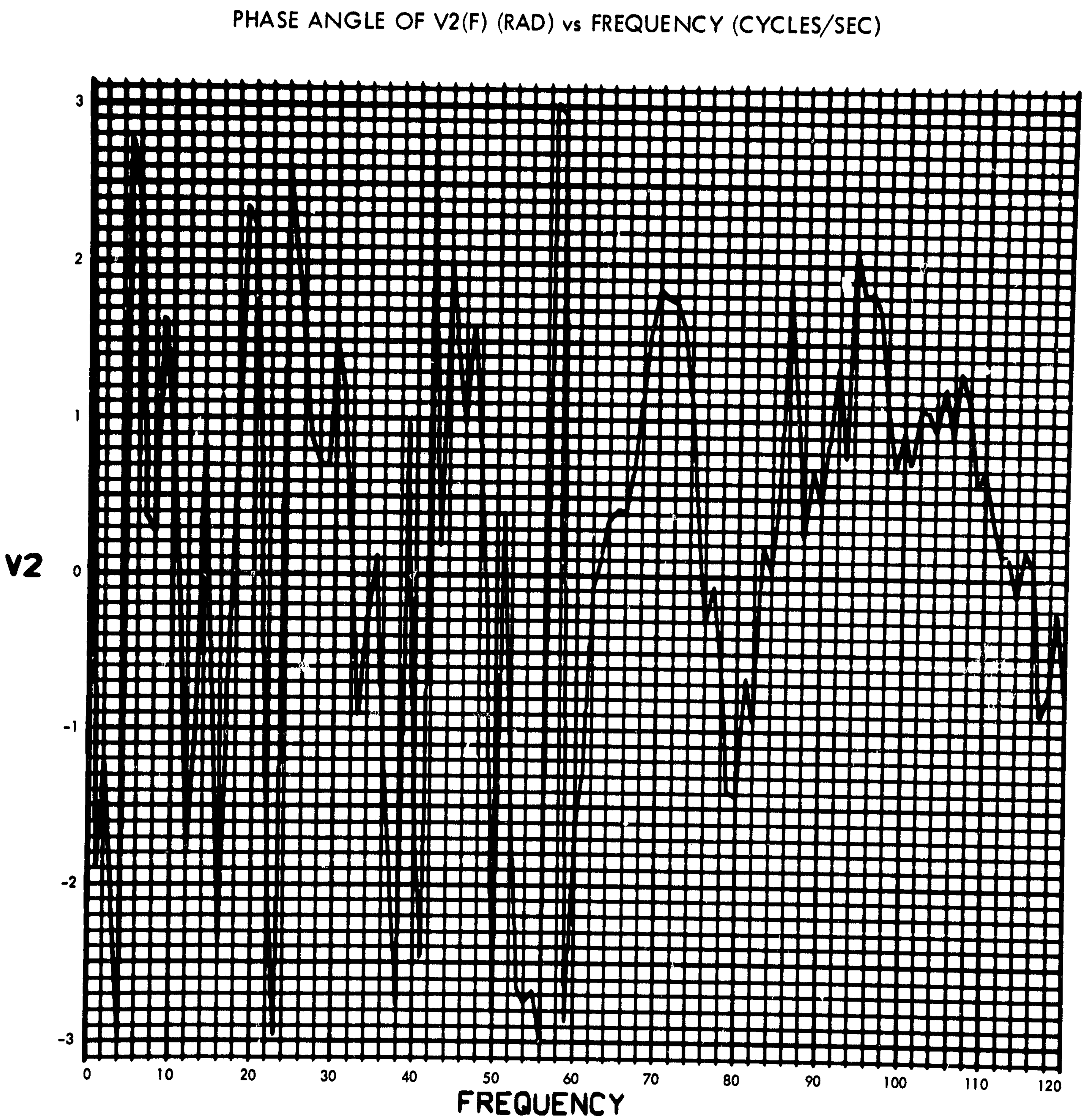

Fig. C-53. Joint 11, acceleration response, Fourier transform, phase angle (pulse 4)

U2(T) (RAD/SEC^2) vs TIME (SEC)

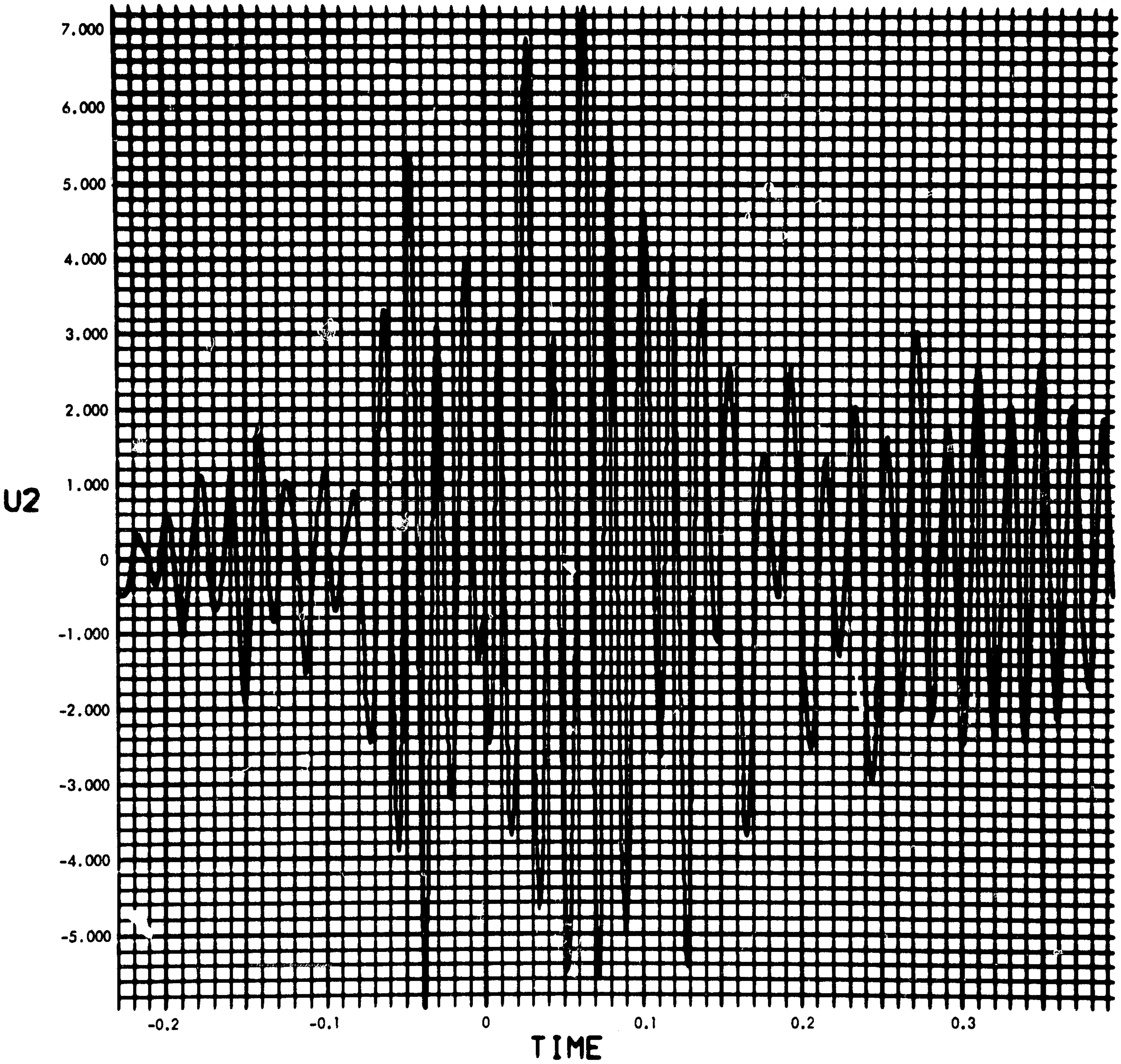

Fig. C-54. Joint 11, acceleration response, time history (pulse 4)

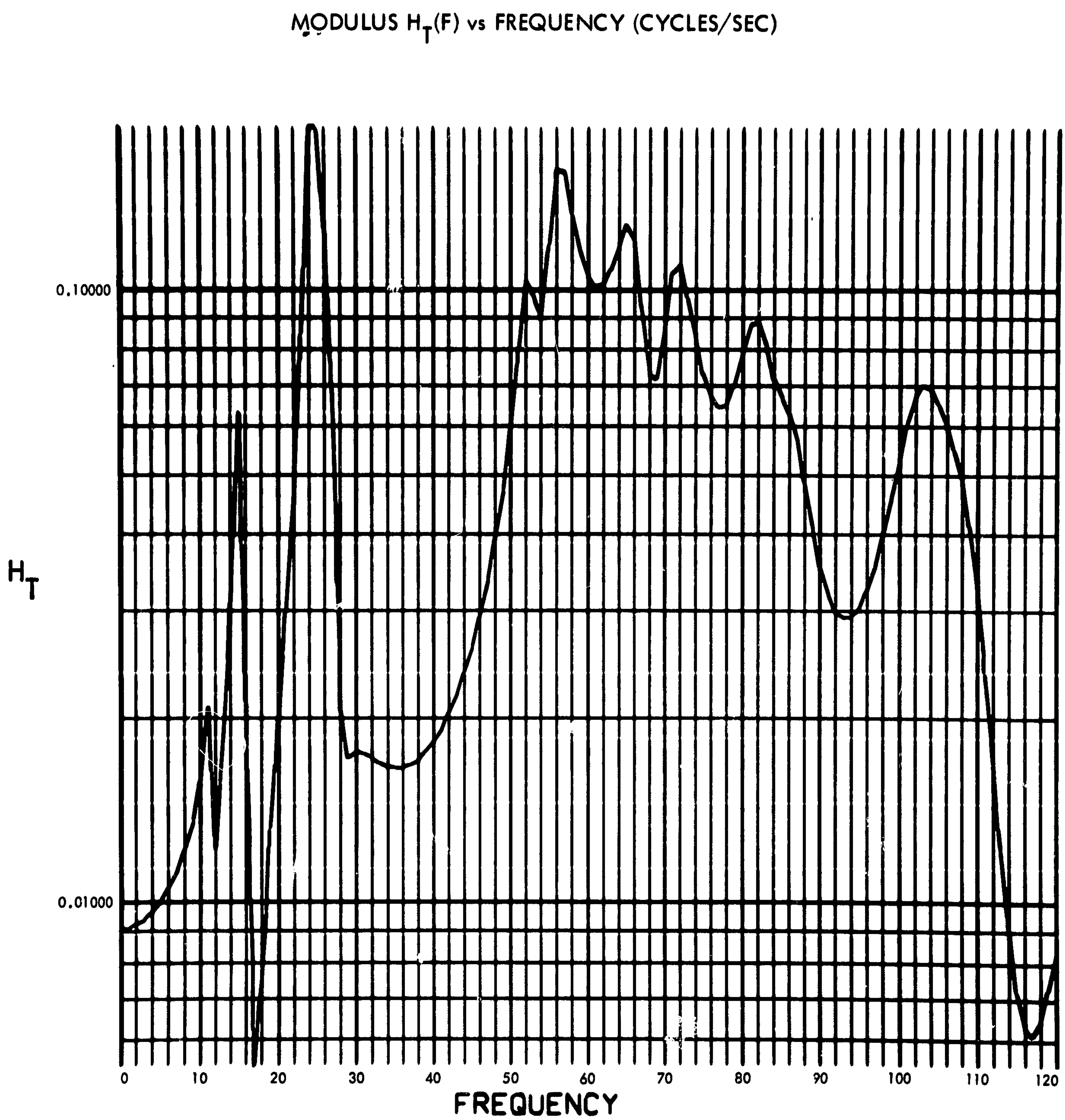

Fig. C-55. Joint 11, torque transfer function, Fourier transform, modulus

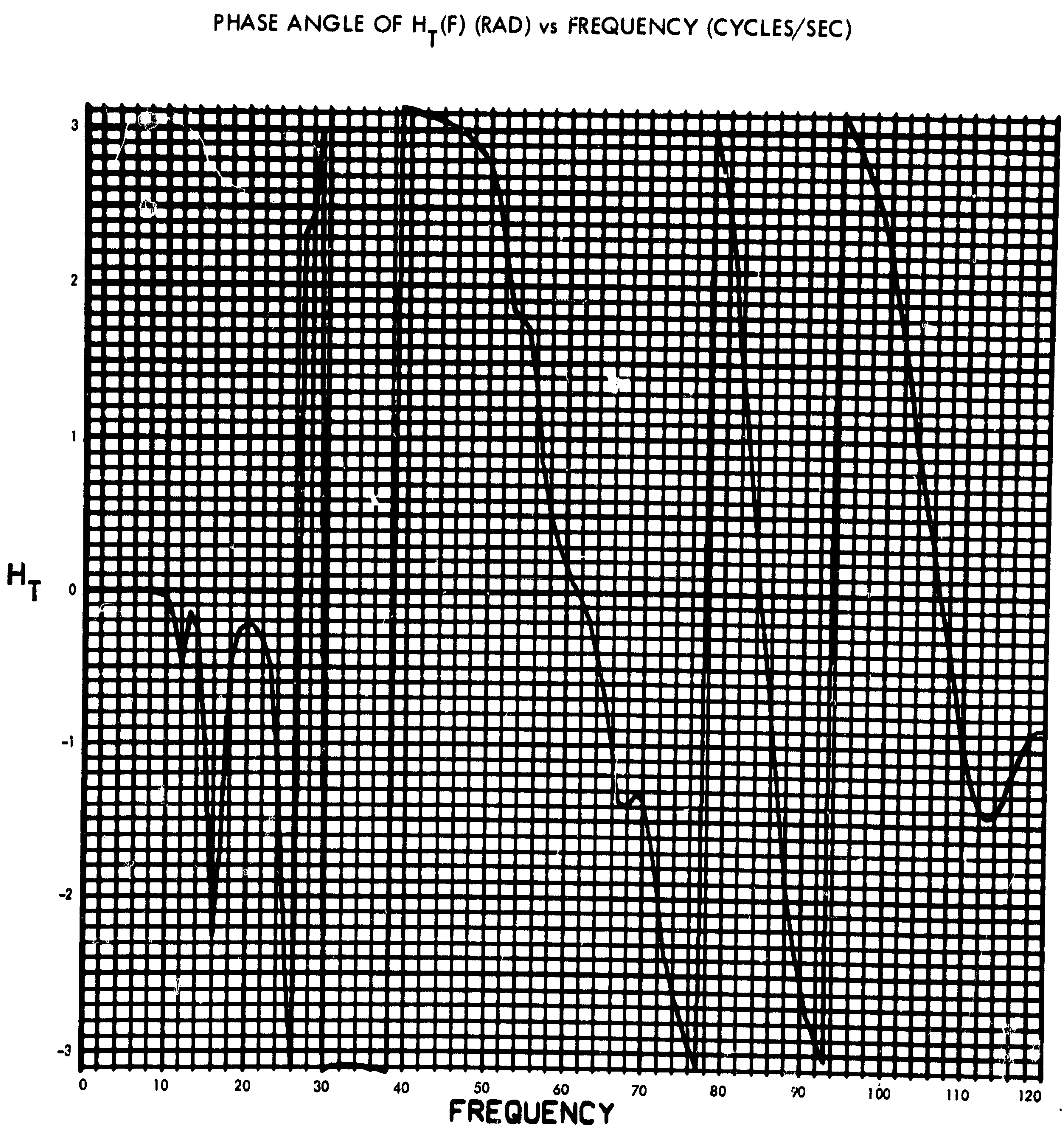

Fig. C-56. Joint 11, torque transfer function, Fourier transform, phase angle

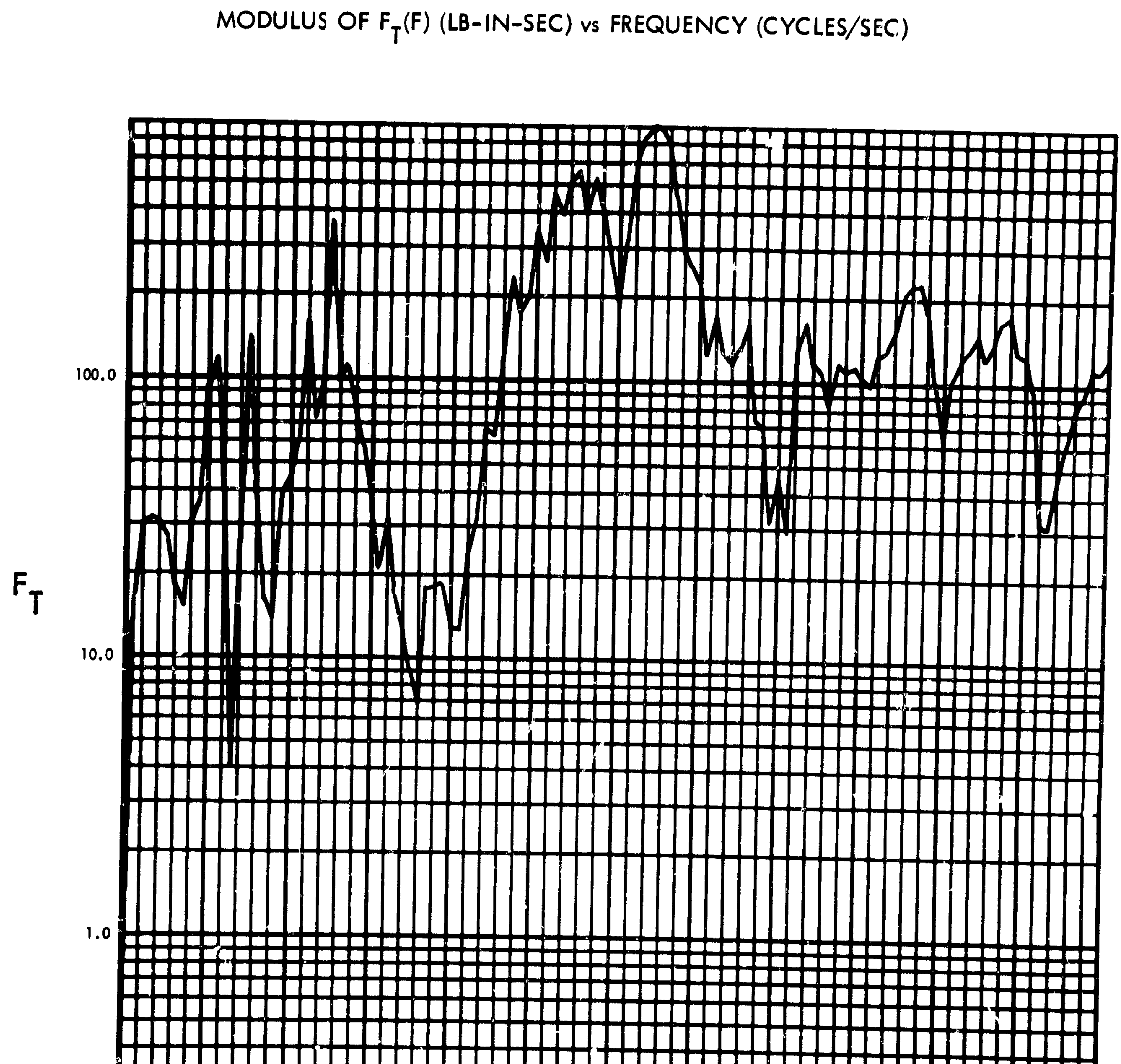

Fig. C-57. Joint 11, torque response, Fourier transform, modulus (pulse 1)

PHASE ANGLE OF $F_T(F)$ (RAD) vs FREQUENCY (CYCLES/SEC)

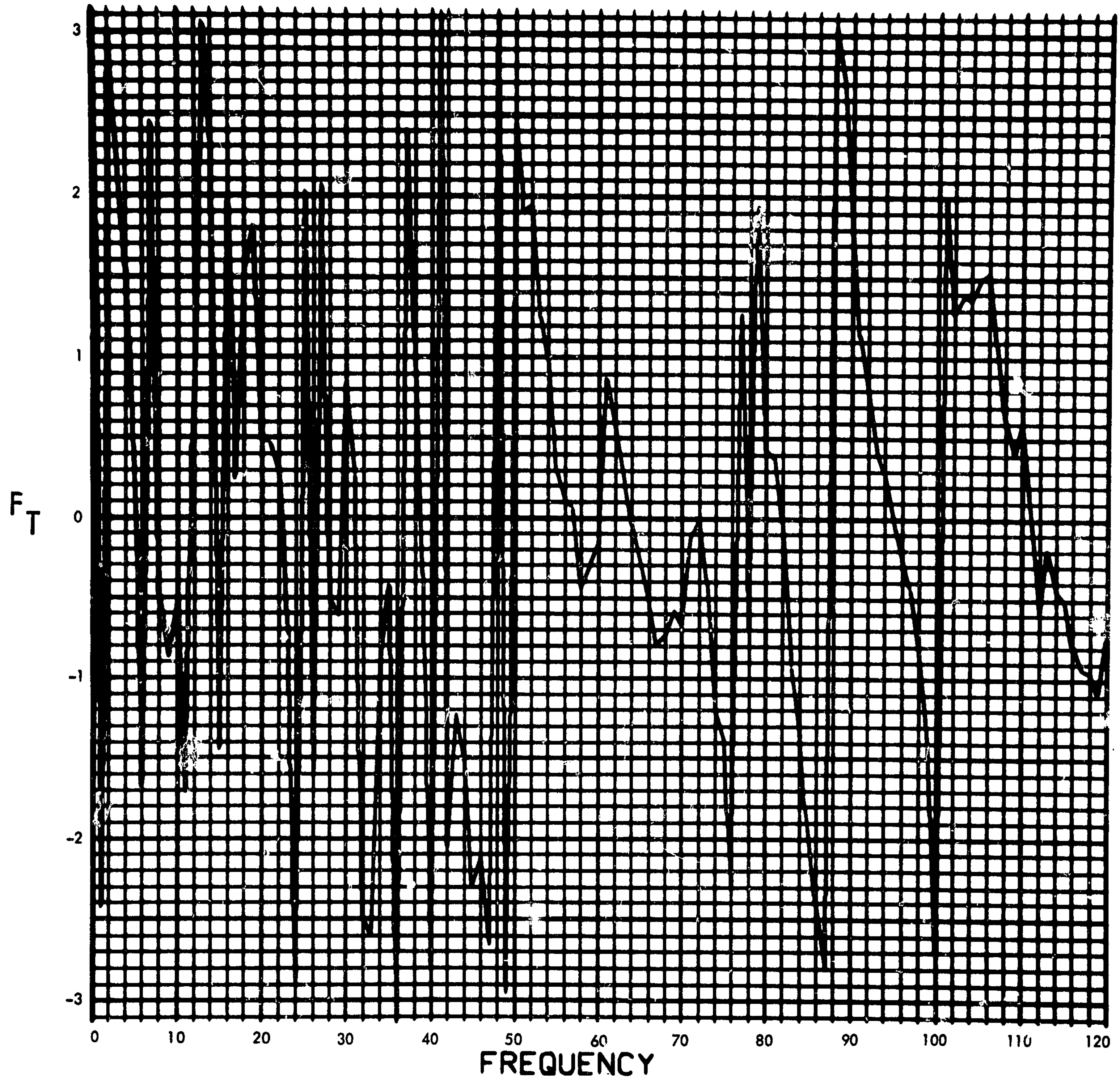

Fig. C-58. Joint 11, torque response, Fourier transform, phase angle (pulse 1)

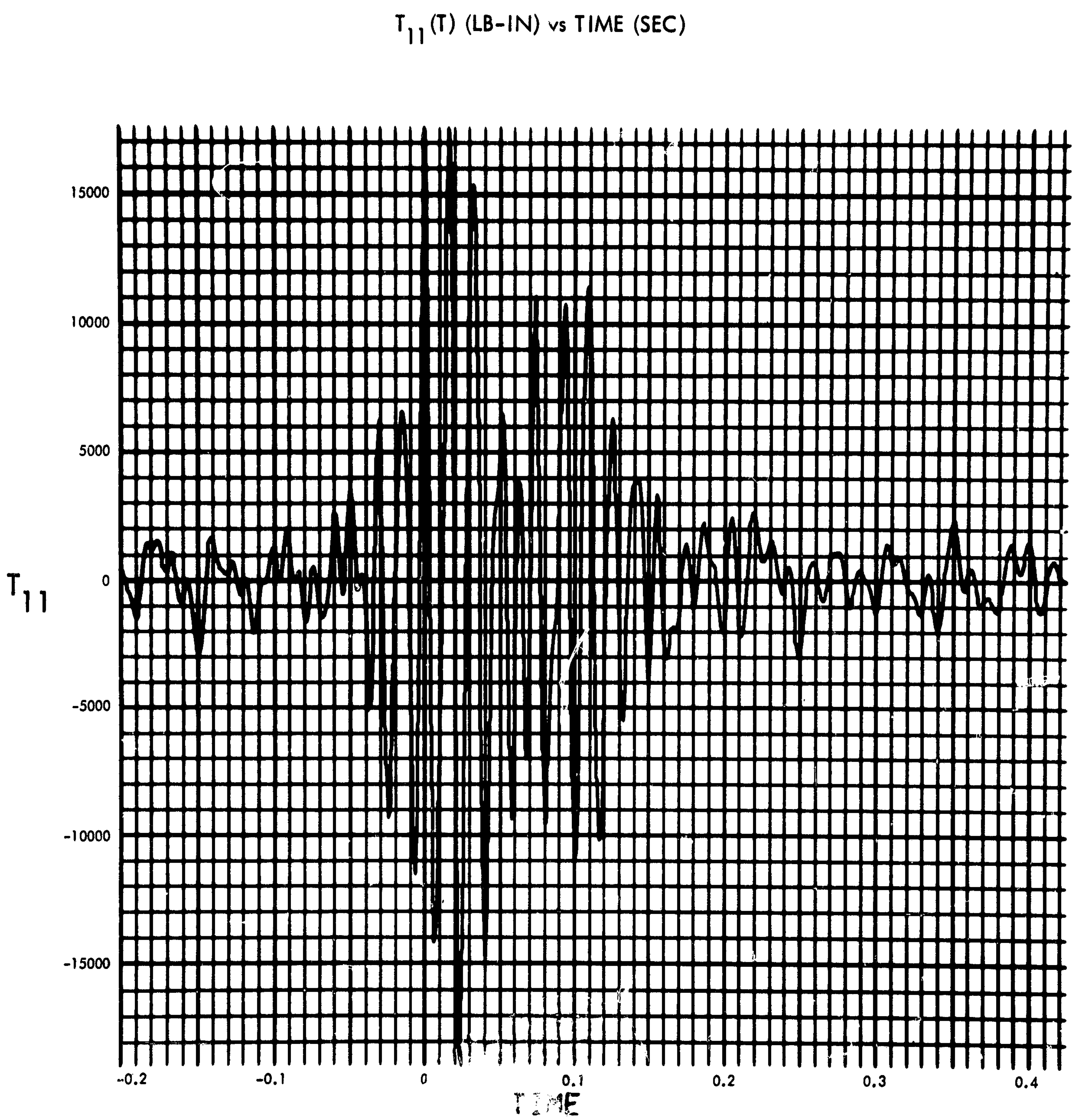

Fig. C-59. Joint 11, torque response, time history (pulse 1)

MODULUS OF $F_T(F)$ (LB-IN-SEC) vs FREQUENCY (CYCLES/SEC)

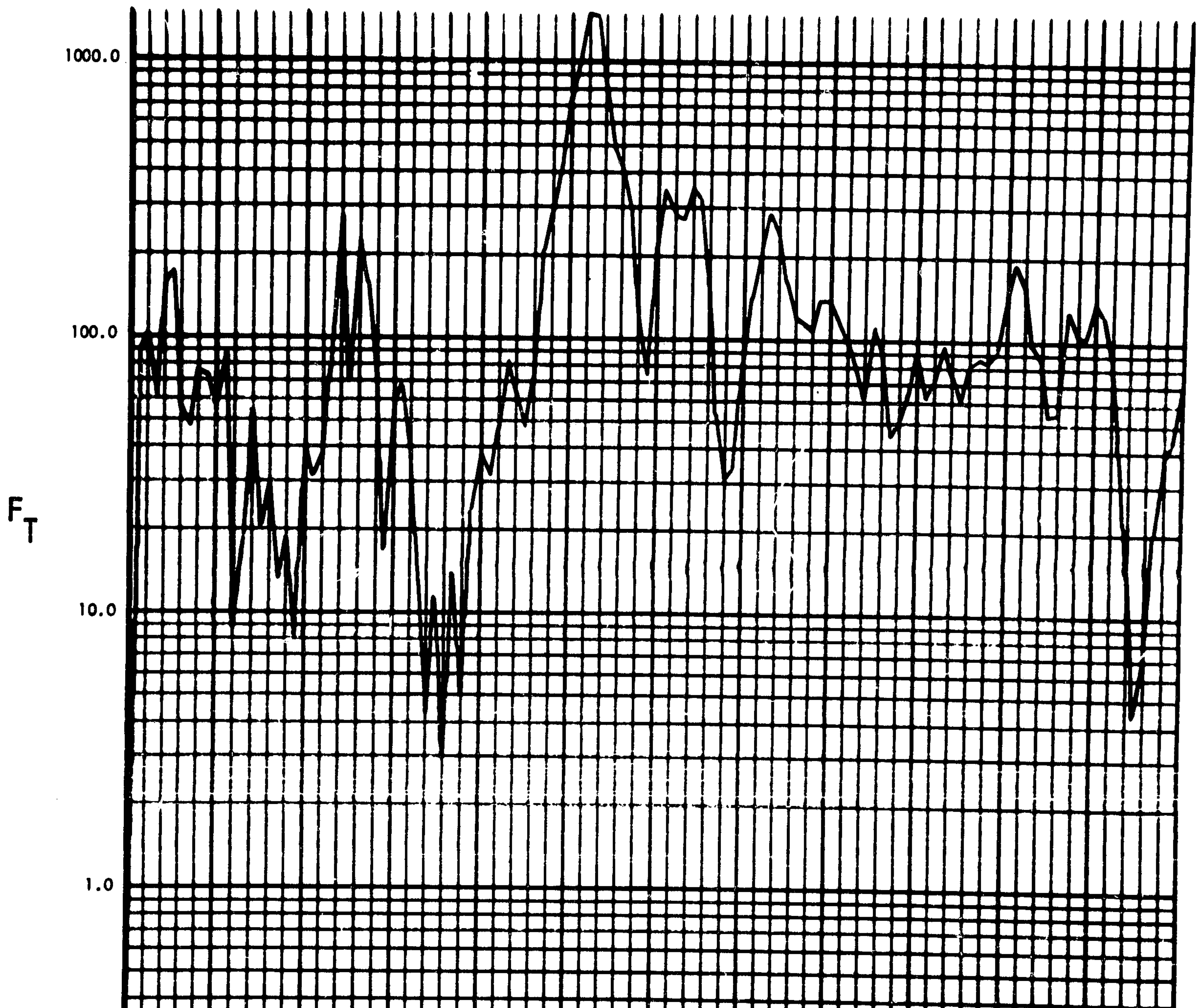

Fig. C-60. Joint 11, torque response, Fourier transform, modulus (pulse 2)

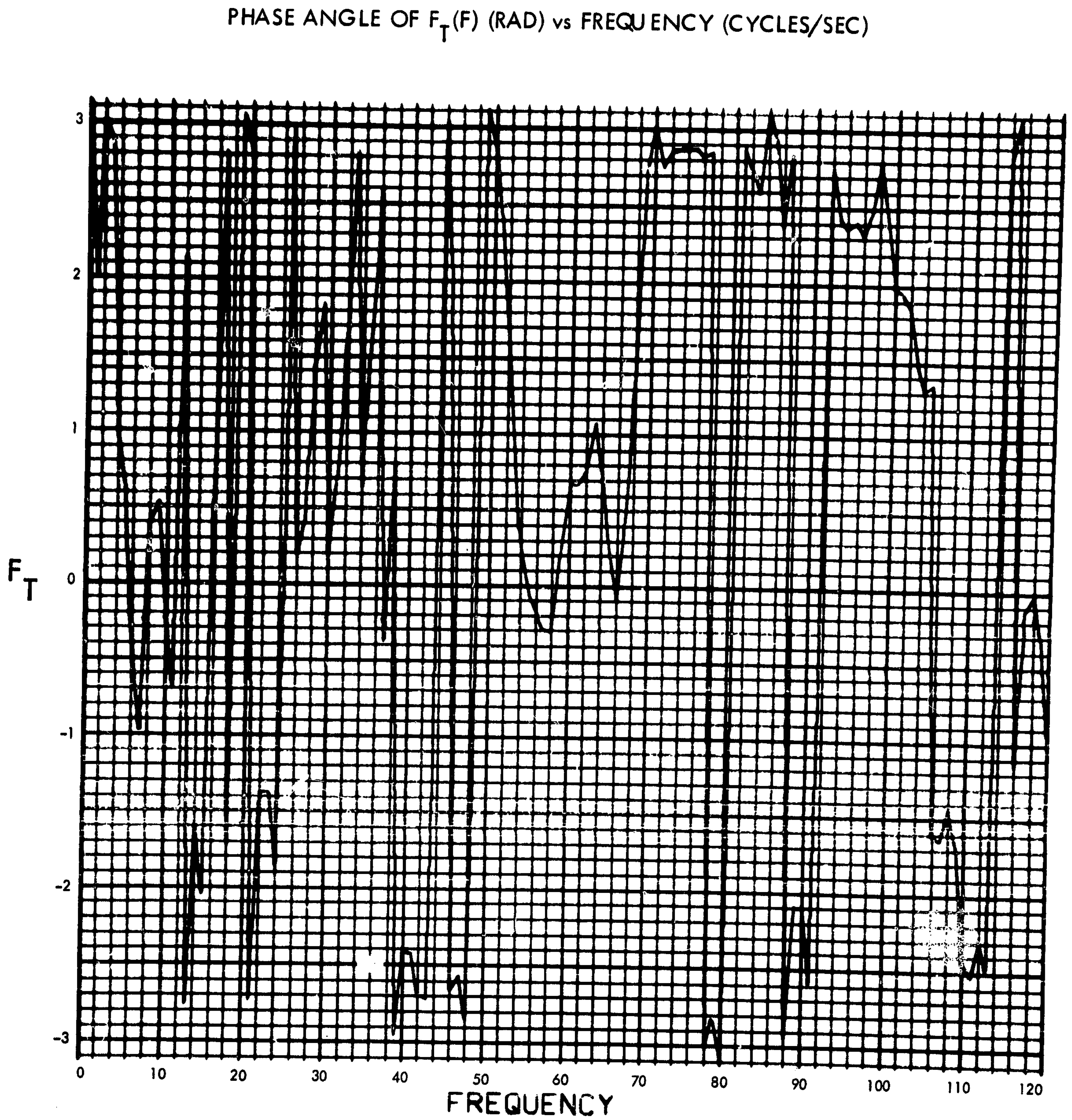

Fig. C-61. Joint 11, torque response, Fourier transform, phase angle (pulse 2)

$T_{11}(T)$ (LB-IN) vs TIME (SEC)

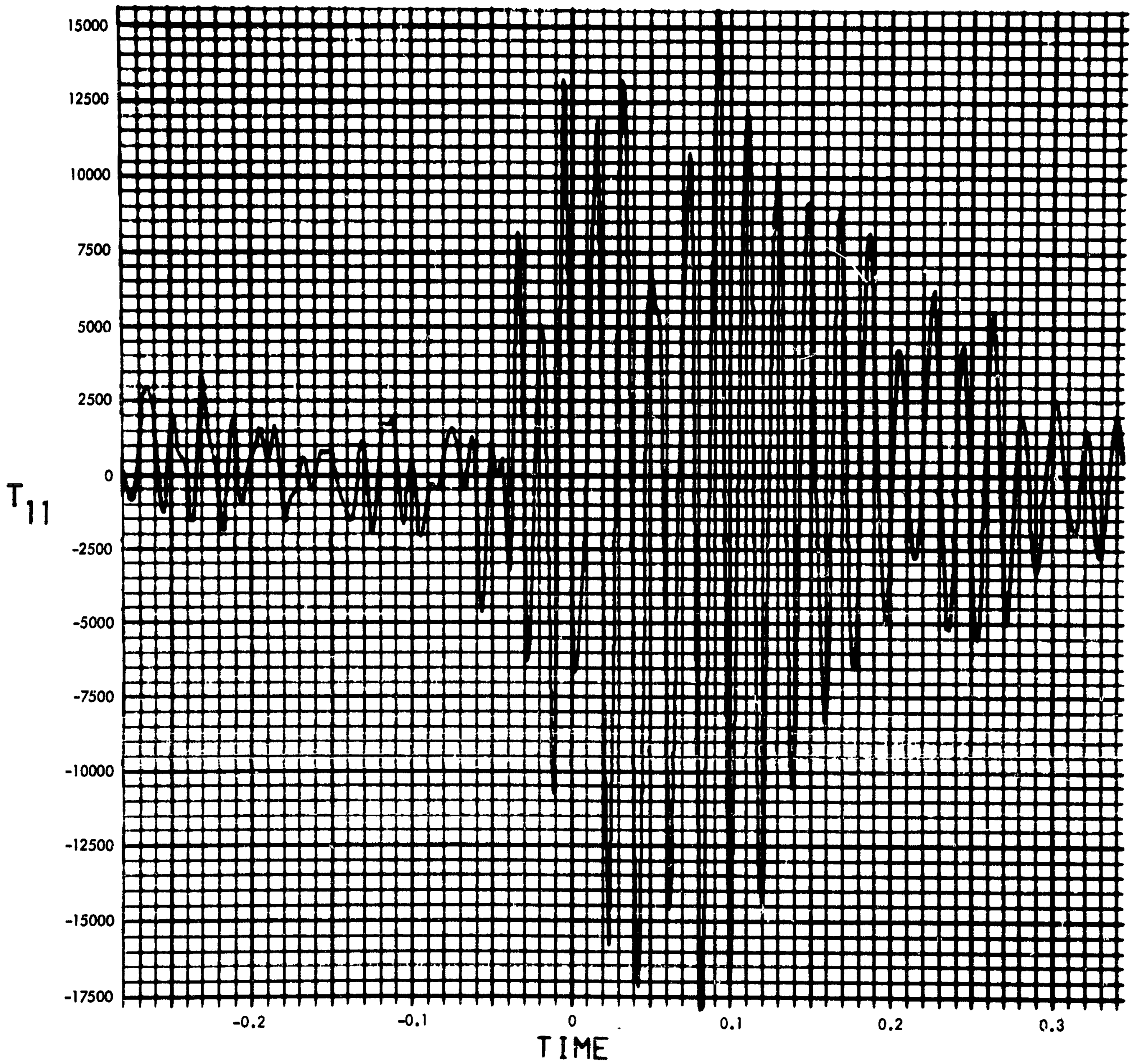

Fig. C-62. Joint 11, torque response, time history (pulse 2)

MODULUS OF $F_T(F)$ (LB-IN-SEC) vs FREQUENCY (CYCLES/SEC)

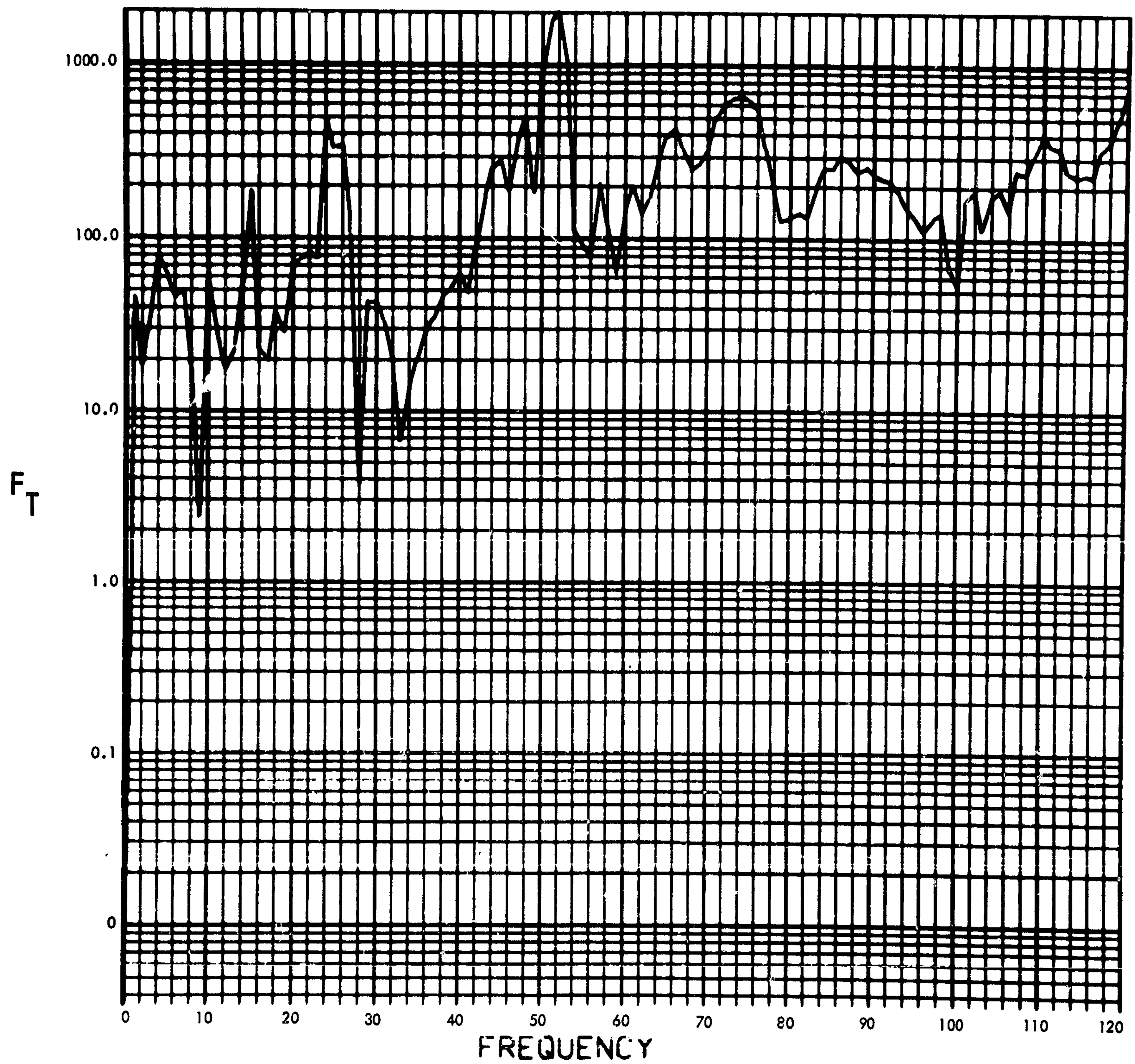

Fig. C-63. Joint 11, torque response, Fourier transform, modulus (pulse 3)

PHASE ANGLE OF $F_T(F)$ (RAD) vs FREQUENCY (CYCLES/SEC)

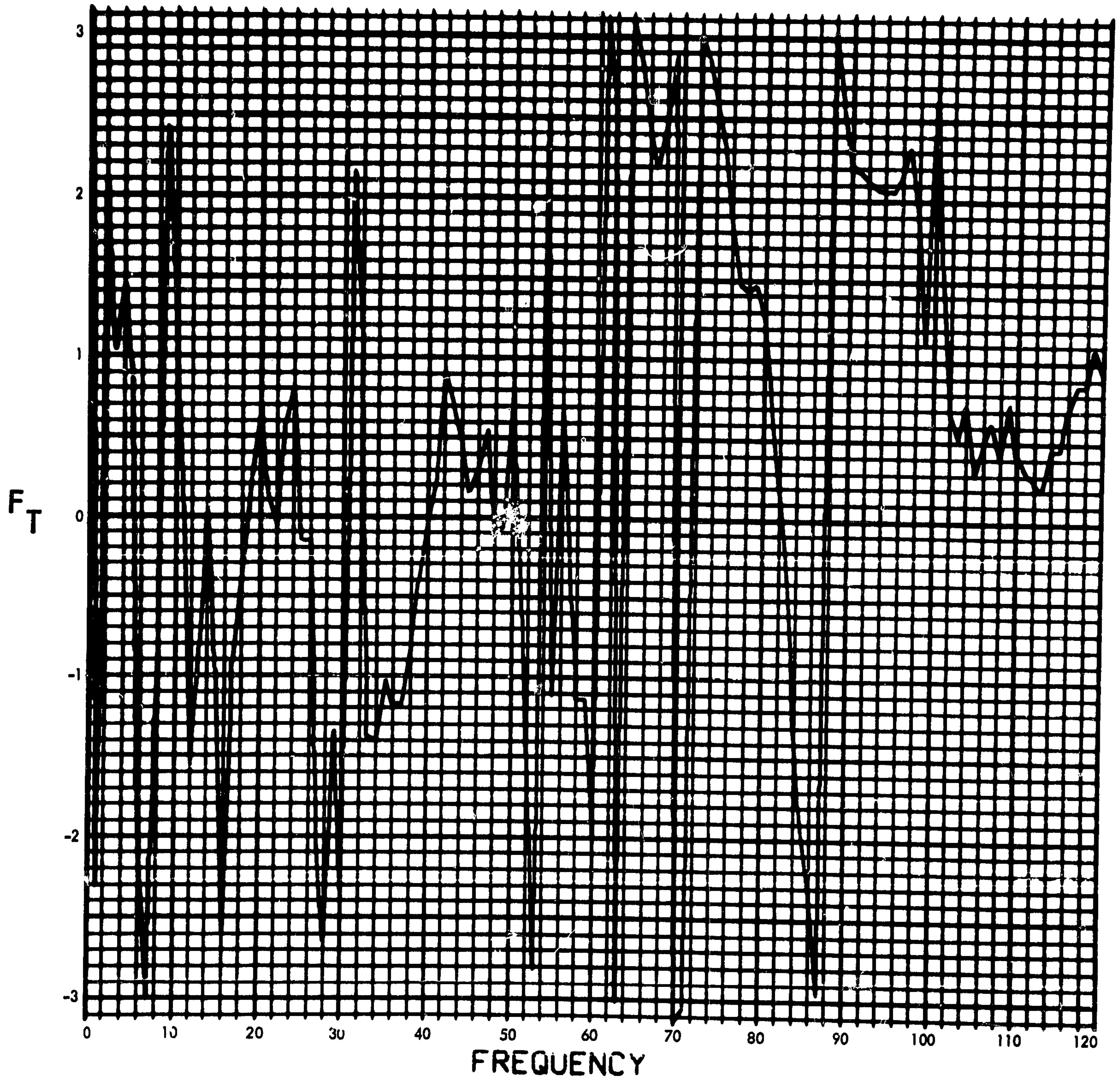

Fig. C-64. Joint 11, torque response, Fourier transform, phase angle (pulse 3)

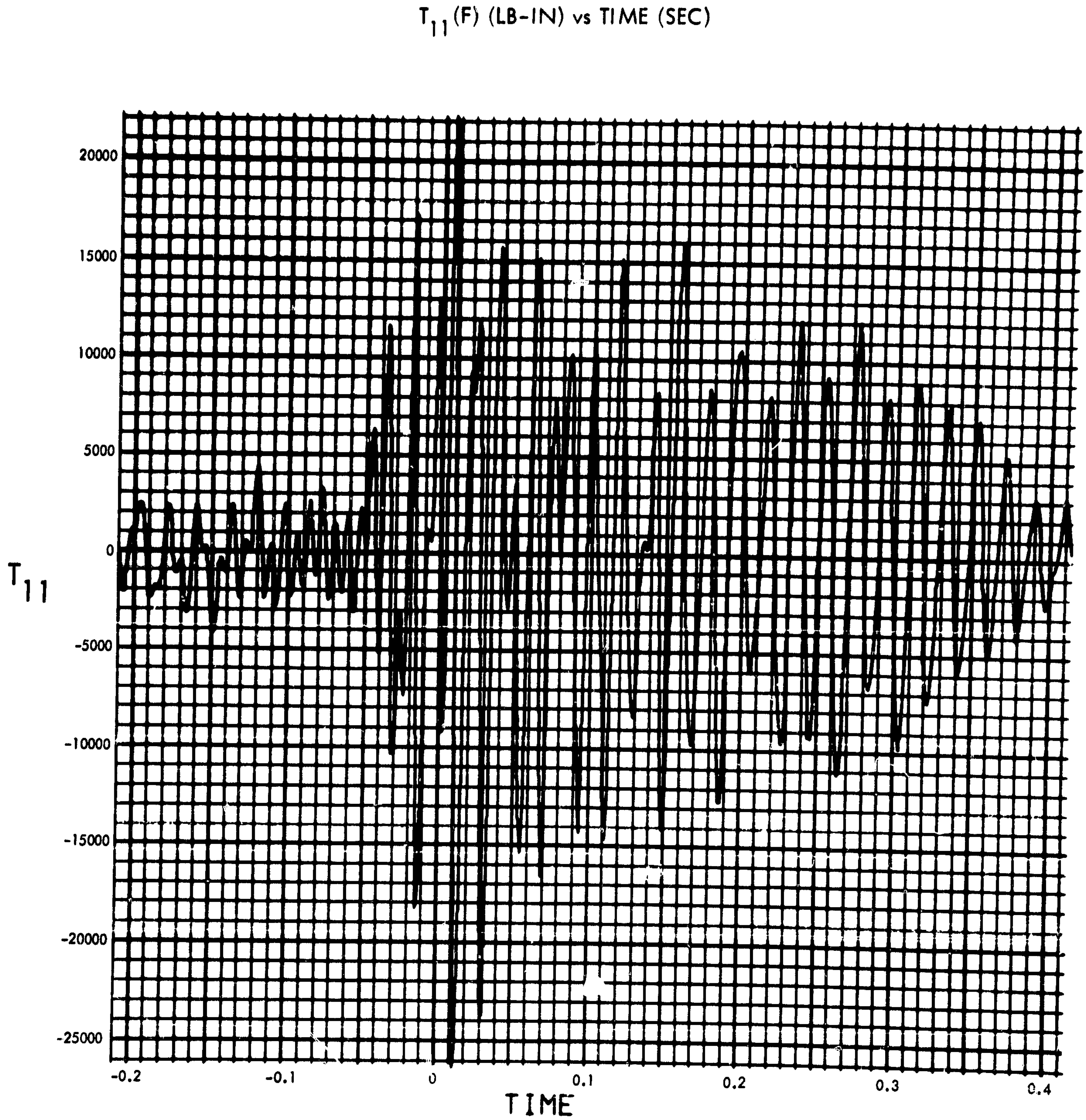

Fig. C-65. Joint 11, torque response, time history (pulse 3)

MODULUS OF $F_T(F)$ (LB-IN-SEC) vs FREQUENCY (CYCLES/SEC)

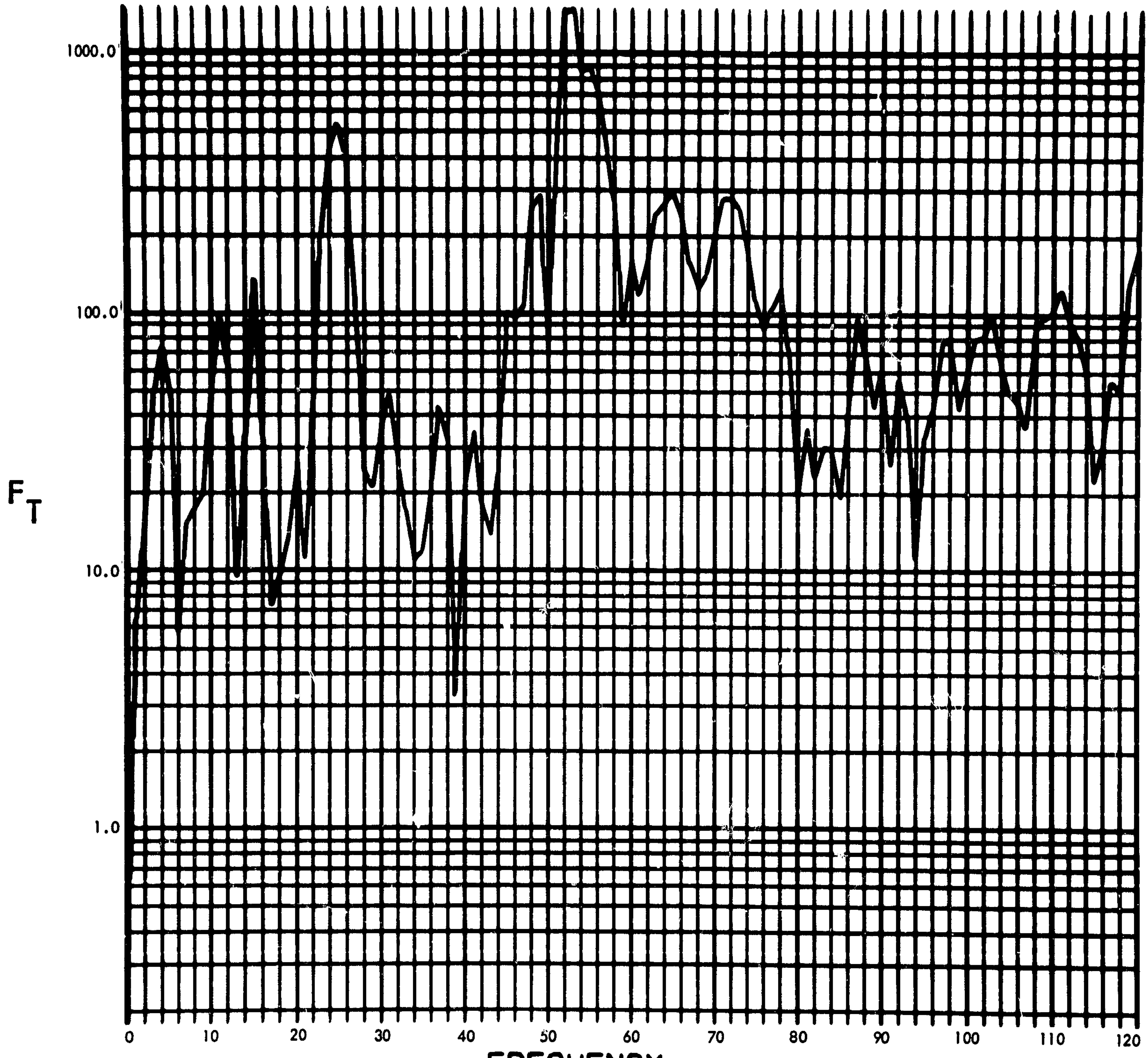

Fig. C-66. Joint 11, torque response, Fourier transform, modulus (pulse 4)

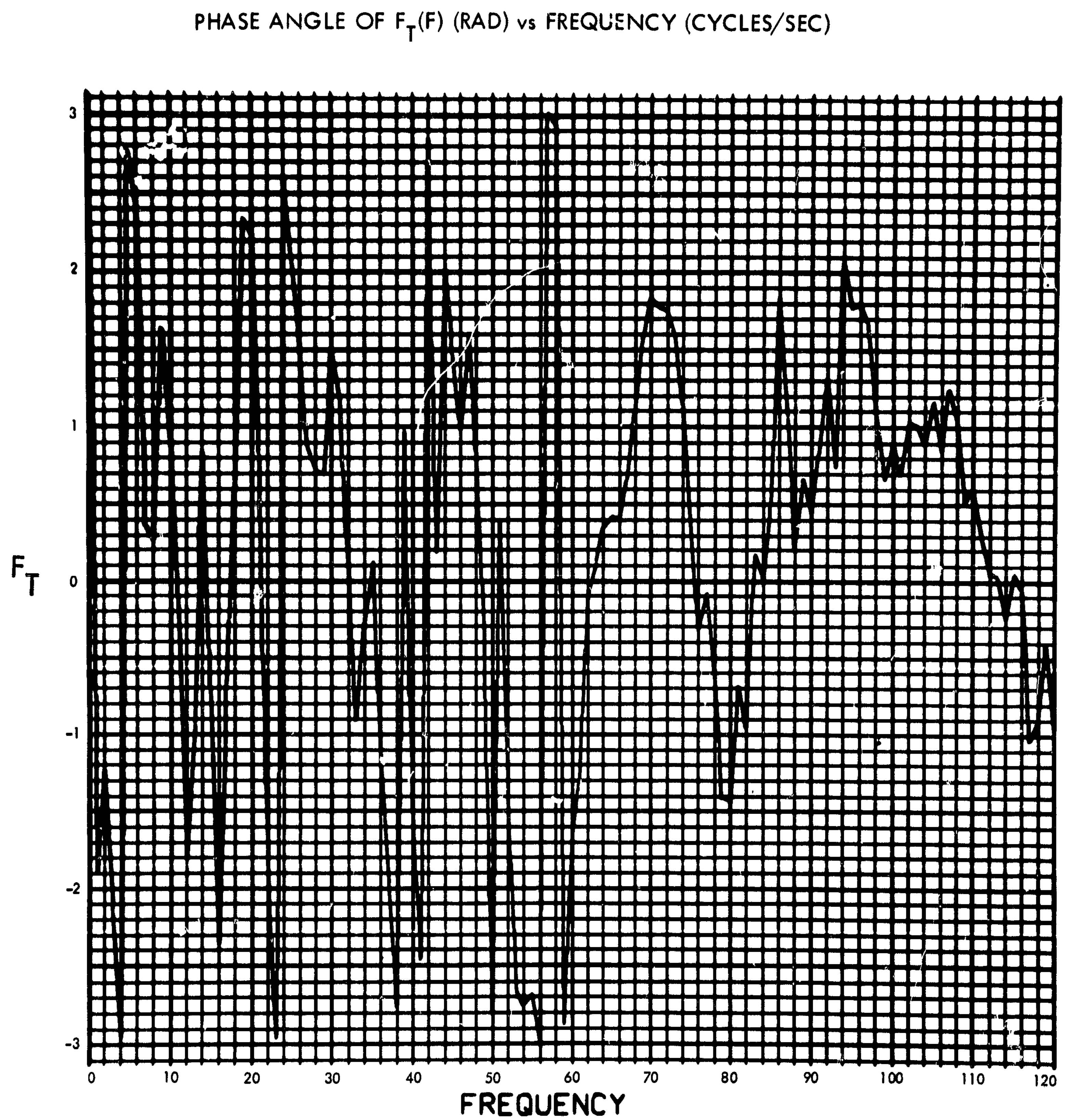

Fig. C-67. Joint 11, torque response, Fourier transform, phase angle (pulse 4)

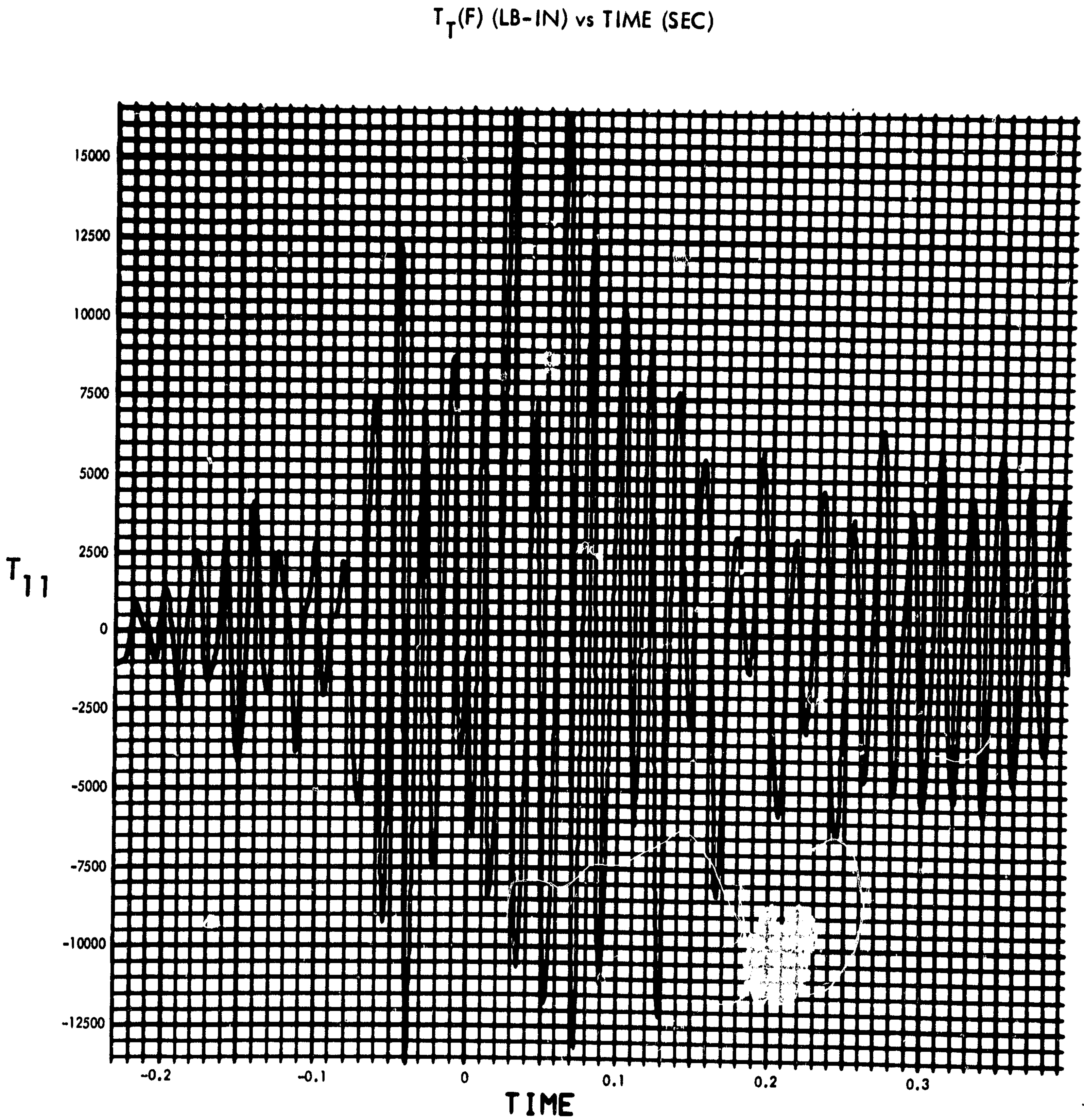

Fig. C-68. Joint 11, torque response, time history (pulse 4)

MODULUS H2(F) (1/LB-IN-SEC^2) vs FREQUENCY (CYCLES/SEC)

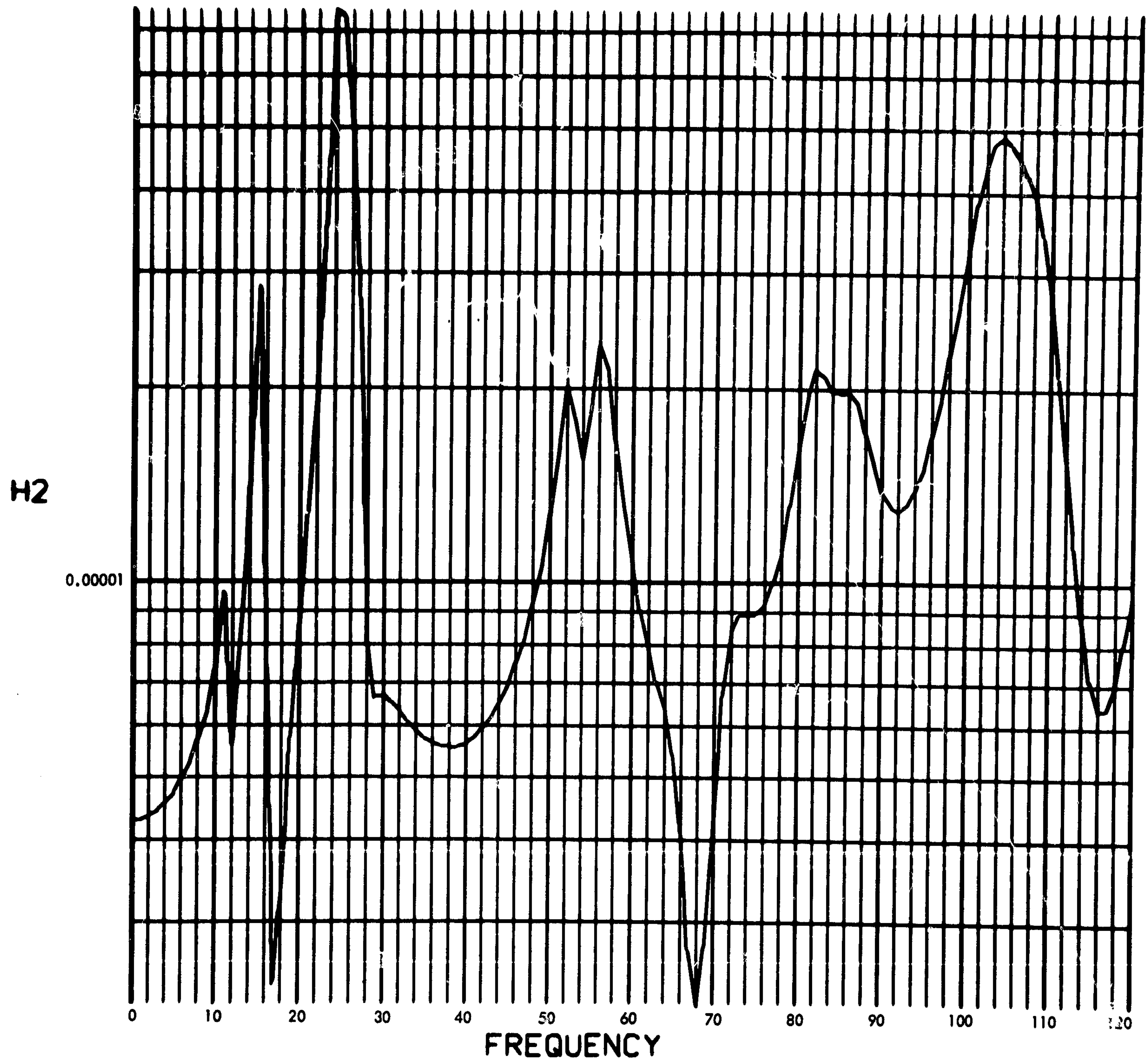

Fig. C-69. Joint 12, acceleration transfer function, Fourier transform, modulus

PHASE ANGLE OF H2(F) (RAD) vs FREQUENCY (CYCLES/SEC)

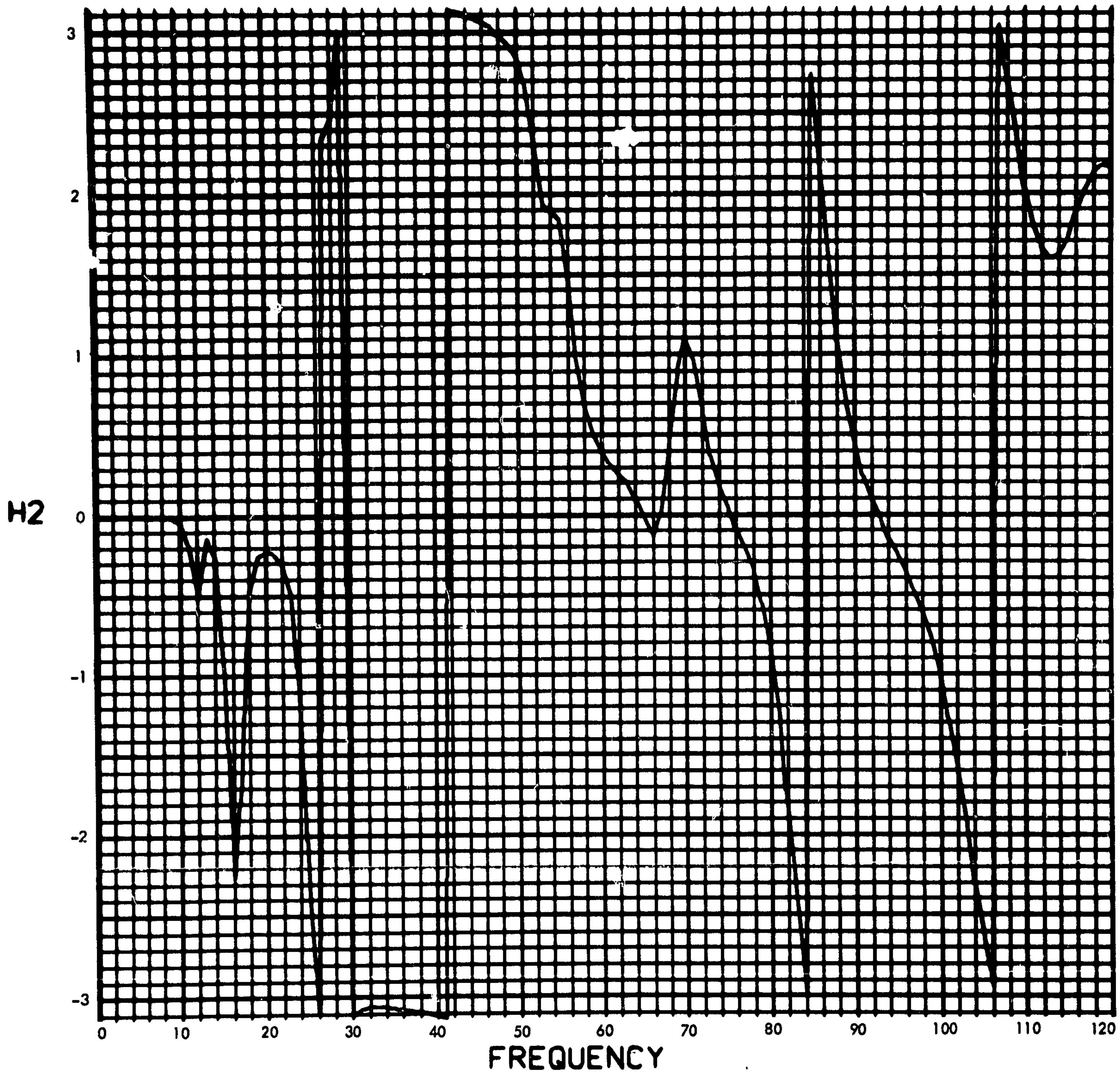

Fig. C-70. Joint 12, acceleration transfer function, Fourier transform, phase angle

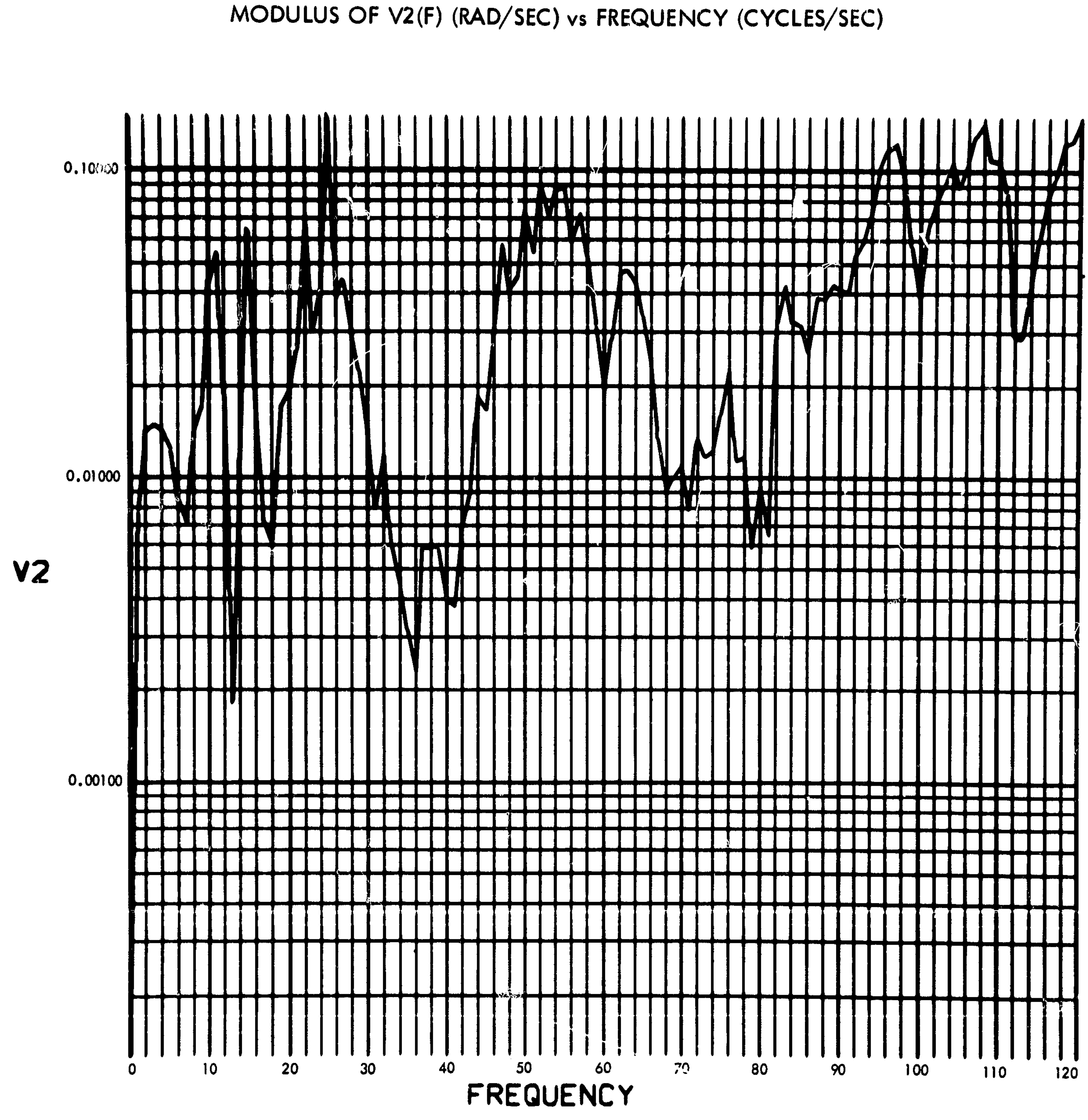

Fig. C-71. Joint 12, acceleration response, Fourier transform, modulus (pulse 1)

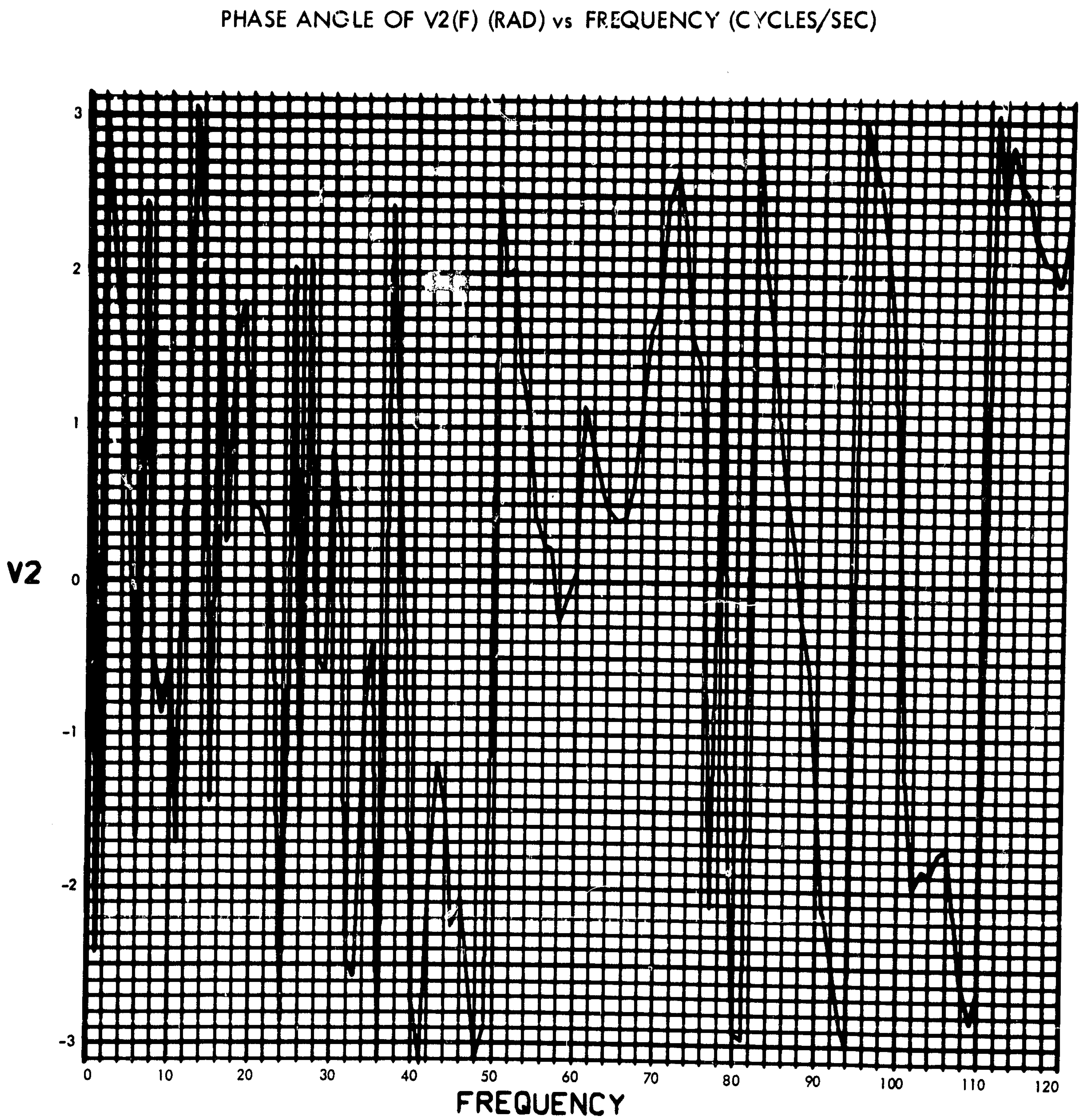

Fig. C-72. Joint 12, acceleration response, Fourier transform, phase angle (pulse 1)

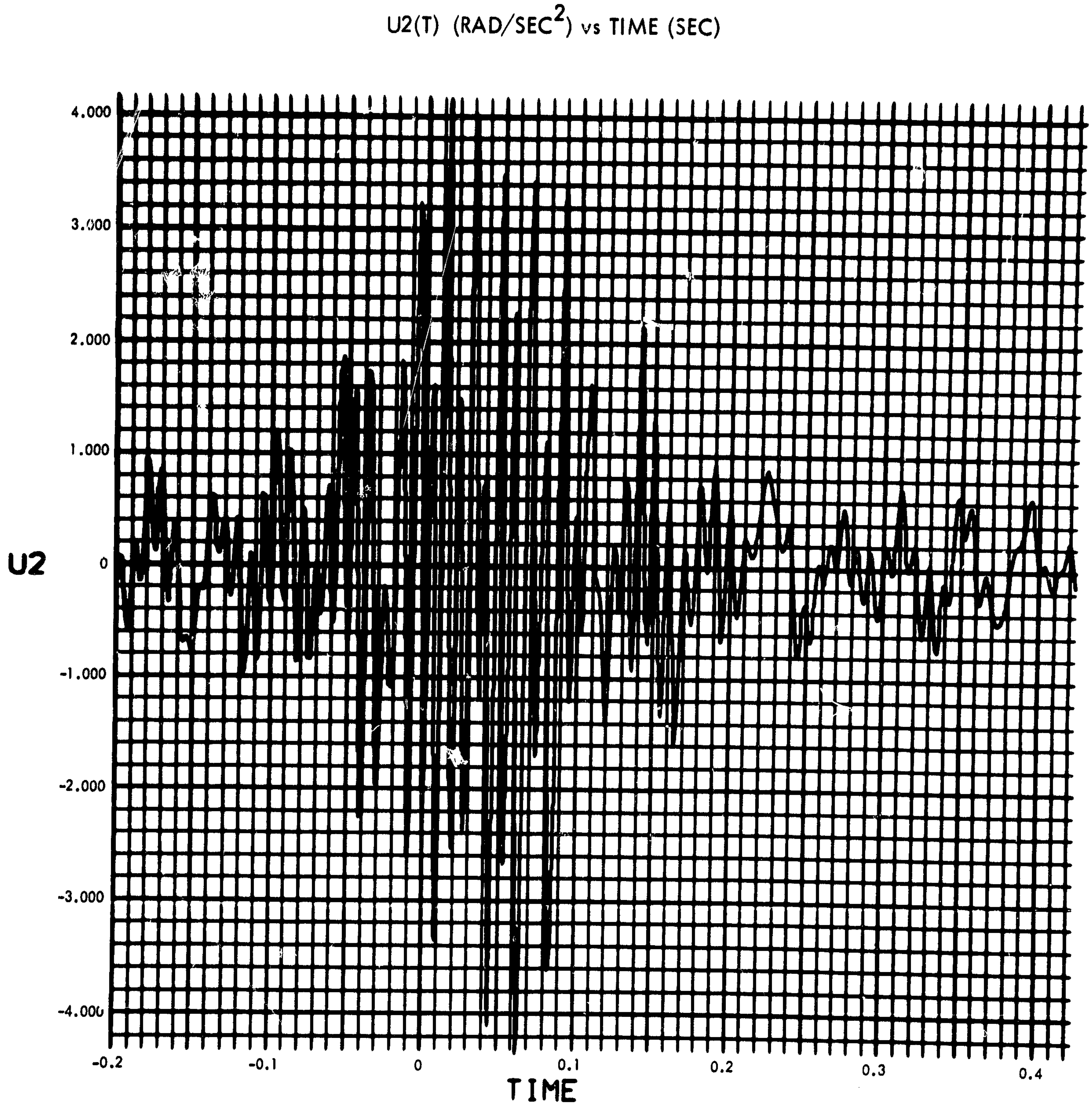

Fig. C-73. Joint 12, acceleration response, time history (pulse 1)

MODULUS OF V2(F) (RAD/SEC) vs FREQUENCY (CYCLES/SEC)

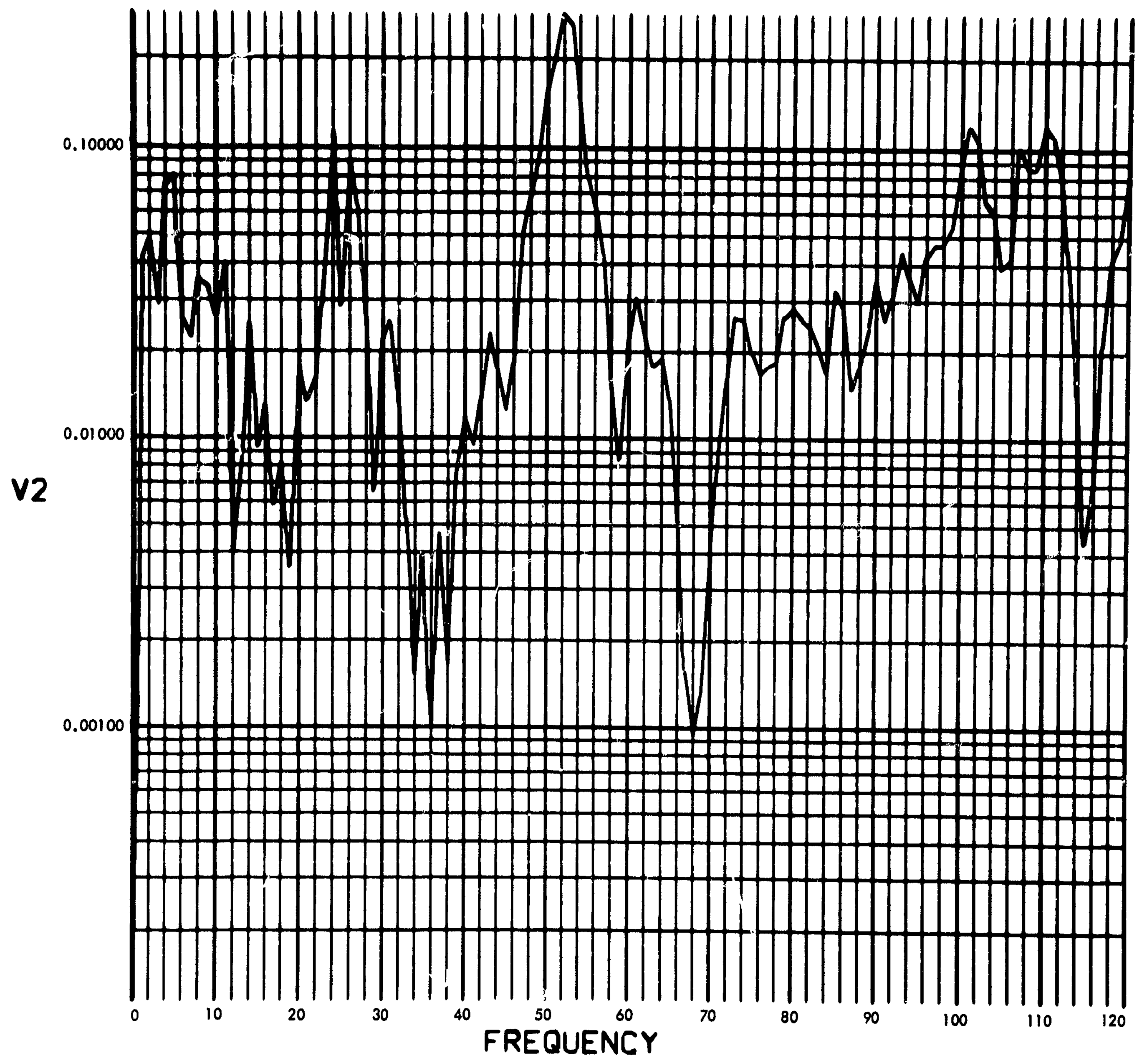

Fig. C-74. Joint 12, acceleration response, Fourier transform, modulus (pulse 2)

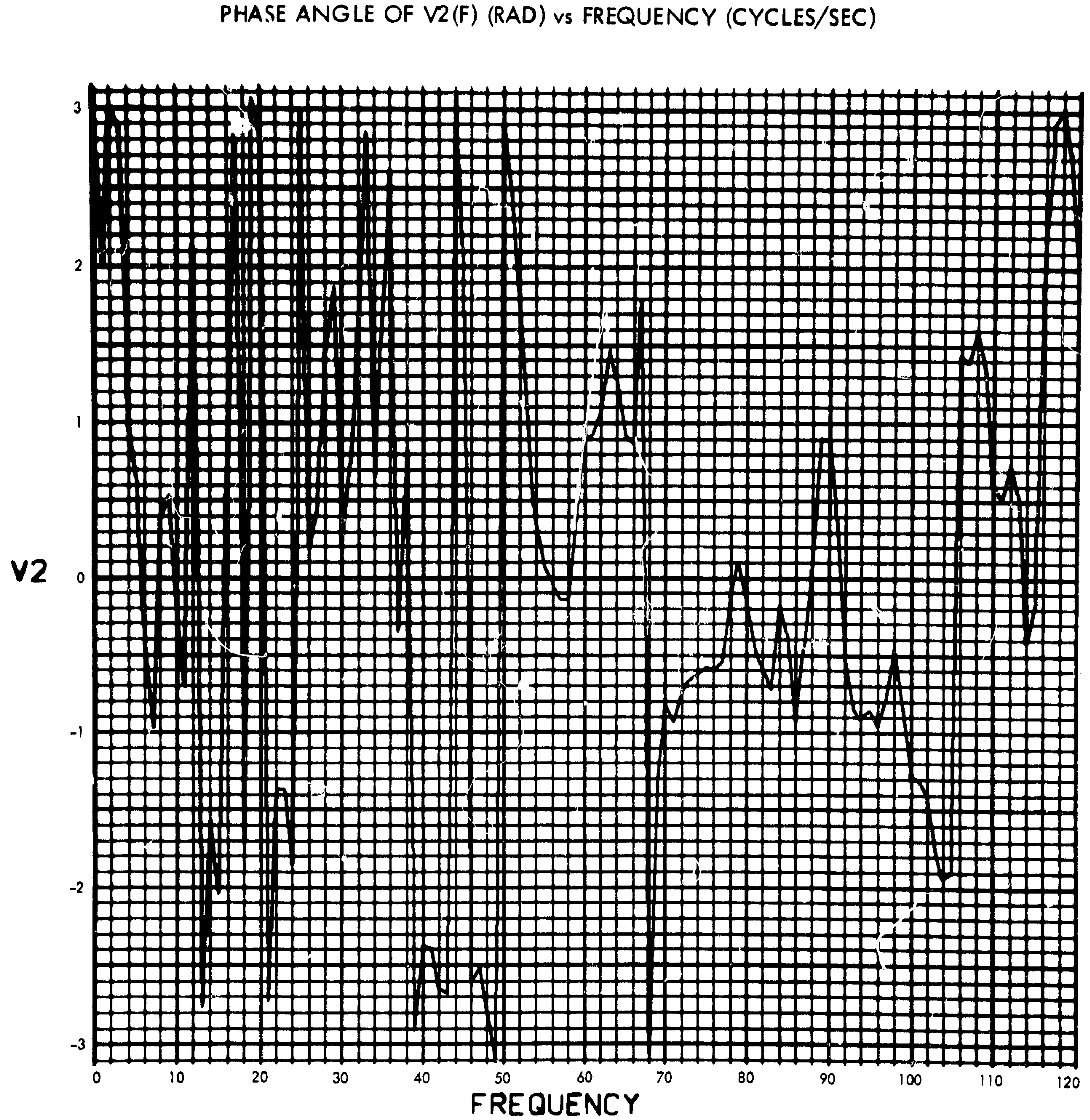

Fig. C-75. Joint 12, acceleration response, Fourier transform, phase angle (pulse 2)

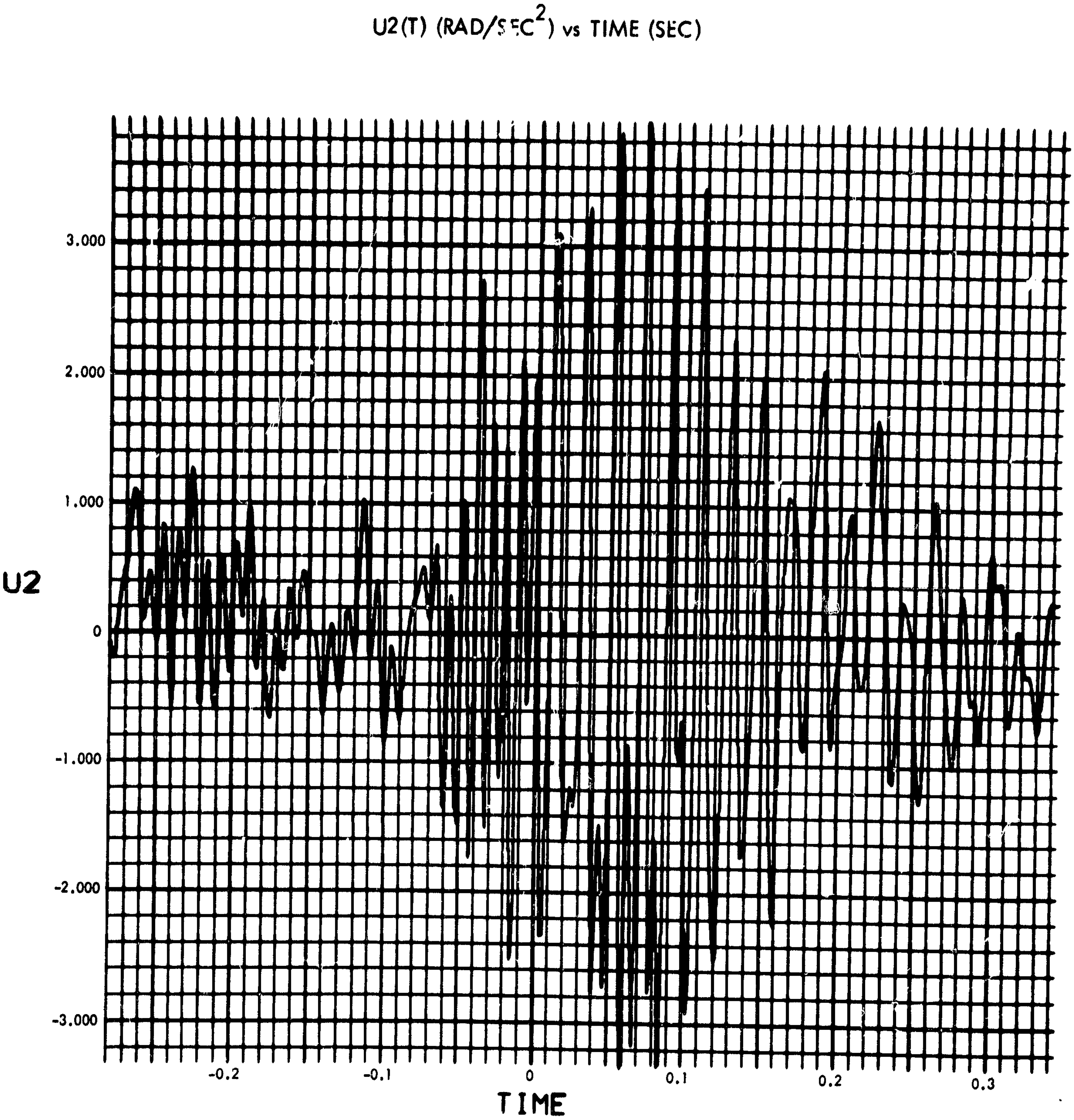

Fig. C-76. Joint 12, acceleration response, time history (pulse 2)

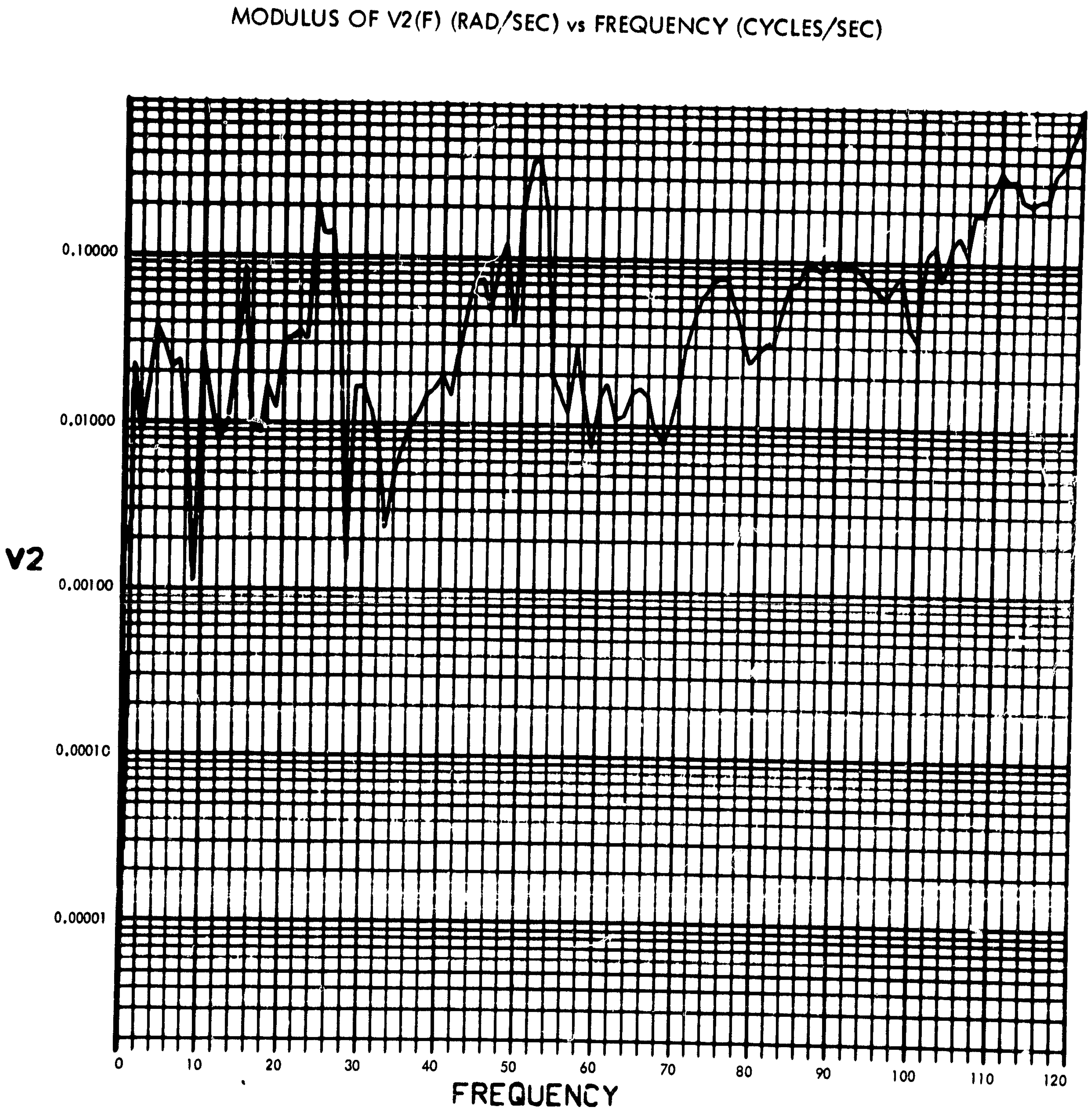

Fig. C-77. Joint 12, acceleration response, Fourier transform, modulus (pulse 3)

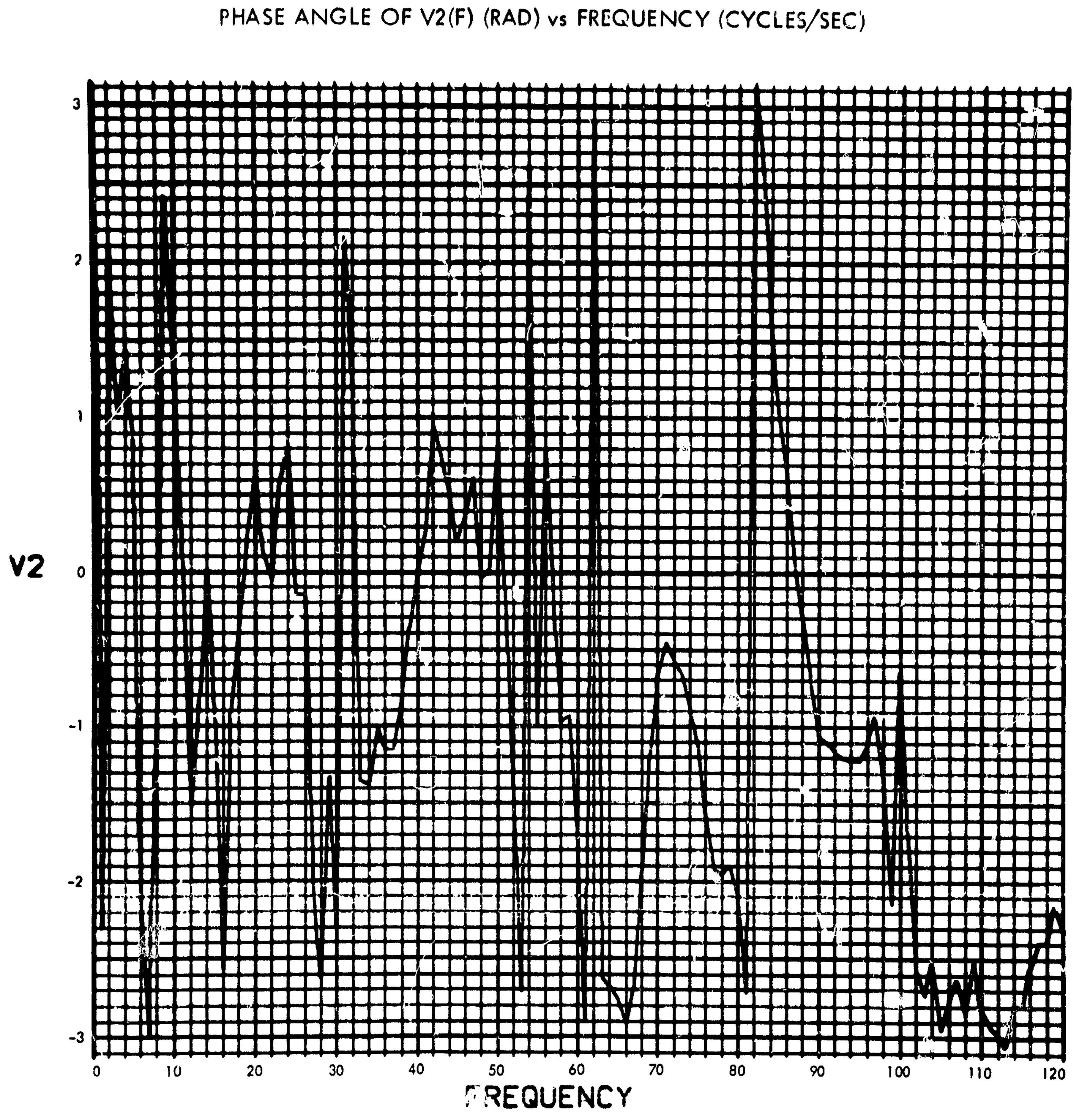

Fig. C-78. Joint 12, acceleration response, Fourier transform, phase angle (pulse 3)

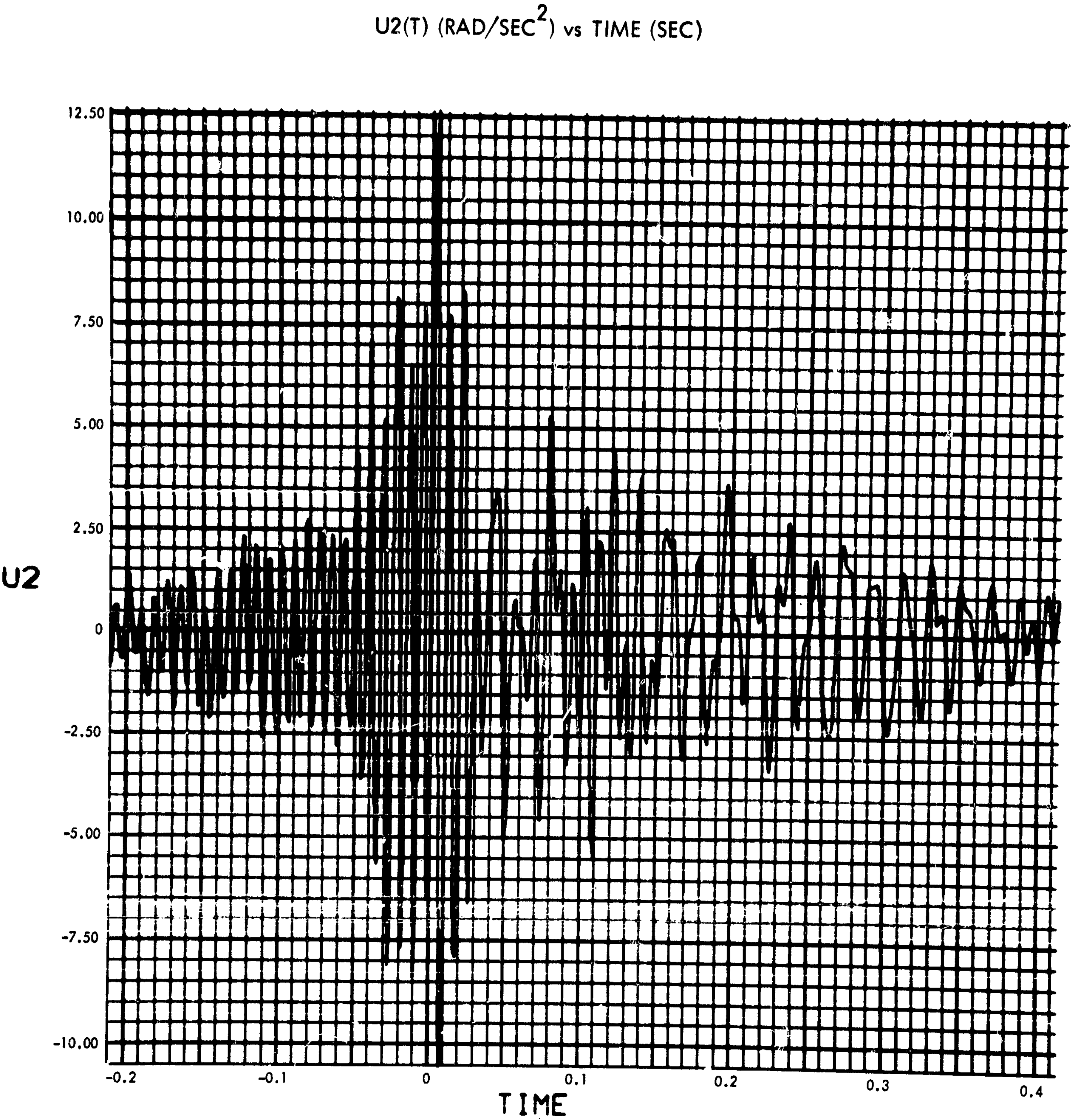

Fig. C-79. Joint 12, acceleration response, time history (pulse 3)

MODULUS OF V2(F) (RAD/SEC) vs FREQUENCY (CYCLES/SEC)

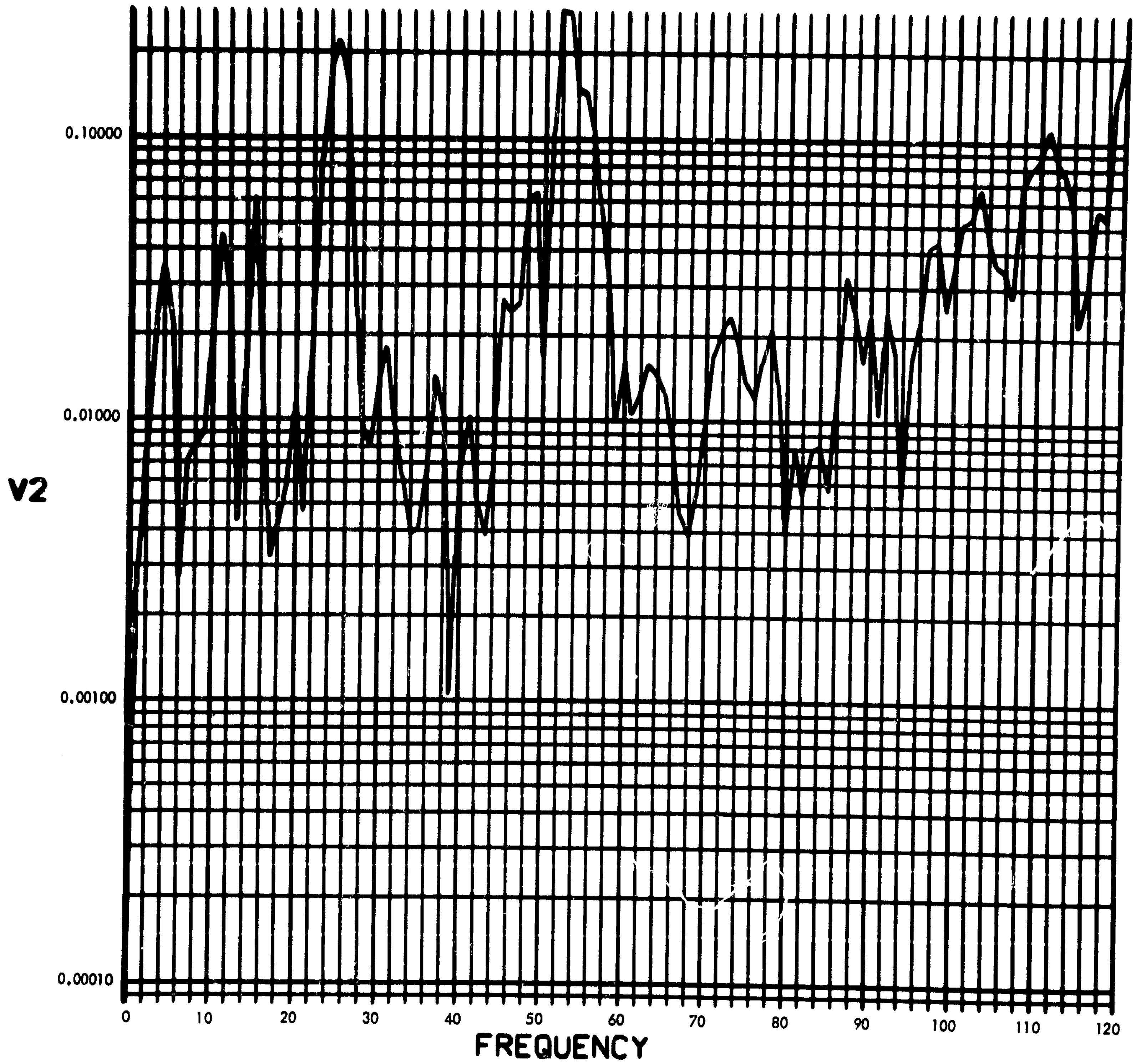

Fig. C-80. Joint 12, acceleration response, Fourier transform, modulus (pulse 4)

PHASE ANGLE OF (V2(F) (RAD) vs FREQUENCY (CYCLES/SEC)

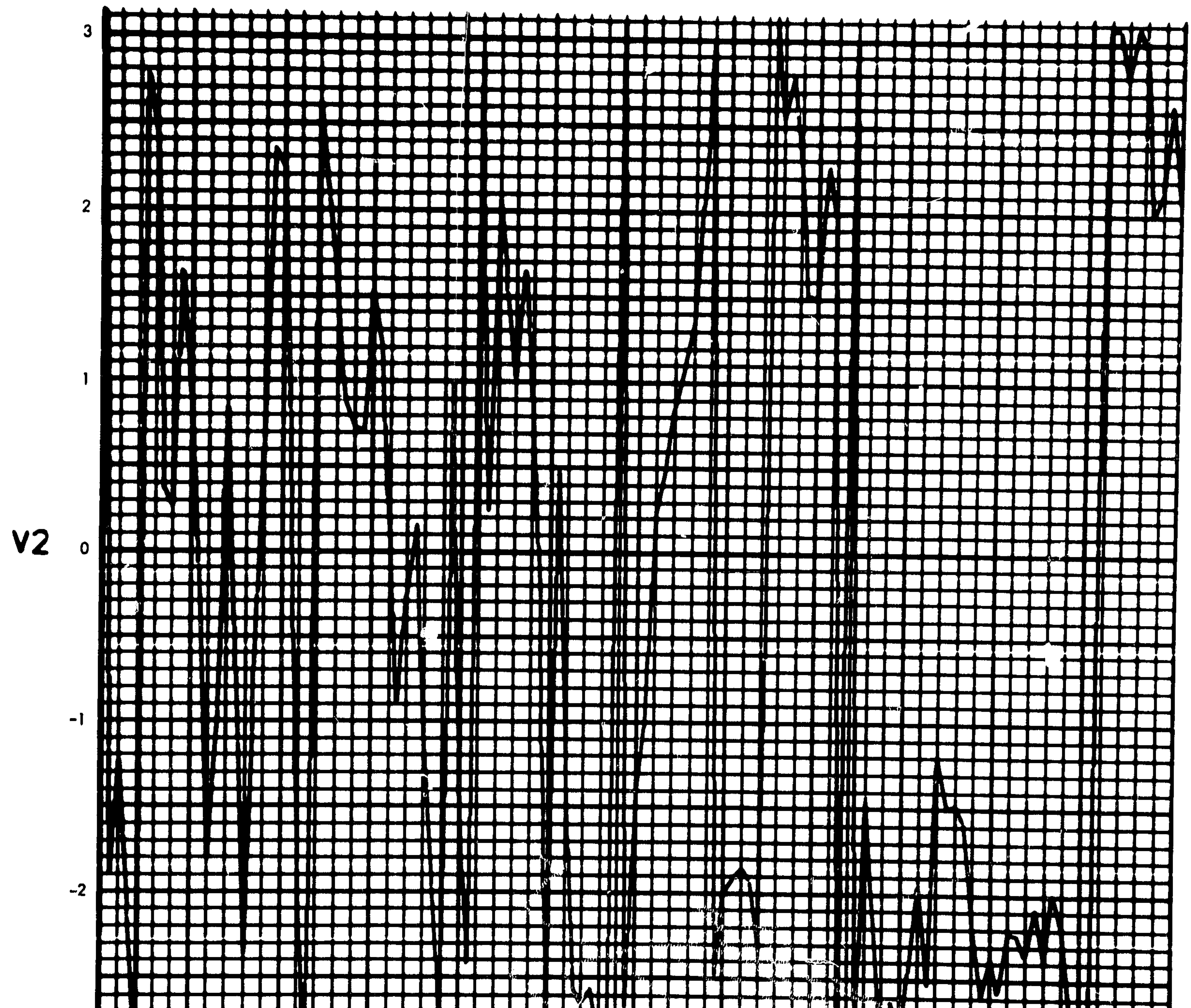

Fig. C-81. Joint 12, acceleration response, Fourier transform, phase angle (pulse 4)

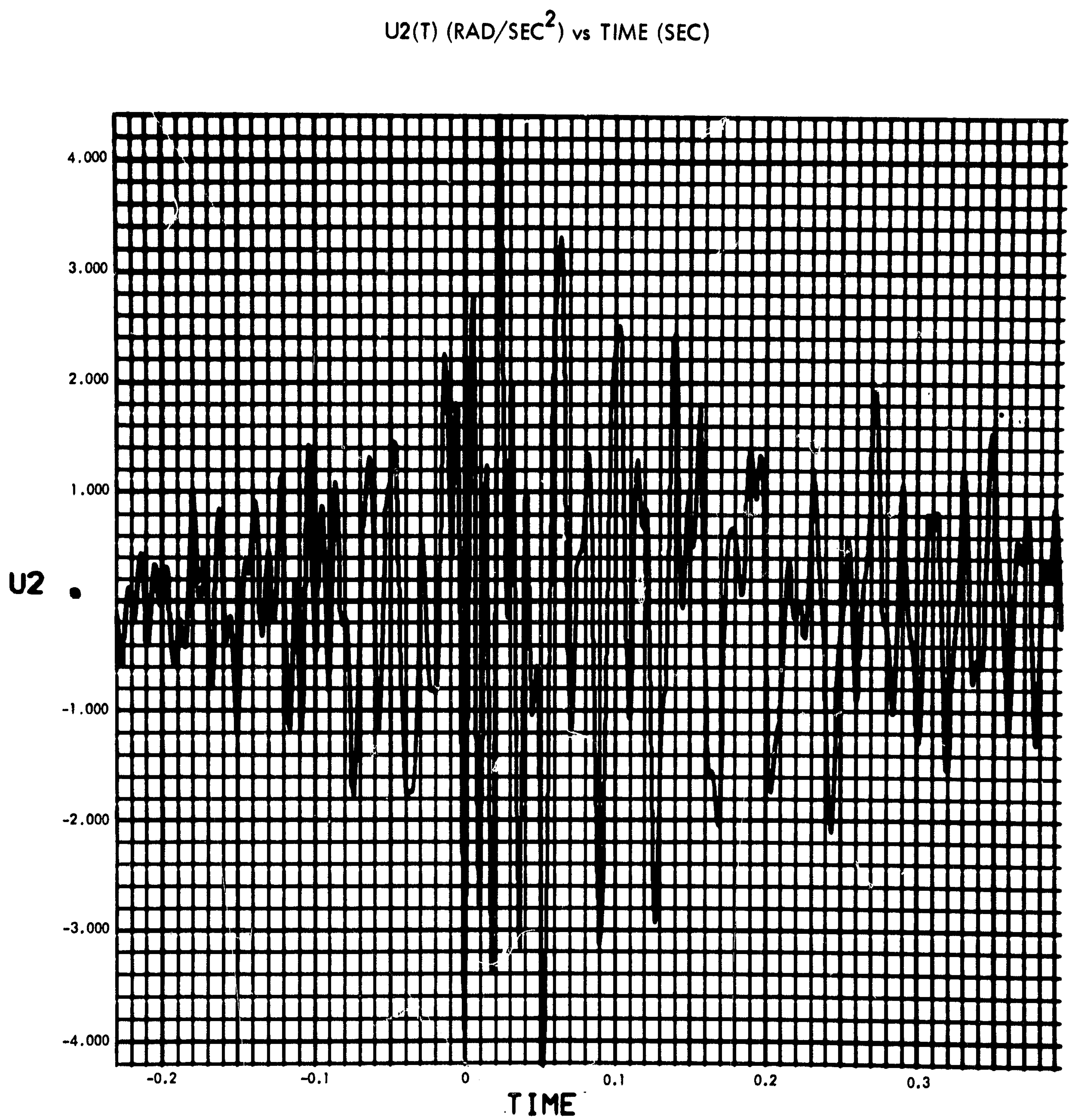

Fig. C-82. Joint 12, acceleration response, time history (pulse 4)

$H_T(F)$ vs FREQUENCY (CYCLES/SEC)

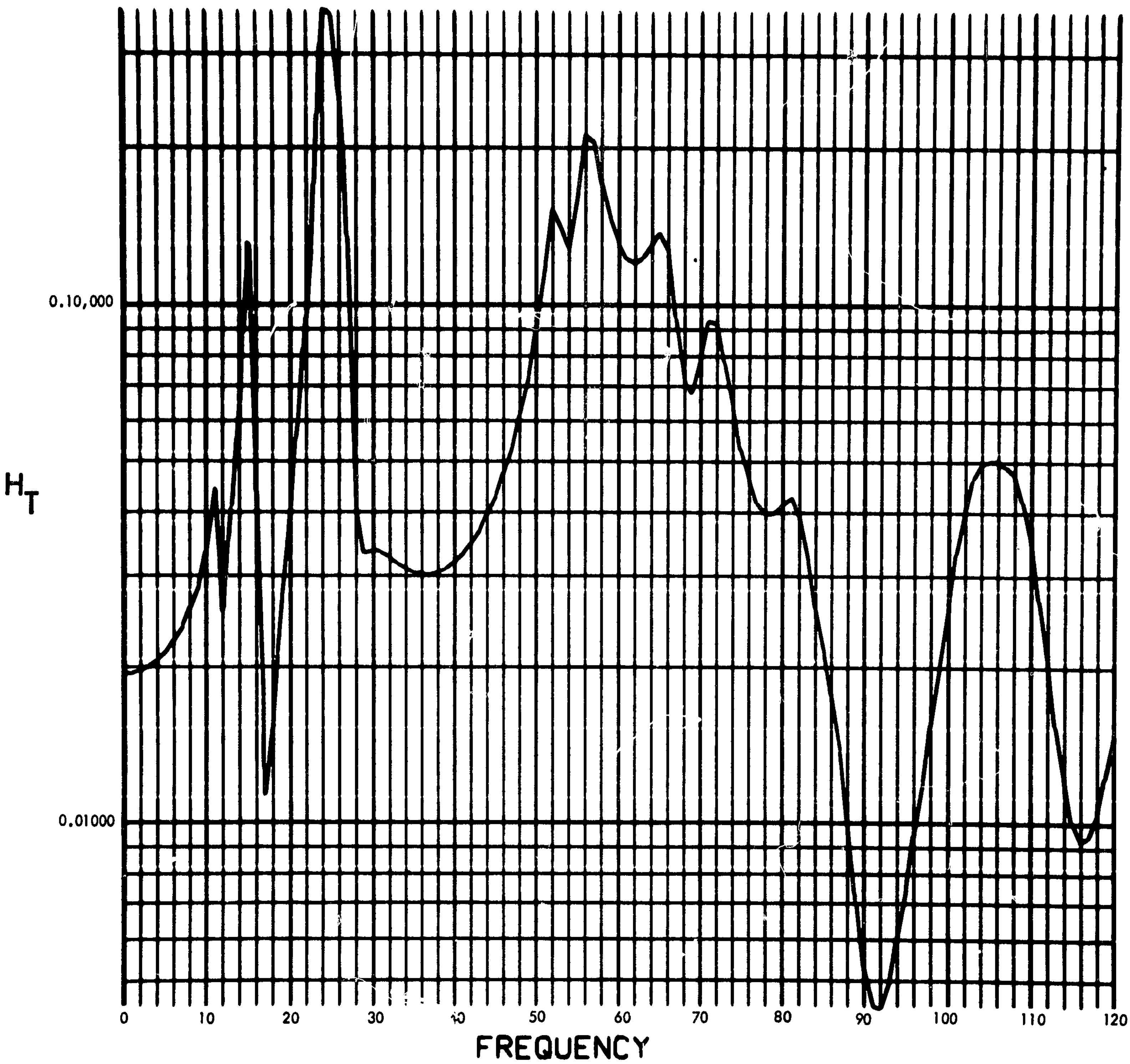

Fig. C-83. Joint 12, torque transfer function, Fourier transform, modulus

PHASE ANGLE OF $H_T(F)$ (RAD) vs FREQUENCY (CYCLES/SEC)

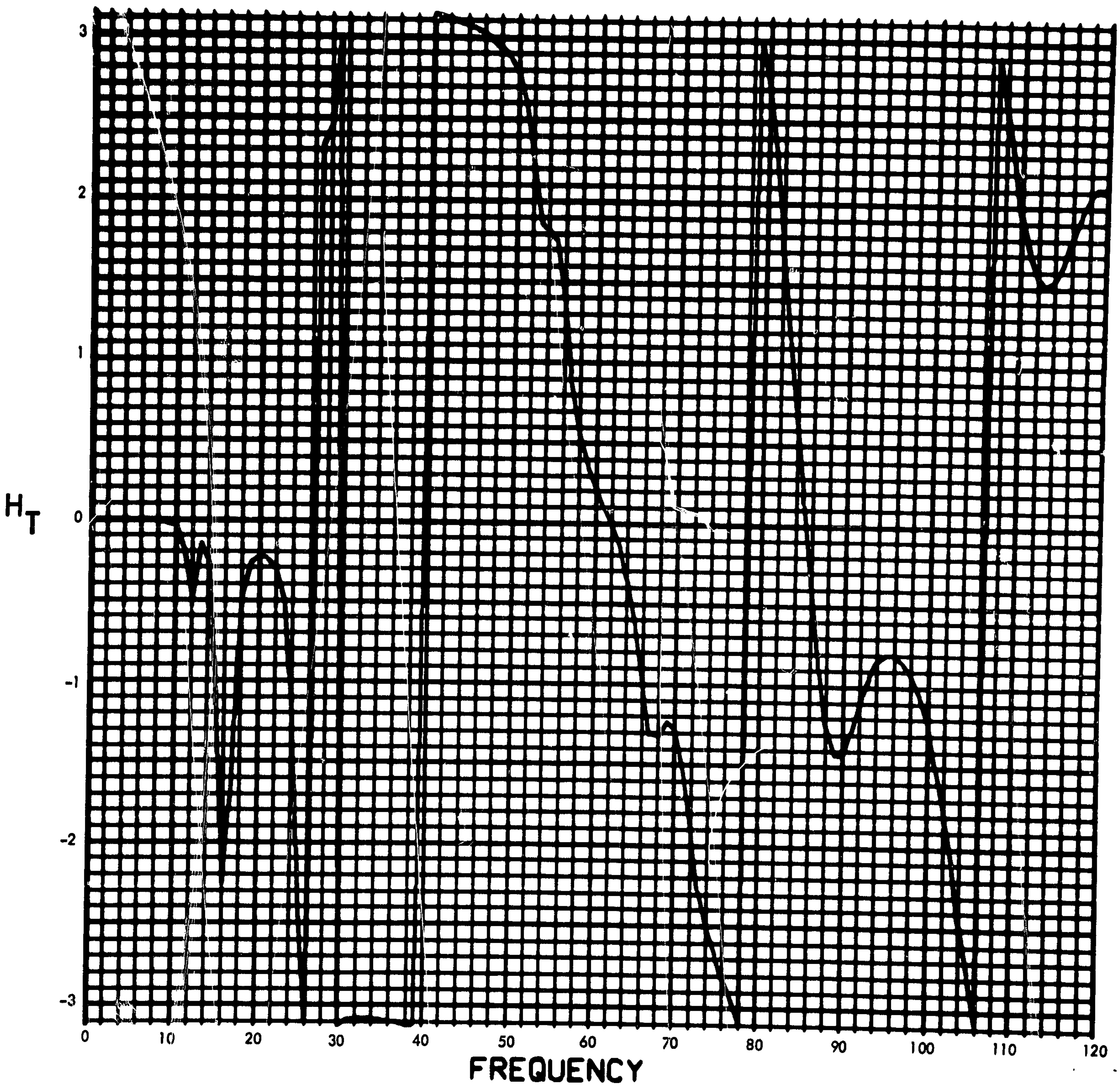

Fig. C-84. Joint 12, torque transfer function, Fourier transform, phase angle

MODULUS OF $F_T(F)$ (LB-IN-SEC) vs FREQUENCY (CYCLES/SEC)

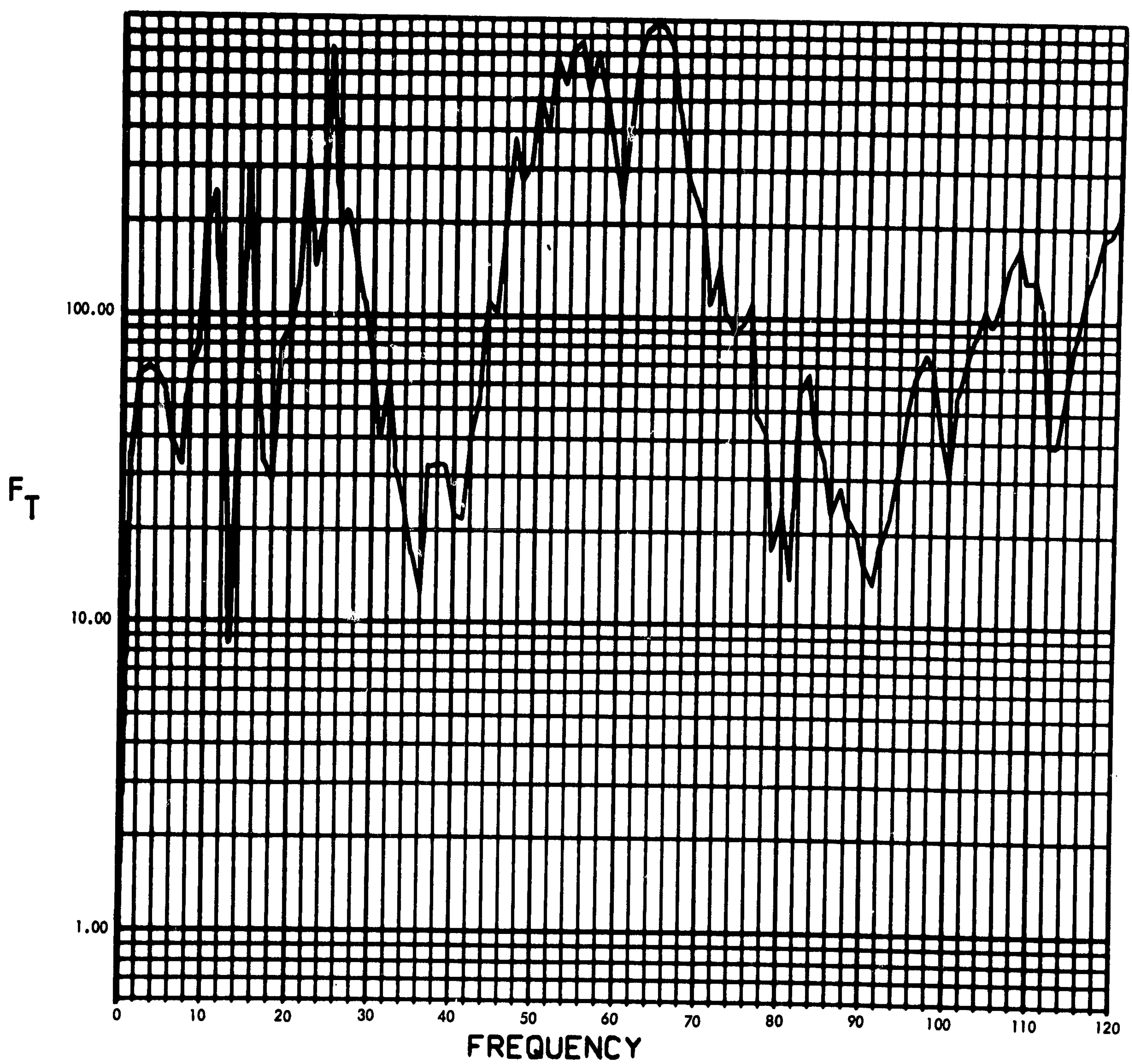

Fig. C-85. Joint 12, torque response function, Fourier transform, modulus (pulse 1)

PHASE ANGLE OF $F_T(F)$ (RAD) vs FREQUENCY (CYCLES/SEC)

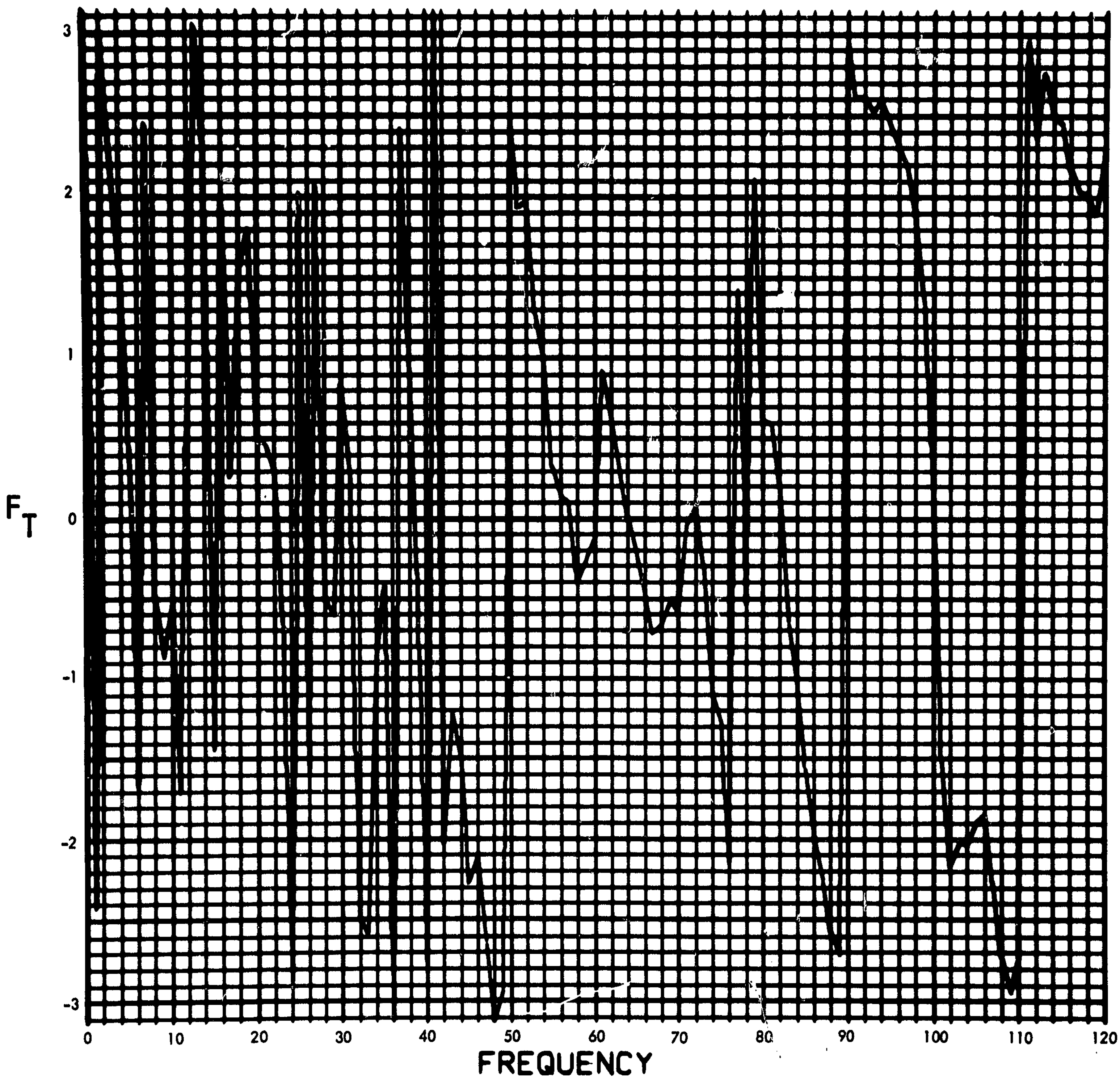

Fig. C-86. Joint 12, torque response function, Fourier transform, phase angle (pulse 1)

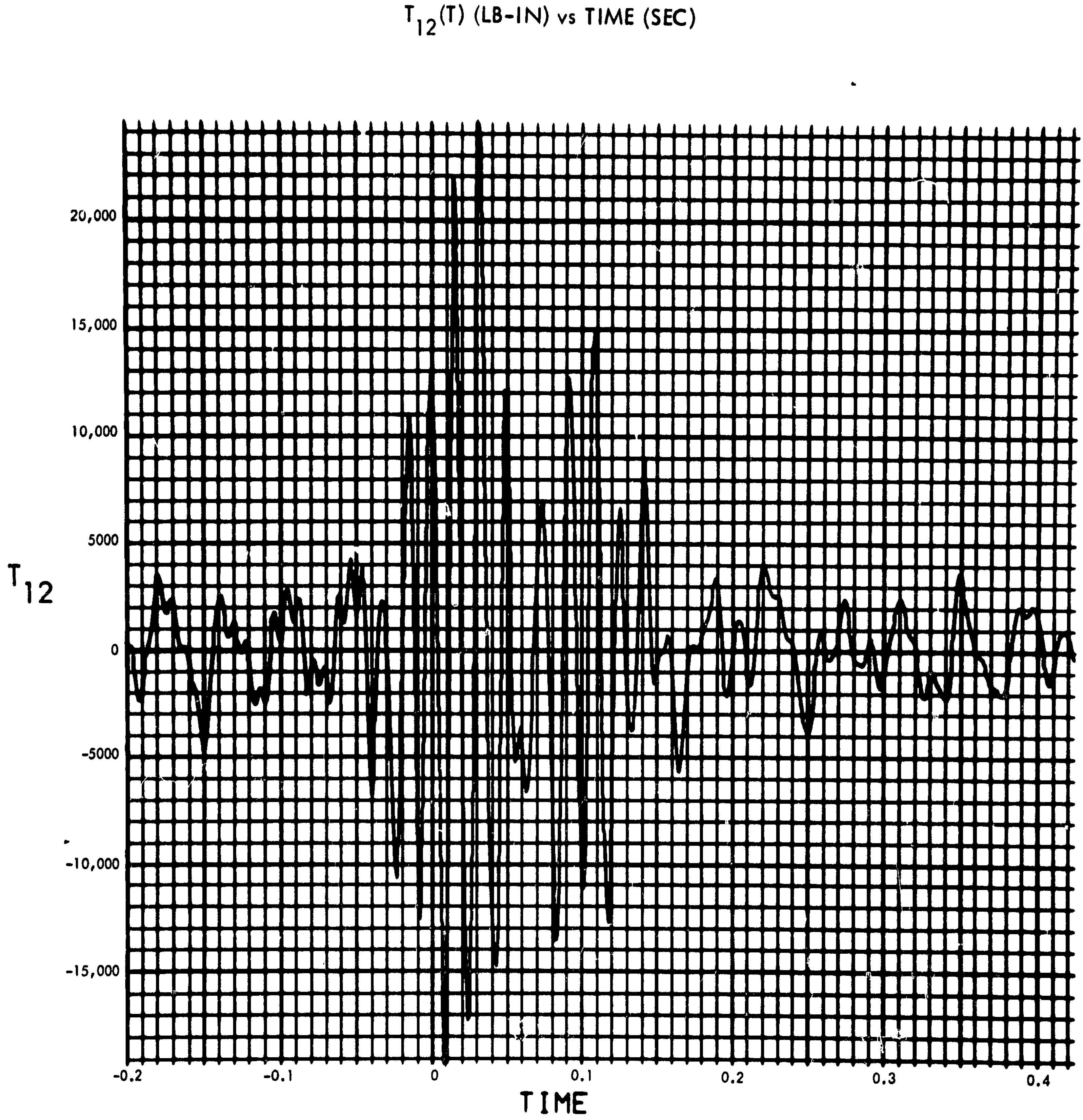

Fig. C-87. Joint 12, torque response, time history (pulse 1)

MODULUS OF $F_T(F)$ (LB-IN-SEC) vs FREQUENCY (CYCLES/SEC)

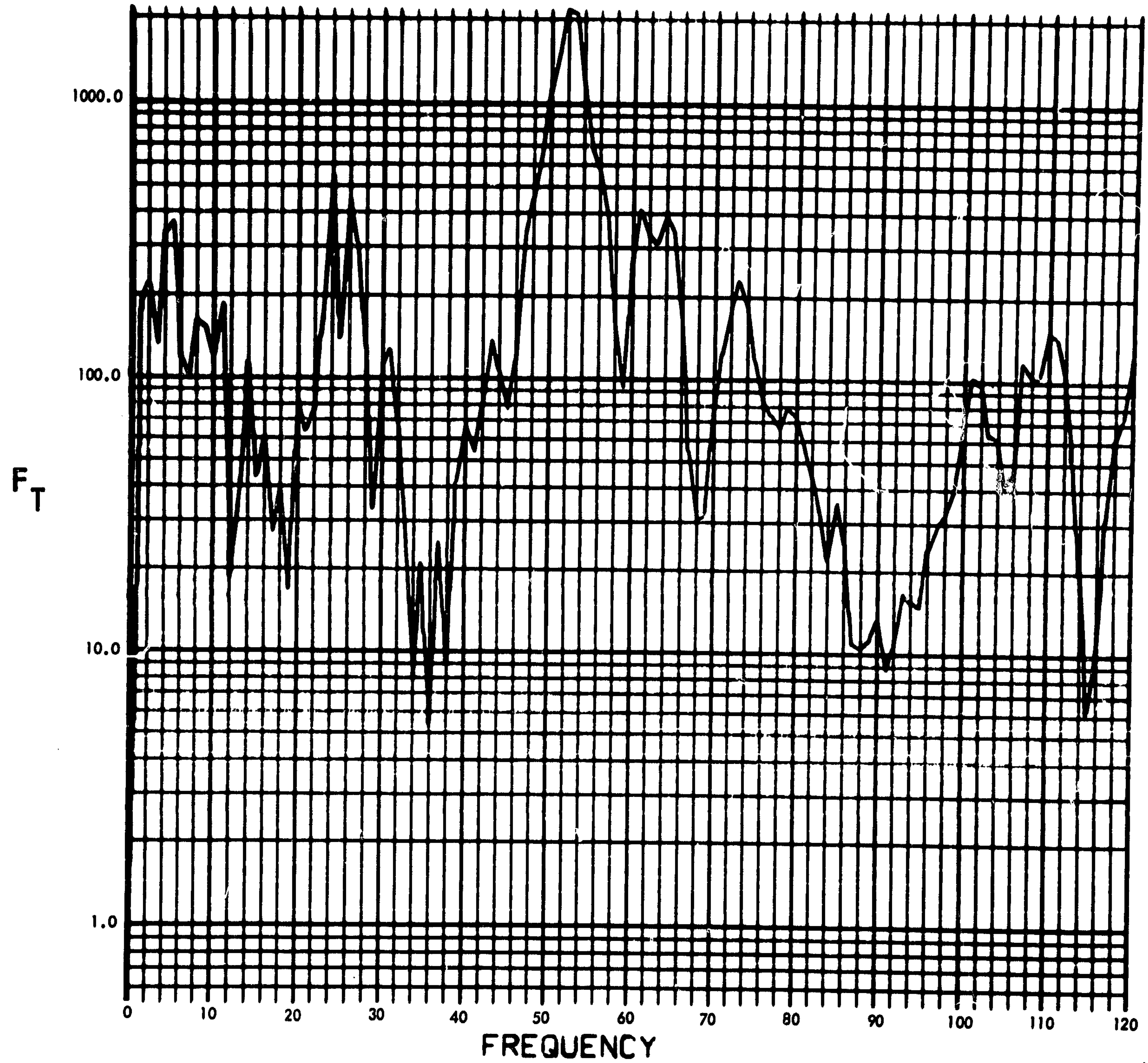

Fig. C-88. Joint 12, torque response function, Fourier transform, modulus (pulse 2)

PHASE ANGLE OF $F_T(F)$ (RAD) vs FREQUENCY (CYCLES/SEC)

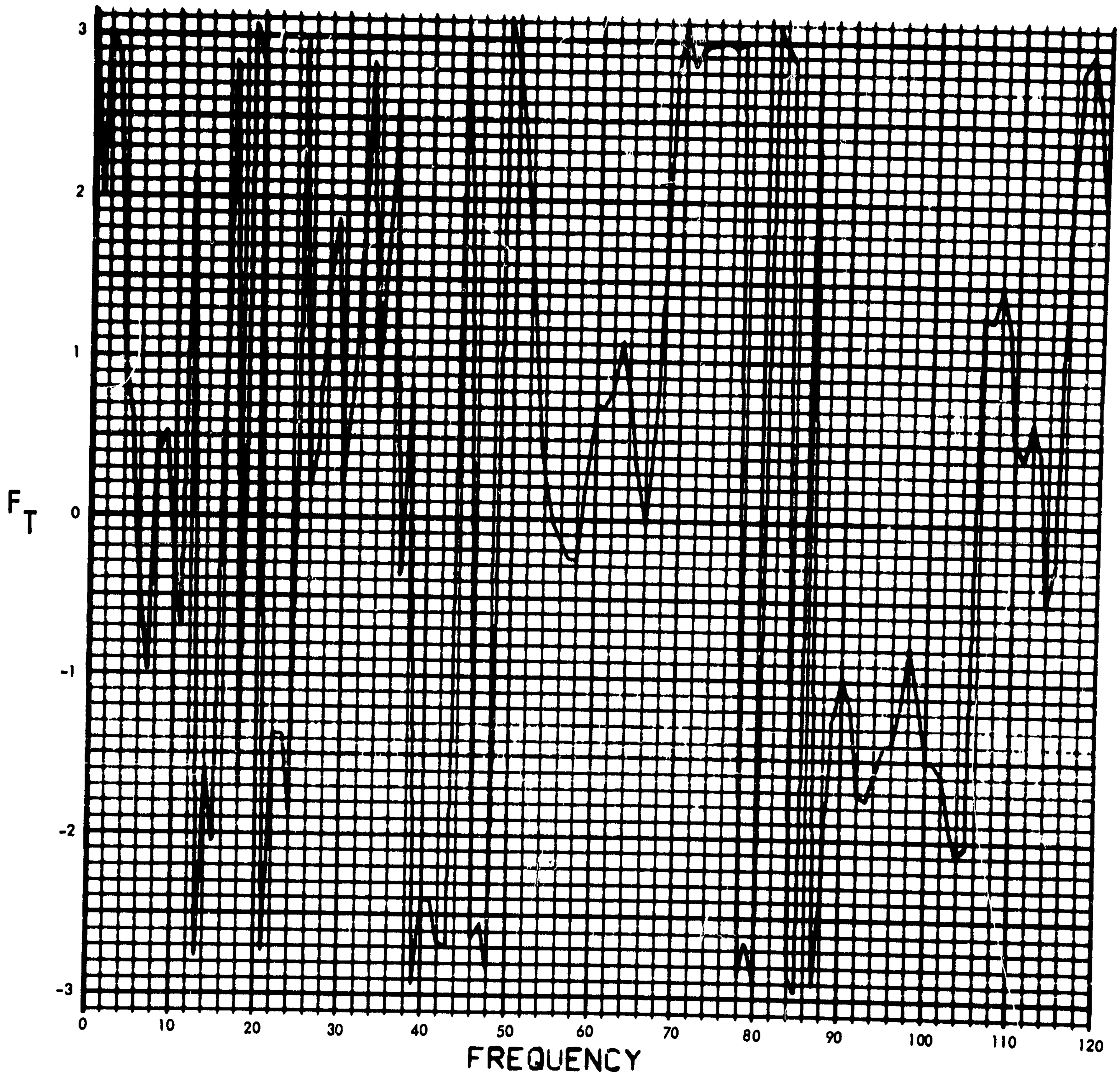

Fig. C-89. Joint 12, torque response function, Fourier transform, phase angle (pulse 2)

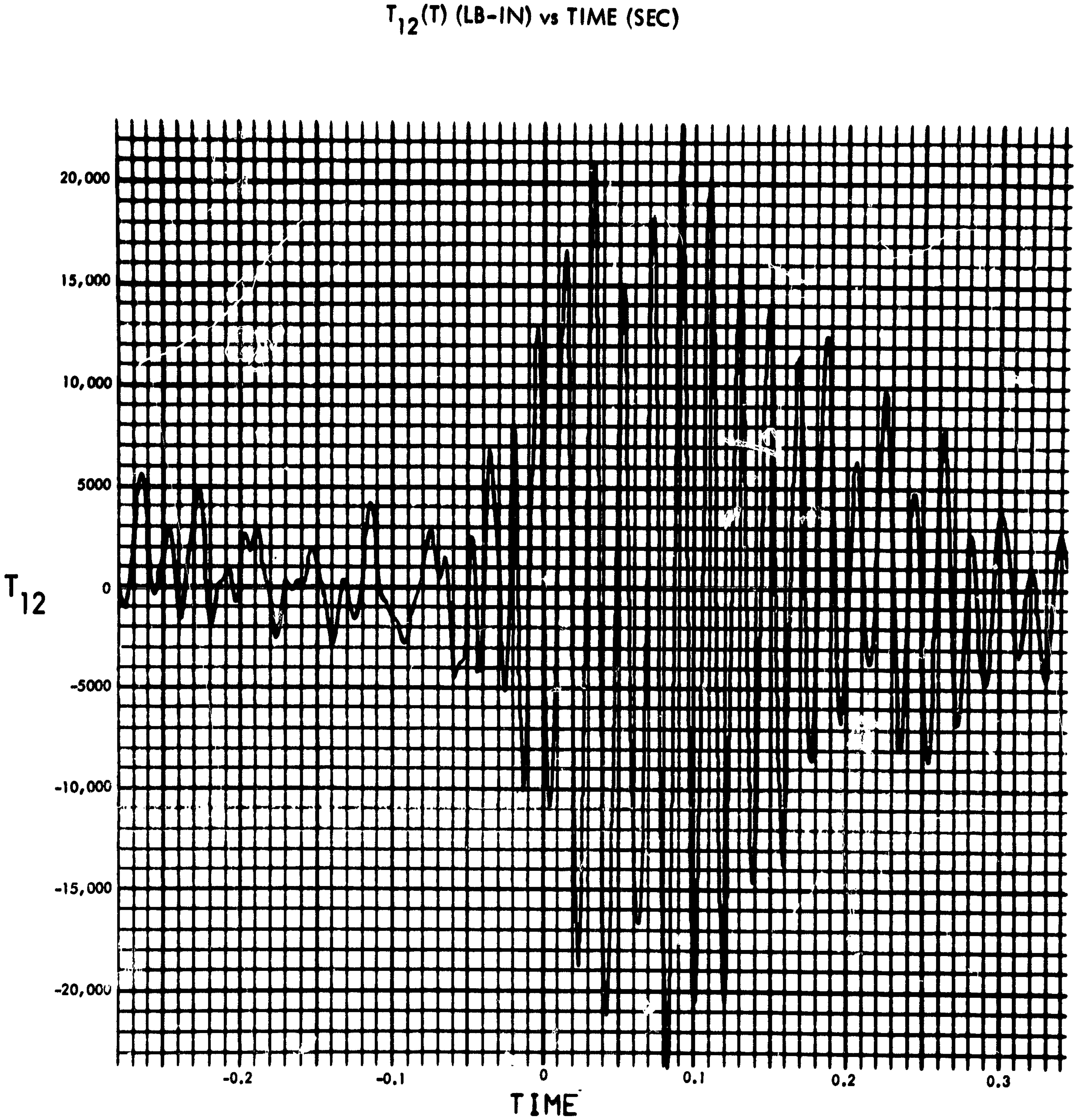

Fig. C-90. Joint 12, torque response, time history (pulse 2)

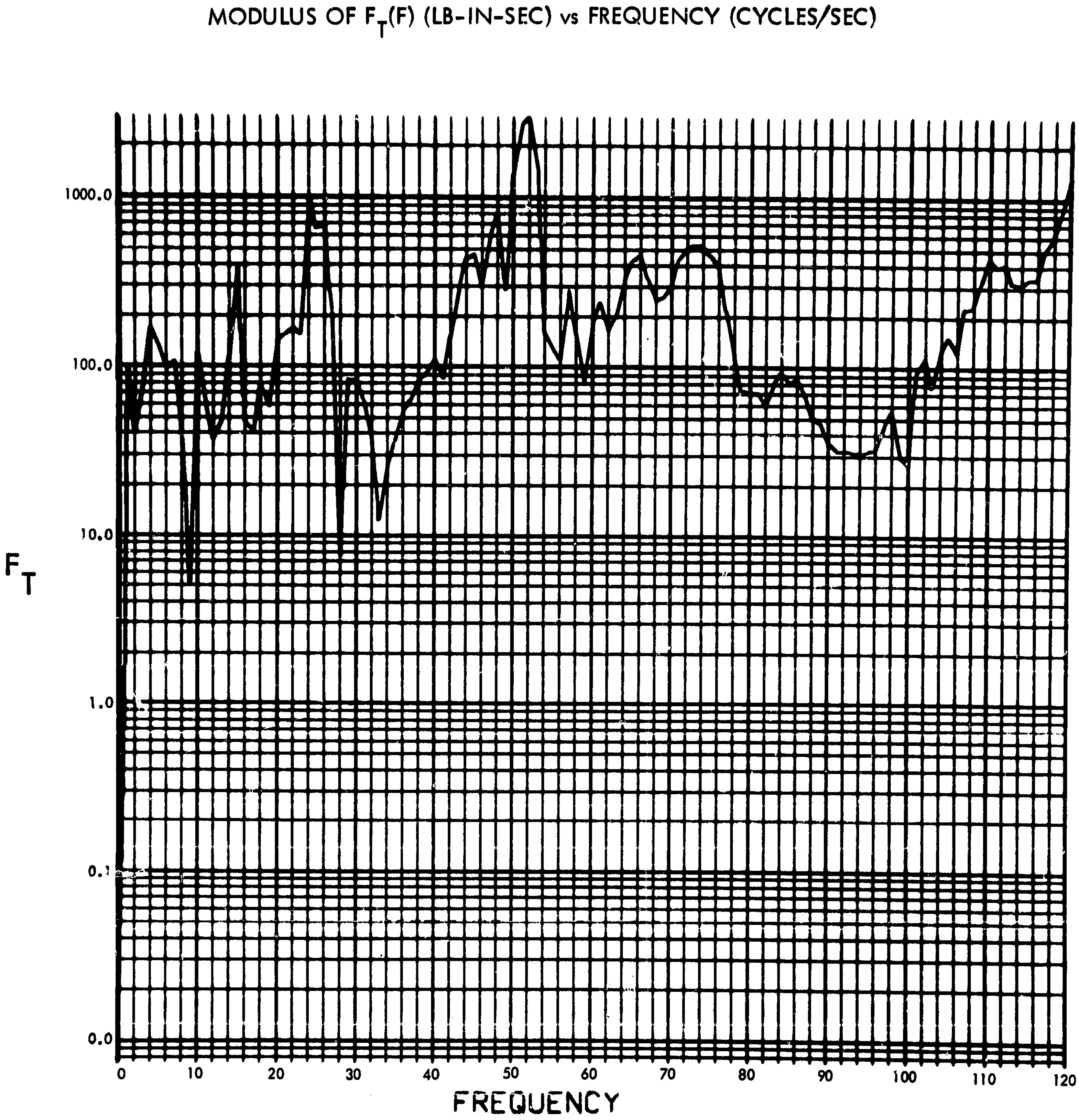

Fig. C-91. Joint 12, torque response function, Fourier transform, modulus (pulse 3)

PHASE ANGLE OF $F_T(F)$ (RAD) vs FREQUENCY (CYCLES/SEC)

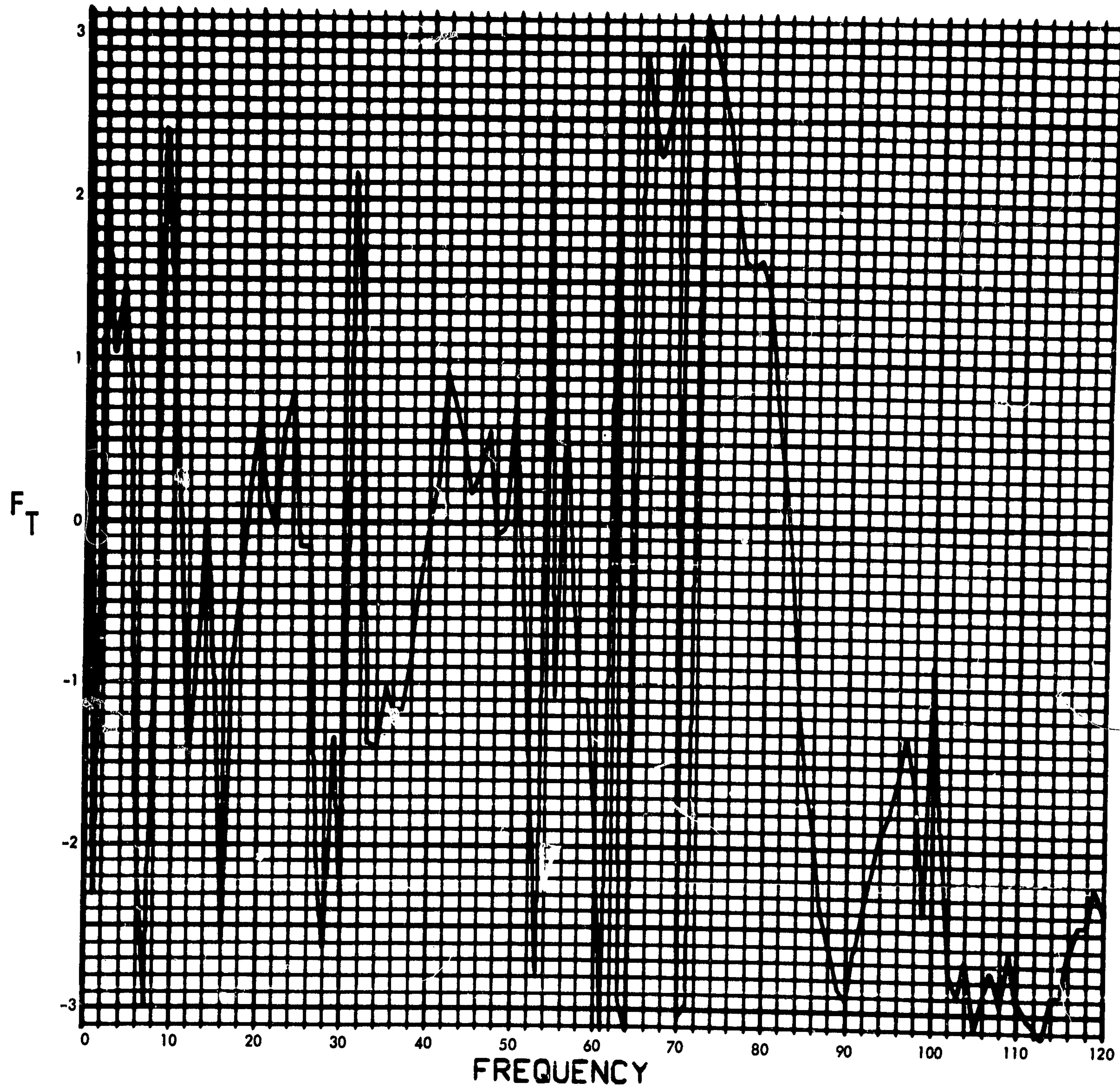

Fig. C-92. Joint 12, torque response function, Fourier transform, phase angle (pulse 3)

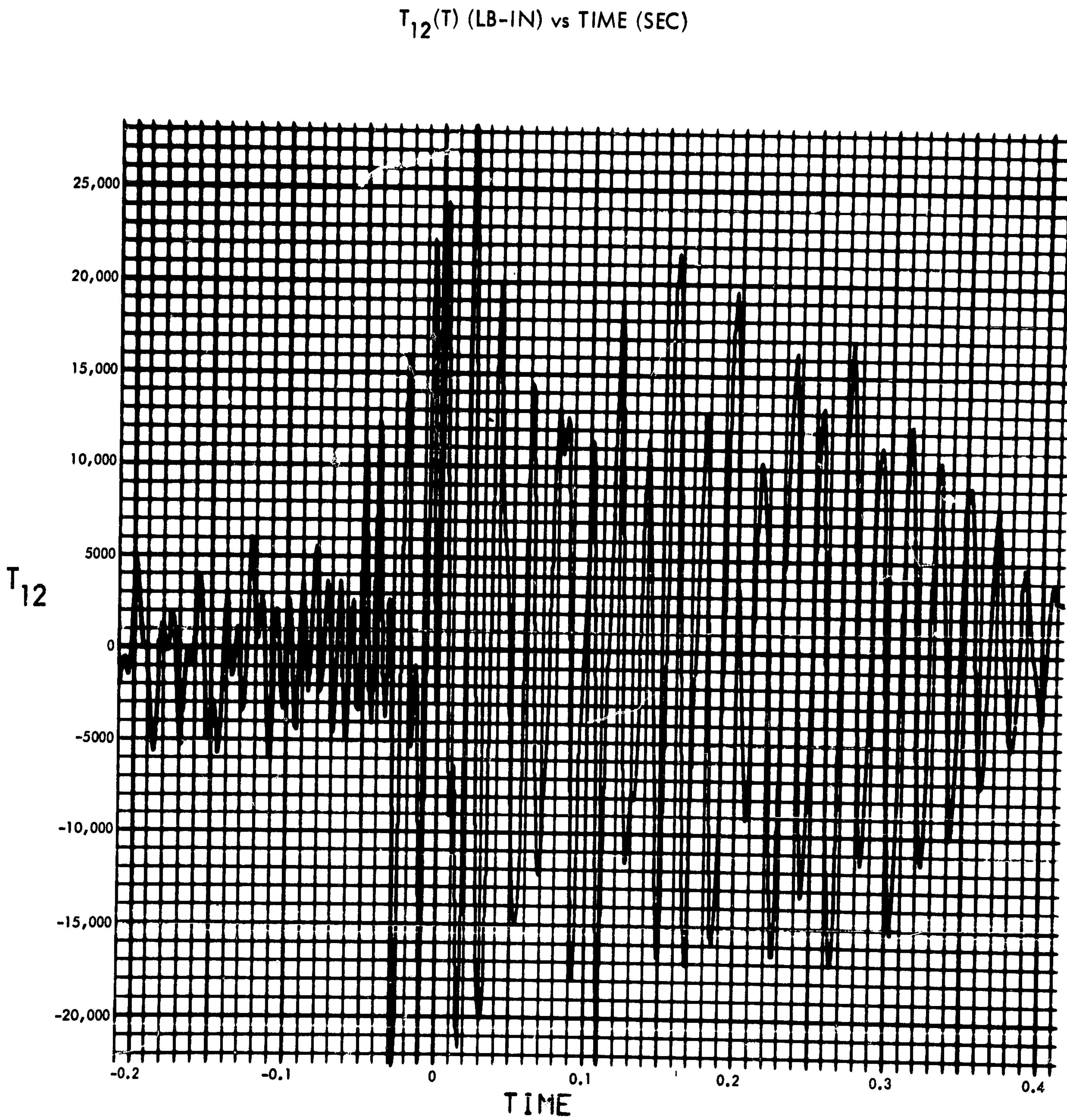

Fig. C-93. Joint 12, torque response, time history (pulse 3)

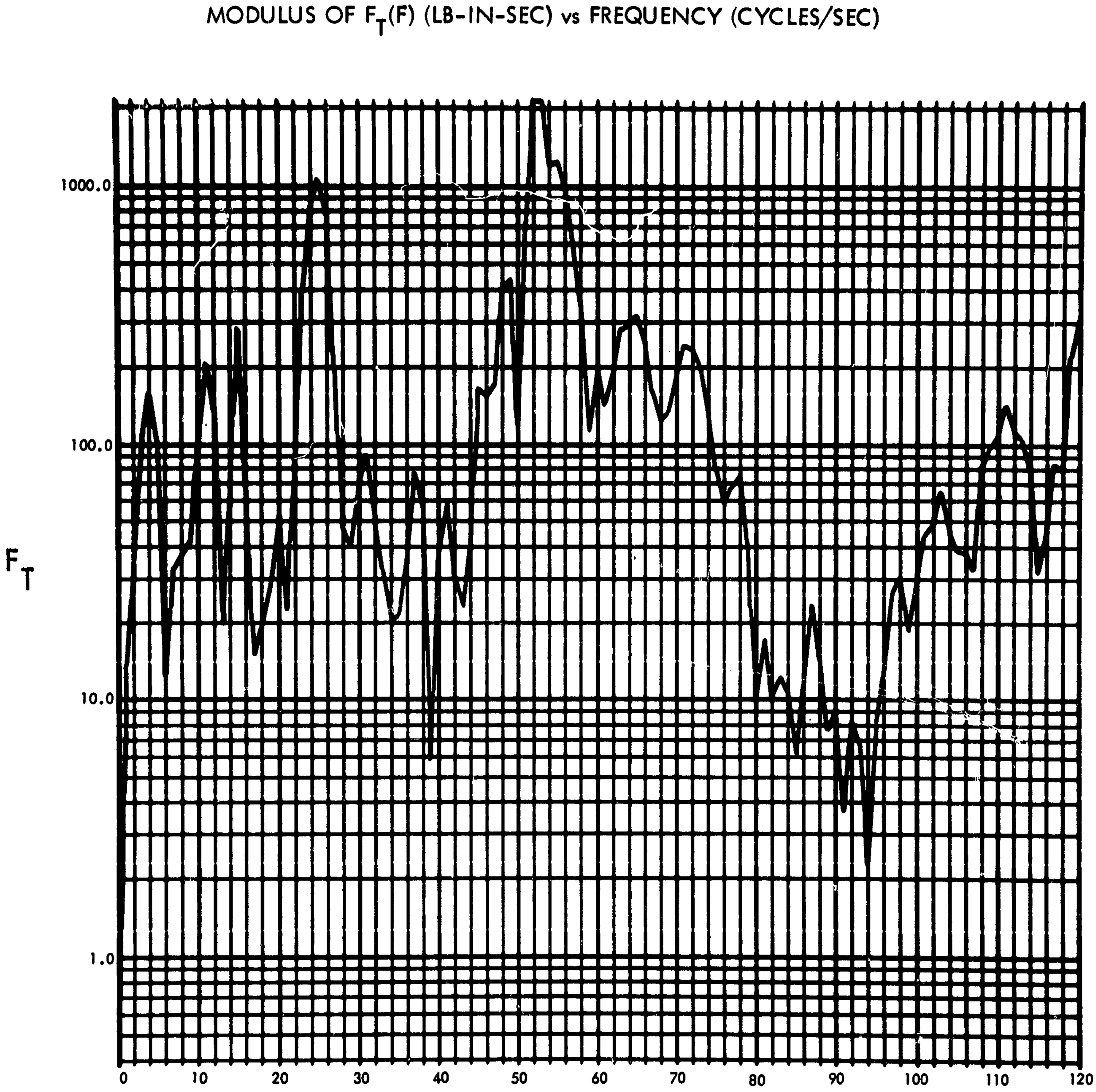

Fig. C-94. Joint 12, torque response function, Fourier transform, modulus (pulse 4)

PHASE ANGLE OF $F_T(F)$ (RAD) vs FREQUENCY (CYCLES/SEC)

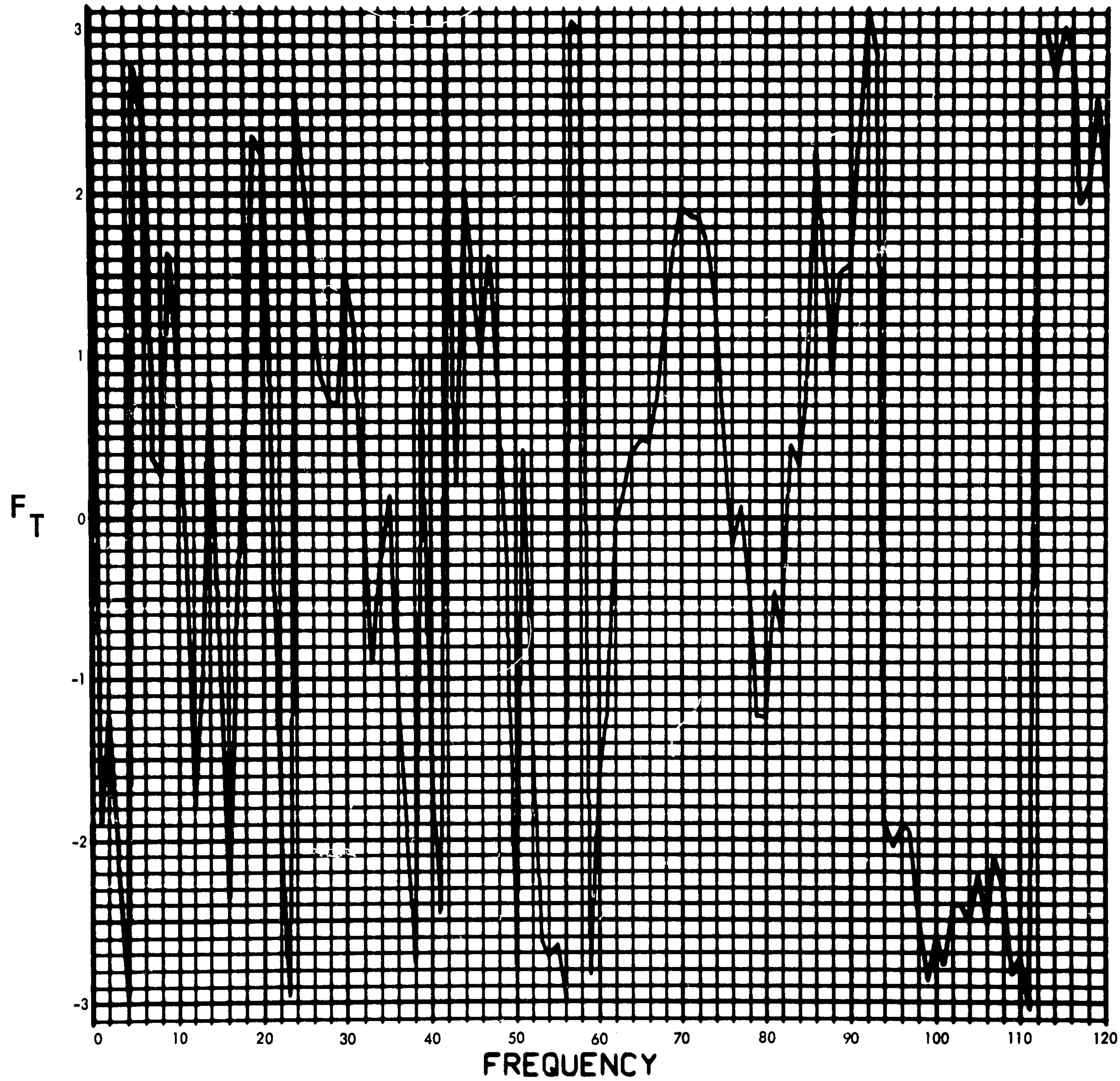

Fig. C-95. Joint 12, torque response function, Fourier transform, phase angle (pulse 4)

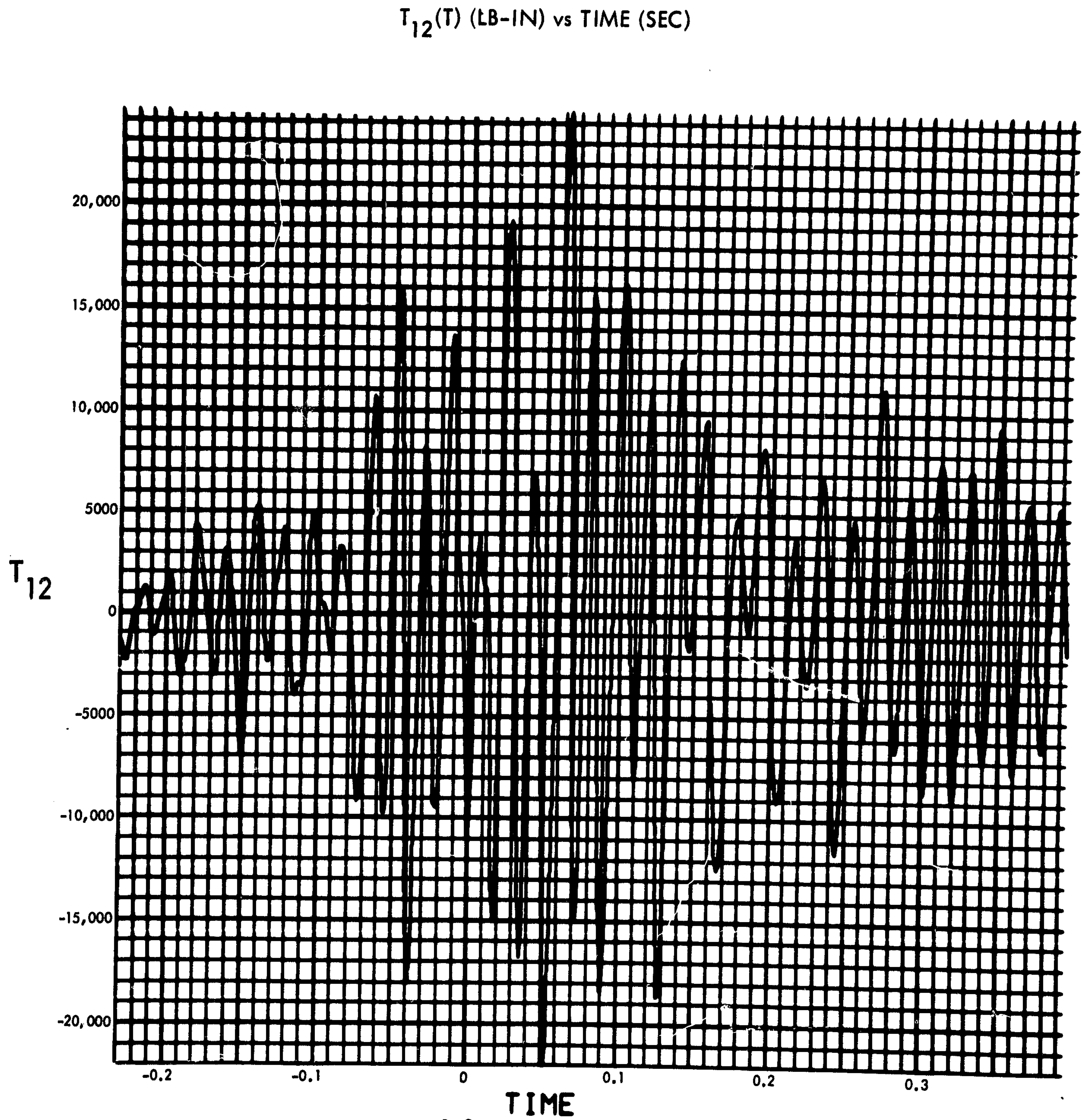

Fig. C-96. Joint 12, torque response, time history (pulse 4)

MODULUS H2(F) (1/LB-IN-SEC^2) vs FREQUENCY (CYCLES/SEC)

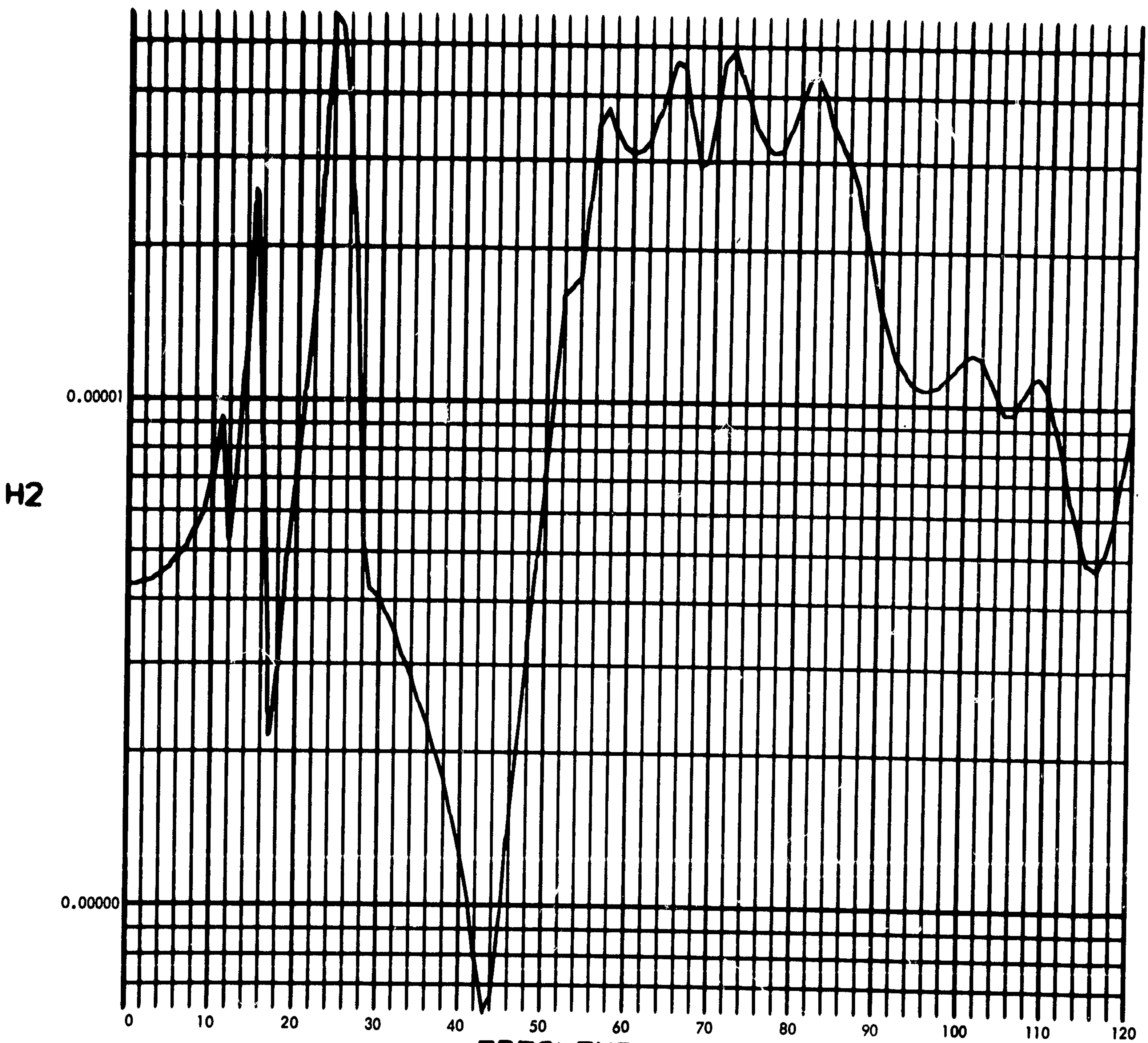

Fig. C-97. Joint 13, acceleration transfer function, Fourier transform, modulus

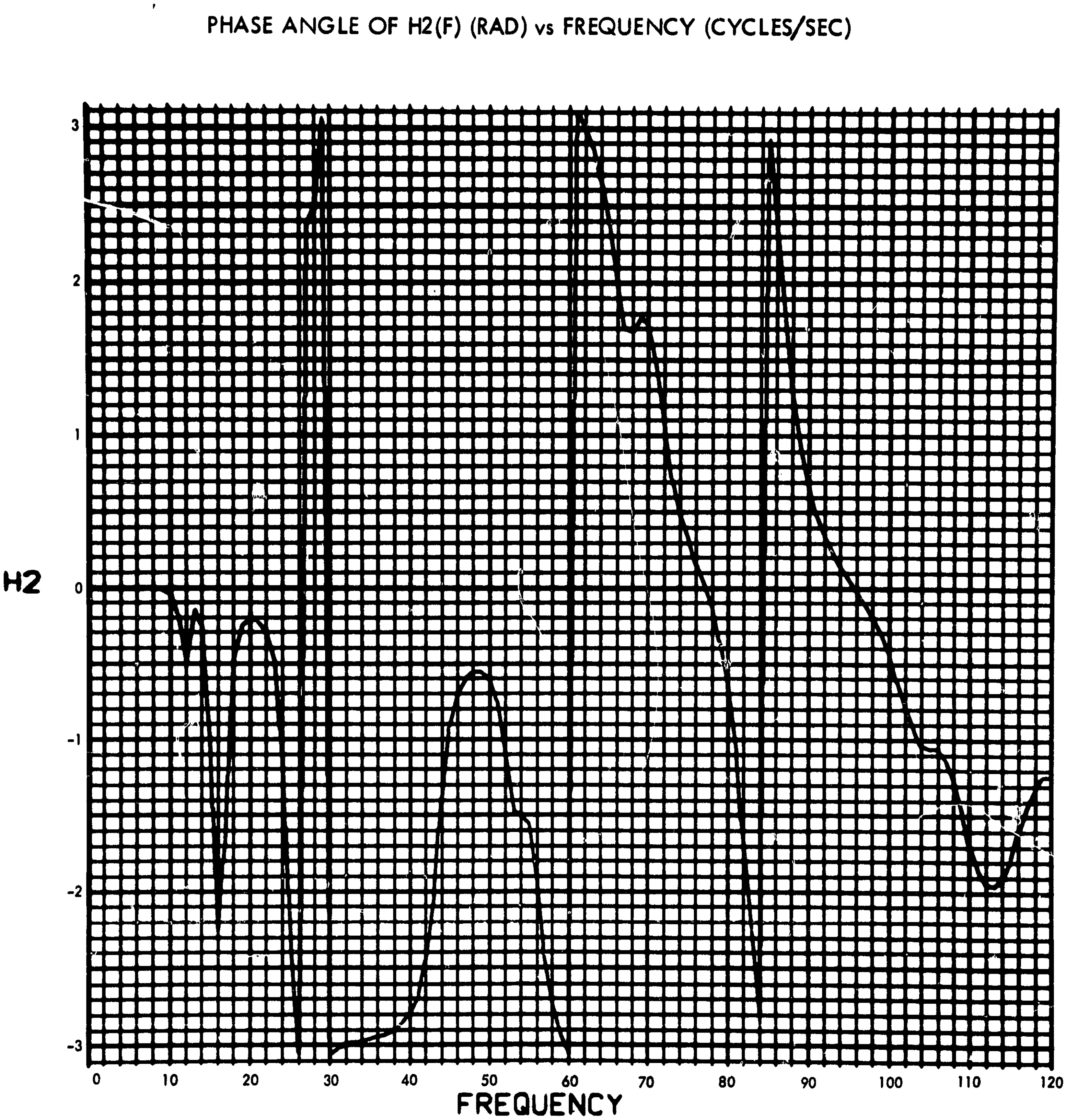

Fig. C-98. Joint 13, acceleration transfer function, Fourier transform, phase angle

MODULUS OF V2(F) (RAD/SEC) vs FREQUENCY (CYCLES/SEC)

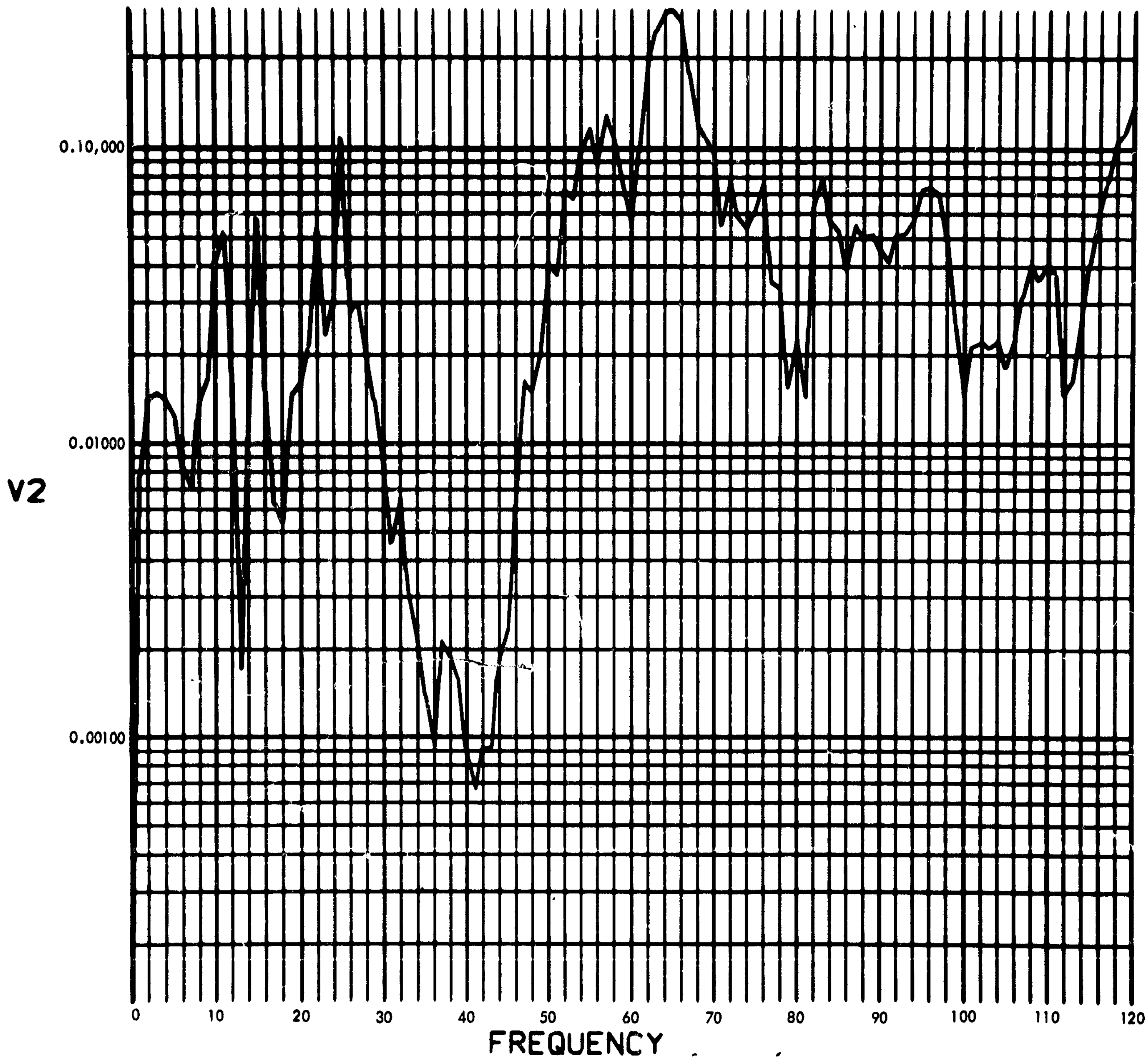

Fig. C-99. Joint 13, acceleration response, Fourier transform, modulus (pulse 1)

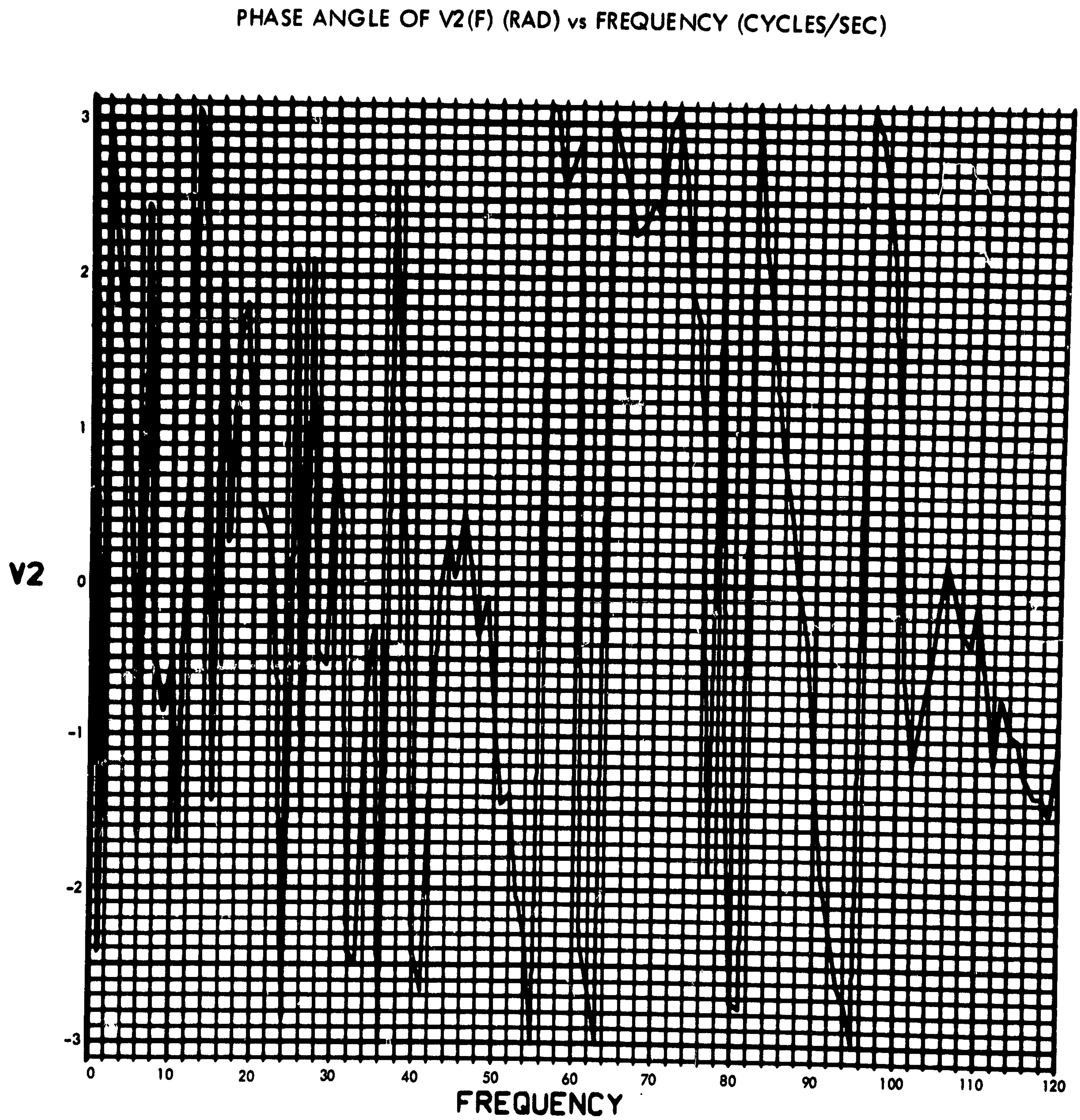

Fig. C-100. Joint 13, acceleration response, Fourier transform, phase angle (pulse 1)

U2(T) (RAD/SEC^2) vs TIME (SEC)

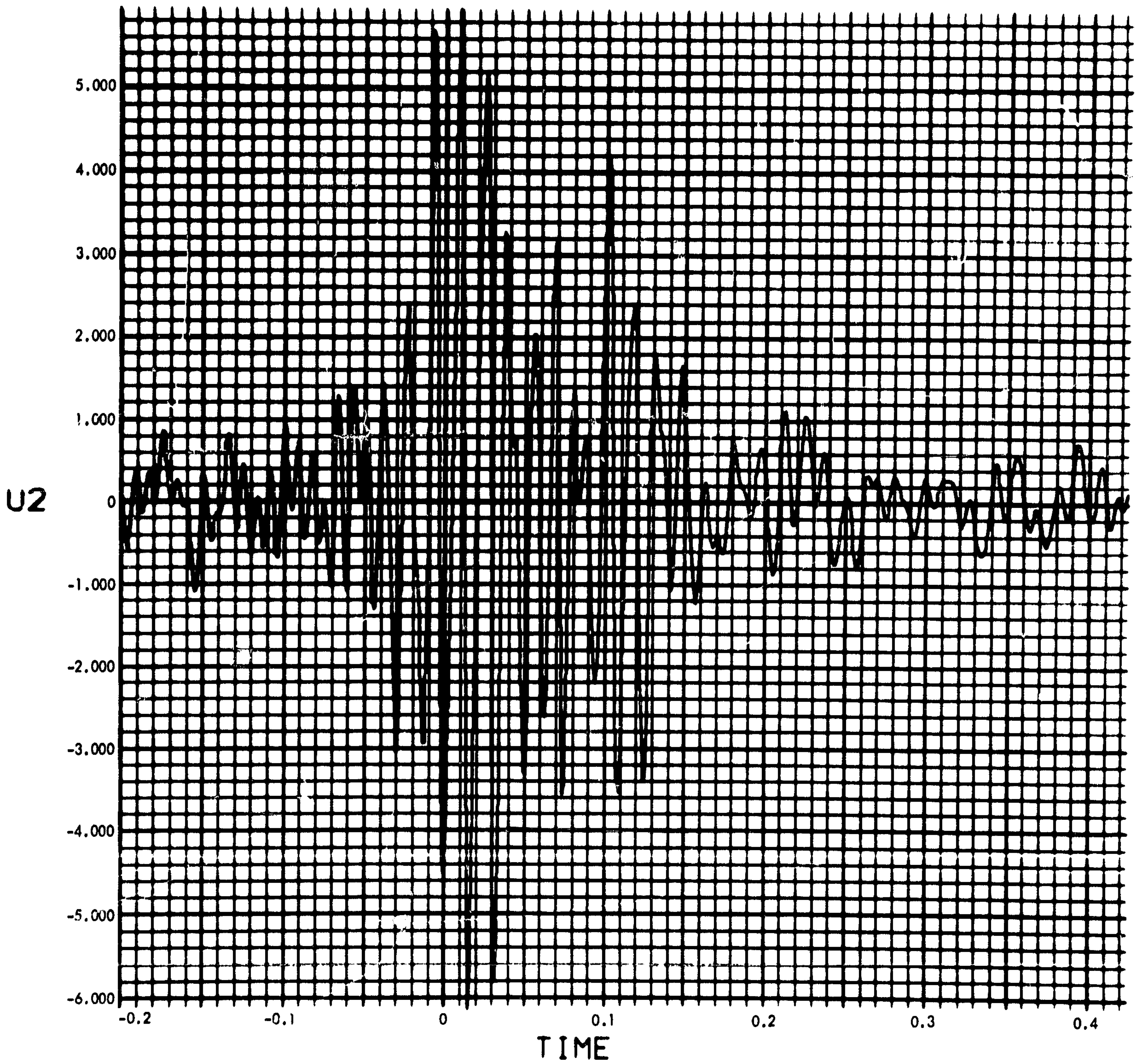

Fig. C-101. Joint 13, acceleration response, time history (pulse 1)

MODULUS OF V2(F) (RAD/SEC) vs FREQUENCY (CYCLES/SEC)

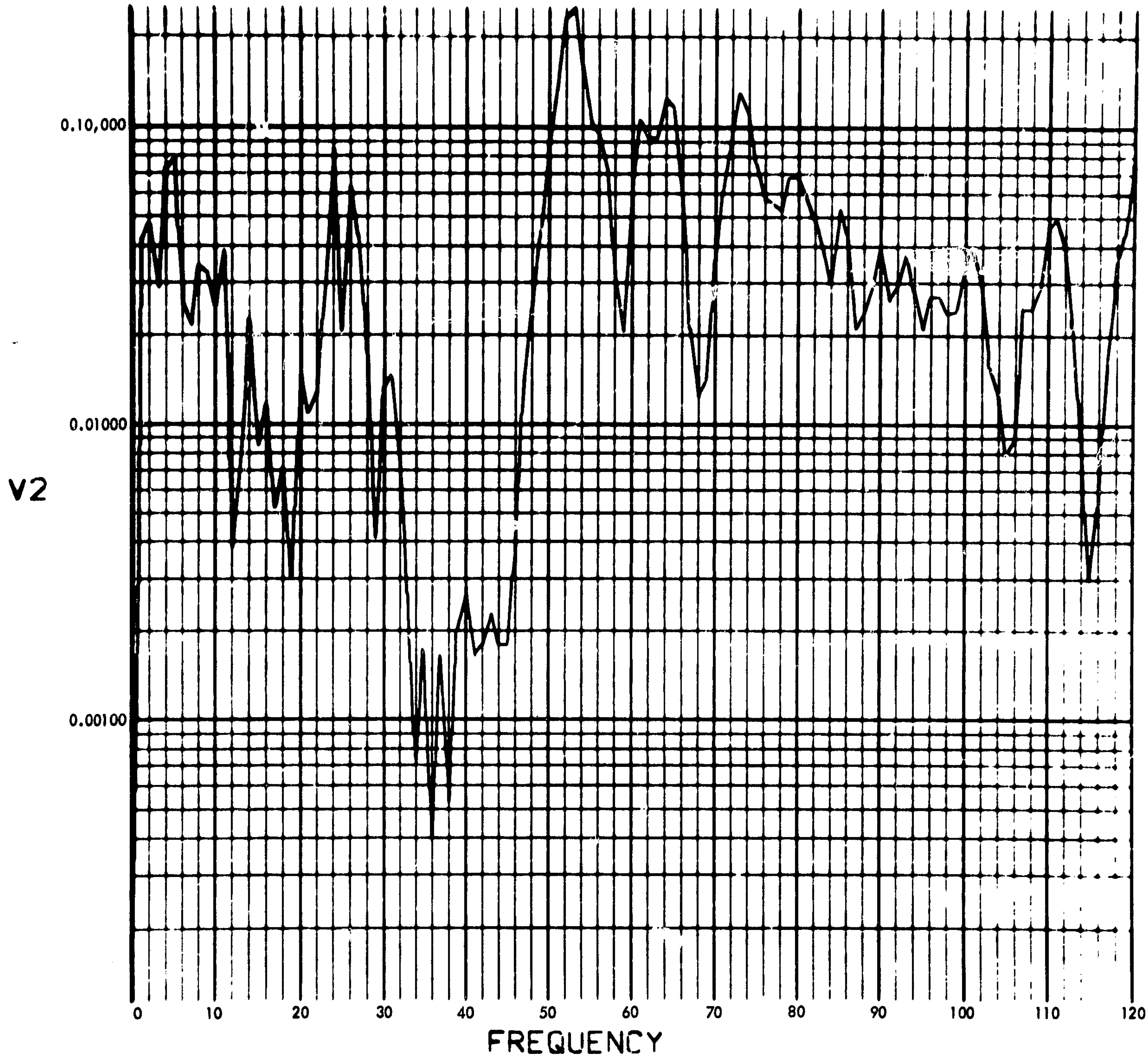

Fig. C-102. Joint 13, acceleration response, Fourier transform, modulus (pulse 2)

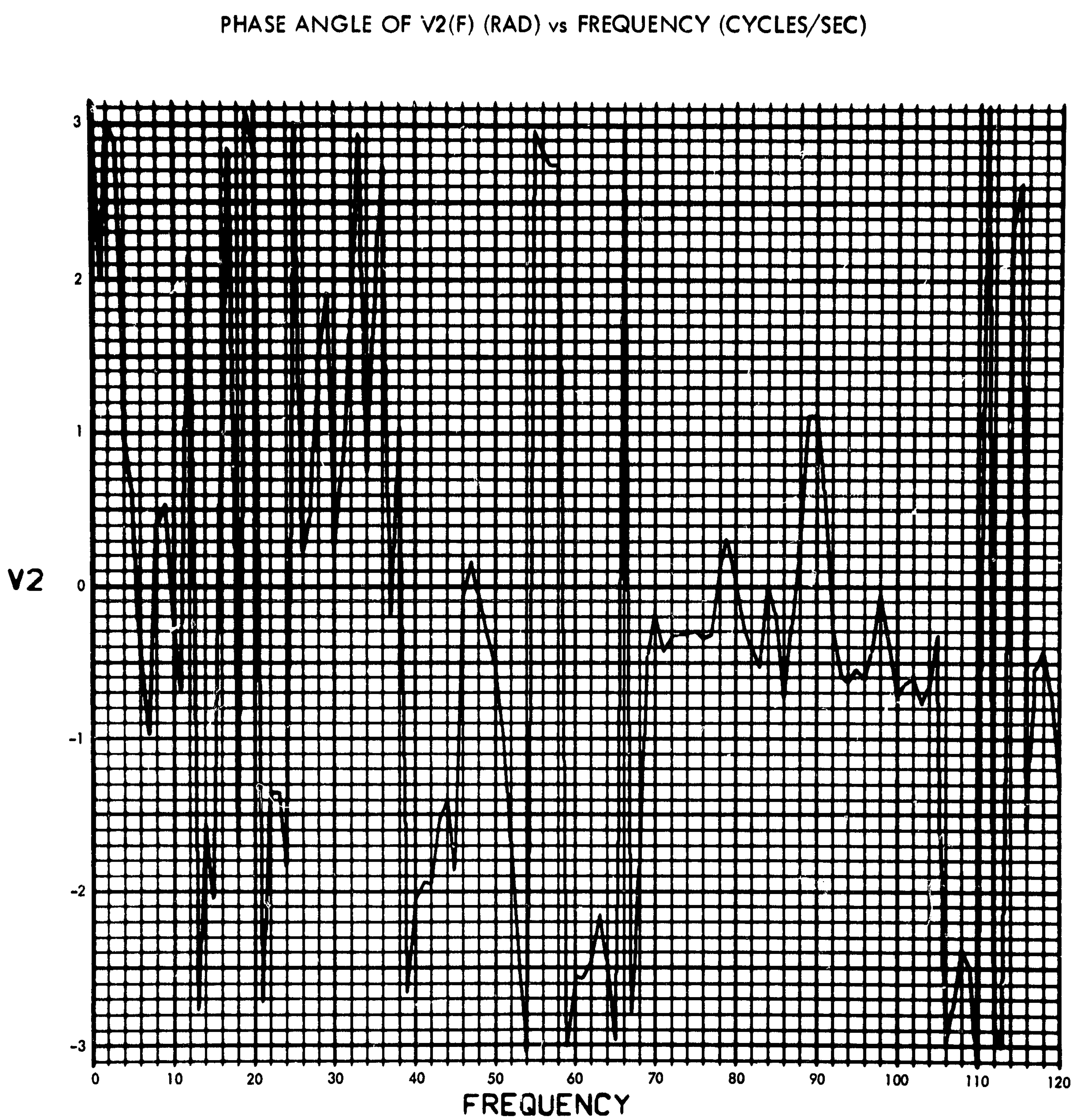

Fig. C-103. Joint 13, acceleration response, Fourier transform, phase angle (pulse 2)

U2(T) (RAD/SEC^2) vs TIME (SEC)

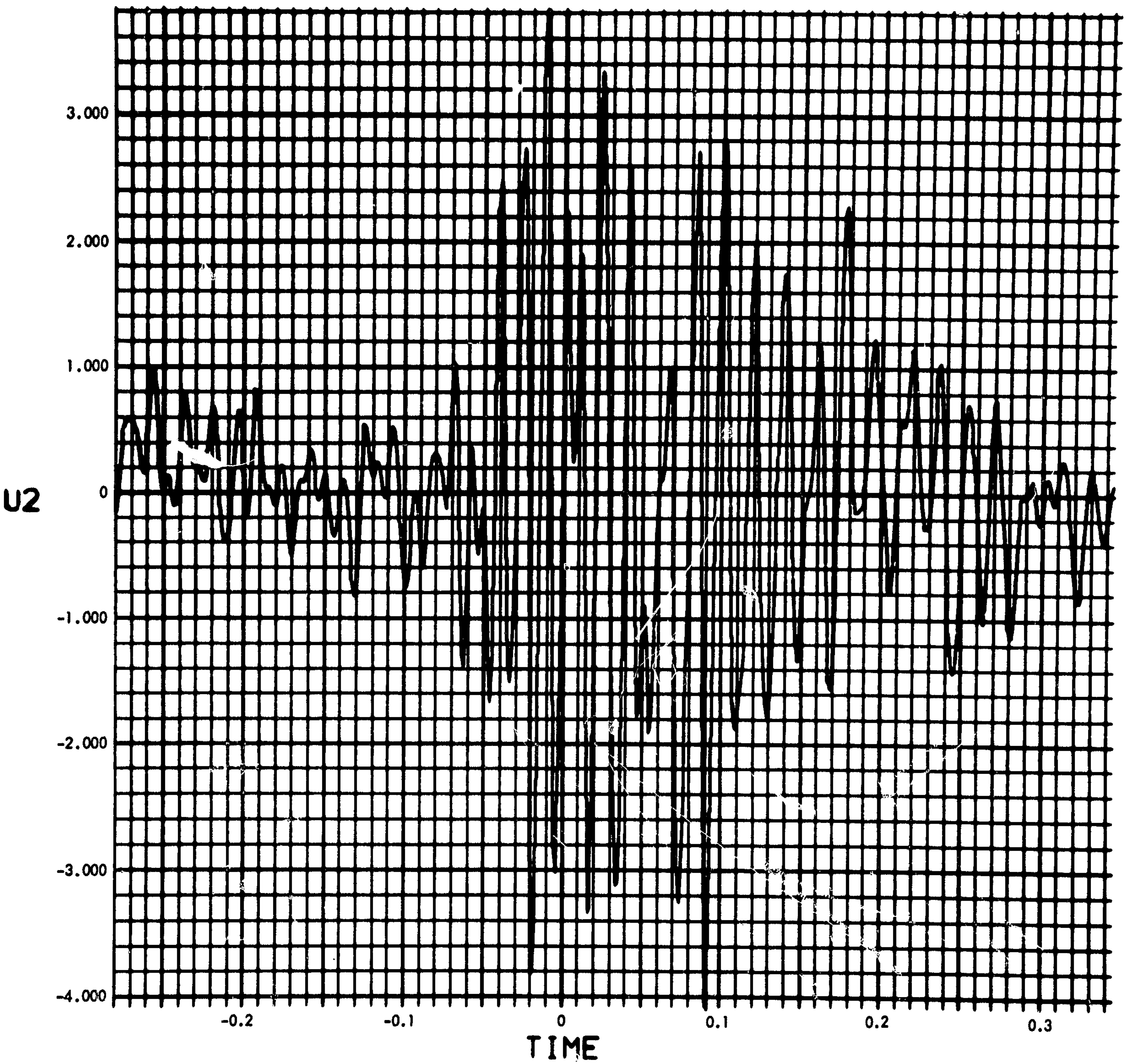

Fig. C-104. Joint 13, acceleration response, time history (pulse 2)

MODULUS OF V2(F) (RAD/SEC) vs FREQUENCY (CYCLES/SEC)

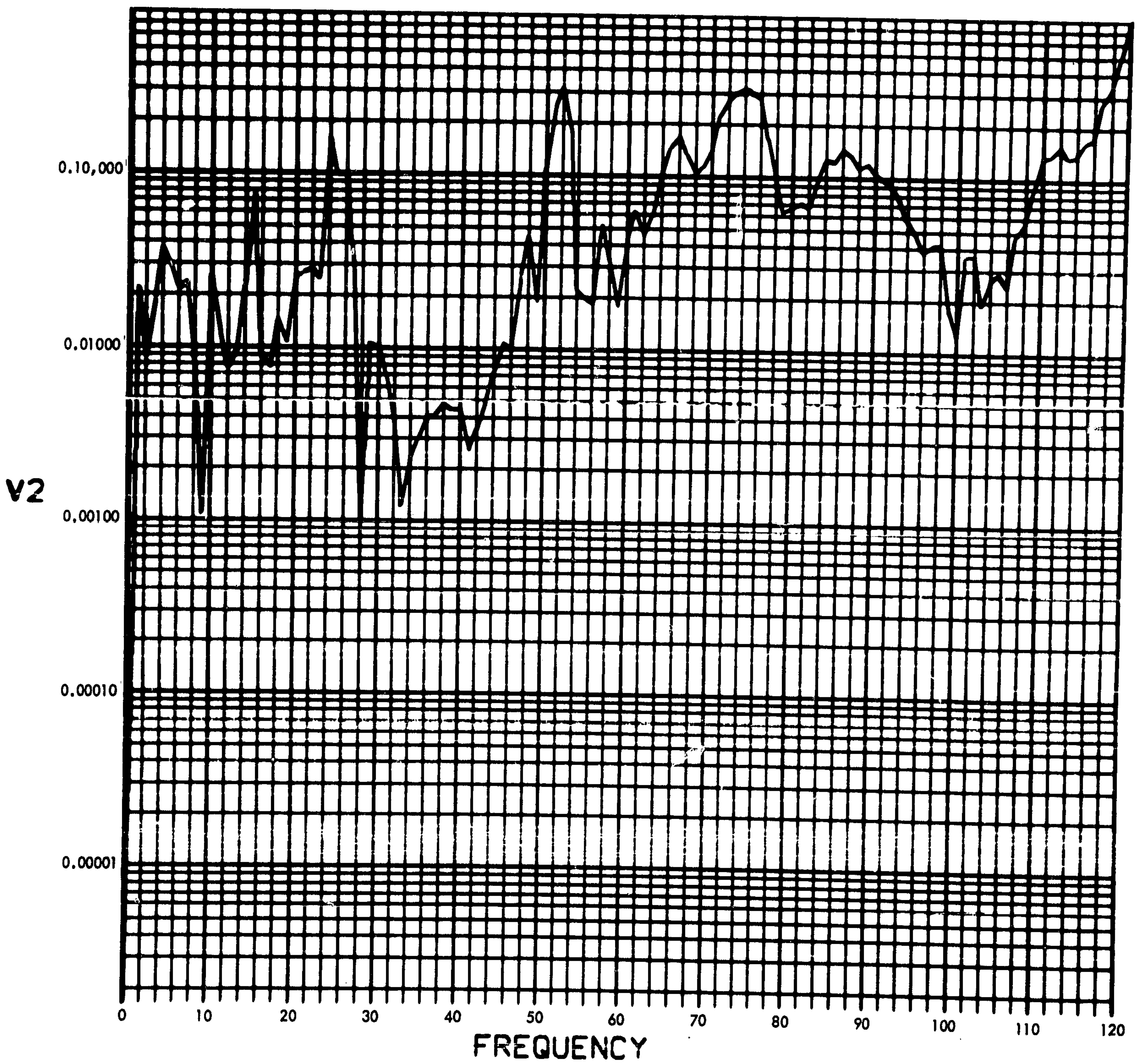

Fig. C-105. Joint 13, acceleration response, Fourier transform, modulus (pulse 3)

PHASE ANGLE OF V2(F) (RAD) vs FREQUENCY (CYCLES/SEC)

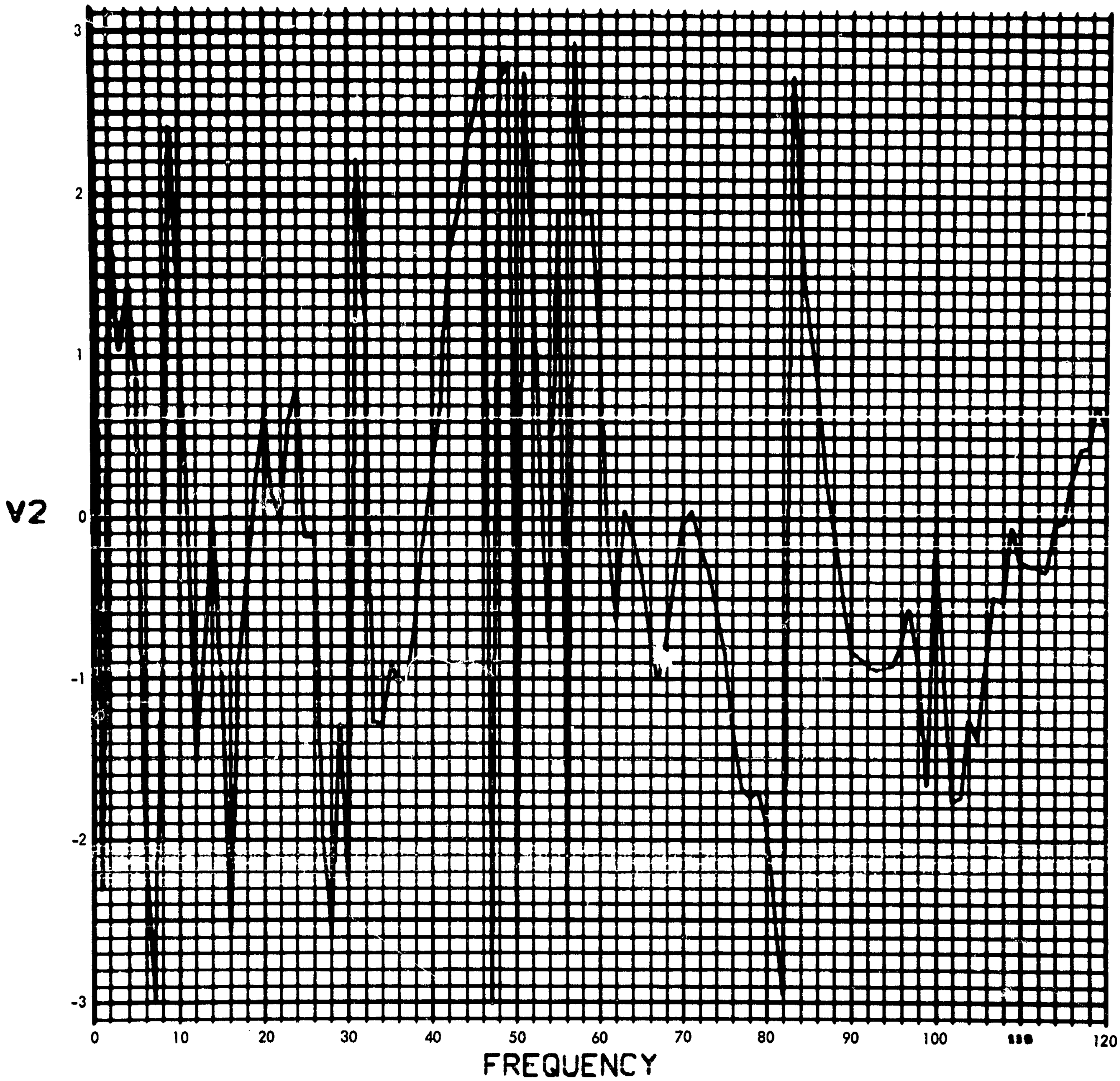

Fig. C-106. Joint 13, acceleration response, Fourier transform, phase angle (pulse 3)

U2(T) (RAD/SEC^2) vs TIME (SEC)

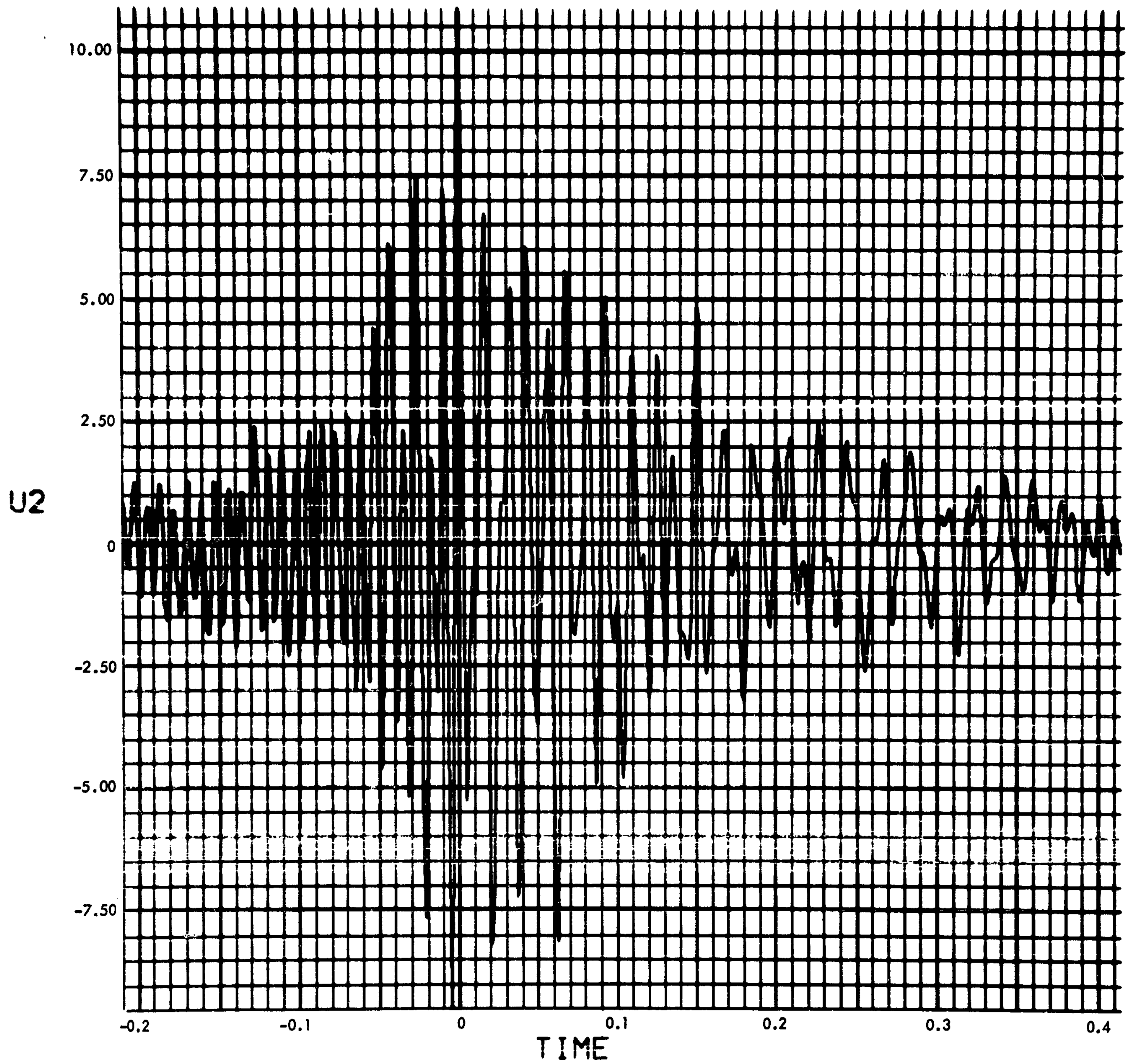

Fig. C-107. Joint 13, acceleration response, time history (pulse 3)

MODULUS OF V2(F) (RAD/SEC) vs FREQUENCY (CYCLES/SEC)

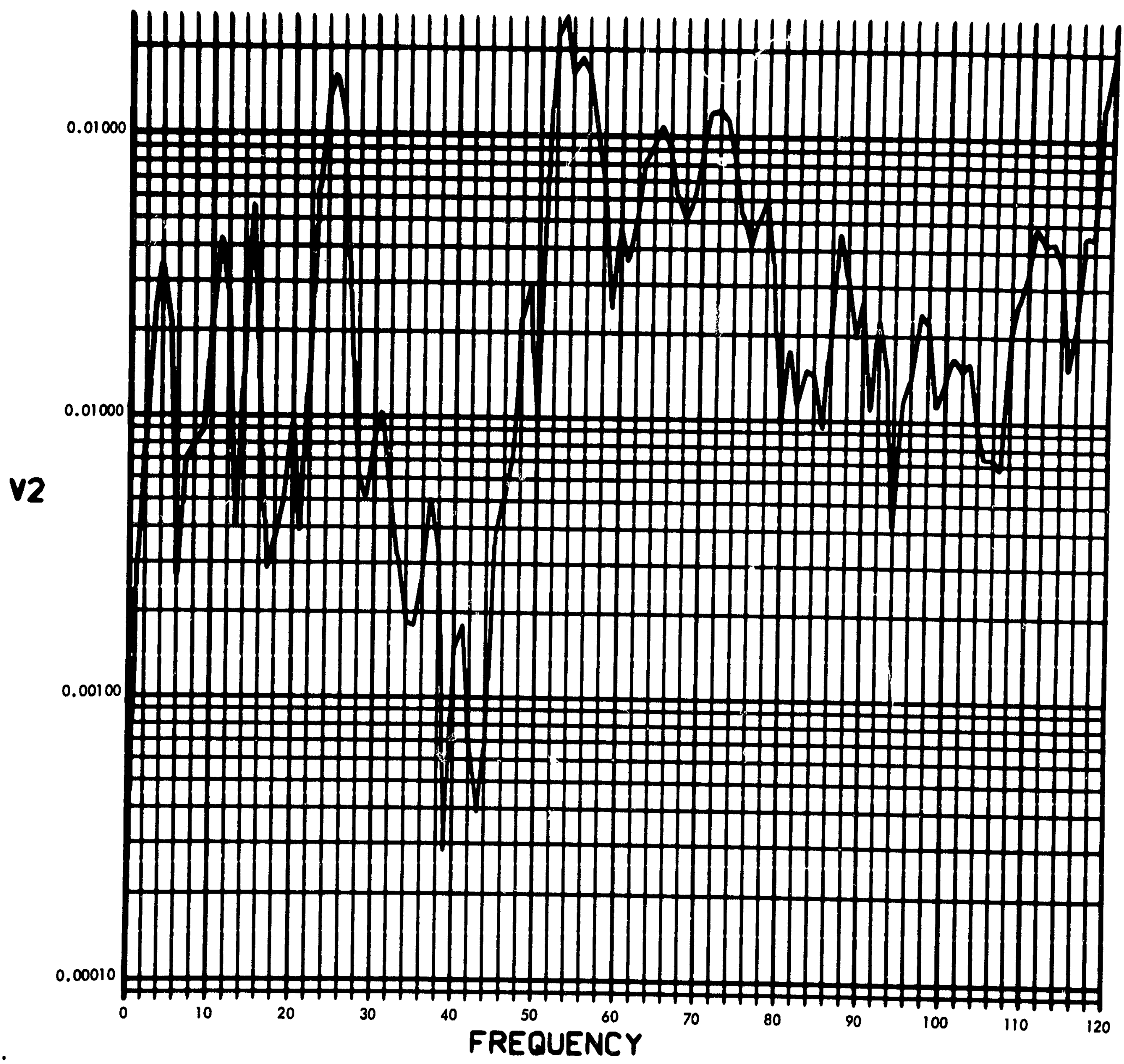

Fig. C-108. Joint 13, acceleration response, Fourier transform, modulus (pulse 4)

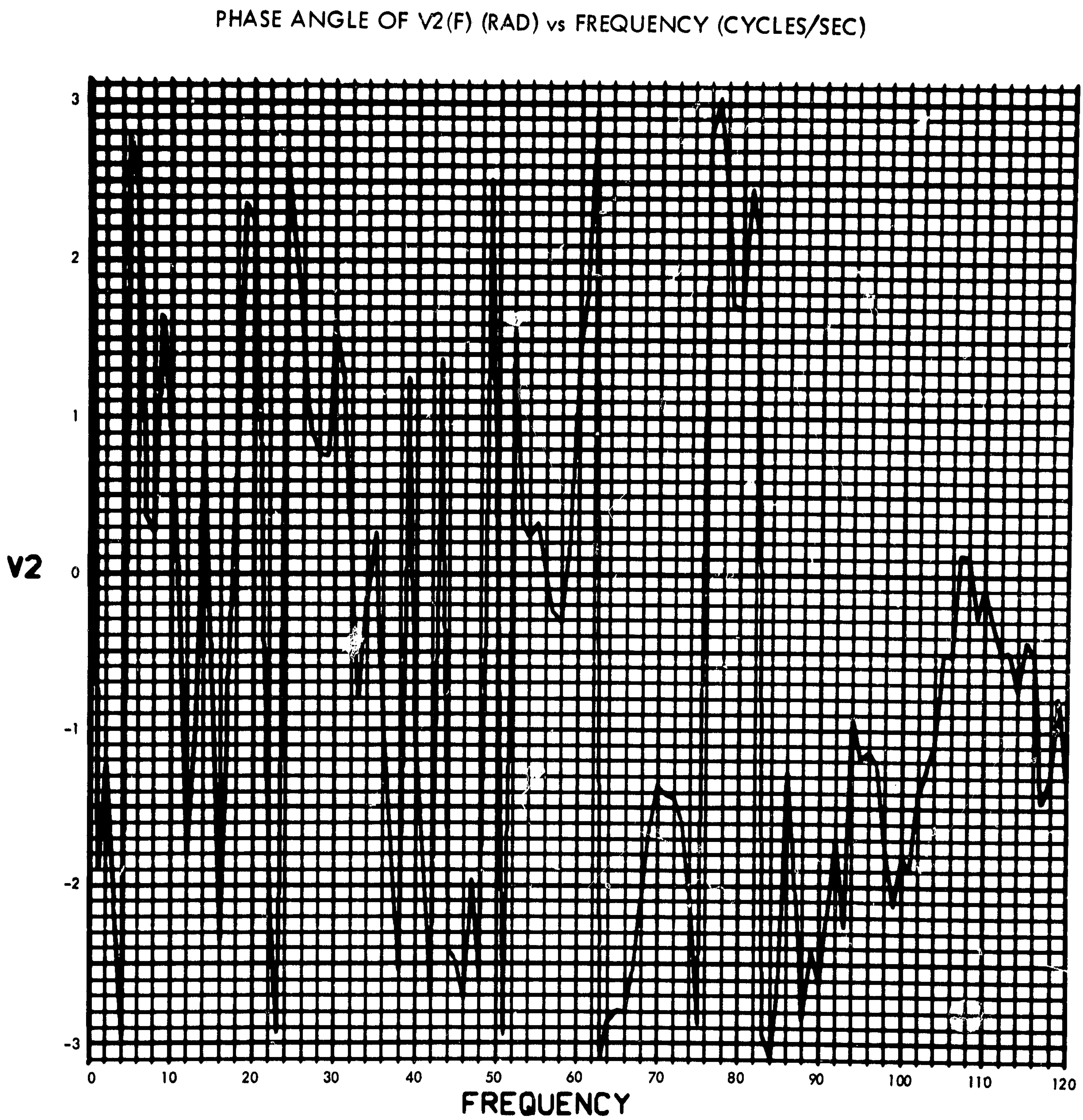

Fig. C-109. Joint 13, acceleration response, Fourier transform, phase angle (pulse 4)

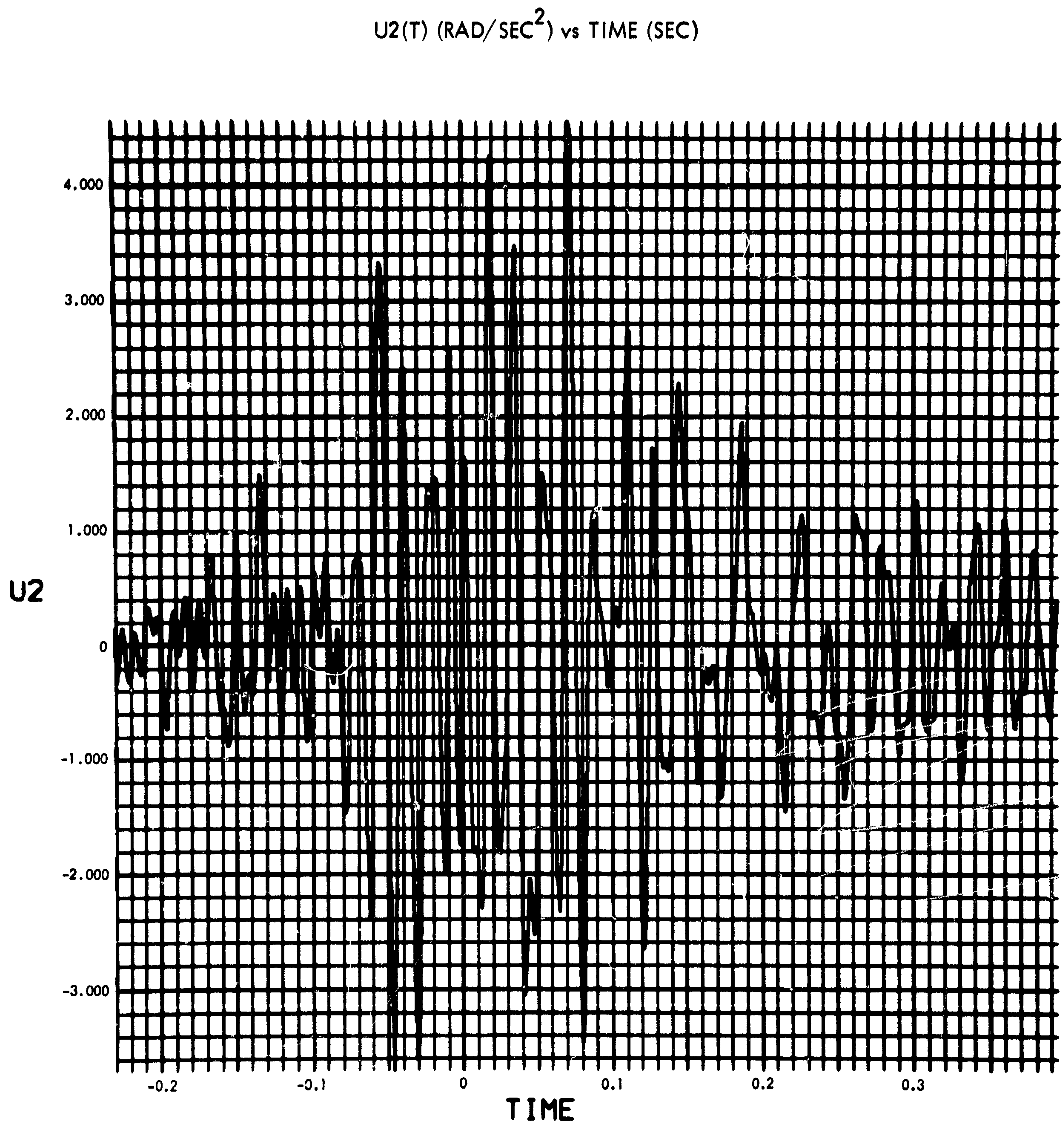

Fig. C-110. Joint 13, acceleration response, time history (pulse 4)

MODULUS H_T(F) (RAD) vs FREQUENCY (CYCLES/SEC)

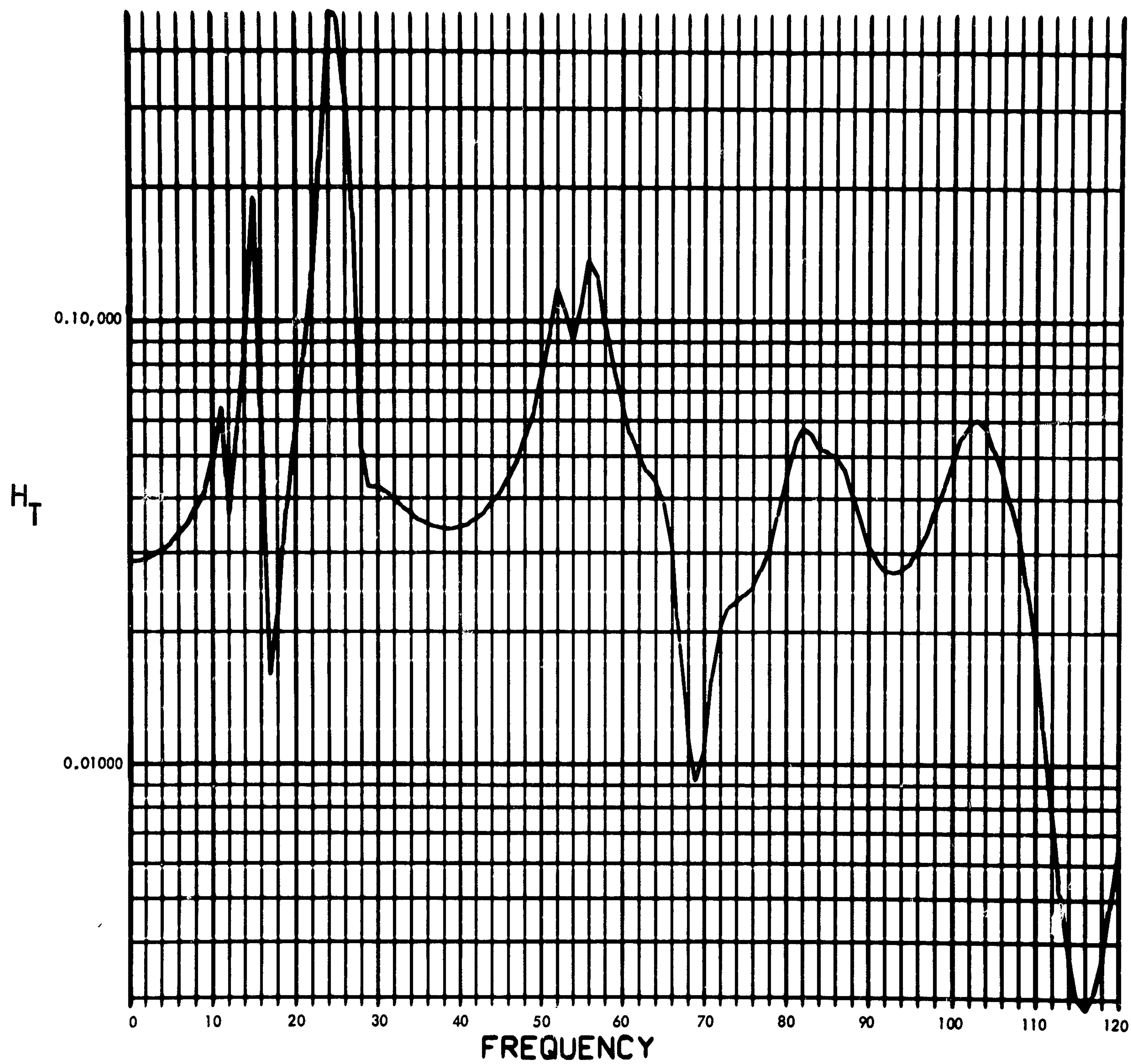

Fig. C-111. Joint 13, torque transfer function, Fourier transform, modulus

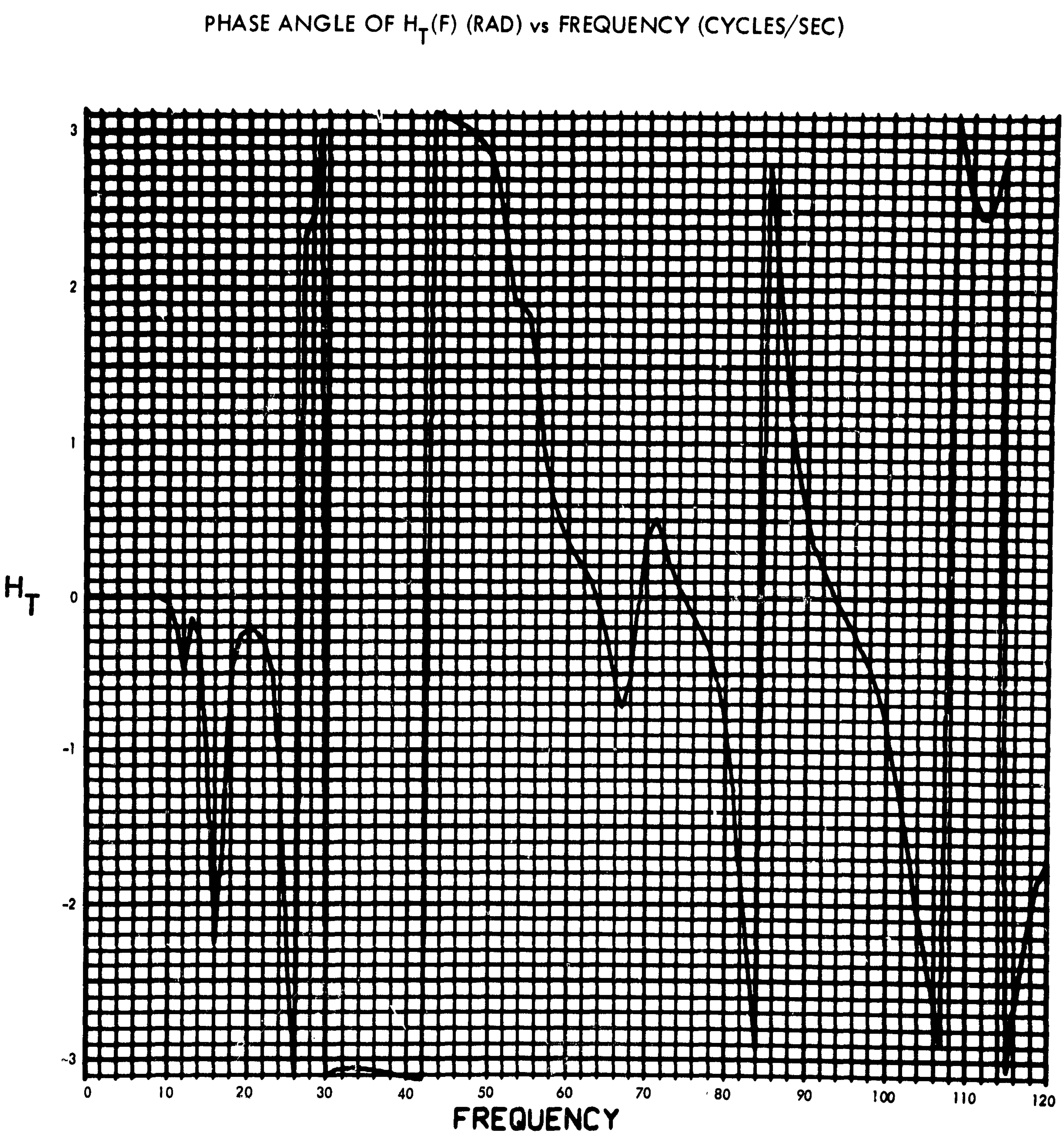

Fig. C-112. Joint 13, torque transfer function, Fourier transform, phase angle

MODULUS OF $F_T(F)$ (LB-IN-SEC) vs FREQUENCY (CYCLES/SEC)

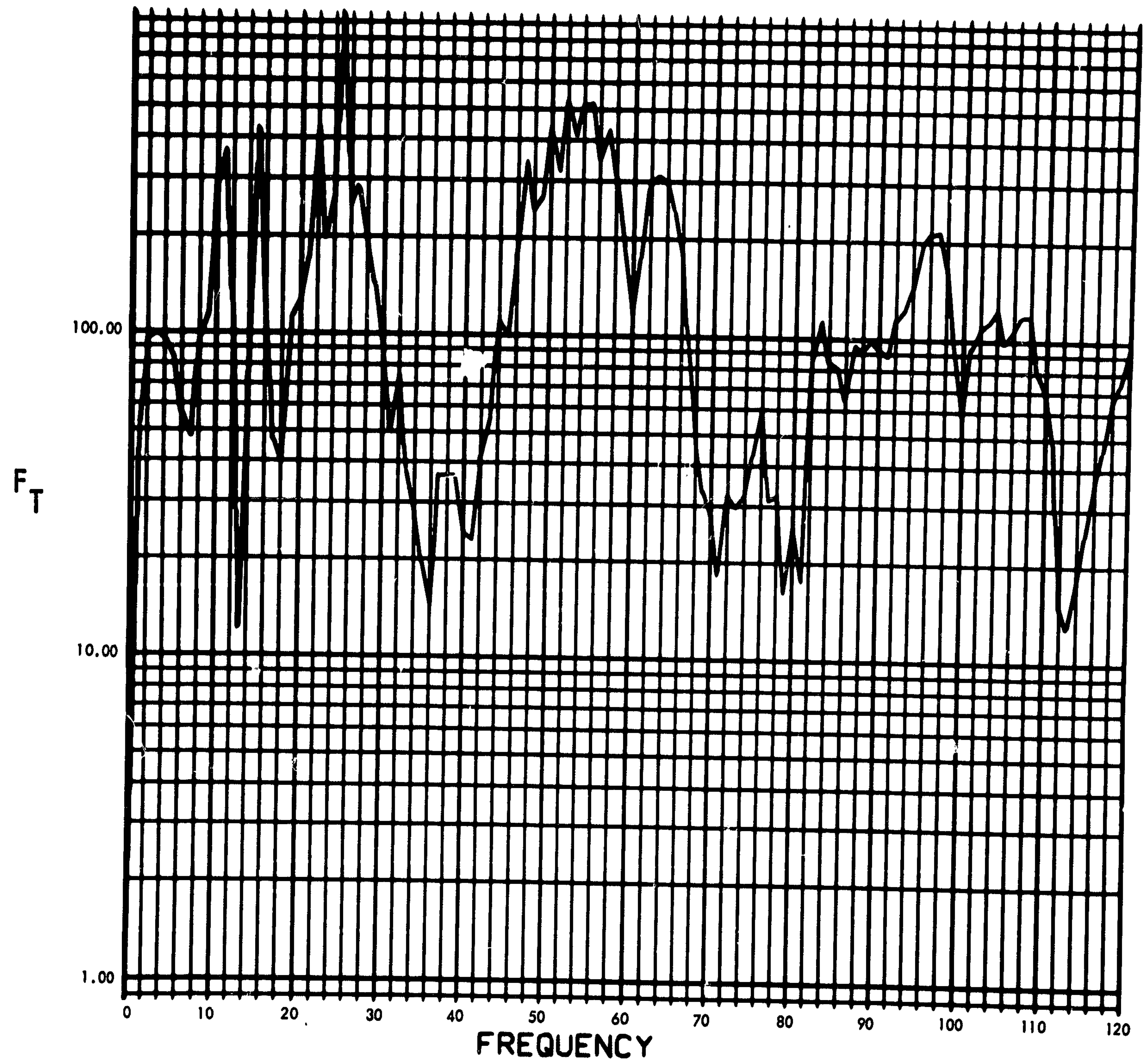

Fig. C-113. Joint 13, torque response function, Fourier transform, modulus (pulse 1)

PHASE ANGLE OF F_T(F) (RAD) vs FREQUENCY (CYCLES/SEC)

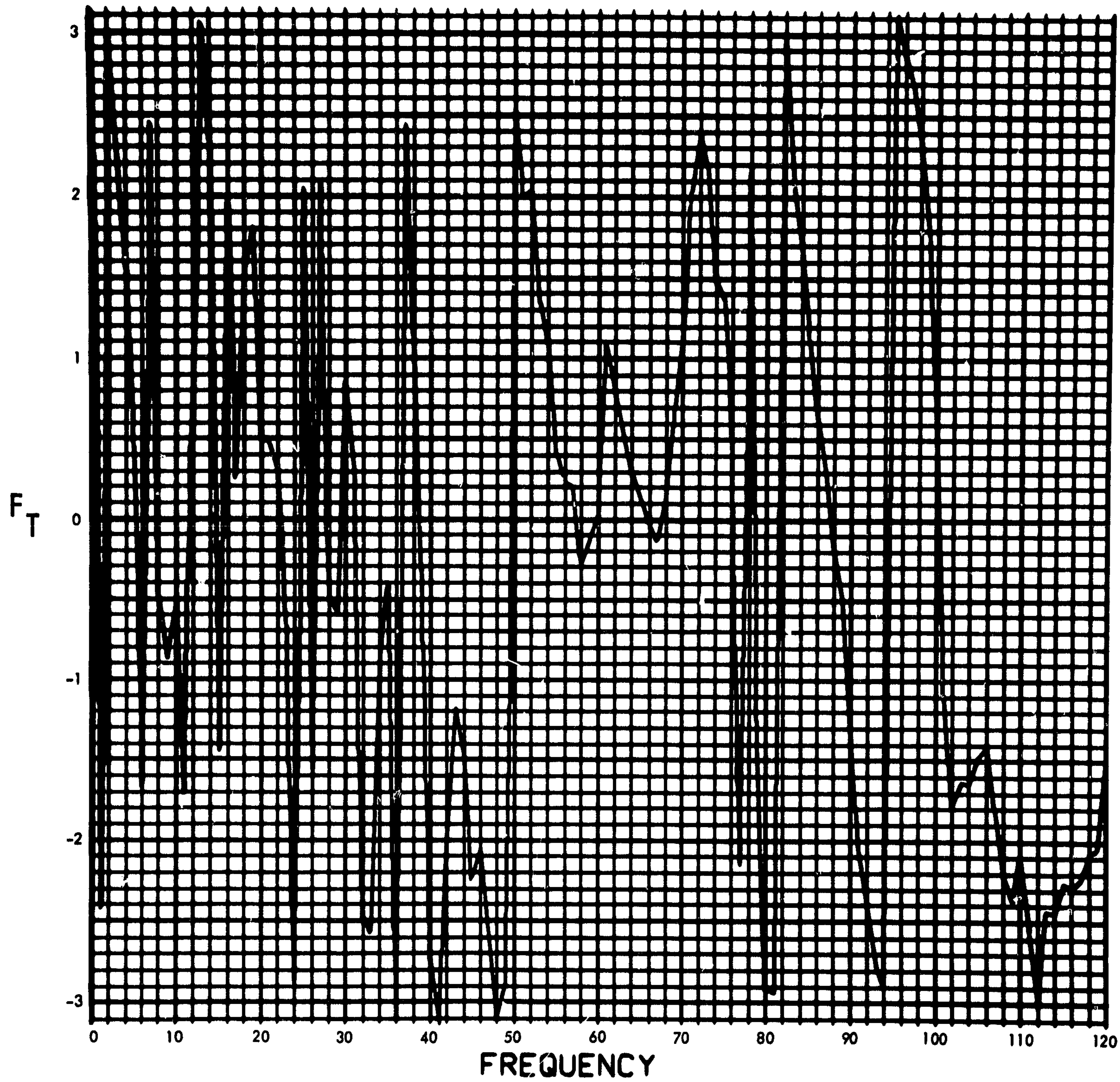

Fig. C-114. Joint 13, torque response function, Fourier transform, phase angle (pulse 1)

$T_{13}(T)$ (LB-IN) vs TIME (SEC)

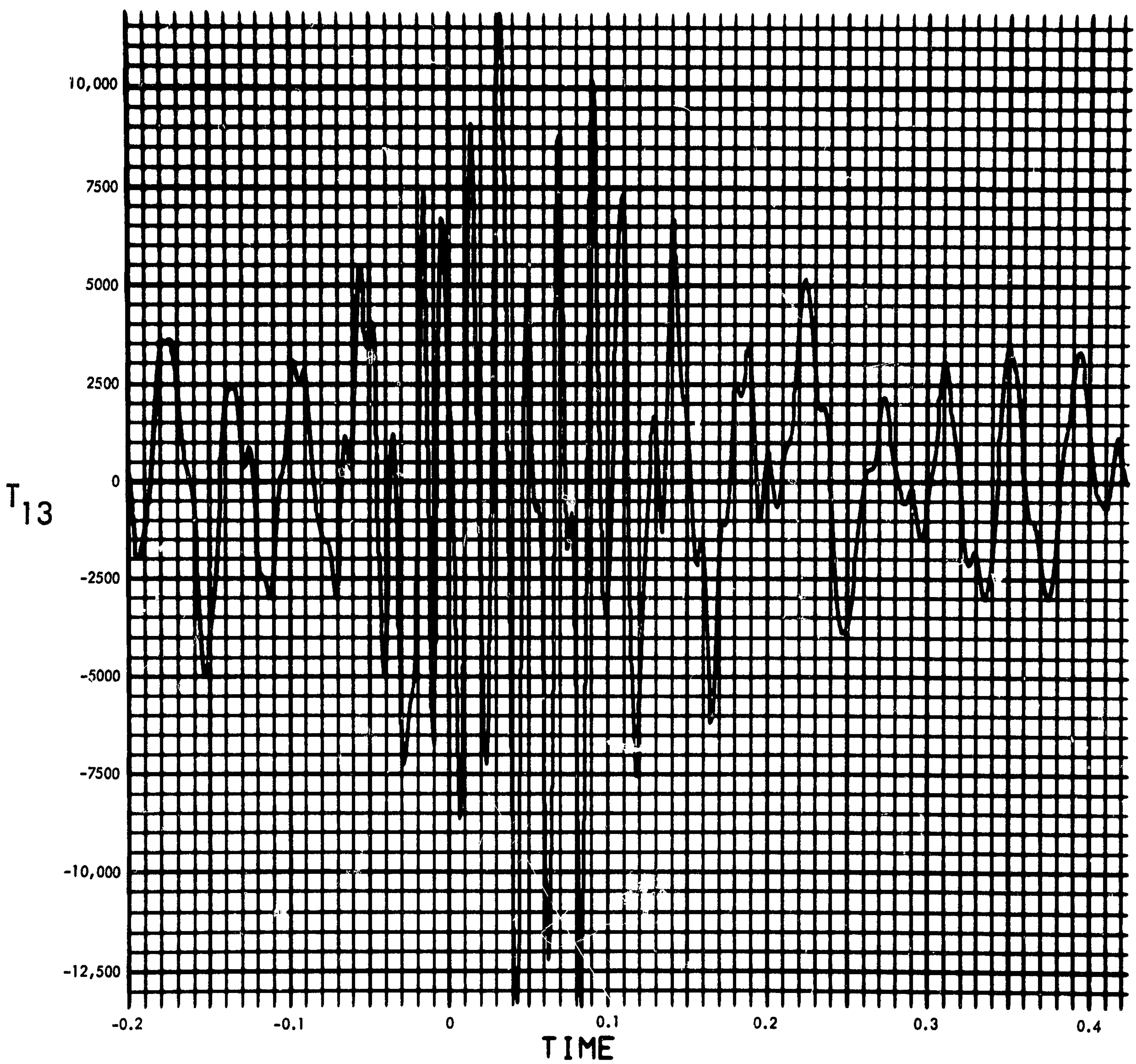

Fig. C-115. Joint 13, torque response, time history (pulse 1)

MODULUS OF $F_T(F)$ (LB-IN-SEC) vs FREQUENCY (CYCLES/SEC)

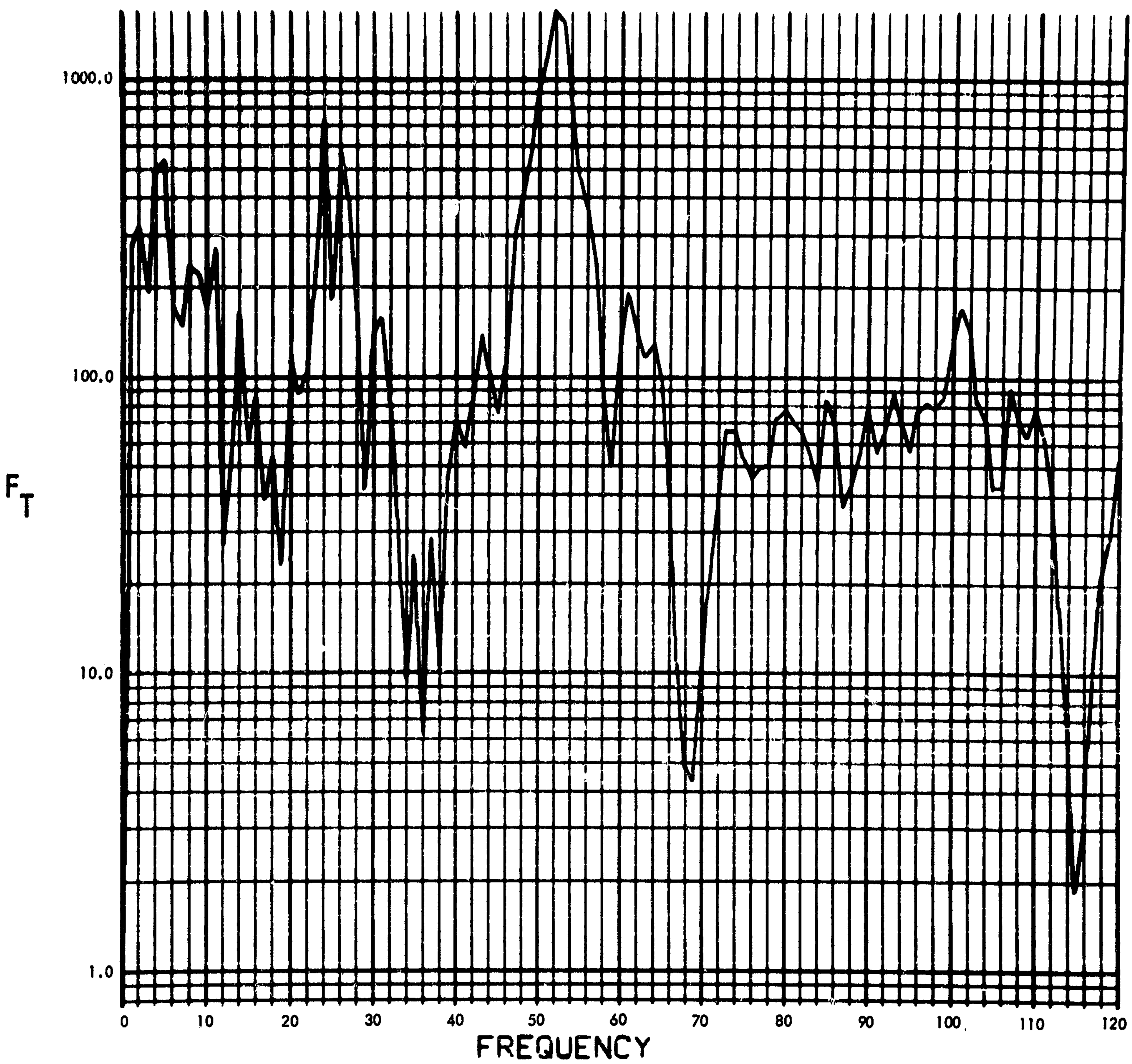

Fig. C-116. Joint 13, torque response function, Fourier transform, modulus (pulse 2)

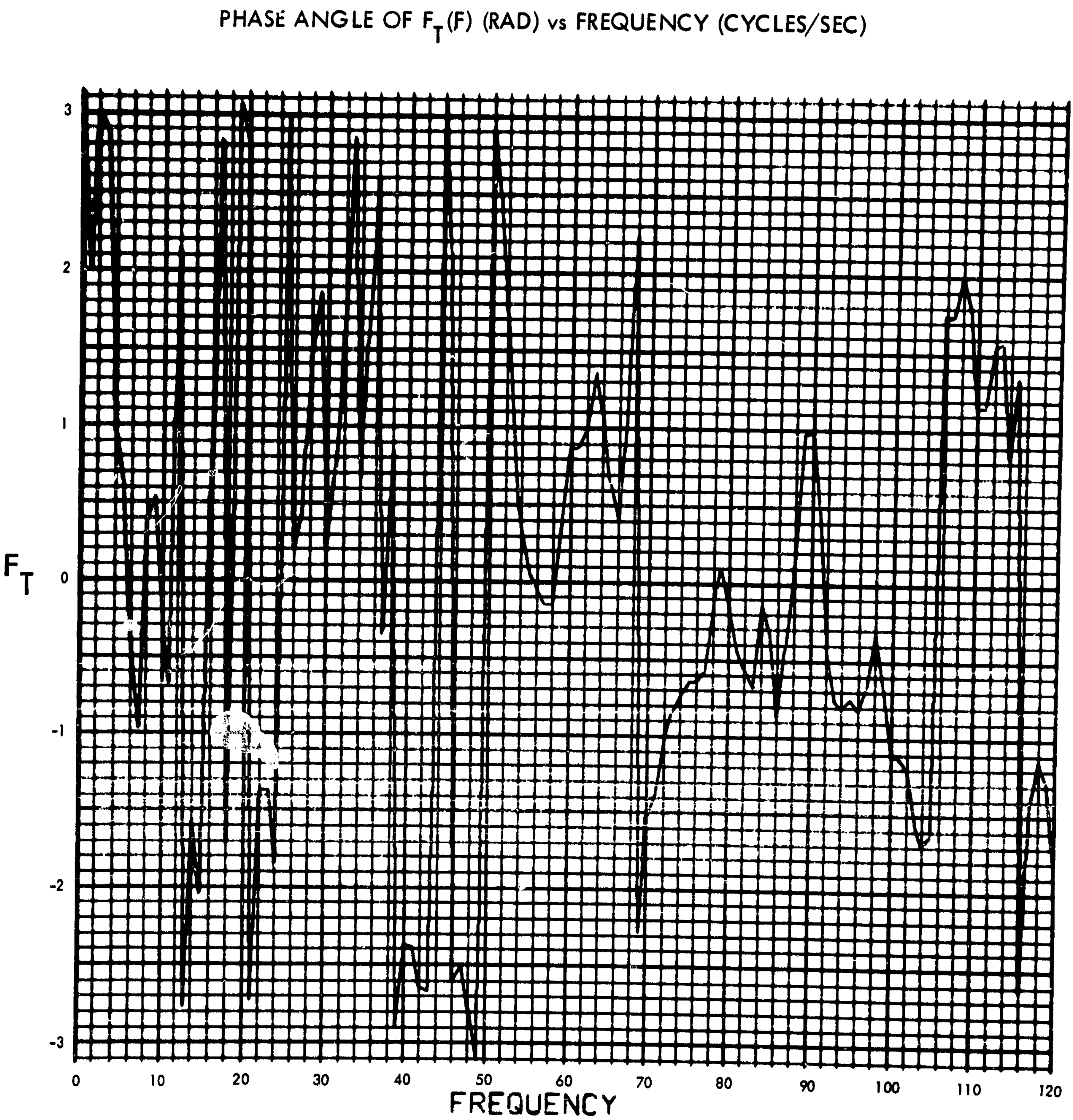

Fig. C-117. Joint 13, torque response function, Fourier transform, phase angle (pulse 2)

$T_{13}(T)$ (LB-IN) vs TIME (SEC)

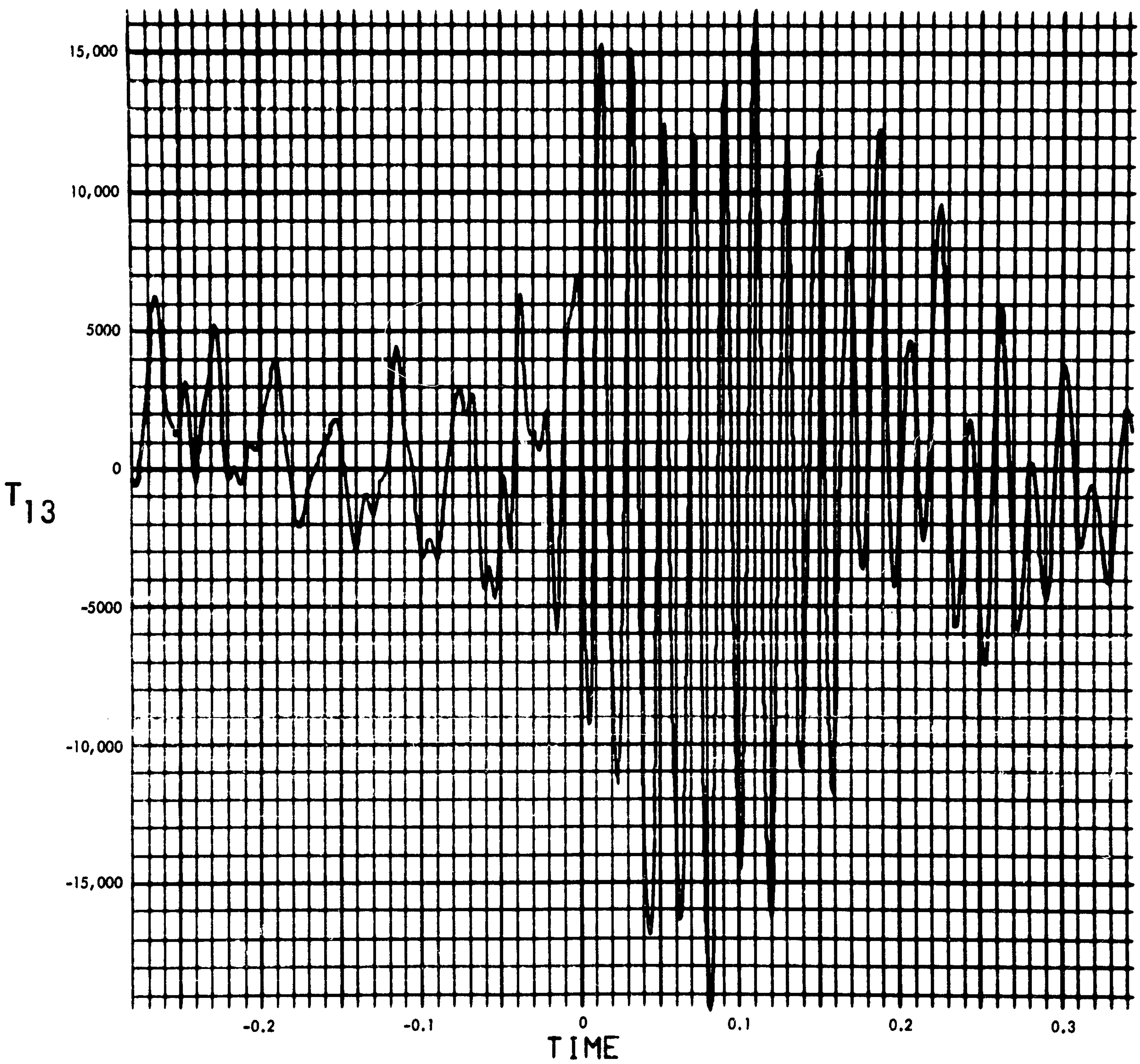

Fig. C-118. Joint 13, torque response, time history (pulse 2)

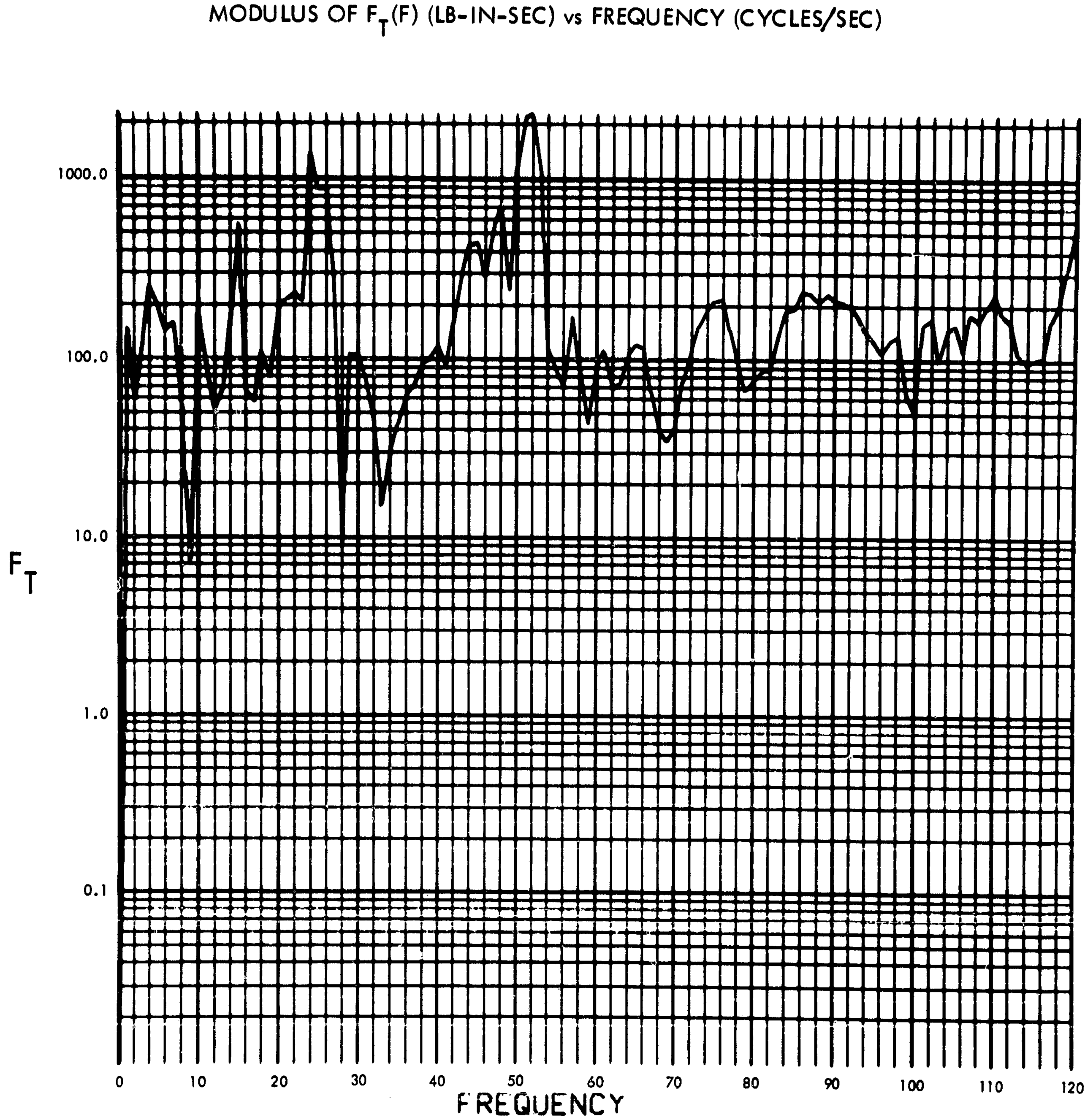

Fig. C-119. Joint 13, torque response function, Fourier transform, modulus (pulse 3)

PHASE ANGLE OF $F_T(F)$ (RAD) vs FREQUENCY (CYCLES/SEC)

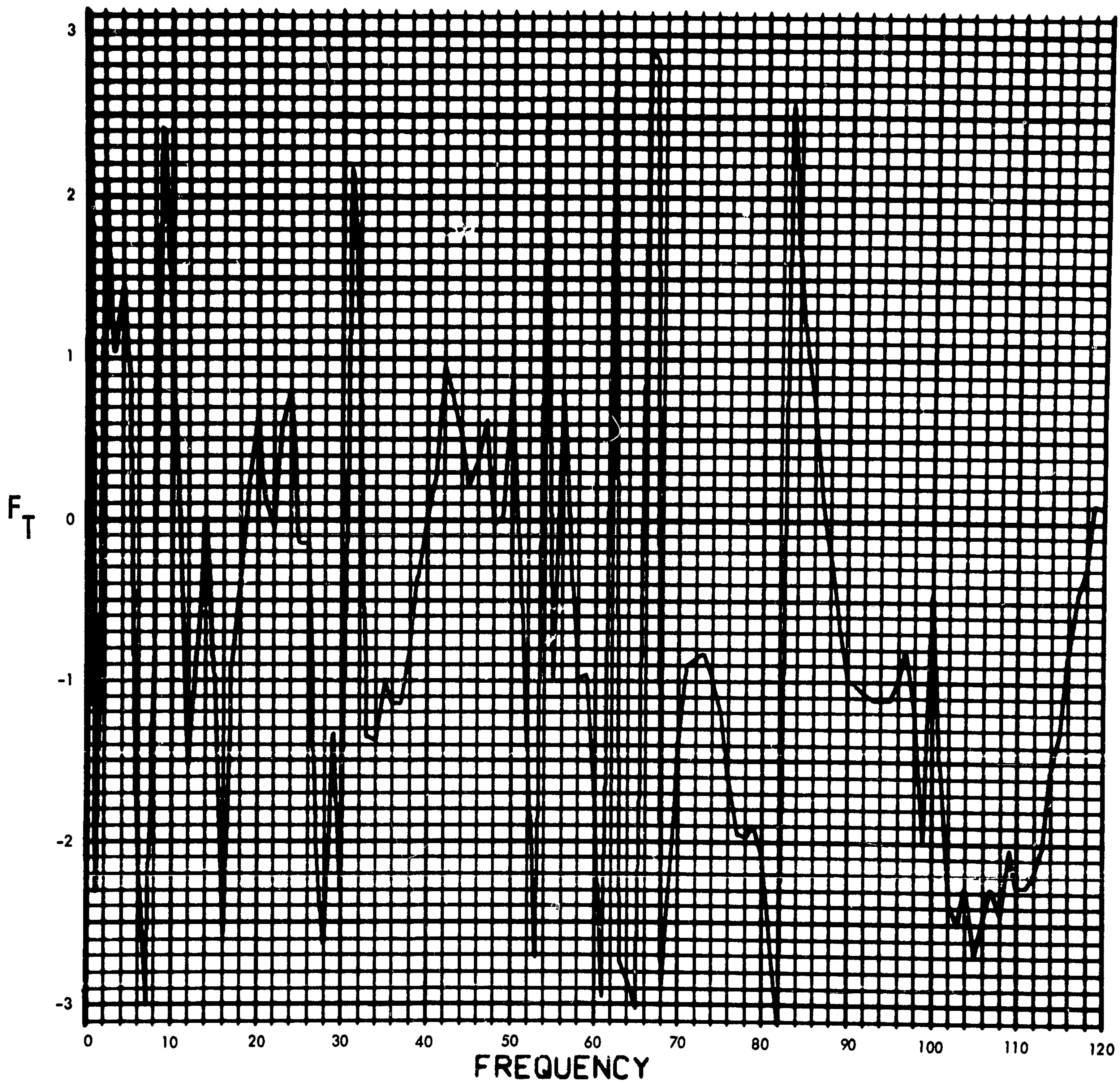

Fig. C-120. Joint 13, torque response function, Fourier transform, phase angle (pulse 3)

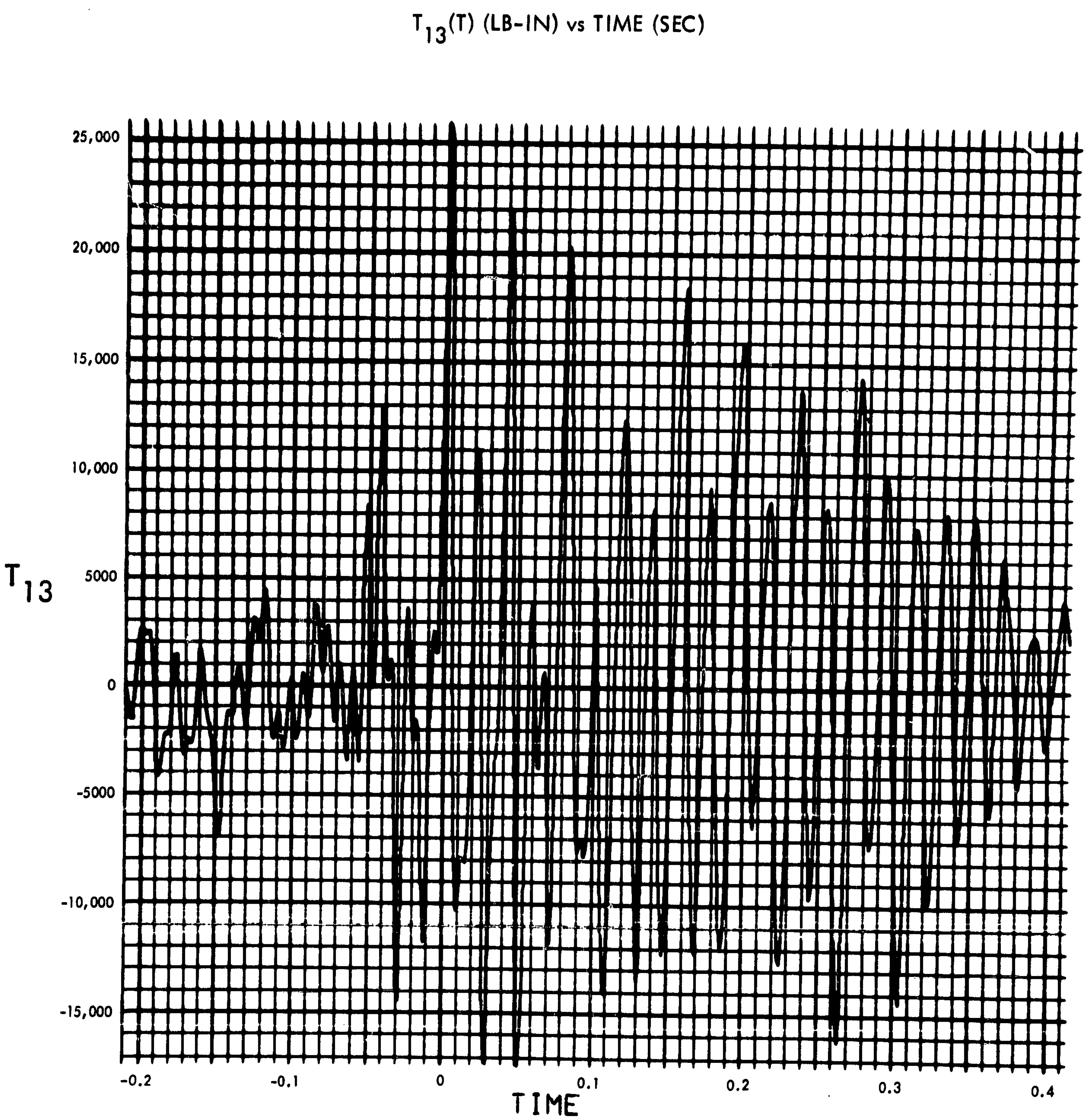

Fig. C-121. Joint 13, torque response, time history (pulse 3)

MODULUS OF $F_T(F)$ (LB-IN-SEC) vs FREQUENCY (CYCLES/SEC)

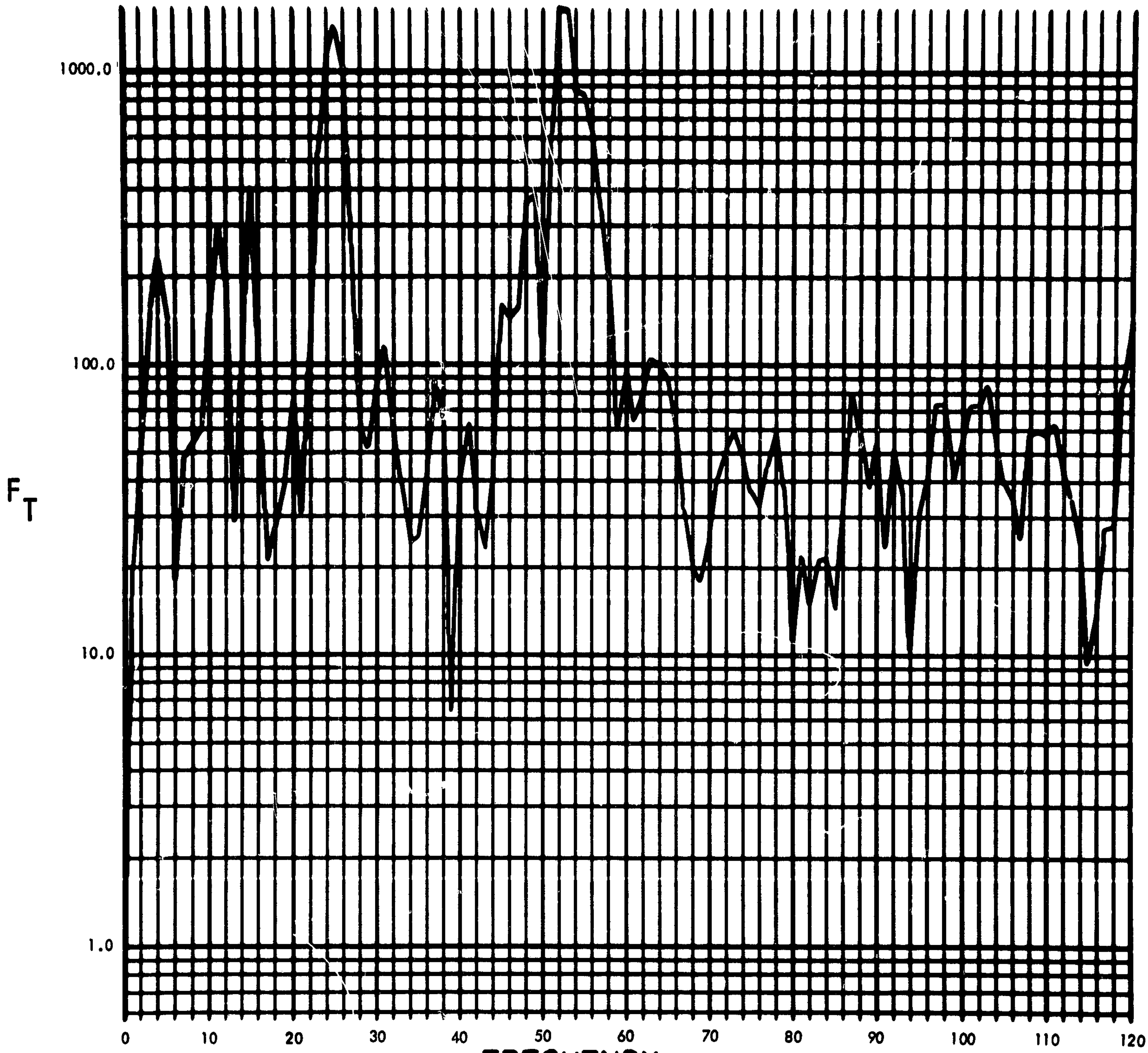

Fig. C-122. Joint 13, torque response function, Fourier transform, modulus (pulse 4)

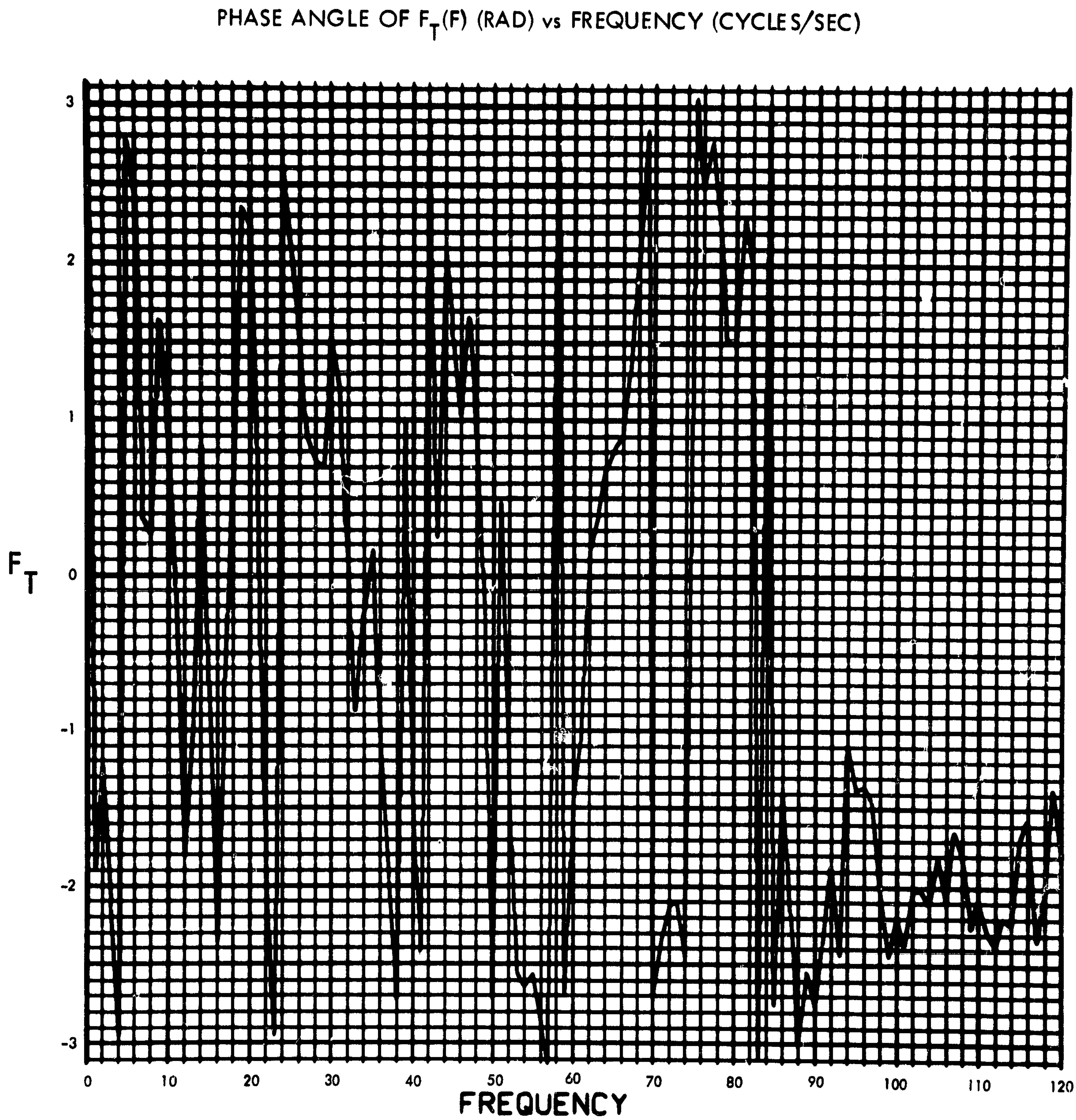

Fig. C-123. Joint 13, torque response function, Fourier transform, phase angle (pulse 4)

$T_{13}(T)$ (LB-IN) vs TIME (SEC)

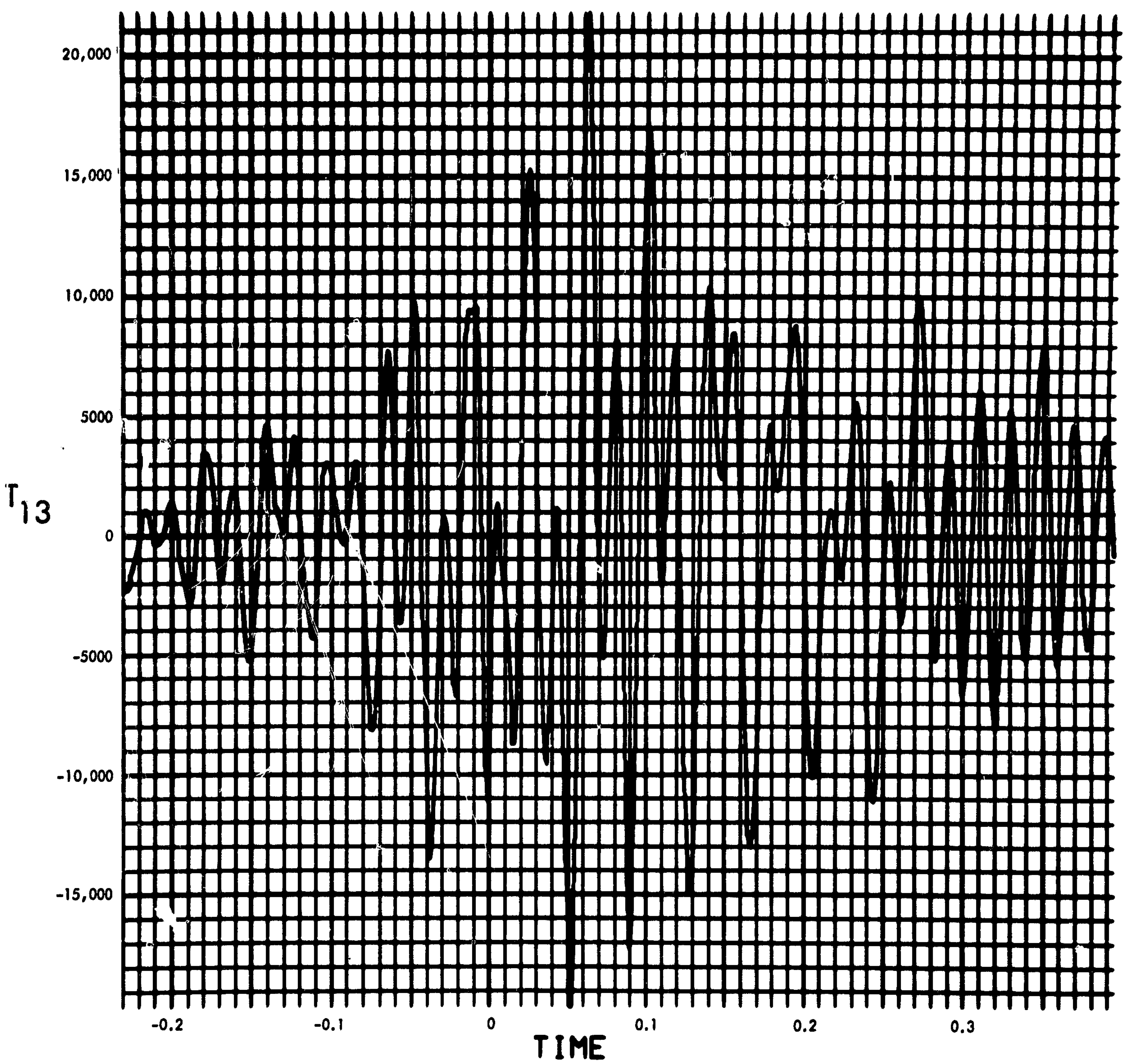

Fig. C-124. Joint 13, torque response, time history (pulse 4)

MODULUS H2(F) (1/LB-IN-SEC^2) vs FREQUENCY (CYCLES/SEC)

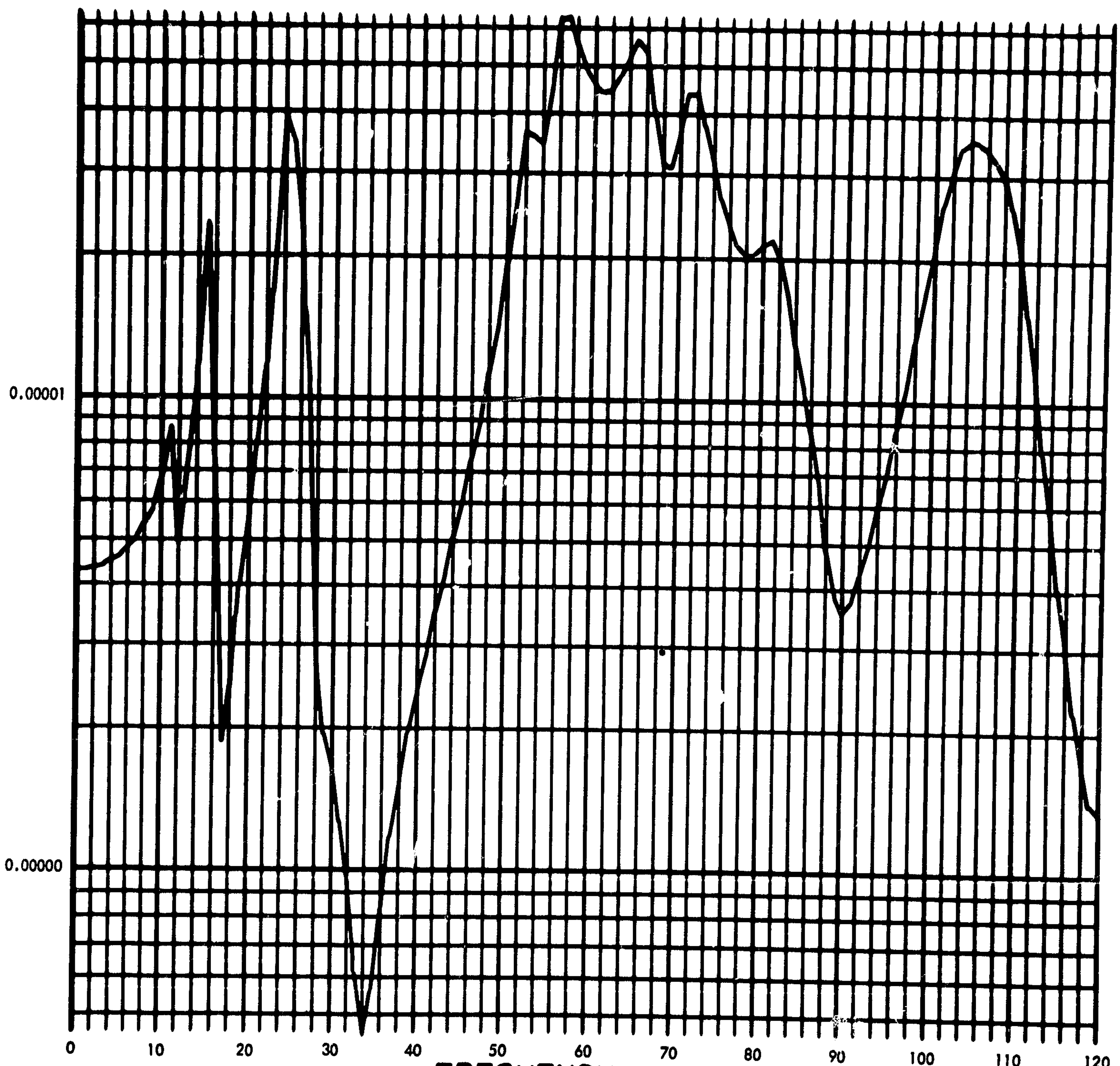

Fig. C-125. Joint 63, acceleration transfer function, Fourier transform, modulus

PHASE ANGLE OF H2(F) (RAD) vs FREQUENCY (CYCLES/SEC)

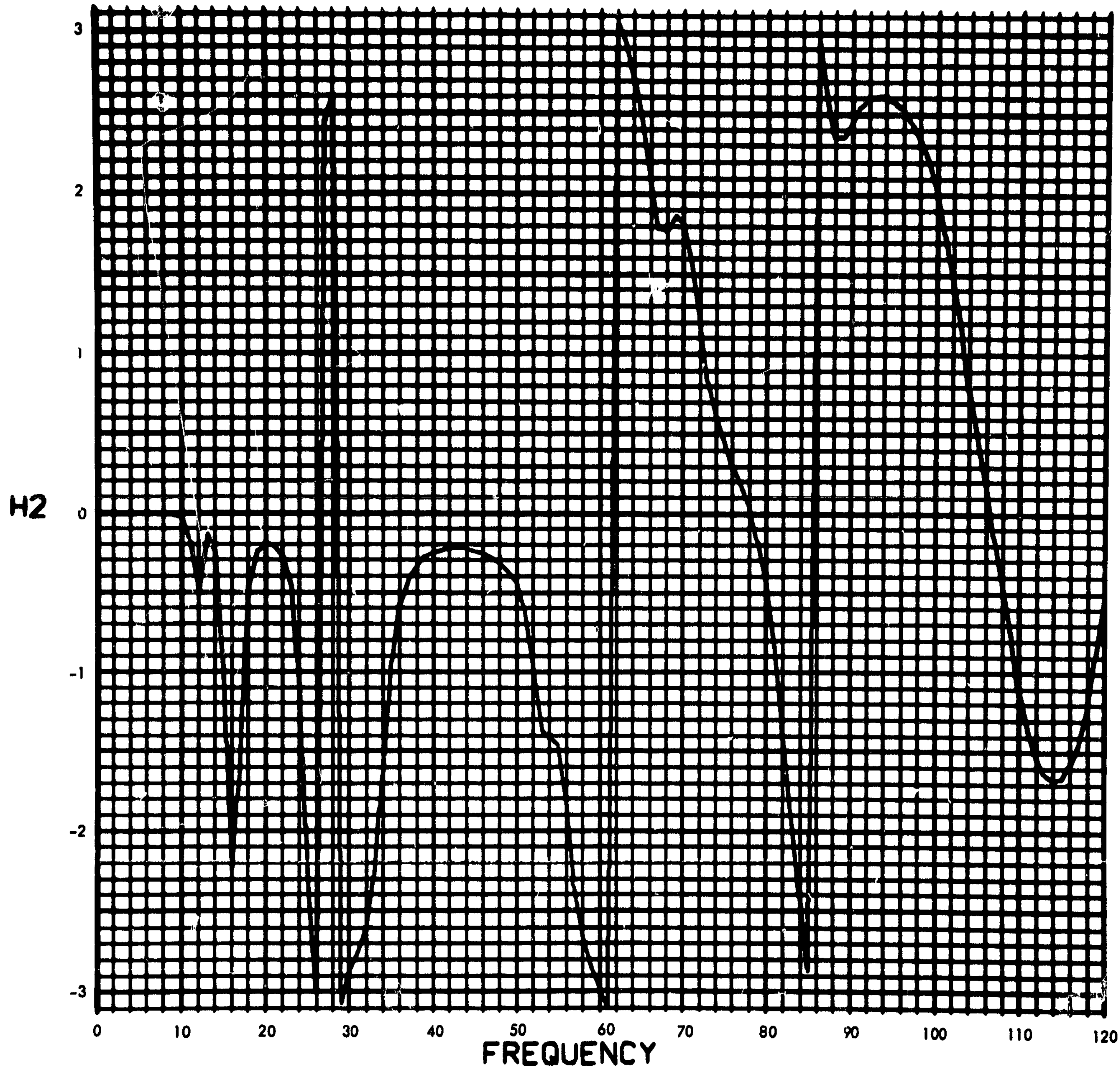

Fig. C-126. Joint 63, transfer function, Fourier transform, phase angle

MODULUS OF V2(F) (RAD/SEC) vs FREQUENCY (CYCLES/SEC)

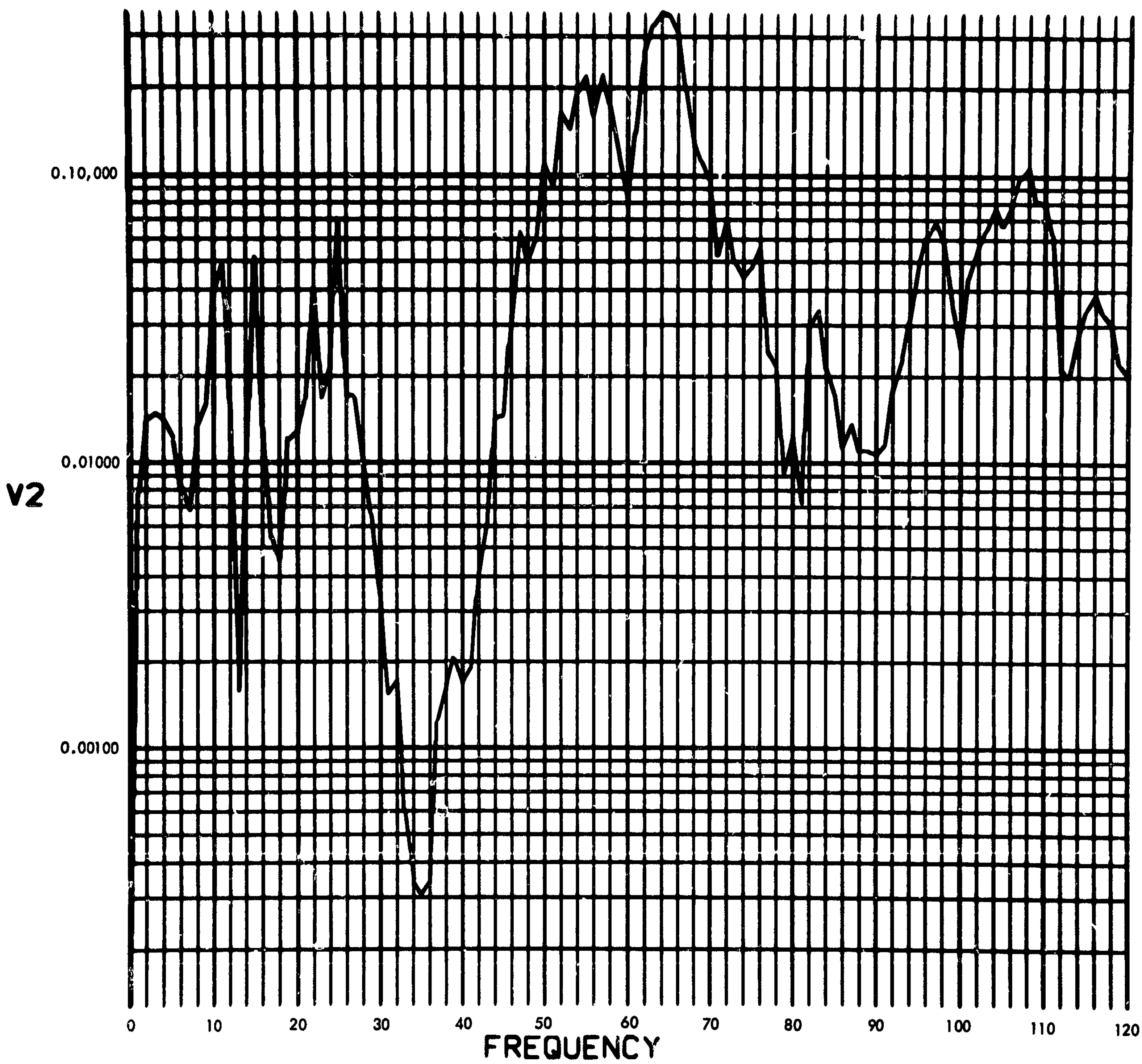

Fig. C-127. Joint 63, acceleration response, Fourier transform, modulus (pulse 1)

PHASE ANGLE OF V2(F) (RAD) vs FREQUENCY (CYCLES/SEC)

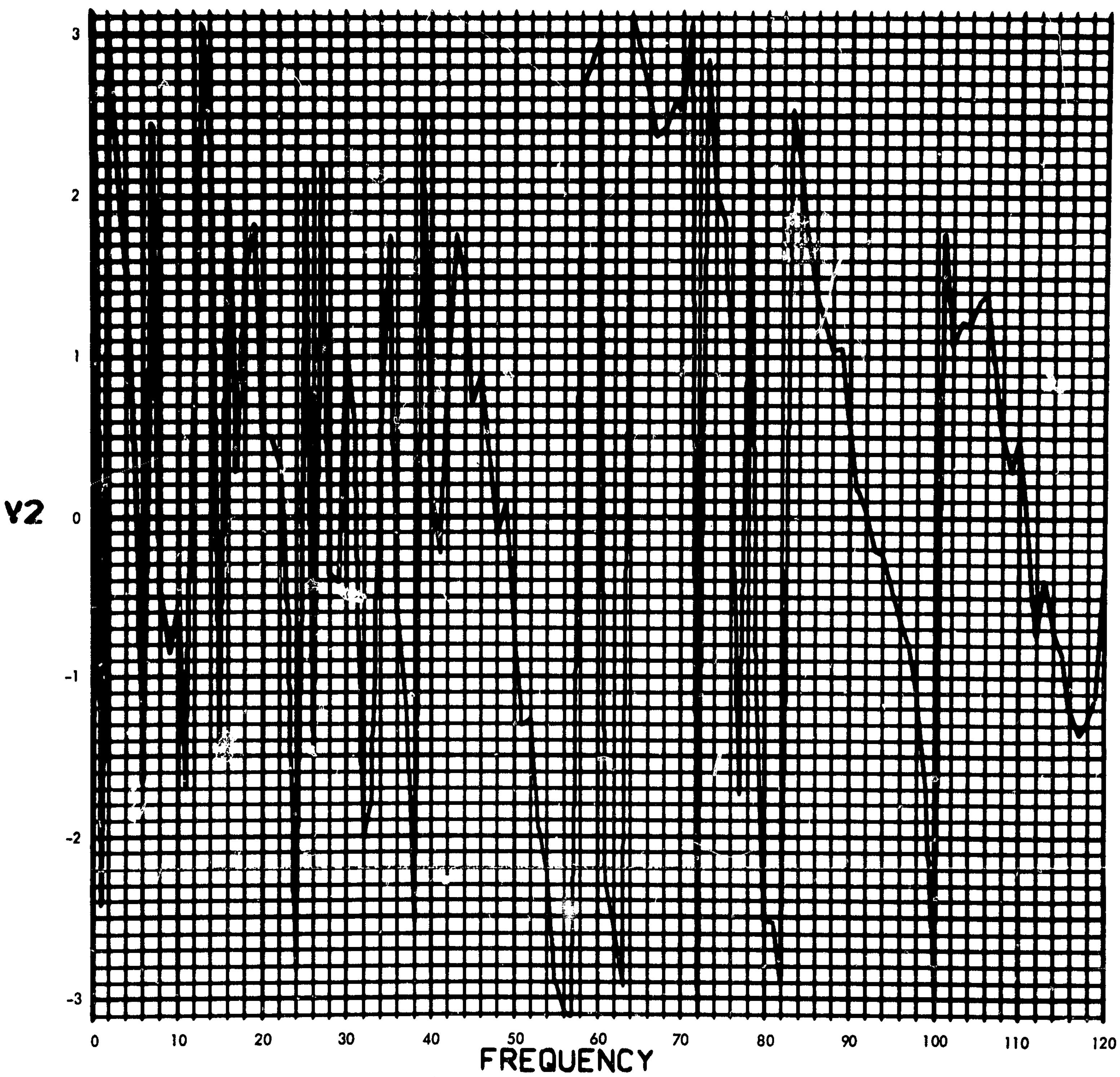

Fig. C-128. Joint 63, acceleration response, Fourier transform, phase angle (pulse 1)

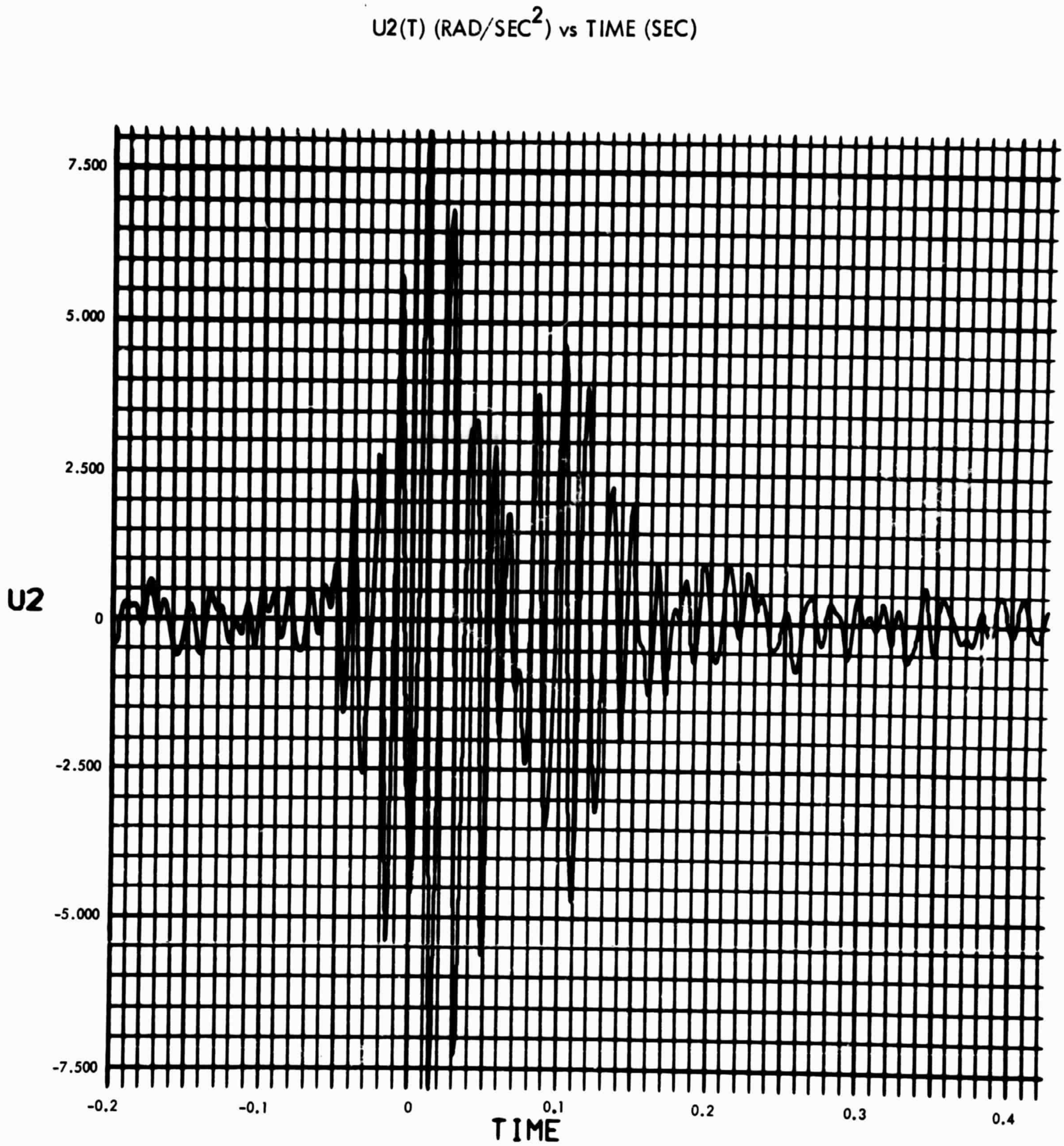

Fig. C-129. Joint 63, acceleration response, time history (pulse 1)

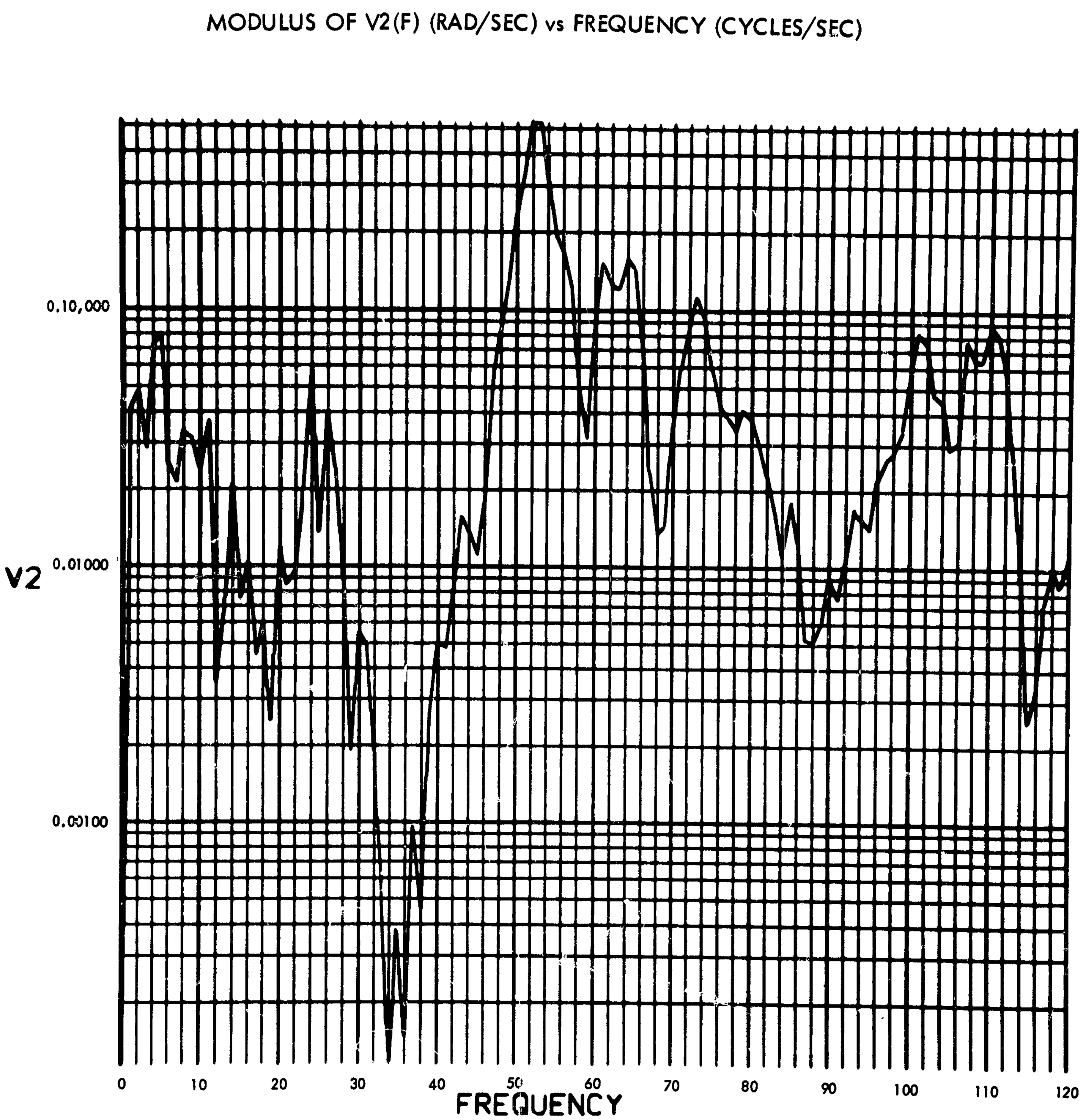

Fig. C-130. Joint 63, acceleration response, Fourier transform, modulus (pulse 2)

PHASE ANGLE OF V2(F) (RAD) vs FREQUENCY (CYCLES/SEC)

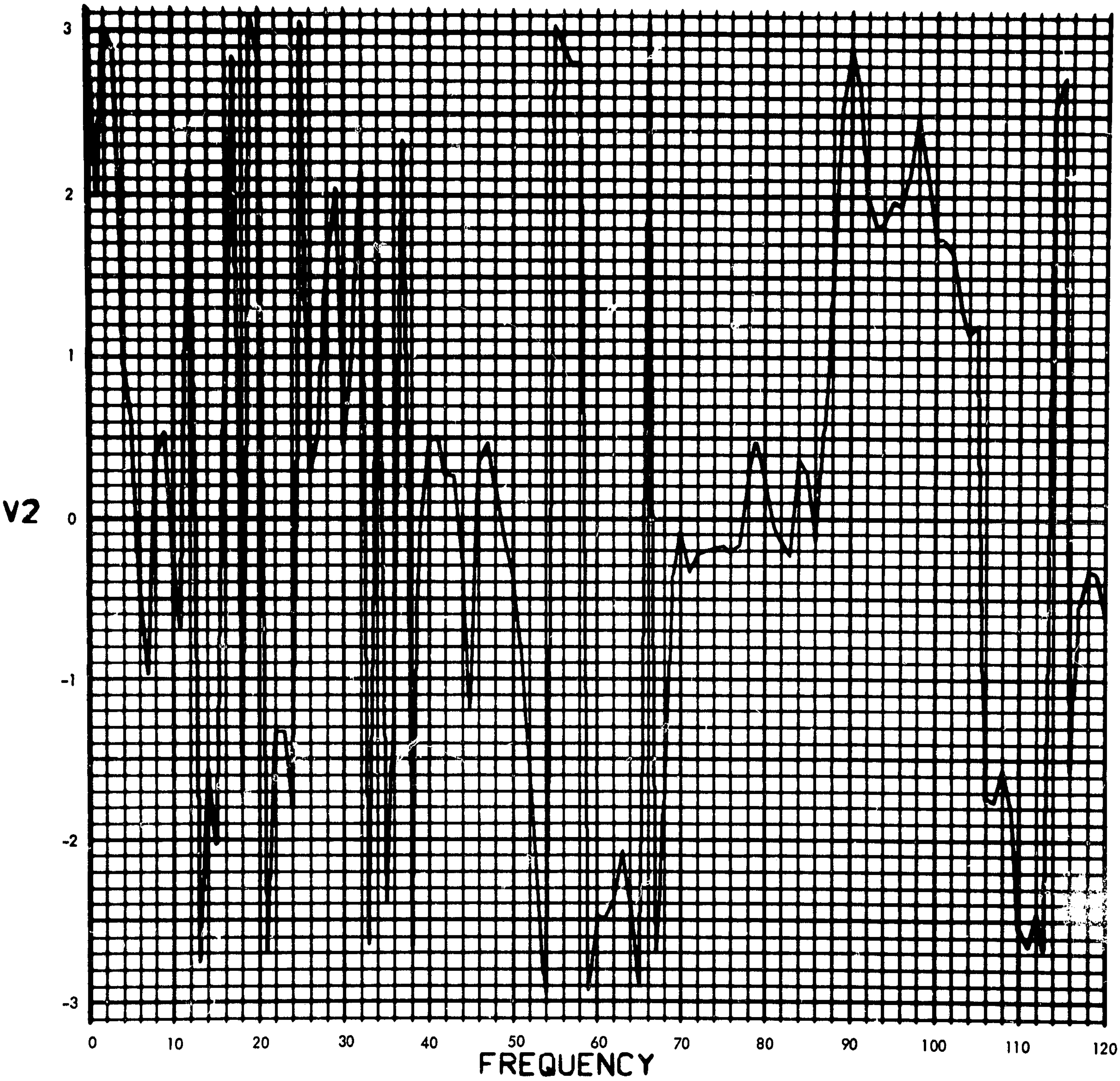

Fig. C-131. Joint 63, acceleration response, Fourier transform, phase angle (pulse 2)

U2(T) (RAD/SEC^2) vs TIME (SEC)

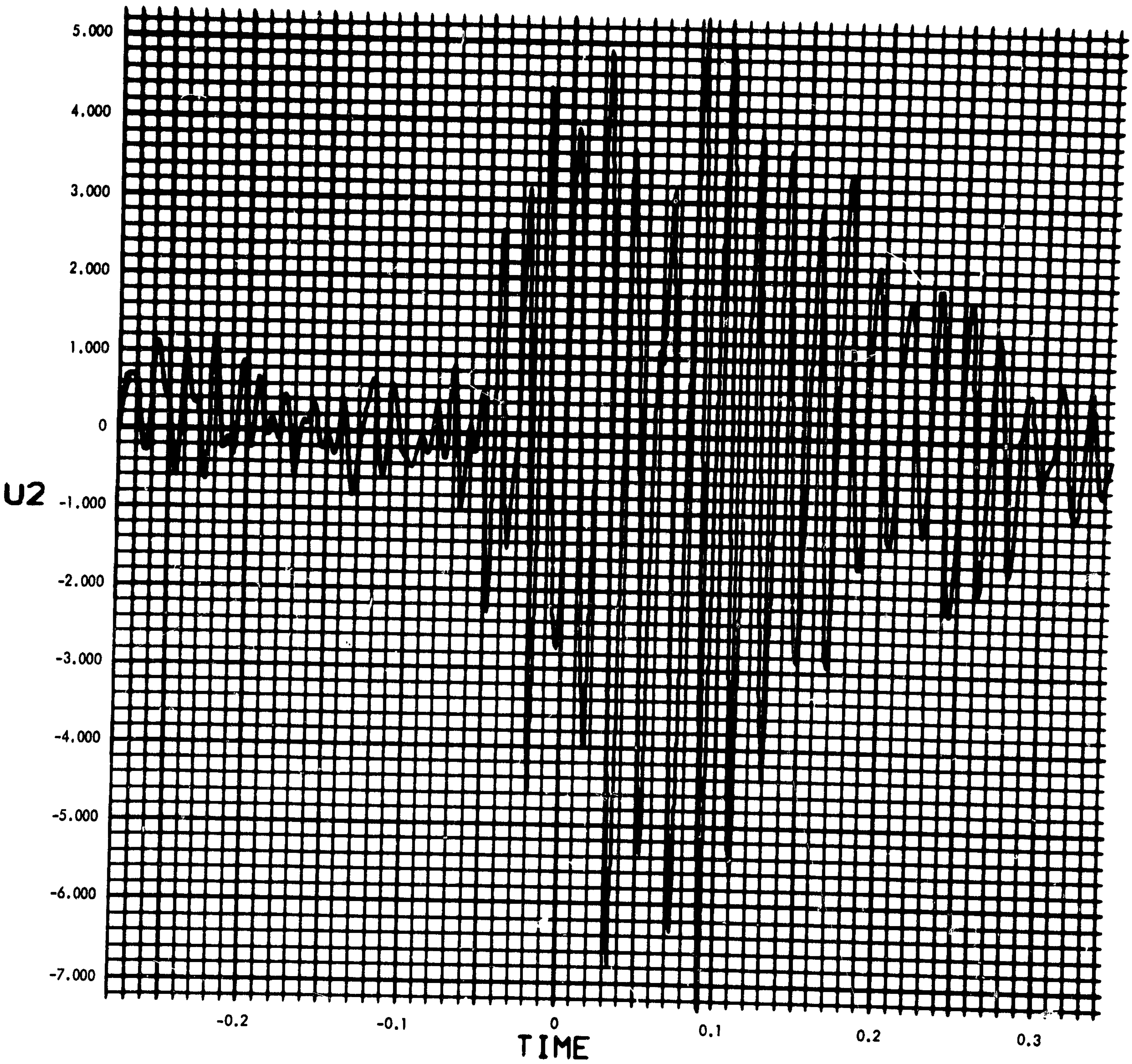

Fig. C-132. Joint 63, acceleration response, time history (pulse 2)

MODULUS OF V2(F) (RAD/SEC) vs FREQUENCY (CYCLES/SEC)

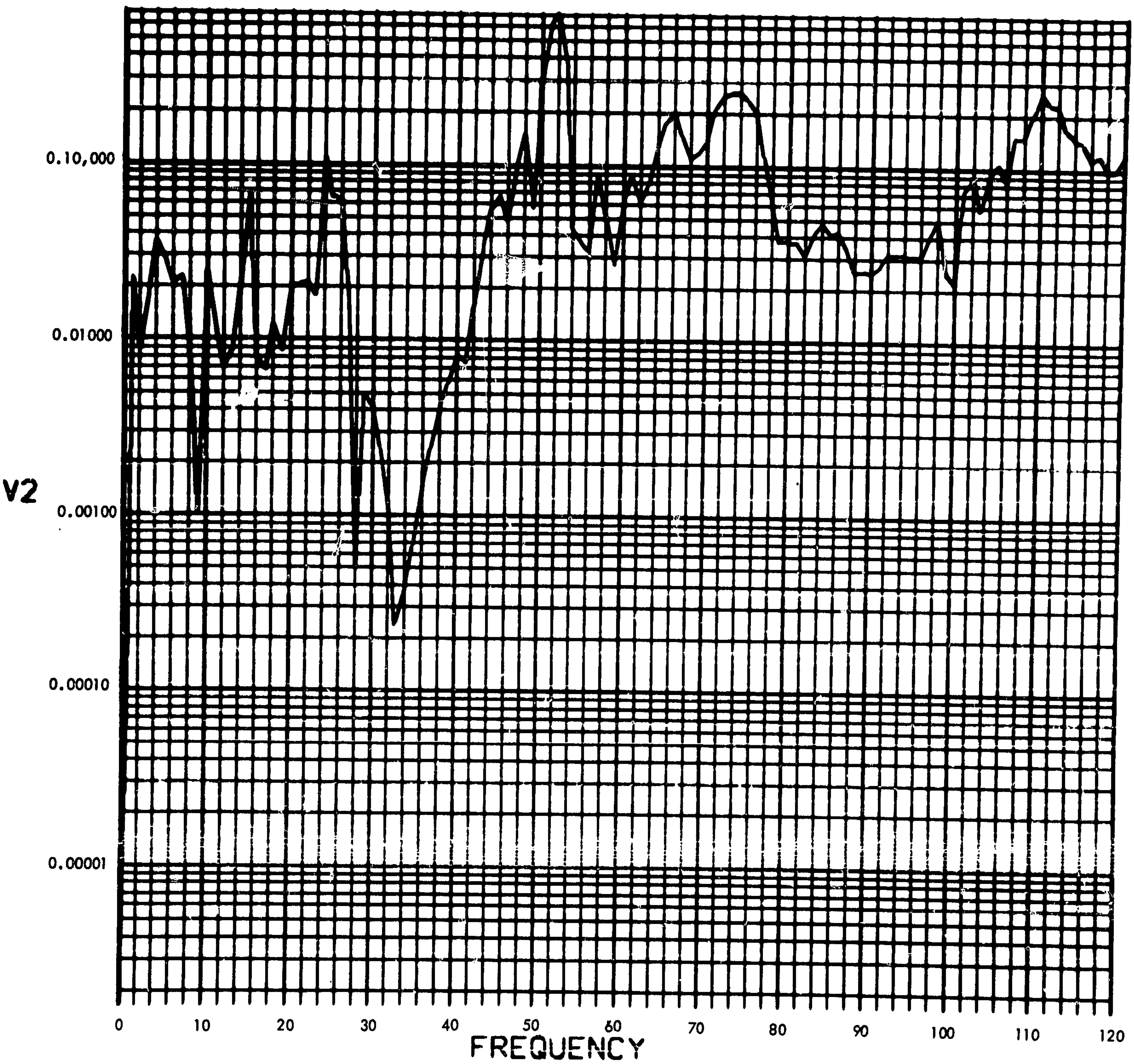

Fig. C-133. Joint 63, acceleration response, Fourier transform, modulus (pulse 3)

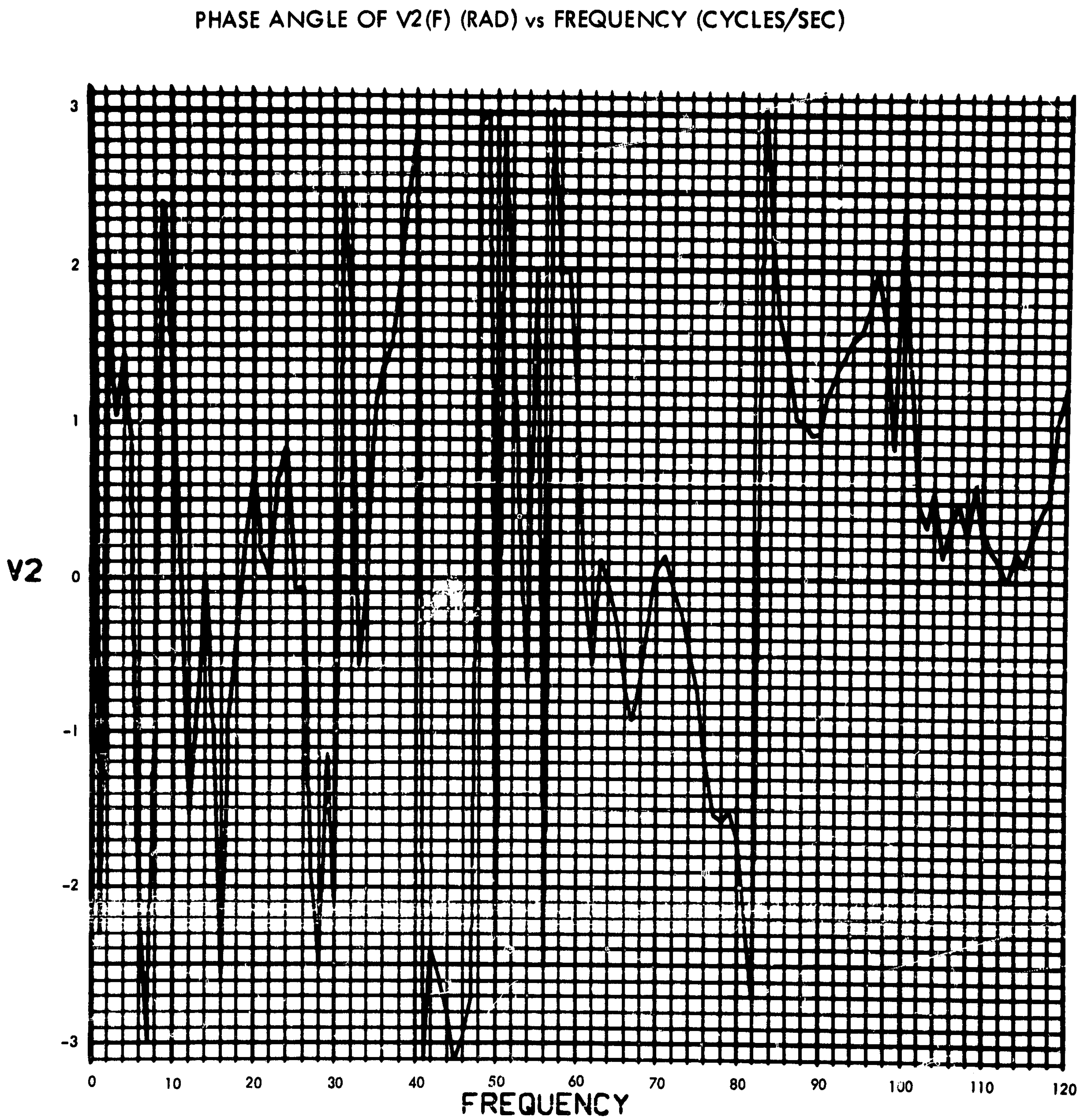

Fig. C-134. Joint 63, acceleration response, Fourier transform, phase angle (pulse 3)

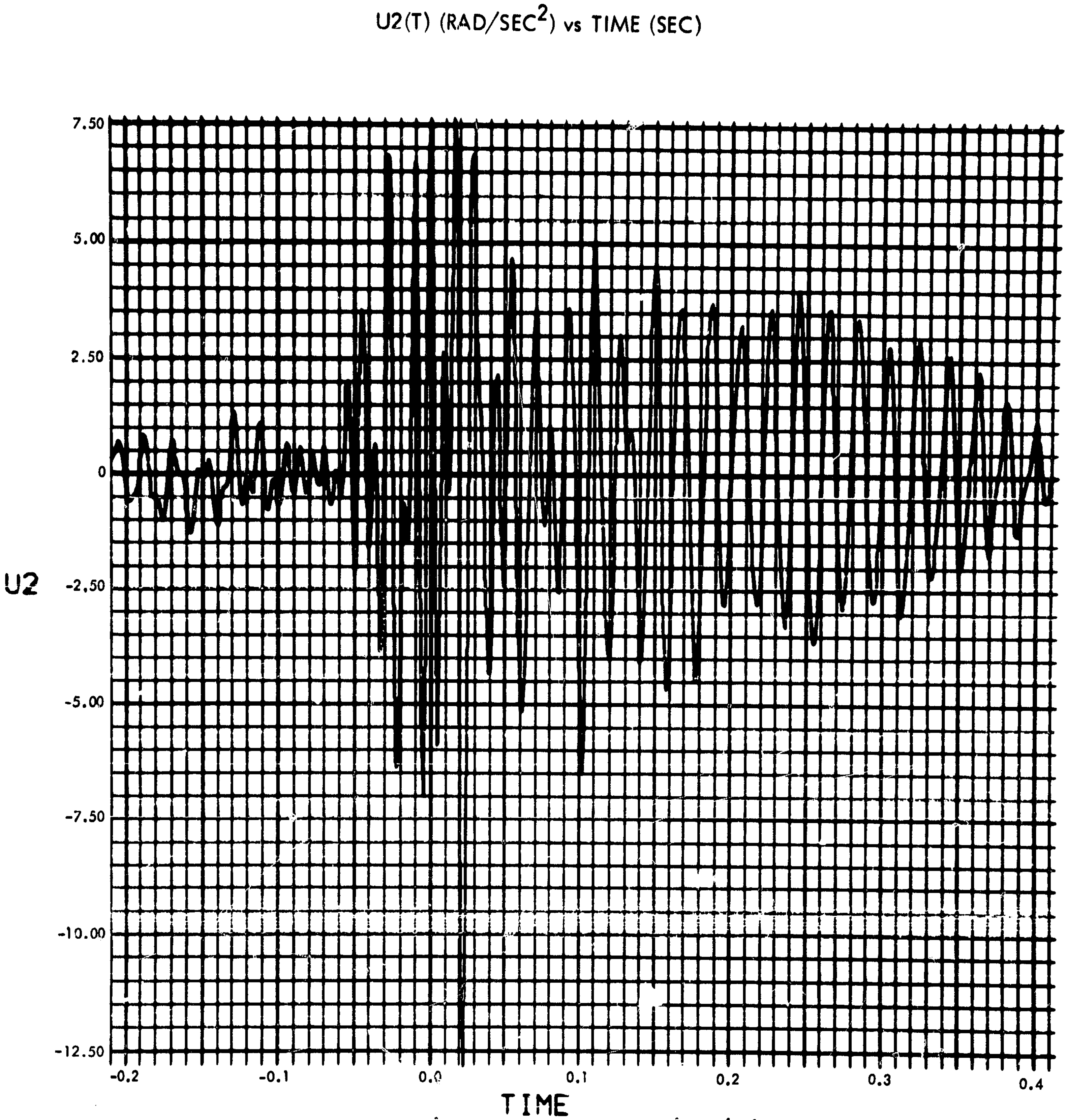

Fig. C-135. Joint 63, acceleration response, time history (pulse 3)

MODULUS OF V2(F) (RAD/SEC vs FREQUENCY (CYCLES/SEC)

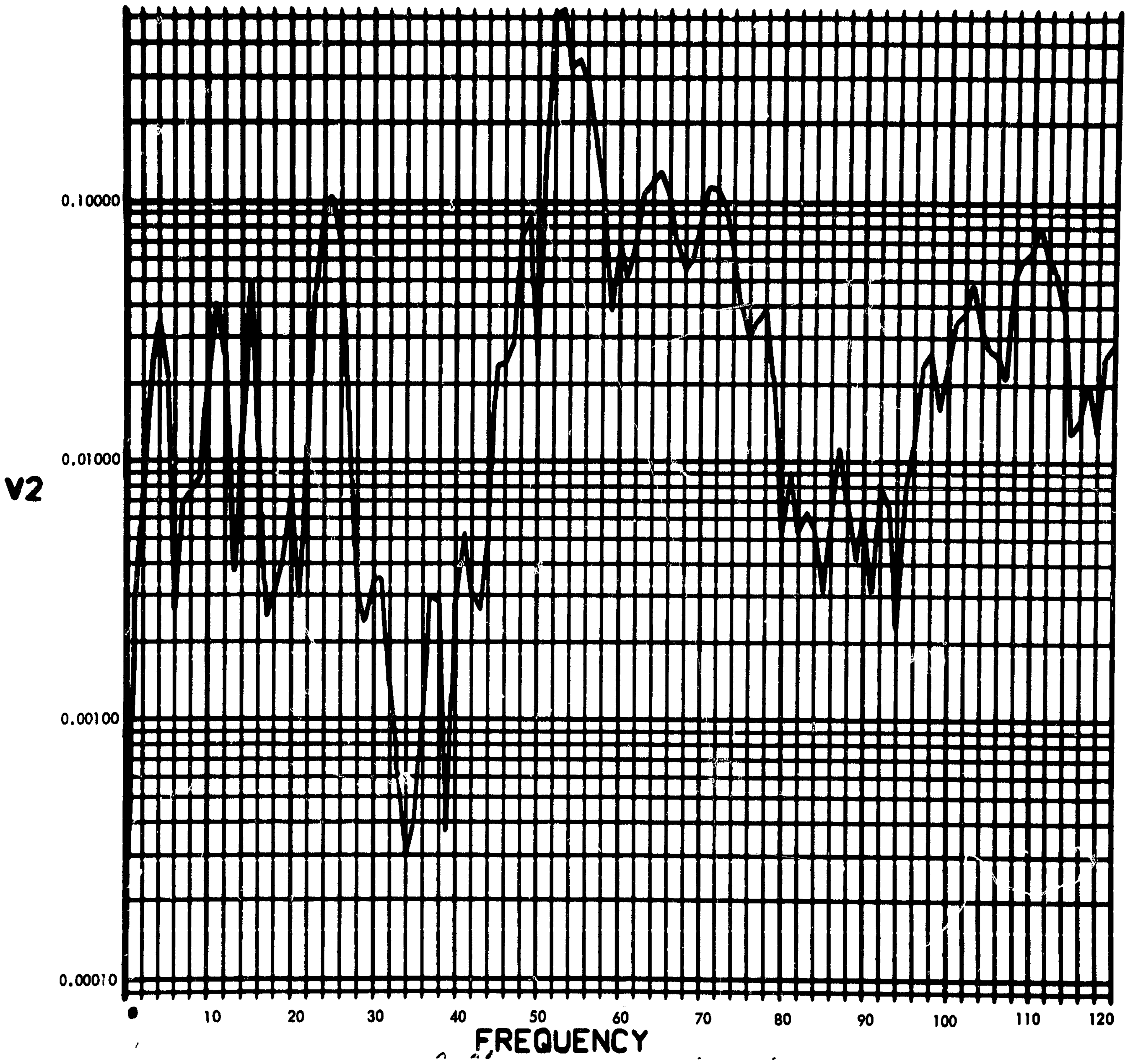

Fig. C-136. Joint 63, acceleration response, Fourier transform, modulus (pulse 4)

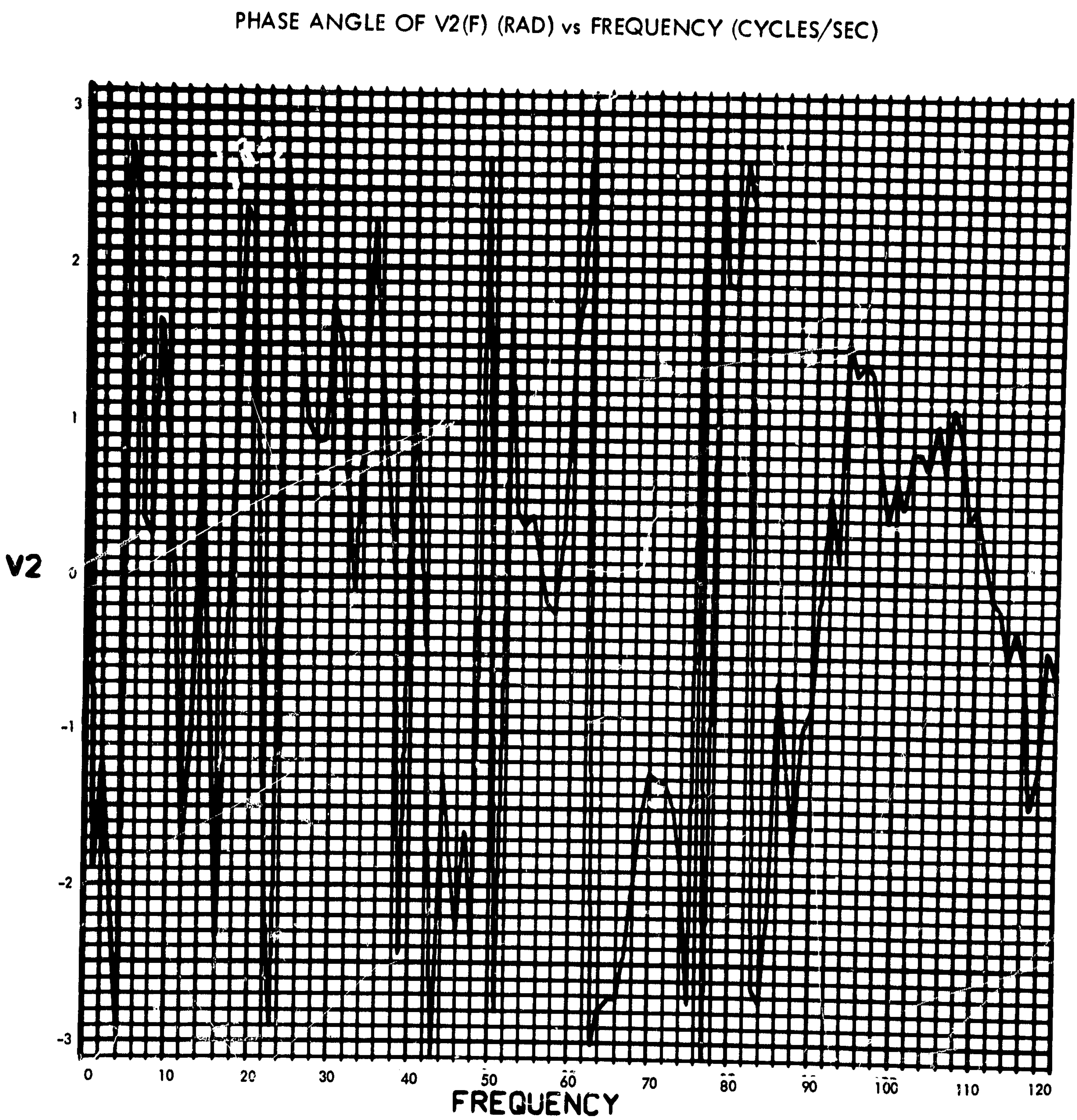

Fig. C-137. Joint 63, acceleration response, Fourier transform, phase angle (pulse 4)

U2(T) (RAD/SEC^2) vs TIME (SEC)

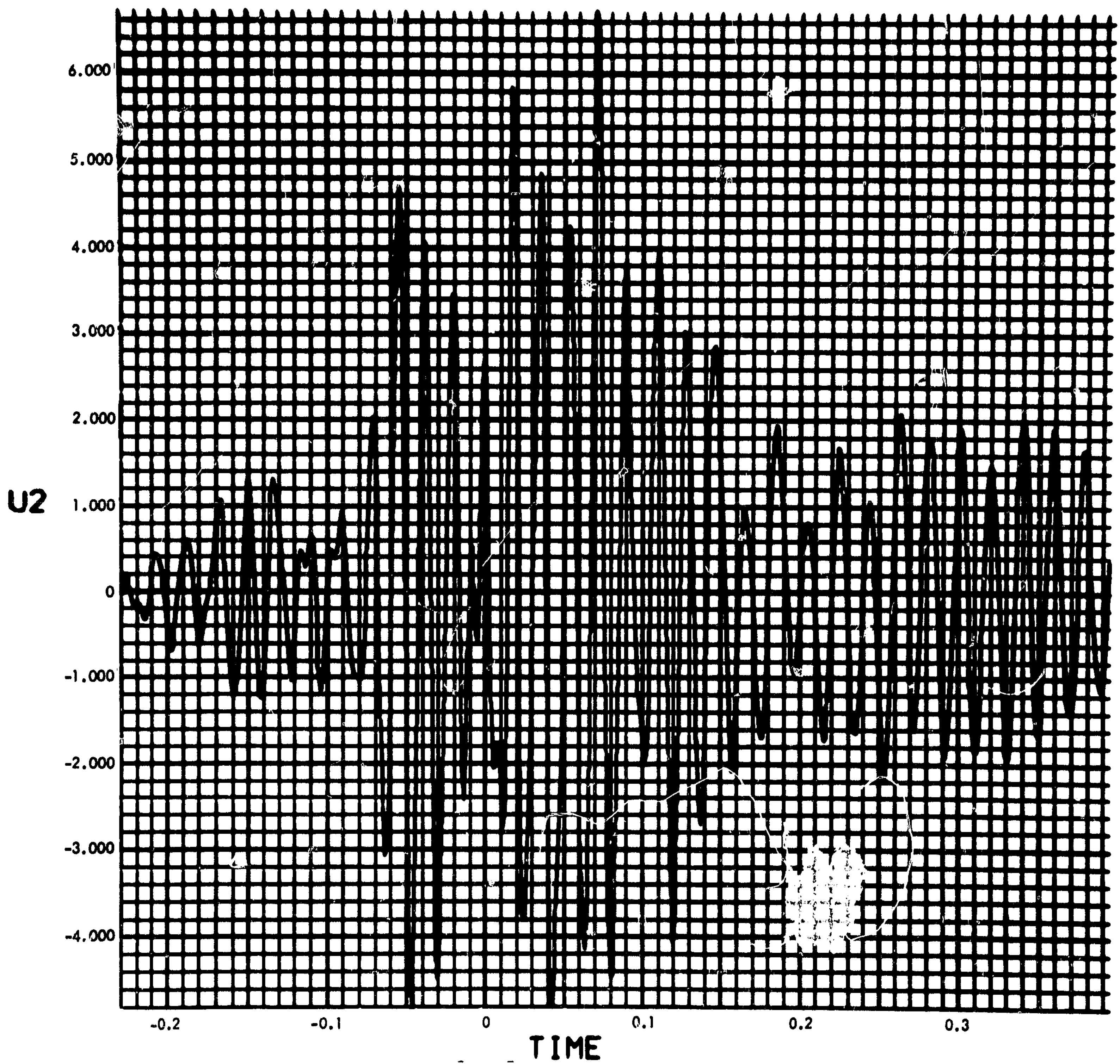

Fig. C-138. Joint 63, acceleration response, time history (pulse 4)

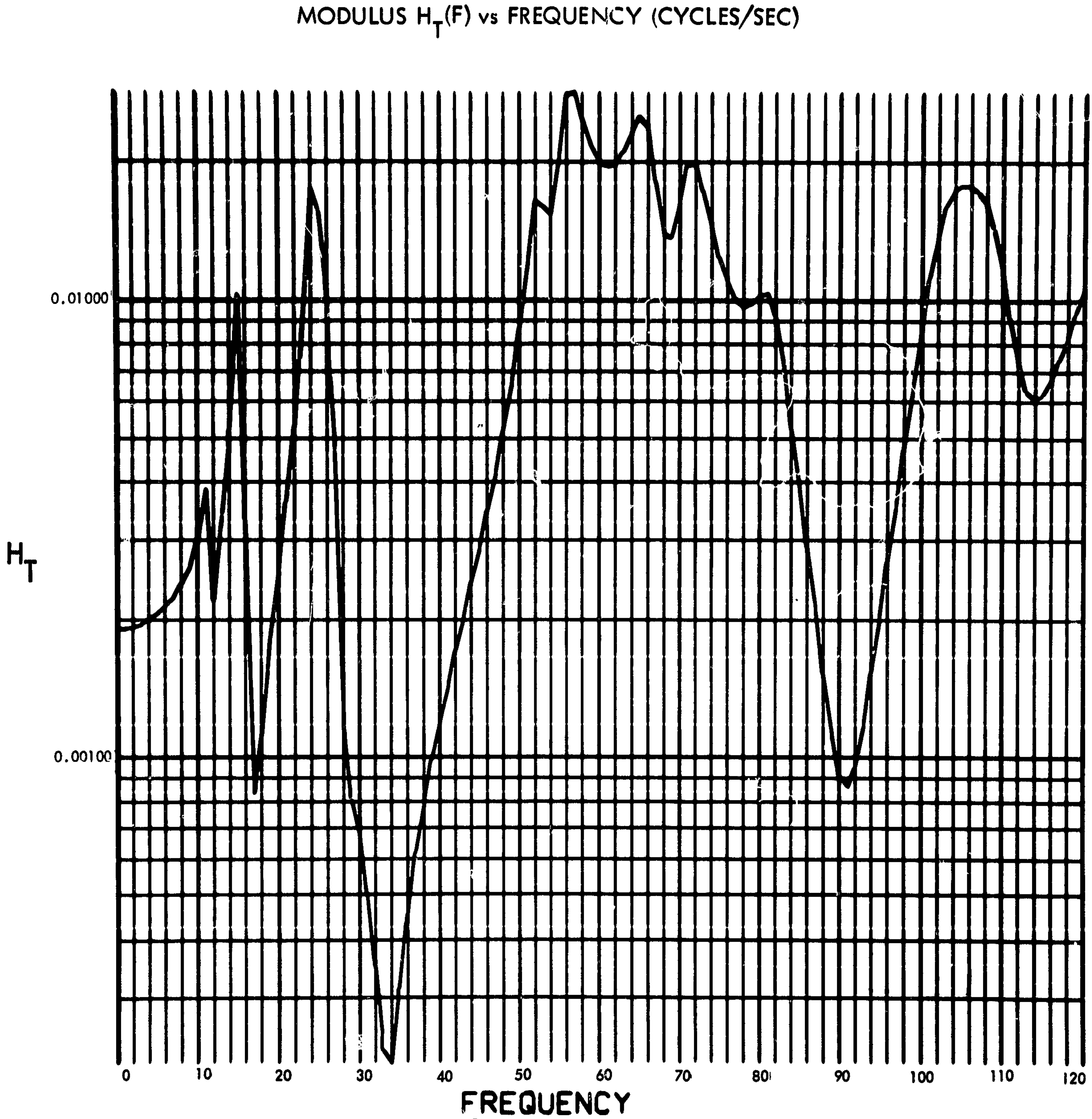

Fig. C-139. Joint 63, torque transfer function, Fourier transform, modulus

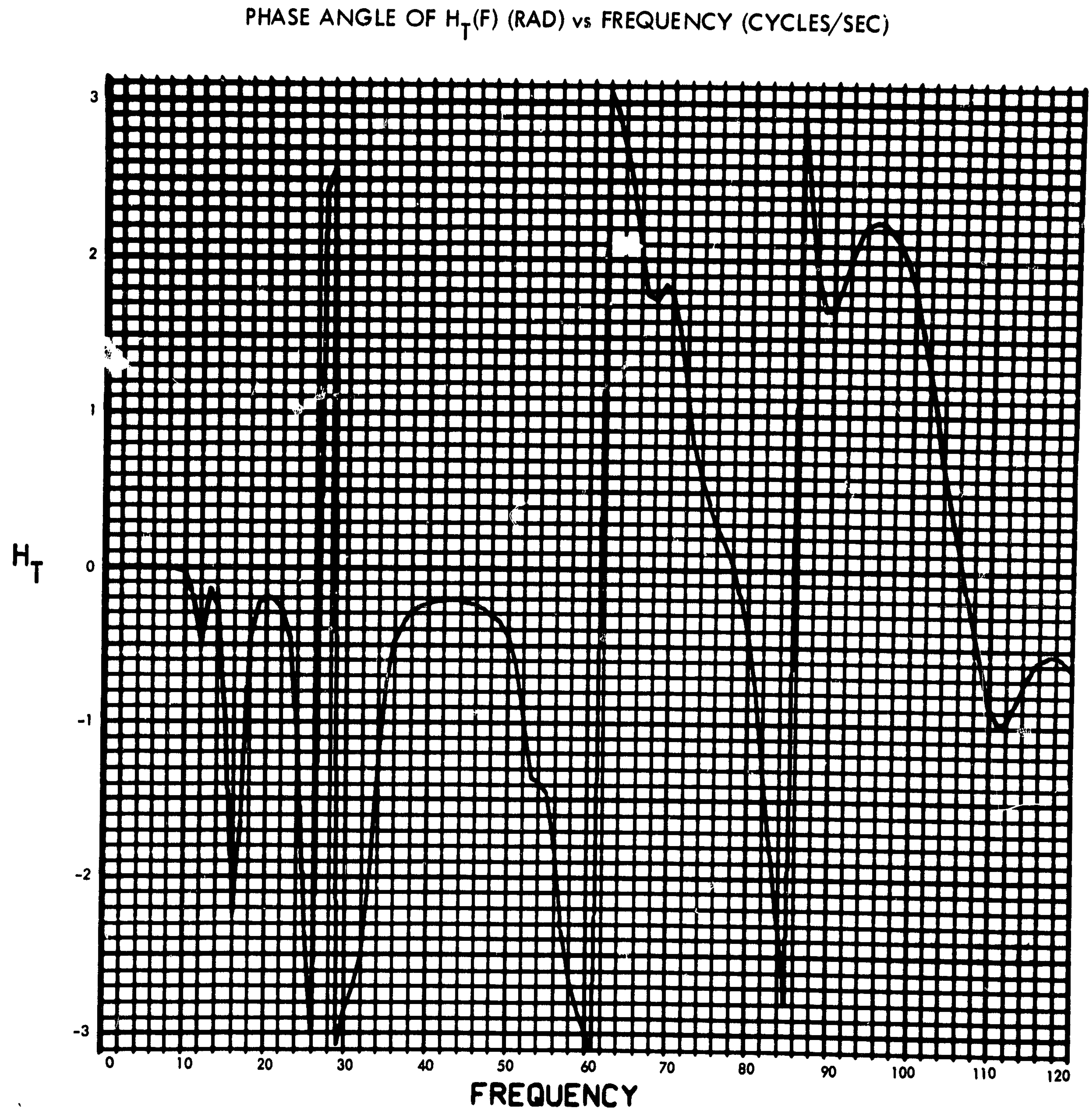

Fig. C-140. Joint 63, torque transfer function, Fourier transform, phase angle

MODULUS OF $F_T(F)$ (LB-IN-SEC) vs FREQUENCY (CYCLES/SEC)

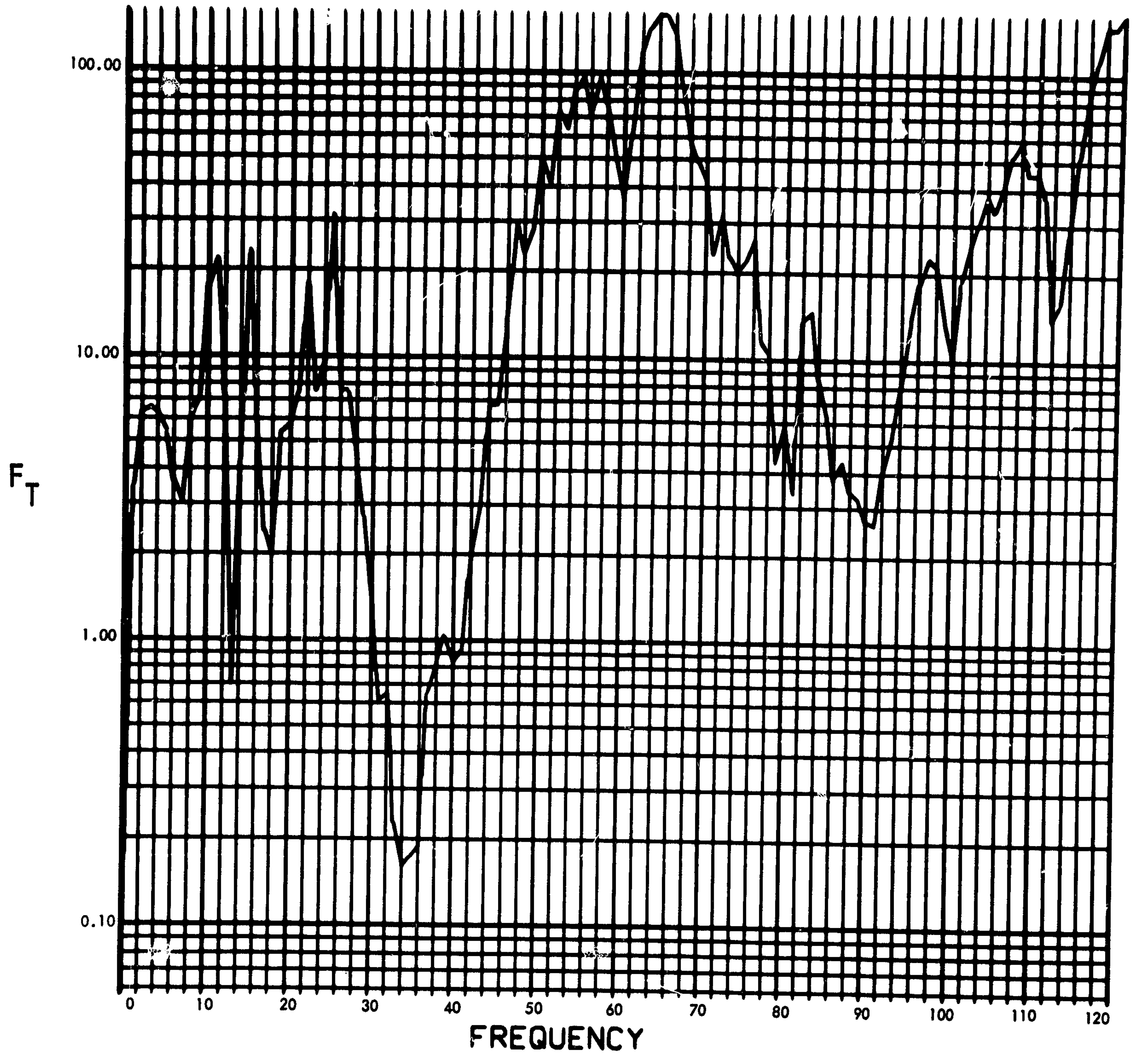

Fig. C-141. Joint 63, torque response function, Fourier transform, modulus (pulse 1)

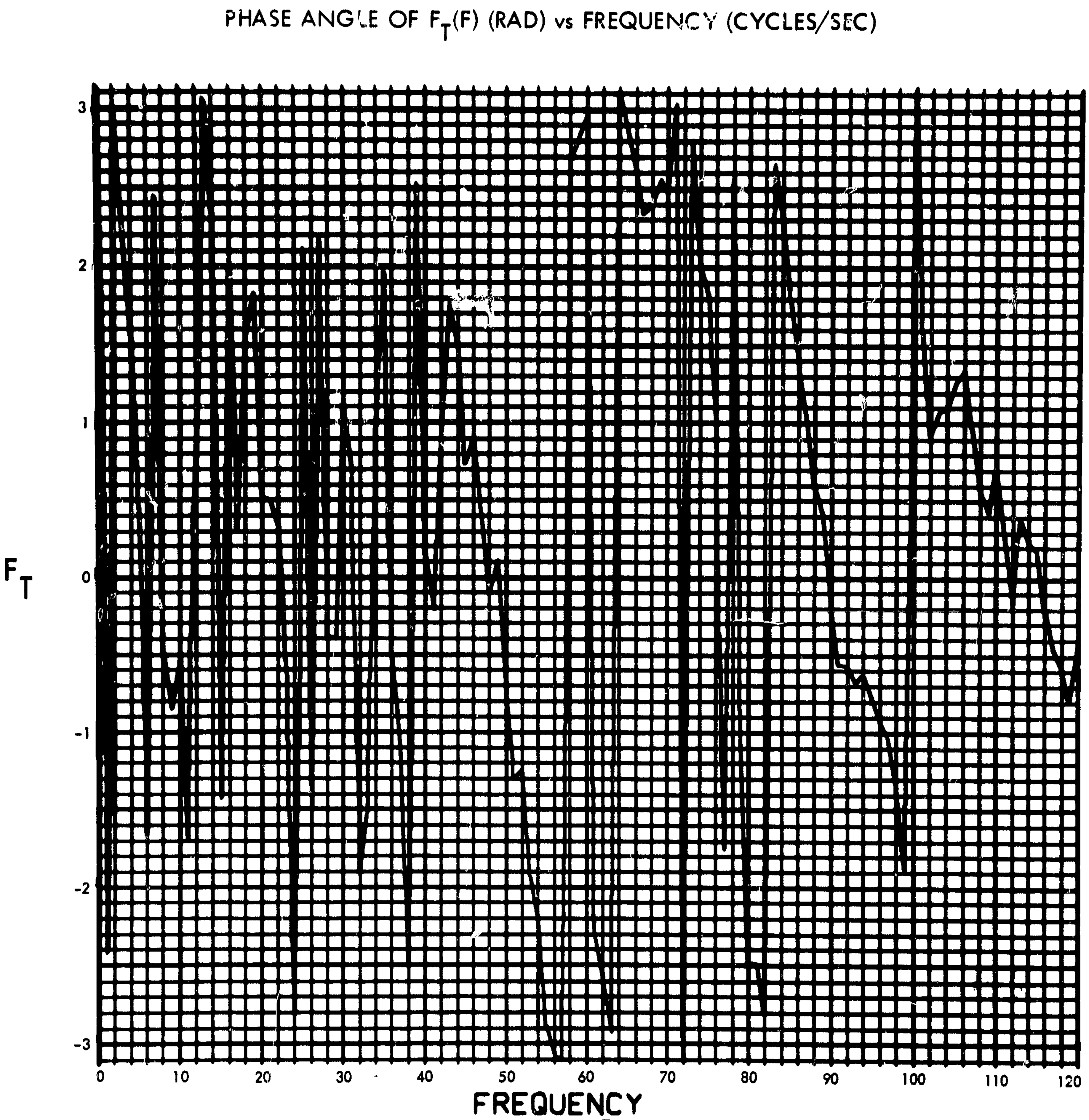

Fig. C-142. Joint 63, torque response function, Fourier transform, phase angle (pulse 1)

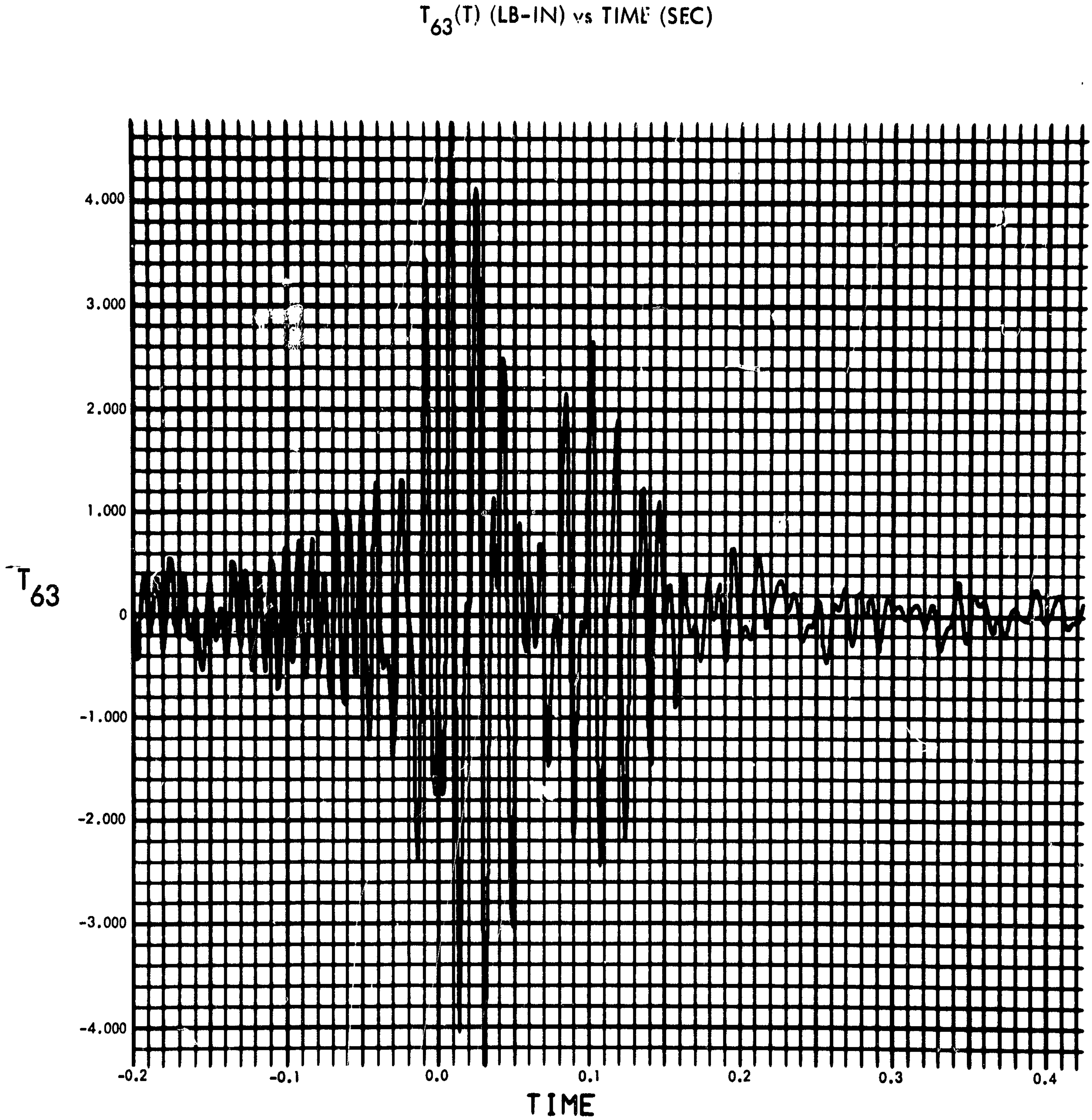

Fig. C-143. Joint 63, torque response, time history (pulse 1)

MODULUS OF $F_T(F)$ (LB-IN-SEC) vs FREQUENCY (CYCLES/SEC)

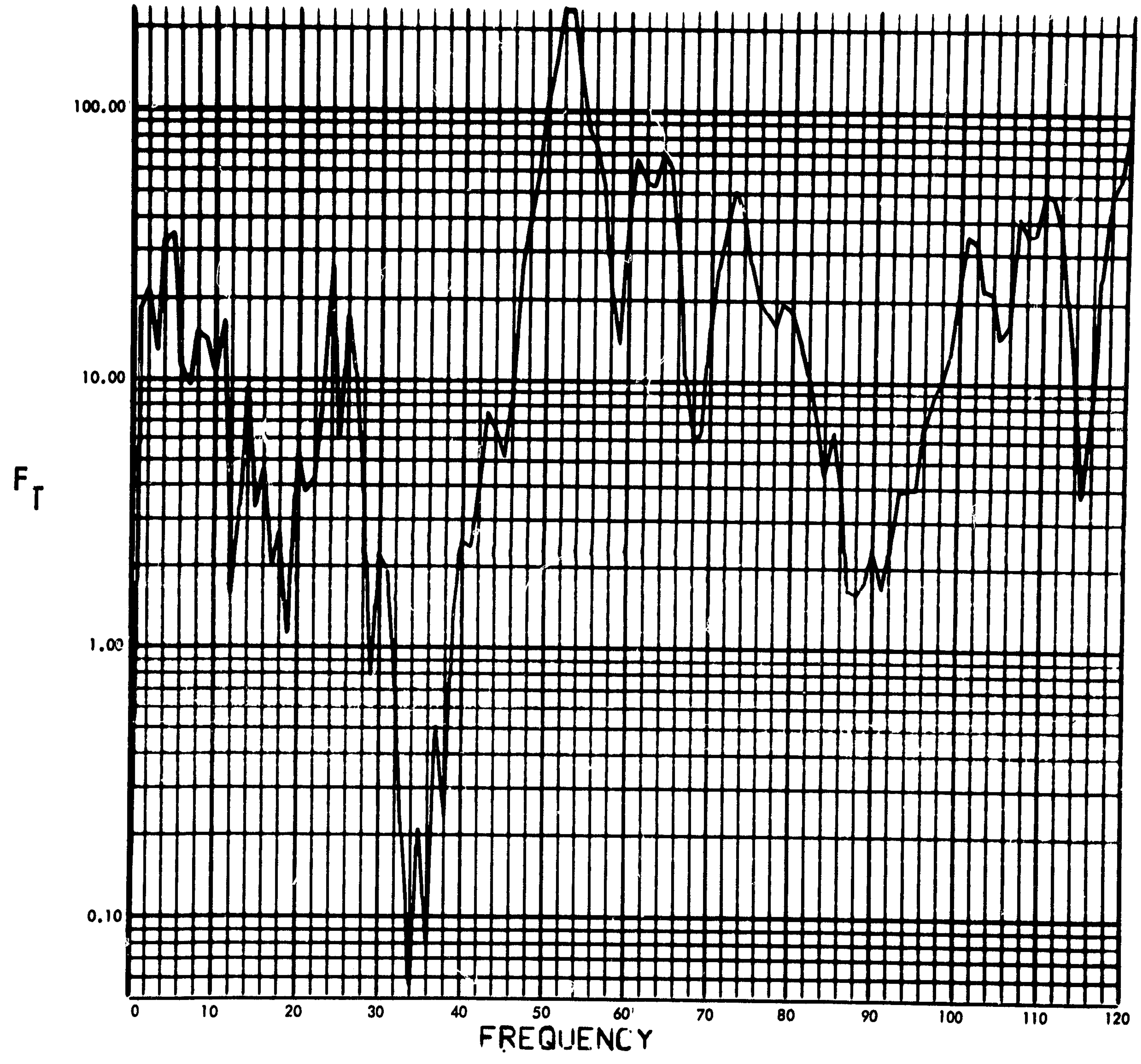

Fig. C-144. Joint 63, torque response function, Fourier transform, modulus (pulse 2)

PHASE ANGLE OF $F_T(F)$ (RAD) vs FREQUENCY (CYCLES/SEC)

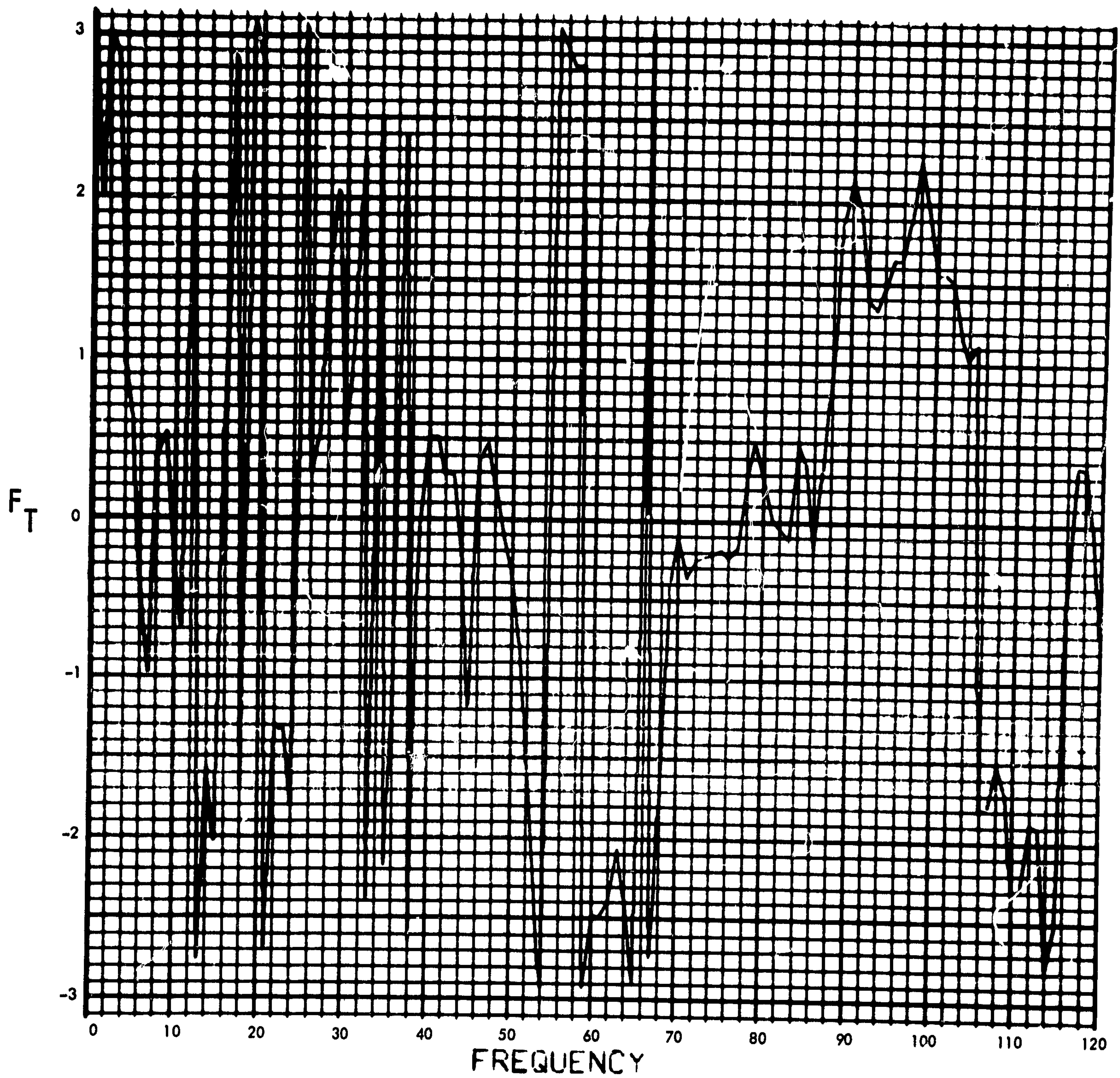

Fig. C-145. Joint 63, torque response function, Fourier transform, phase angle (pulse 2)

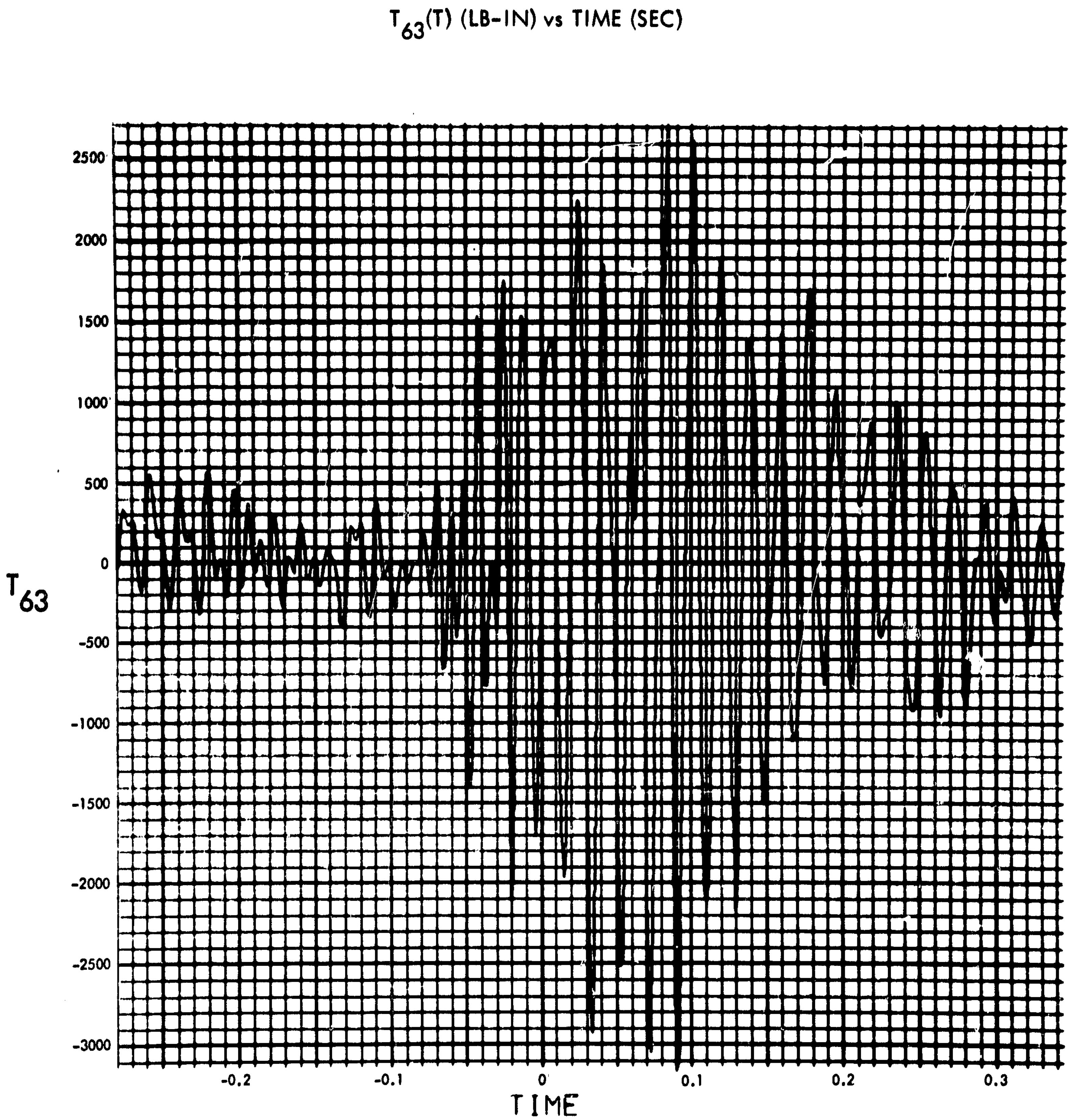

Fig. C-146. Joint 63, torque response, time history (pulse 2)

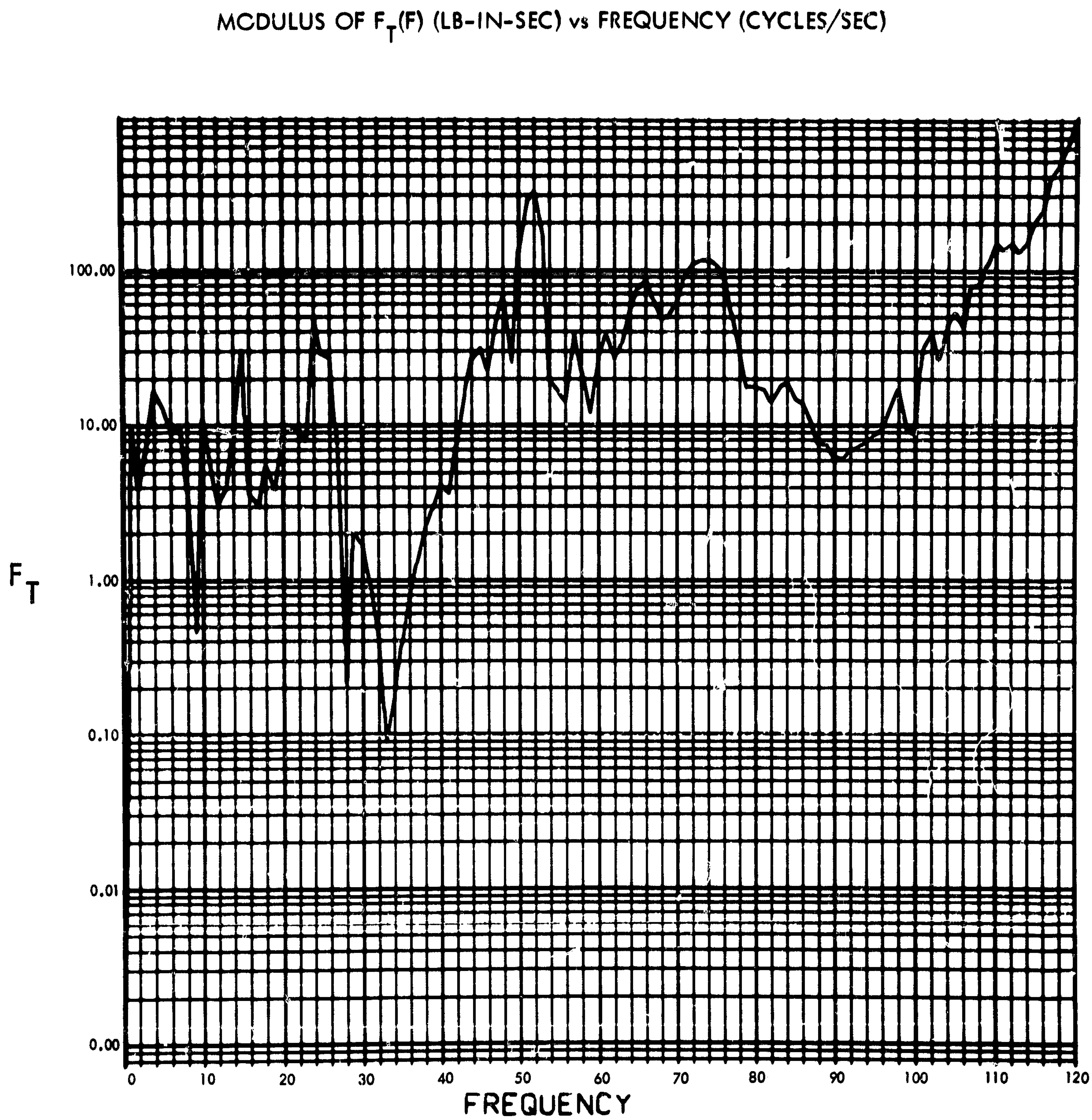

Fig. C-147. Joint 63, torque response function, Fourier transform, modulus (pulse 3)

PHASE ANGLE OF $F_T(F)$ (RAD) vs FREQUENCY (CYCLES/SEC)

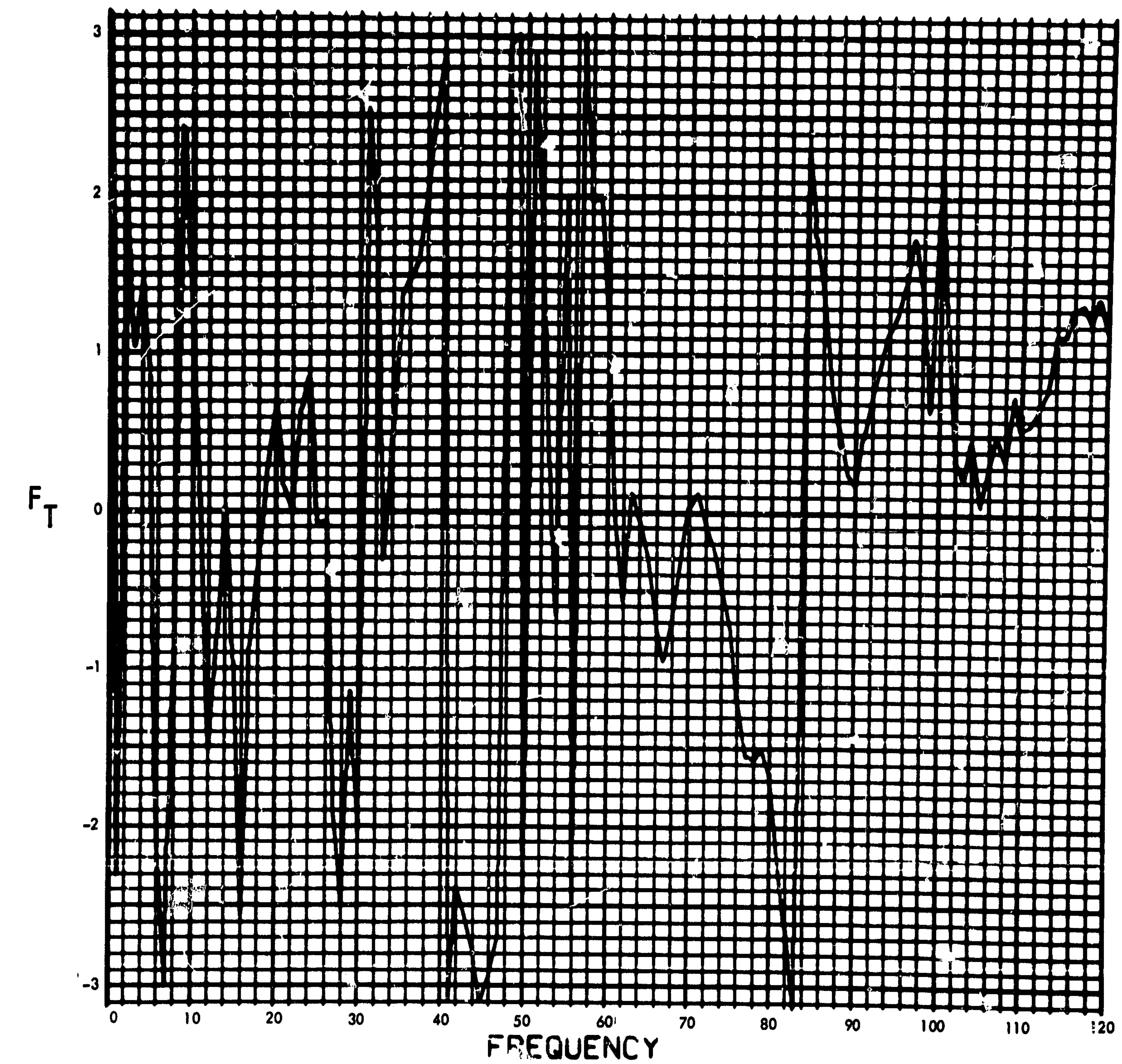

Fig. C-148. Joint 63, torque response function, Fourier transform, phase angle (pulse 3)

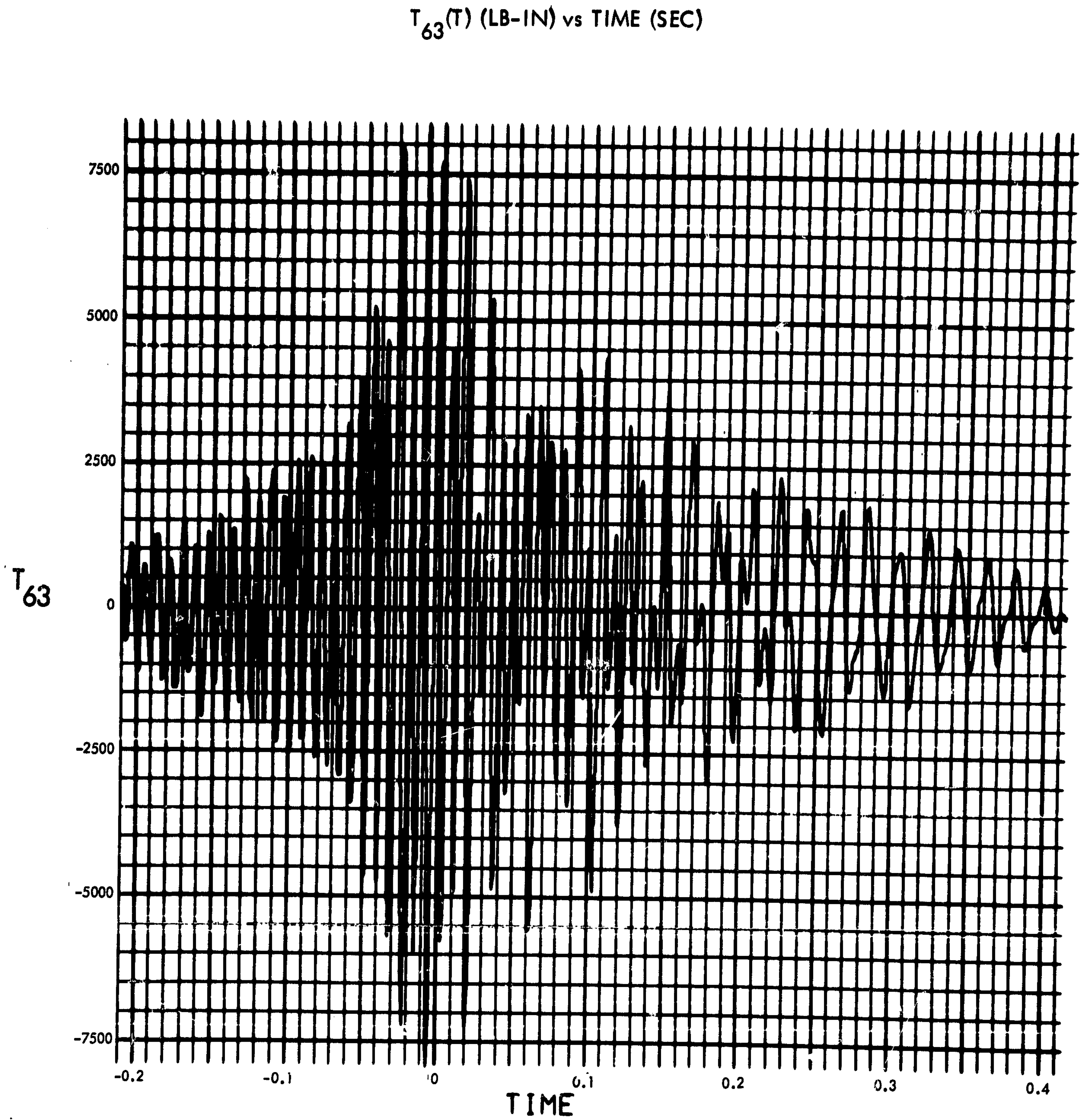

Fig. C-149. Joint 63, torque response, time history (pulse 3)

MODULUS OF $F_T(F)$ (LB-IN-SEC) vs FREQUENCY (CYCLES/SEC)

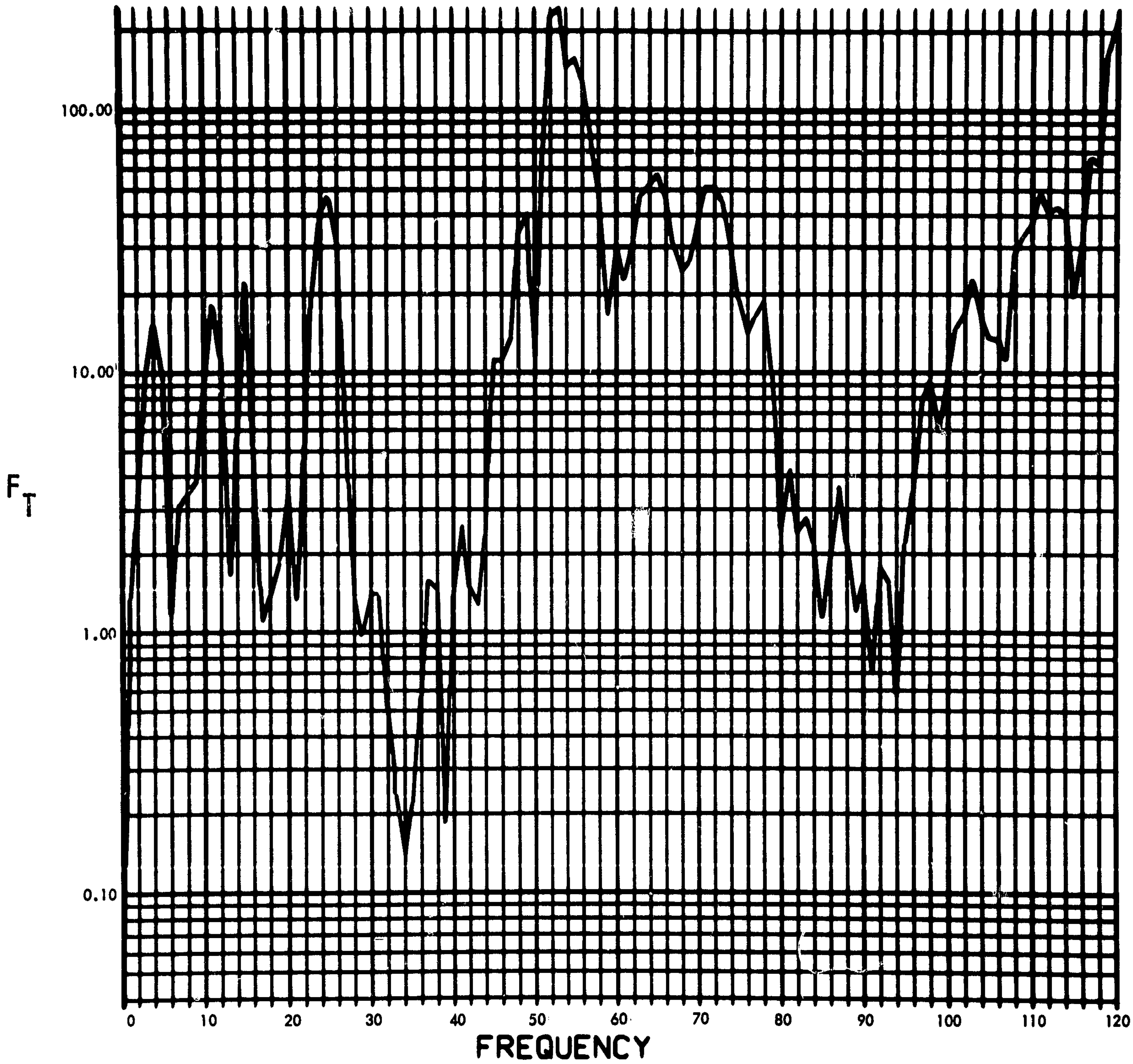

Fig. C-150. Joint 63, torque response function, Fourier transform, modulus (pulse 4)

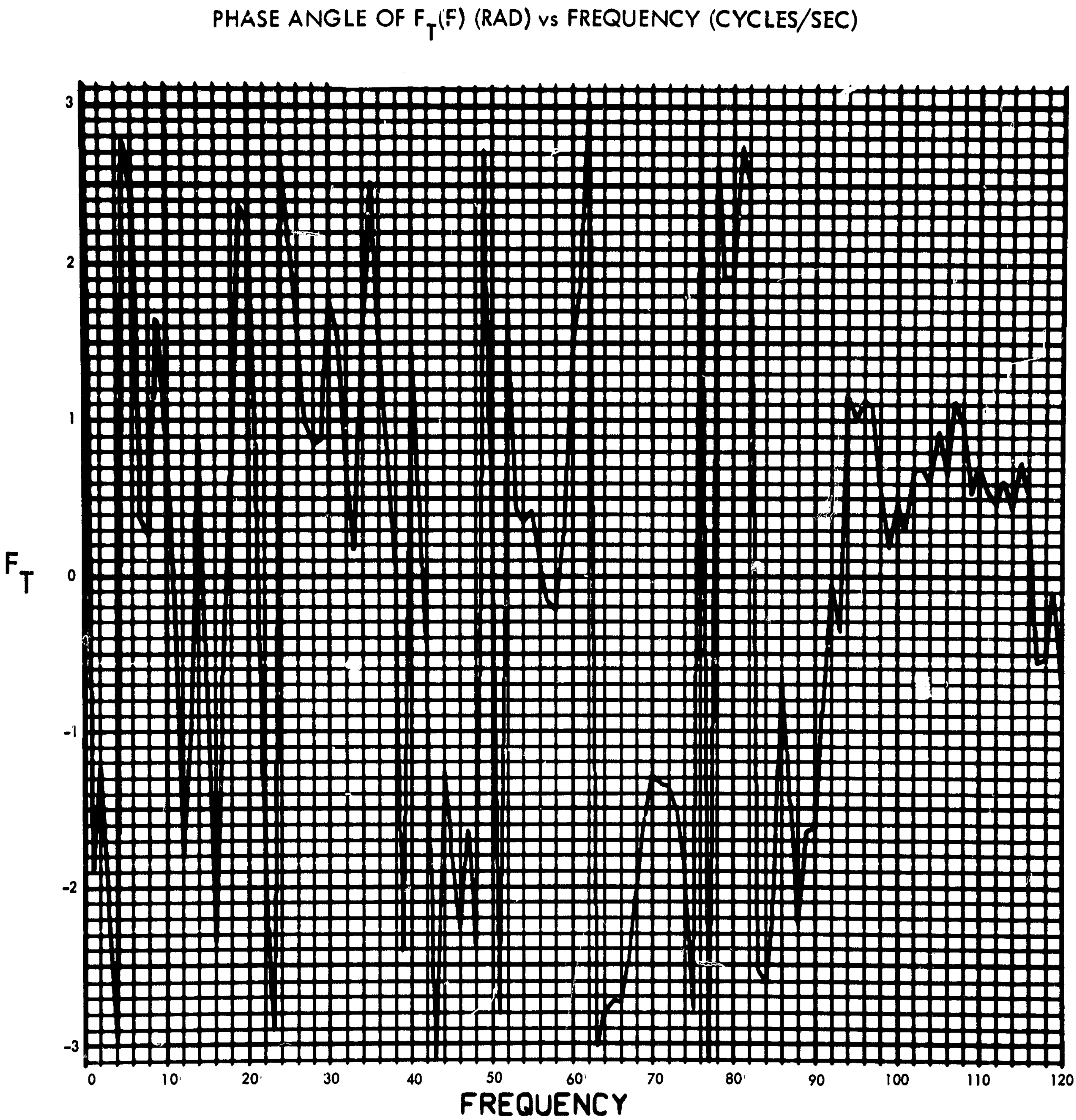

Fig. C-151. Joint 63, torque response function, Fourier transform, phase angle (pulse 4)

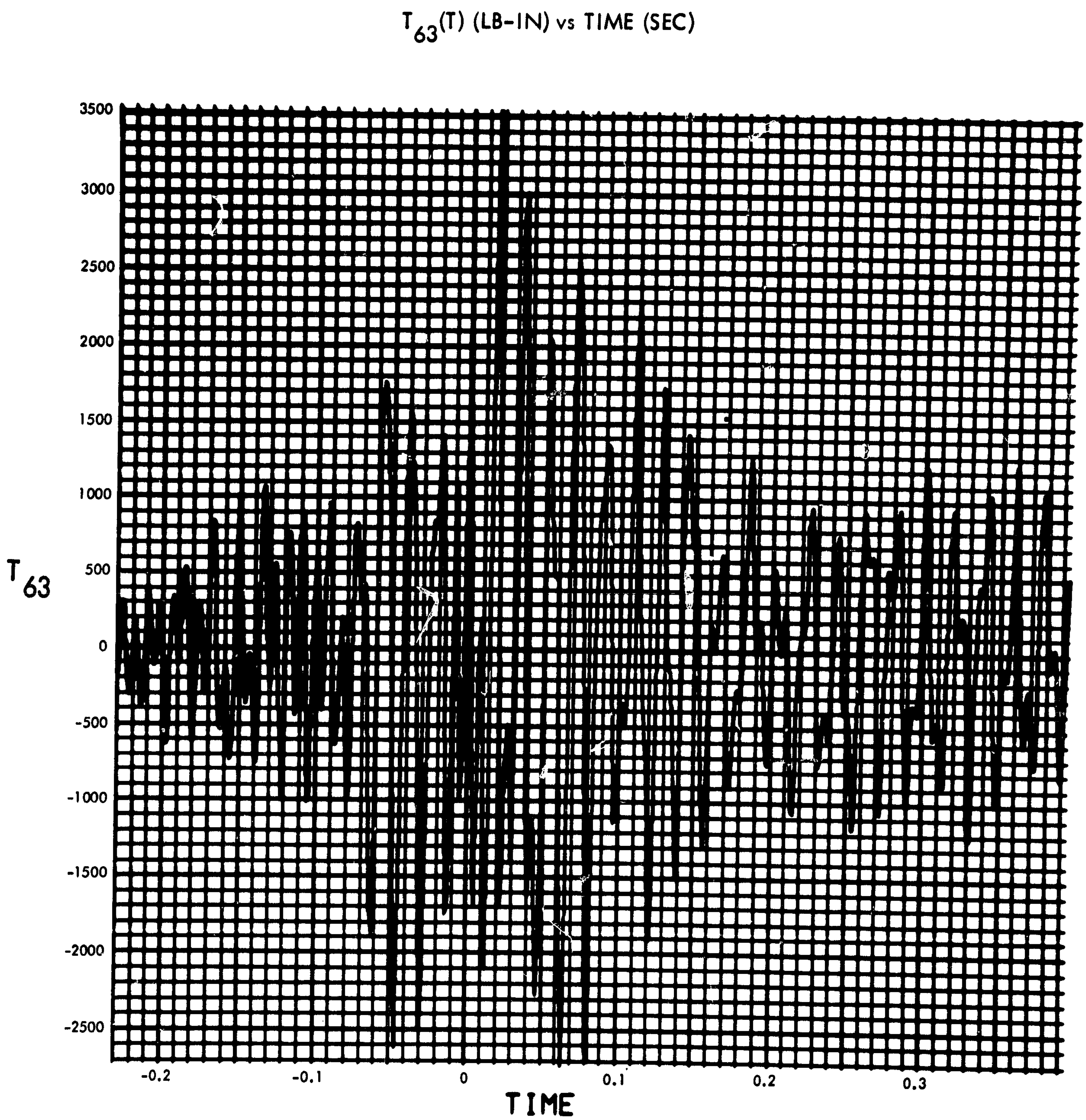

Fig. C-152. Joint 63, torque response, time history (pulse 4)

MODULUS H2(F) (1/LB-IN-SEC^2) vs FREQUENCY (CYCLES/SEC)

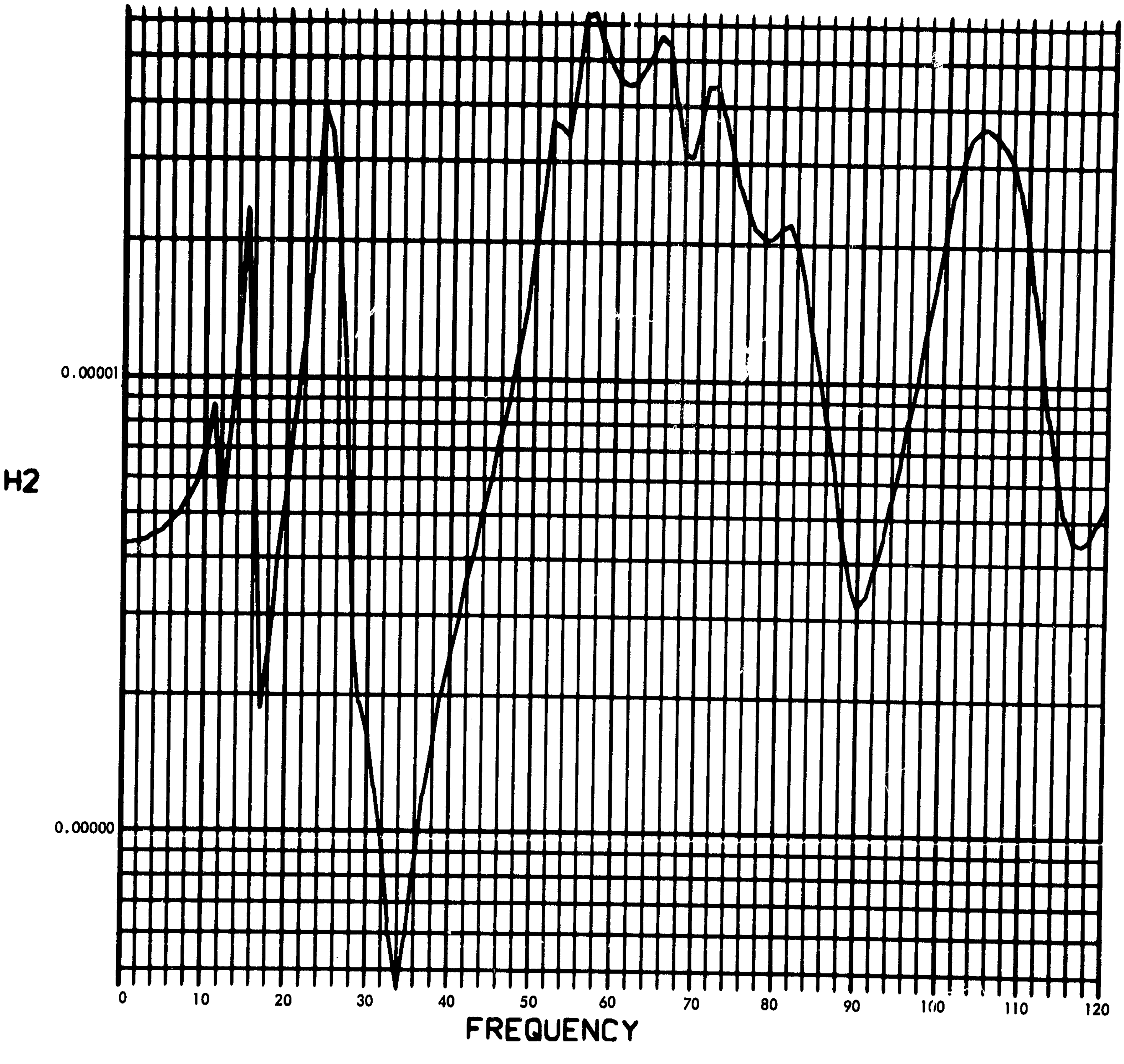

Fig. C-153. Joint 14, acceleration transfer function, Fourier transform, modulus

PHASE ANGLE OF H2(F) (RAD) vs FREQUENCY (CYCLES/SEC)

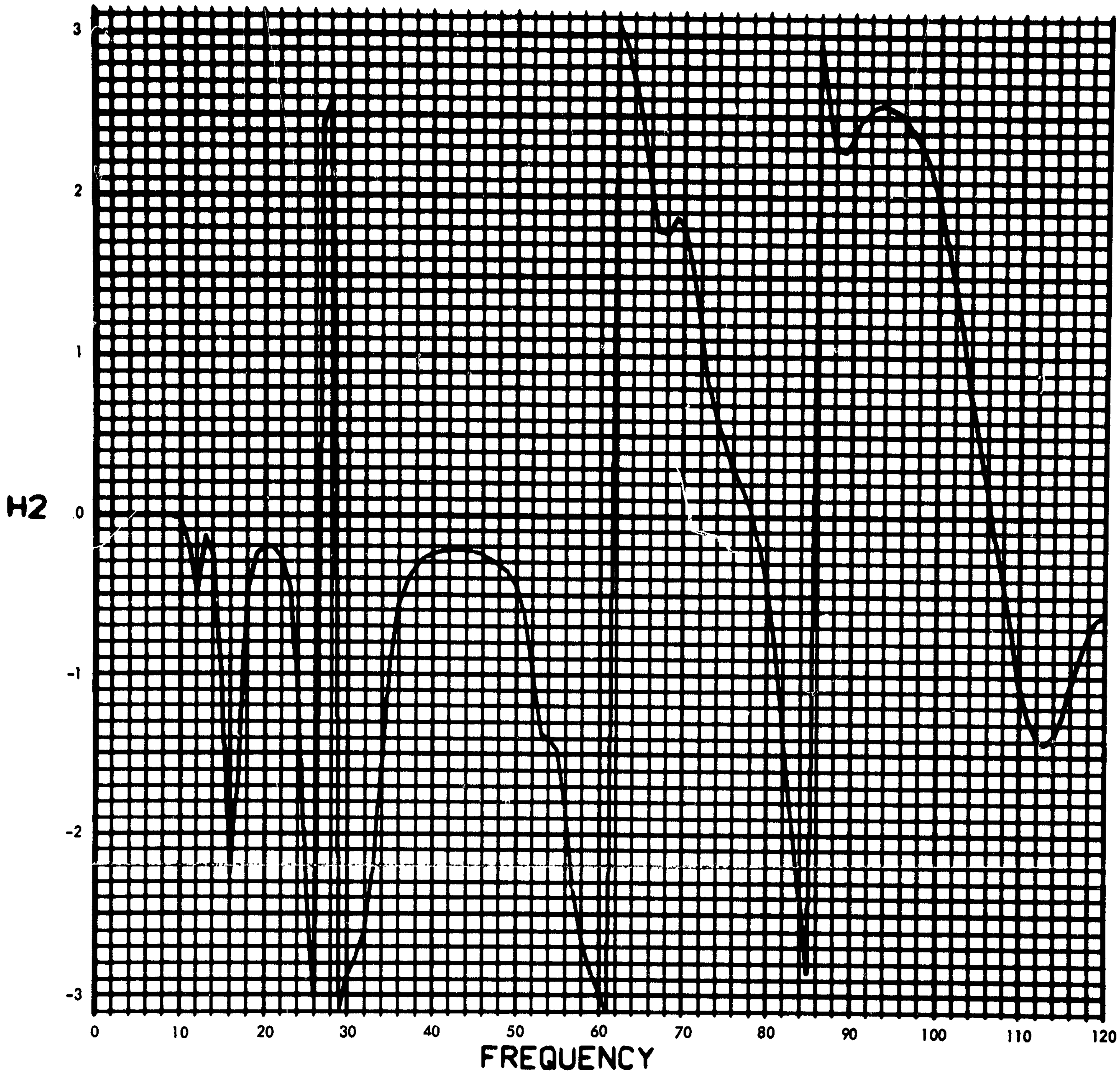

Fig. C-154. Joint 14, acceleration transfer function, Fourier transform, phase angle

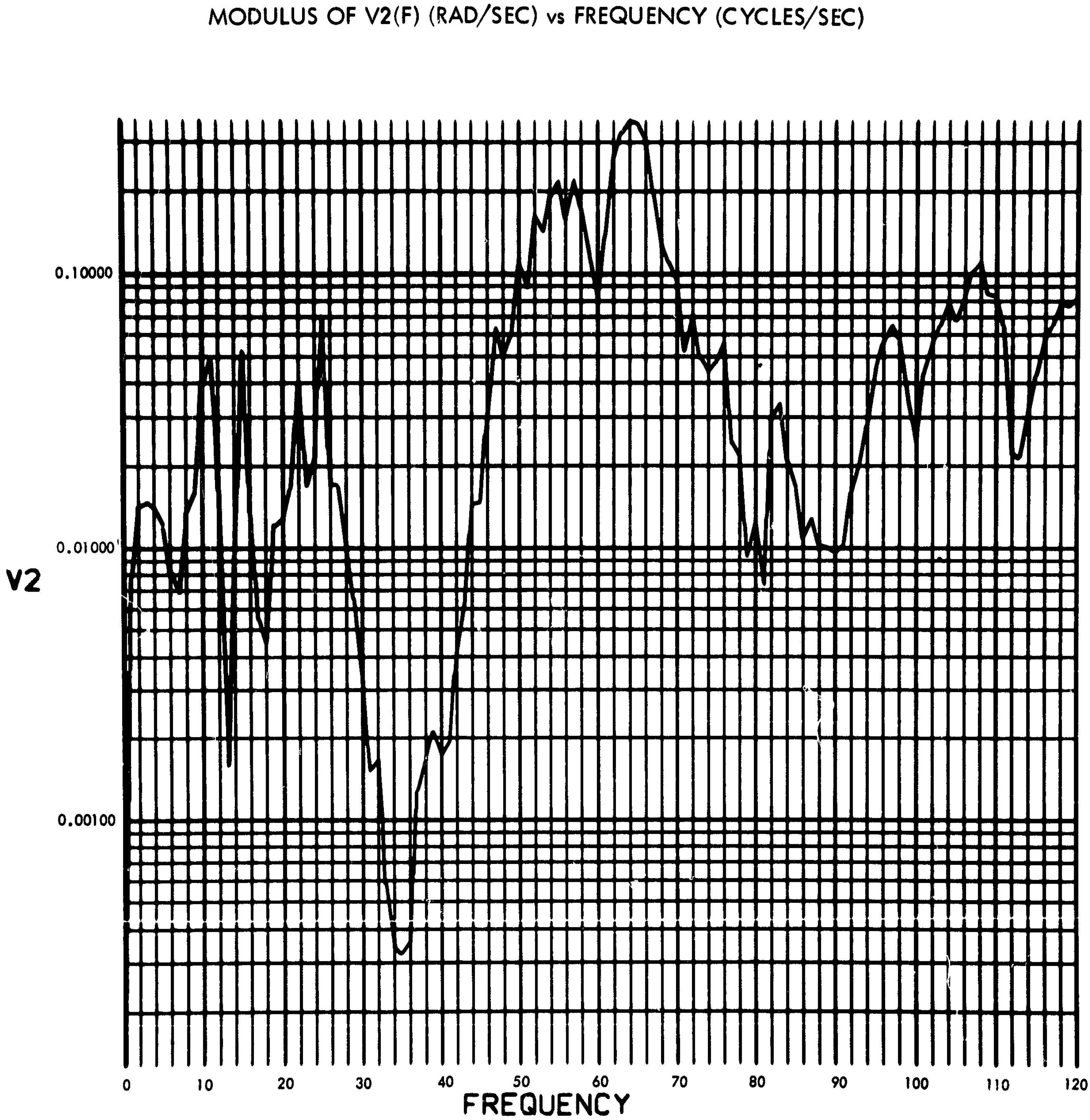

Fig. C-155. Joint 14, acceleration response, Fourier transform, modulus (pulse 1)

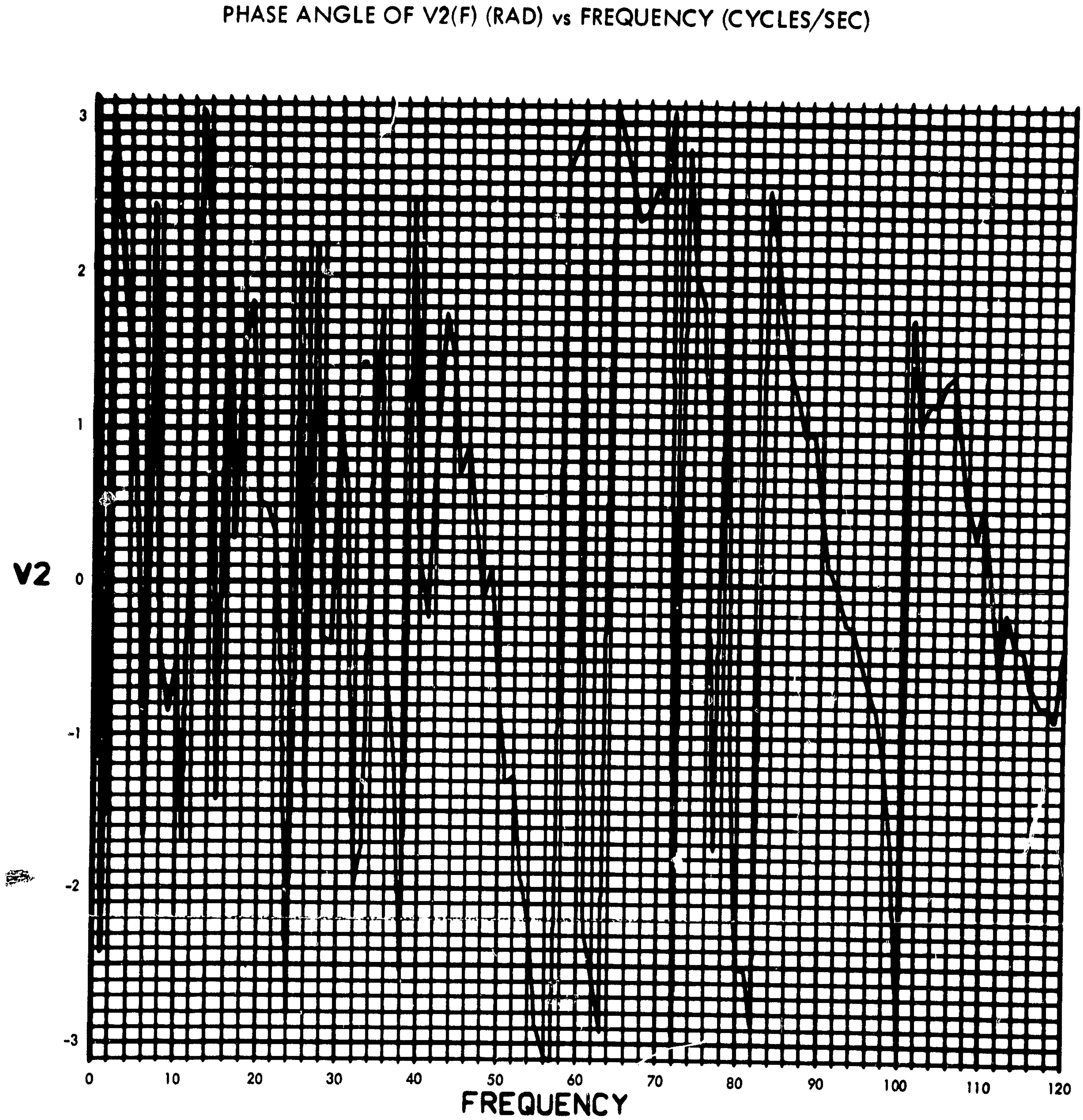

Fig. C-156. Joint 14, acceleration response, Fourier transform, phase angle (pulse 1)

U2(T) (RAD/SEC^2) vs TIME (SEC)

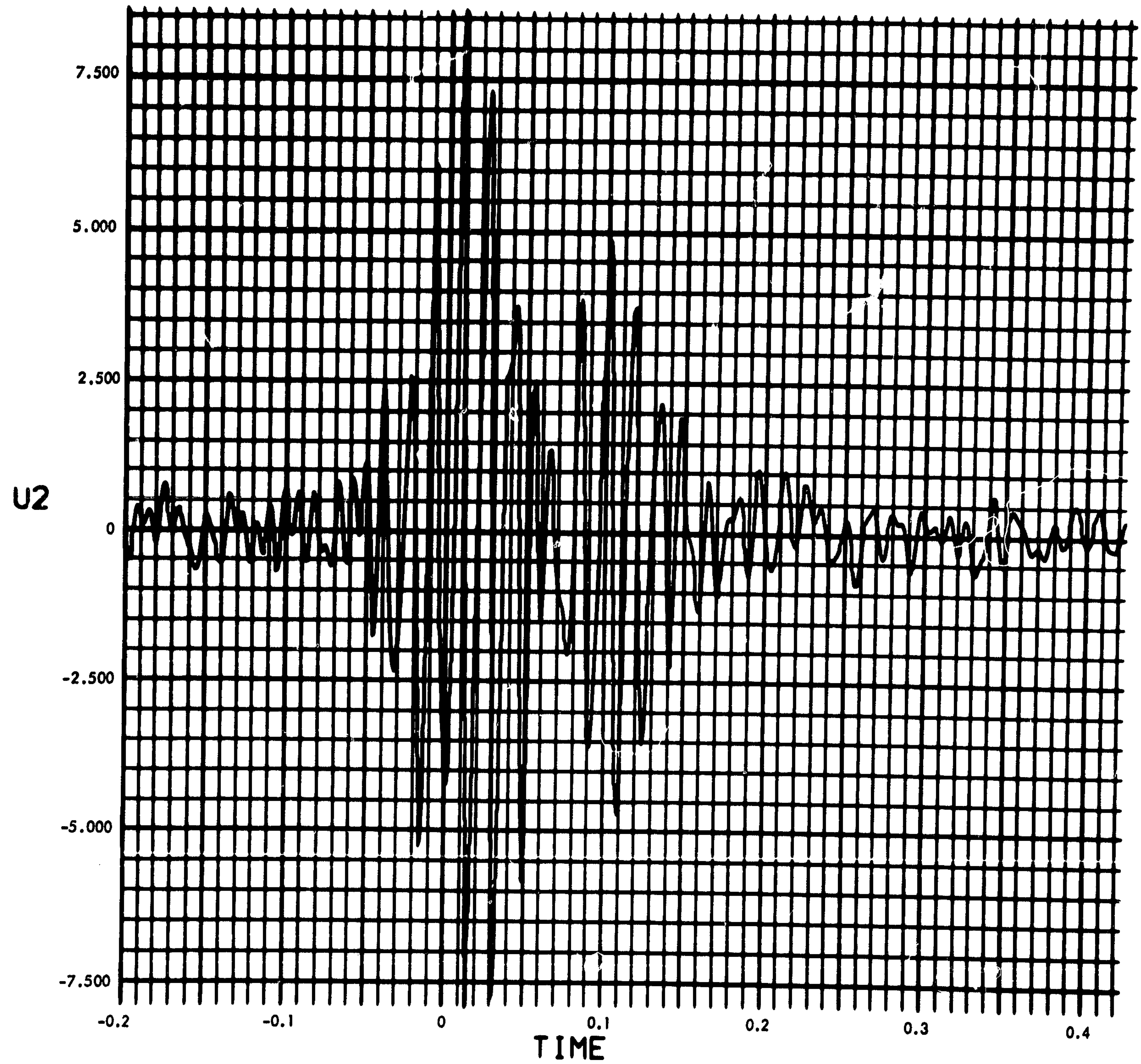

Fig. C-157. Joint 14, acceleration response, time history (pulse 1)

MODULUS OF V2(F) (RAD/SEC) vs FREQUENCY (CYCLES/SEC)

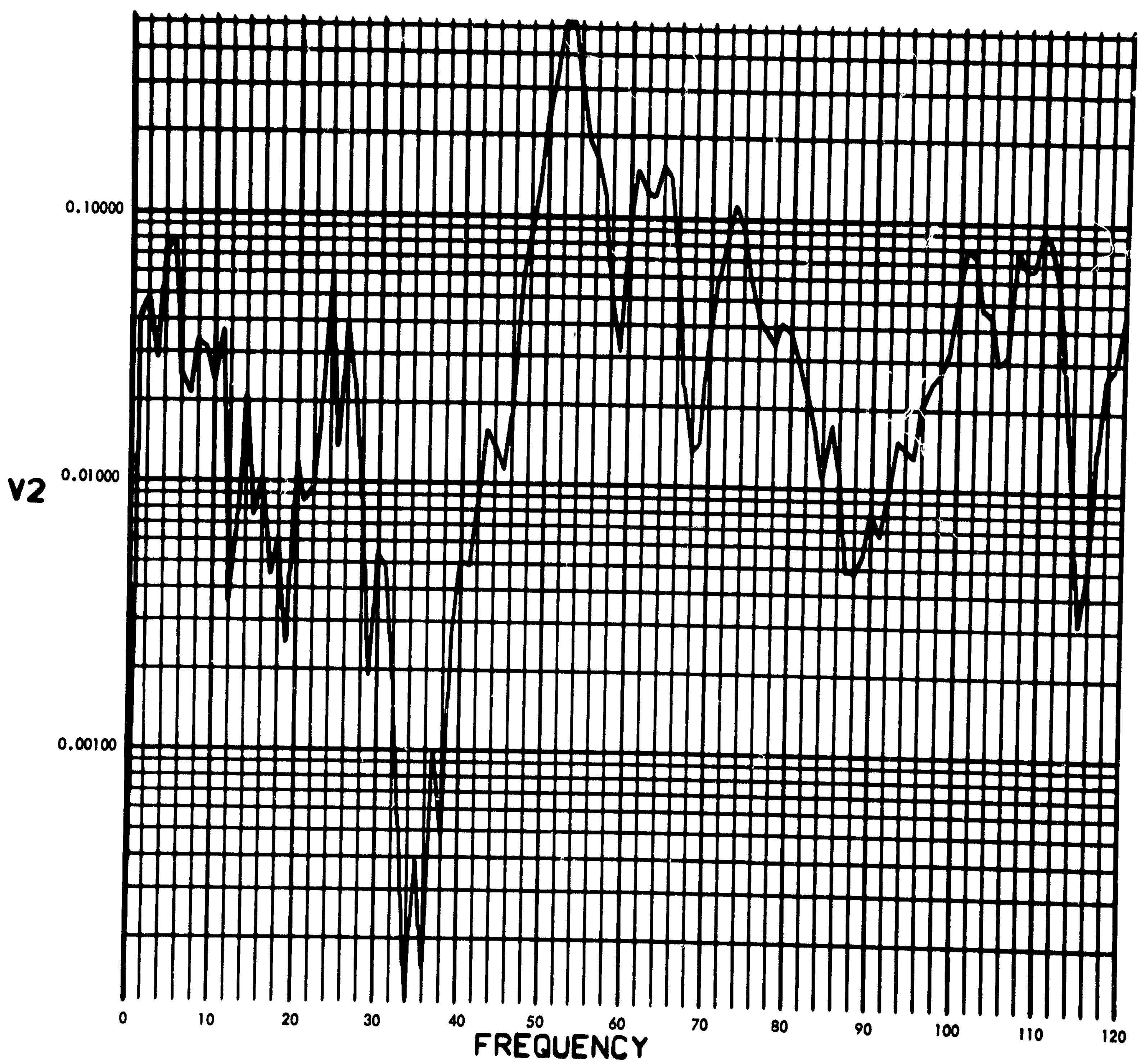

Fig. C-158. Joint 14, acceleration response, Fourier transform, modulus (pulse 2)

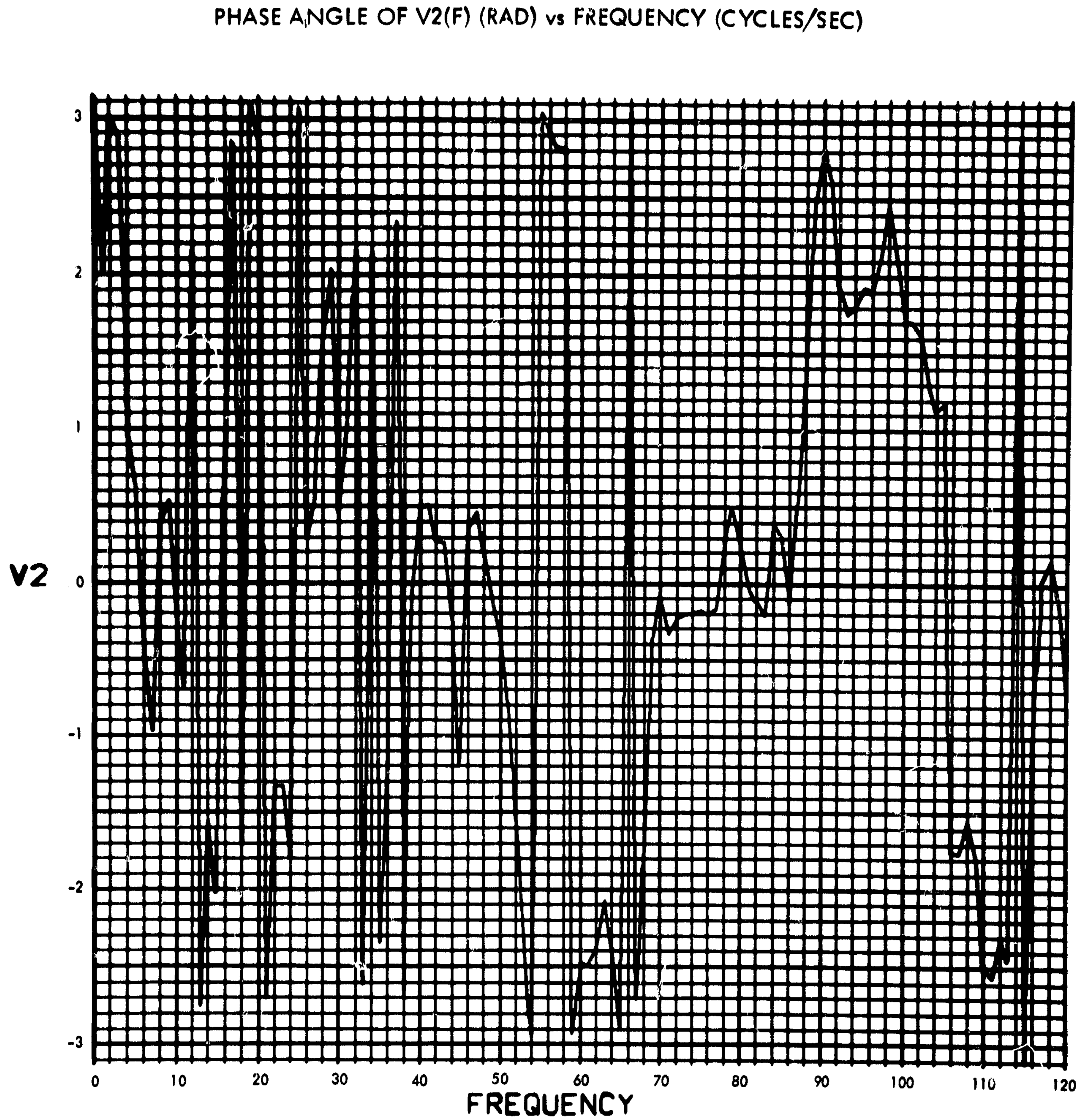

Fig. C-159. Joint 14, acceleration response, Fourier transform, phase angle (pulse 2)

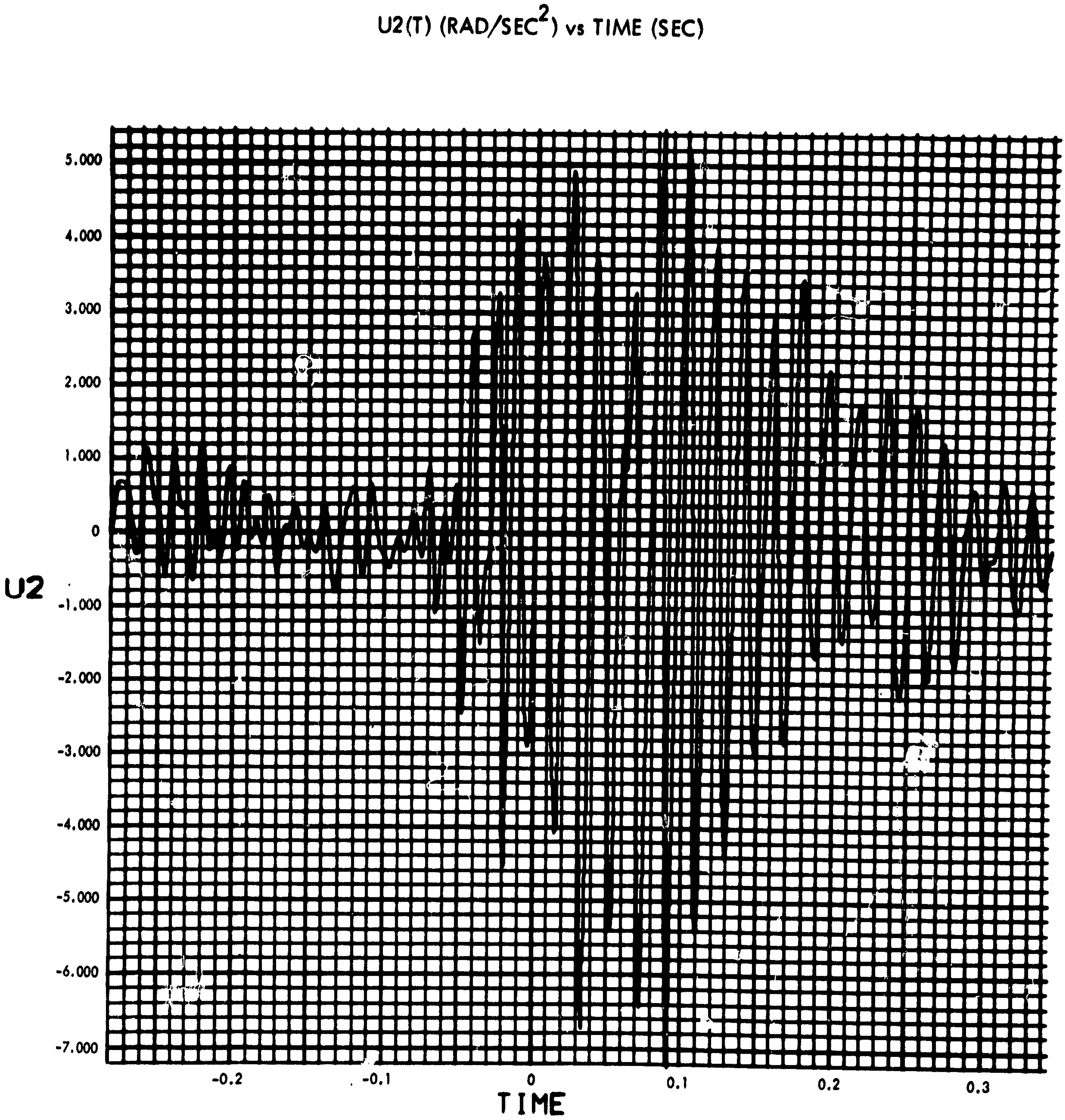

Fig. C-160. Joint 14, acceleration response, time history (pulse 2)

MODULUS OF V2(F) (RAD/SEC) vs FREQUENCY (CYCLES/SEC)

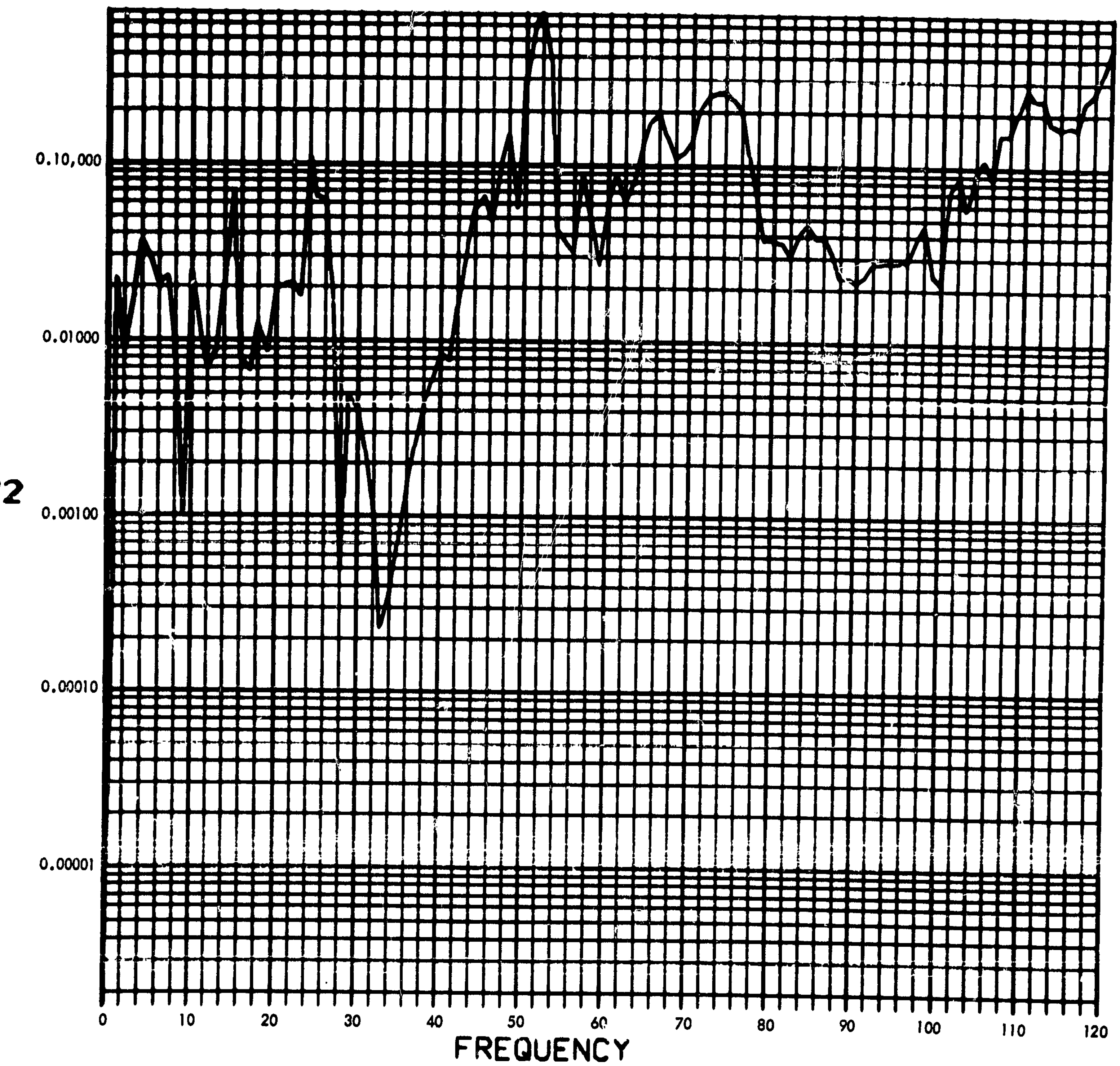

Fig. C-161. Joint 14, acceleration response, Fourier transform, modulus (pulse 3)

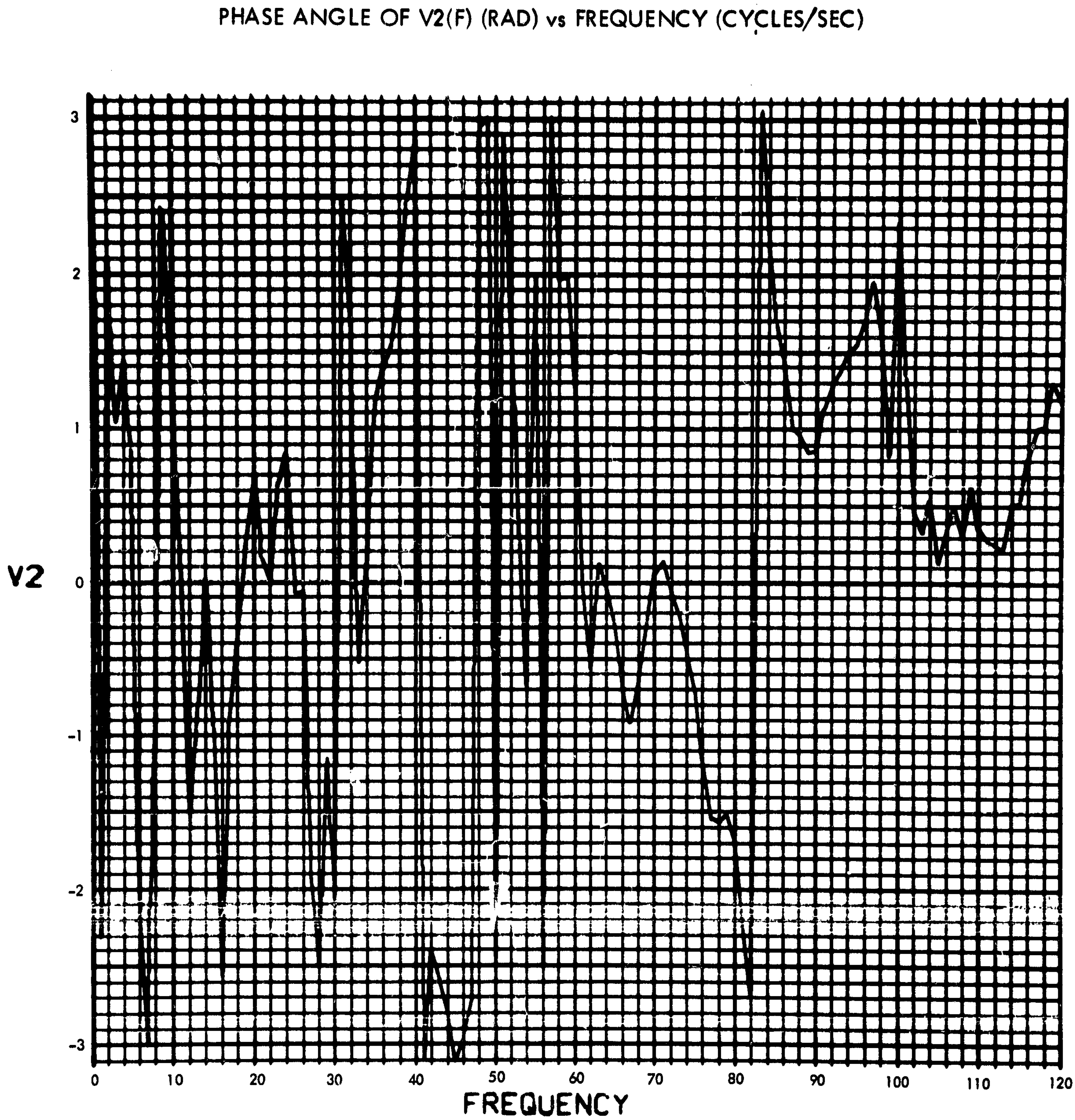

Fig. C-162. Joint 14, acceleration response, Fourier transform, phase angle (pulse 3)

U2(T) (RAD/SEC^2) vs TIME (SEC)

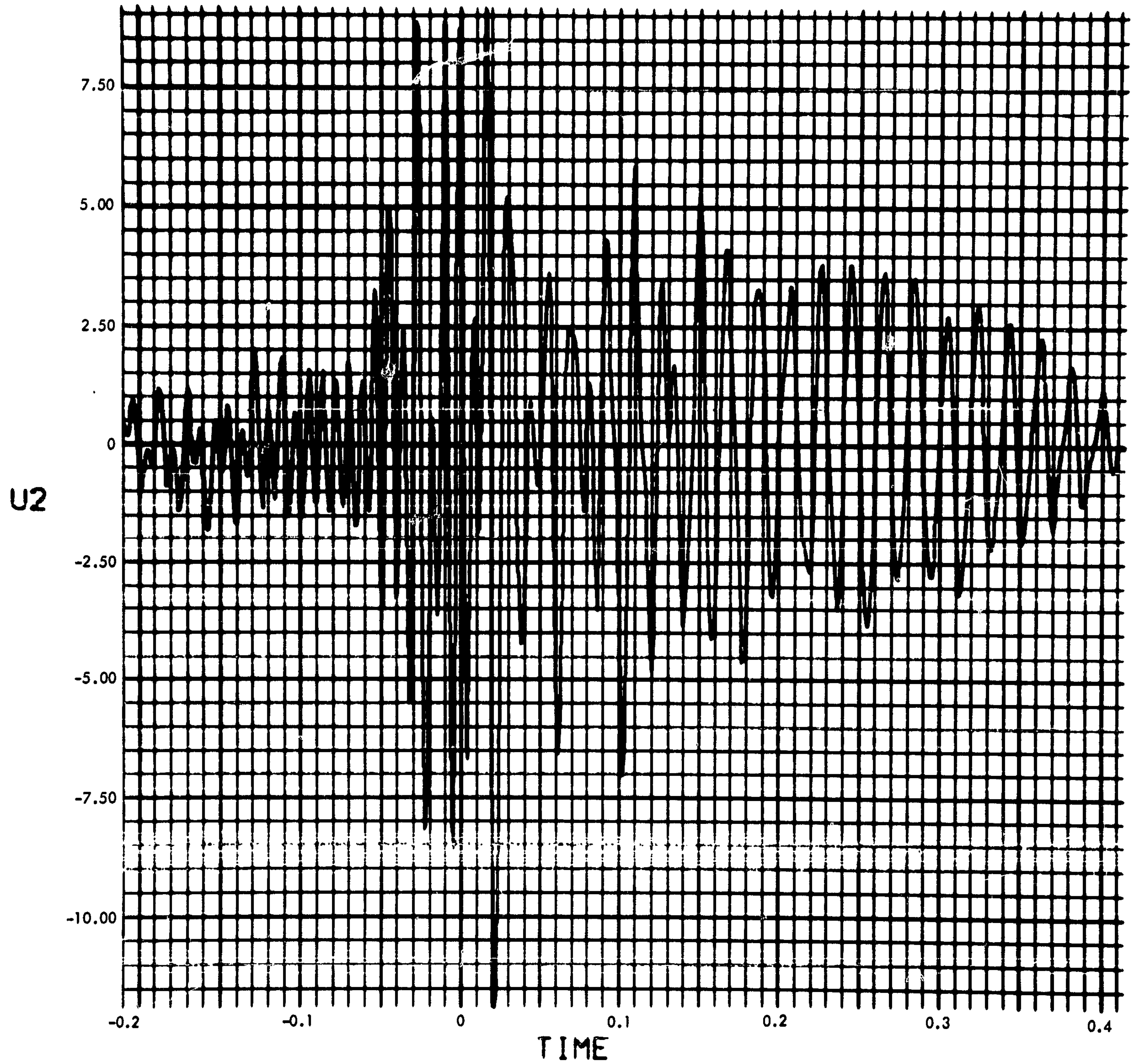

Fig. C-163. Joint 14, acceleration response, time history (pulse 3)

MODULUS OF V2(F) (RAD/SEC) vs FREQUENCY (CYCLES/SEC)

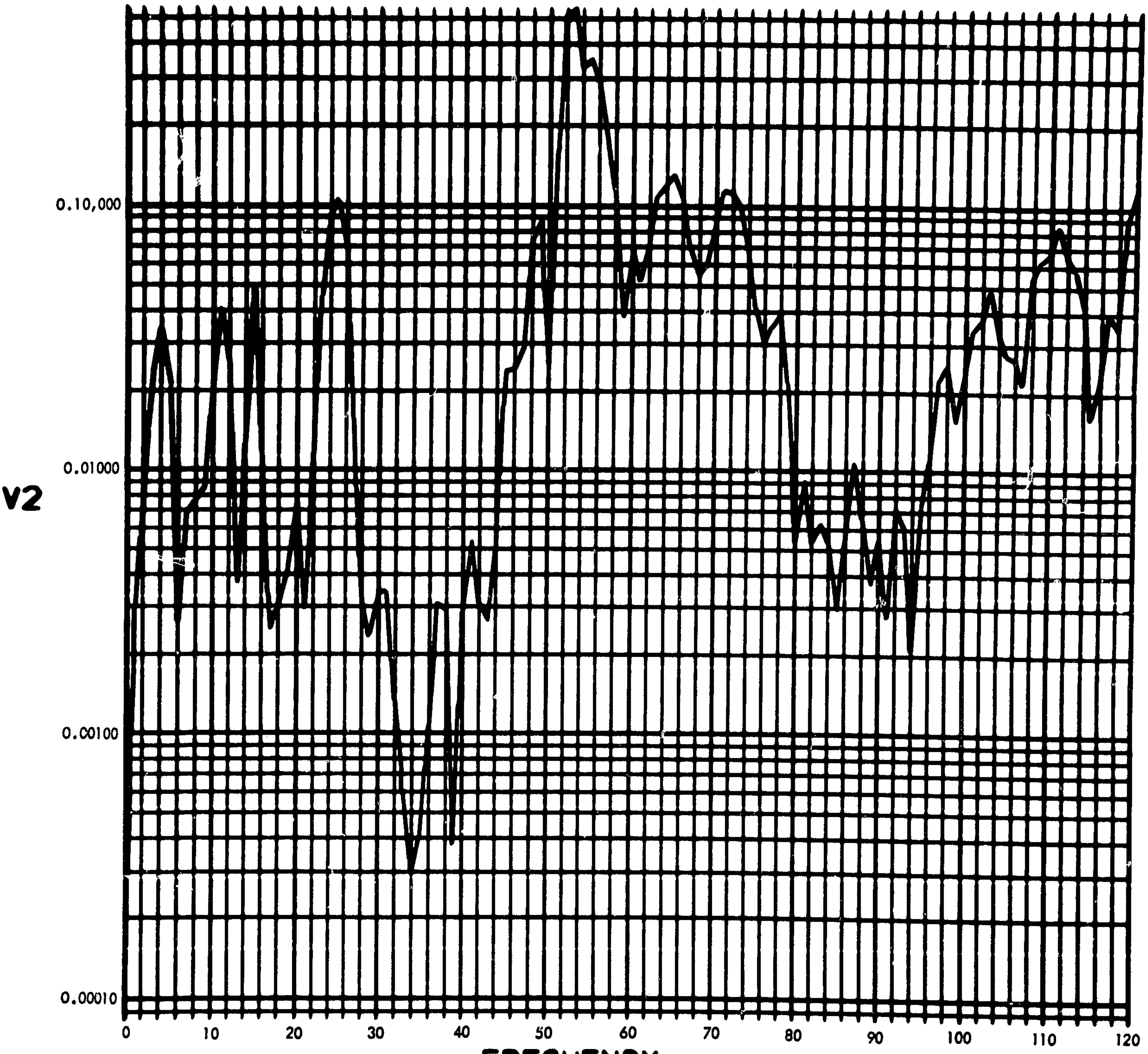

Fig. C-164. Joint 14, acceleration response, Fourier transform, modulus (pulse 4)

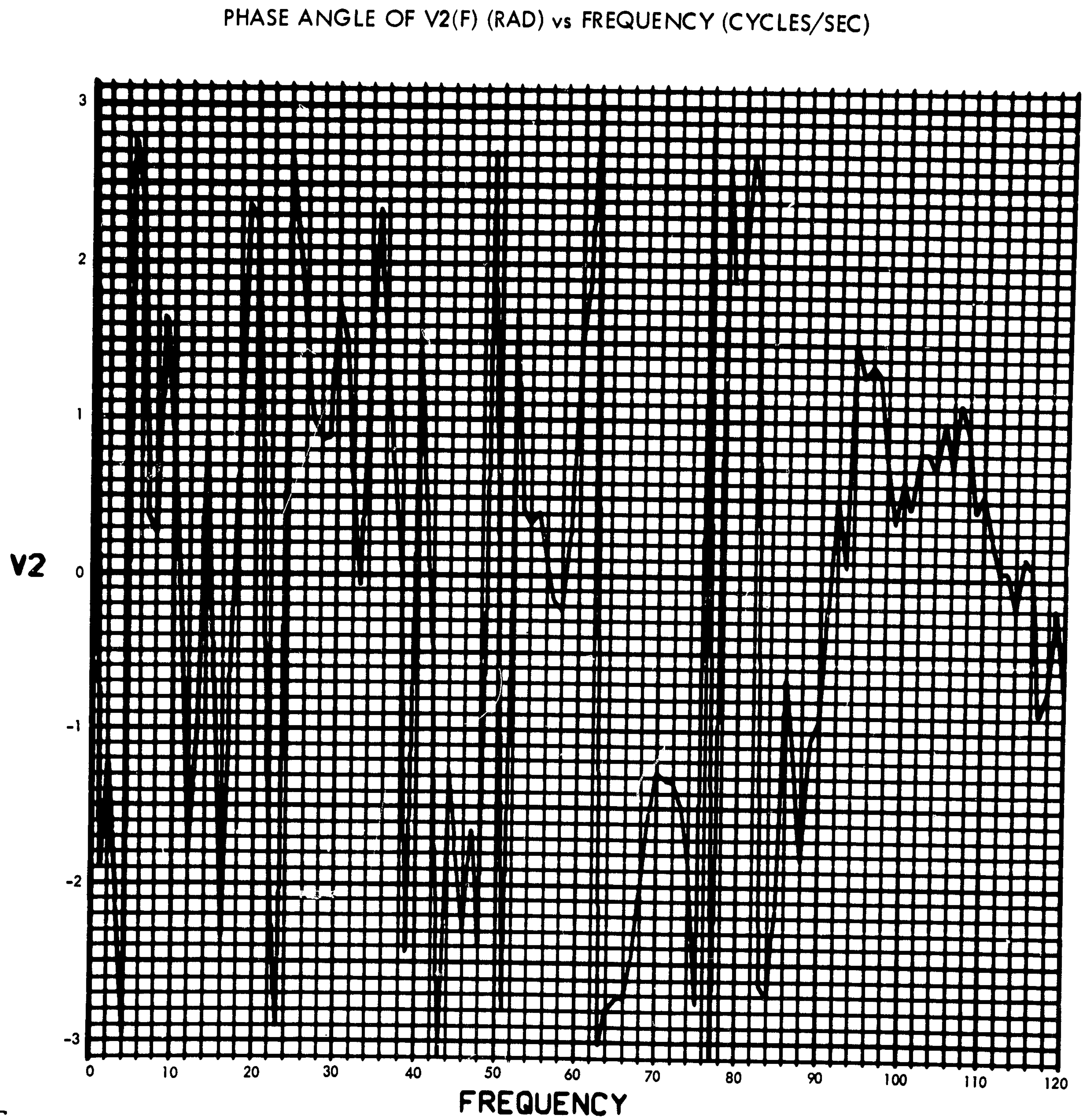

Fig. C-165. Joint 14, acceleration response, Fourier transform, phase angle (pulse 4)

U2(T) (RAD/SEC^2) vs TIME (SEC)

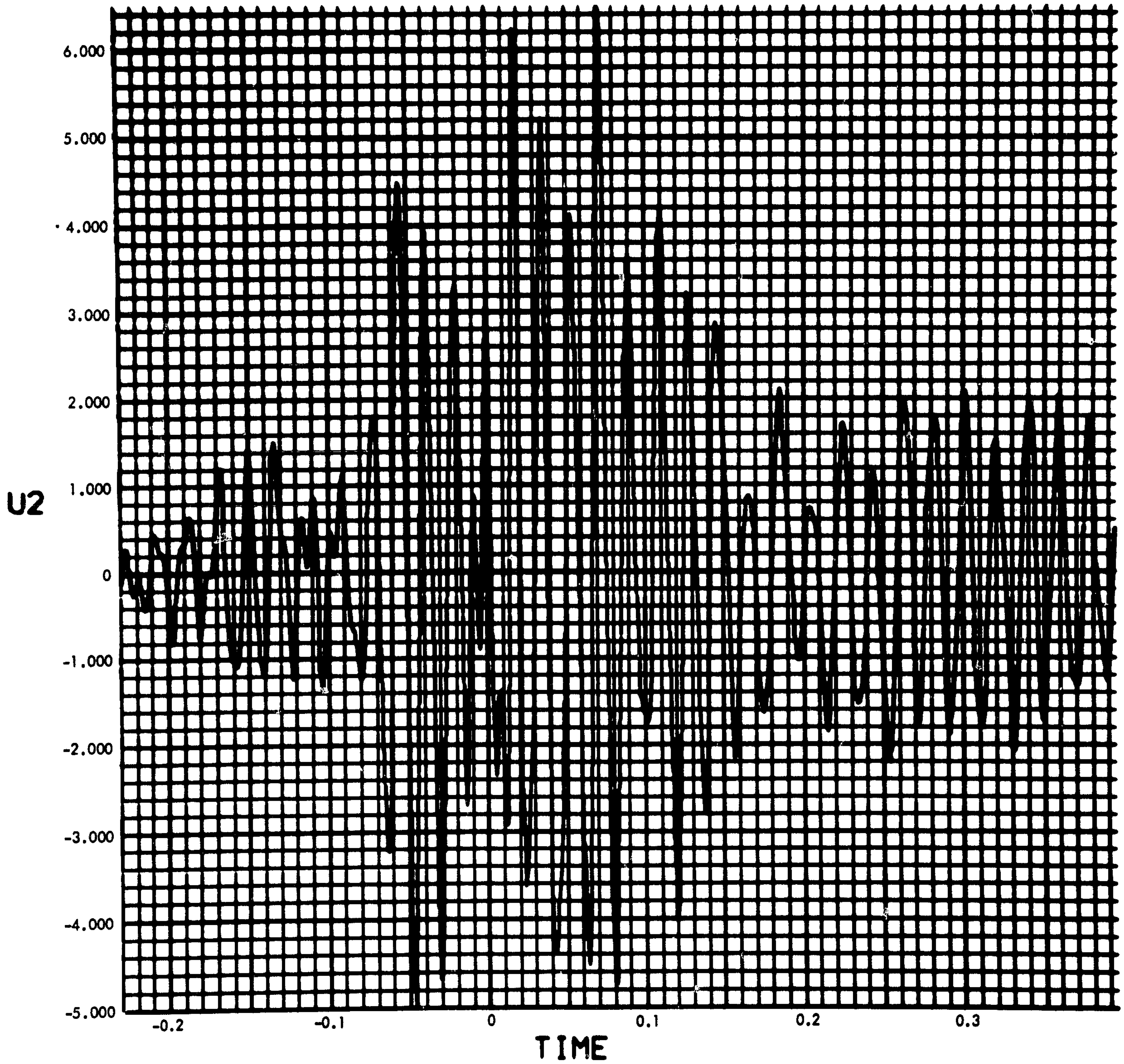

Fig. C-166. Joint 14, acceleration response, time history (pulse 4)

MODULUS $H_T(F)$ vs FREQUENCY (CYCLES/SEC)

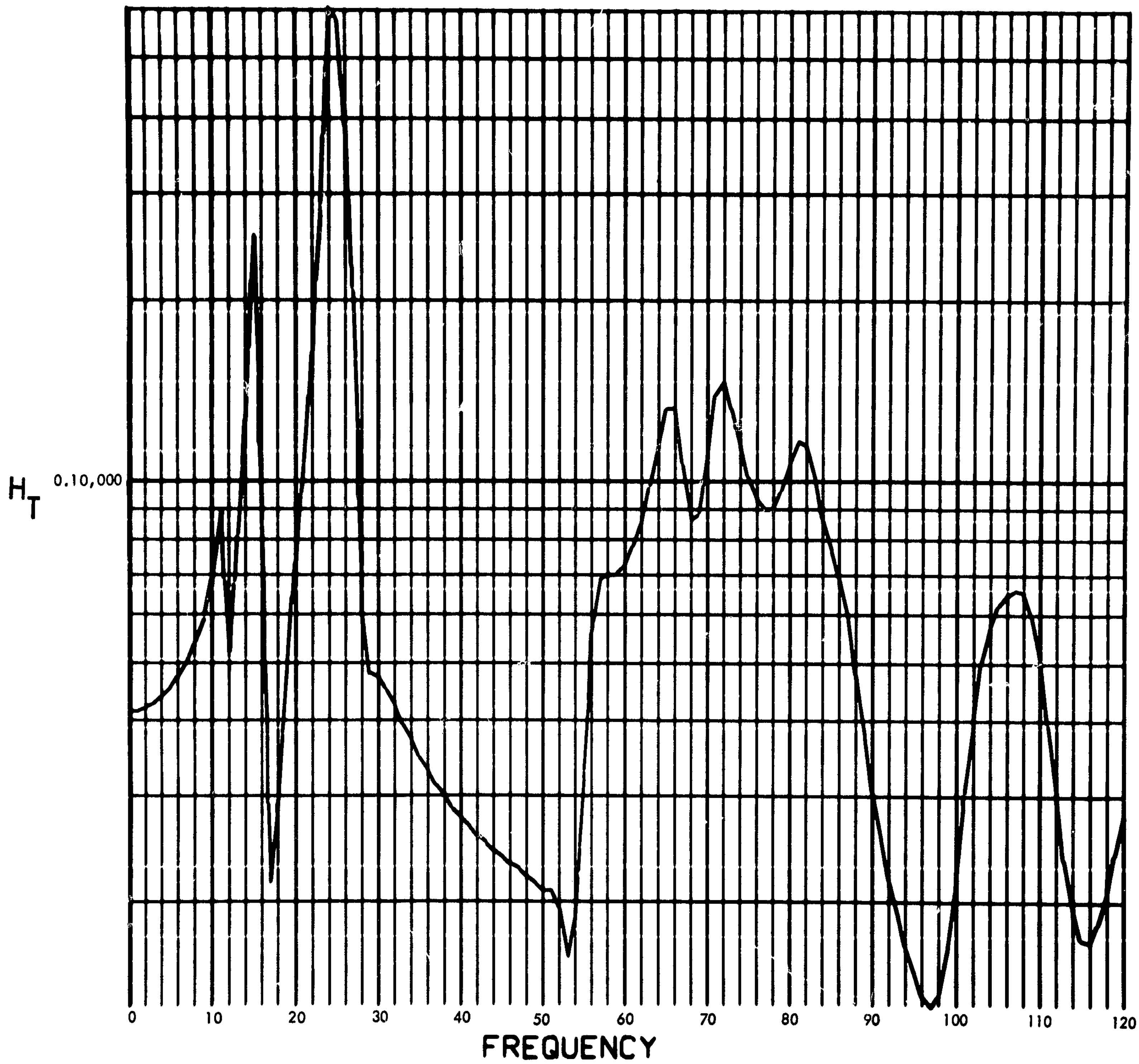

Fig. C-167. Joint 14, torque transfer function, Fourier transform, modulus

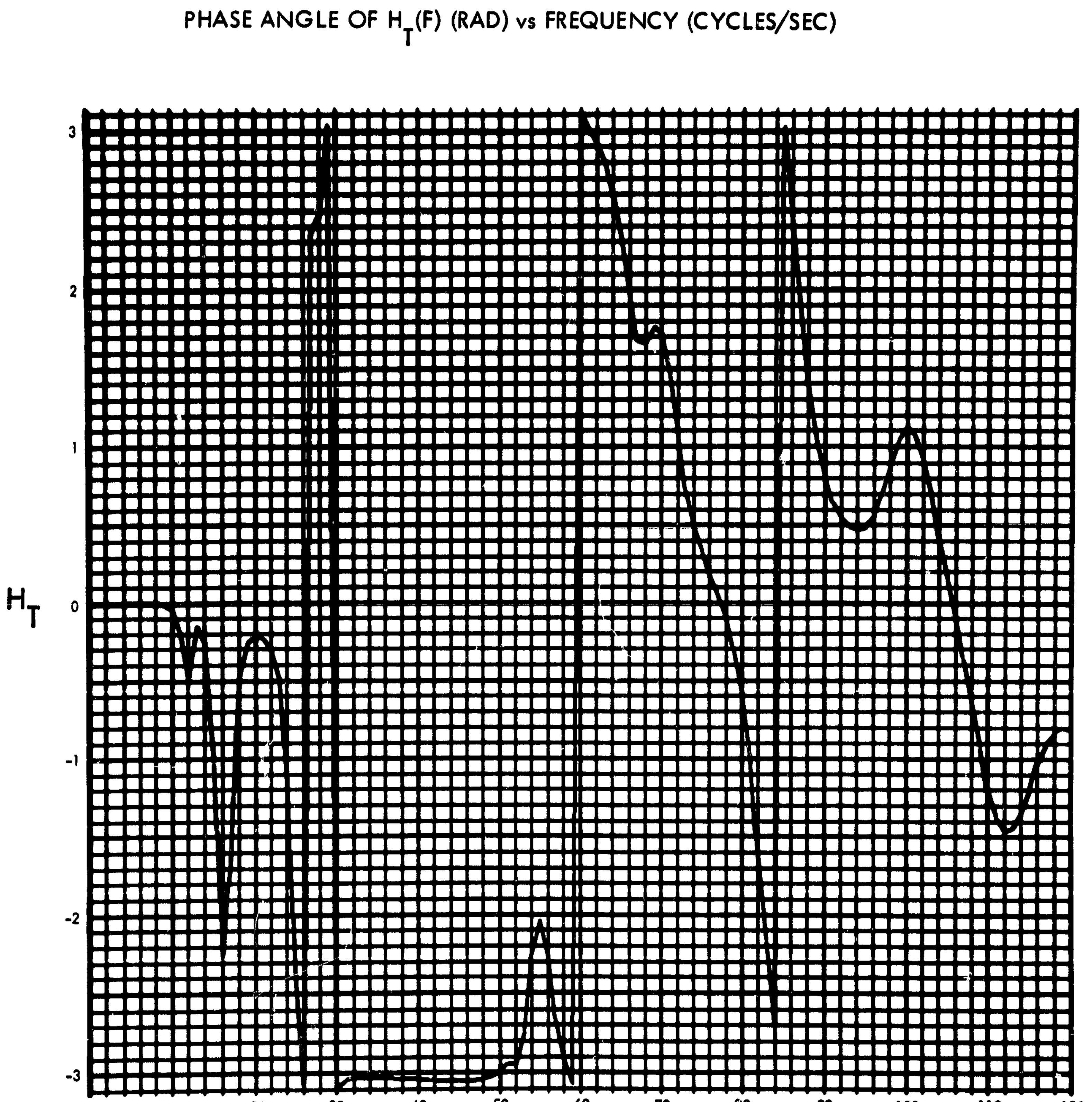

Fig. C-168. Joint 14, torque transfer function, Fourier transform, phase angle

MODULUS OF $F_T(F)$ (LB-IN-SEC) vs FREQUENCY (CYCLES/SEC)

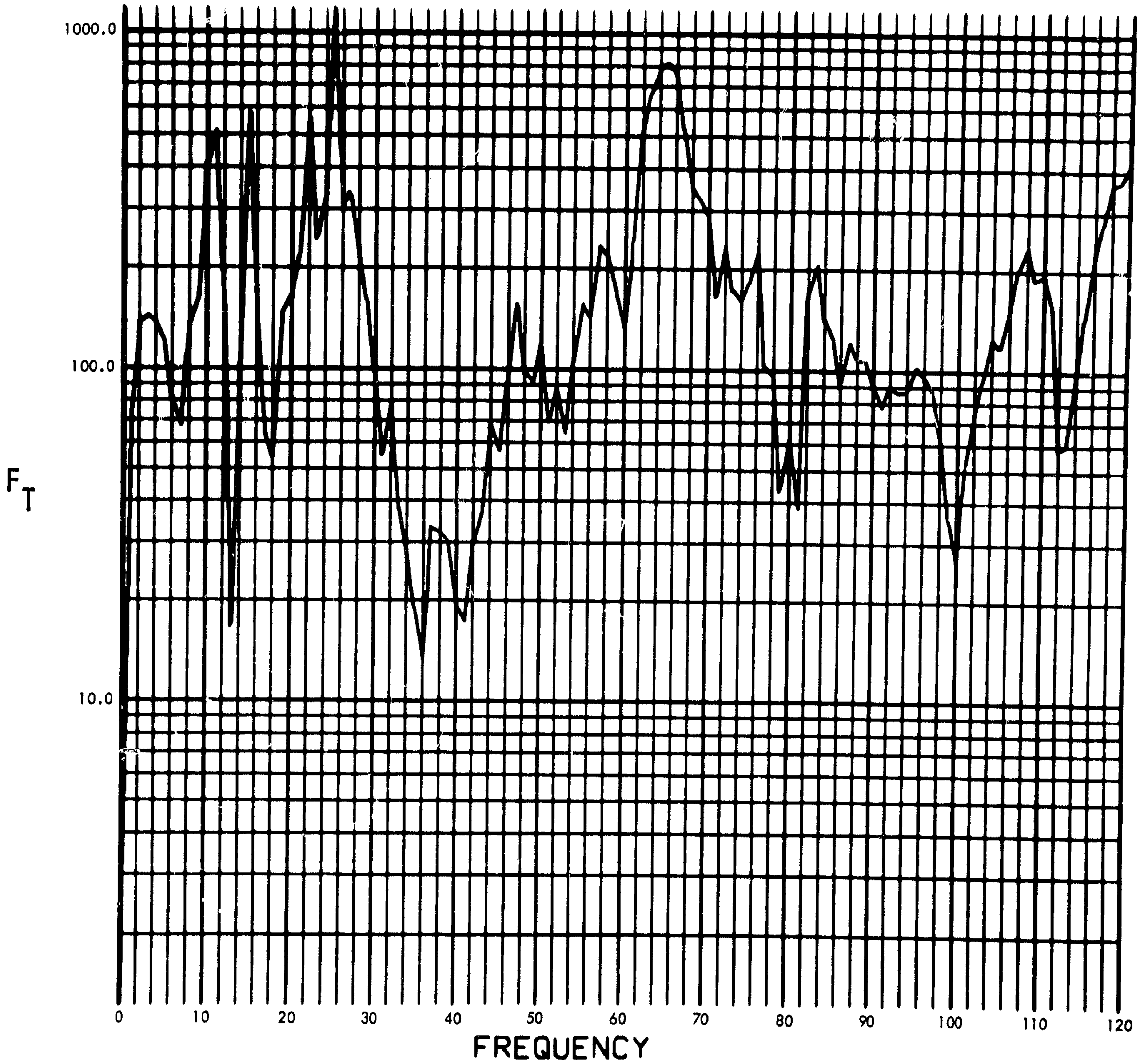

Fig. C-169. Joint 14, torque response, Fourier transform, modulus (pulse 1)

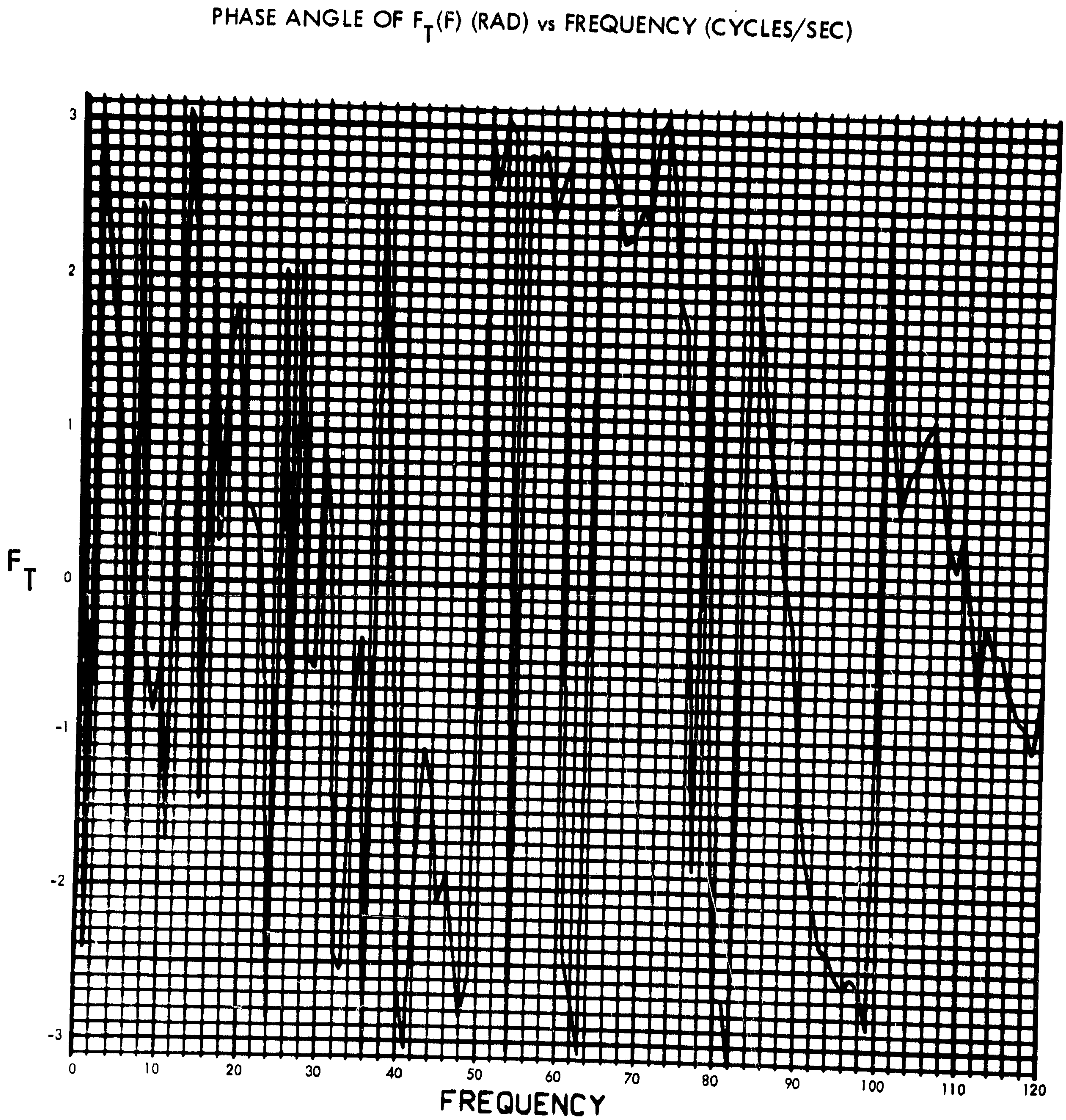

Fig. C-170. Joint 14, torque response, Fourier transform, phase angle (pulse 1)

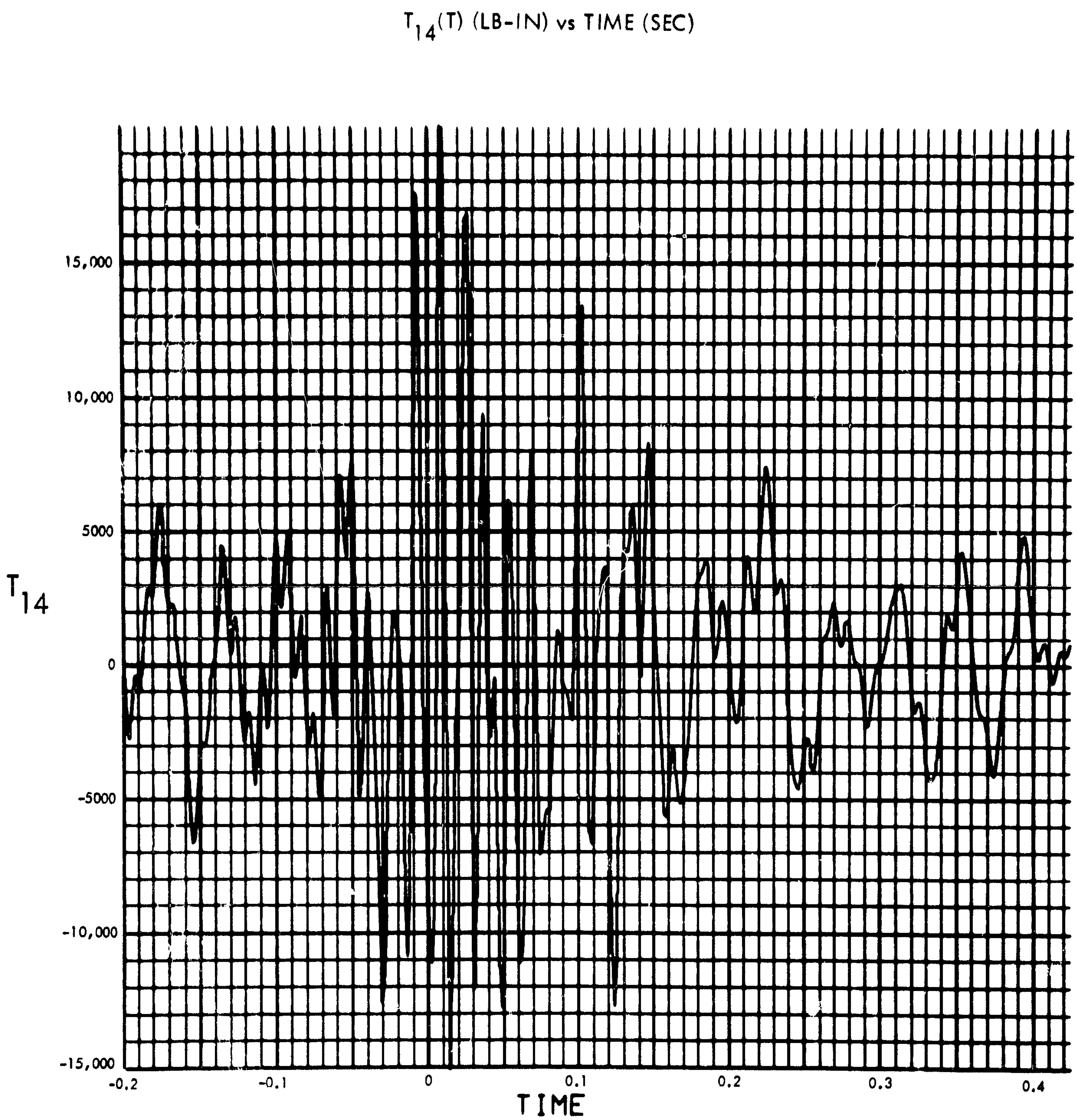

Fig. C-171. Joint 14, torque response, time history (pulse 1)

MODULUS OF $F_T(F)$ (LB-IN-SEC) vs FREQUENCY (CYCLES/SEC)

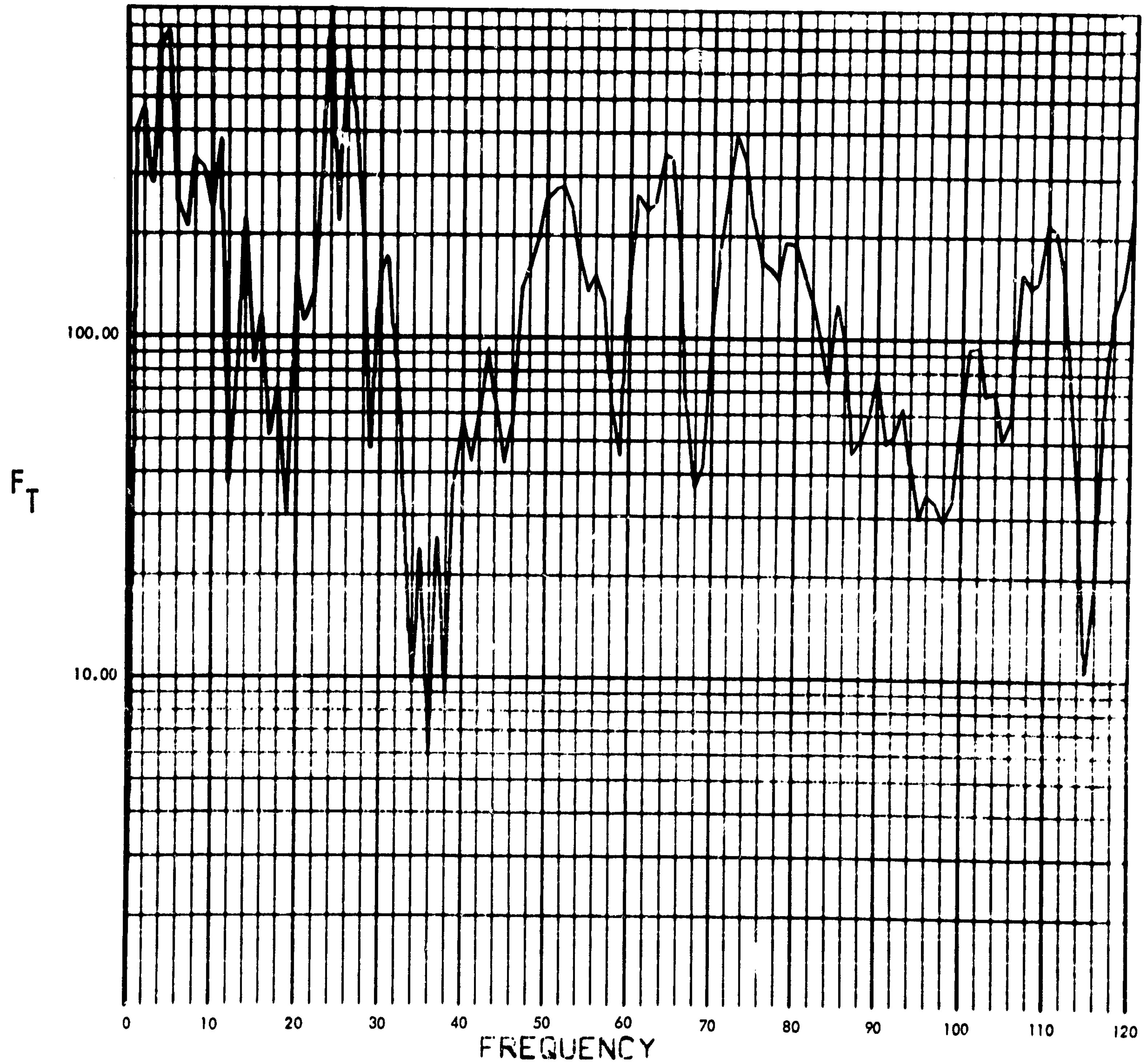

Fig. C-172. Joint 14, torque response, Fourier transform, modulus (pulse 2)

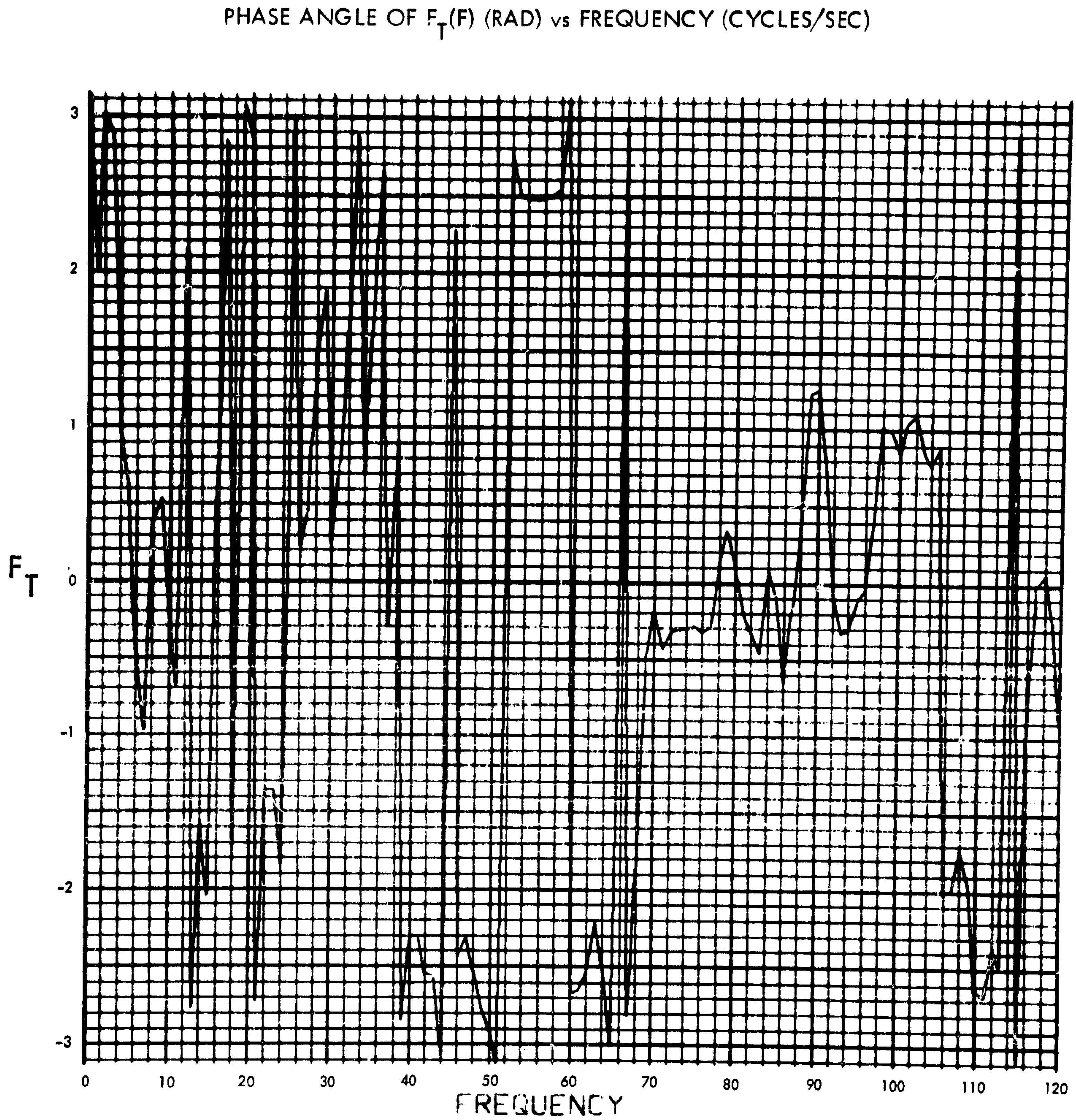

Fig. C-173. Joint 14, torque response, Fourier transform, phase angle (pulse 2)

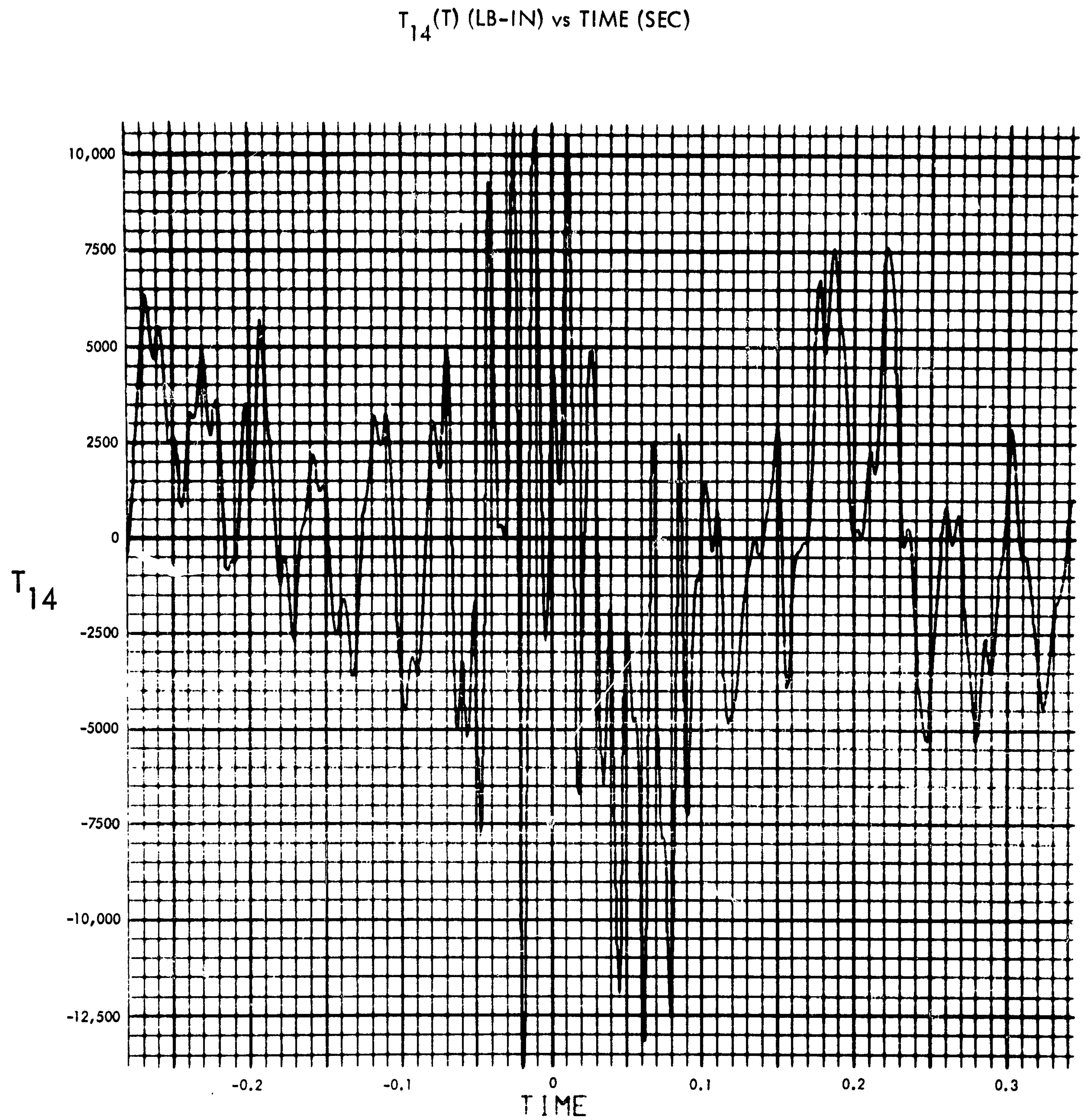

Fig. C-174. Joint 14, torque response, time history (pulse 2)

MODULUS OF $F_T(F)$ (LB-IN-SEC) vs FREQUENCY (CYCLES/SEC)

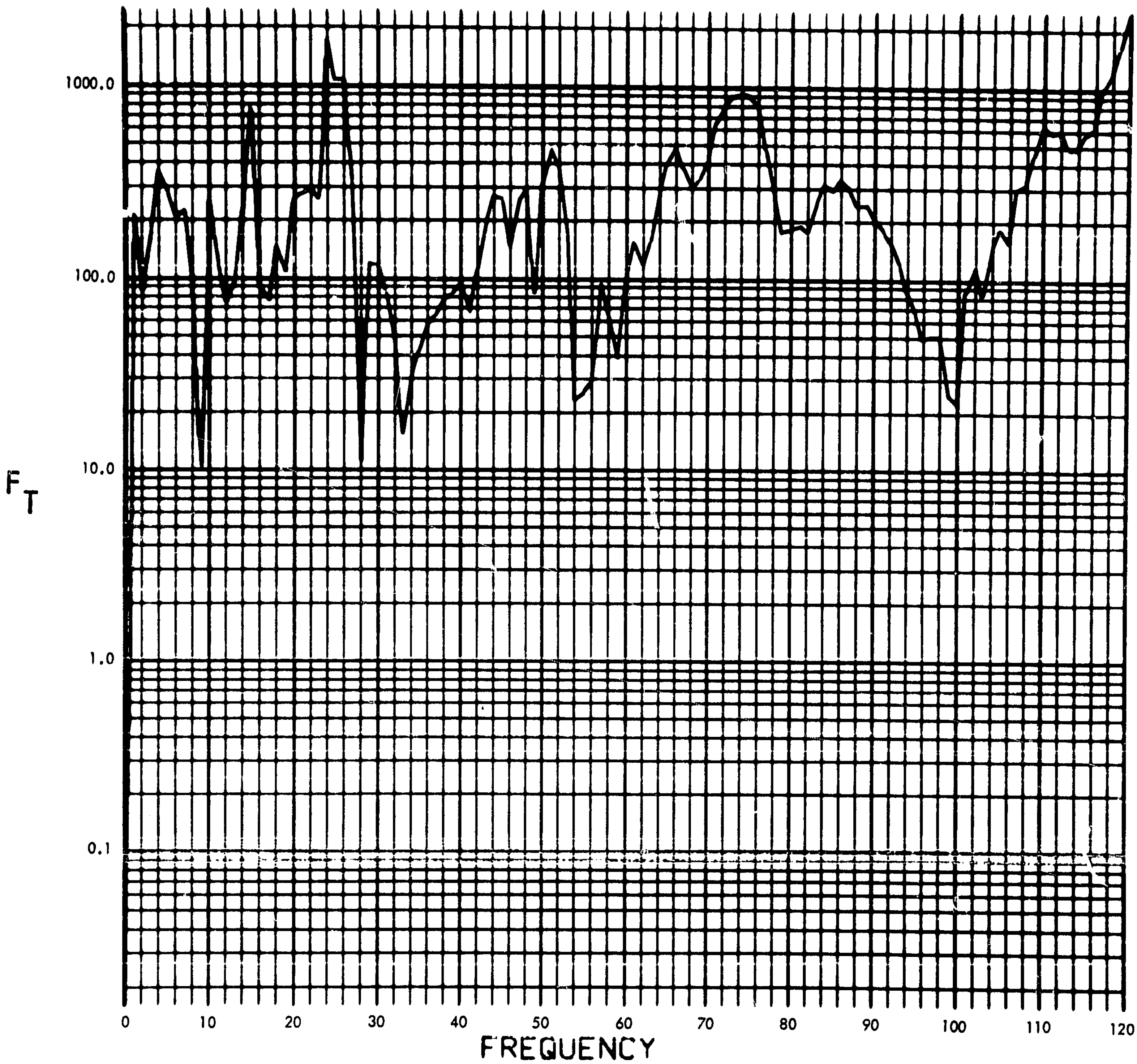

Fig. C-175. Joint 14, torque response, Fourier transform, modulus (pulse 3)

PHASE ANGLE OF $F_T(F)$ (RAD) vs FREQUENCY (CYCLES/SEC)

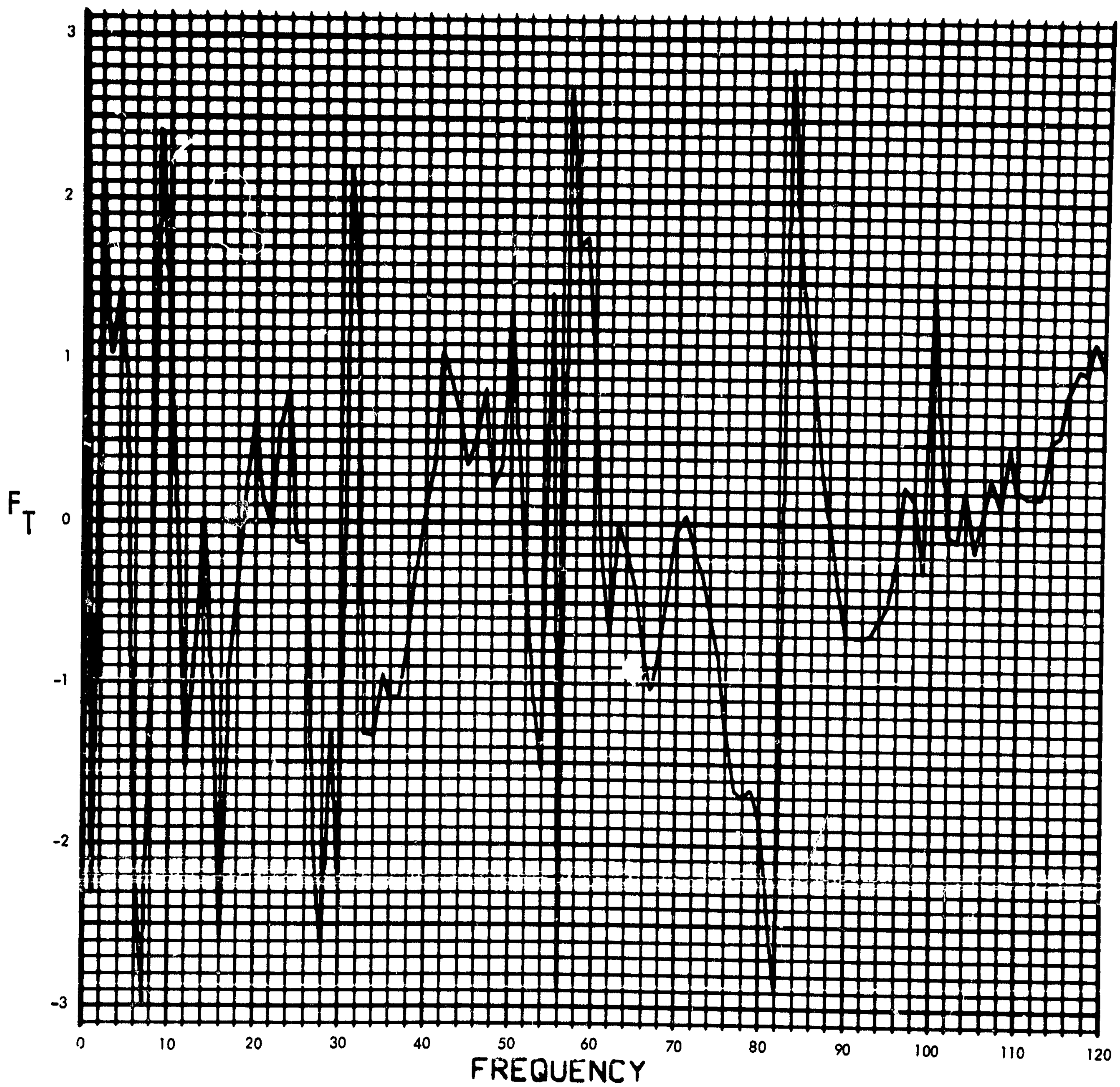

Fig. C-176. Joint 14, torque response, Fourier transform, phase angle (pulse 3)

$T_{14}(T)$ (LB-IN) vs TIME (SEC)

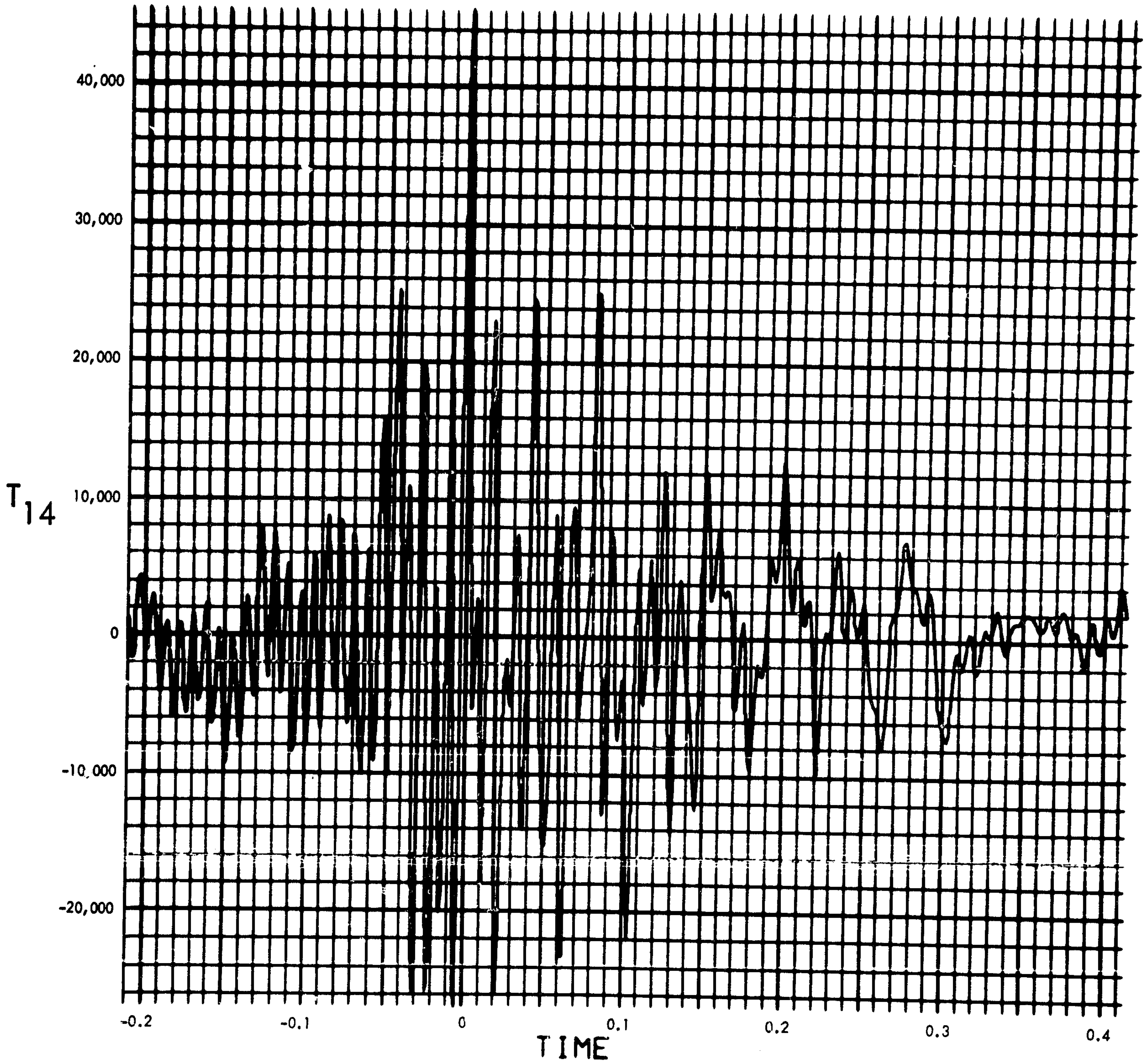

Fig. C-177. Joint 14, torque response, time history (pulse 3)

MODULUS OF $F_T(F)$ (LB-IN-SEC) vs FREQUENCY (CYCLES/SEC)

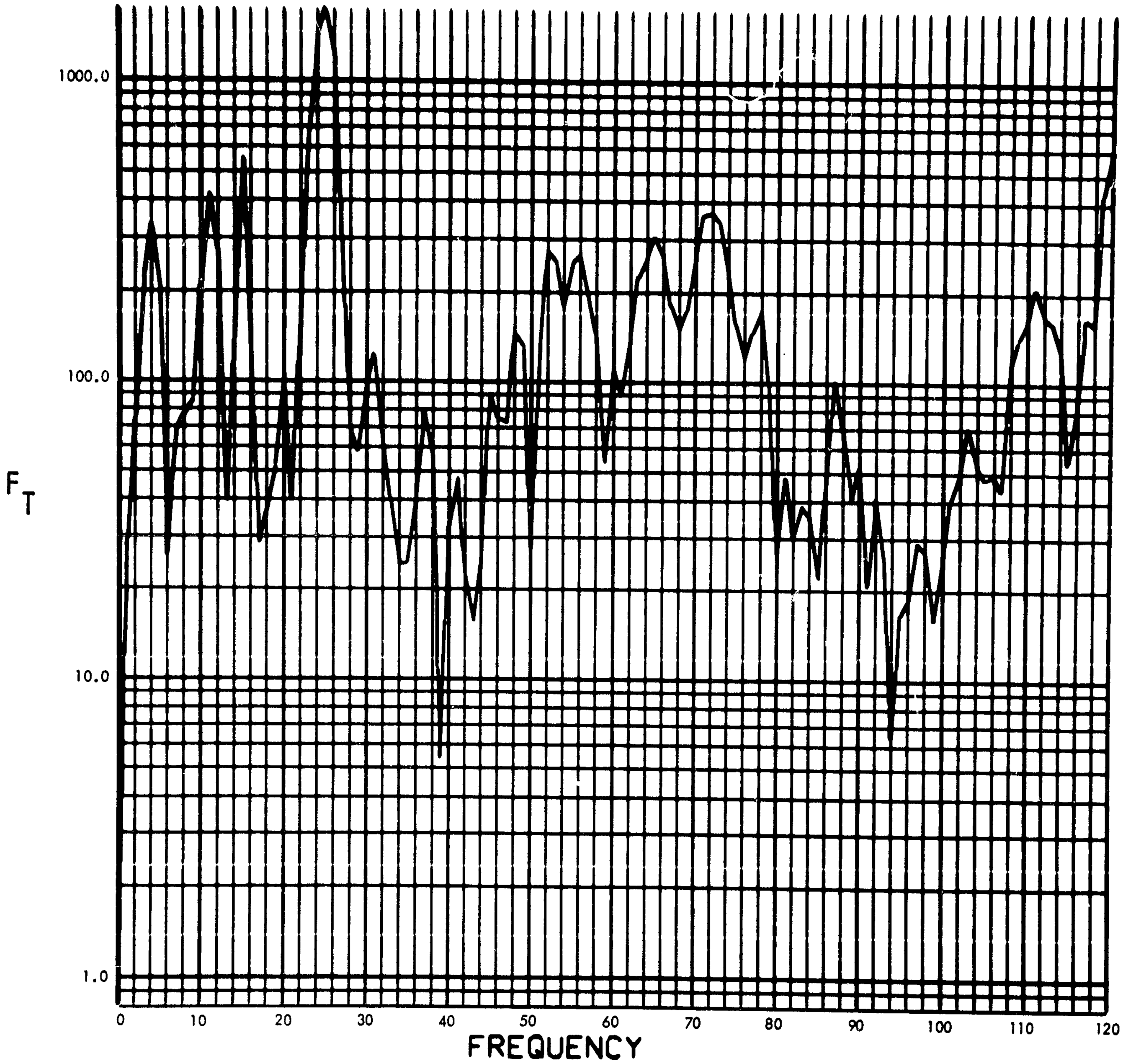

Fig. C-178. Joint 14, torque response, Fourier transform, modulus (pulse 4)

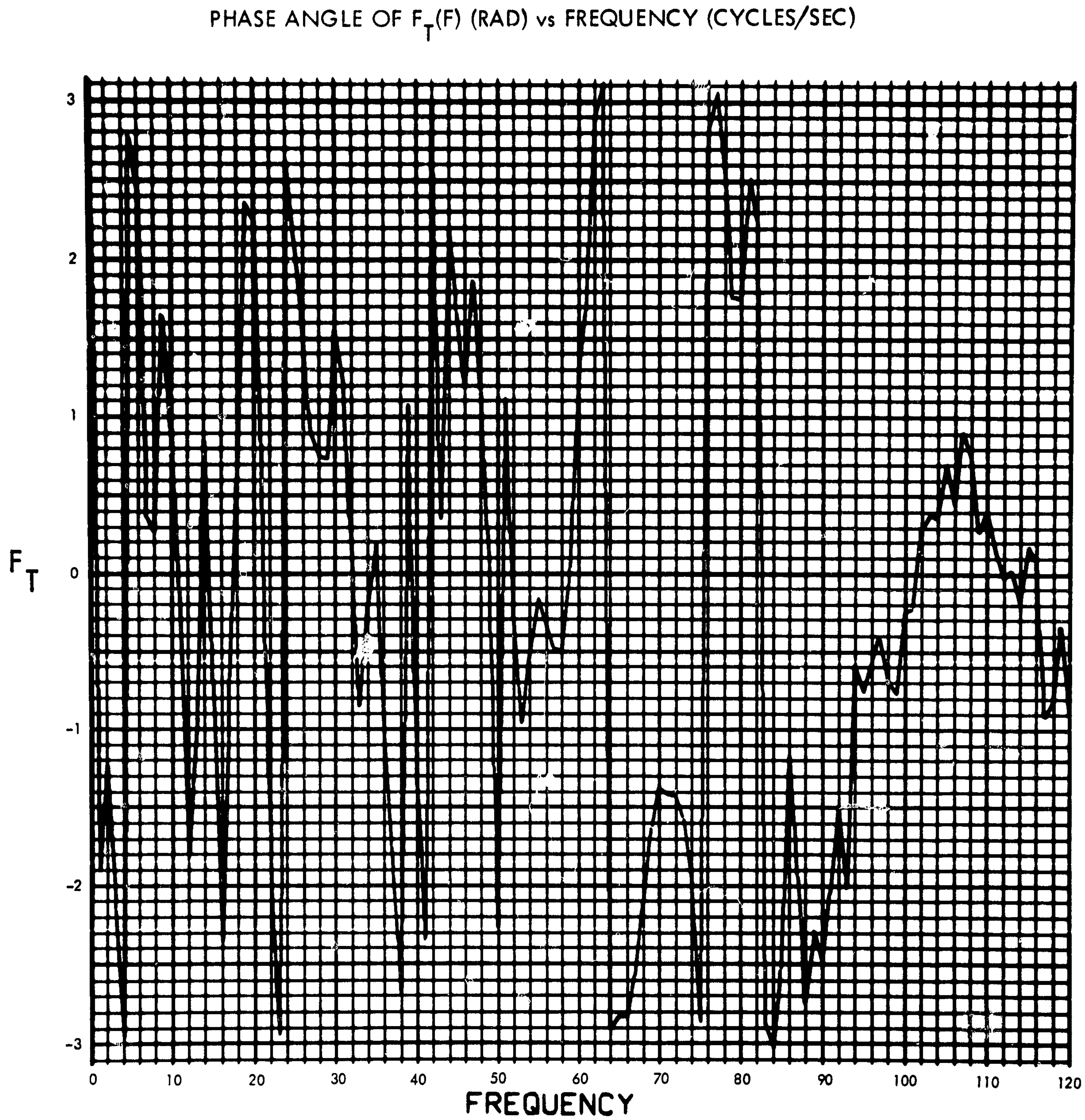

Fig. C-179. Joint 14, torque response, Fourier transform, phase angle (pulse 4)

T_{14}(T) (LB-IN) vs TIME (SEC)

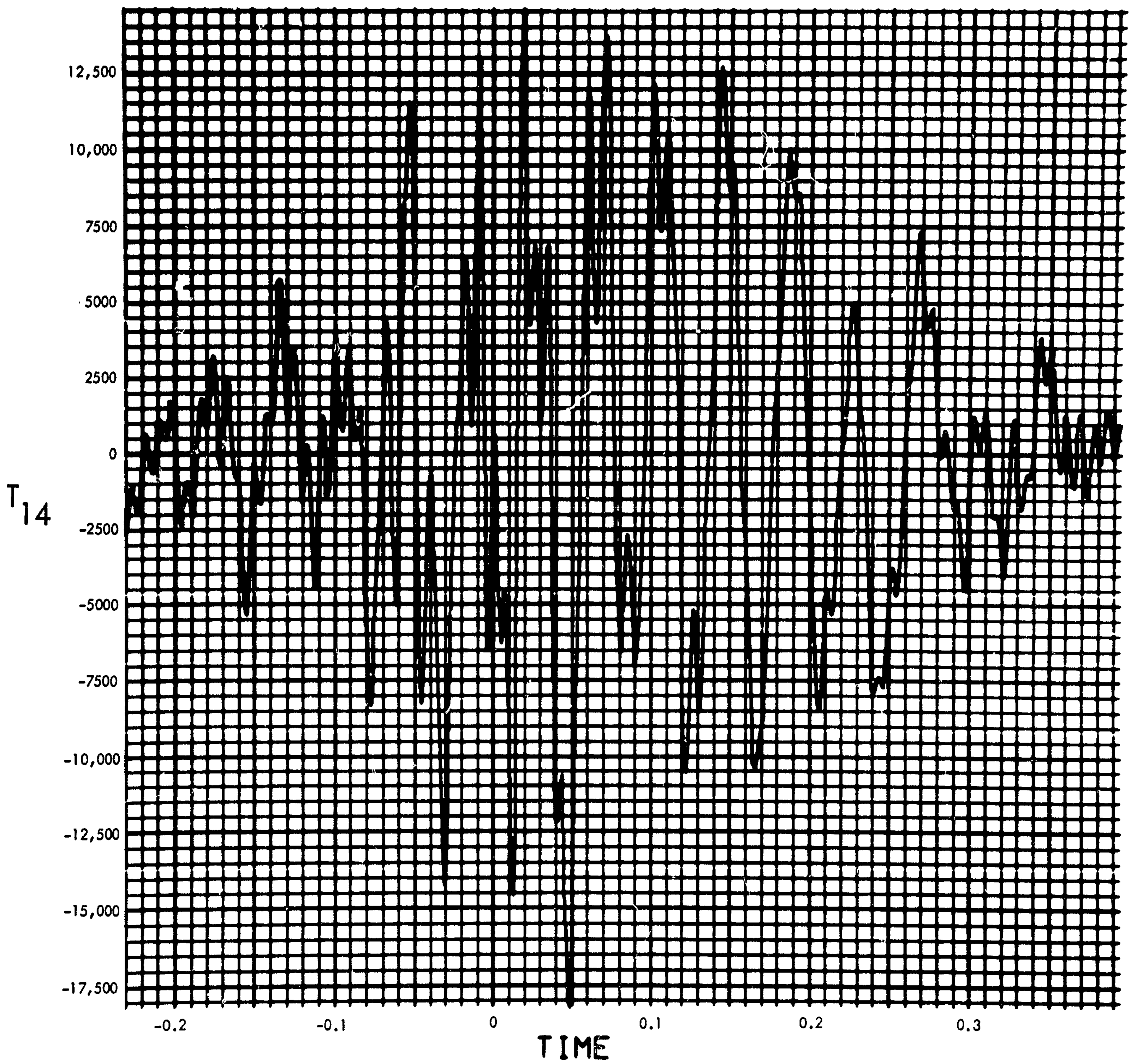

Fig. C-180. Joint 14, torque response, time history (pulse 4)

MODULUS H2(F) (1/LB-IN-SEC^2) vs FREQUENCY (CYCLES/SEC)

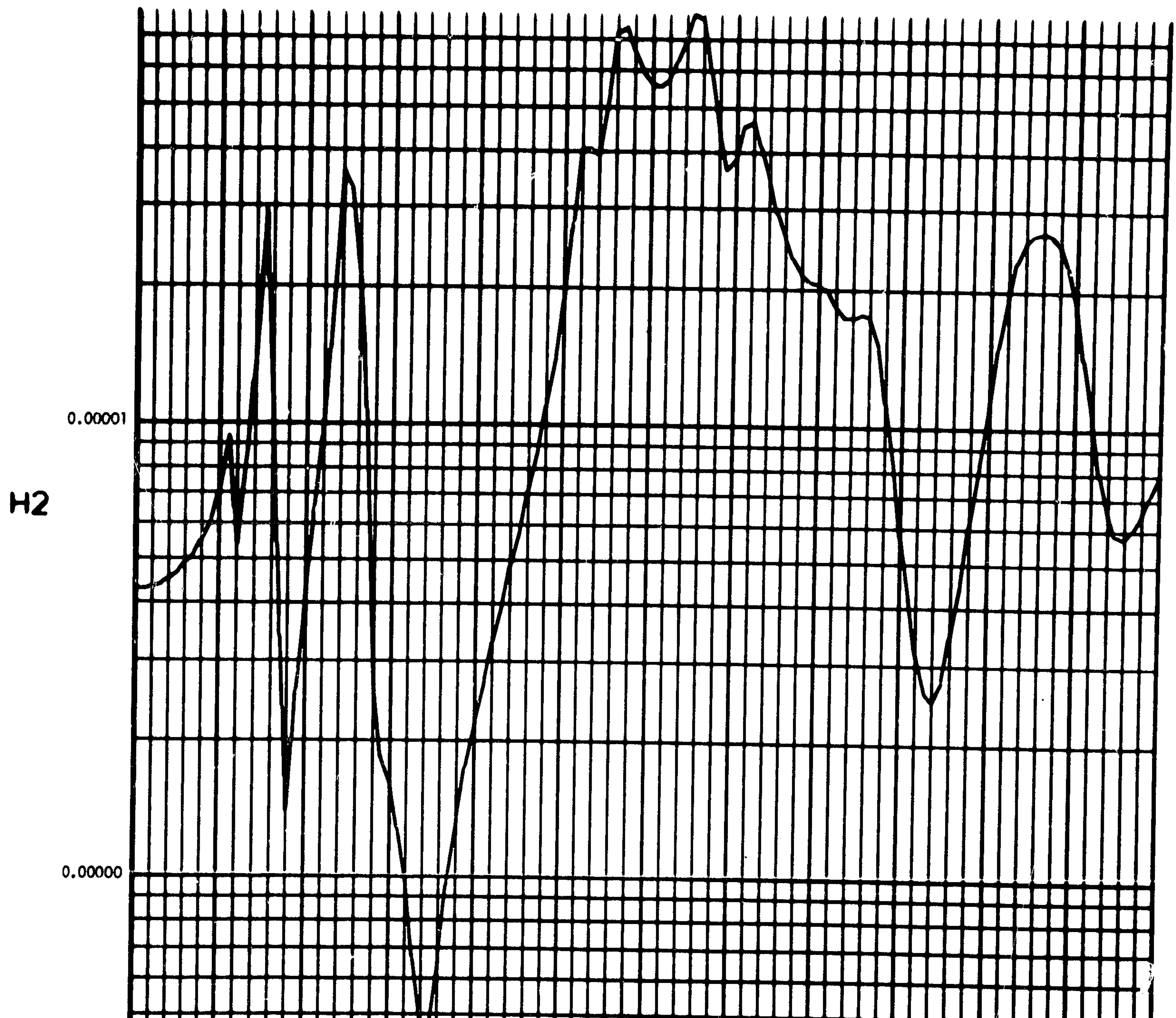

Fig. C-181. Joint 15, acceleration transfer function, Fourier transform, modulus

PHASE ANGLE OF H2(F) (RAD) vs FREQUENCY (CYCLES/SEC)

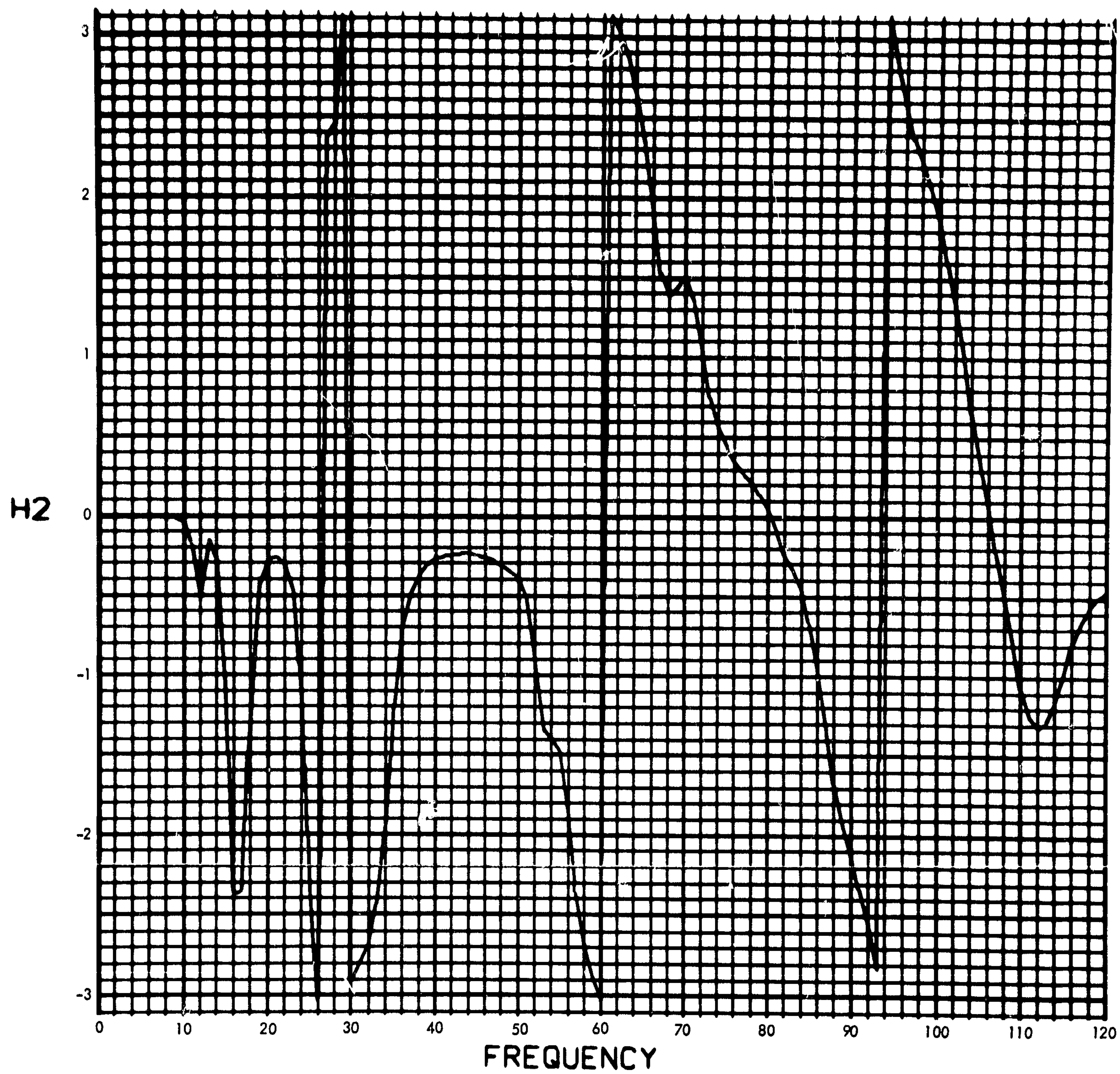

Fig. C-182. Joint 15, acceleration transfer function, Fourier transform, phase angle

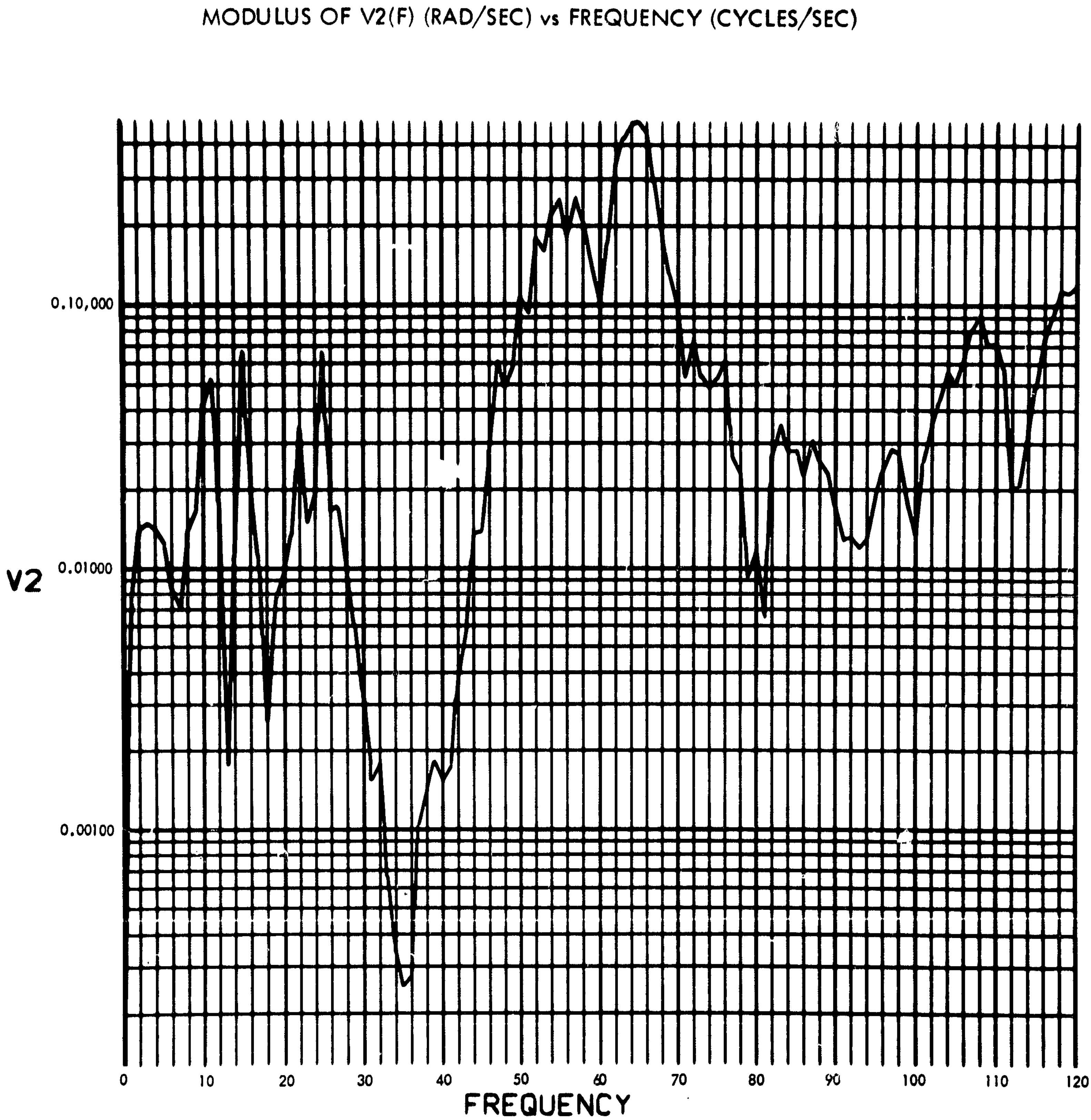

Fig. C-183. Joint 15, acceleration response, Fourier transform, modulus (pulse 1)

PHASE ANGLE OF V2(F) (RAD) vs FREQUENCY (CYCLES/SEC)

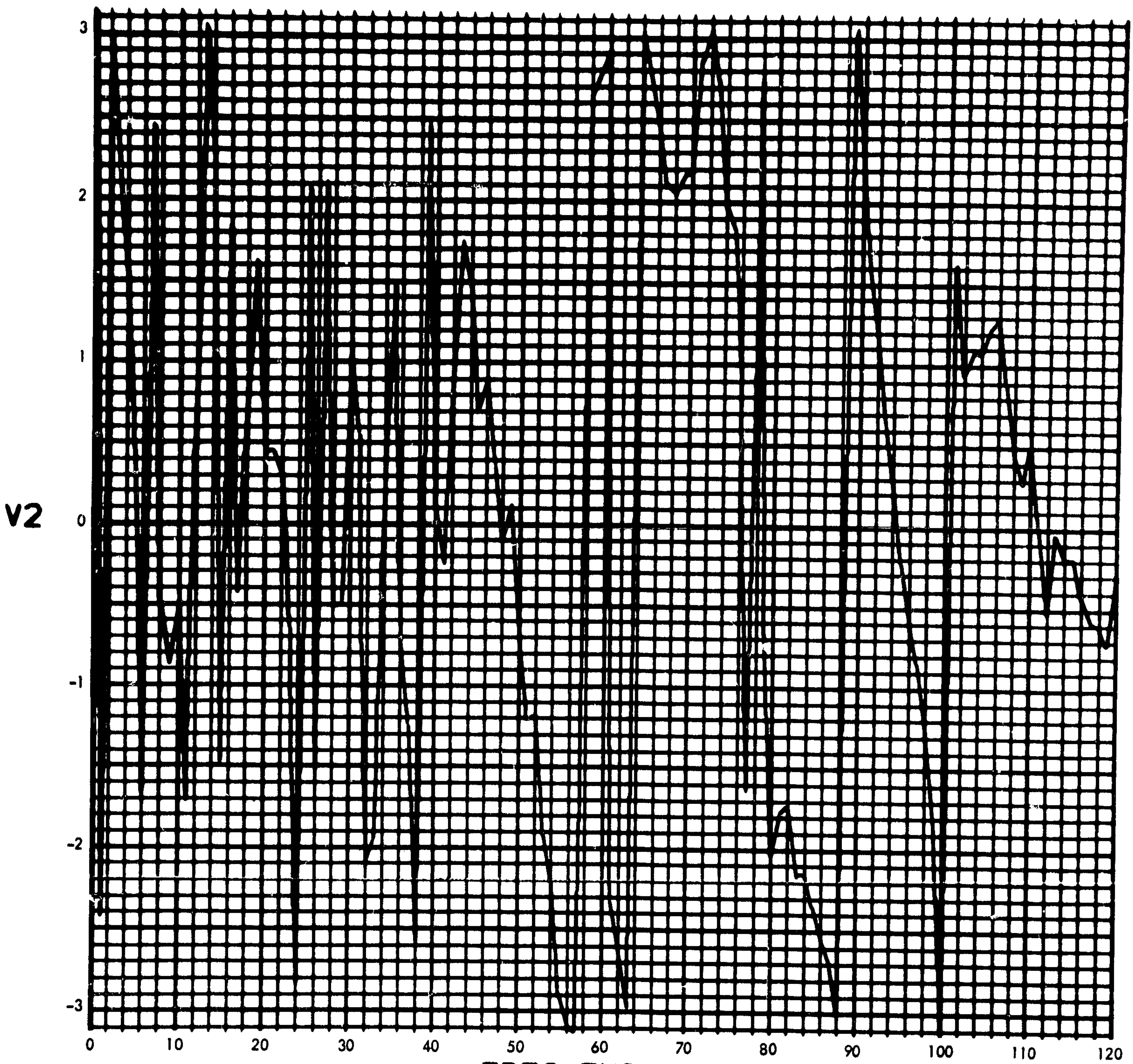

Fig. C-184. Joint 15, acceleration response, Fourier transform, phase angle (pulse 1)

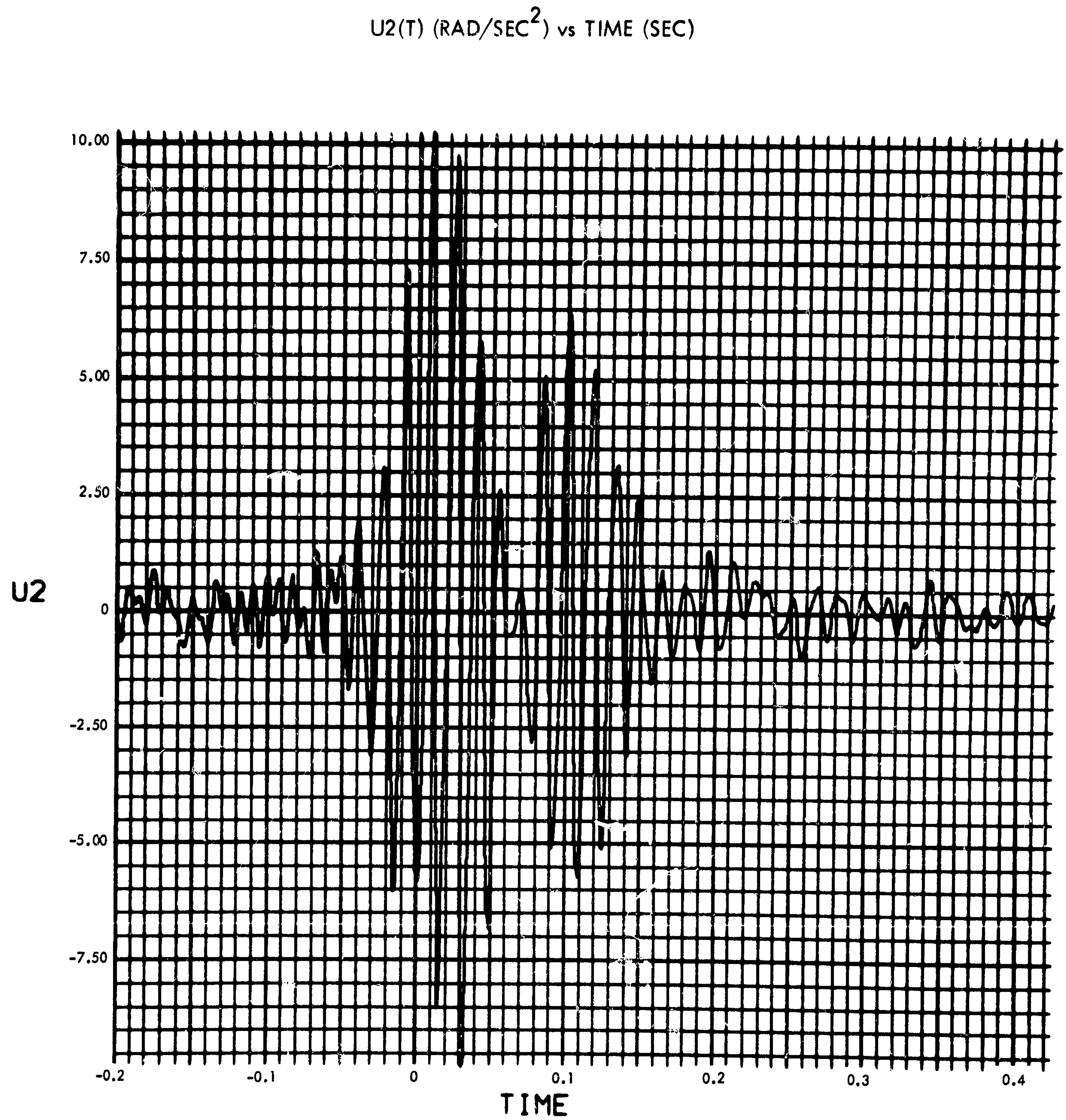

Fig. C-185. Joint 15, acceleration response, time history (pulse 1)

MODULUS OF V2(F) (RAD/SEC) vs FREQUENCY (CYCLES/SEC)

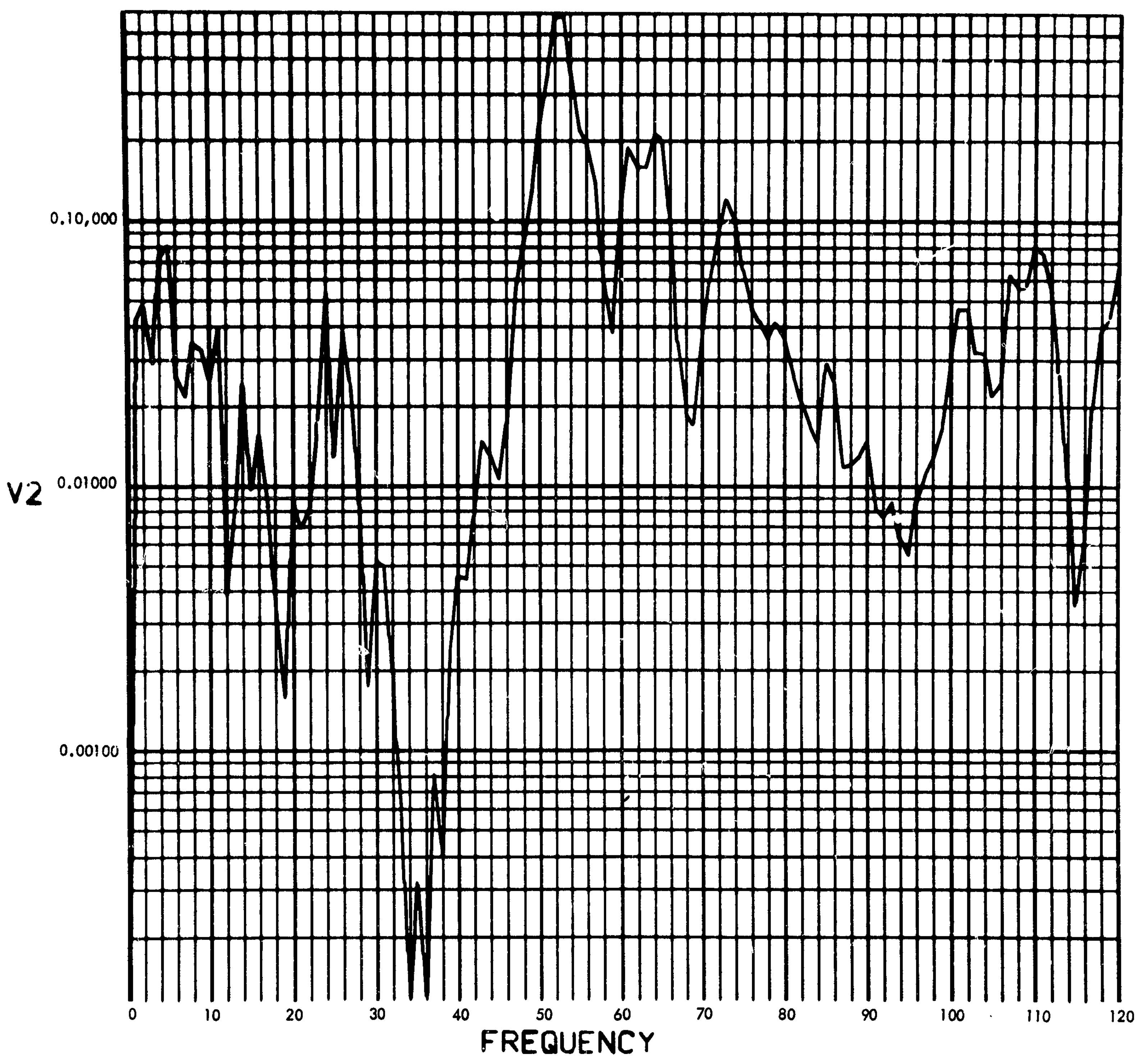

Fig. C-186. Joint 15, acceleration response, Fourier transform, modulus (pulse 2)

PHASE ANGLE OF V2(F) (RAD) vs FREQUENCY (CYCLES/SEC)

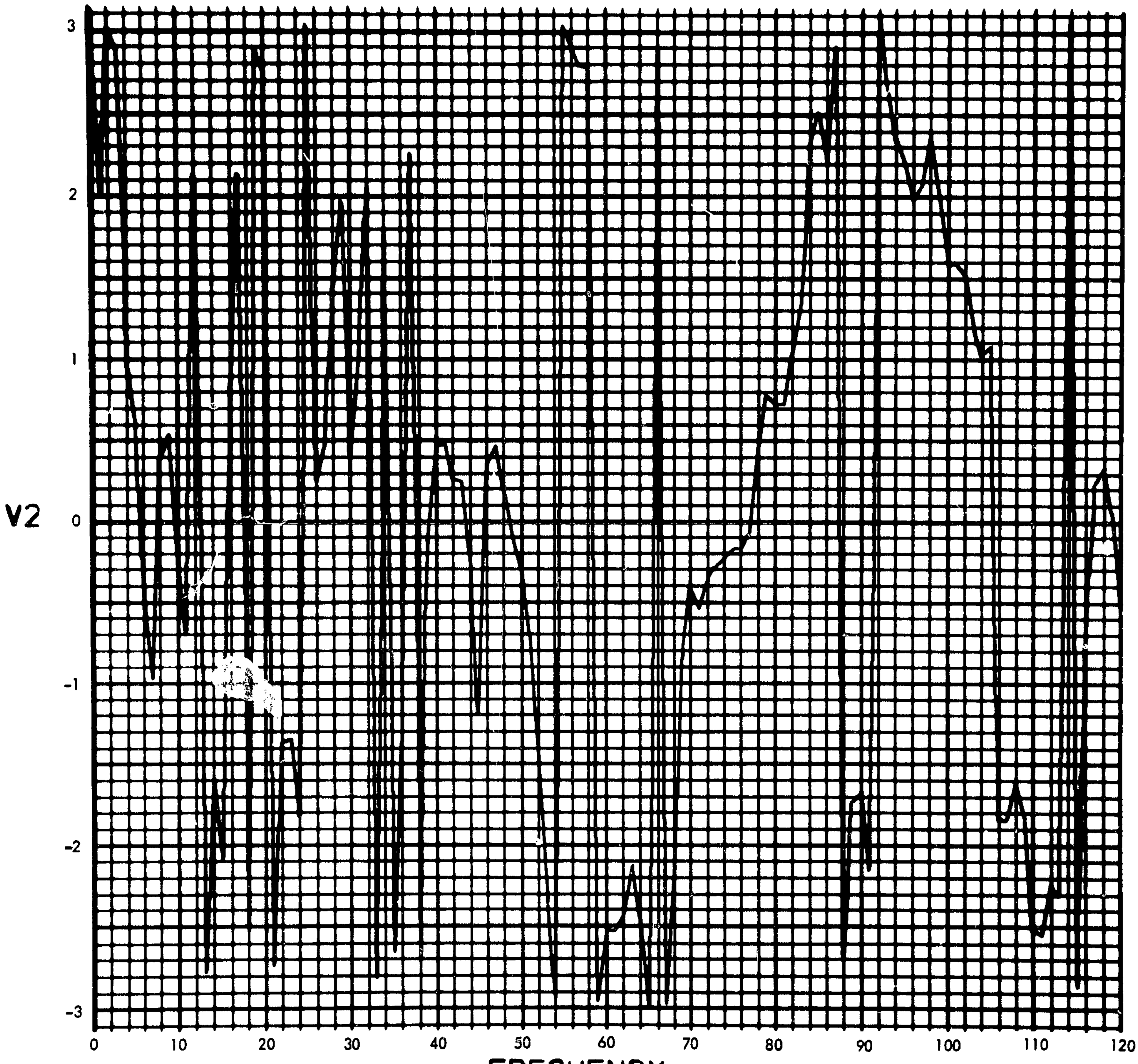

Fig. C-187. Joint 15, acceleration response, Fourier transform, phase angle (pulse 2)

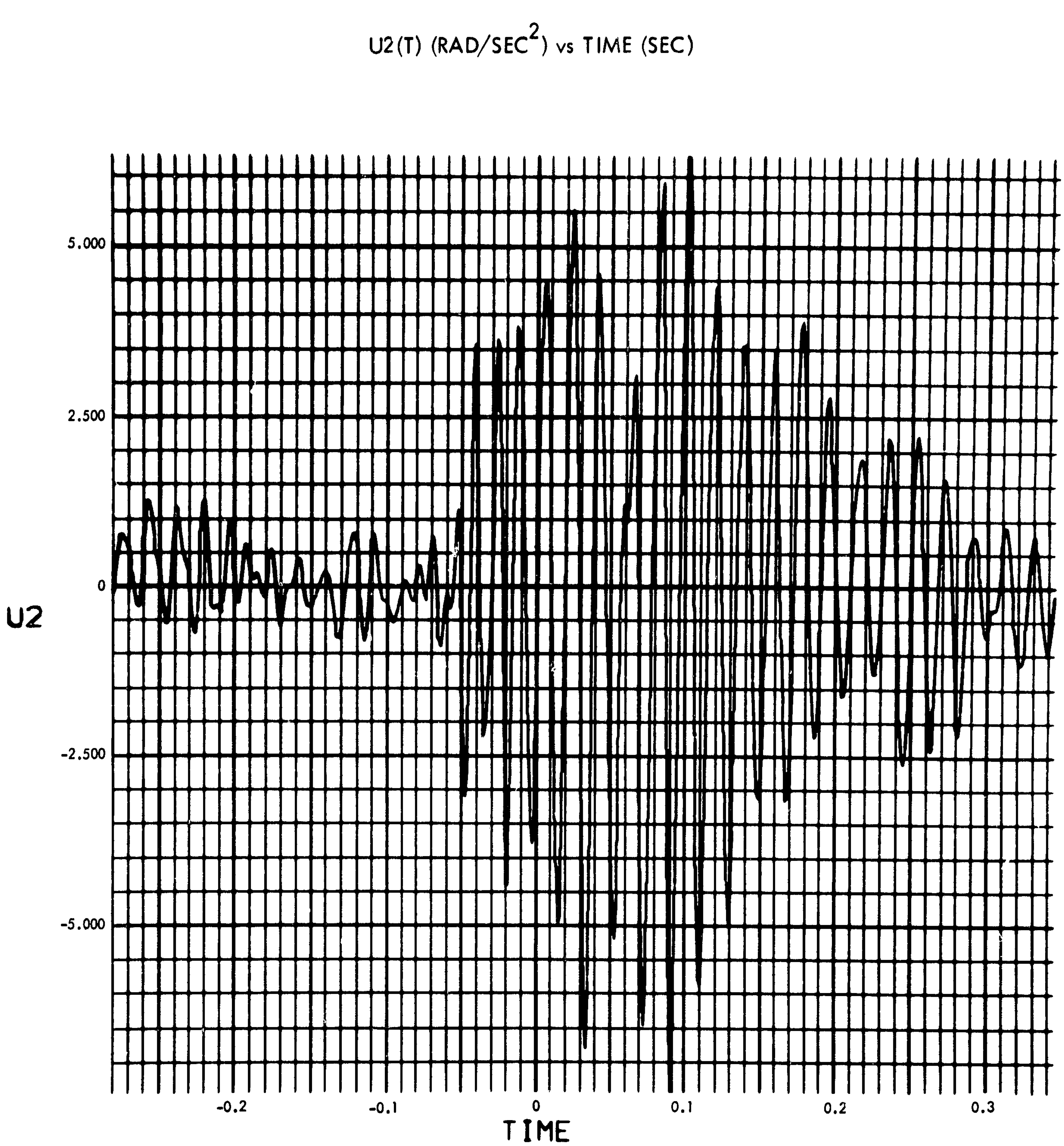

Fig. C-188. Joint 15, acceleration response, time history (pulse 2)

MODULUS OF V2(F) (RAD/SEC) vs FREQUENCY (CYCLES/SEC)

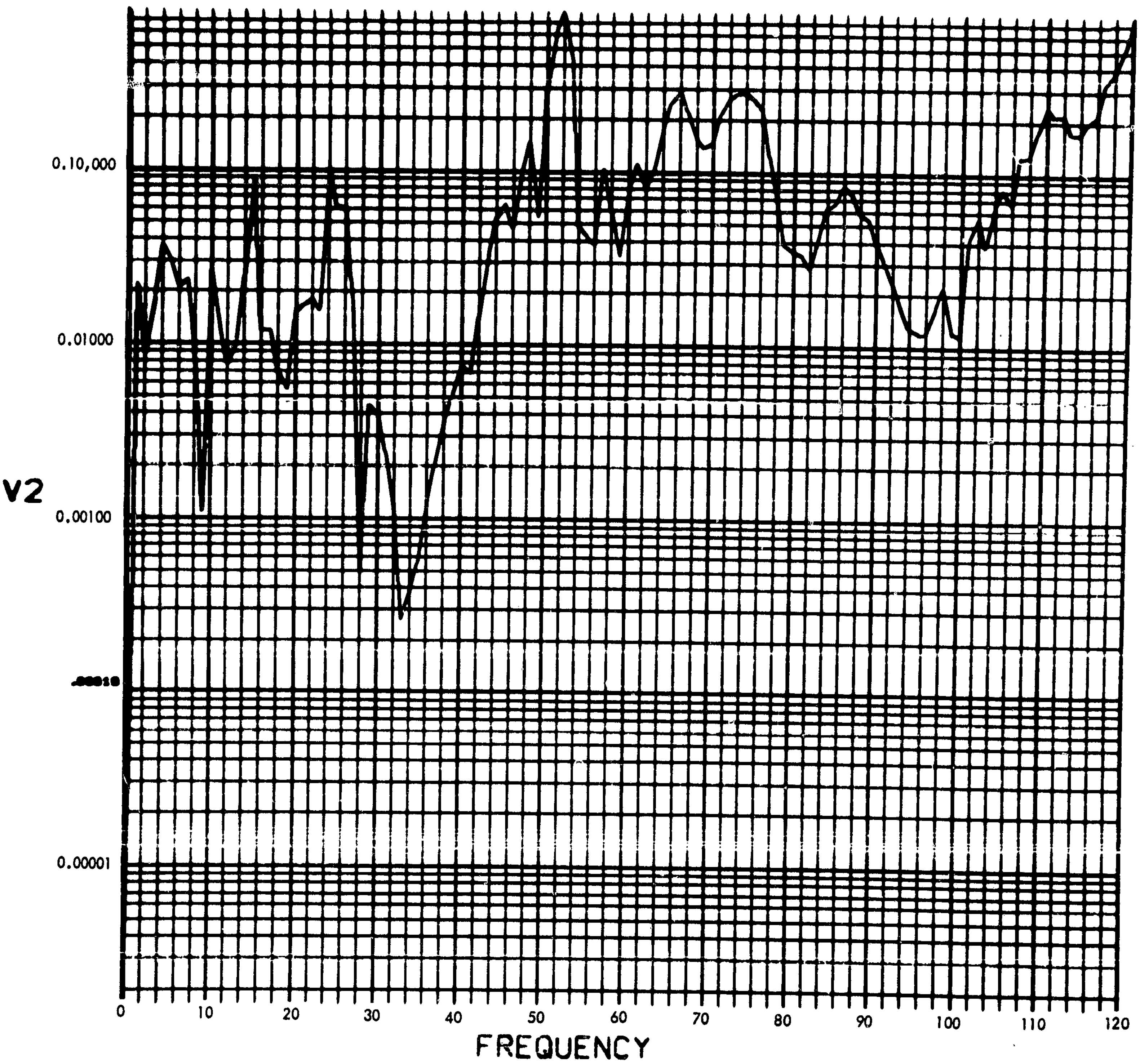

Fig. C-189. Joint 15, acceleration response, Fourier transform, modulus (pulse 3)

PHASE ANGLE OF V2(F) (RAD) vs FREQUENCY (CYCLES/SEC)

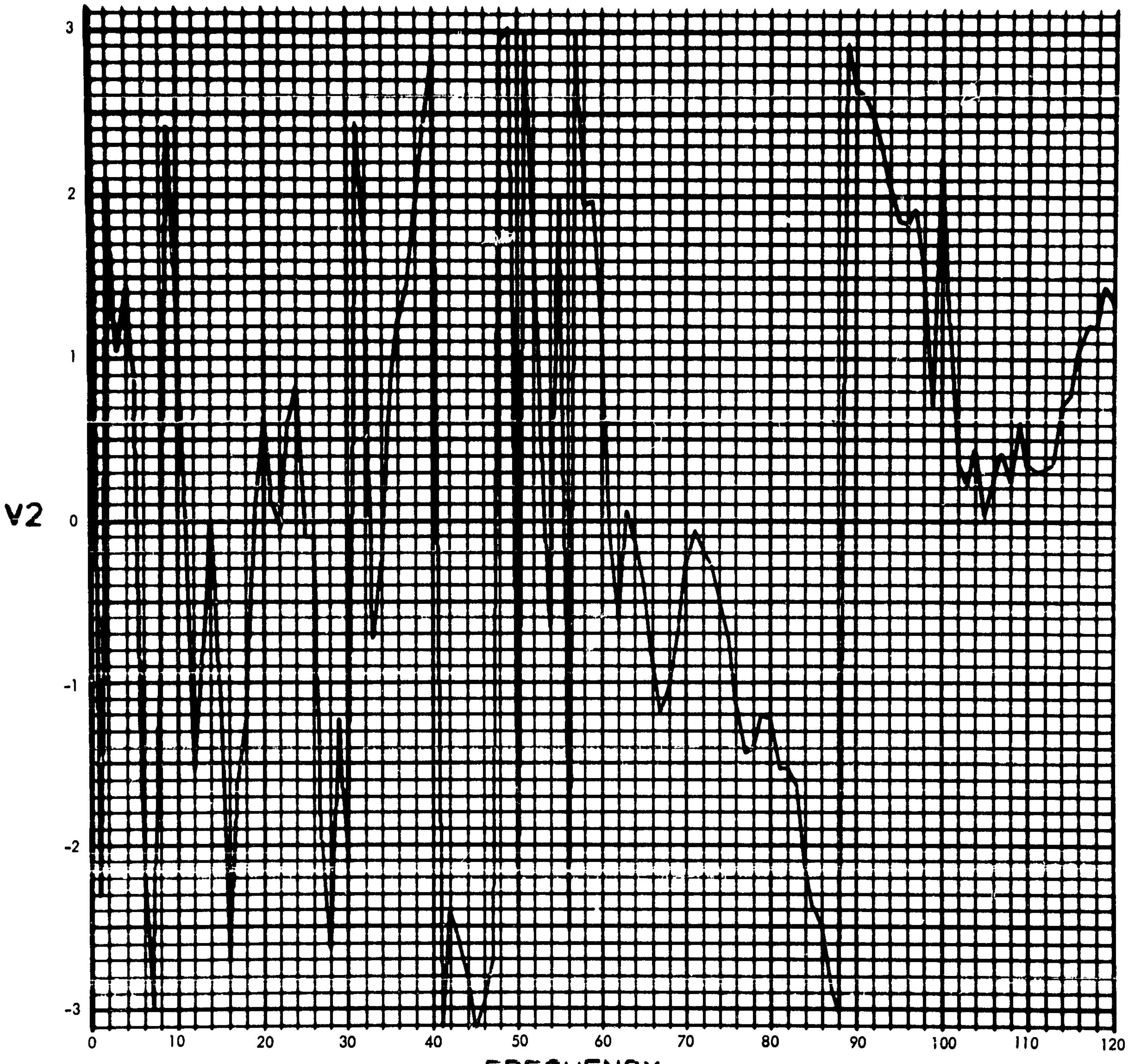

Fig. C-190. Joint 15, acceleration response, Fourier transform, phase angle (pulse 3)

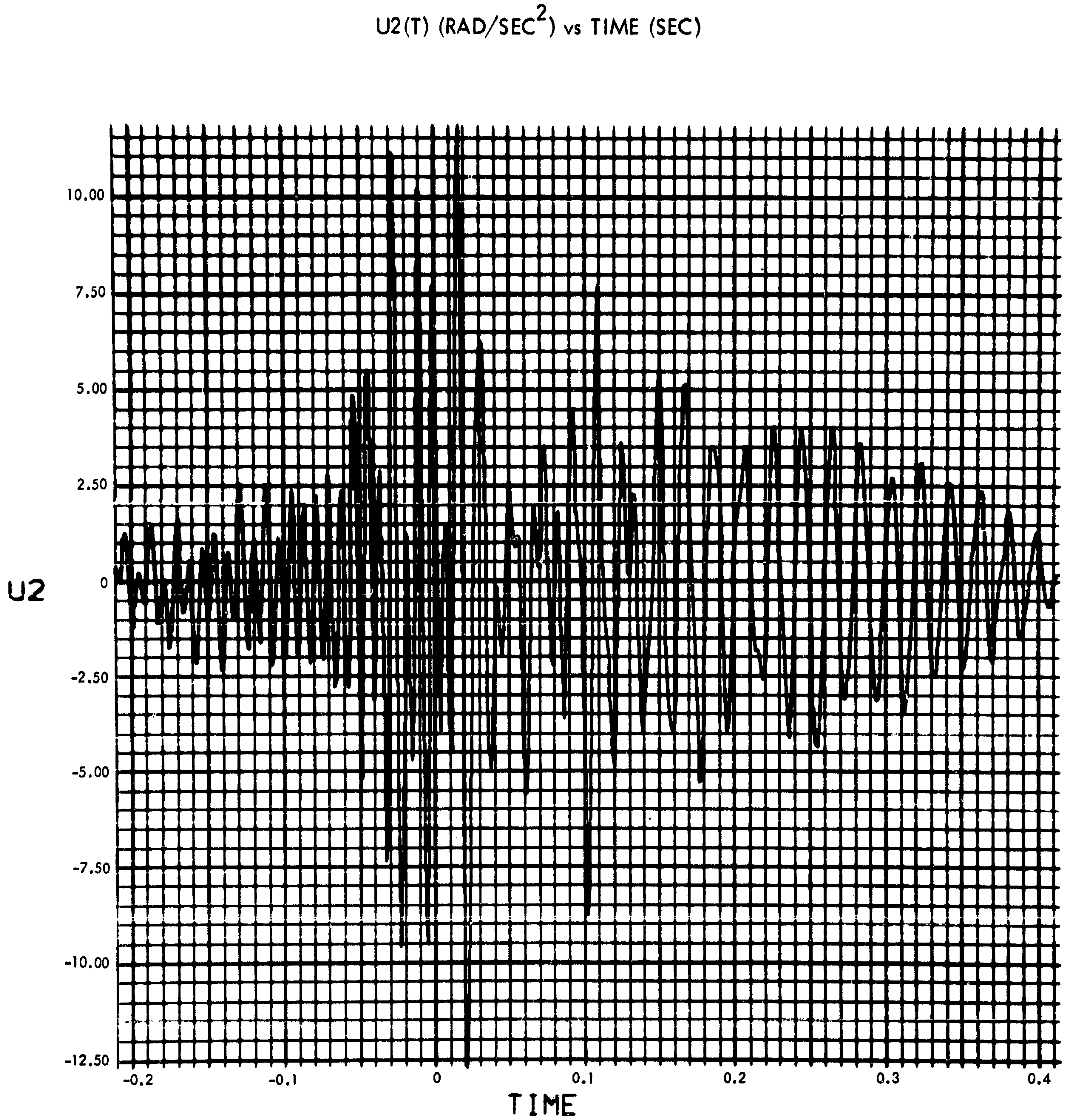

Fig. C-191. Joint 15, acceleration response, time history (pulse 3)

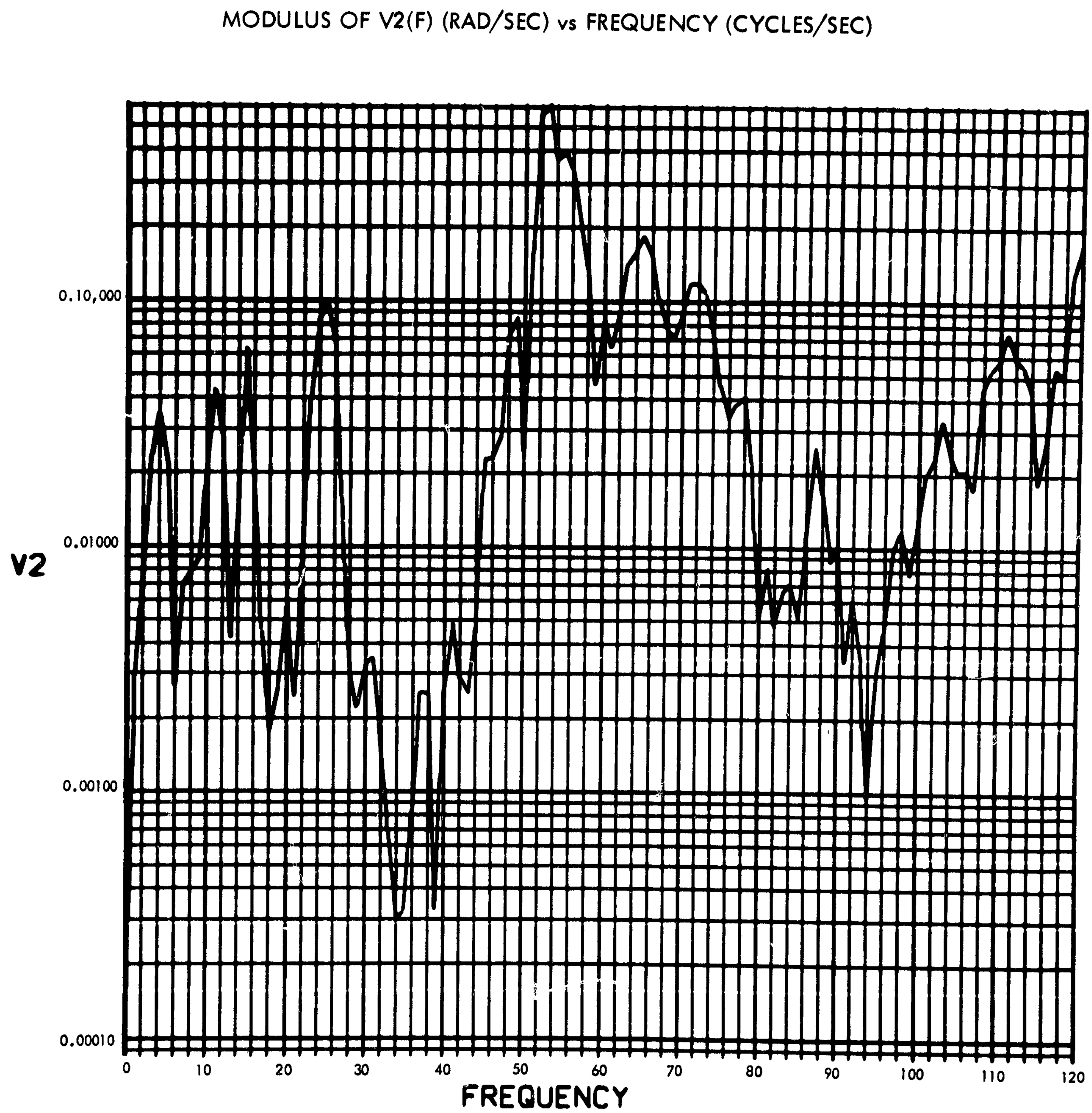

Fig. C-192. Joint 15, acceleration response, Fourier transform, modulus (pulse 4)

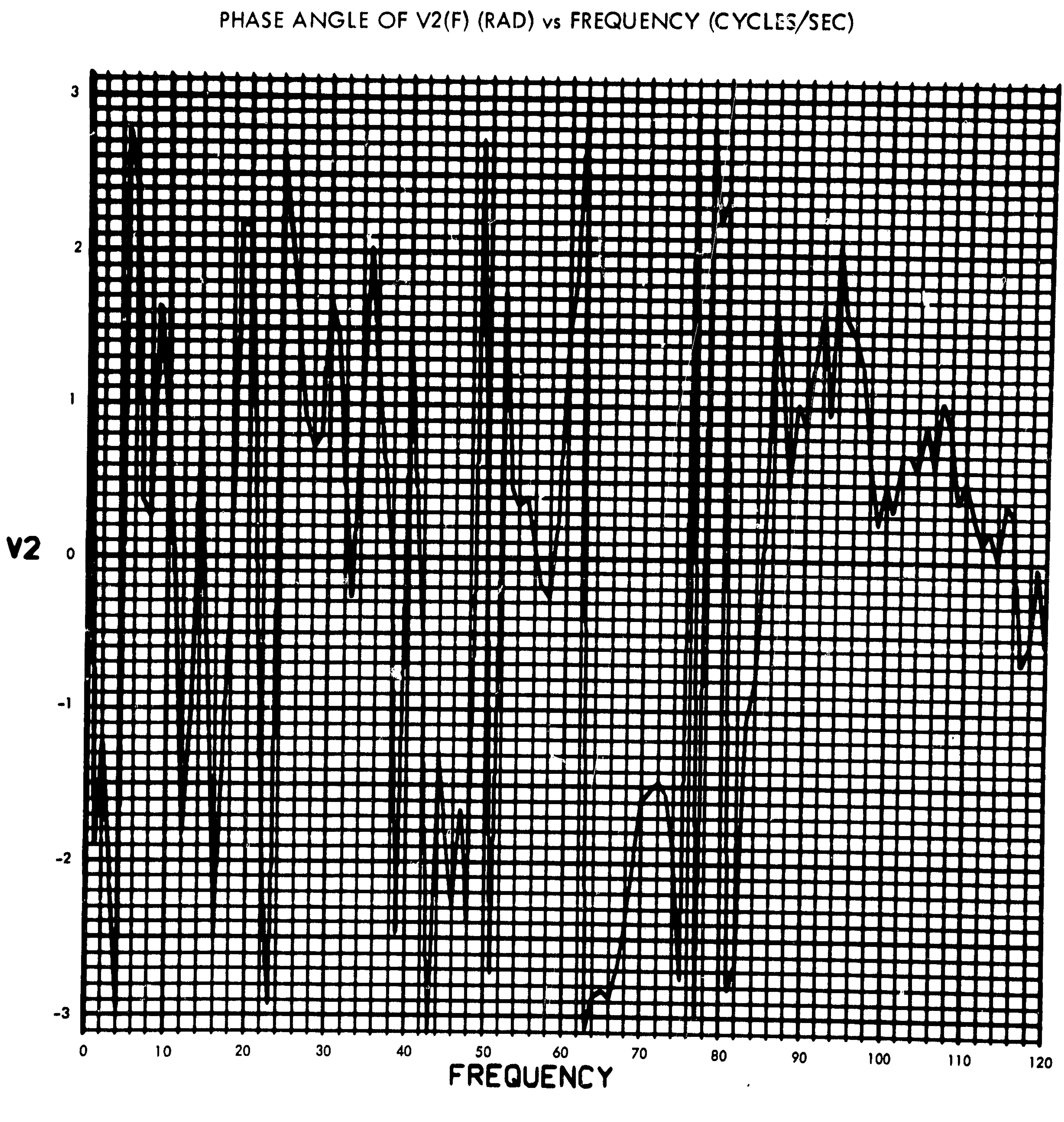

Fig. C-193. Joint 15, acceleration response, Fourier transform, phase angle (pulse 4)

U2(T) (RAD/SEC^2) vs TIME (SEC)

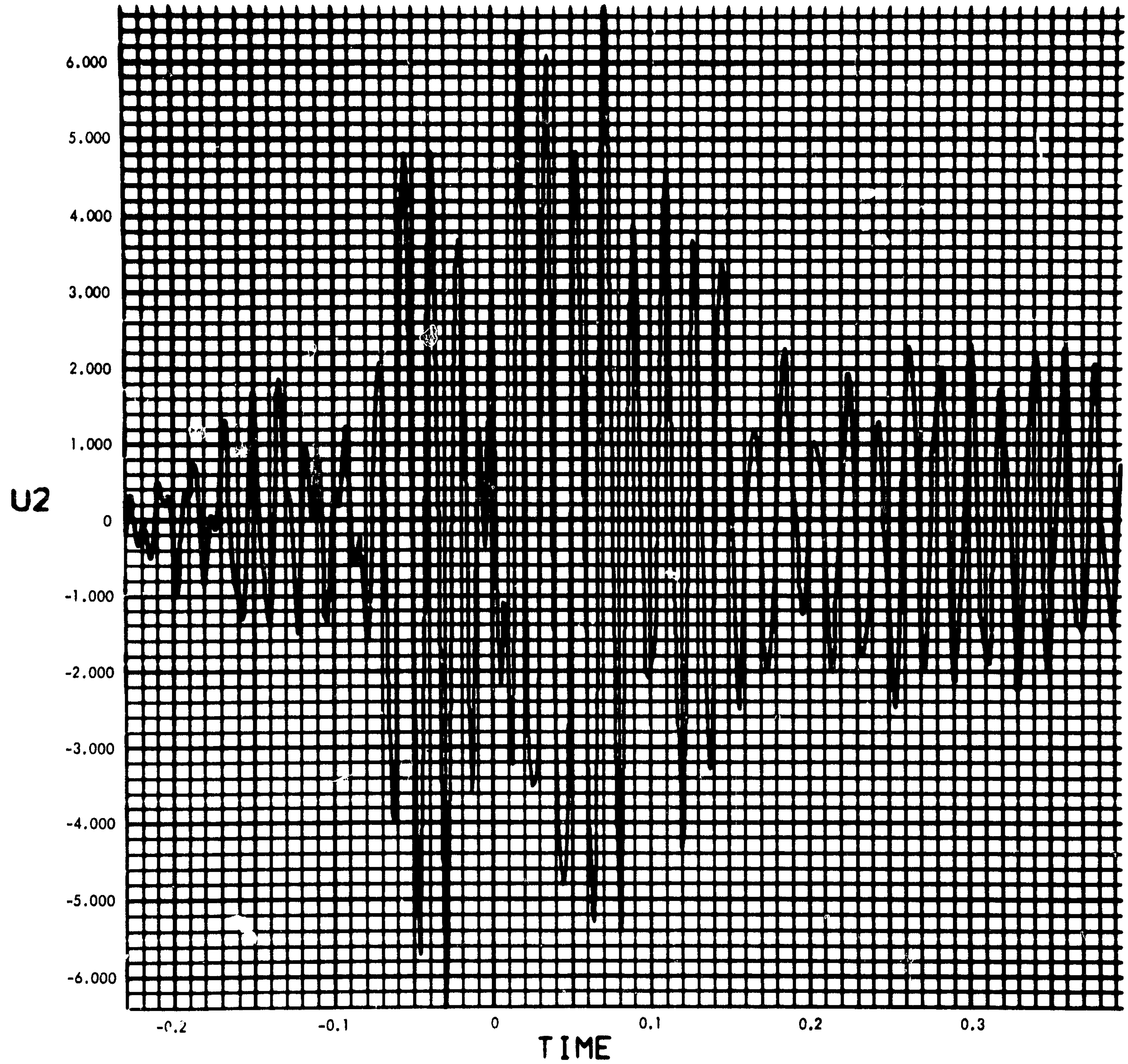

Fig. C-194. Joint 15, acceleration response, time history (pulse 4)

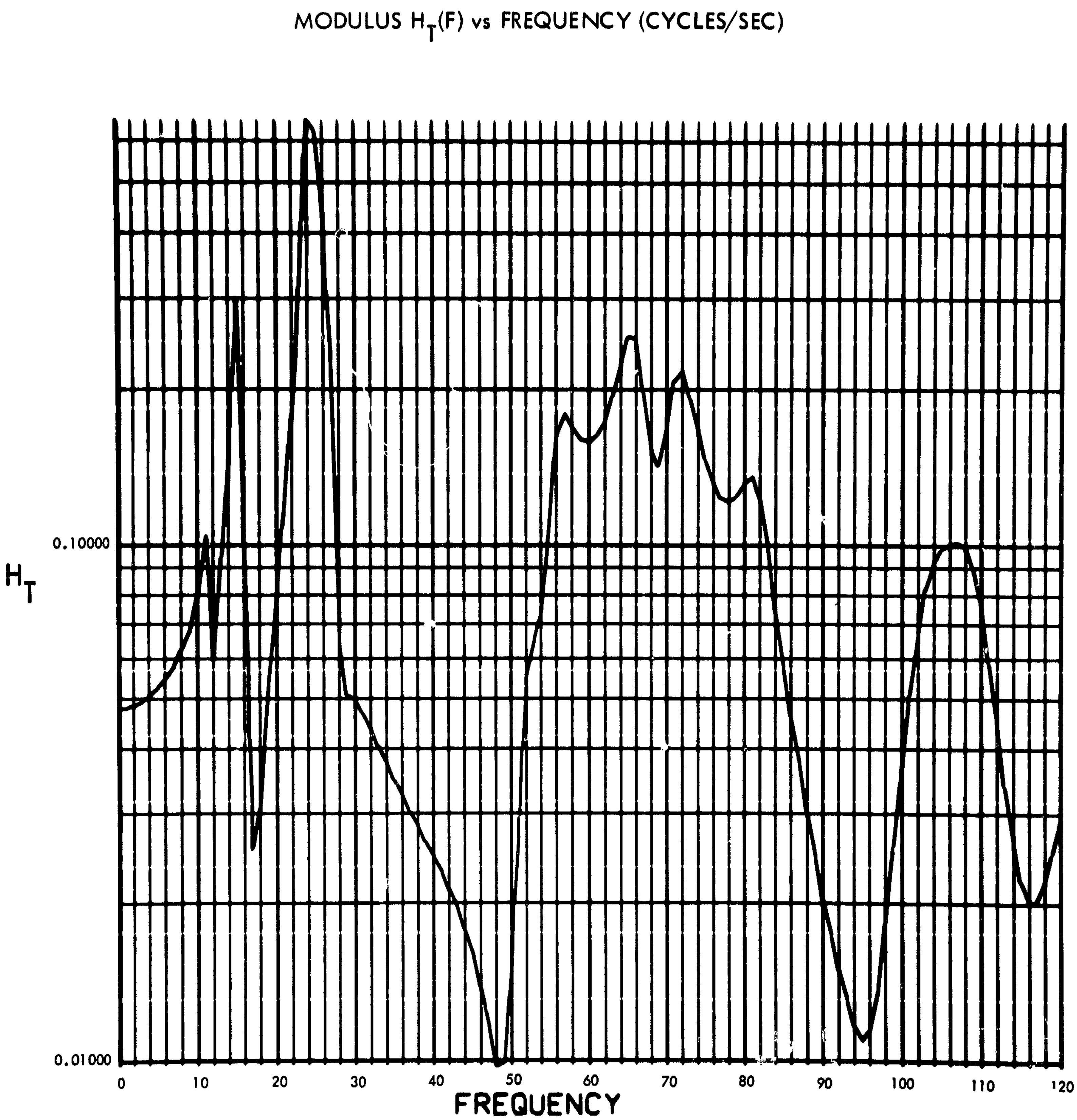

Fig. C-195. Joint 15, torque transfer function, Fourier transform, modulus

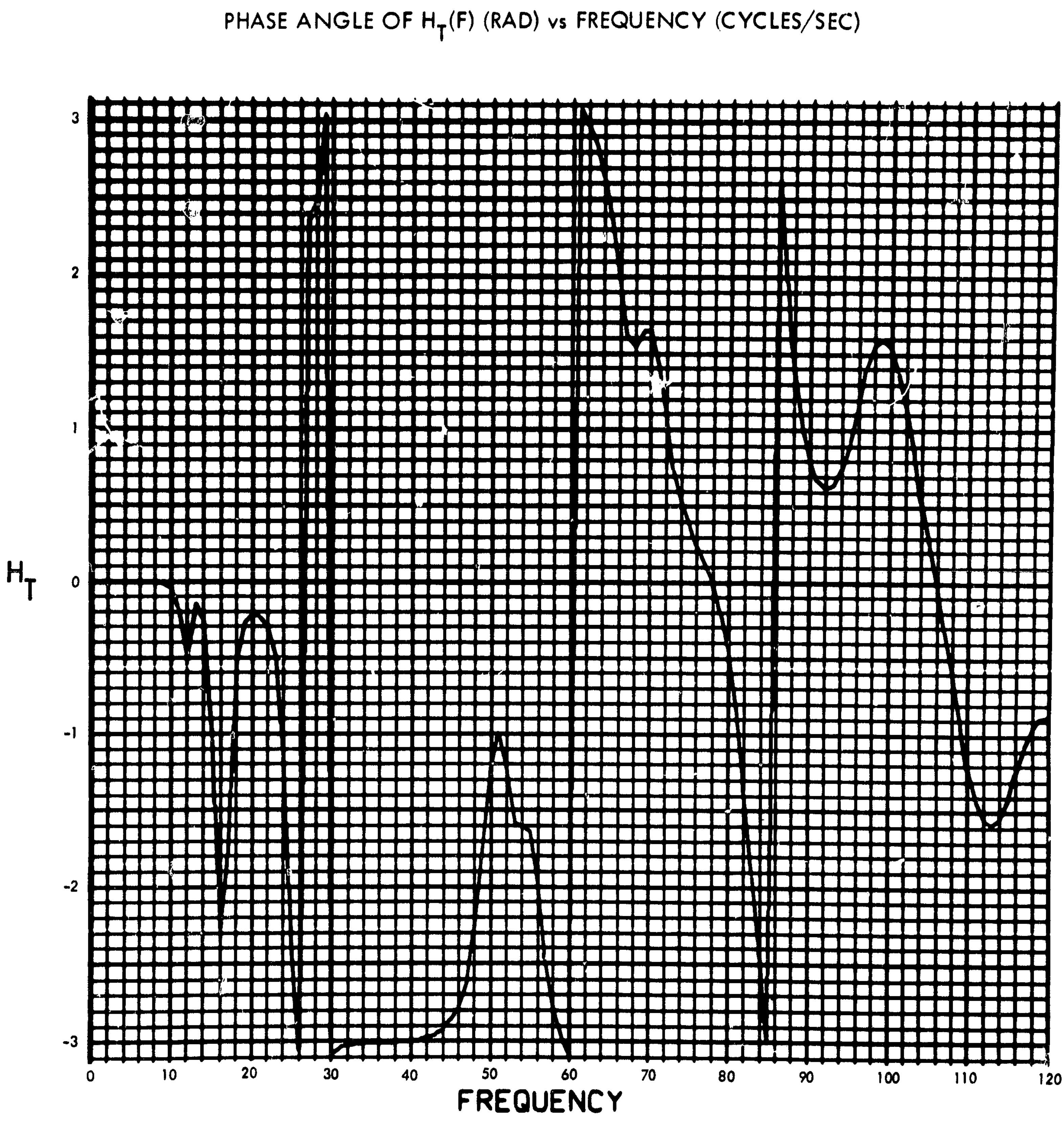

Fig. C-196. Joint 15, torque transfer function, Fourier transform, phase angle

MODULUS OF $F_T(F)$ (LB-IN-SEC) vs FREQUENCY (CYCLES/SEC)

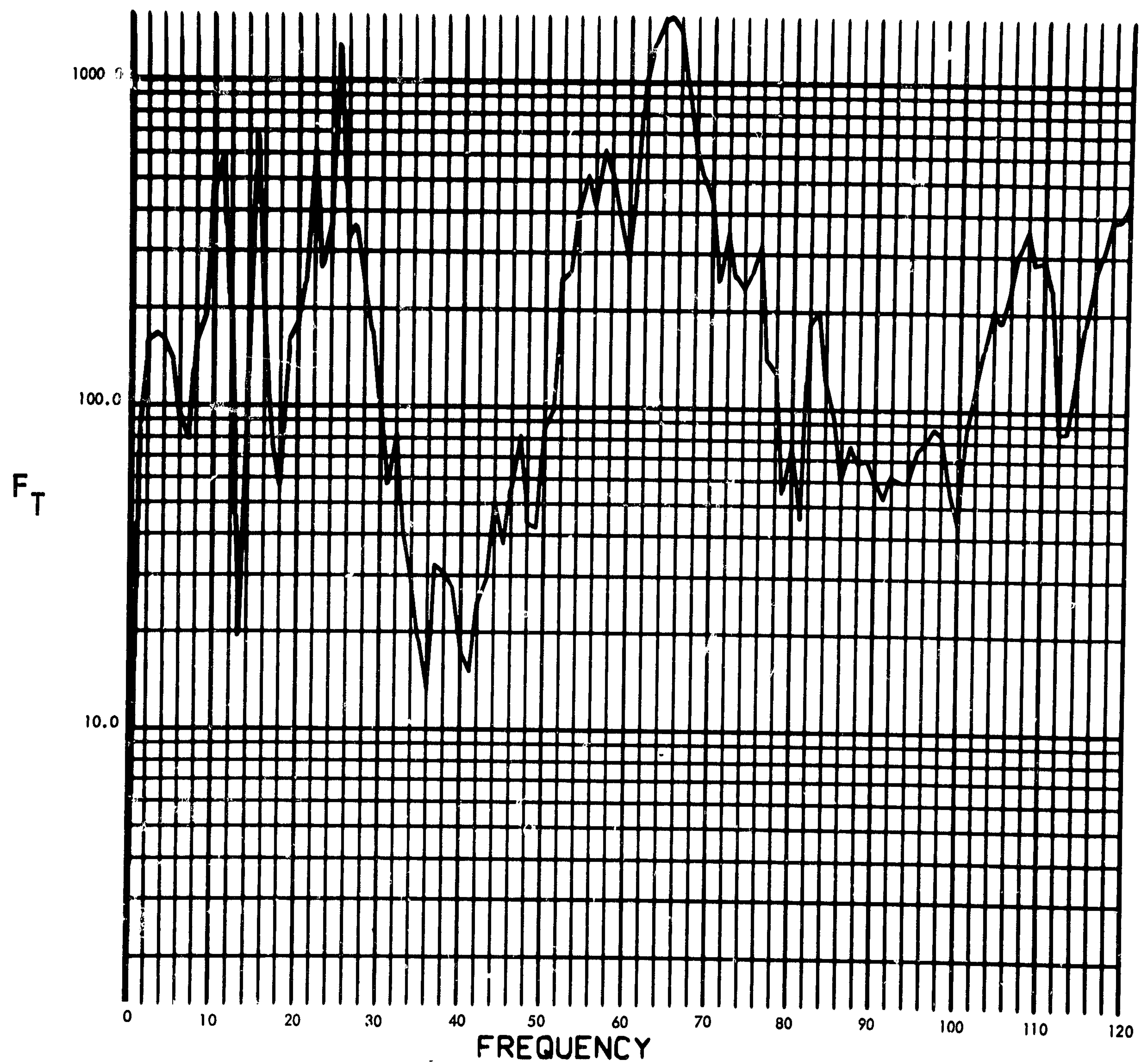

Fig. C-197. Joint 15, torque response function, Fourier transform, modulus (pulse 1)

PHASE ANGLE OF $F_T(F)$ (RAD) vs FREQUENCY (CYCLES/SEC)

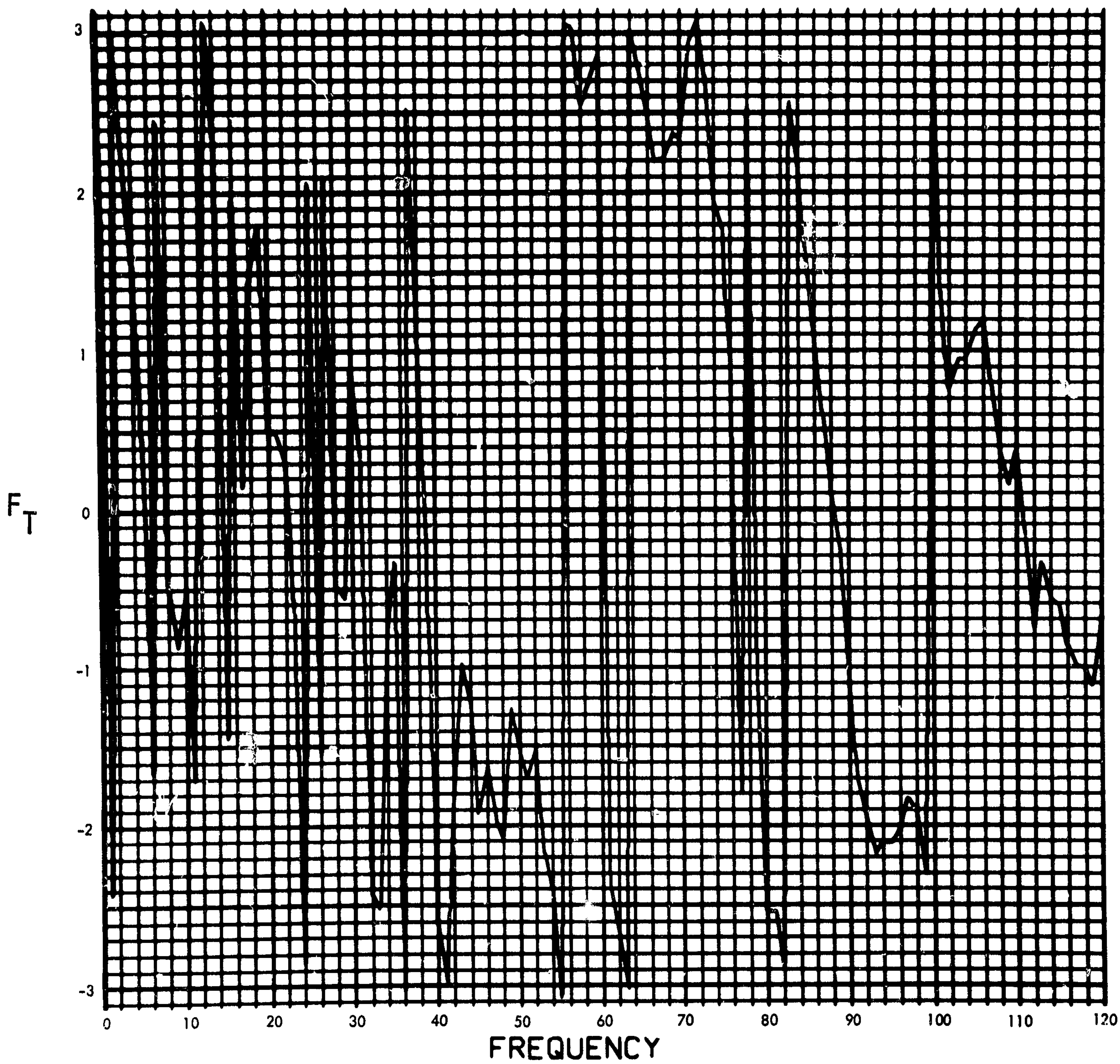

Fig. C-198. Joint 15, torque response function, Fourier transform, phase angle (pulse 1)

MODULUS OF $F_T(F)$ (LB-IN-SEC) vs FREQUENCY (CYCLES/SEC)

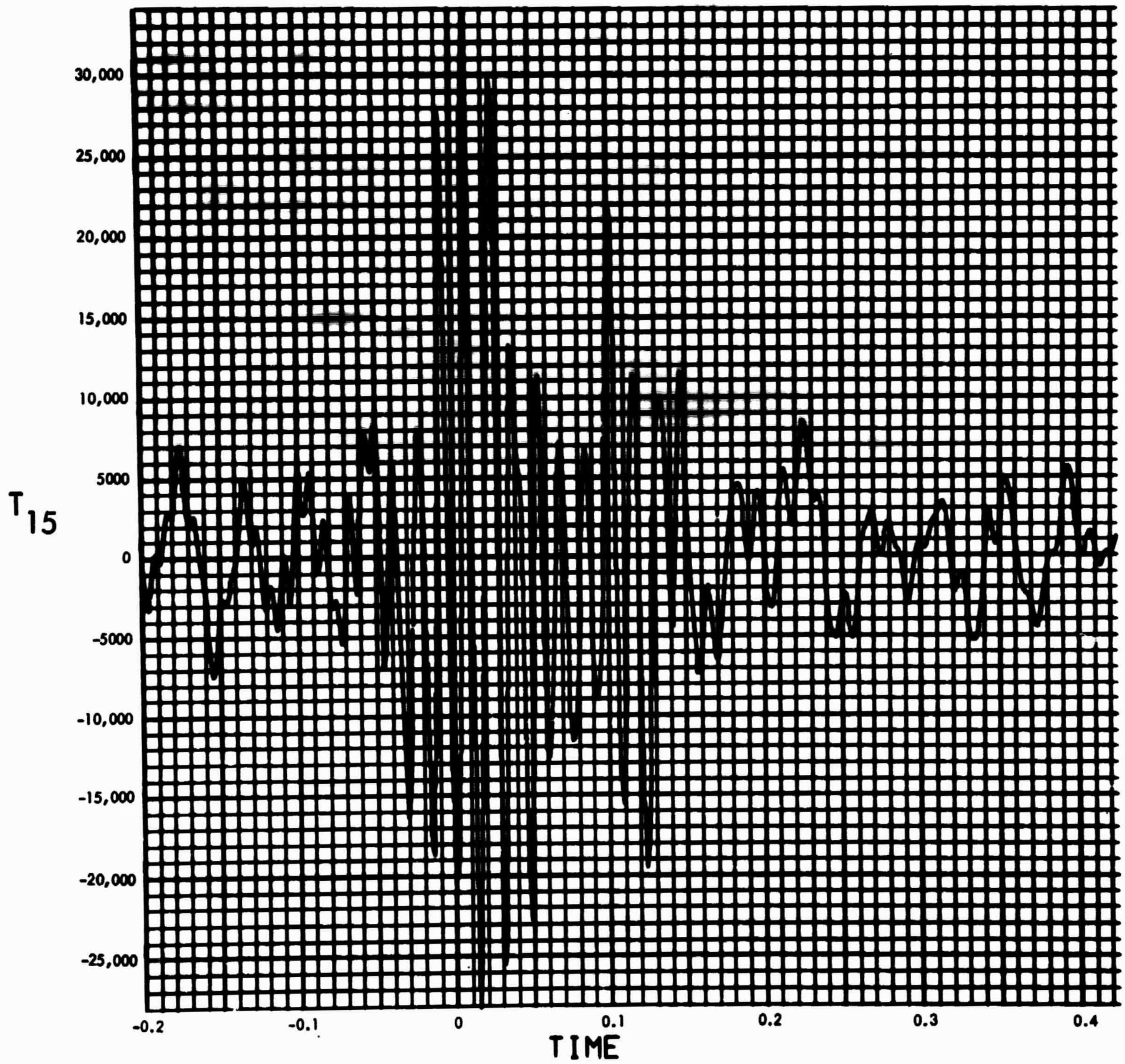

Fig. C-199. Joint 15, torque response, time history (pulse 1)

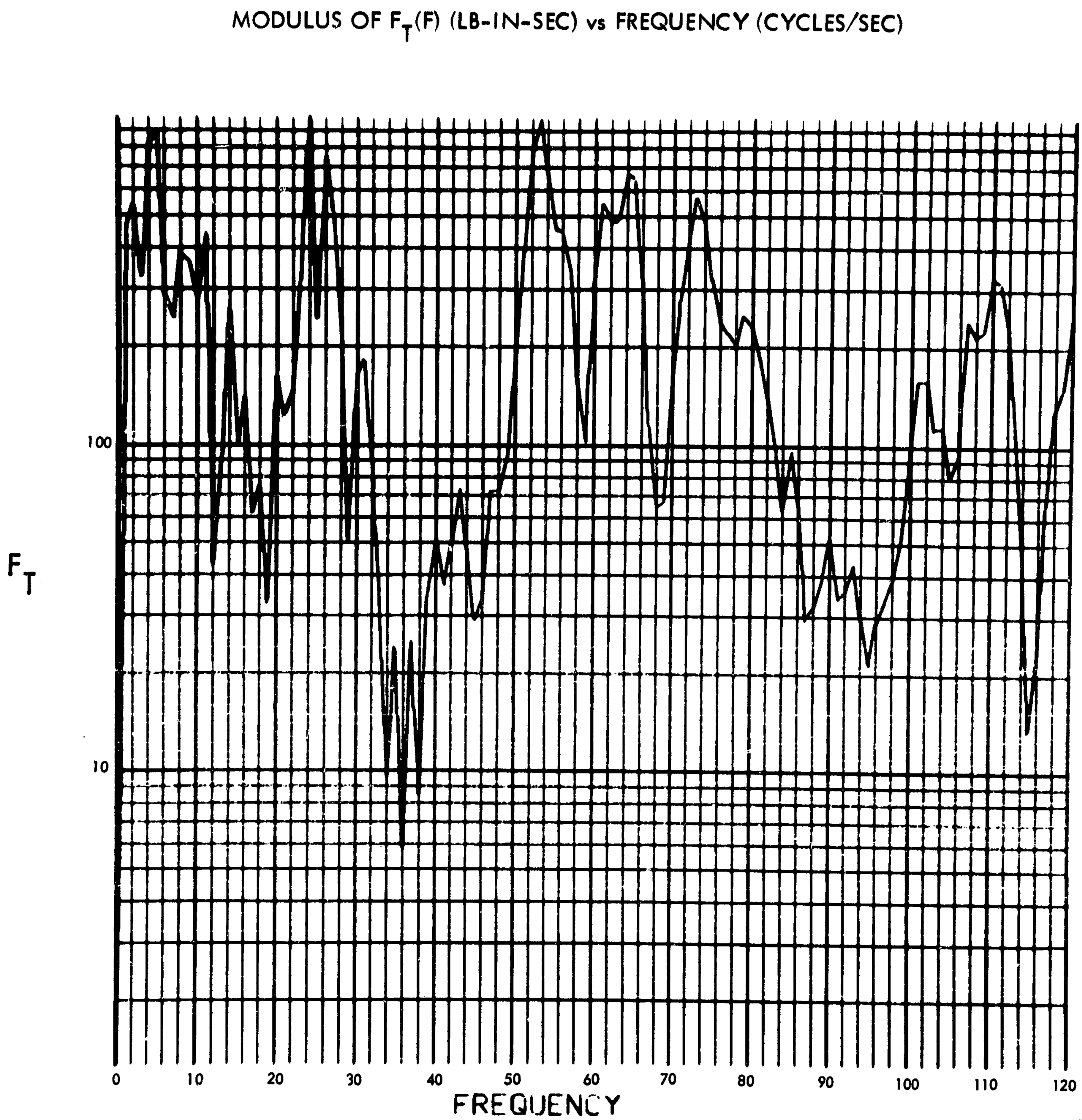

Fig. C-200. Joint 15, torque response function, Fourier transform, modulus (pulse 2)

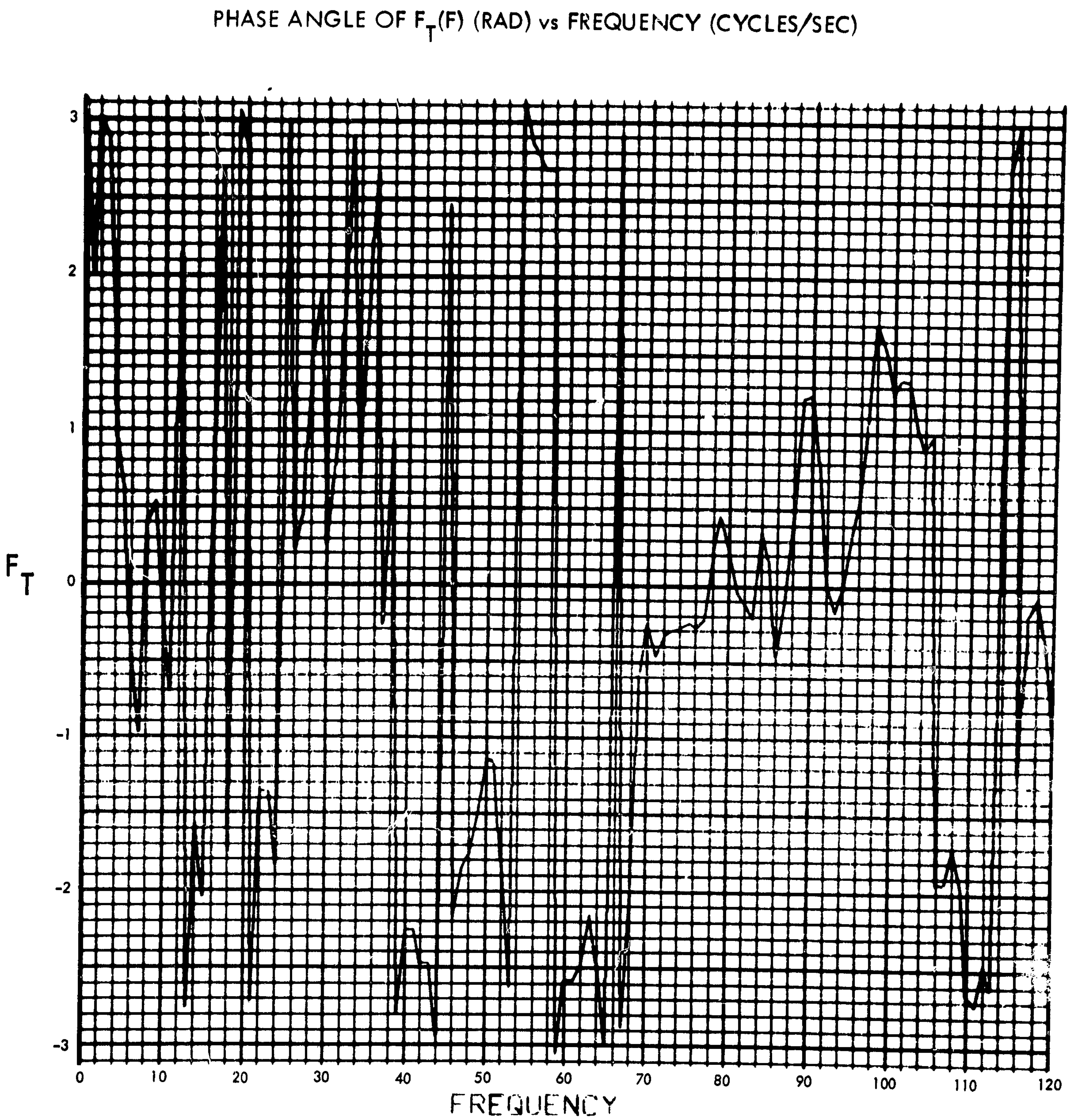

Fig. C-201. Joint 15, torque response function, Fourier transform phase angle (pulse 2)

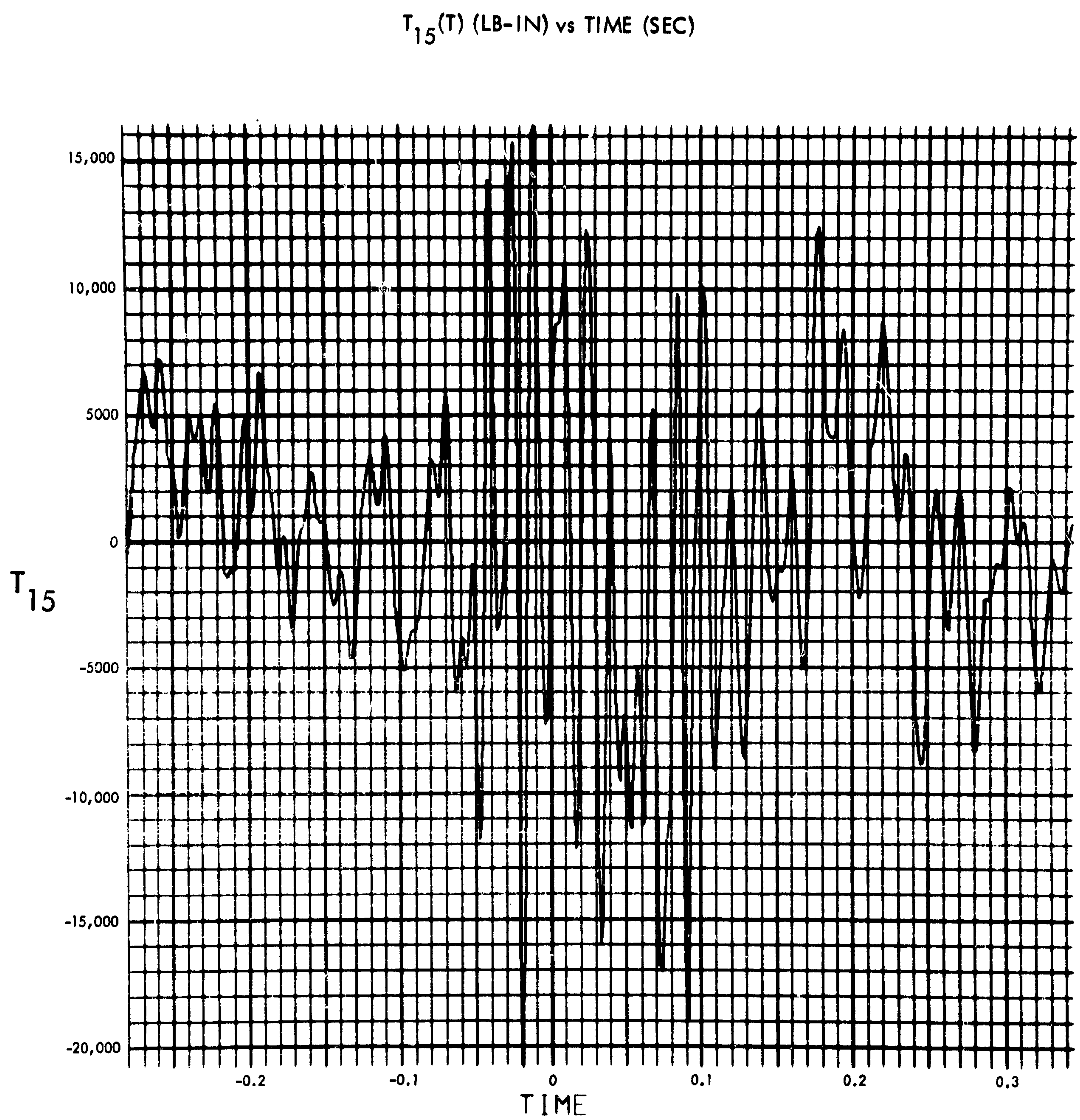

Fig. C-202. Joint 15, torque response, time history (pulse 2)

MODULUS OF $F_T(F)$ (LB-IN-SEC) vs FREQUENCY (CYCLES/SEC)

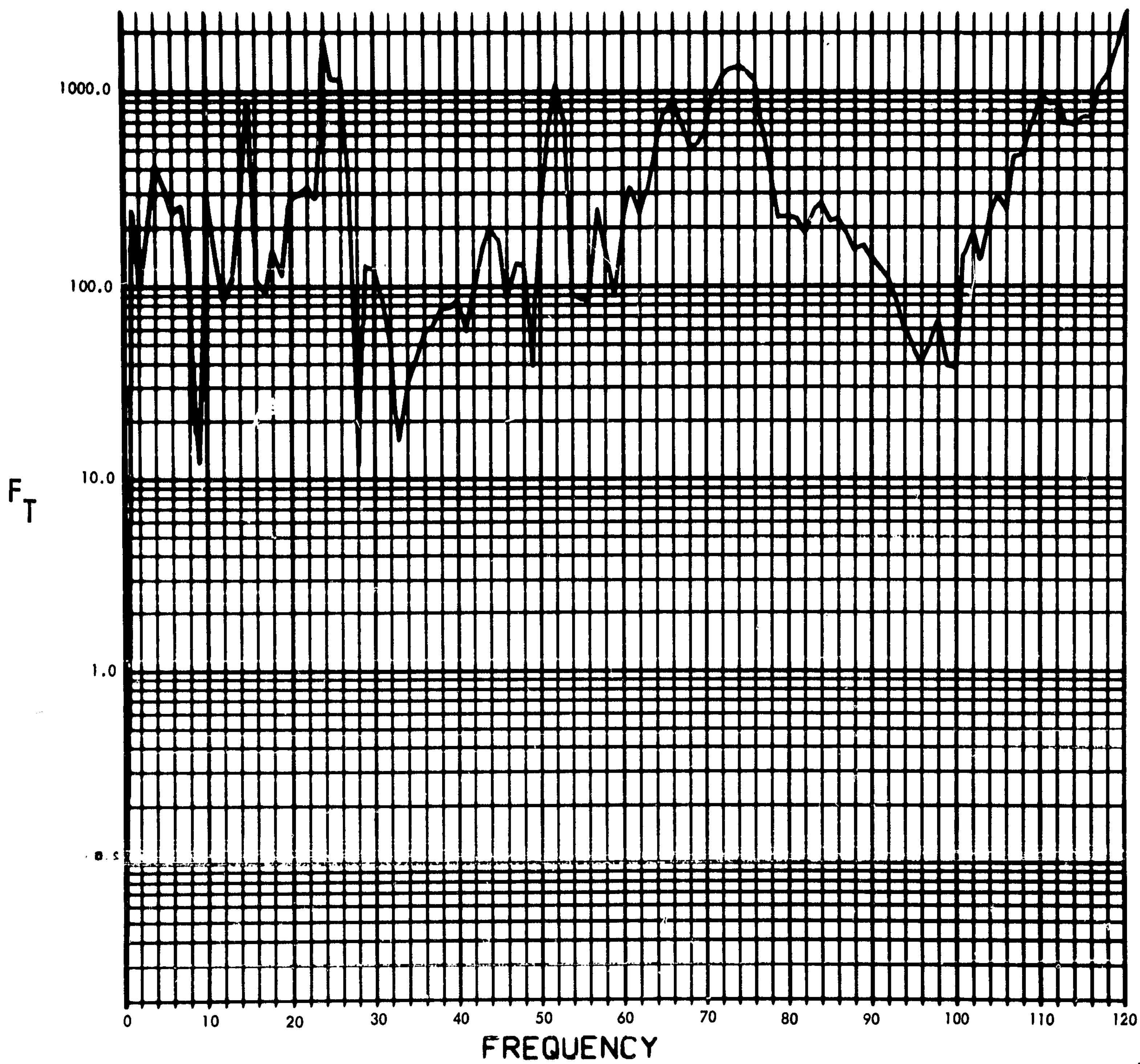

Fig. C-203. Joint 15, torque response function, Fourier transform, modulus (pulse 3)

PHASE ANGLE OF $F_T(F)$ (RAD) vs FREQUENCY (CYCLES/SEC)

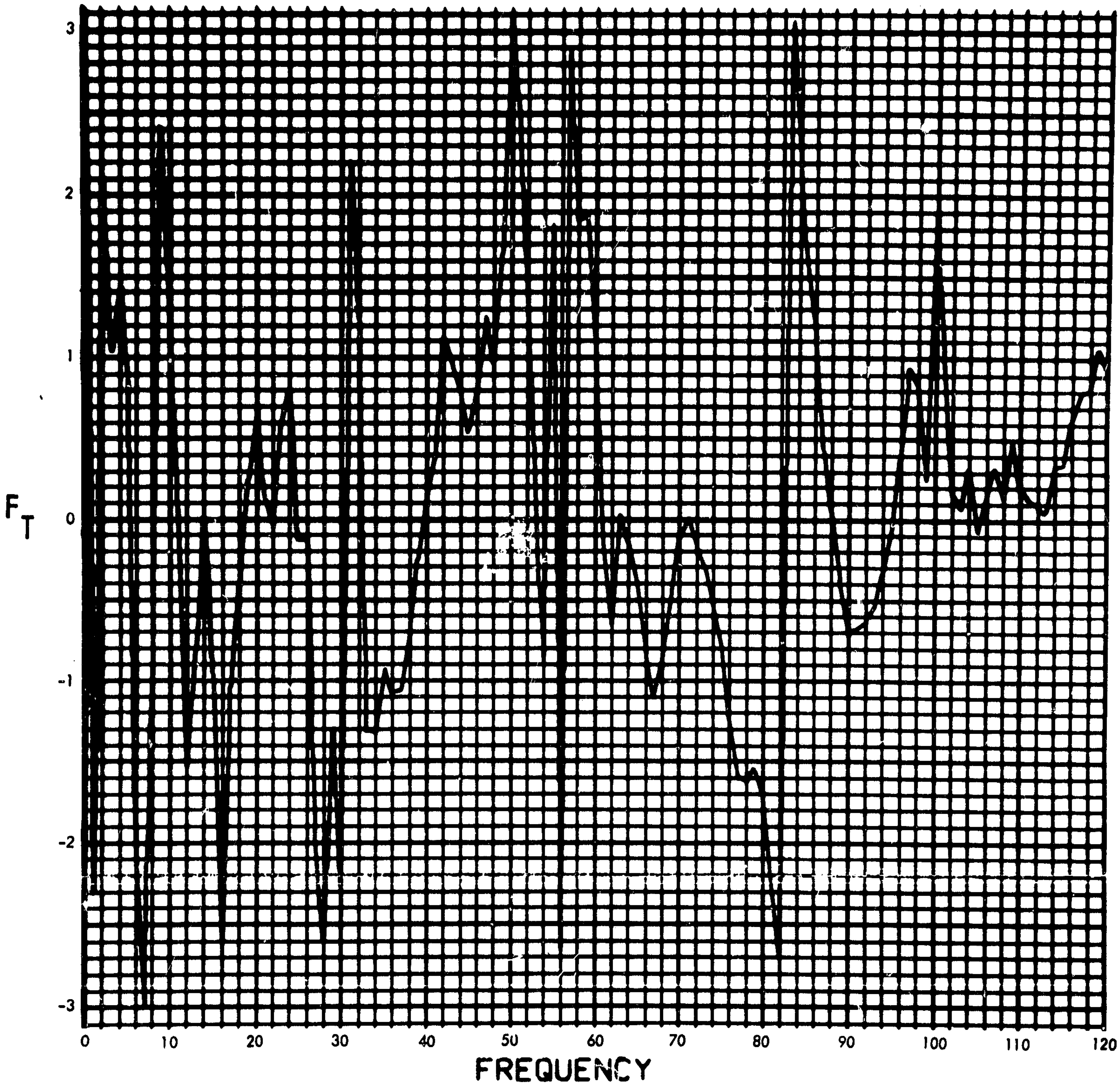

Fig. C-204. Joint 15, torque response function, Fourier transform, phase angle (pulse 3)

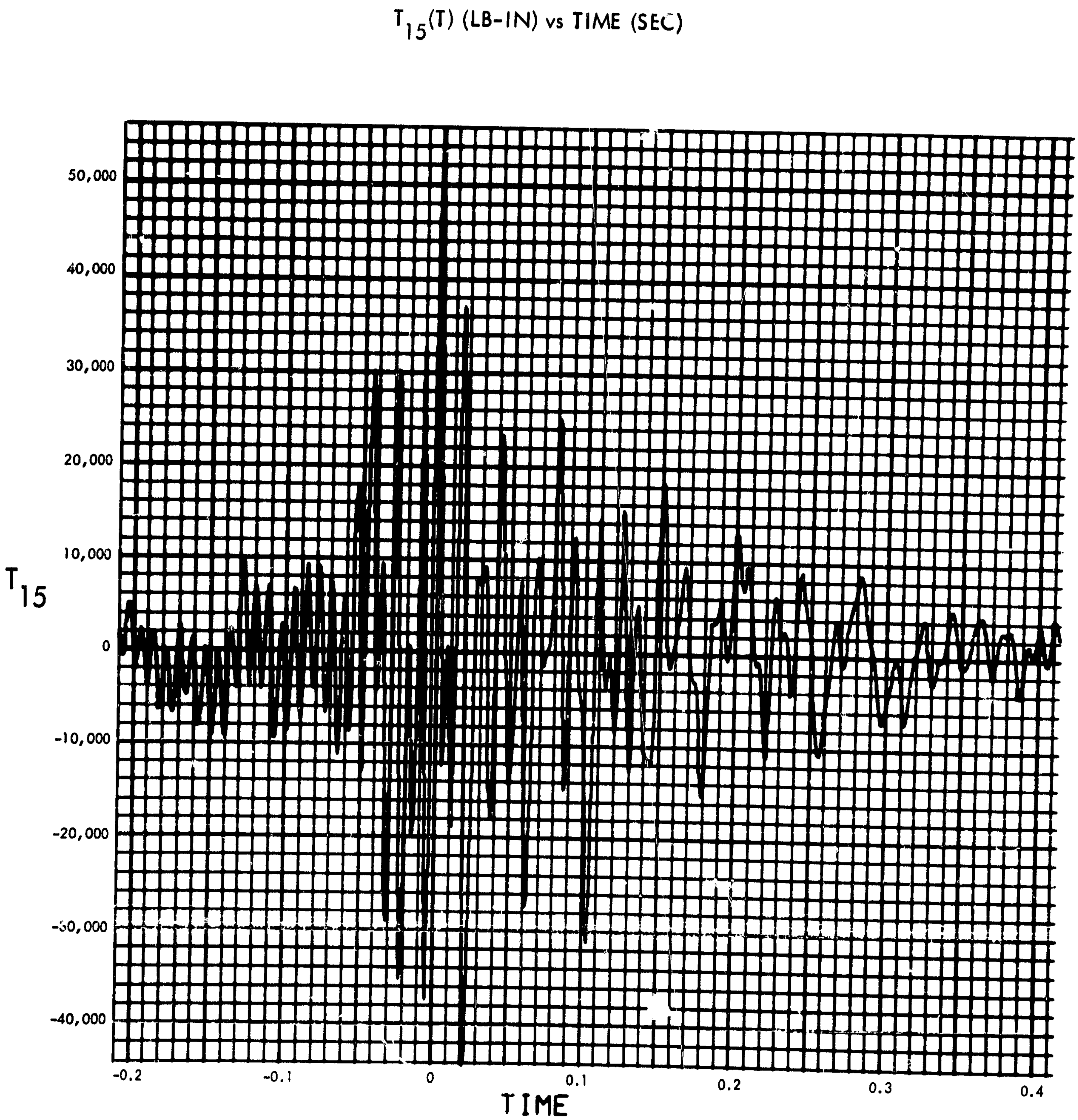

Fig. C-205. Joint 15, torque response, time history (pulse 3)

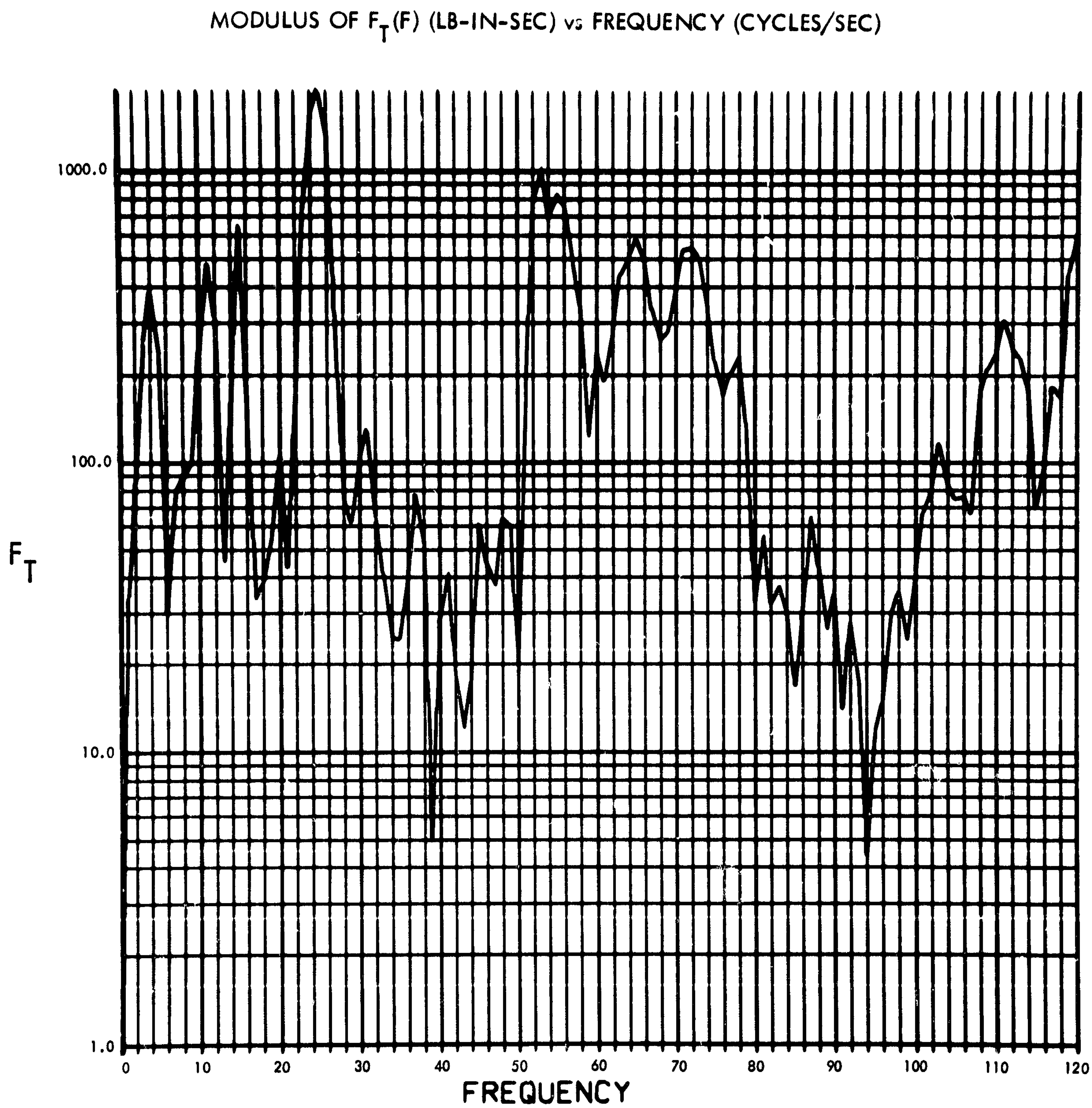

Fig. C-206. Joint 15, torque response function, Fourier transform, modulus (pulse 4)

PHASE ANGLE OF $F_T(F)$ (RAD) vs FREQUENCY (CYCLES/SEC)

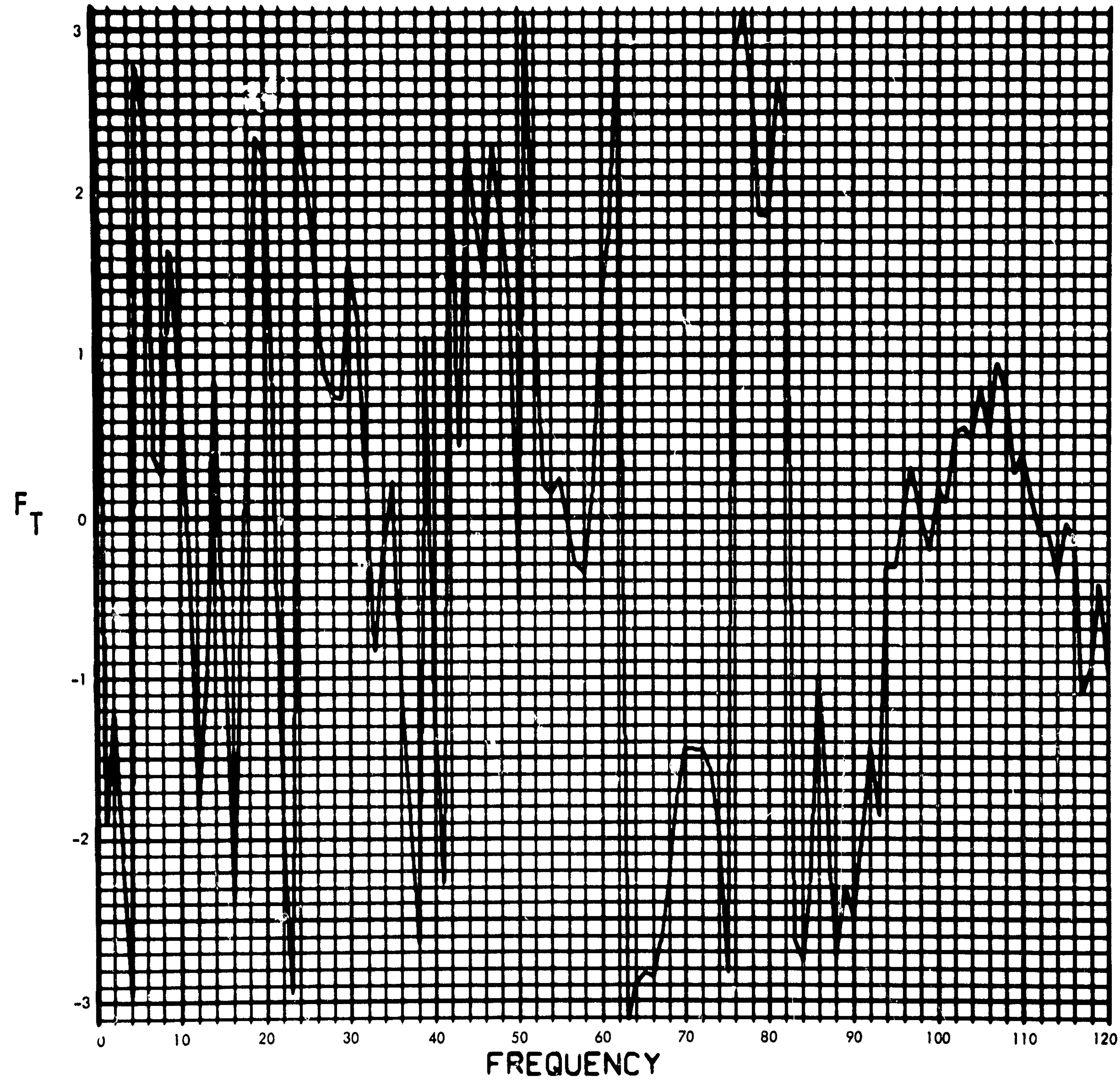

Fig. C-207. Joint 15, torque response function, Fourier transform, phase angle (pulse 4)

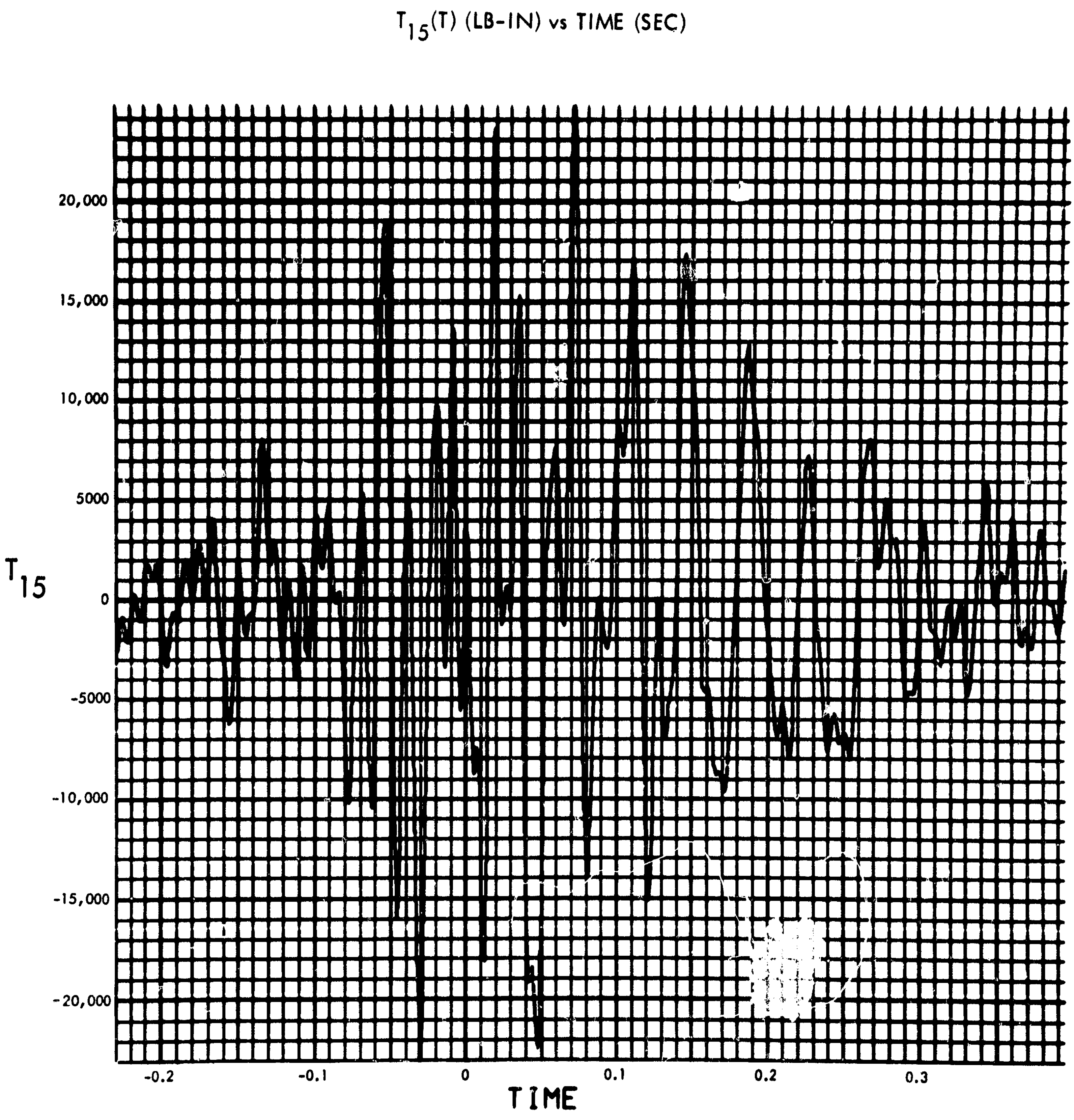

Fig. C-208. Joint 15, torque response, time history (pulse 4)

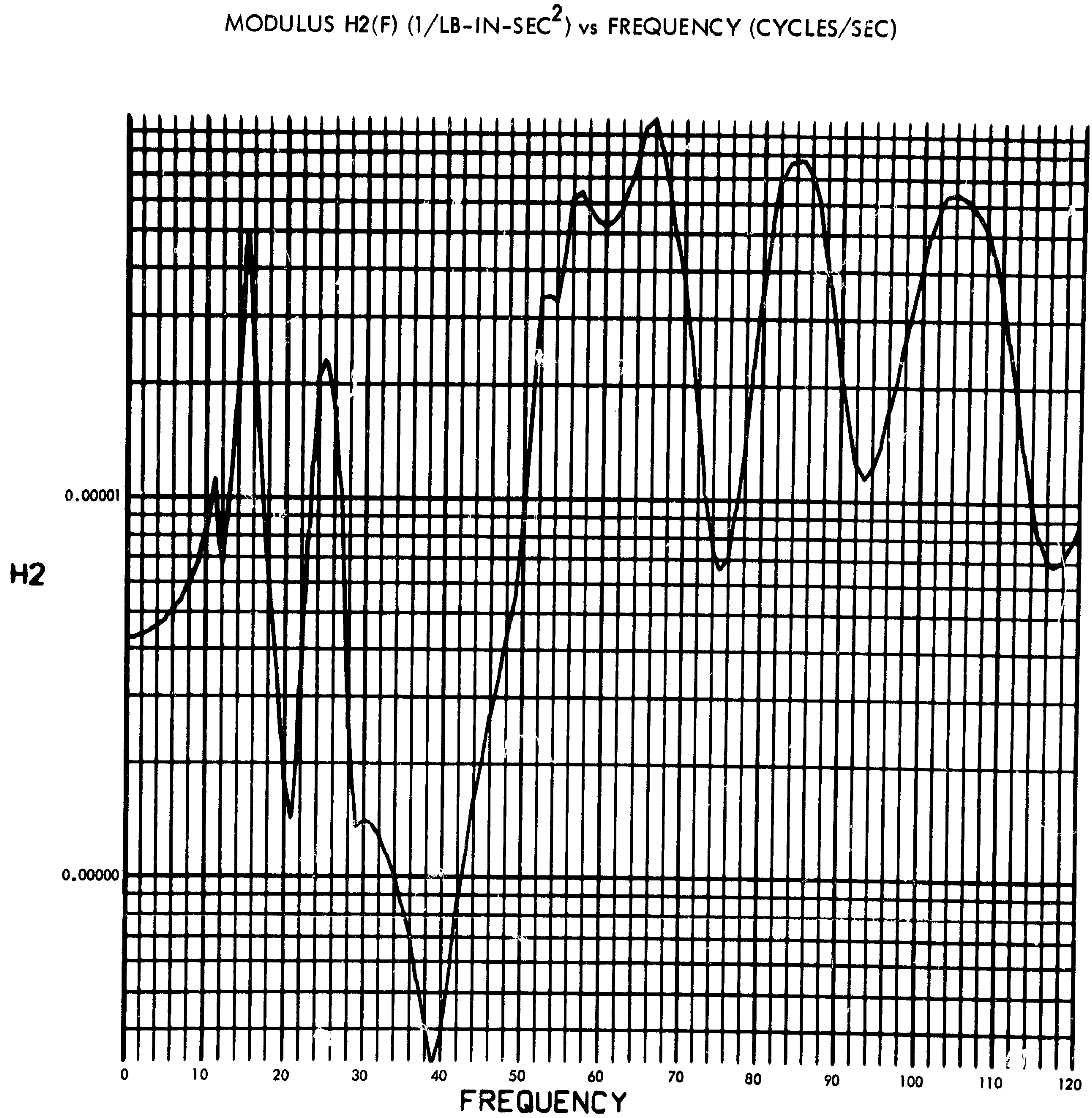

Fig. C-209. Joint 16, acceleration transfer function, Fourier transform, modulus

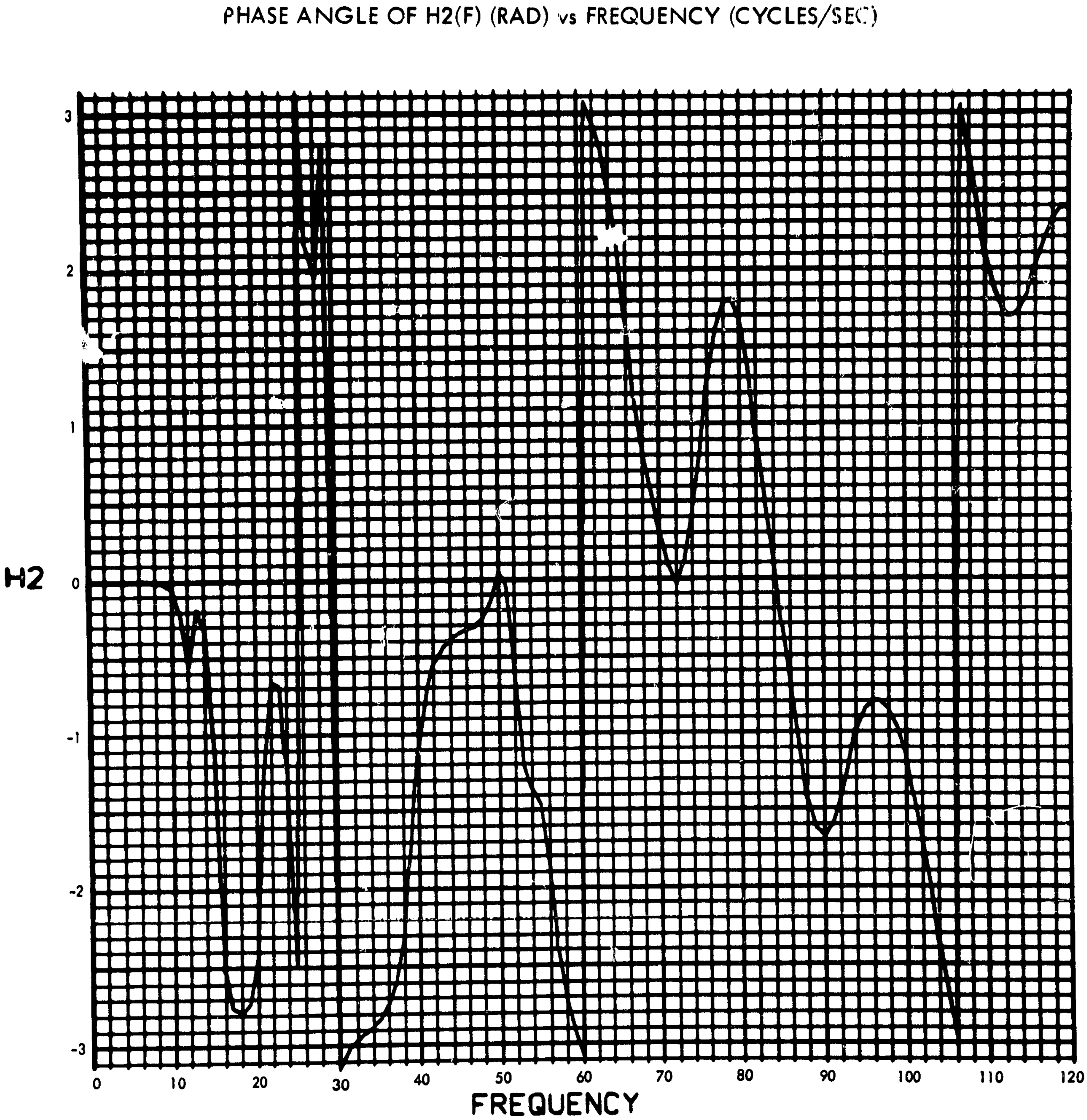

Fig. C-210. Joint 16, acceleration transfer function,
Fourier transform, phase angle

MODULUS OF V2(F) (RAD/SEC) vs FREQUENCY (CYCLES/SEC)

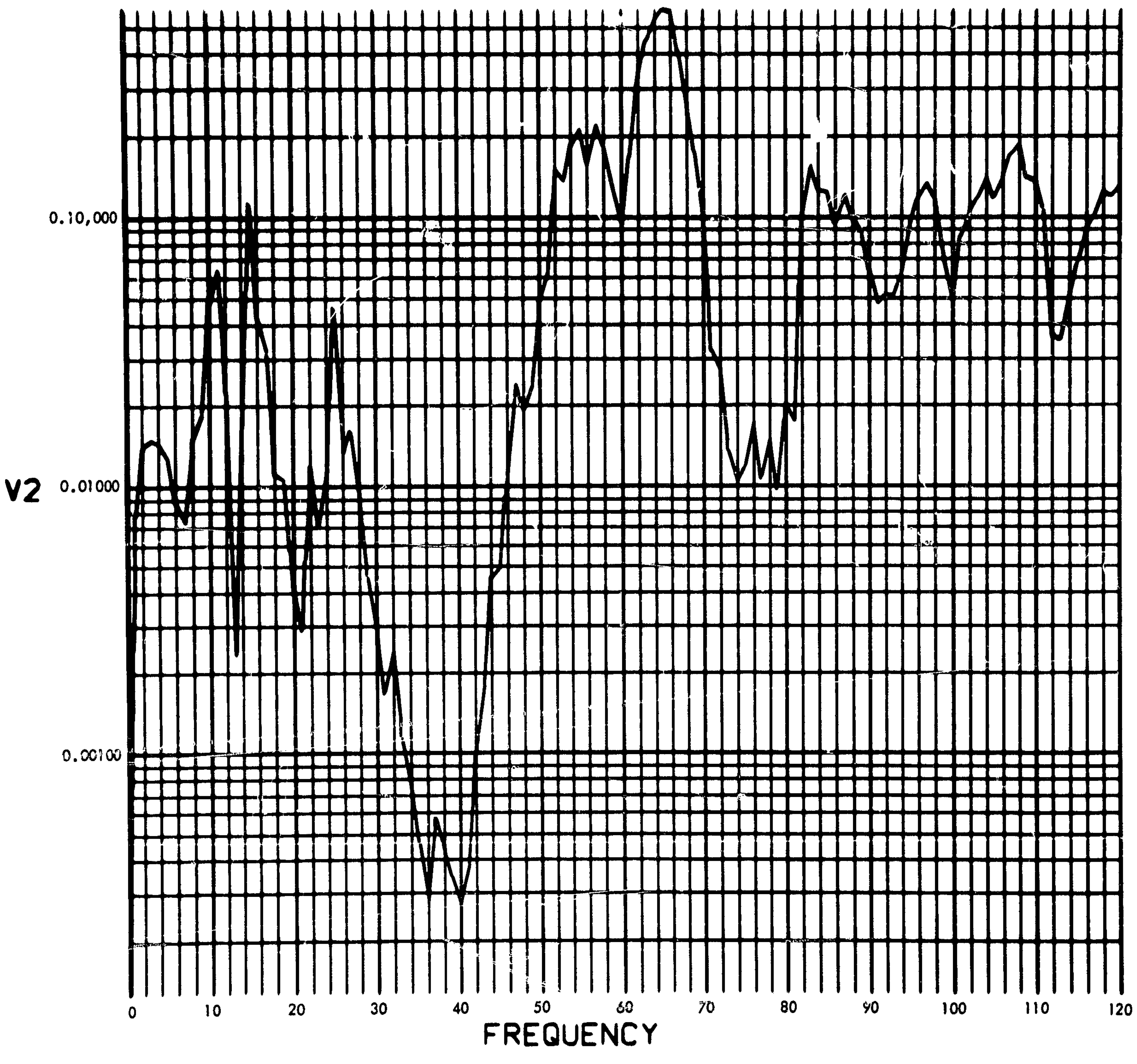

Fig. C-211. Joint 16, acceleration response, Fourier transform, modulus (pulse 1)

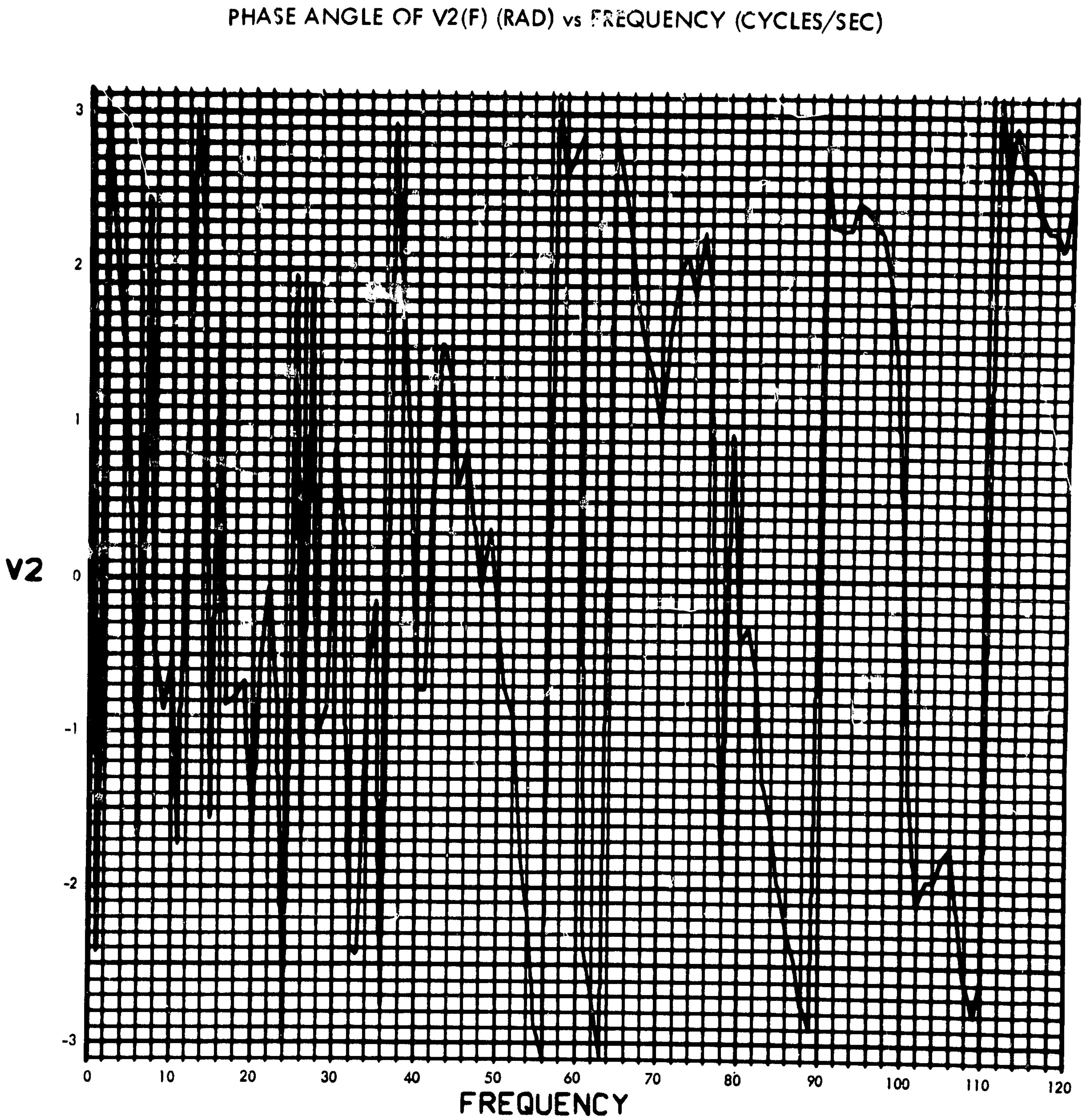

Fig. C-212. Joint 16, acceleration response, Fourier transform, phase angle (pulse 1)

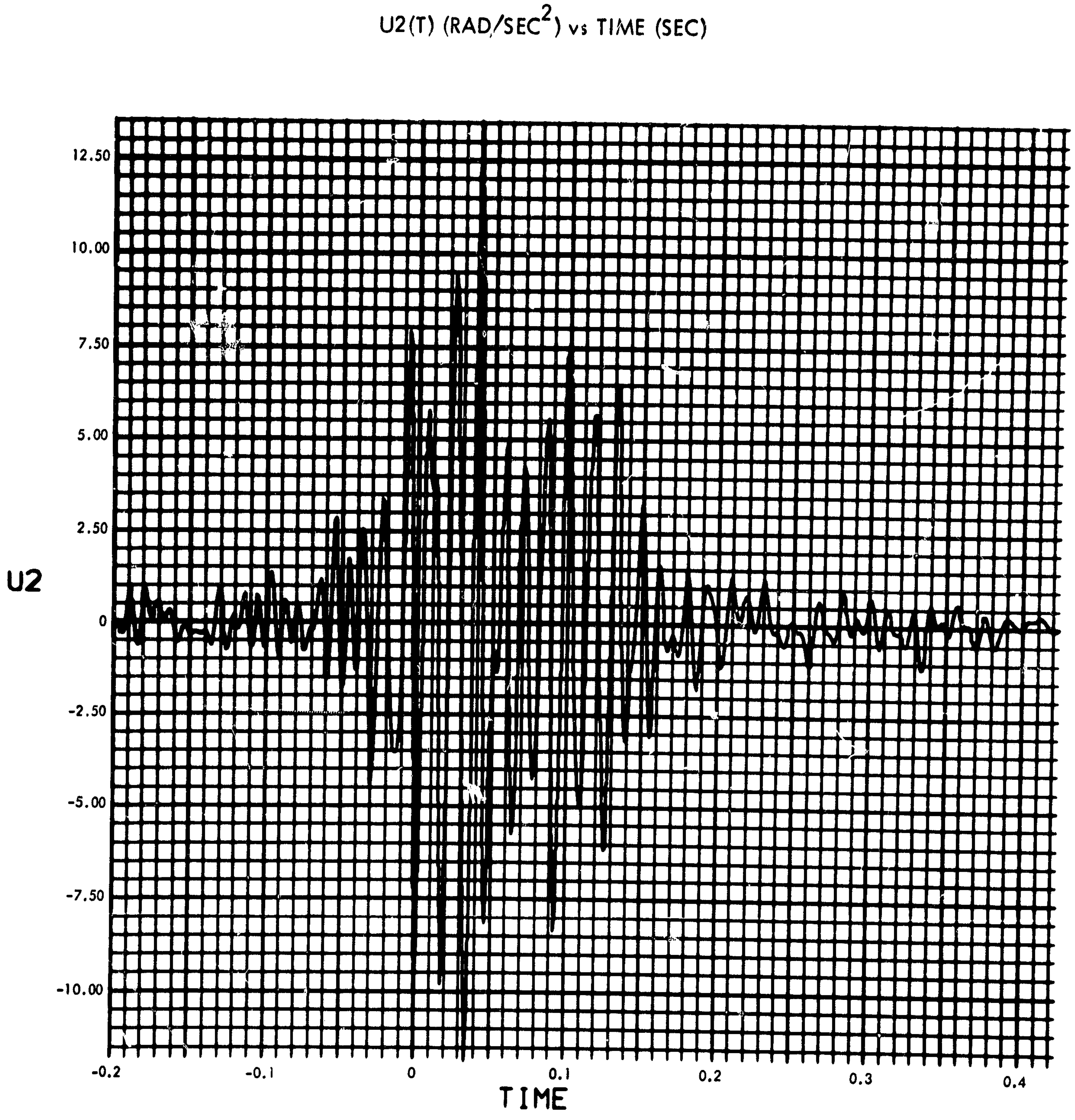

Fig. C-213. Joint 16, acceleration response, time history (pulse 1)

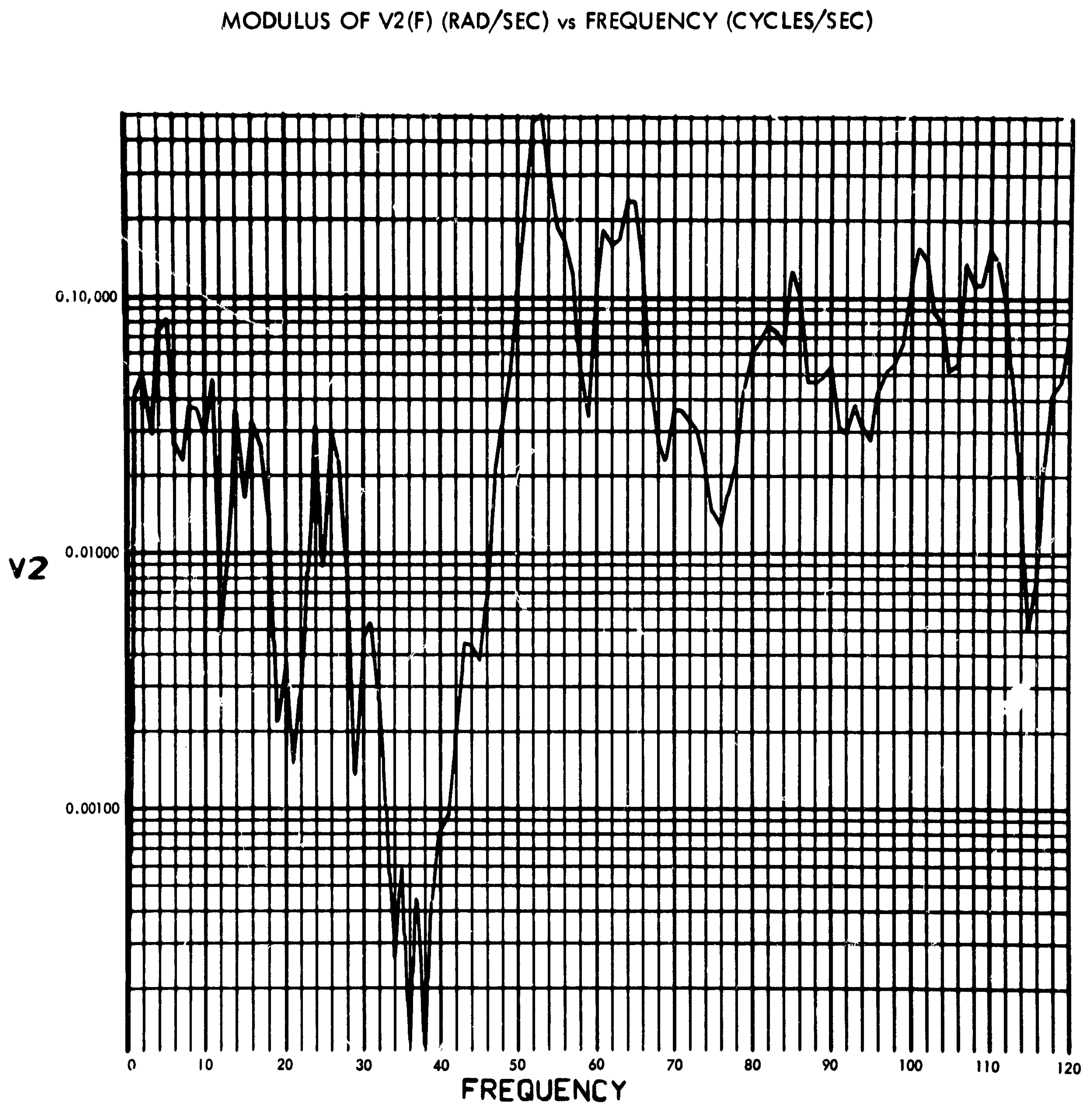

Fig. C-214. Joint 16, acceleration response, Fourier transform, modulus (pulse 2)

PHASE ANGLE OF V2(F) (RAD) vs FREQUENCY (CYCLES/SEC

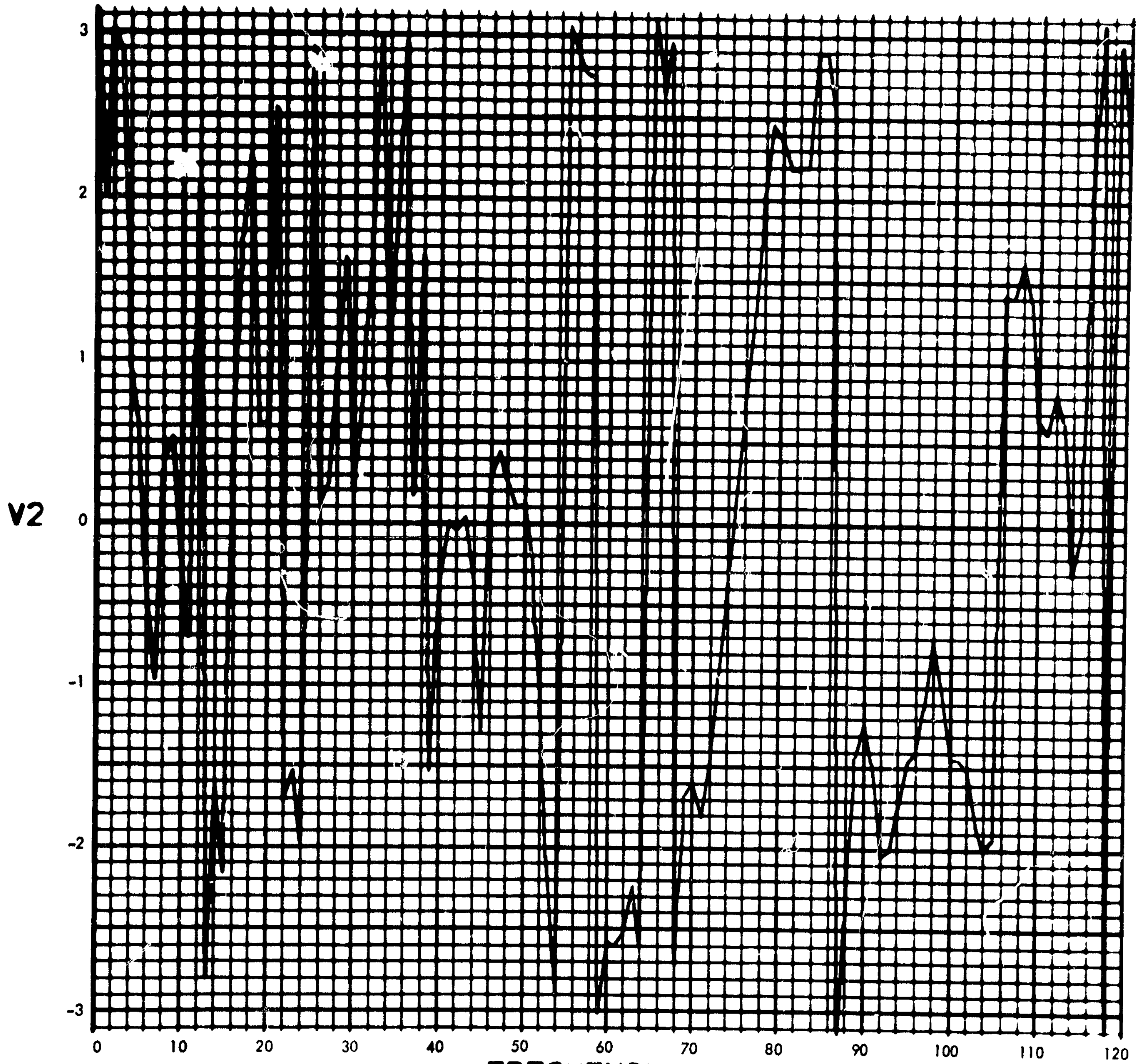

Fig. C-215. Joint 16, acceleration response, Fourier transform, phase angle (pulse 2)

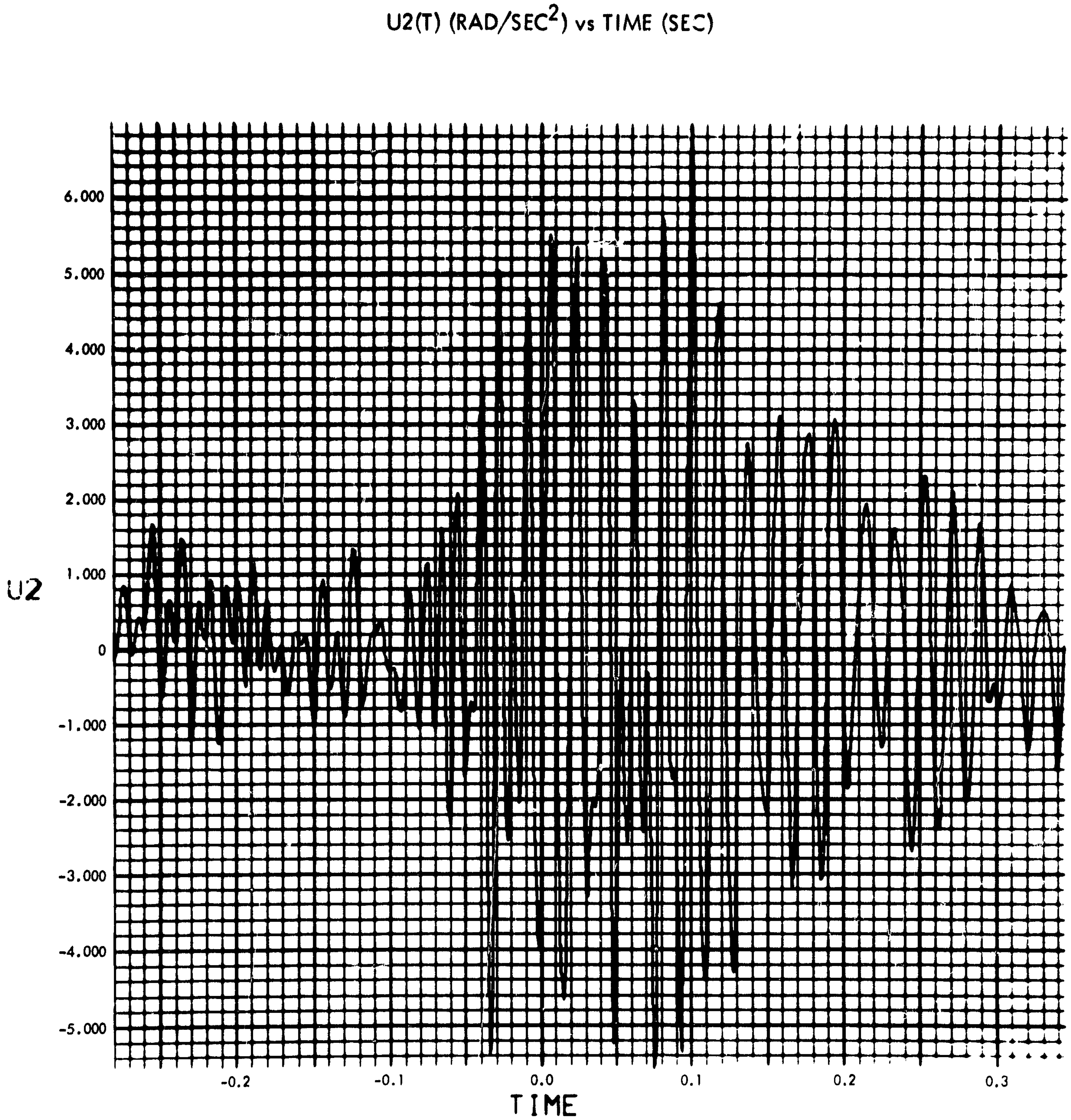

Fig. C-216. Joint 16, acceleration response, time history (pulse 2)

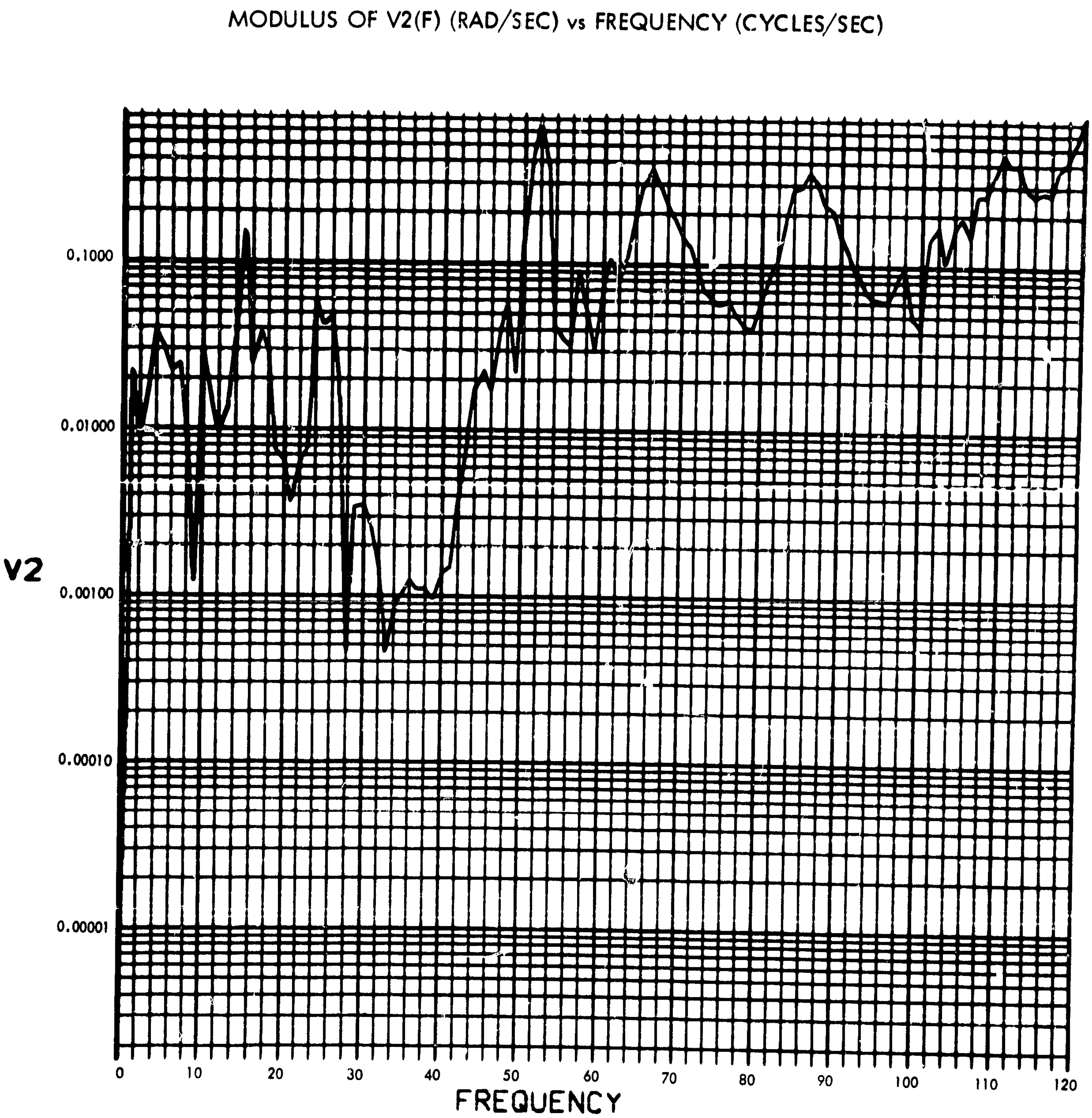

Fig. C-217. Joint 16, acceleration response, Fourier transform, modulus (pulse 3)

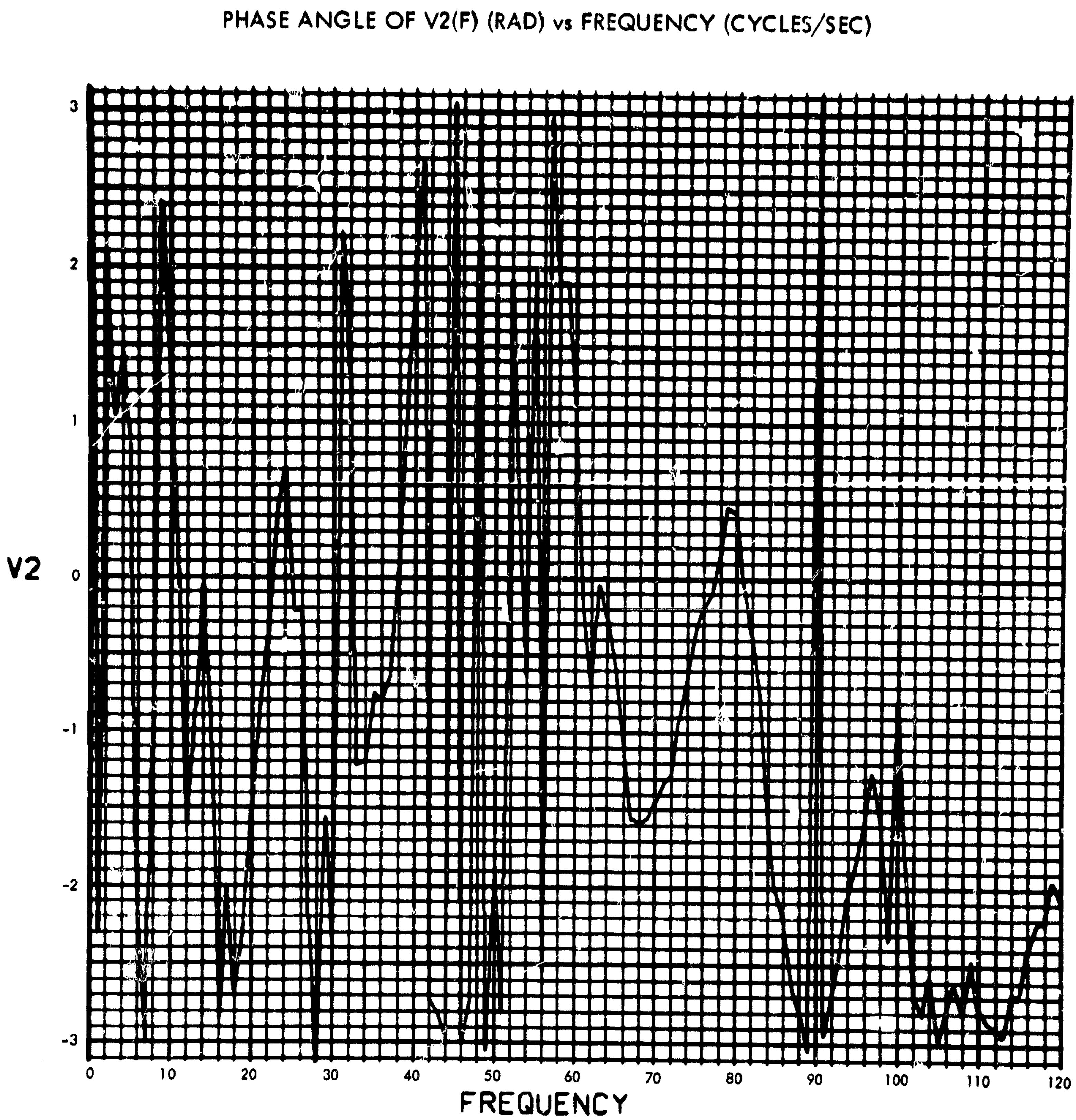

Fig. C-218. Joint 16, acceleration response, Fourier transform, phase angle (pulse 3)

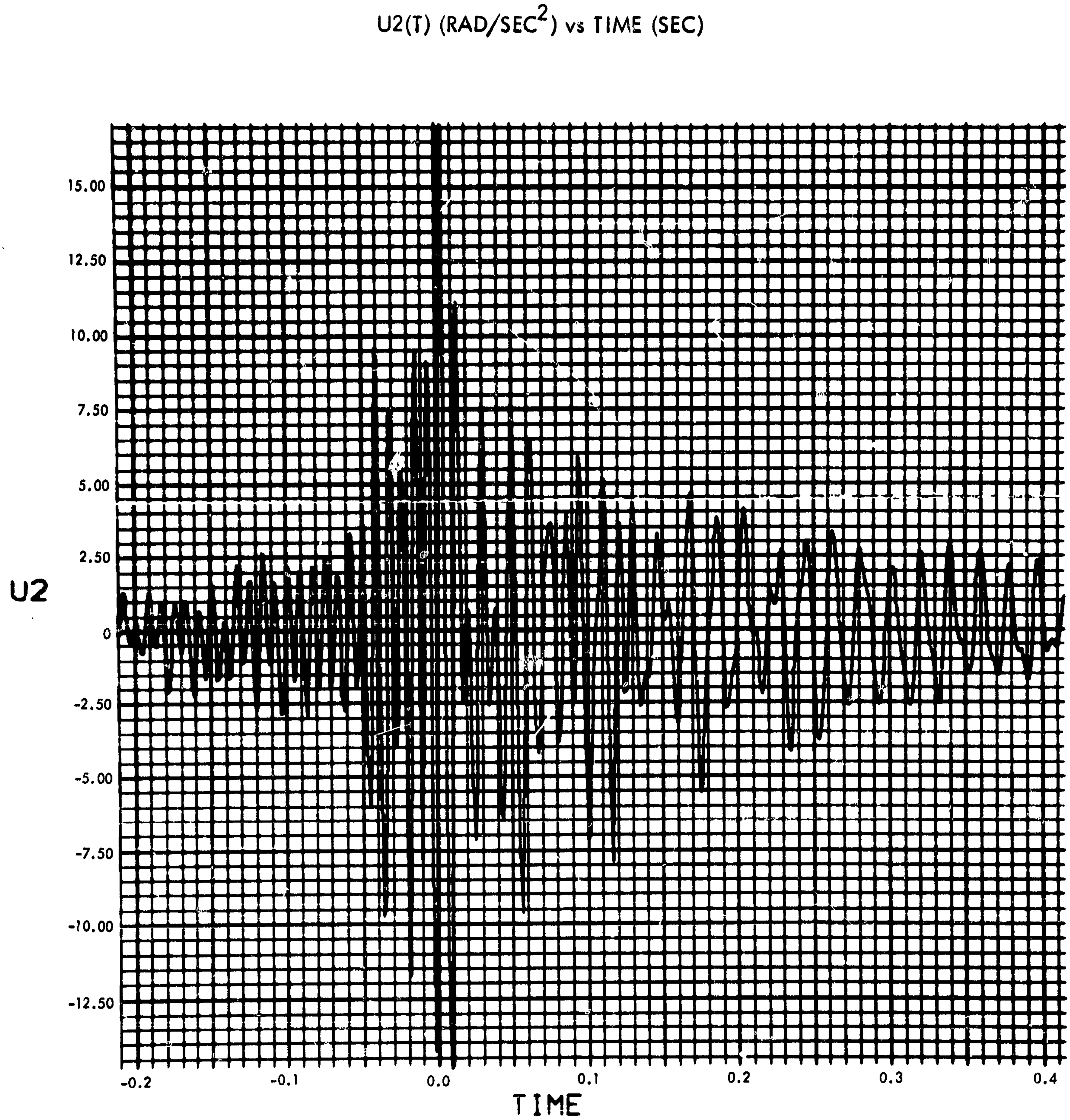

Fig. C-219. Joint 16, acceleration response, time history (pulse 3)

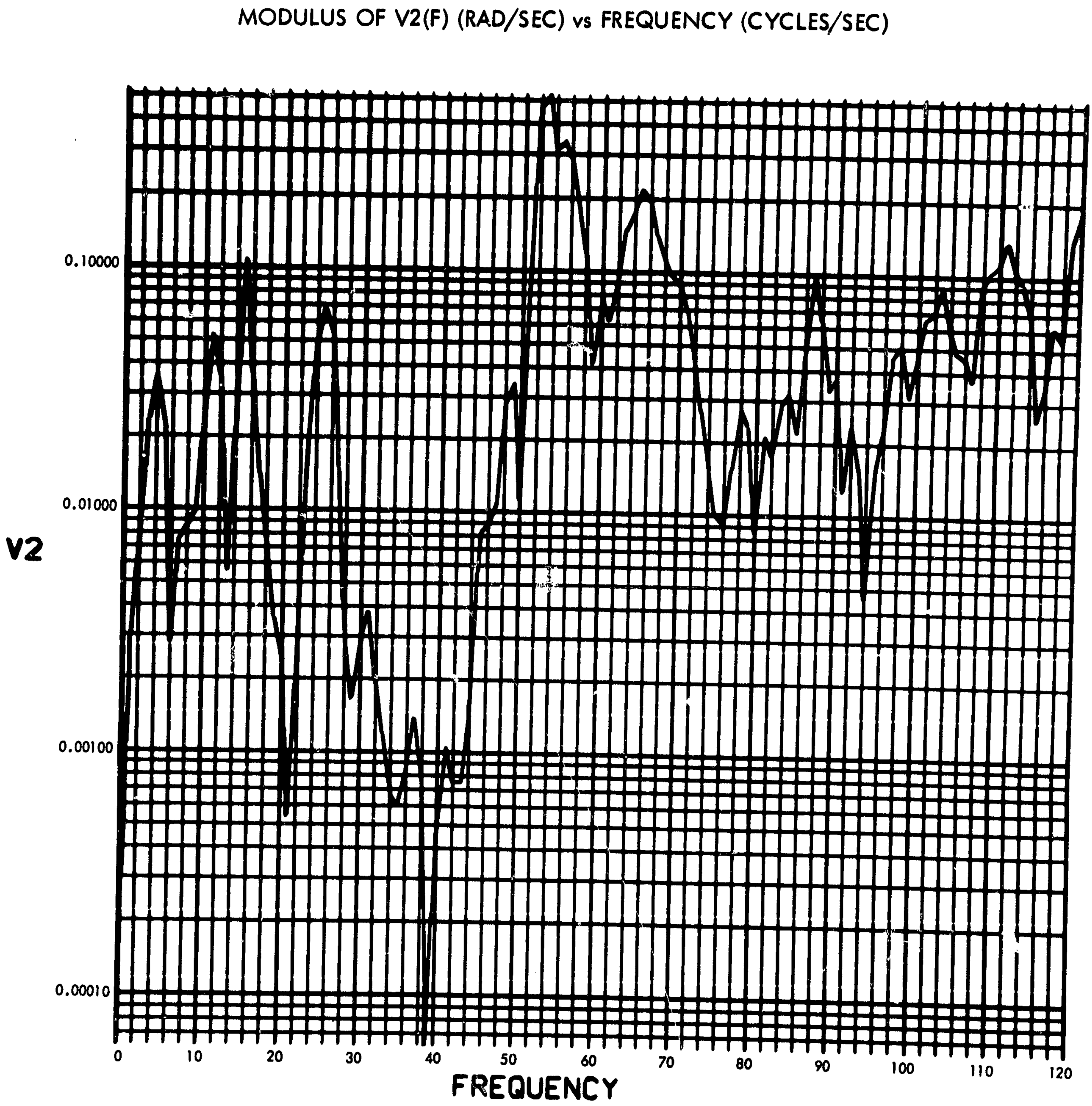

Fig. C-220. Joint 16, acceleration response, Fourier transform, modulus (pulse 4)

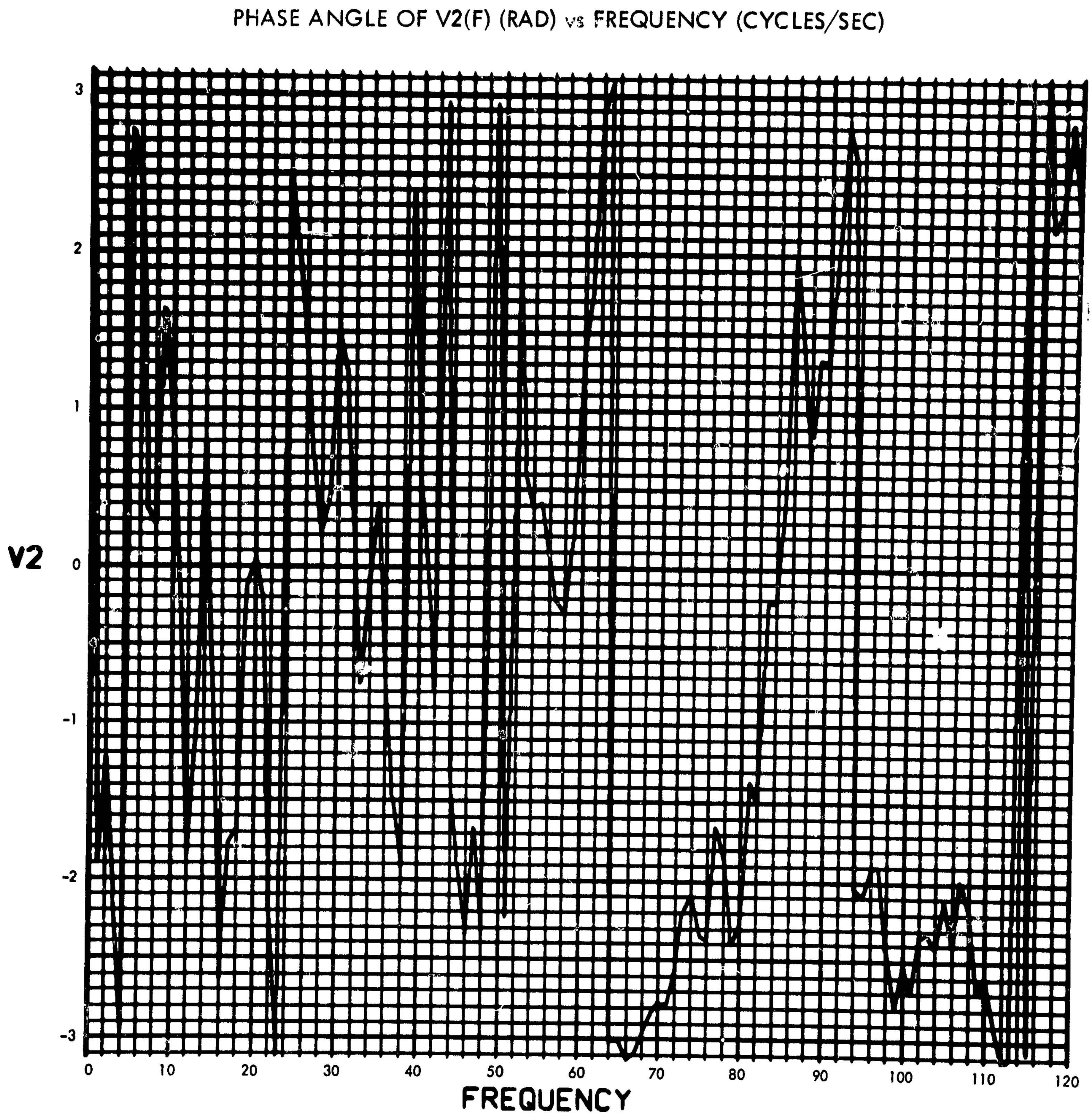

Fig. C-221. Joint 16, acceleration response, Fourier transform, phase angle (pulse 4)

U2(T) (RAD/SEC^2) vs TIME (SEC)

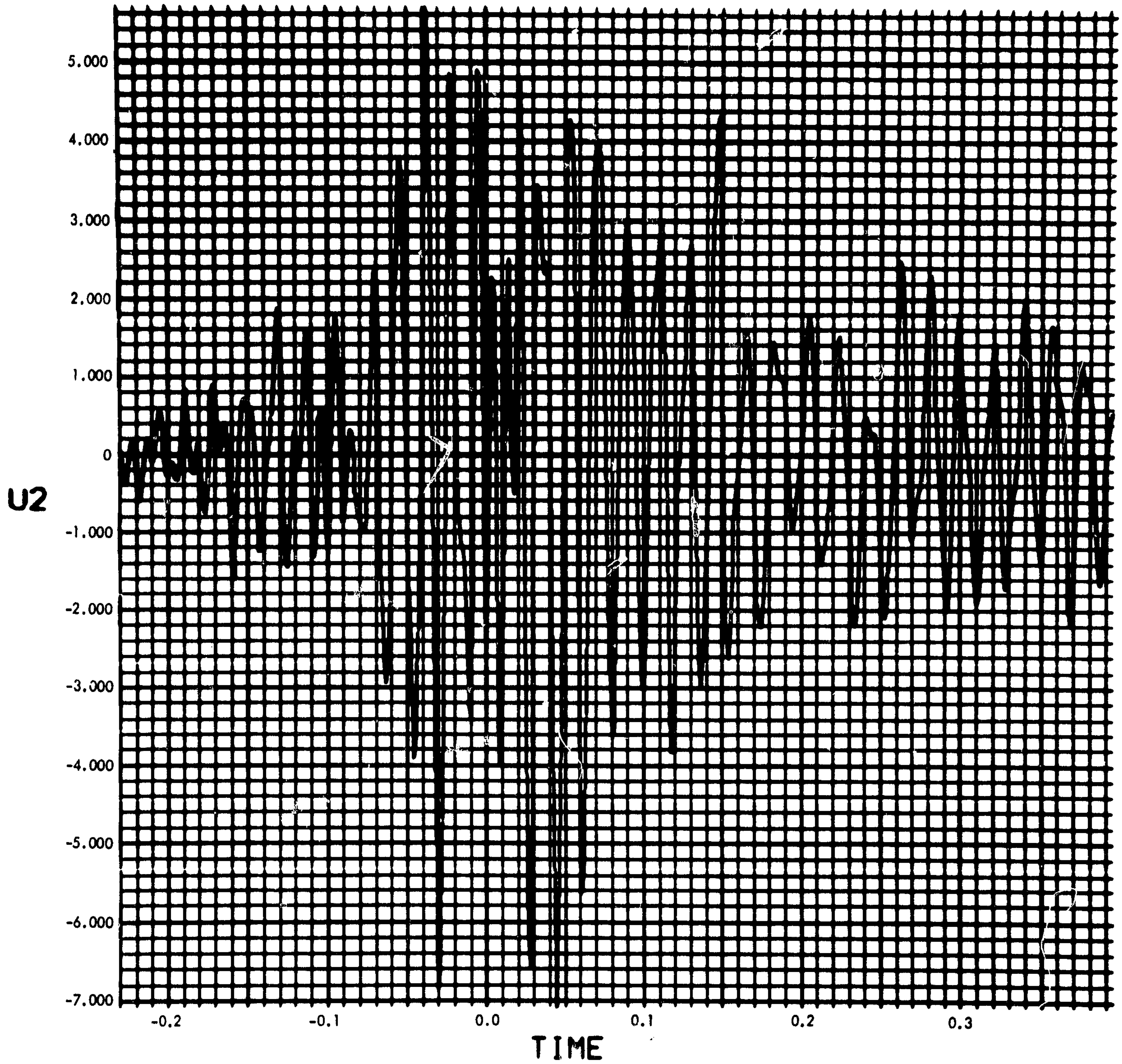

Fig. C-222. Joint 16, acceleration response, timehistory (pulse 4)

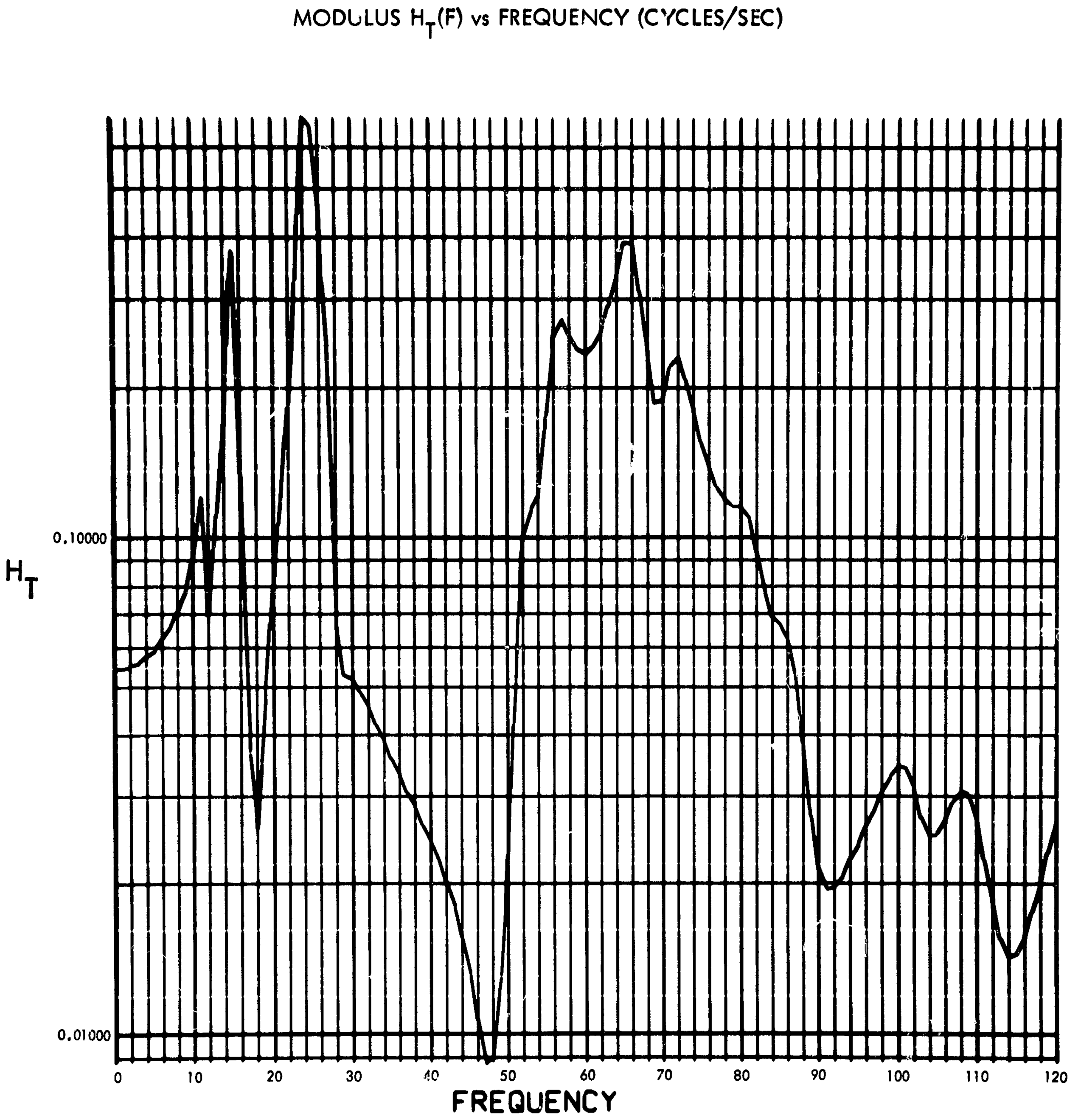

Fig. C-223. Joint 16, torque transfer function, Fourier transform, modulus

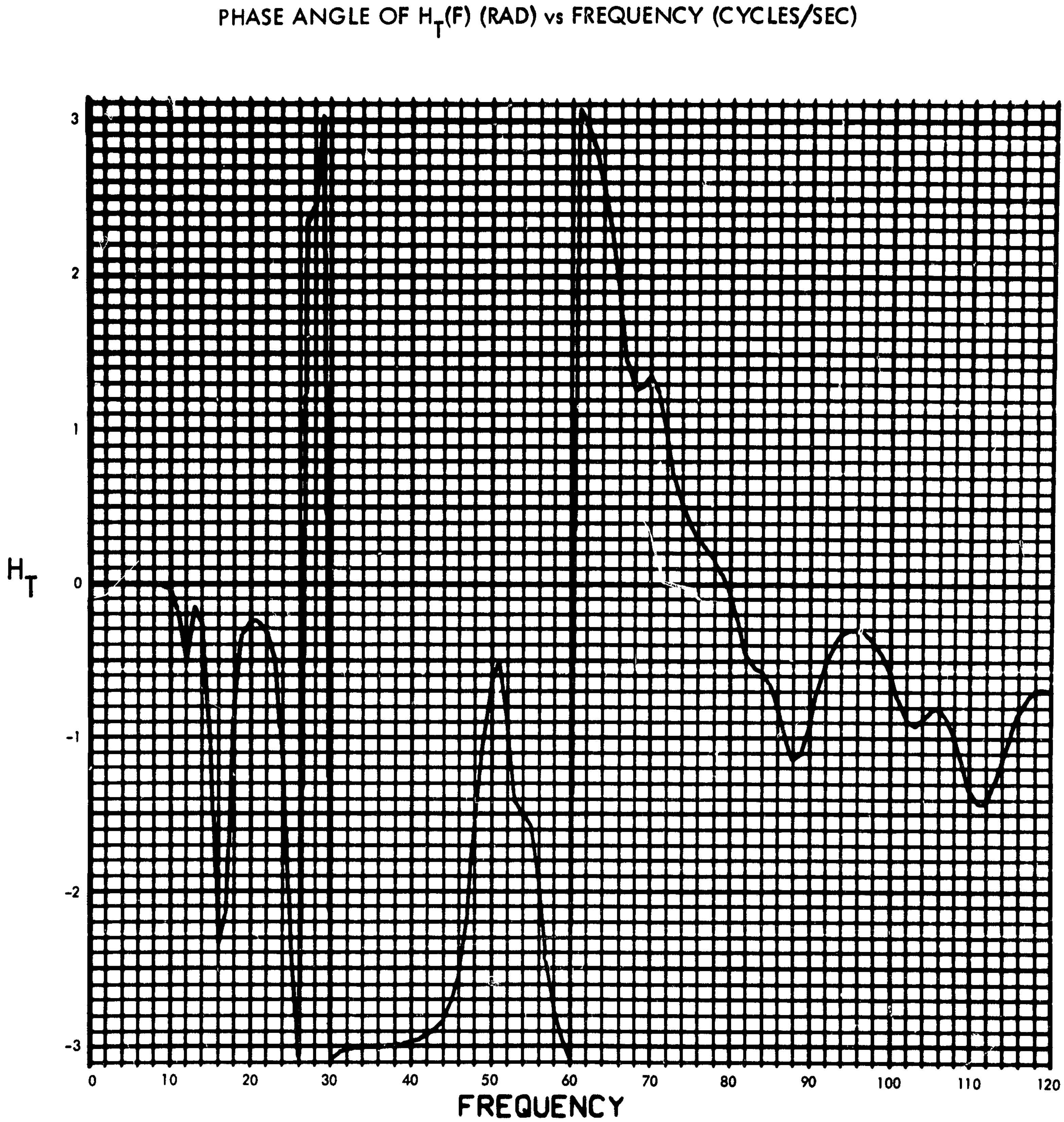

Fig. C-224. Joint 16, torque transfer function, Fourier transform, phase angle

MODULUS OF $F_T(F)$ (LB-IN-SEC) vs FREQUENCY (CYCLES/SEC)

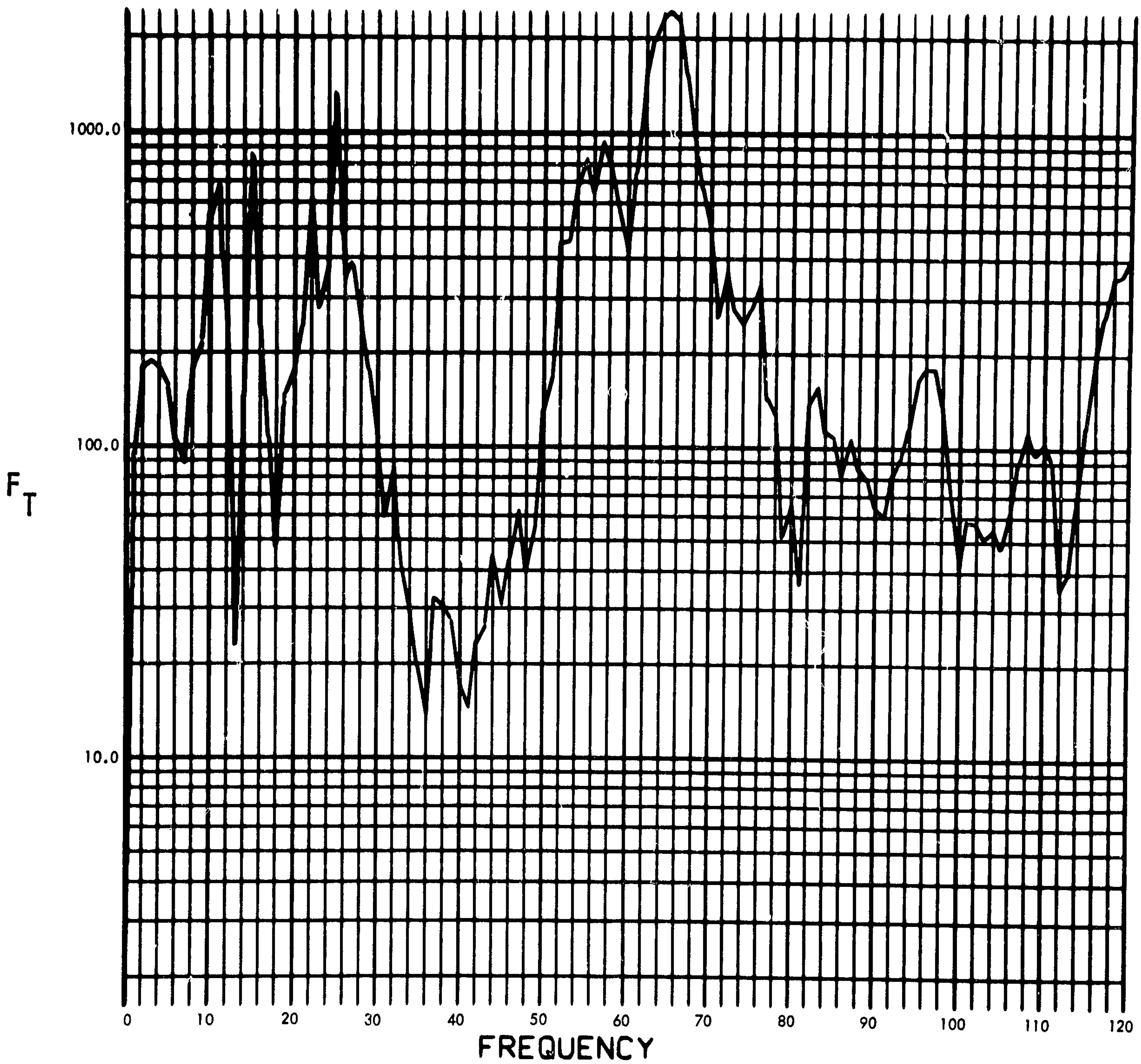

Fig. C-225. Joint 16, torque response function, Fourier transform, modulus (pulse 1)

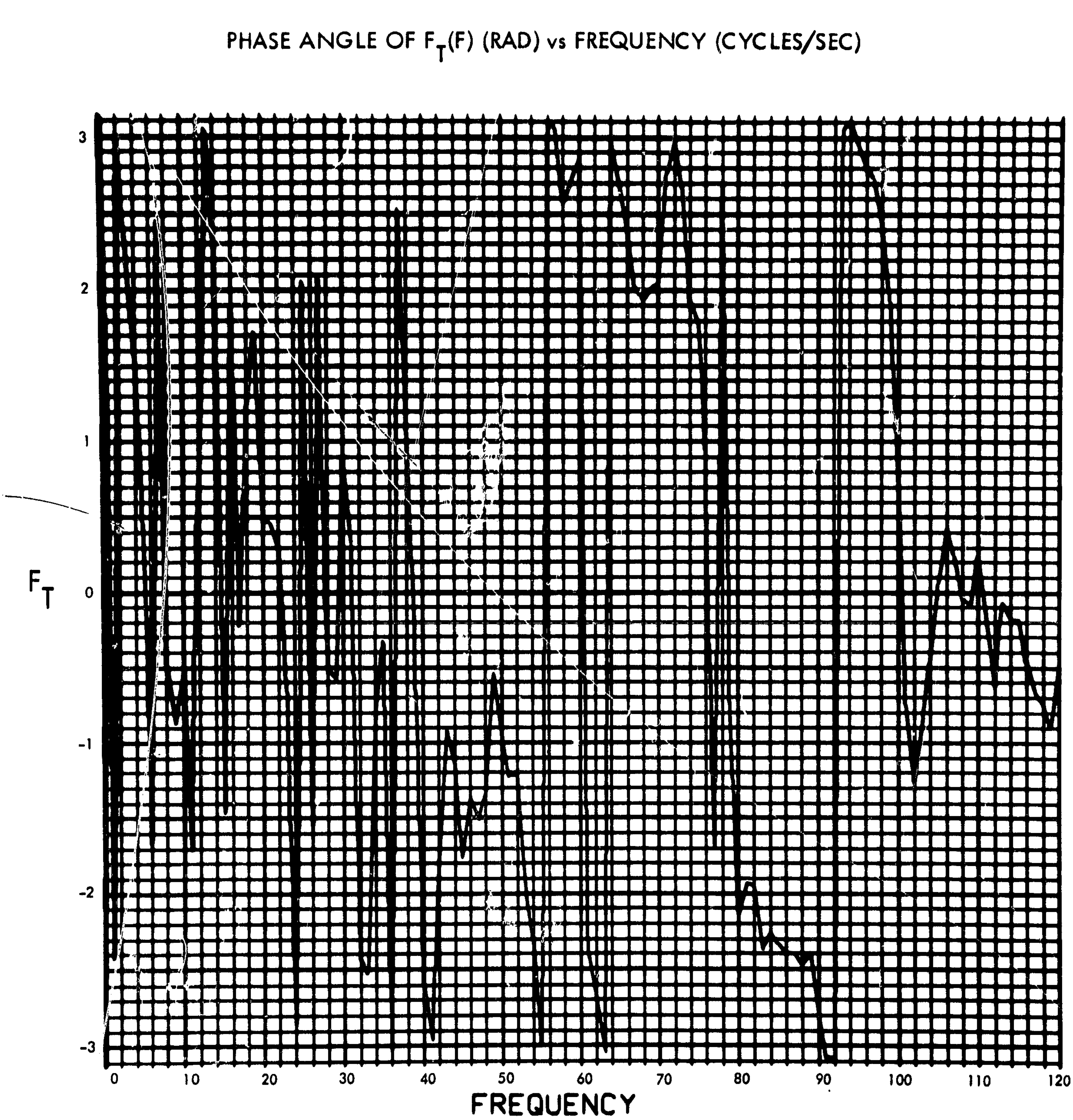

Fig. C-226. Joint 16, torque response function, Fourier transform, phase angle (pulse 1)

T$_{16}$(F) (LB-IN) vs TIME (SEC)

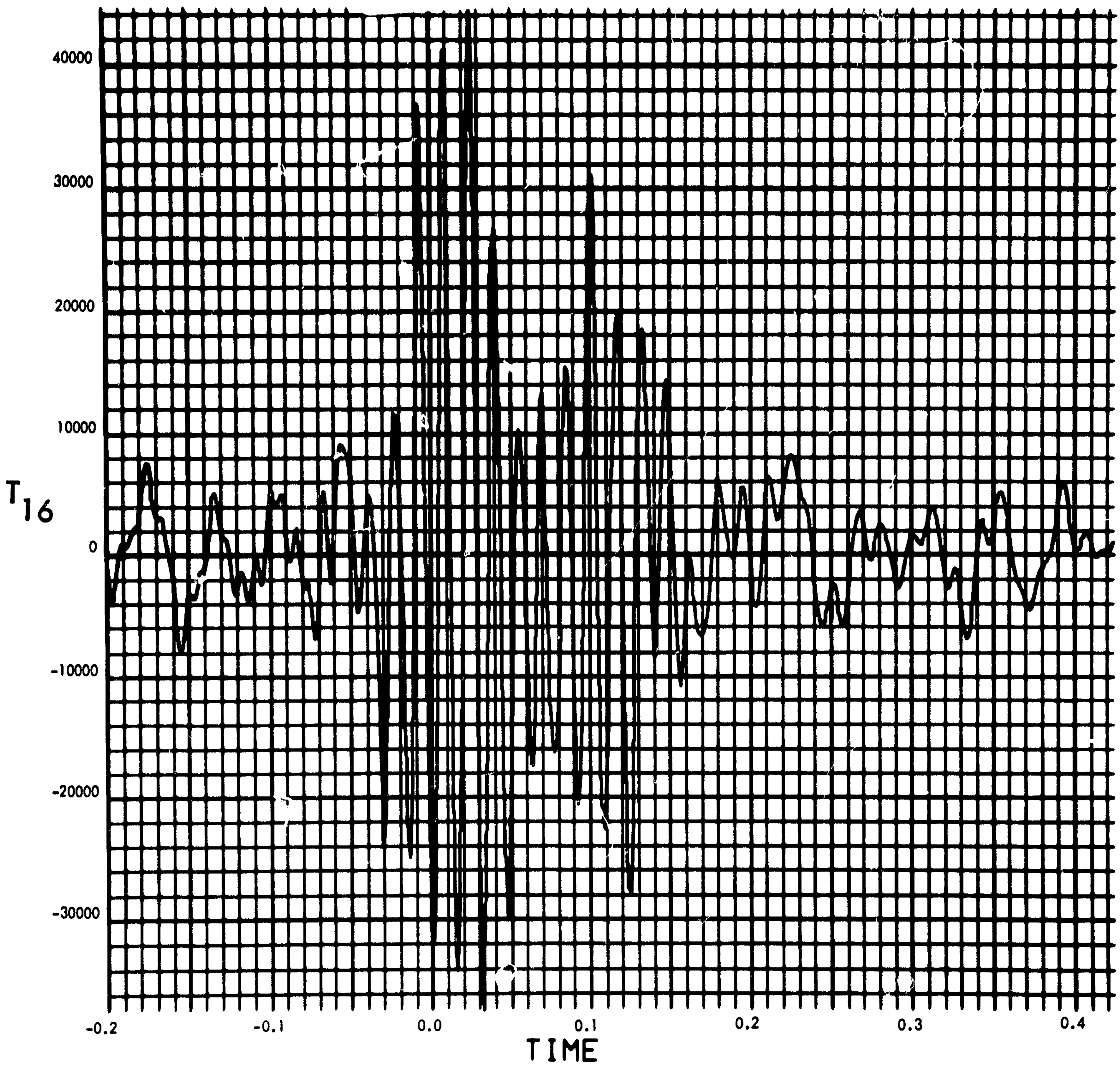

Fig. C-227. Joint 16, torque response, time history (pulse 1)

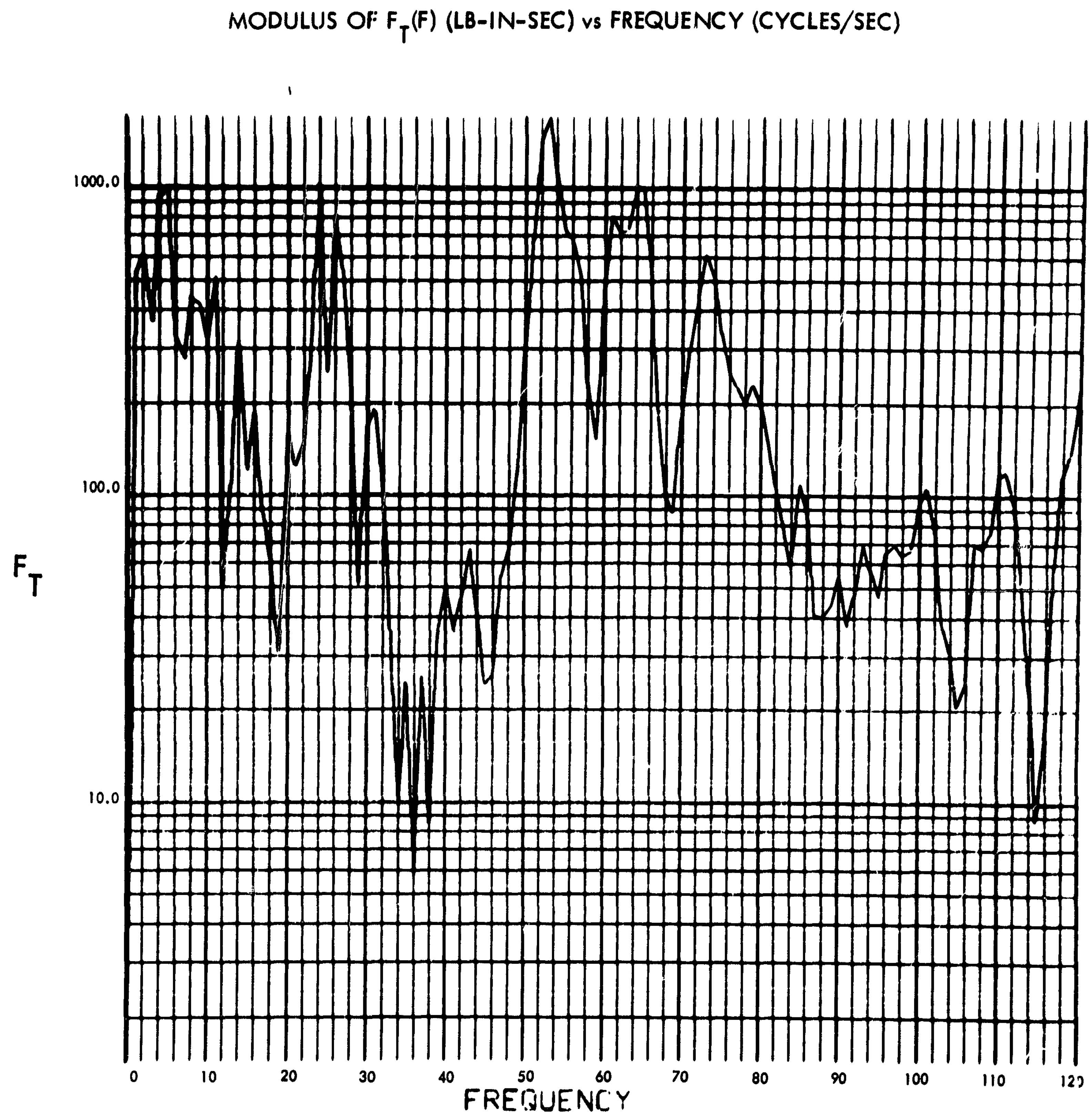

Fig. C-228. Joint 16, torque response function, Fourier transform, modulus (pulse 2)

PHASE ANGLE OF $F_T(F)$ (RAD) vs FREQUENCY (CYCLES/SEC)

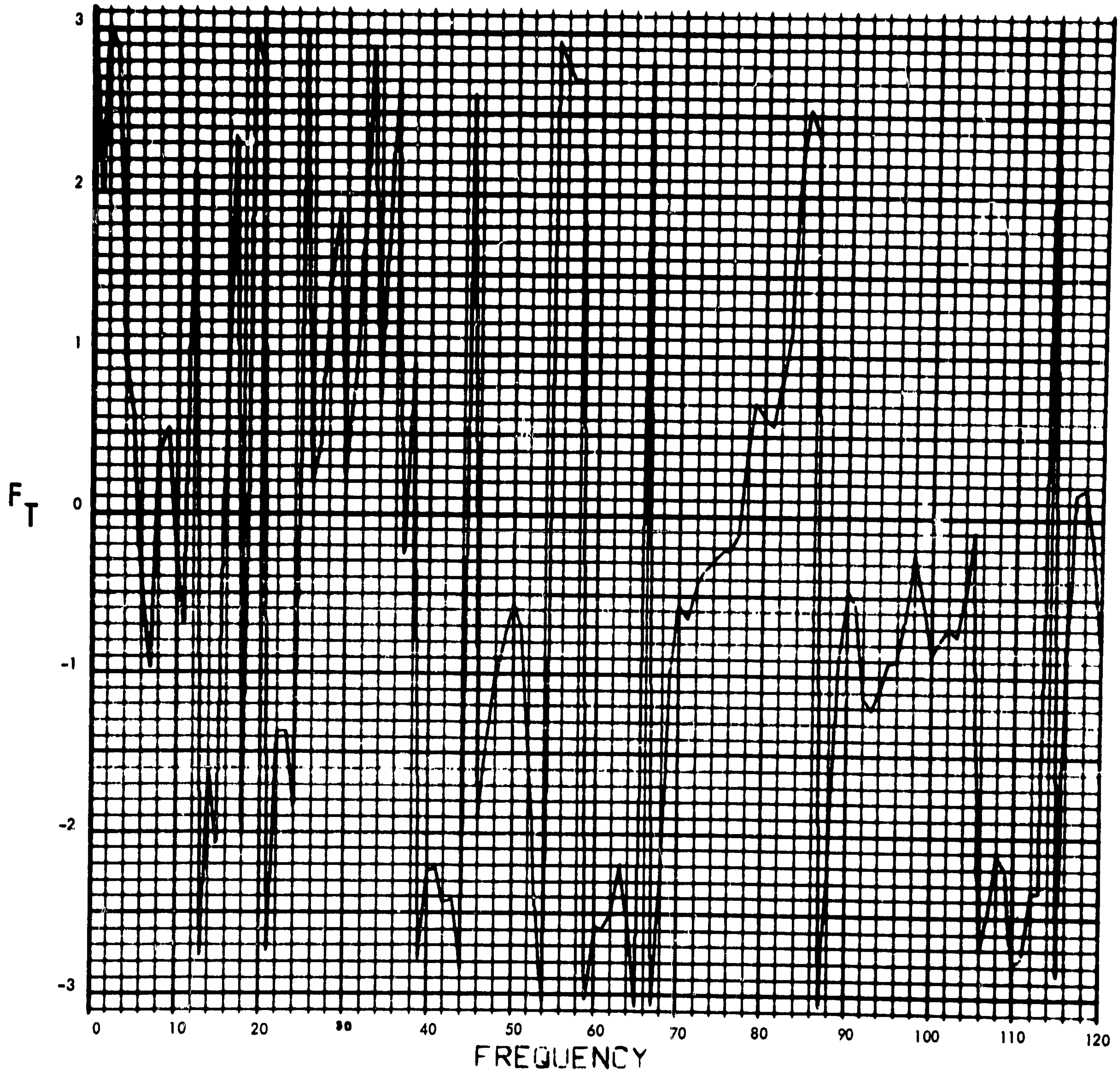

Fig. C-229. Joint 16, torque response function, Fourier transform, phase angle (pulse 2)

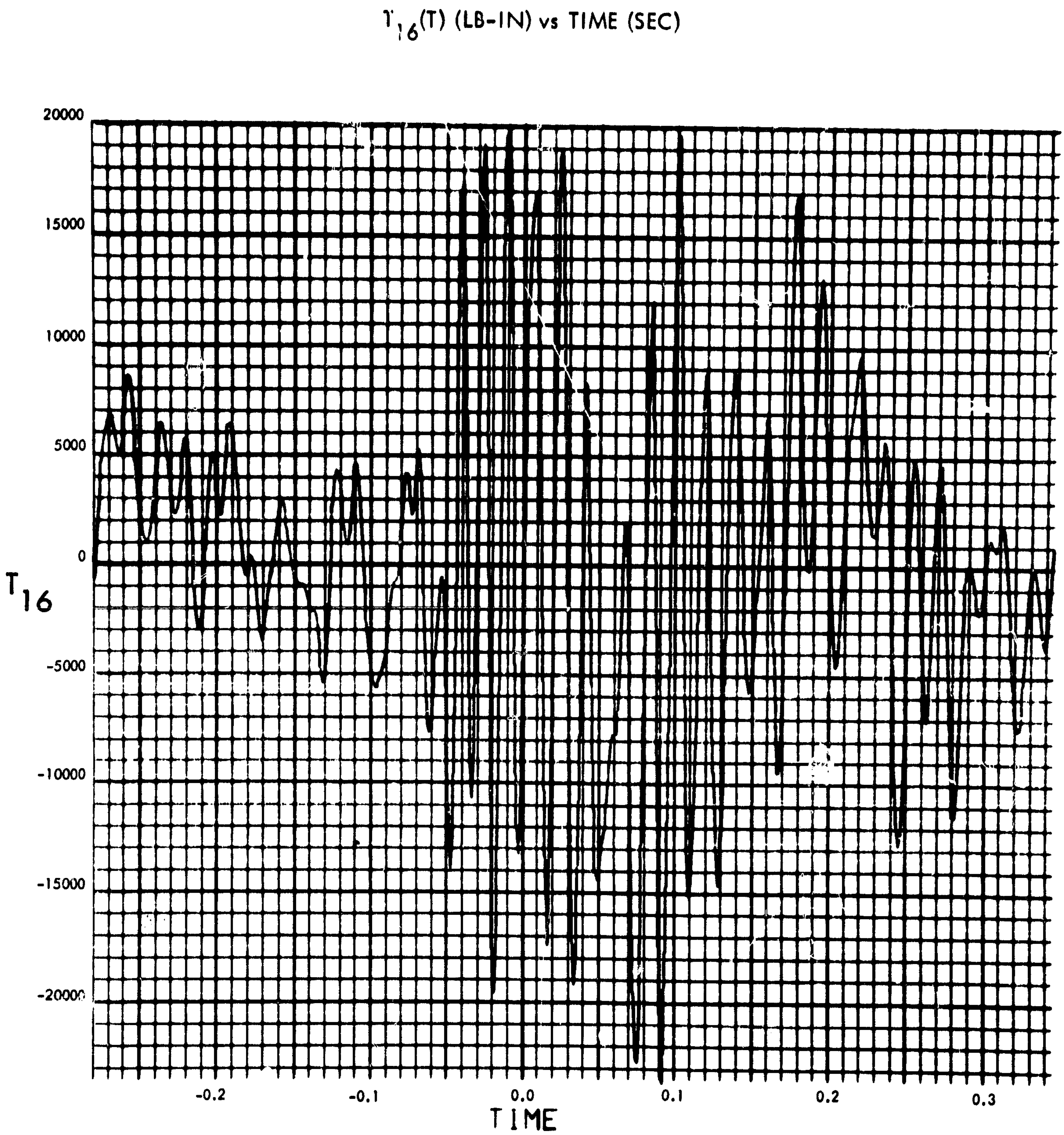

Fig. C-230. Joint 16, torque response, time history (pulse 2)

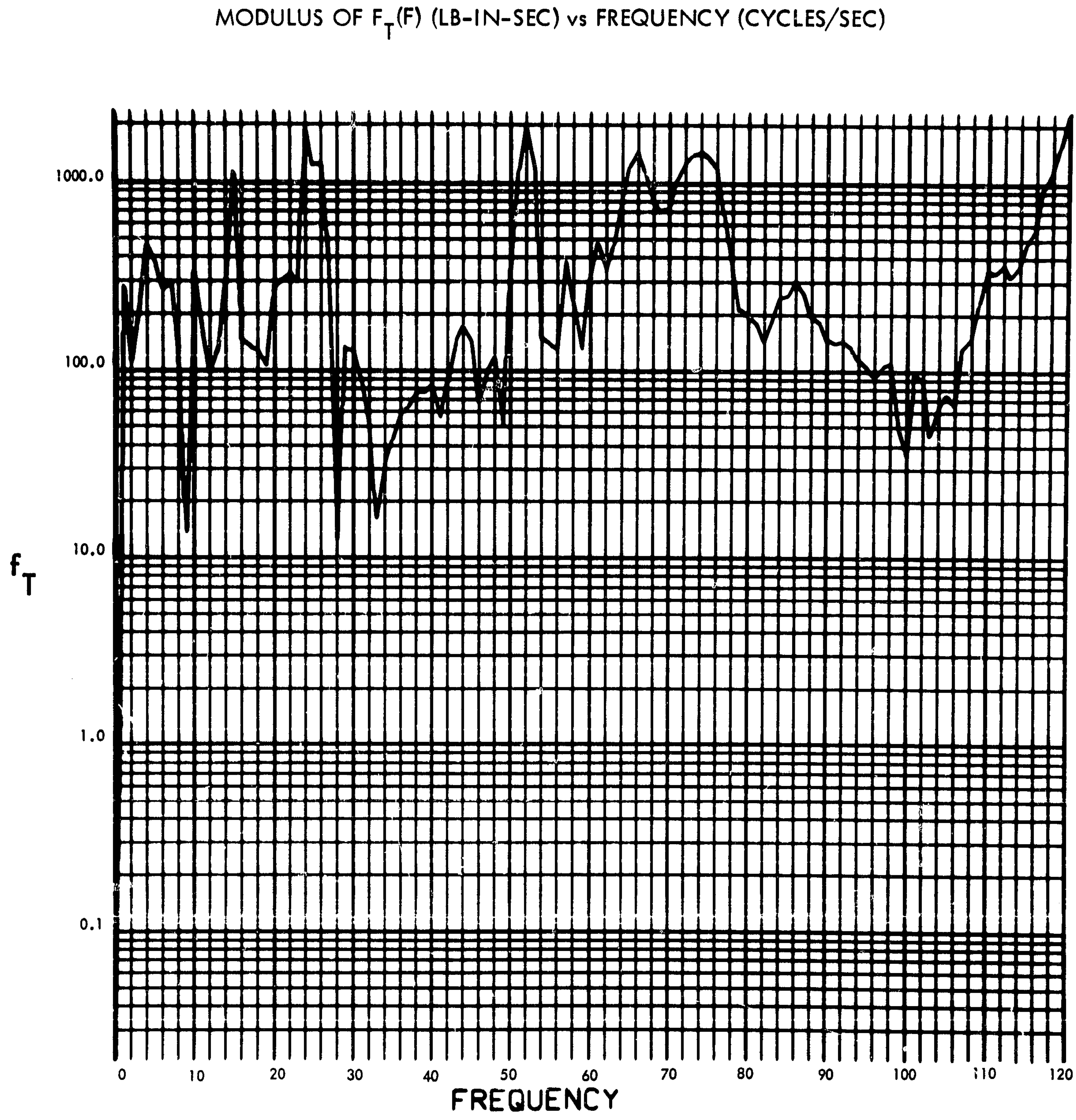

Fig. C-231. Joint 16, torque response function, Fourier transform, modulus (pulse 3)

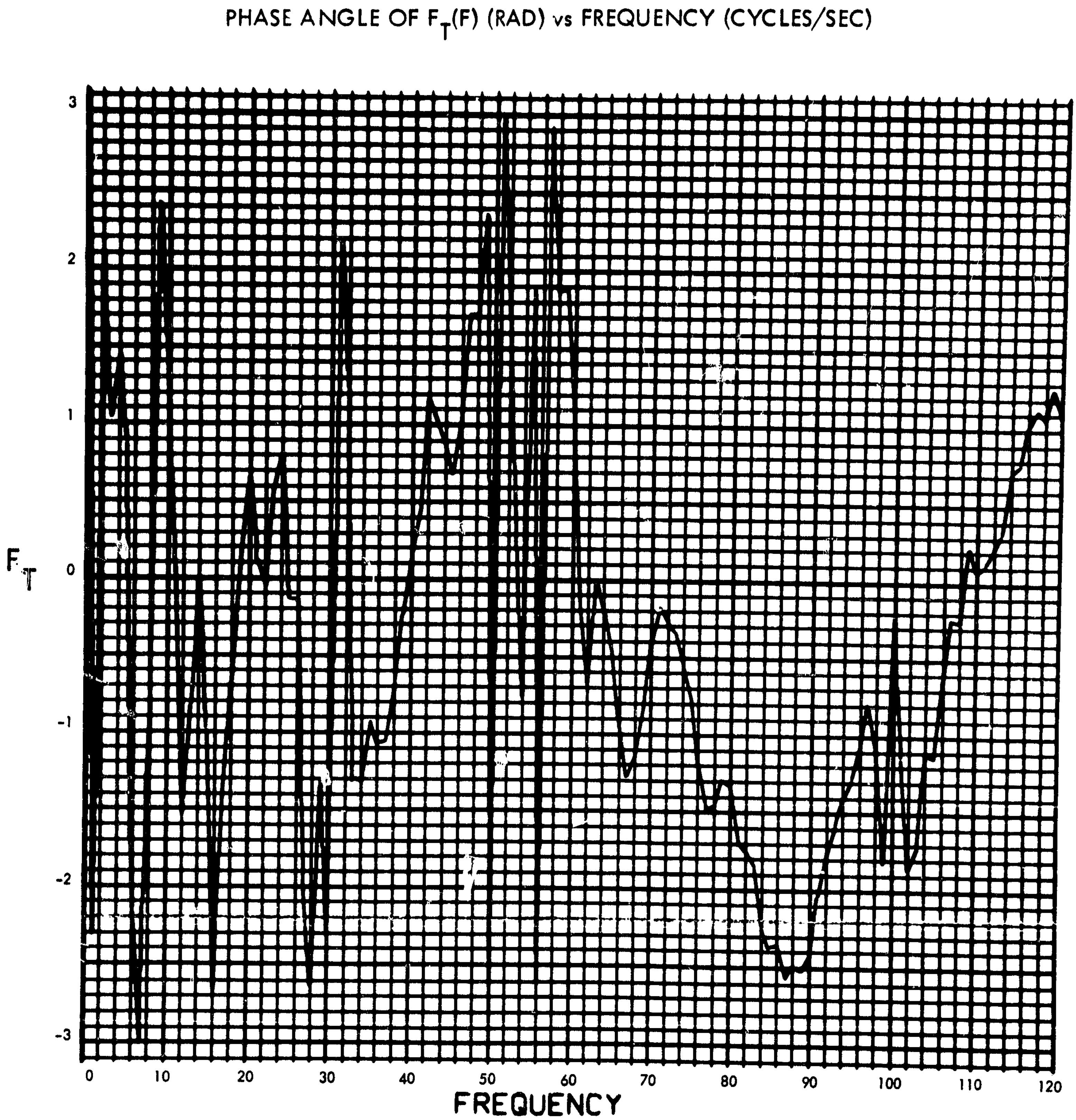

Fig. C-232. Joint 16, torque response function, Fourier transform, phase angle (pulse 3)

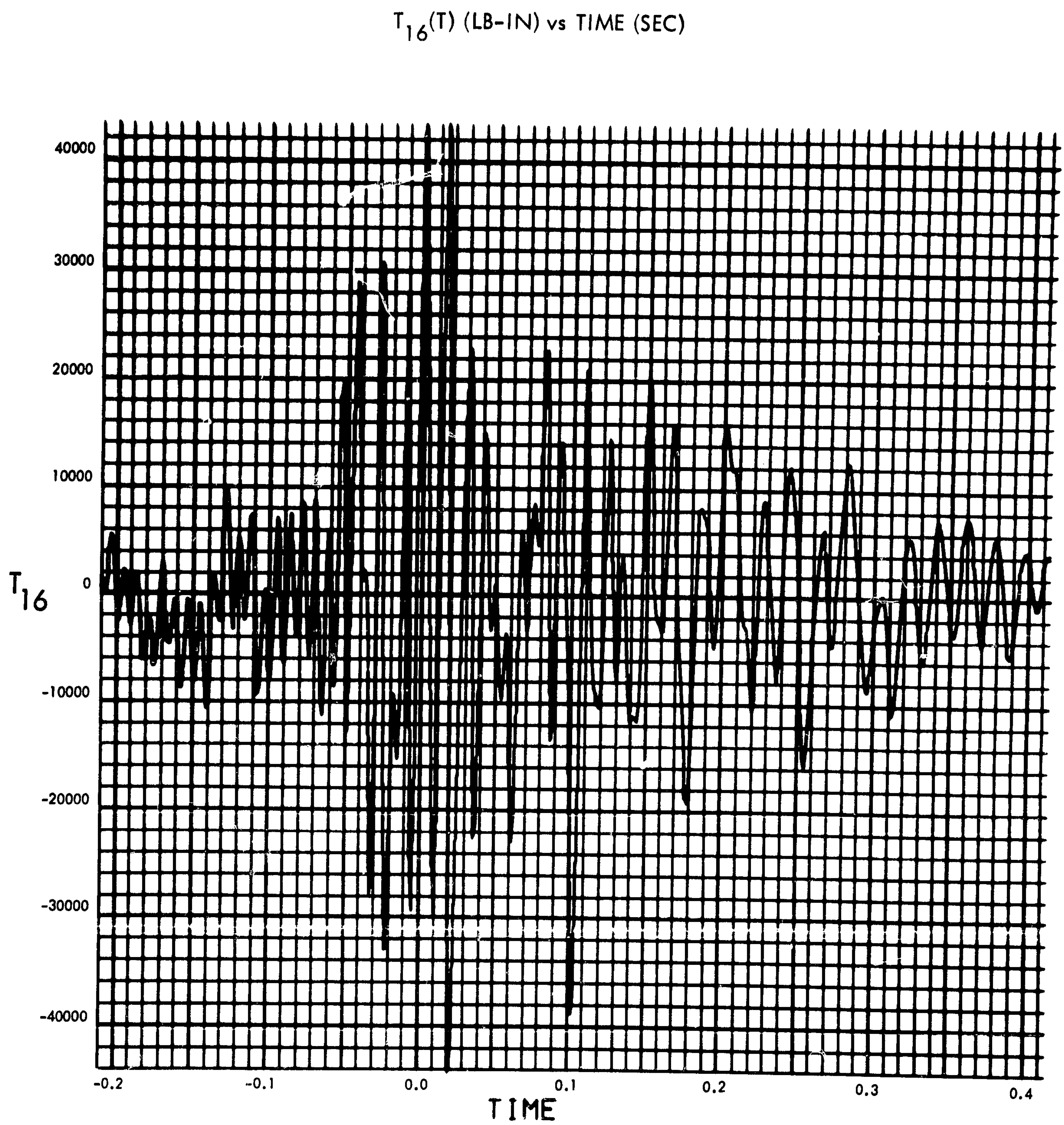

Fig. C-233. Joint 16, torque response, time history (pulse 3)

MODULUS OF $F_T(F)$ (LB-IN-SEC) vs FREQUENCY (CYCLES/SEC)

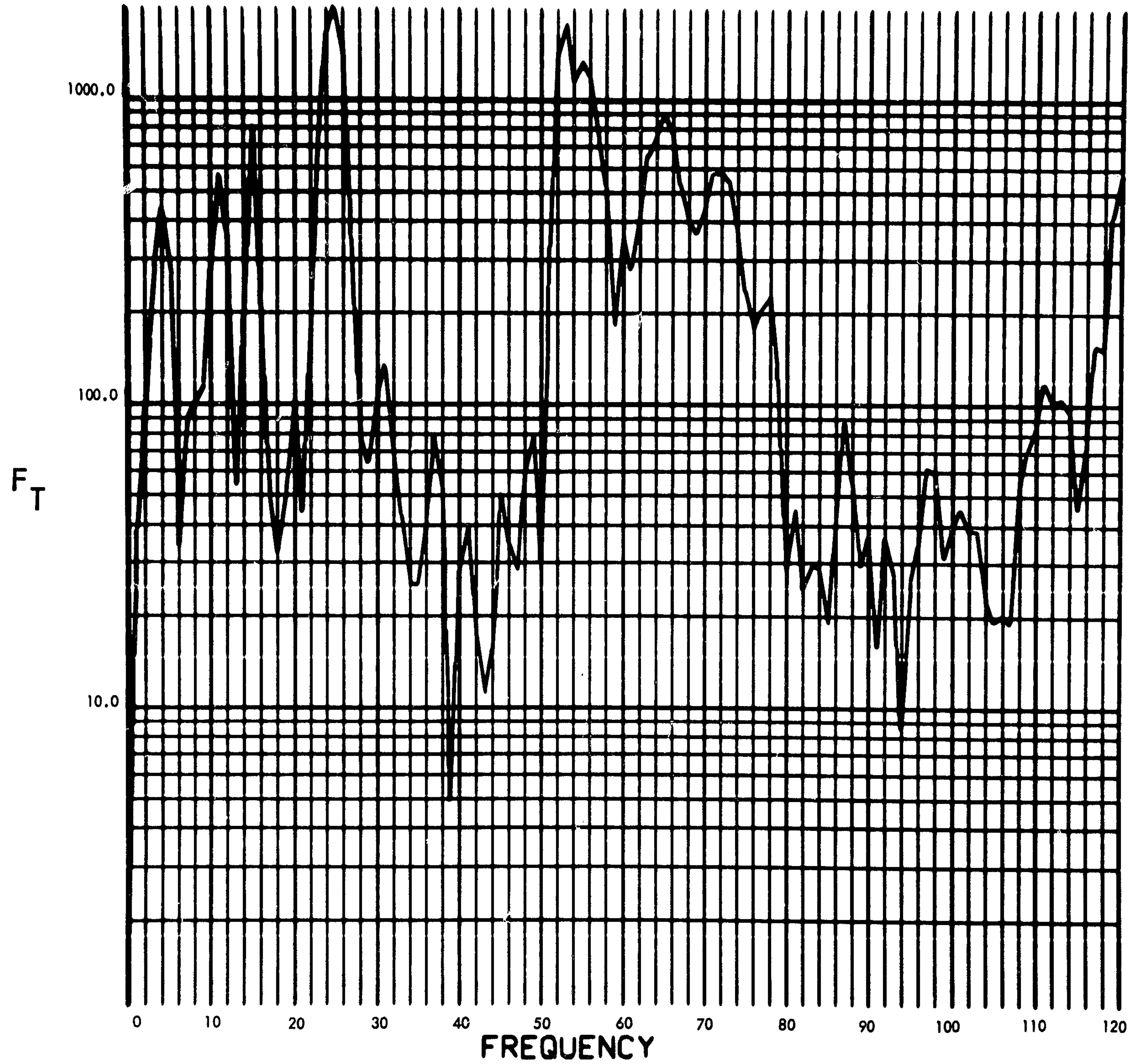

Fig. C-234. Joint 16, torque response function, Fourier transform, modulus (pulse 4)

PHASE ANGLE OF $F_T(F)$ (RAD) vs FREQUENCY (CYCLES/SEC)

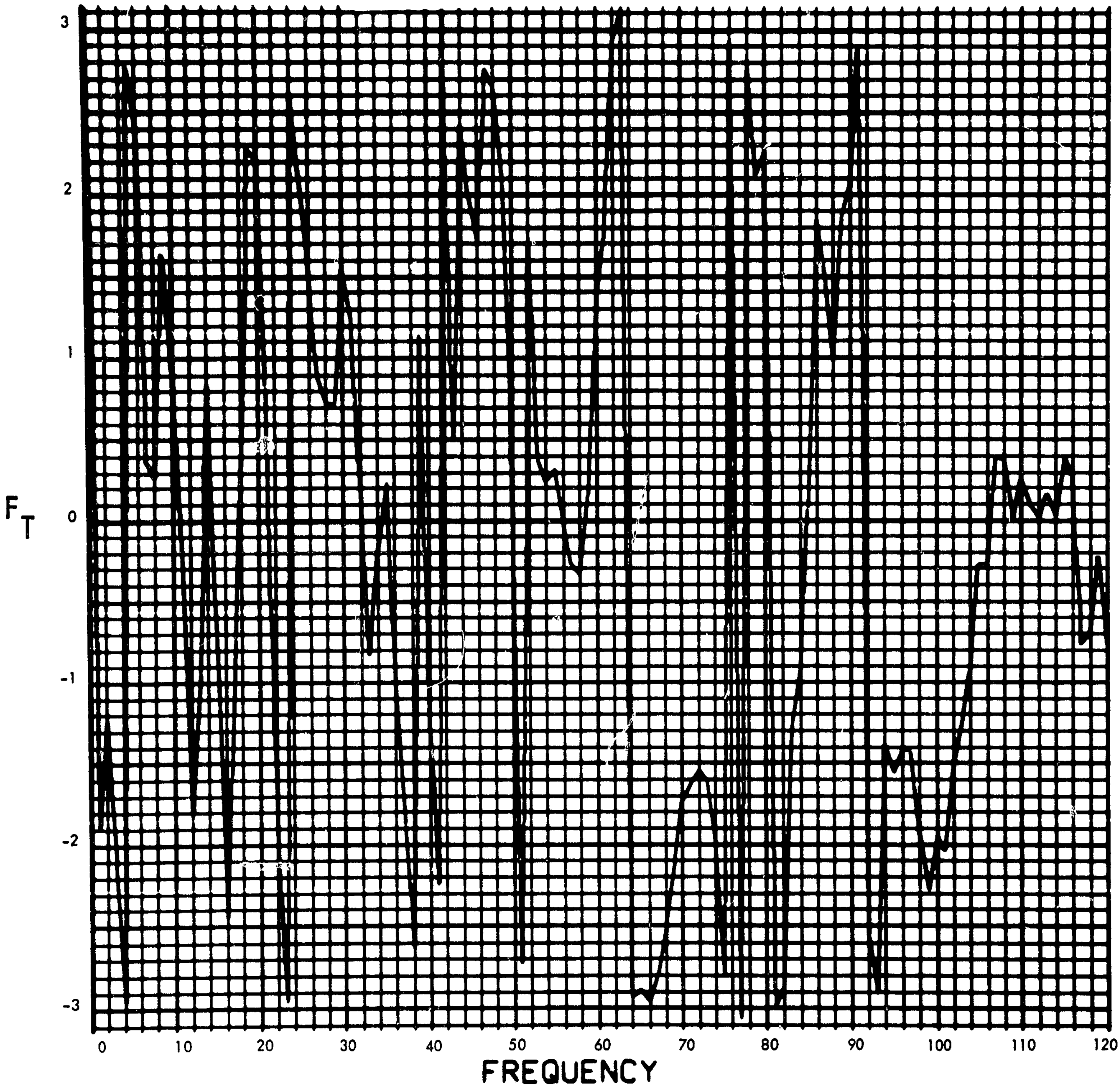

Fig. C-235. Joint 16, torque response function, Fourier transform, phase angle (pulse 4)

$T_{16}(T)$ (LB-IN) vs TIME (SEC)

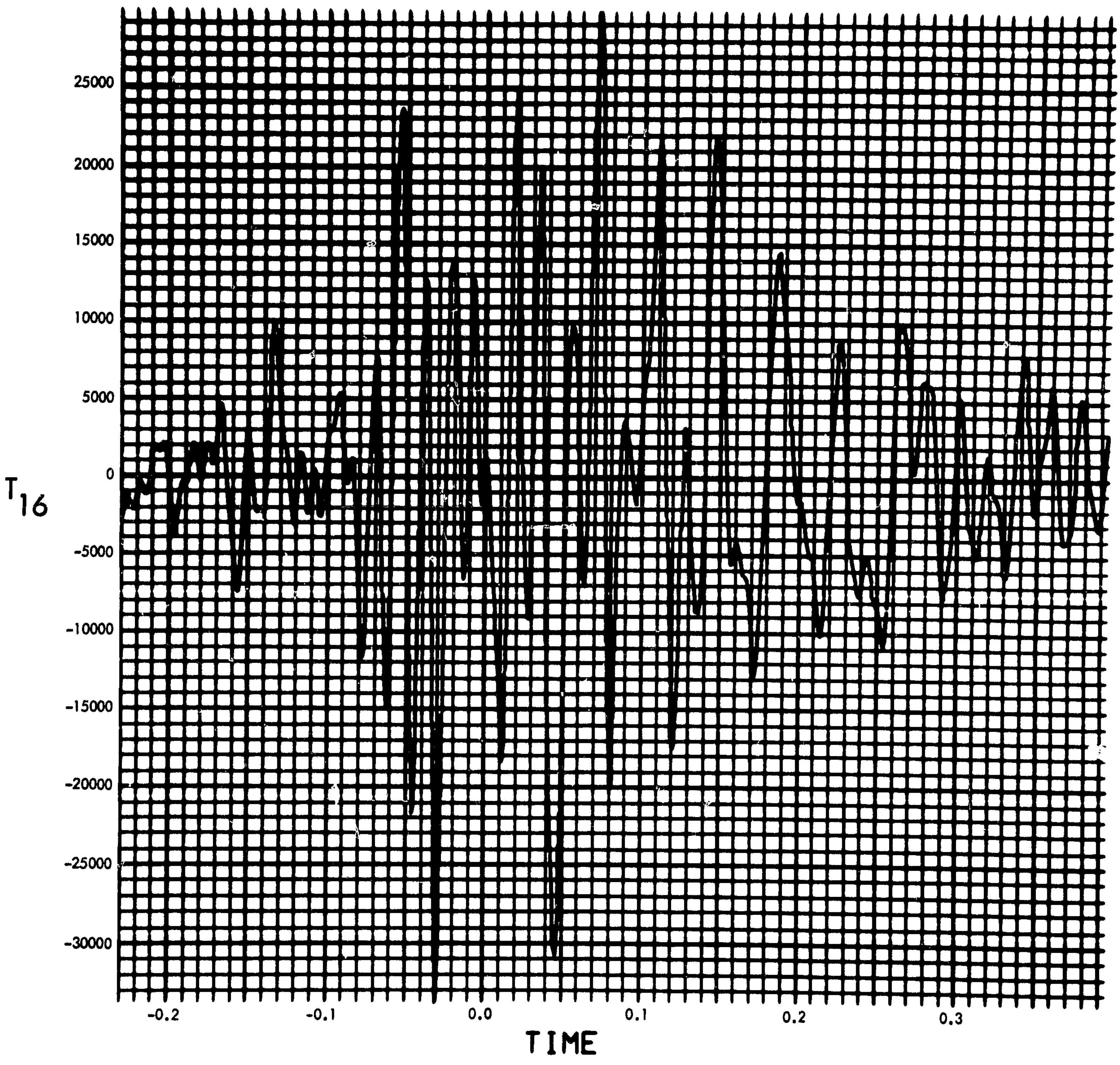

Fig. C-236. Joint 16, torque response, time history (pulse 4)

MODULUS H2(F) (1/LB-IN-SEC^2) vs FREQUENCY (CYCLES/SEC)

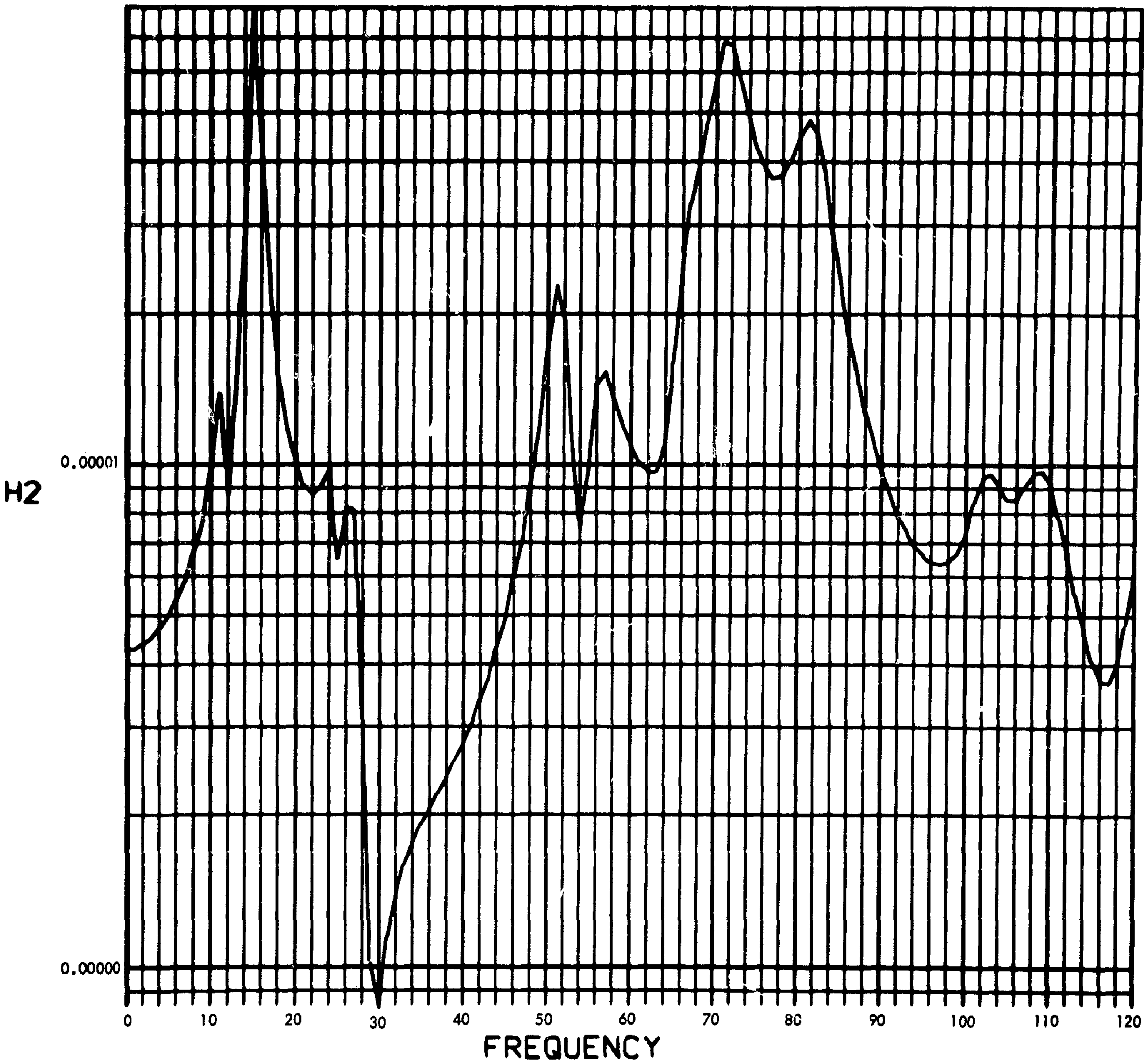

Fig. C-237. Joint 16, acceleration transfer function, Fourier transform, modulus

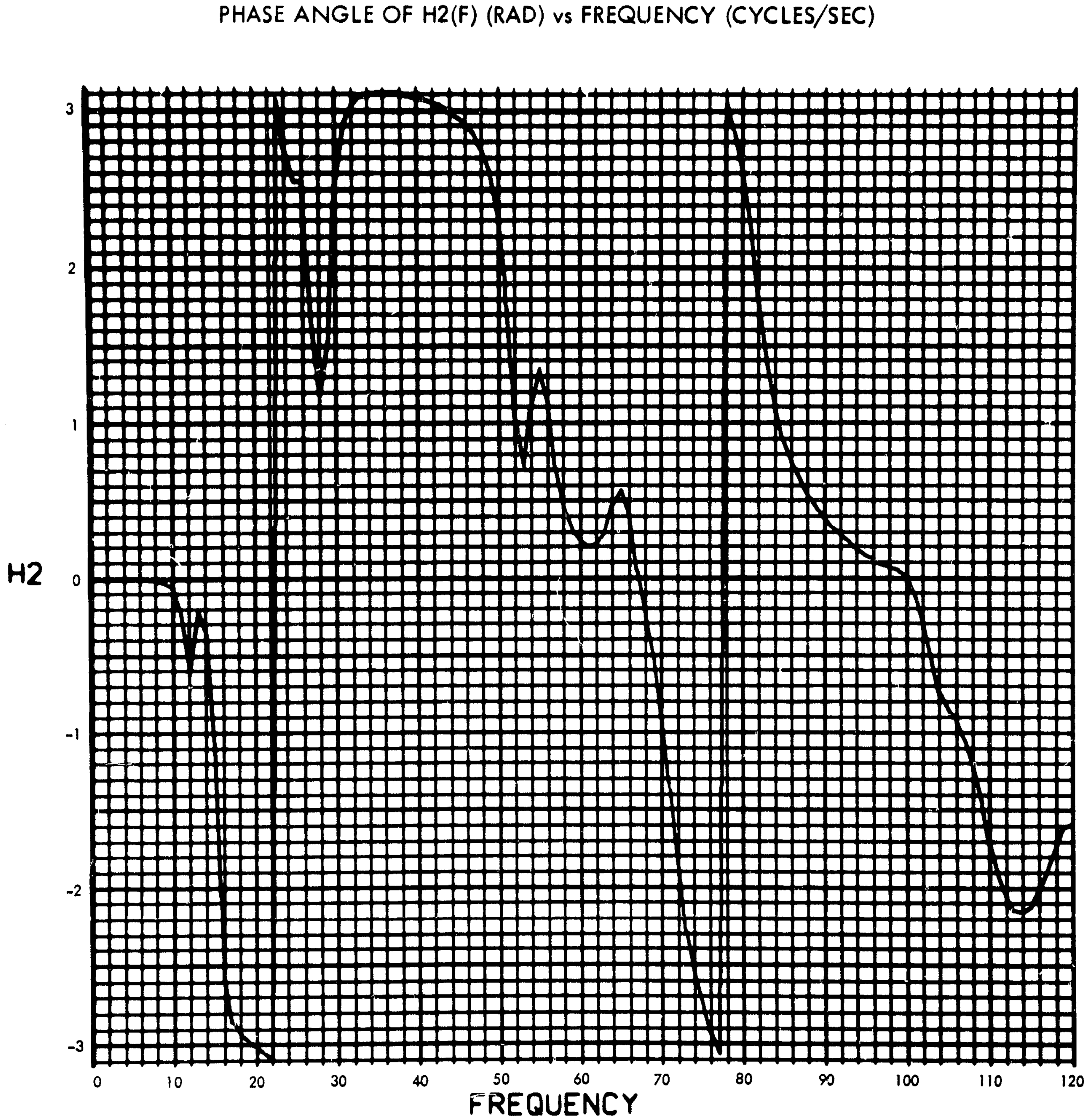

Fig. C-238. Joint 17, acceleration transfer function, Fourier transform, phase angle

MODULUS OF V2(F) (RAD/SEC) vs FREQUENCY (CYCLES/SEC)

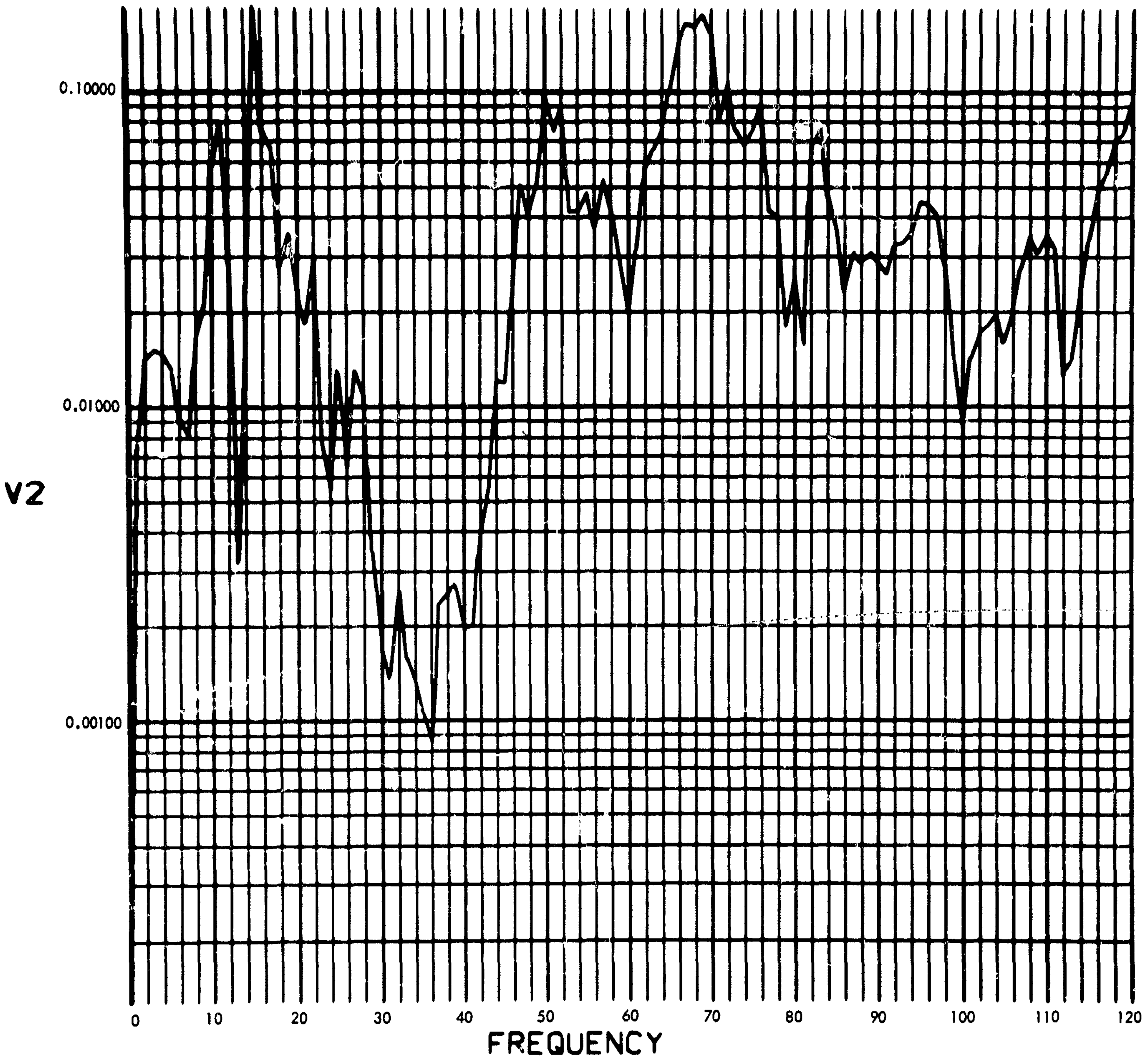

Fig. C-239. Joint 17, acceleration response, Fourier transform, modulus (pulse 1)

PHASE ANGLE OF V2(F) (RAD) vs FREQUENCY (CYCLES/SEC)

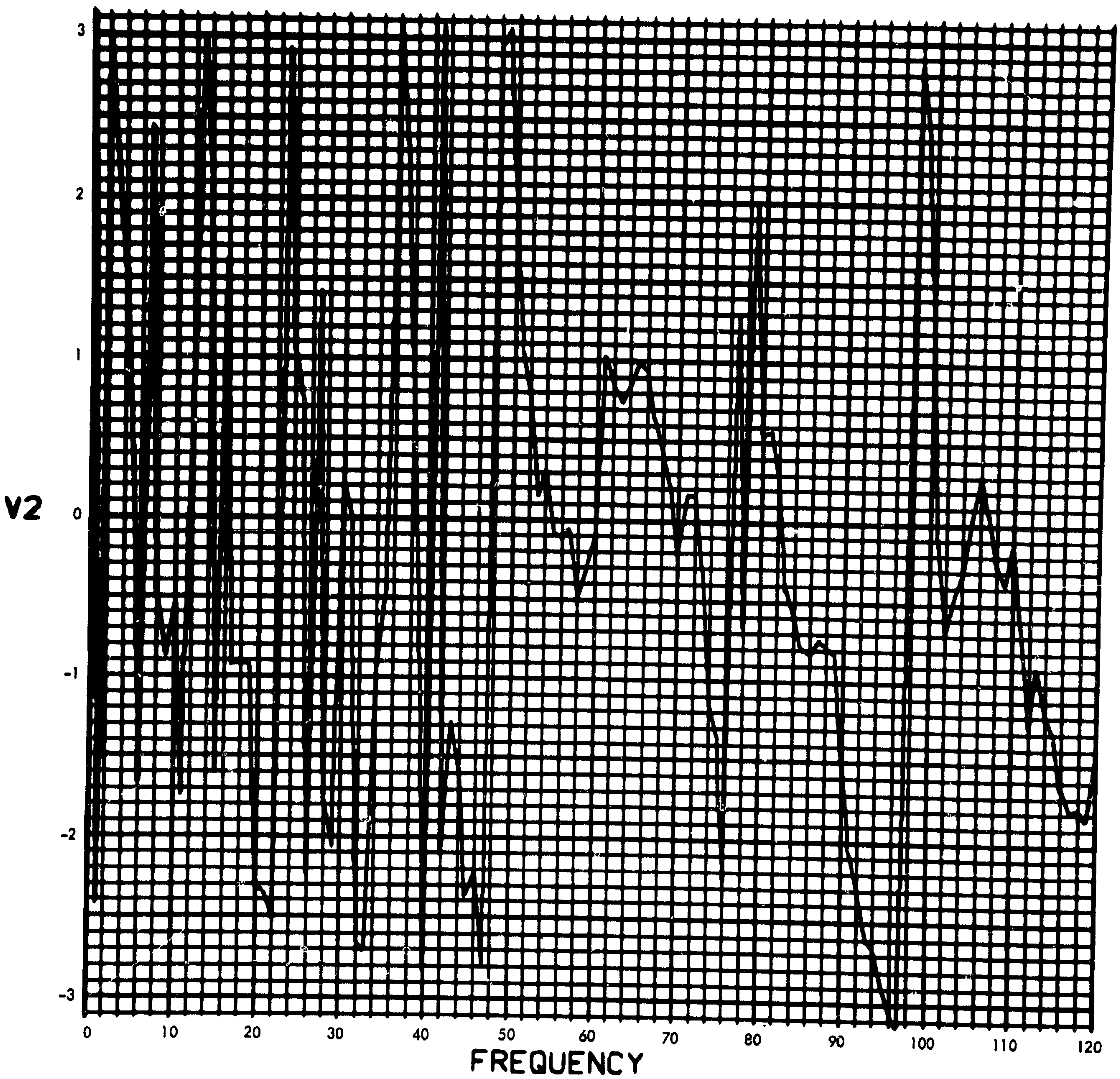

Fig. C-240. Joint 17, acceleration response, Fourier transform, phase angle (pulse 1)

U2(T) (RAD/SEC^2) vs TIME (SEC)

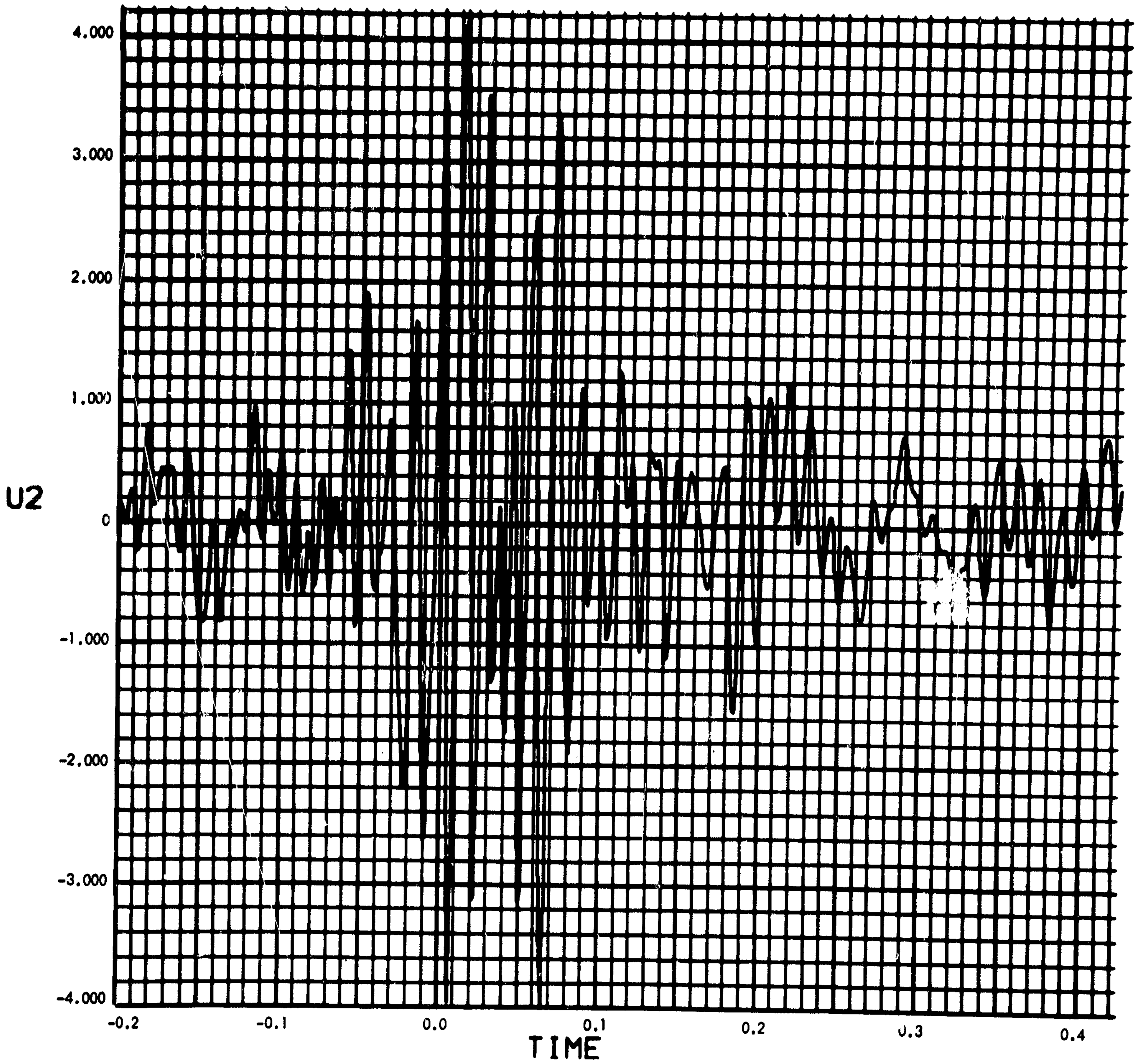

Fig. C-241. Joint 17, acceleration response, time history (pulse 1)

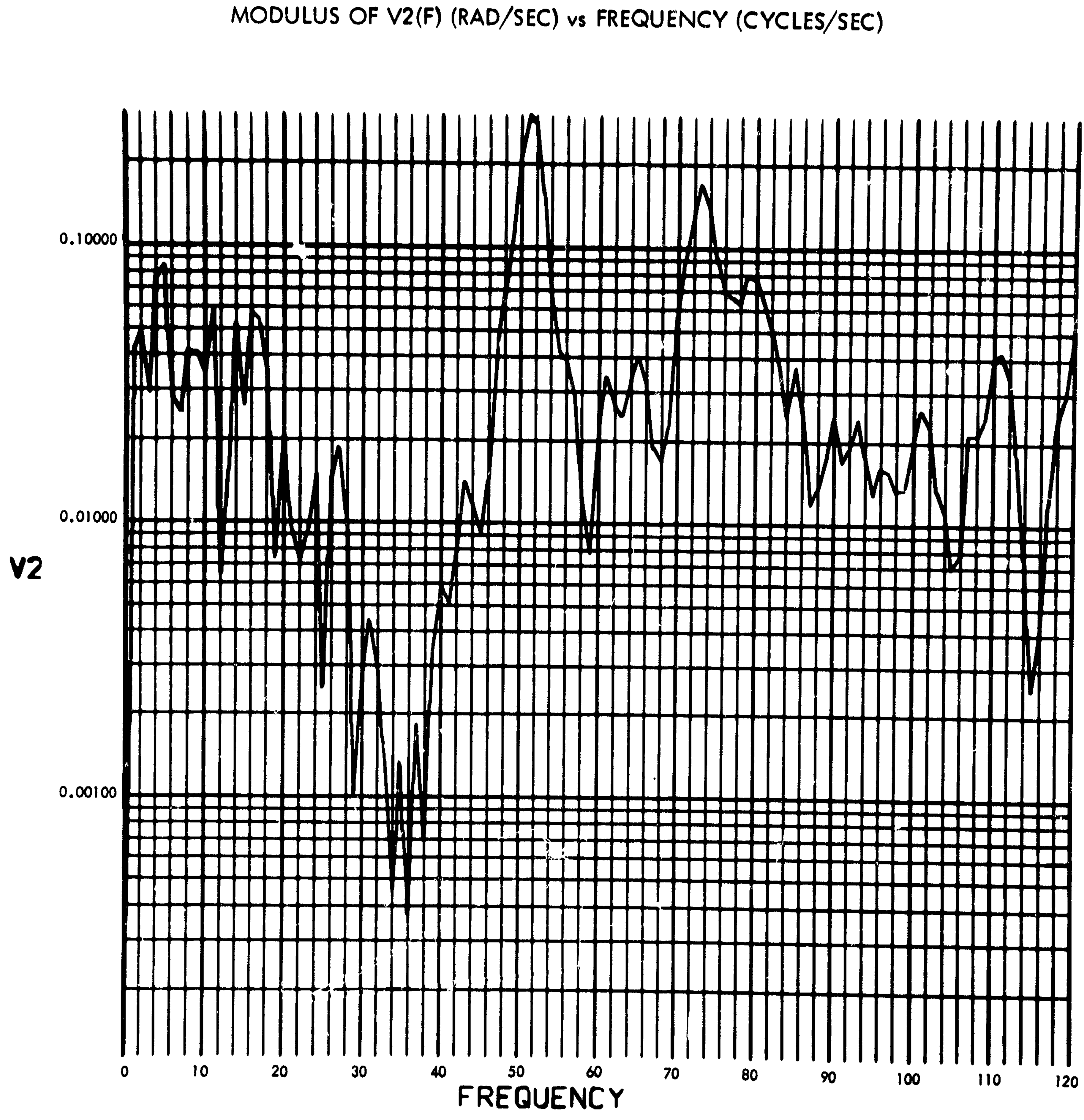

Fig. C-242. Joint 17, acceleration response, Fourier transform, modulus (pulse 2)

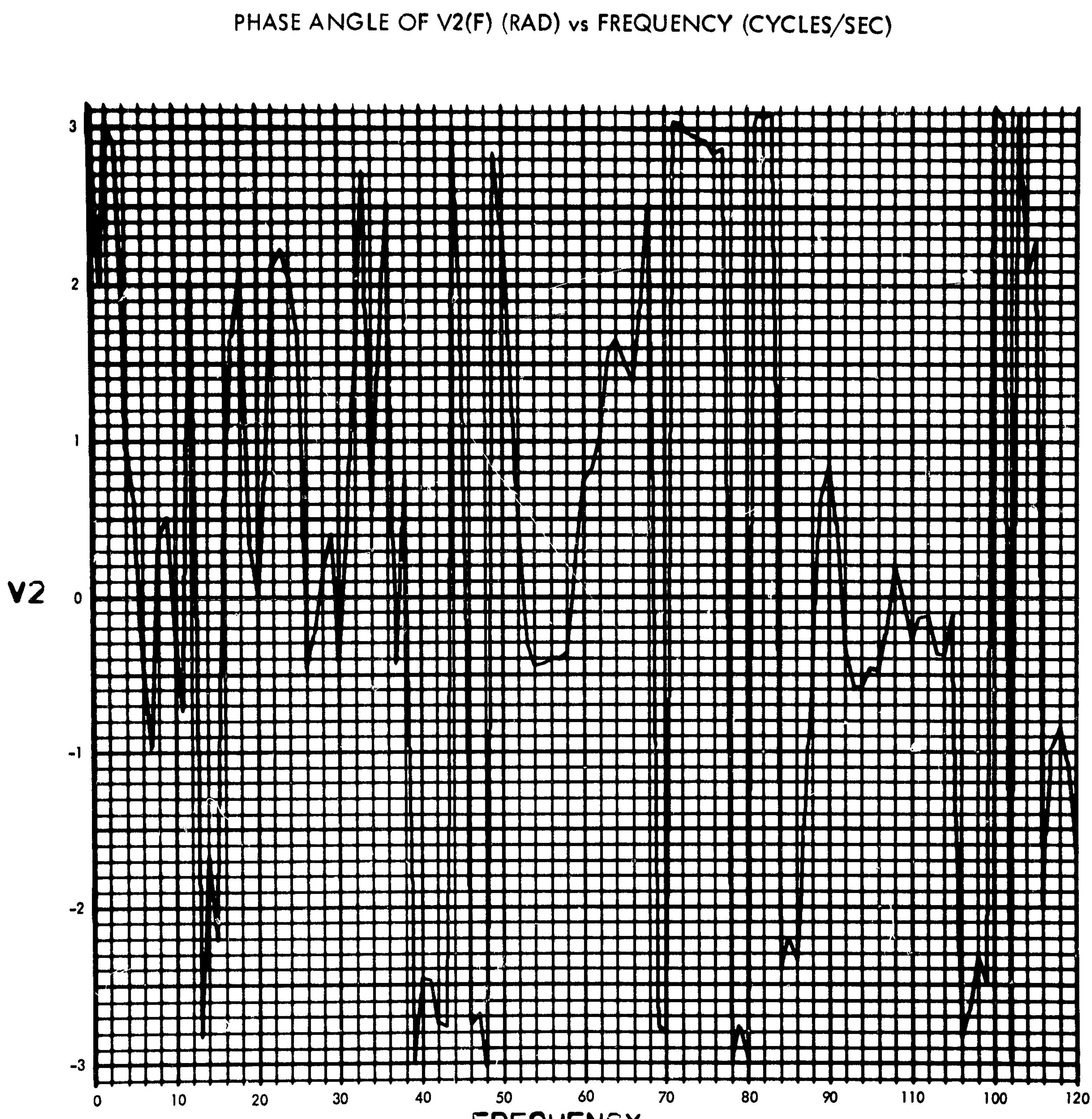

Fig. C-243. Joint 17, acceleration response, Fourier transform, phase angle (pulse 2)

U2(T) (RAD/SEC^2) vs TIME (SEC)

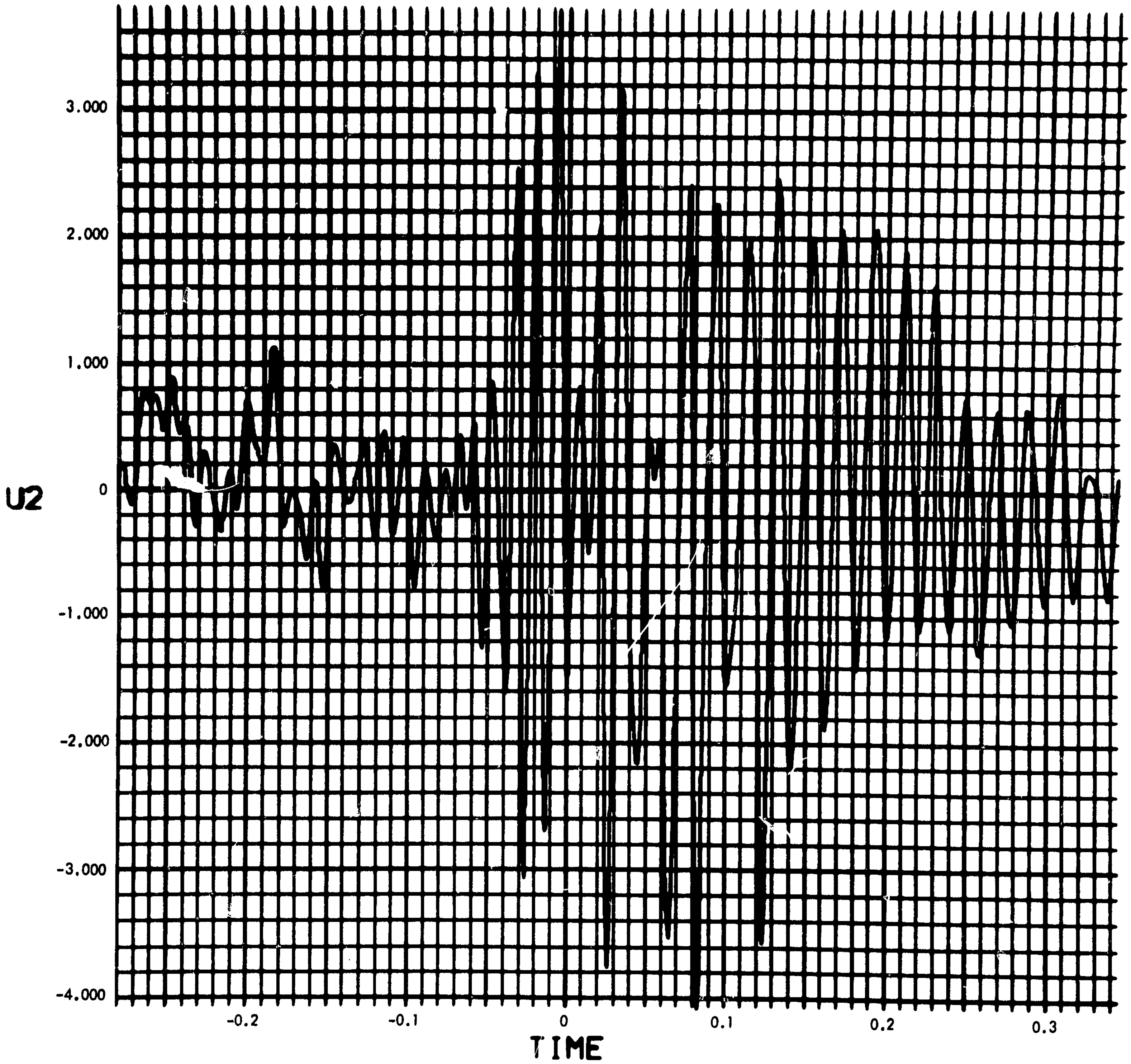

Fig. C-244. Joint 17, acceleration response, time history (pulse 2)

MODULUS OF V2(F) (RAD/SEC) vs FREQUENCY (CYCLES/SEC)

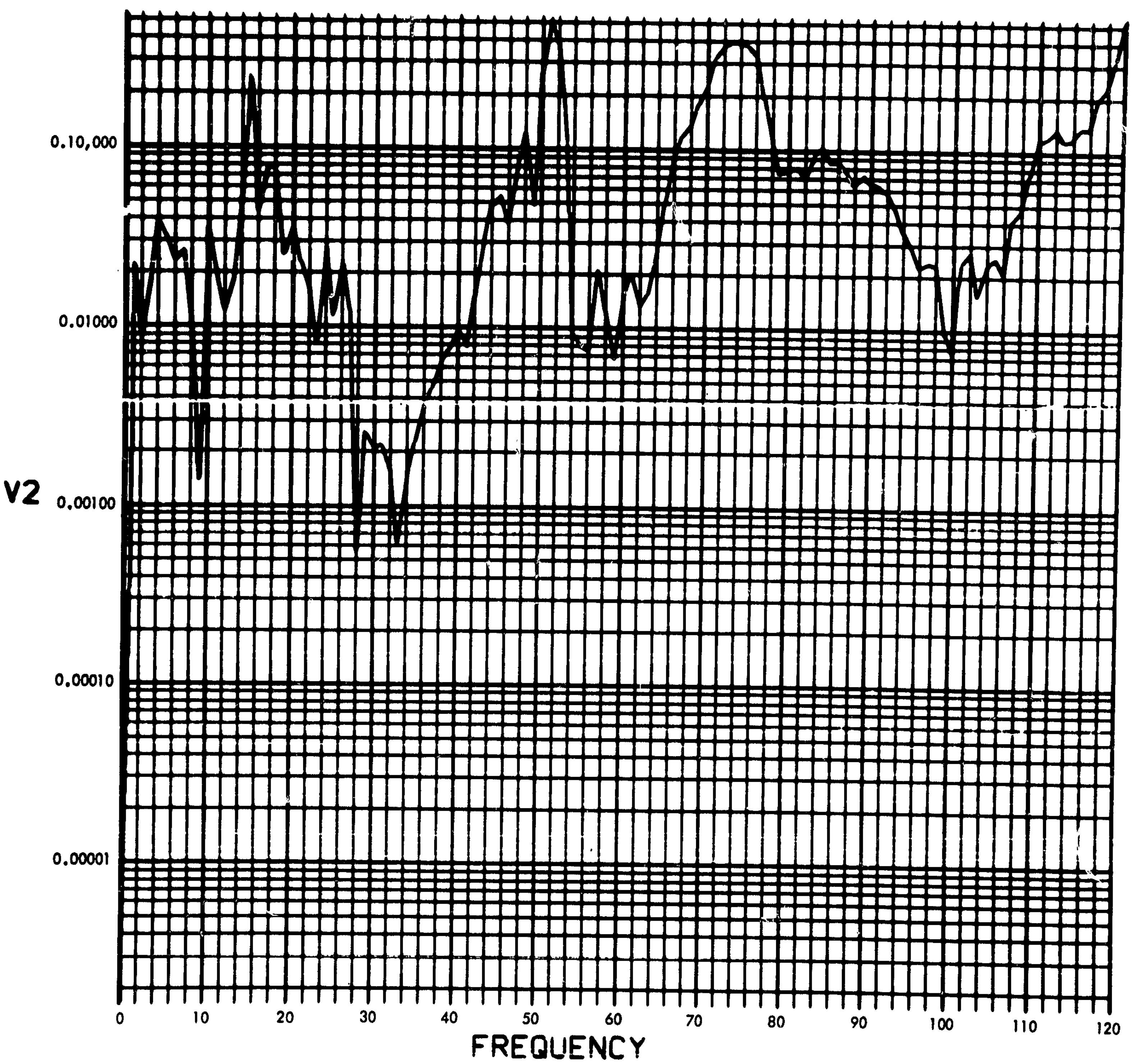

Fig. C-245. Joint 17, acceleration response, Fourier transform, modulus (pulse 3)

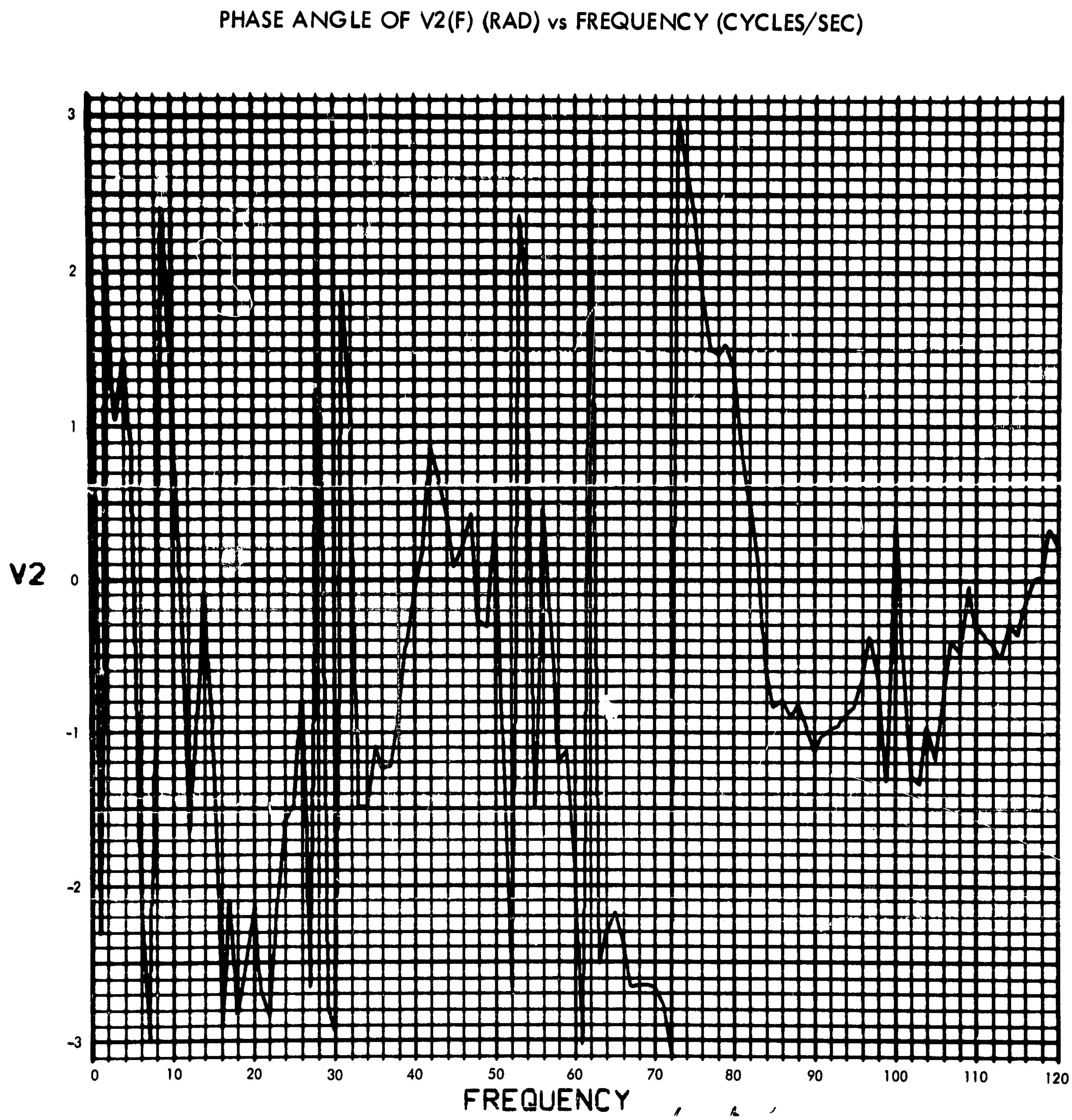

Fig. C-246. Joint 17, acceleration response, Fourier transform, phase angle (pulse 3)

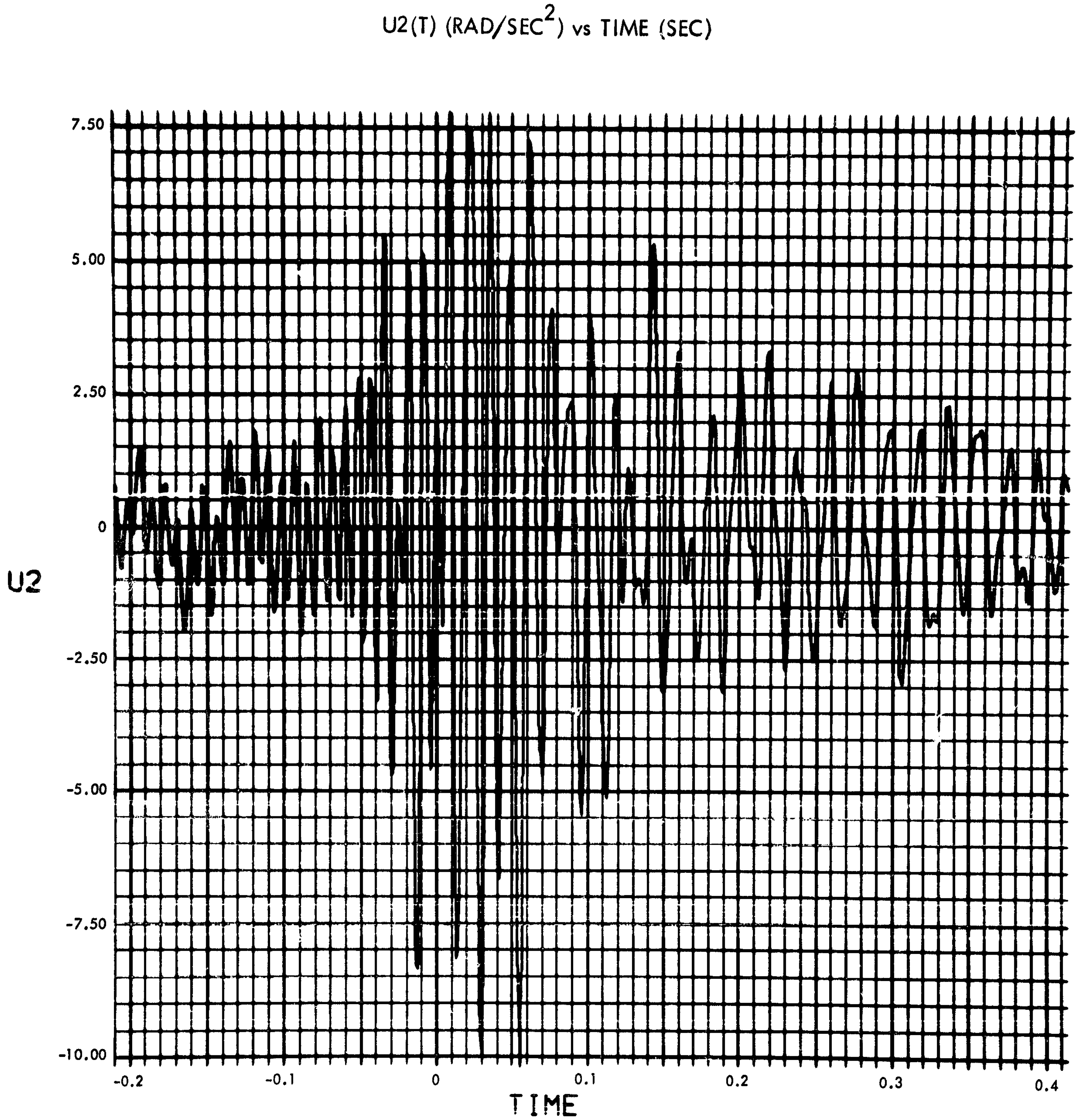

Fig. C-247. Joint 17, acceleration response, time history (pulse 3)

MODULUS OF V2(F) (RAD/SEC) vs FREQUENCY (CYCLES/SEC)

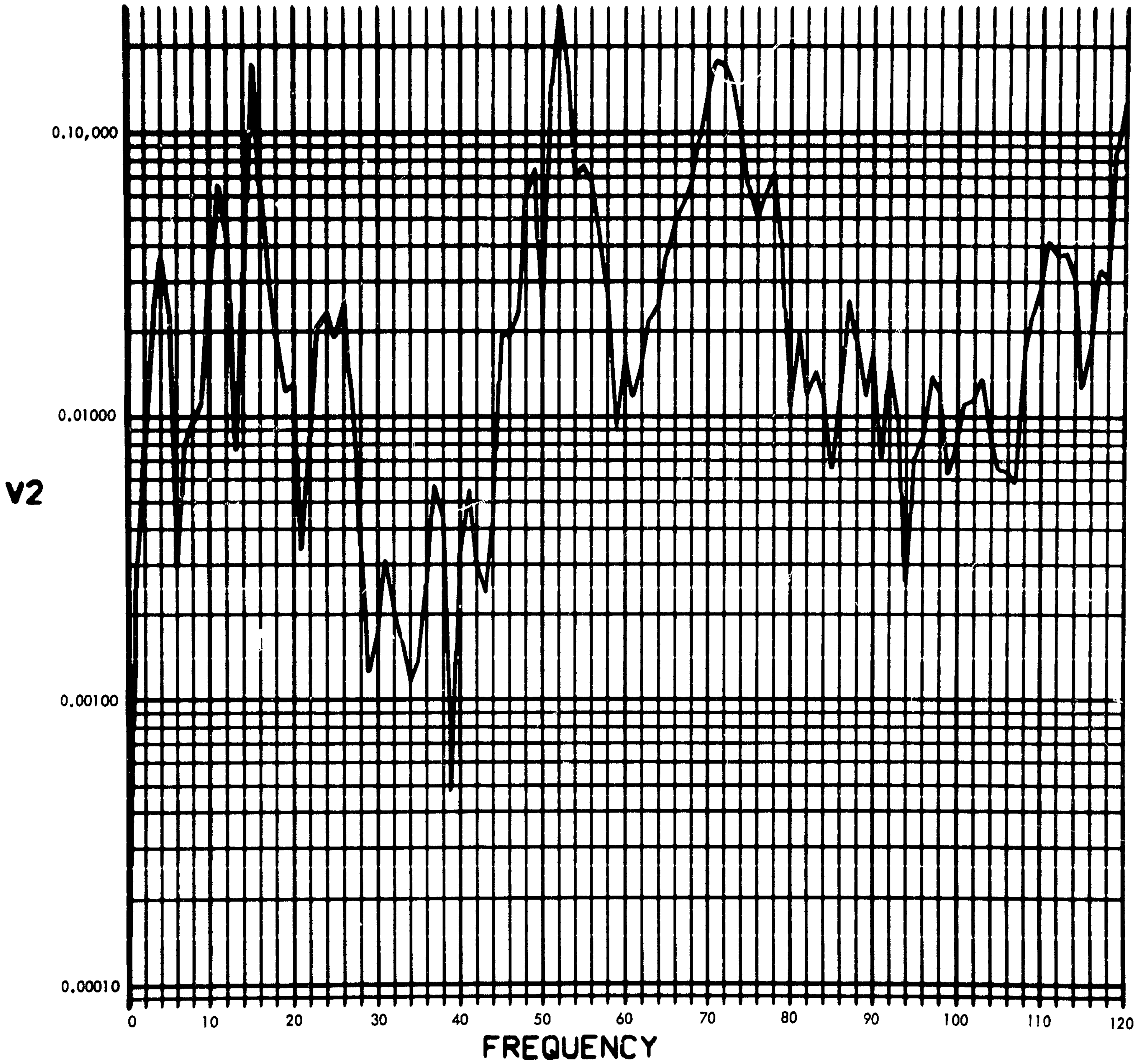

Fig. C-248. Joint 17, acceleration response, Fourier transform, modulus (pulse 4)

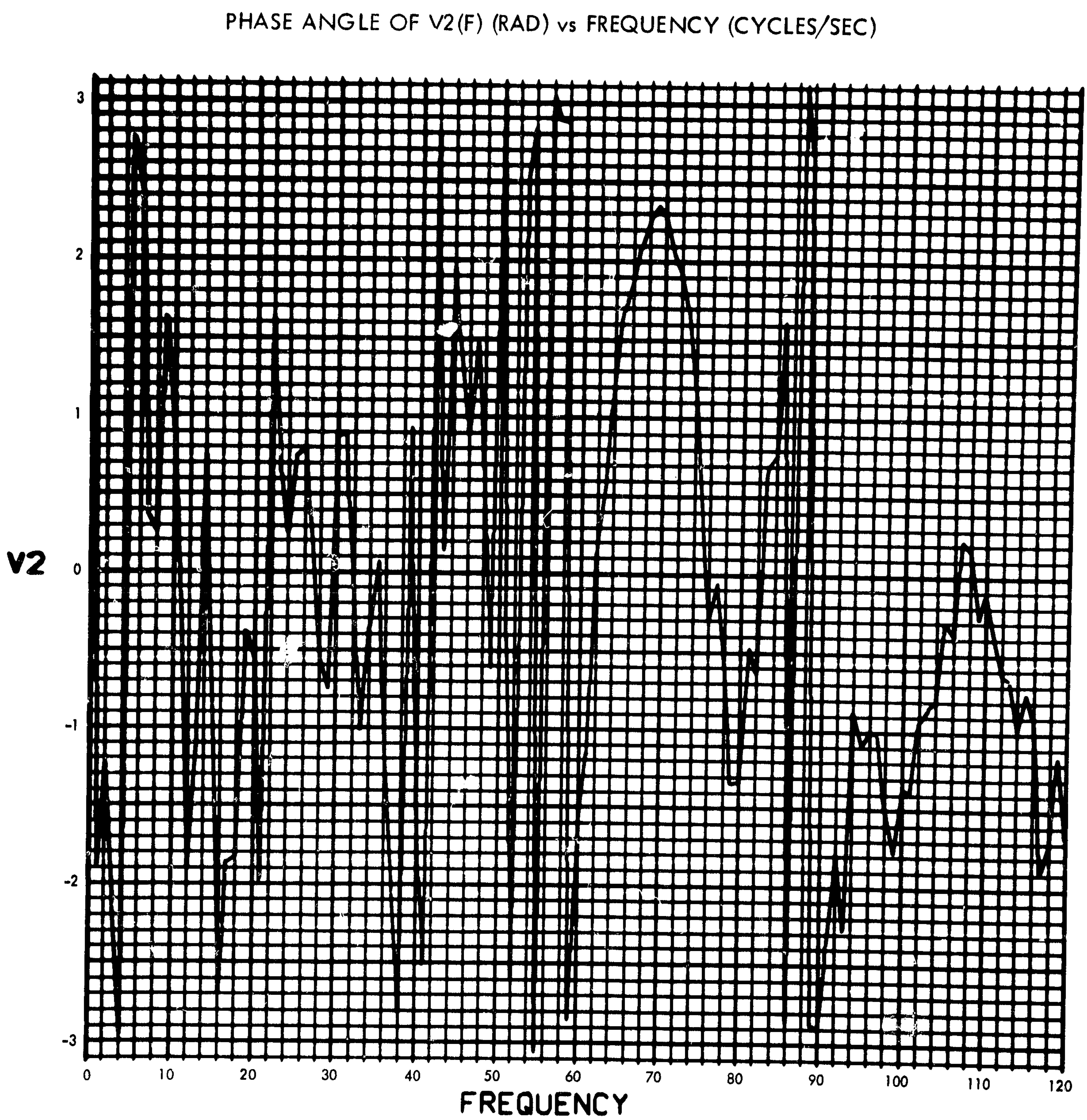

Fig. C-249. Joint 17, acceleration response, Fourier transform, phase angle (pulse 4)

U2(T) (RAD/SEC^2) vs TIME (SEC)

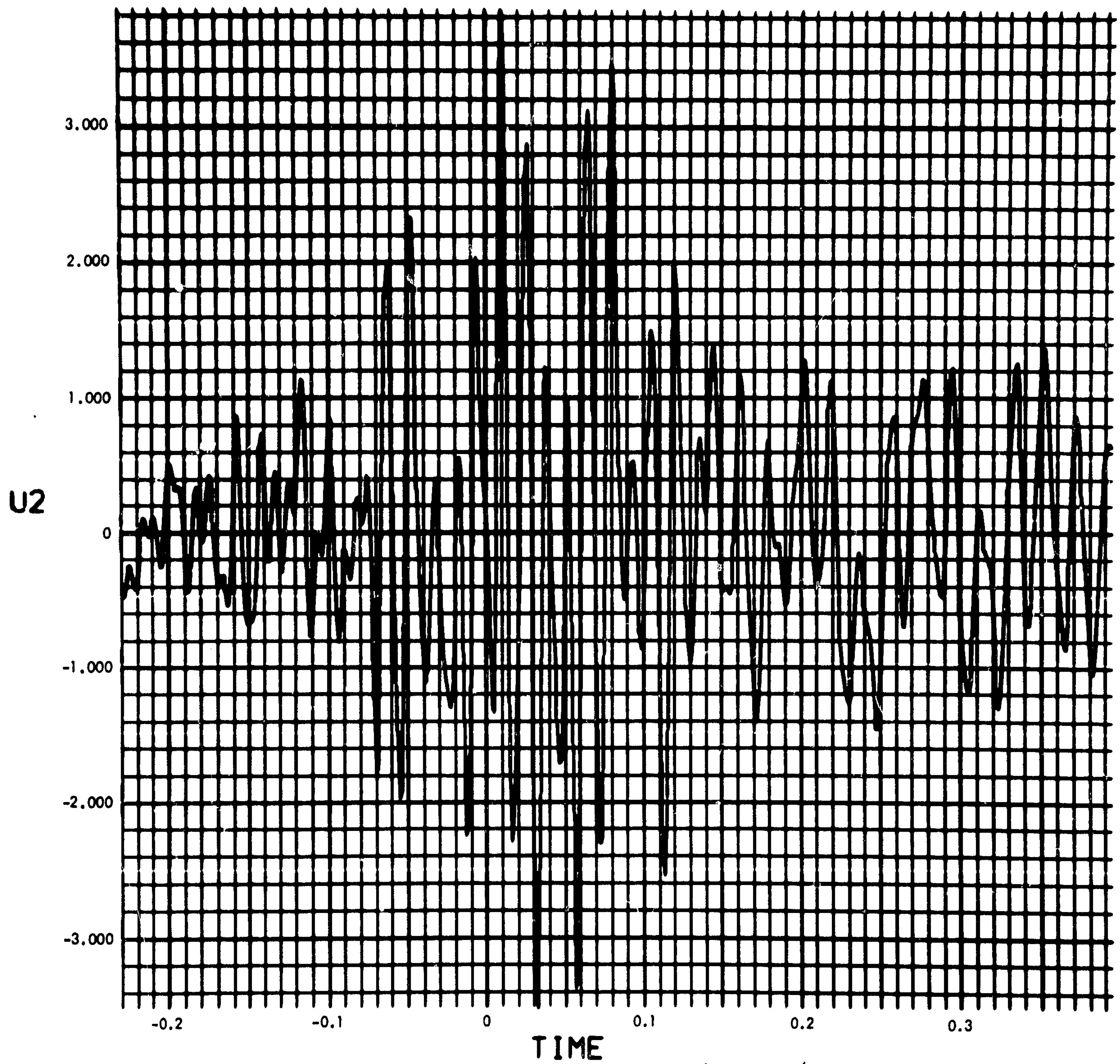

Fig. C-250. Joint 17, acceleration response, time history (pulse 4)

MODULUS $H_T(F)$ vs FREQUENCY (CYCLES/SEC)

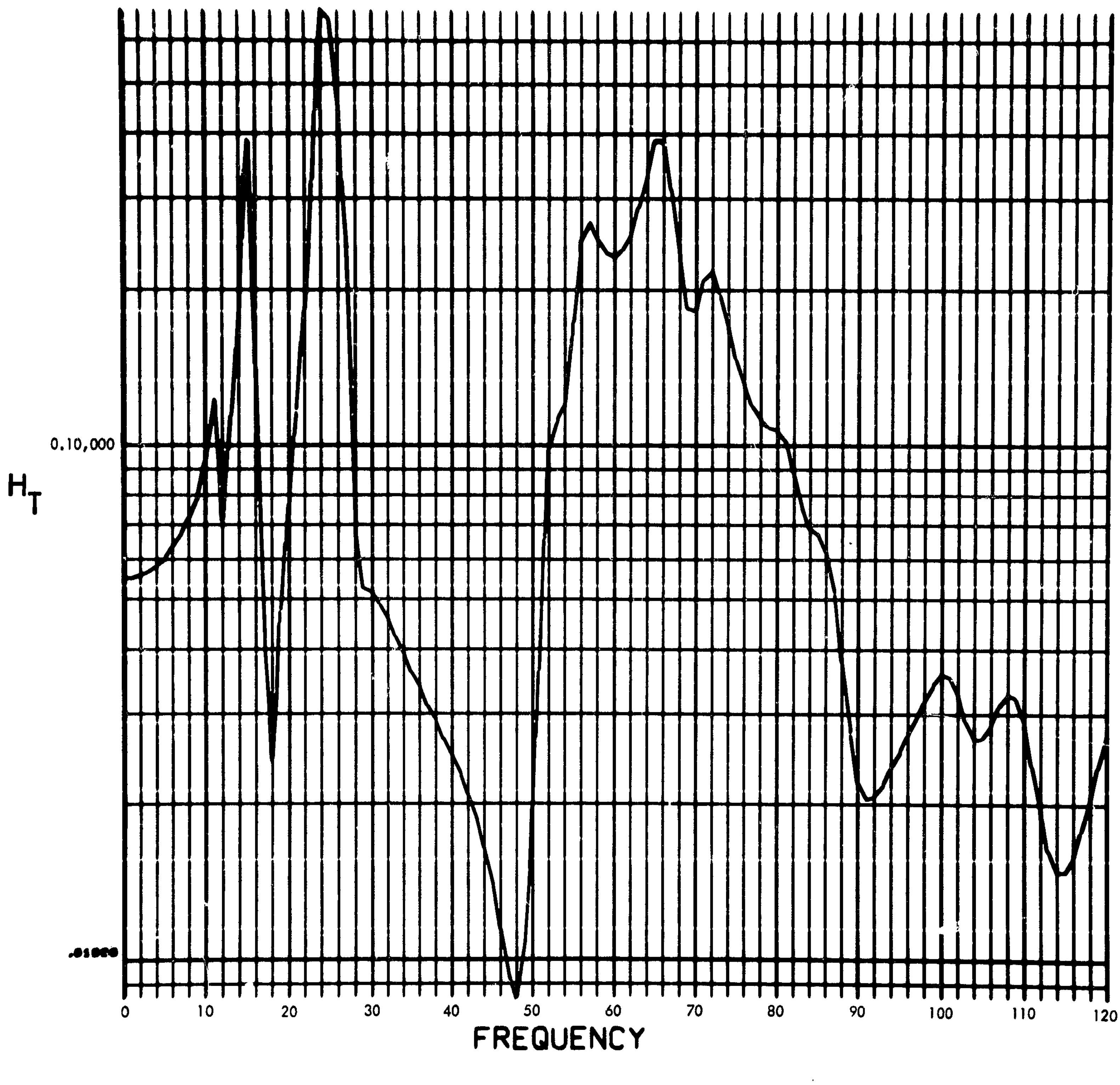

Fig. C-251. Joint 17, torque transfer function, Fourier transform, modulus

PHASE ANGLE OF $H_T(F)$ (RAD) vs FREQUENCY (CYCLES/SEC)

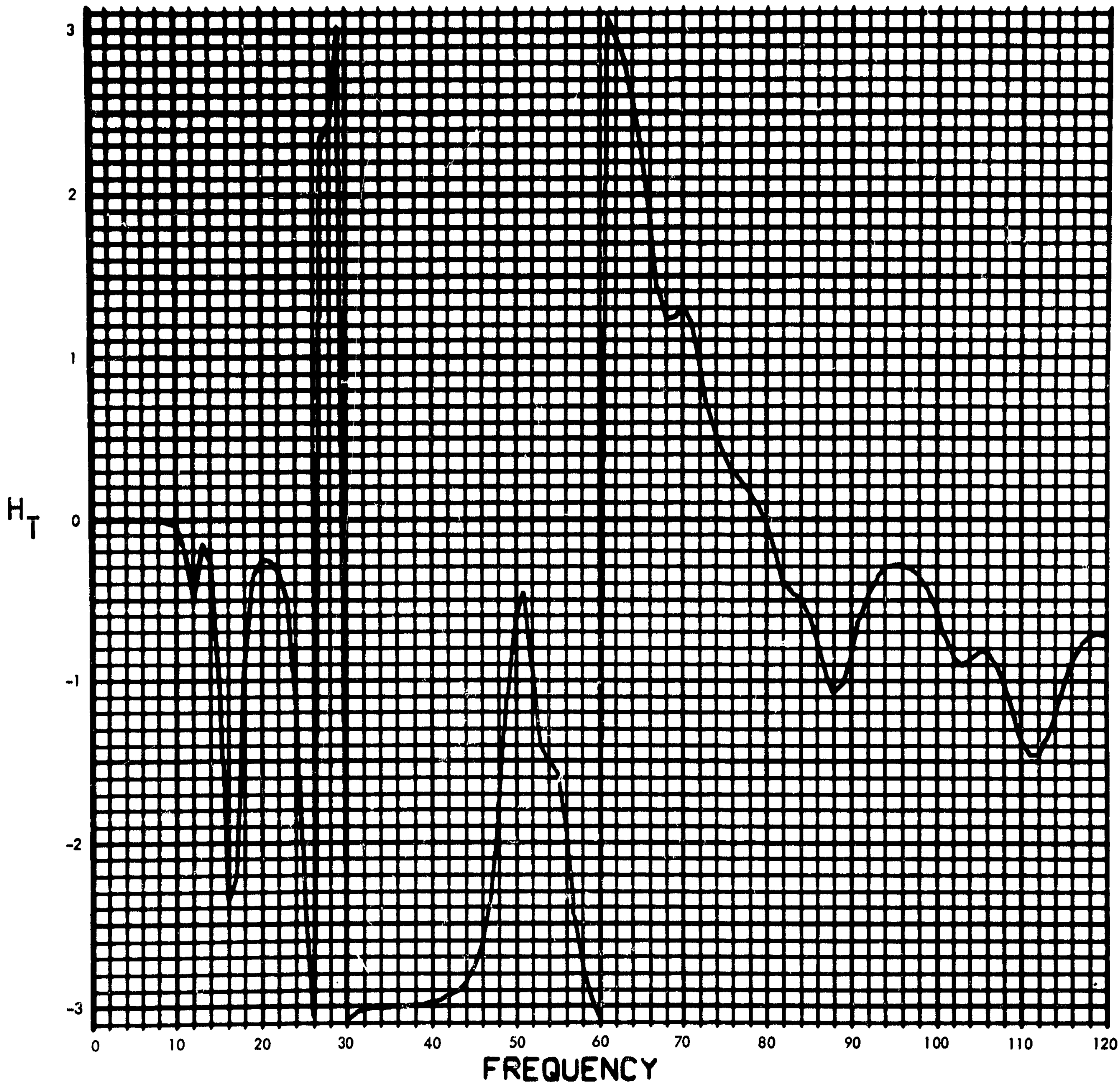

Fig. C-252. Joint 17, torque transfer function, Fourier transform, phase angle

MODULUS OF $F_T(F)$ (LB-IN-SEC) vs FREQUENCY (CYCLES/SEC)

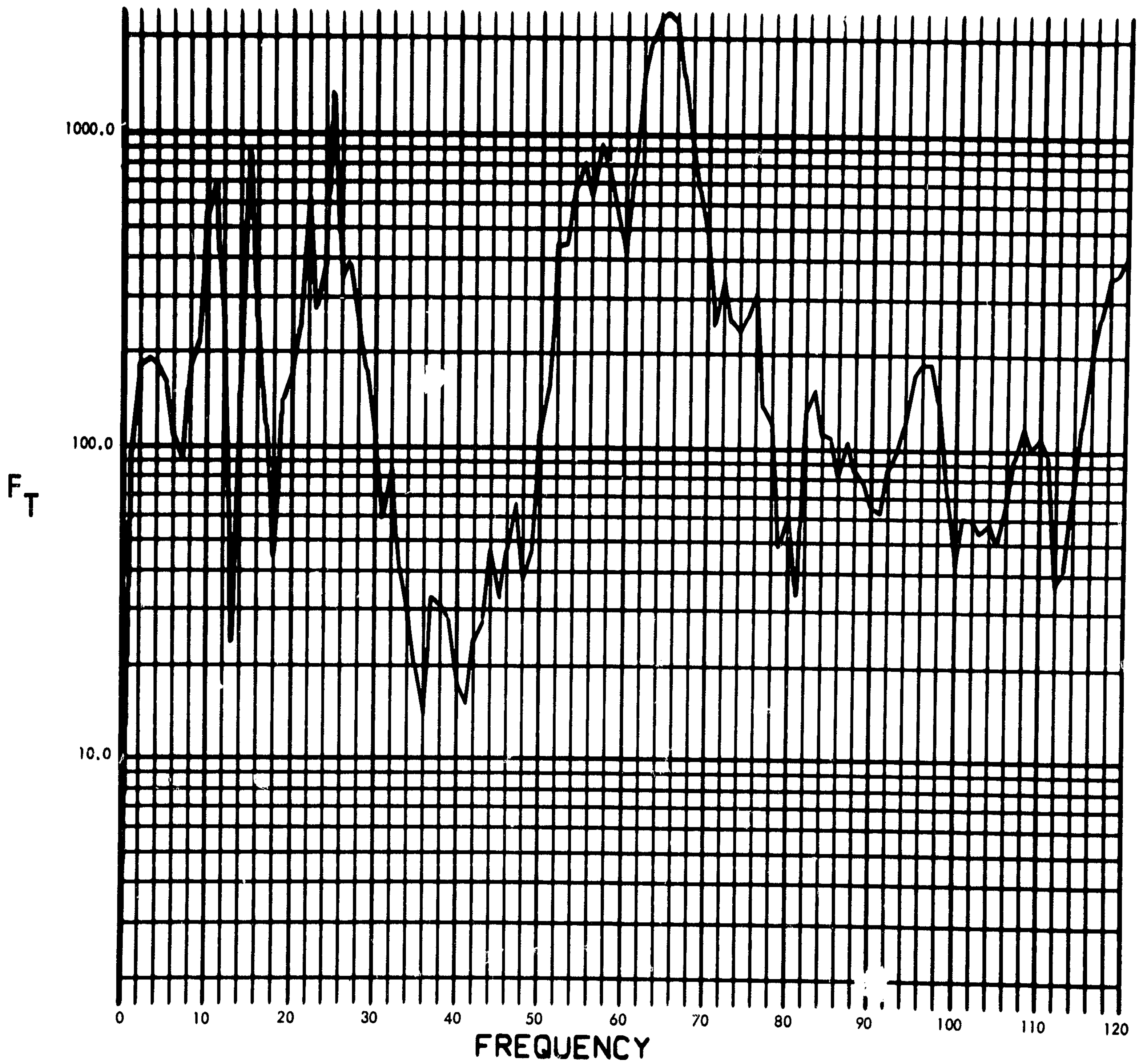

Fig. C-253. Joint 17, torque response, Fourier transform, modulus (pulse 1)

PHASE ANGLE OF $F_T(F)$ (RAD) vs FREQUENCY (CYCLES/SEC)

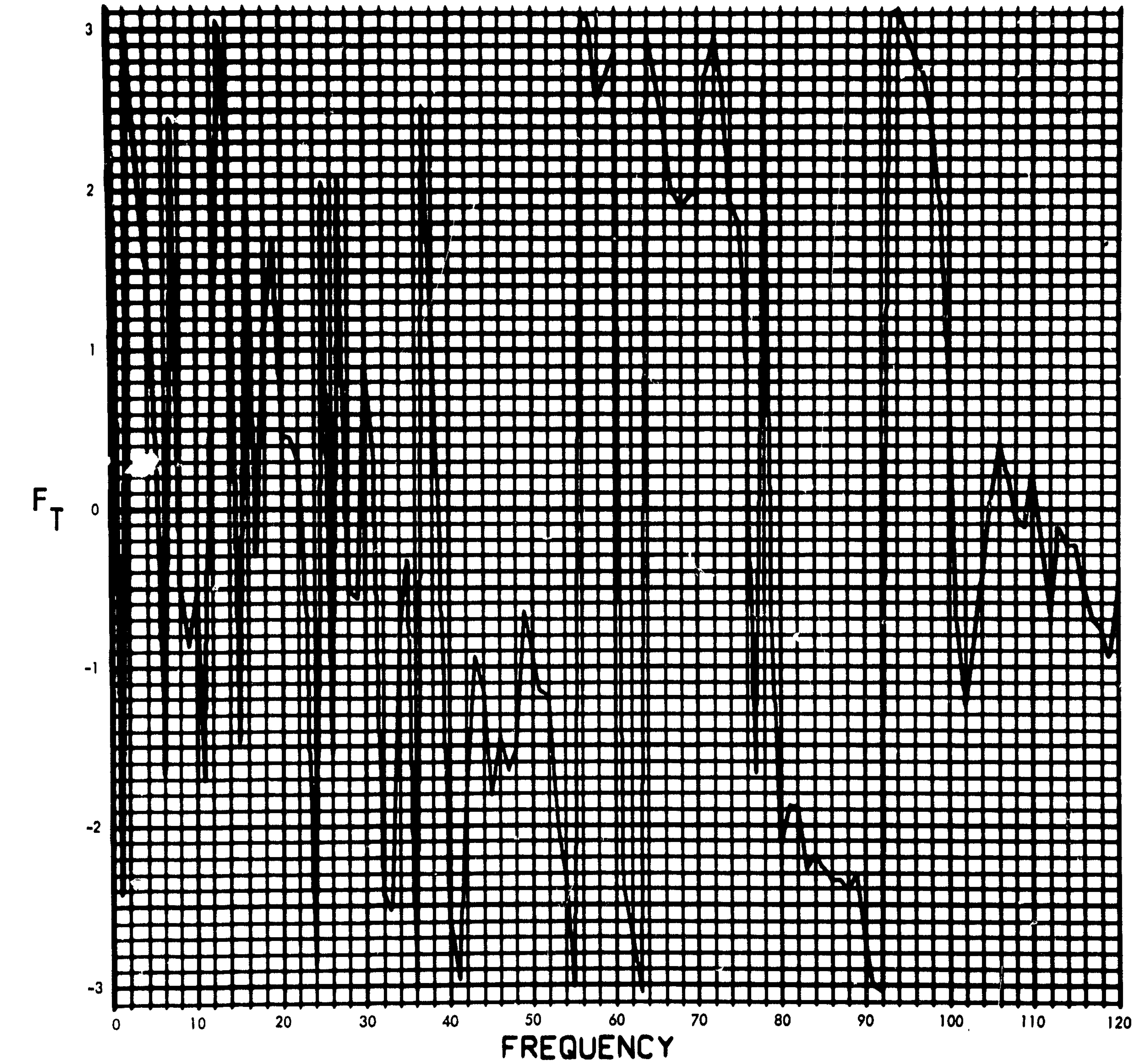

Fig. C-254. Joint 17, torque response, Fourier transform, phase angle (pulse 1)

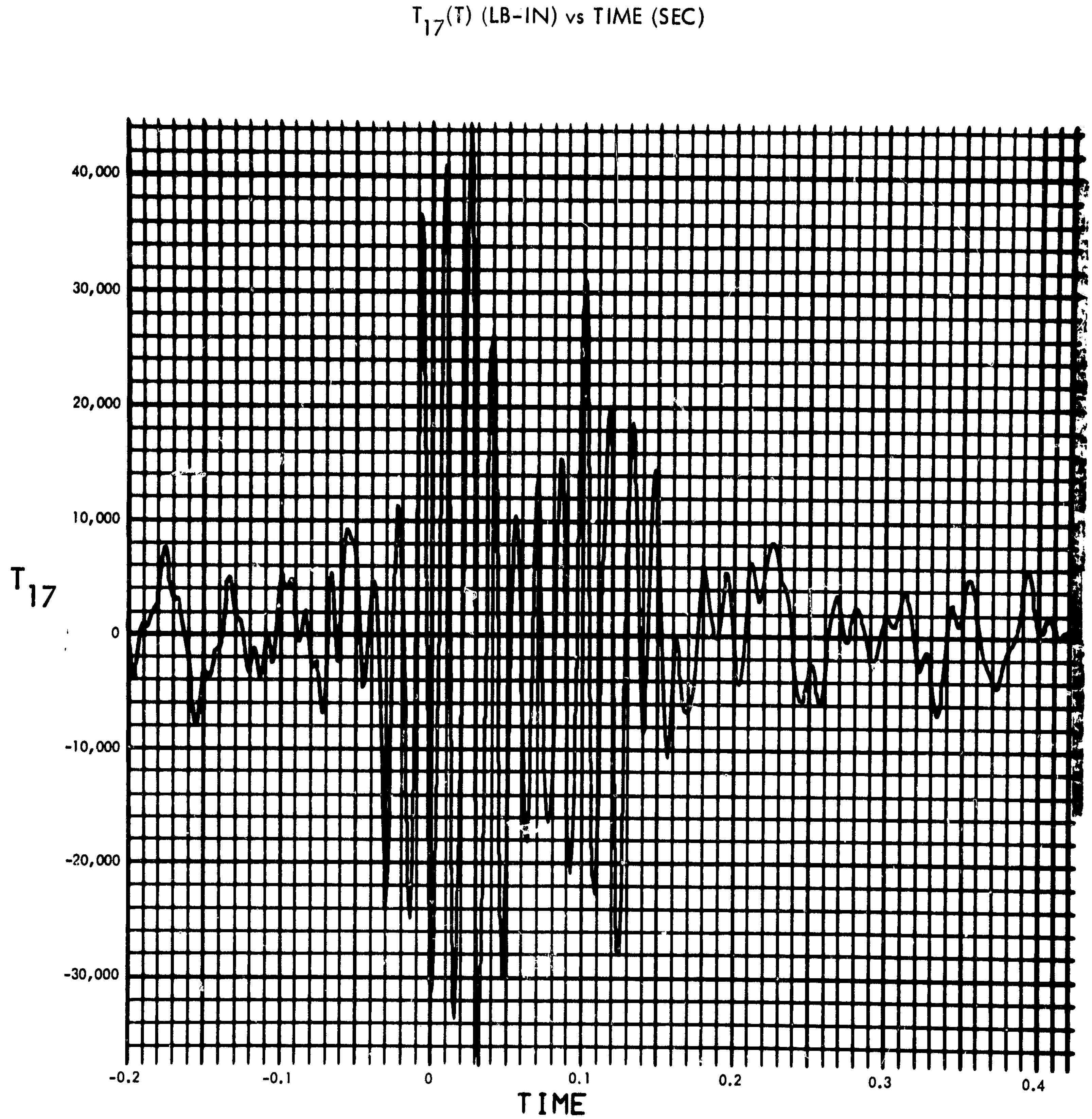

Fig. C-255. Joint 17, torque response, time history (pulse 1)

MODULUS OF $F_T(F)$ (LB-IN-SEC) vs FREQUENCY (CYCLES/SEC)

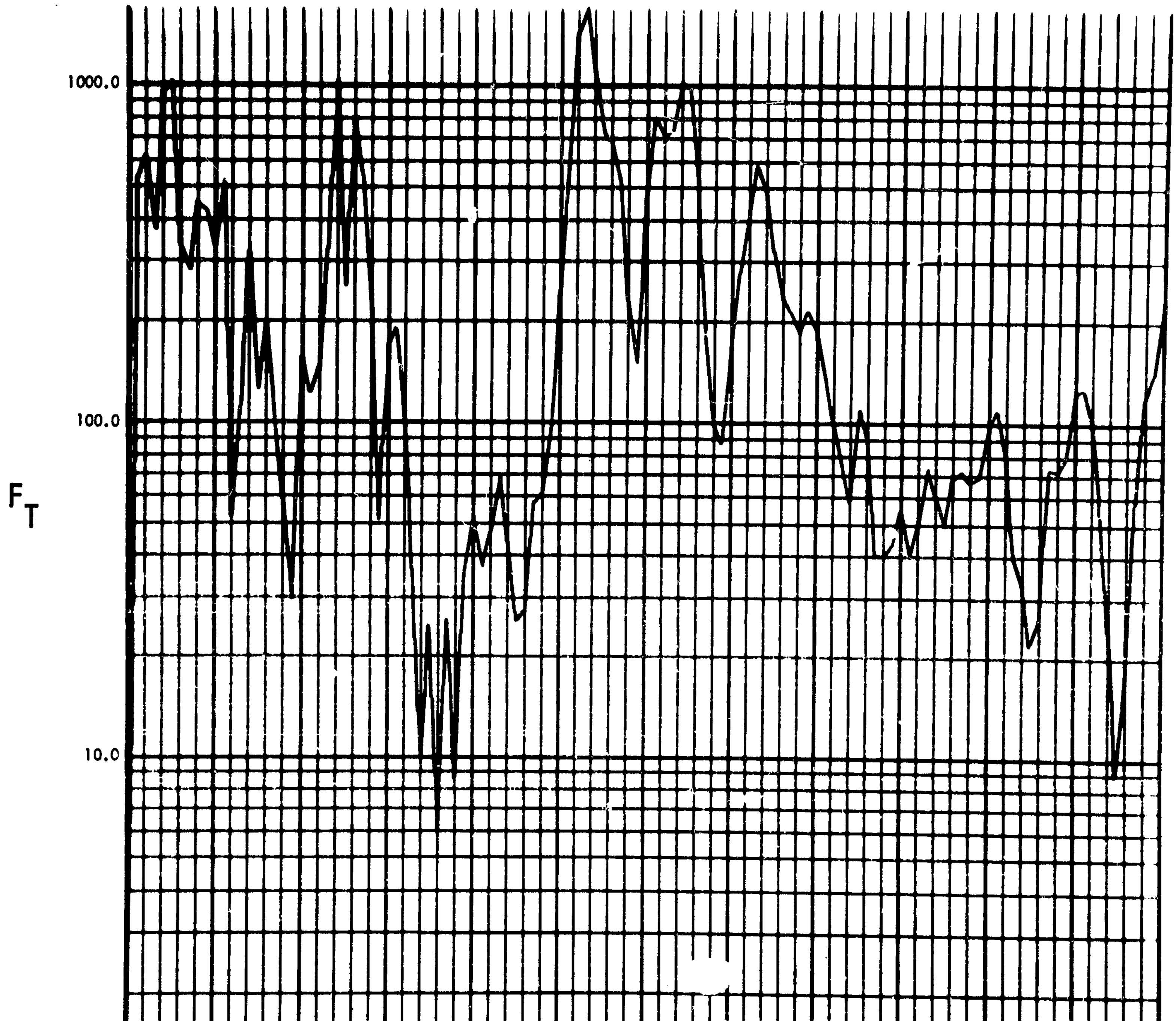

Fig. C-256. Joint 17, torque response, Fourier transform, modulus (pulse 2)

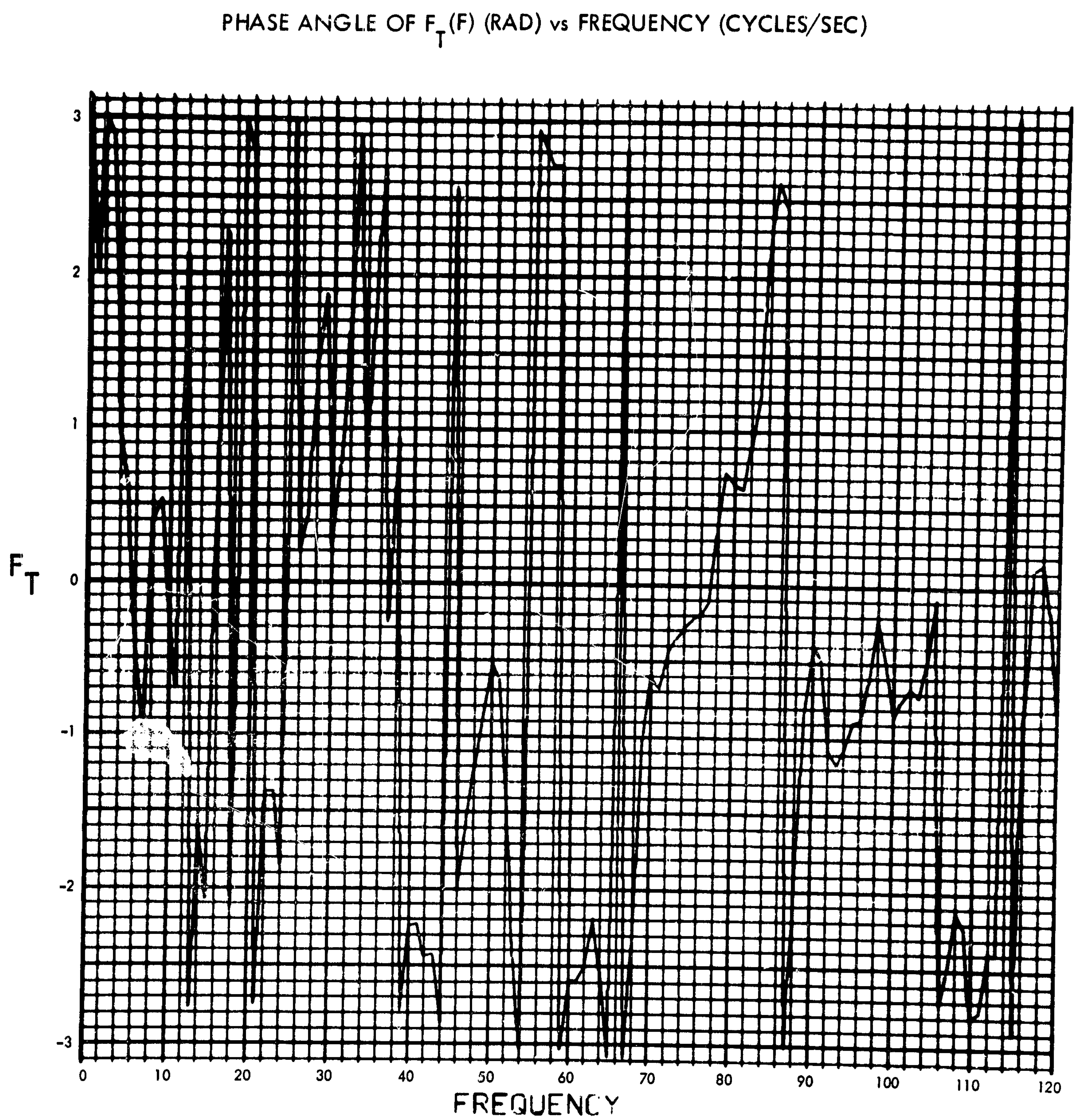

Fig. C-257. Joint 17, torque response, Fourier transform, phase angle (pulse 2)

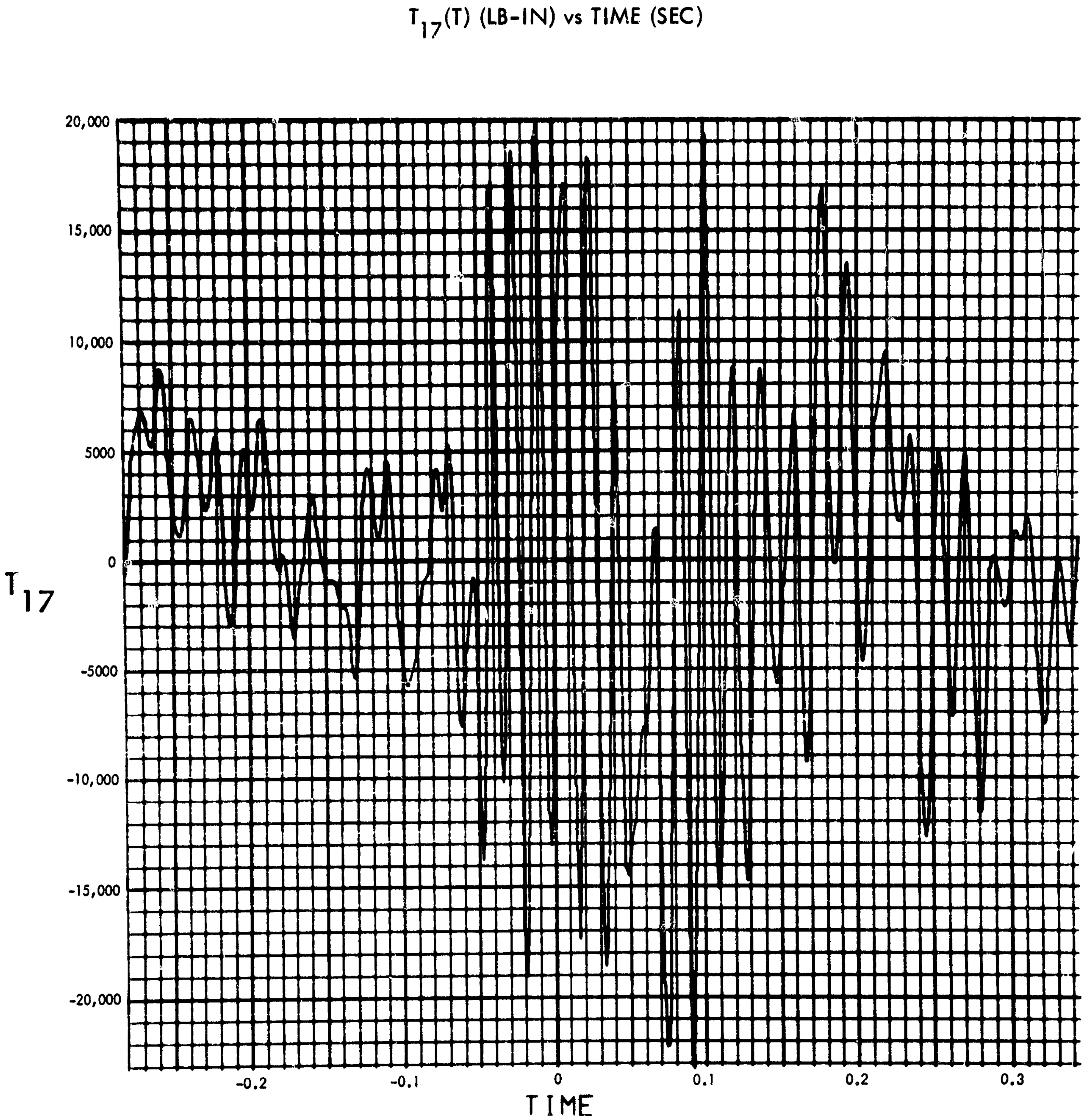

Fig. C-258. Joint 17, torque response, time history (pulse 2)

MODULUS OF $F_T(F)$ (LB-IN-SEC) vs FREQUENCY (CYCLES/SEC)

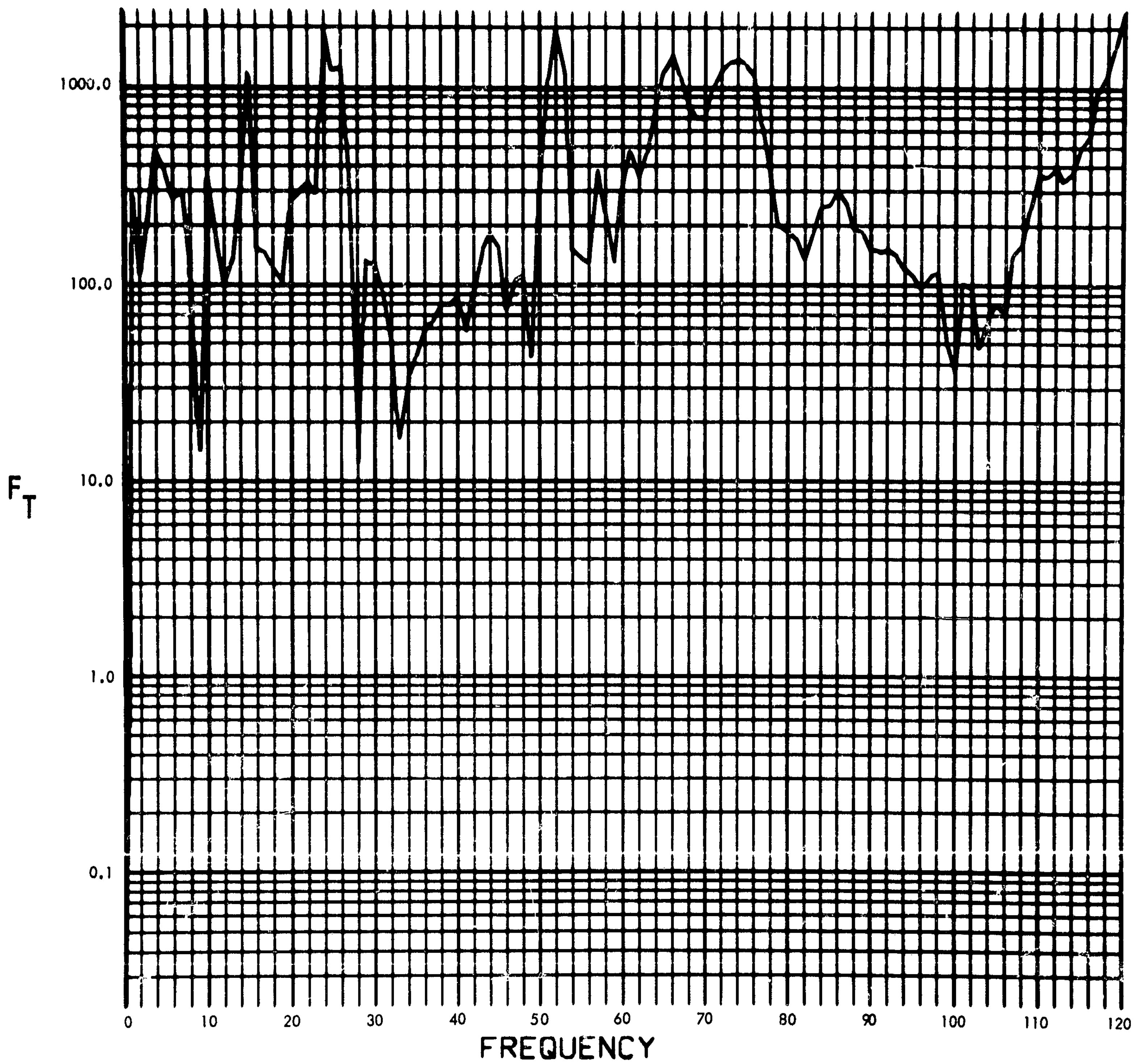

Fig. C-259. Joint 17, torque response, Fourier transform, modulus (pulse 3)

PHASE ANGLE OF $F_T(F)$ (RAD) vs FREQUENCY (CYCLES/SEC)

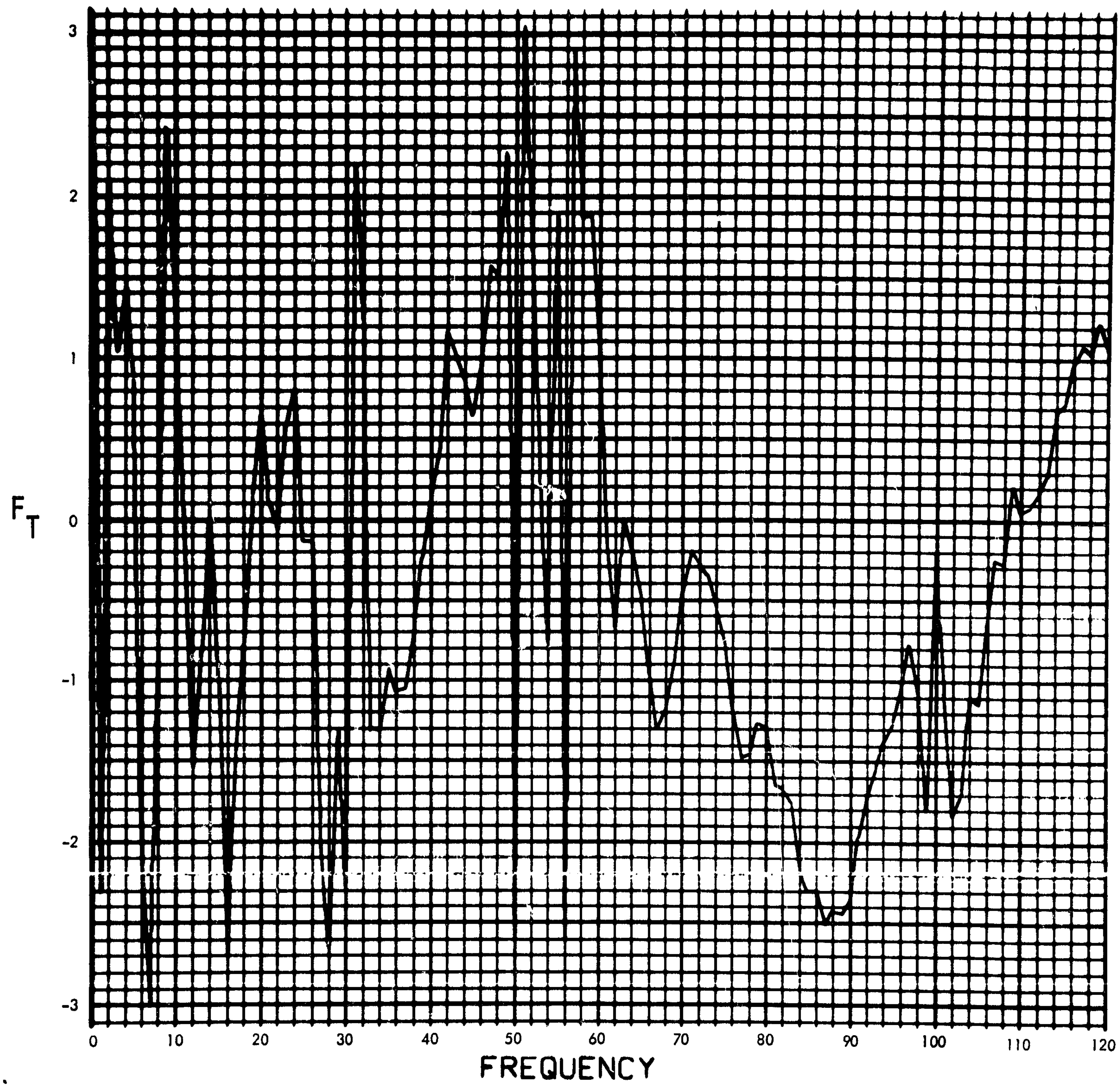

Fig. C-260. Joint 17, torque response, Fourier transform, phase angle (pulse 4)

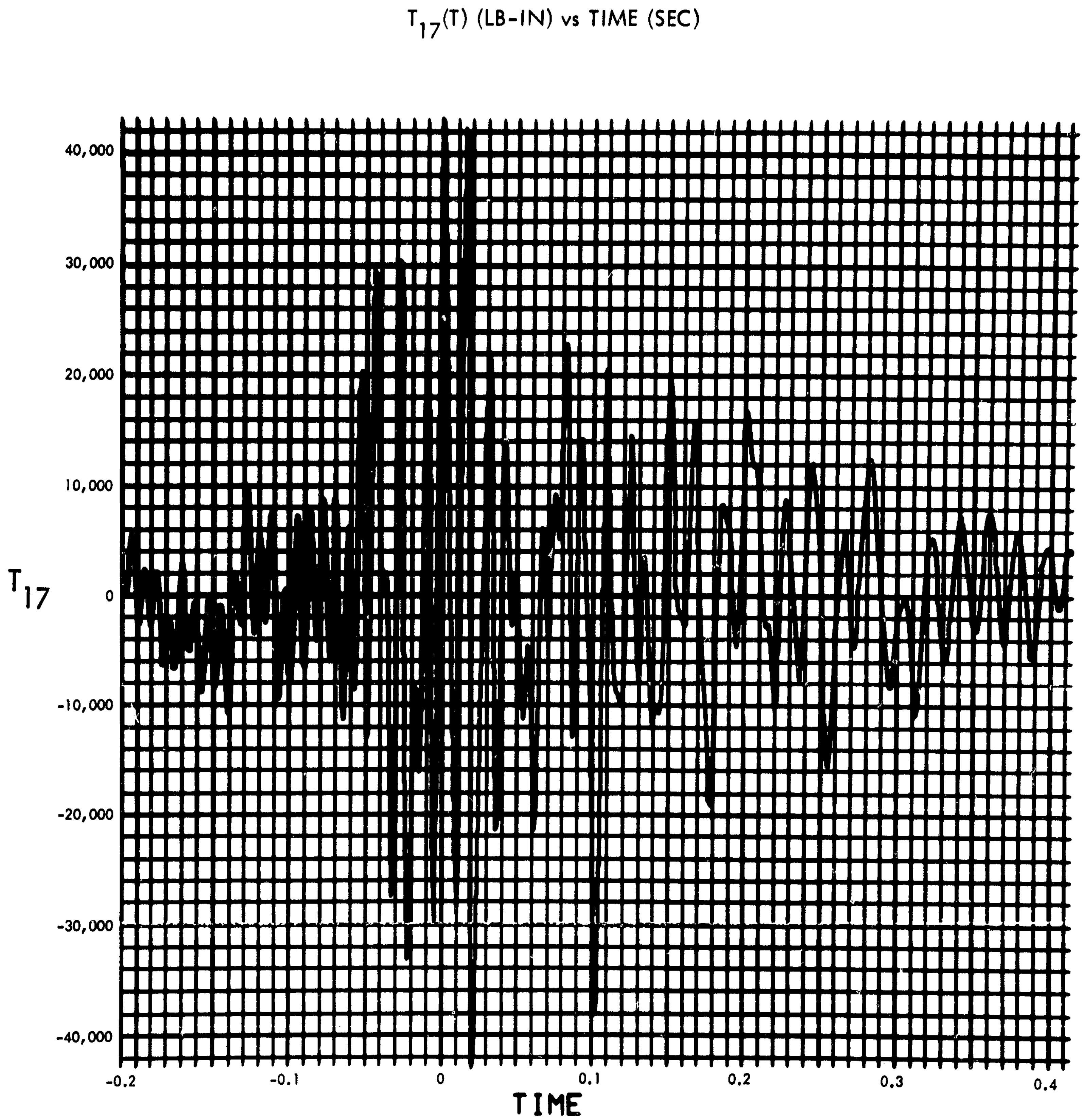

Fig. C-261. Joint 1', torque response, time history (pulse 3)

MODULUS OF $F_T(F)$ (LB-IN-SEC) vs FREQUENCY (CYCLES/SEC)

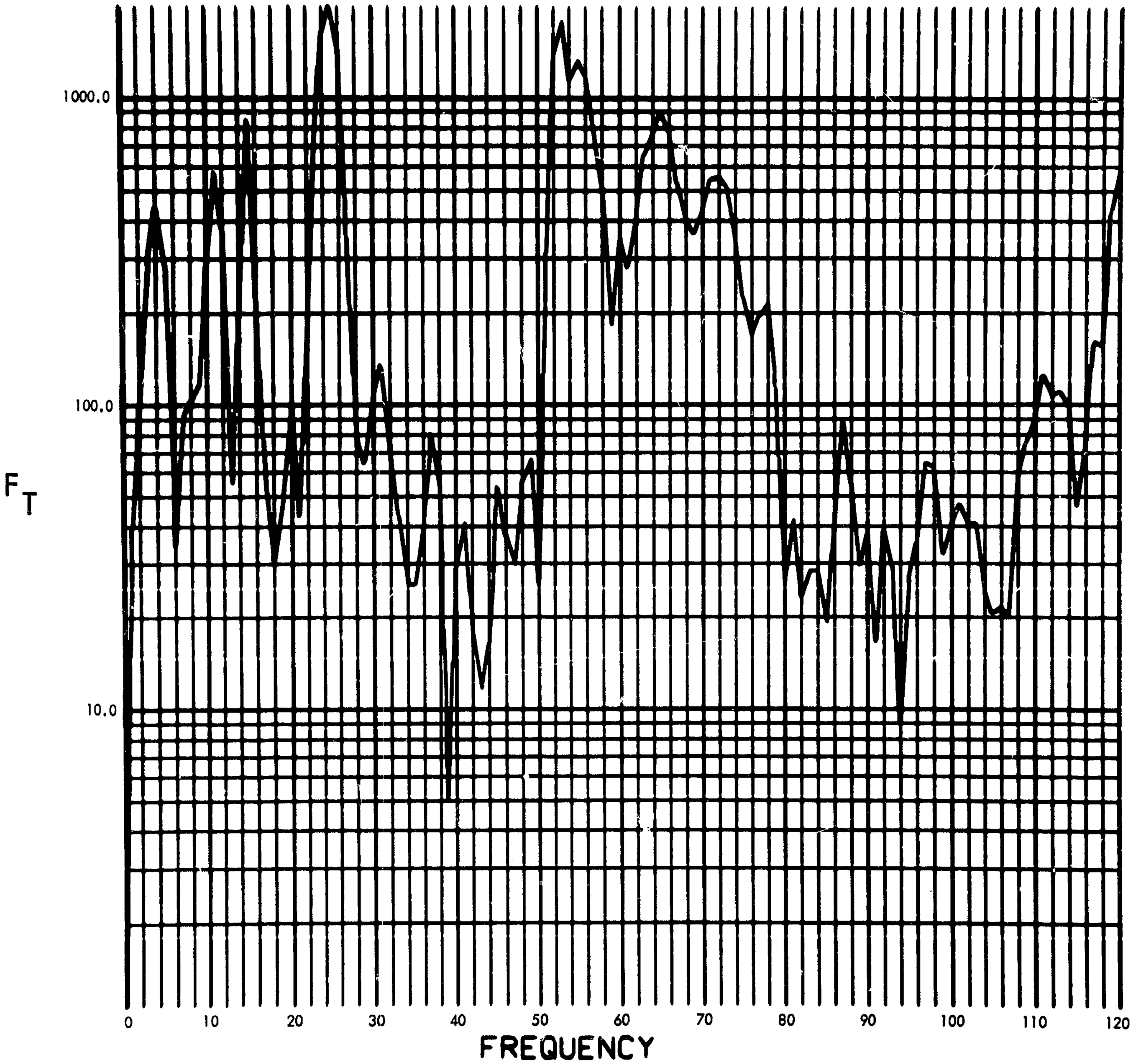

Fig. C-262. Joint 17, torque response, Fourier transform, modulus (pulse 4)

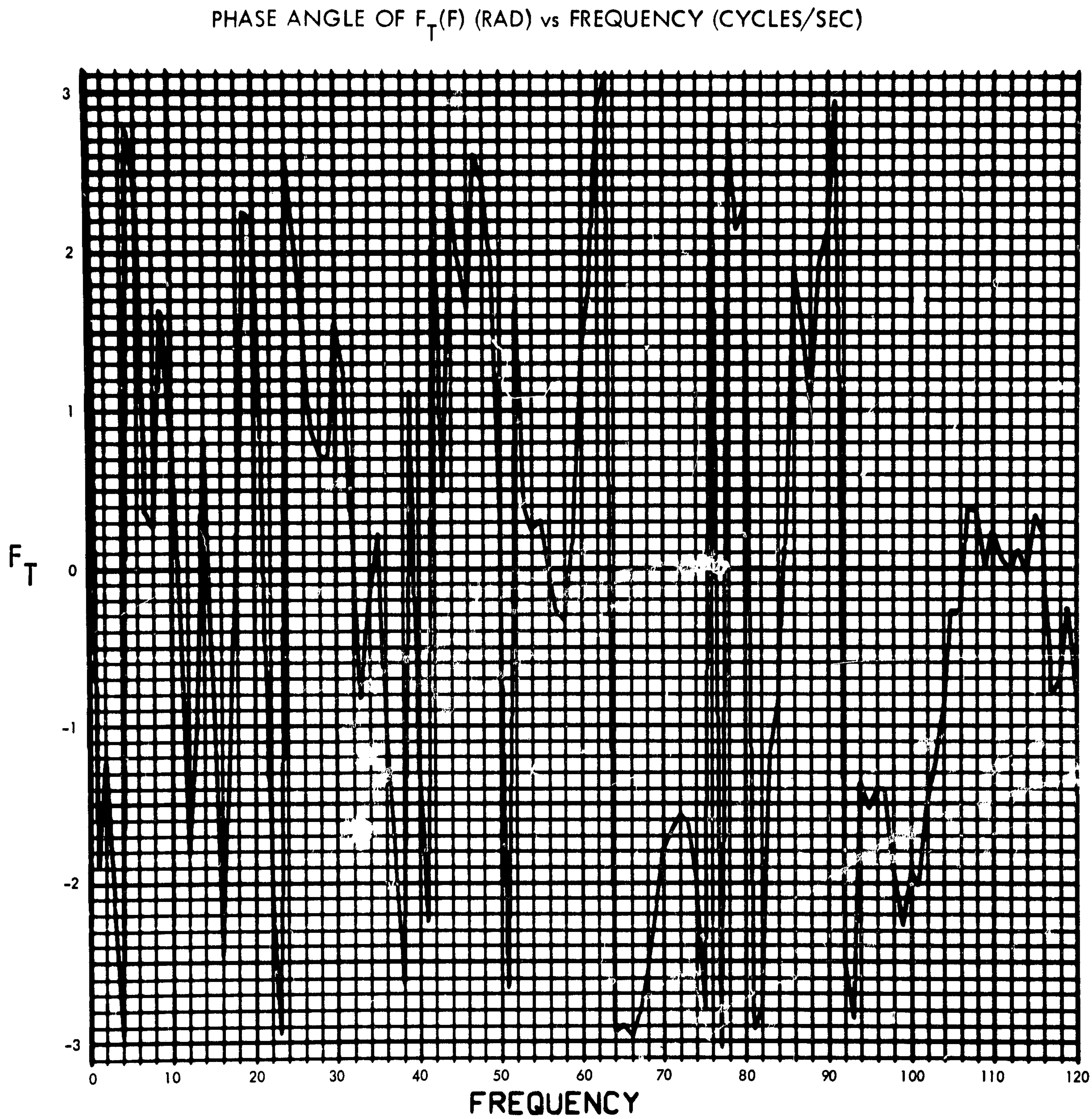

Fig. C-263. Joint 17, torque response, Fourier transform, phase angle (pulse 4)

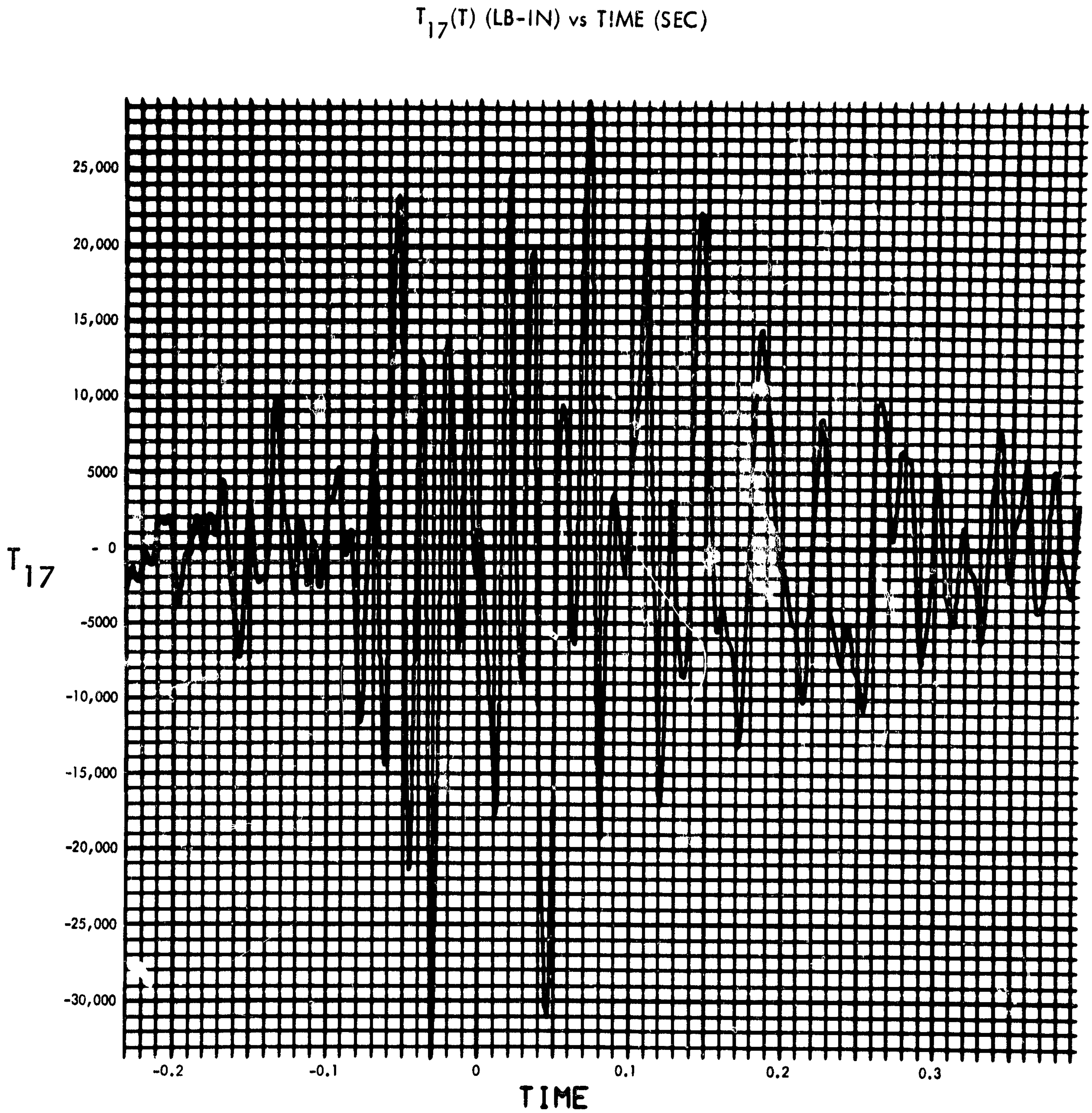

Fig. C-264. Joint 17, torque response, time history (pulse 4)